Enclosure 3 to E-46110

NUHOMS®-MP197 Transportation Package Safety Analysis Report, Revision 17A Consolidated Appendix A.1.4.8, Appendix A.1.4.9, Appendix A.2.13.11, Chapter A.3, and Chapter A.5

(Non-Proprietary)

Appendix A.1.4.8
NUHOMS®-61BTH DSC

TABLE OF CONTENTS

A.1.4.8.1 NUHOMS®-61BTH DSC Description A.1.4.8-1
A.1.4.8.2 NUHOMS®-61BTH DSC Fuel Basket A.1.4.8-1
A.1.4.8.3 NUHOMS®-61BTH DSC Contents A.1.4.8-2
A.1.4.8.4 References A.1.4.8-3a

LIST OF TABLES

Table A.1.4.8-1 Key Design Parameters of the NUHOMS®-61BTH System A.1.4.8-4
Table A.1.4.8-2 BWR Fuel Specification for the Fuel to be Transported in the NUHOMS®-61BTH DSC A.1.4.8-5
Table A.1.4.8-3 BWR Fuel Assembly Design Characteristics for the NUHOMS®-61BTH DSC A.1.4.8-7
Table A.1.4.8-4 BWR Fuel Assembly Lattice Average Initial Enrichment v/s Minimum B10 Requirements for the NUHOMS®-61BTH DSC Poison Plates (Intact Fuel) A.1.4.8-9
Table A.1.4.8-5 BWR Fuel Assembly Lattice Average Initial Enrichment v/s Minimum B10 Requirements for the NUHOMS®-61BTH DSC Poison Plates (Damaged/Failed Fuel) A.1.4.8-10
Table A.1.4.8-6 BWR Fuel Qualification Table for NUHOMS®-61BTH Type 1 DSC. A.1.4.8-11
Table A.1.4.8-7 BWR Fuel Qualification Table for NUHOMS®-61BTH Type 2 DSC. A.1.4.8-12
Table A.1.4.8-7a "B" Parameters to Determine Additional Cooling Time for Fuel in Peripheral Compartments (years) A.1.4.8-13a
Table A.1.4.8-8 BWR Assembly Decay Heat for Heat Load Configurations A.1.4.8-14

LIST OF FIGURES

Figure A.1.4.8-1 Heat Load Zoning Configuration No. 1 for Type 1 or Type 2 61BTH DSCs A.1.4.8-15
Figure A.1.4.8-2 Heat Load Zoning Configuration No. 2 for Type 1 or Type 2 61BTH DSCs A.1.4.8-16
Figure A.1.4.8-3 Heat Load Zoning Configuration No. 3 for Type 1 or Type 2 61BTH DSCs A.1.4.8-17
Figure A.1.4.8-4 Heat Load Zoning Configuration No. 4 for Type 1 or Type 2 61BTH DSCs A.1.4.8-18
Figure A.1.4.8-5 Heat Load Zoning Configuration No. 5 for Type 2 61BTH DSC(2) A.1.4.8-19
Figure A.1.4.8-6 Heat Load Zoning Configuration No. 6 for Type 2 61BTH DSC A.1.4.8-20
Figure A.1.4.8-7 Heat Load Zoning Configuration No. 7 for Type 2 61BTH DSC A.1.4.8-21
Figure A.1.4.8-8 Heat Load Zoning Configuration No. 8 for Type 2 61BTH DSC A.1.4.8-22
Figure A.1.4.8-9 Location of Damaged and Failed Fuel Assemblies Inside 61BTH DSC A.1.4.8-23
Figure A.1.4.8-10 Peripheral and Inner Fuel Locations for the 61BTH DSC A.1.4.8-24

Appendix A.1.4.8
NUHOMS®-61BTH DSC

NOTE: References in this Appendix are shown as [1], [2], etc. and refer to the reference list in Section A.1.4.8.4.

A.1.4.8.1 NUHOMS®-61BTH DSC Description

Each NUHOMS®-61BTH DSC consists of a DSC shell assembly and basket assembly. The shell assembly consists of a cylindrical shell, the inner cover plates of the top and bottom shield plug assemblies and outer top cover plate. The DSC shell assembly is designed, fabricated and inspected in accordance with ASME B&PV Code Subsection NB [1]. Alternatives to the code are provided in Chapter A.2, Appendix A.2.13.13. The 61BTH DSC system consists of three design configurations, depending upon the type of fuel and heat load, as follows:

- 61BTH Type 1
- 61BTH Type 2
- 61BTHF, accommodates up to 4 Failed Fuel Cans with Failed Fuel

Table A.1.4.8-1 provides the overall lengths and outer diameters for each 61BTH DSC configuration. The shell assemblies are high integrity stainless steel welded pressure vessels that provide confinement of radioactive materials, encapsulate the fuel in an inert atmosphere (the canister is back-filled with helium before being seal welded closed), and provide biological shielding (in the axial direction). The 61BTH DSCs have double redundant seal welds that join the shell and the top and bottom cover plate assemblies to seal the canister. The bottom end assembly welds are made during fabrication of the 61BTH DSCs. The top end closure welds are made after fuel loading. Both top plug penetrations (siphon and vent ports) are redundantly sealed after the 61BTH DSC drying operations are complete.

The canister is designed to contain its fuel basket and fuel assemblies, and is completely supported by the transport cask. Under normal conditions, the canister rests on four canister rails attached to the inside surface of the aluminum inner sleeve of the transport cask.

A.1.4.8.2 NUHOMS®-61BTH DSC Fuel Basket

The basket structure is designed, fabricated and inspected in accordance with ASME B&PV Code Subsection NG[1]. Alternatives to the code are provided in Chapter A.2, Appendix A.2.13.13. The overall lengths and outer diameters of the baskets, including the hold down rings, are provided in Table A.1.4.8-1. The details of the 61BTH fuel baskets are shown in the drawings in Section A.1.4.10.9 of Appendix A.1.4.10. The 61BTH baskets are designed to accommodate 61 intact, or up to 16 damaged with up to four (4) Failed Fuel Cans (FFCs) loaded with failed fuel with the remainder intact BWR fuel assemblies with or without fuel channels. The basket structure consists of a welded assembly of stainless steel tubes (fuel compartments) separated by poison plates and surrounded by larger stainless steel boxes and support rails.

The basket structure is open at each end. Therefore, longitudinal fuel assembly loads are applied directly to the canister/cask body and not the fuel basket structure. The fuel assemblies are

laterally supported by the stainless steel structural boxes. The basket is laterally supported by the basket rails and the canister shell. The stainless steel basket rails are oriented parallel to the axis of the canister, and are attached to the periphery of the basket to provide support, and to establish and maintain basket orientation.

The failed fuel assemblies are to be placed in individual Failed Fuel Cans (FFCs). Each FFC is constructed of sheet metal and is provided with a welded bottom closure and a removable top closure which allows lifting of the FFC with the enclosed damaged assembly/debris. The FFC is provided with screens at the bottom and top to contain fuel debris and allow fill/drainage of water from the FFC during loading operations. The FFC is protected by the fuel compartment tubes and its only function is to confine the failed fuel.

Shear keys, welded to the inner wall of the DSC, mate with notches in the basket support rails to prevent the basket from rotating during normal operations. Also a hold down ring is installed above the basket to prevent the basket from moving axially during transport.

The NUHOMS®-61BTH DSC is designed with six alternate basket configurations based on the boron content in the poison plates as listed in Table A.1.4.8-4 or Table A.1.4.8-5 (designated as "A" for the poison plates with the lowest B10 loading to "F" for the highest B10 loading). Three alternate poison materials are allowed: (a) Borated Aluminum alloy, (b) Boron Carbide/Aluminum Metal Matrix Composite (MMC), or (c) Boral®. The poison plates provide a heat conduction path from the fuel assemblies to the canister wall, as well as the necessary criticality control.

A.1.4.8.3 NUHOMS®-61BTH DSC Contents

Each of the NUHOMS®-61BTH DSC Type 1 and Type 2 configurations is designed to transport intact (including reconstituted) and/or damaged BWR fuel assemblies as specified in Table A.1.4.8-2 and Table A.1.4.8-3. In addition, the 61BTHF can transport up to four failed fuel assemblies placed in Failed Fuel Cans as described in Table A.1.4.8-2. The fuel to be transported is limited to a maximum lattice average initial enrichment of 5.0 wt. % U-*235*. The maximum allowable fuel assembly average burnup is limited to 62 GWd/MTU and the minimum cooling time requirement is given in Table A.1.4.8-2.

Reconstituted fuel assemblies containing up to four replacement irradiated stainless steel rods per assembly or 61 lower enrichment UO_2 rods instead of Zircaloy clad enriched UO_2 rods are acceptable for storage in 61BTH DSCs as intact fuel assemblies. The stainless steel rods are assumed to have two-thirds the irradiation time as the remaining fuel rods of the assembly. The reconstituted UO_2 rods are assumed to have the same irradiation history as the entire fuel assembly. The reconstituted rods can be at any location in the fuel assemblies. The maximum number of reconstituted fuel assemblies per DSC is four with irradiated stainless steel rods or 61 with UO_2 rods or Zr rods or Zr pellets or unirradiated stainless steel rods.

The NUHOMS®-61BTH DSCs can also accommodate up to a maximum of 16 damaged fuel assemblies placed in the 2x2 compartments located at the outer edge of the DSC as shown in Figure A.1.4.8-9. Damaged BWR fuel assemblies are assemblies containing missing or partial fuel rods, or fuel rods with known or suspected cladding defects greater than hairline cracks or

pinhole leaks. The extent of damage in the fuel rods is to be limited such that the fuel assembly will still be able to be handled by normal means. Missing fuel rods are allowed. The DSC basket cells which accommodate damaged fuel assemblies are provided with top and bottom end caps.

The NUHOMS®-61BTHF DSC, an alternative version of NUHOMS®-61BTH DSC discussed in Section A.1.4.8.2 is designed to accommodate up to a maximum of four failed fuel assemblies in failed fuel cans placed in cells located at the outer edge of the DSC as shown in Figure A.1.4.8-9. Failed fuel is defined as ruptured fuel rods, severed fuel rods, loose fuel pellets, or fuel assemblies that cannot be handled by normal means. Fuel assemblies may contain breached rods, grossly breached rods, and other defects such as missing or partial rods, missing grid spacers, or damaged spacers to the extent that the assembly cannot be handled by normal means.

Fuel debris and damaged fuel rods that have been removed from a damaged fuel assembly and placed in a rod storage basket are also considered as failed fuel, and therefore shall be encapsulated in individual failed fuel cans as described above. *The rod storage baskets consist of an array (typically 6x6) of hollow cylindrical steel tubes axially supported by perforated plates that has approximately the same width of a fuel assembly and span the length of fuel rods. A maximum of 36 BWR fuel rods can be stored in each rod storage basket.* The tubes of the rod storage basket shall have a provision to allow for the drainage of water, by using either a screen mesh opening or a drainage hole on the bottom of the tubes, or by some other equivalent effective mean. Loose fuel debris, not contained in a rod storage basket may also be placed in a failed fuel can for storage, provided the size of the debris is larger than the failed fuel can screen mesh opening and it is located at a position of at least 10″ above the top of the bottom shield plug of the DSC.

Fuel debris may be associated with any type of UO_2 fuel provided that the maximum uranium content and initial enrichment limits are met. The total weight of each failed fuel can plus all its content shall be less than 705 lb.

A 61BTH DSC containing less than 61 fuel assemblies may contain dummy fuel assemblies in the empty slots. The dummy assemblies are unirradiated, stainless steel encased structures that approximate the weight and center of gravity of a fuel assembly.

The NUHOMS®-61BTH DSC may transport up to 61 BWR fuel assemblies arranged in any of the eight alternate heat load zoning configurations shown in Figure A.1.4.8-1 through A.1.4.8-8.

The basket is divided into inner and peripheral zones, as shown in Figure A.1.4.8-10. Fuel in the inner zone is governed by the cooling times presented in Table A.1.4.8-6 and Table A.1.4.8-7 for the Type 1 and 2 basket, respectively. These cooling times are determined to meet dose rate limits. For fuel in the peripheral zone, certain burnup and enrichment combinations require additional cooling time governed by the following equation:

Peripheral Compartment Cooling = Fuel Qualification Table Cooling + Δt

$$\Delta t = 26.13 \cdot \ln\left(\frac{m}{198}\right) + B \qquad \text{(A.1.4.8-1)}$$

Where,

Δt = cooling time to be added to the appropriate value in Table A.1.4.8-6 or Table A.1.4.8-7 (years)
m = the uranium loading of the fuel assembly to be shipped (kg), and
B = additional cooling time (years), obtain from Table A.1.4.8-7a

This equation applies only if the "B" value is defined in Table A.1.4.8-7a. Additional cooling is not required for burnup and enrichment combinations that fall in the zone labeled "no additional cooling time required." Therefore, no additional cooling is required for burnups < *49* GWd/MTU.

This equation can return a negative value for Δt, which indicates that no additional cooling is required. In such a scenario, $\Delta t \equiv 0$ years. Application of the method is illustrated in the following examples.

Example #1: Fuel with a burnup of 62 GWd/MTU, enrichment of 2.6 wt. % U-235, and uranium loading of 198 kgU is to be loaded in the peripheral zone of the Type 1 DSC. From Table A.1.4.8-6, the minimum cooling time is 29.5 years. From the equation above, $\Delta t = 26.13*\ln(1) + 10.5 = 10.5$ years. Therefore, the minimum required cooling time for this fuel assembly in the peripheral zone is $29.5+10.5 = 40.0$ years.

Example #2: Fuel with a burnup of *58* GWd/MTU, enrichment of 4.0 wt. % U-235, and uranium loading of 185 kgU is to be loaded in the peripheral zone of the Type 1 DSC. From Table A.1.4.8-6, the minimum cooling time is *11.5* years. From the equation above, $\Delta t = 26.13*\ln(185/198)+1.0$ years = -0.8 years $\equiv$ 0 years. Therefore, the minimum required cooling time for this fuel assembly in the peripheral zone is *11.5* years. No additional cooling time is required because the reduction in uranium loading is sufficient to reduce the dose rate to acceptable levels.

The cooling times determined by Table A.1.4.8-6 or Table A.1.4.8-7 (as supplemented by equation A.1.4.8-1) are developed to meet dose rate limits only. The minimum cooling time for an assembly is the longer of that given by these supplemented FQT tables and the cooling time required to meet the decay heat restrictions provided in Figure A.1.4.8-1 through Figure A.1.4.8-8 for the heat load zoning configuration selected.

A.1.4.8.4 References

1. American Society of Mechanical Engineers, ASME Boiler and Pressure Vessel Code, Section III, Division 1 - Subsections NB, NG and NF, 1998 edition including 2000 Addenda.

Table A.1.4.8-1
Key Design Parameters of the NUHOMS®-61BTH System

Parameter	61BTH Type 1 DSC	61BTH Type 2 DSC
DSC Length (in.)	196.04 (Maximum)	196.04 (Maximum)
DSC Outside Diameter (in.)	67.25	67.25
DSC Cavity Length (in.)	179.50	179.50
Basket length (including holddown ring) (in.)	178.50	178.50
Basket OD (in.)	66.00	66.00

Note: Unless stated otherwise, nominal values are provided.

Table A.1.4.8-2
BWR Fuel Specification for the Fuel to be Transported in the NUHOMS®-61BTH DSC
(Part 1 of 2)

PHYSICAL PARAMETERS:	
Fuel Class	Intact or damaged or failed 7x7, 8x8, 9x9 or 10x10 BWR assemblies manufactured by General Electric or Exxon/ANF or FANP or ABB or reload fuel manufactured by same or other vendors that are enveloped by the fuel assembly design characteristics listed in Table A.1.4.8-3. Damaged fuel assemblies beyond the definition contained below are not authorized for transport in damaged fuel locations shown in Figure A.1.4.8-9.
Damaged Fuel	Damaged BWR fuel assemblies are assemblies containing fuel rods with known or suspected cladding defects greater than hairline cracks or pinhole leaks. The extent of damage in the fuel rods is to be limited such that the fuel assembly will still be able to be handled by normal means. Missing fuel rods are allowed. Damaged fuel assemblies shall also contain top and bottom end fittings or nozzles or tie plates depending on the fuel type.
Failed Fuel	Failed fuel is defined as ruptured fuel rods, severed fuel rods, loose fuel pellets, or fuel assemblies that cannot be handled by normal means. Fuel assemblies may contain breached rods, grossly breached rods, and other defects such as missing or partial rods, missing grid spacers, or damaged spacers to the extent that the assembly cannot be handled by normal means. Fuel debris and damaged fuel rods that have been removed from a damaged fuel assembly and placed in a rod storage basket(3) are also considered as failed fuel, and therefore shall be encapsulated in individual failed fuel cans. Loose fuel debris, not contained in a rod storage basket may also be placed in a failed fuel can for storage, provided the size of the debris is larger than the failed fuel can screen mesh opening and it is located at a position of at least 10" above the top of the bottom shield plug of the DSC. Fuel debris may be associated with any type of UO_2 fuel provided that the maximum uranium content and initial enrichment limits are met. The total weight of each failed fuel can plus all its content shall be less than 705 lb.
RECONSTITUTED FUEL ASSEMBLIES(2):	
• Maximum Number of Reconstituted Assemblies per DSC with Irradiated Stainless Steel Rods	4
• Maximum Number of Irradiated Stainless Steel Rods per Reconstituted Fuel Assembly	4
• Maximum Number of Reconstituted Assemblies per DSC with unlimited number of low enriched UO_2 rods or Zr Rods or Zr Pellets or Unirradiated Stainless Steel Rods	61
Number of Intact Assemblies	≤61

Table A.1.4.8-2
BWR Fuel Specification for the Fuel to be Transported in the NUHOMS®-61BTH DSC
(Part 2 of 2)

Number and Location of Damaged Assemblies	Up to 16 damaged fuel assemblies, with balance intact or dummy assemblies, are authorized for transport in 61BTH DSC. Damaged fuel assemblies may only be transported in the 2x2 compartments as shown in Figure A.1.4.8-9. The DSC basket cells which accommodate damaged fuel assemblies are provided with top and bottom end caps.
Number and Location of Failed Assemblies	Up to 4 failed fuel assemblies. Balance may be intact and/or damaged fuel assemblies, empty slots, or dummy assemblies depending on the specific heat load zoning configuration. Failed fuel assemblies are to be placed as shown in Figure A.1.4.8-9. Failed fuel assembly/fuel debris is to be encapsulated in an individual failed fuel can (FFC) provided with a welded bottom closure and a removable top closure.
Channels	Fuel may be transported with or without channels, channel fasteners, or finger springs.
Maximum Assembly Weight with Channels	705 lb
THERMAL/RADIOLOGICAL PARAMETERS[(1)]**:** Maximum Lattice Average Initial Enrichment (wt. % U-235)	Per Table A.1.4.8-4 or Table A.1.4.8-5.
Fuel Assembly Average Burnup and minimum Cooling Time	Type 1 Per Table A.1.4.8-6 (as supplemented by equation A.1.4.8-1 for peripheral compartments).
	Type 2 Per Table A.1.4.8-7 (as supplemented by equation A.1.4.8-1 for peripheral compartments).
Decay Heat per DSC	≤22.0 kW for Type 1 DSC, per Figures A.1.4.8-1 through A.1.4.8-4
	≤24.0 kW for Type 2 DSC, per Figures A.1.4.8-1 through A.1.4.8-8
Minimum B10 Content in Poison Plates	Per Table A.1.4.8-4 or Table A.1.4.8-5.

(1) Minimum cooling time is the longer of that given in Table A.1.4.8-6 or Table A.1.4.8-7 (as supplemented by equation A.1.4.8-1 for peripheral compartments), and that required to meet the decay heat restrictions provided in Figures A.1.4.8-1 through A.1.4.8-8.

(2) Reconstituted rods shall displace an amount of water equal to or greater than that displaced by the original fuel rods in the active fuel region of the fuel assembly.

(3) *A maximum of 36 BWR fuel rods can be stored in each rod storage basket.*

Table A.1.4.8-3
BWR Fuel Assembly Design Characteristics for the NUHOMS®-61BTH DSC
(Part 1 of 2)

Transnuclear ID	**7x7-49/0**	**8x8-63/1**	**8x8-62/2**	**8x8-60/4**	**8x8-60/1**	**9x9-74/2**
Initial Design or Reload Fuel Designation	GE1	GE4	GE5	GE8 Type II	GE9	GE11
	GE2		GE6		GE10	GE13
	GE3		GE7			
			GE8 Type I			
			FANP 8x8-2			
Length (in) (Unirradiated)	≤ 176.6	≤ 176.6	≤ 176.6	≤ 176.6	≤ 176.6	≤ 176.6
Maximum Active-Fuel Length (in)	*144*	*146*	*150*	*150*	*150*	*146*
Fissile Material	UO_2	UO_2	UO_2	UO_2	UO_2	UO_2
Number of Fuel Rods	≤ 49	≤ 63	≤ 62	≤ 60	≤ 60	≤ 74
Initial Uranium Content (kg)	≤ 198	≤ 192	≤ 192	≤ 192	≤ 192	≤ 192
Rod Pitch (in)	≤ 0.738	≤ 0.640	≤ 0.640	≤ 0.640	≤ 0.640	≤ 0.566
Pellet Diameter (in)	≤ 0.487	≤ 0.416	≤ 0.411	≤ 0.411	≤ 0.411	≤ 0.376
Clad Outer Diameter (in)	≥ 0.563	≥ 0.493	≥ 0.483	≥ 0.483	≥ 0.483	≥ 0.440
Clad Thickness (in)	≥ 0.032	≥ 0.034	≥ 0.032	≥ 0.032	≥ 0.032	≥ 0.028

Transnuclear ID	**10x10-92/2**	**7x7-49/0Z**	**7x7-48/1Z**	**8x8-60/4Z**	**FANP 9x9**	**Siemens**
Initial Design or Reload Fuel Designation	GE12	ENC-IIIA	ENC-III	ENC Va	FANP 9x9-72	QFA 9x9
	GE14		ENC-IIIE	ENC Vb	FANP 9x9-79	
			ENC-IIIF		FANP 9x9-80	
					FANP 9x9-81	
Length (in) (Unirradiated)	≤ 176.6	≤ 176.6	≤ 176.6	≤ 176.6	≤ 176.6	≤ 176.6
Maximum Active-Fuel Length (in)	*150*	*144*	*144*	*144*	*150*	*145.24*
Fissile Material	UO_2	UO_2	UO_2	UO_2	UO_2	UO_2
Number of Fuel Rods	≤ 92	≤ 49	≤ 48	≤ 60	≤ 81	≤ 72
Initial Uranium Content (kg)	≤ 192	≤ 198	≤ 198	≤ 192	≤ 192	≤ 192
Rod Pitch (in)	≤ 0.510	≤ 0.738	≤ 0.738	≤ 0.642	≤ 0.572	≤ 0.570
Pellet Diameter (in)	≤ 0.345	≤ 0.491	≤ 0.491	≤ 0.420	≤ 0.357	≤ 0.374
Clad Outer Diameter (in)	≥ 0.404	≥ 0.570	≥ 0.570	≥ 0.501	≥ 0.424	≥ 0.433
Clad Thickness (in)	≥ 0.026	≥ 0.035	≥ 0.035	≥ 0.035	≥ 0.030	≥ 0.026

Table A.1.4.8-3
BWR Fuel Assembly Design Characteristics for the NUHOMS®-61BTH DSC
(Part 2 of 2)

Transnuclear ID	**10x10-91/1**	**LACROSSE10**	**ABB-8x8**	**ABB-10x10-1**	**ABB-10x10-2**
Initial Design or Reload Fuel Designation	ATRIUM-10	ALLIS CHALMERS	SVEA-64	SVEA-92	SVEA-100
	ATRIUM-10XM	EXXON/ANF		SVEA-96	
				SVEA-96 +/L	
				SVEA-OPTIMA	
				SVEA-OPTIMA 2	
Length (in) (Unirradiated)	≤ 176.6	≤ 130	≤ 176.6	≤ 176.6	≤ 176.6
Maximum Active-Fuel Length (in)	*150*	*100*	*151*	*151*	*151*
Fissile Material	UO_2	UO_2	UO_2	UO_2	UO_2
Number of Fuel Rods	≤ 91	≤ 100	≤ 64	≤ 96	≤ 100
Initial Uranium Content (kg)	≤ 192	≤ 150	≤ 192	≤ 192	≤ 192
Rod Pitch (in)	≤ 0.510	≤ 0.565	≤ 0.622	≤ 0.512	≤ 0.512
Pellet Diameter (in)	≤ 0.350	≤ 0.350	≤ 0.411	≤ 0.346	≤ 0.375
Clad Outer Diameter (in)	≥ 0.395	≥ 0.394	≥ 0.462	≥ 0.378	≥ 0.443
Clad Thickness (in)	≥ 0.023	≥ 0.020	≥ 0.027	≥ 0.022	≥ 0.024

Notes:
(1) The fuel assembly fabrication documentation may be used to demonstrate compliance with these fuel assembly parameters. The fuel assembly parameters are design nominal values. The maximum and minimum dimensions are specified to bound variations in design nominal values among fuel assemblies within a fuel assembly class (or an array type).
(2) Any fuel channel average thickness up to 0.120 inch is acceptable on any of the fuel designs. Fuel channels are required for loading intact fuel assemblies with an assembly average burnup greater than 45 GWd/MTU.

Table A.1.4.8-4
BWR Fuel Assembly Lattice Average Initial Enrichment v/s Minimum B10 Requirements for the NUHOMS®-61BTH DSC Poison Plates (Intact Fuel)

61BTH DSC Type	Basket Type	Maximum Lattice Average *Initial* Enrichment(1) (wt. % U-235)	Minimum B10 Areal Density, gram/cm²	
			Borated Aluminum/MMC	Boral®
1	A	3.7	0.021	0.025
	B	4.1	0.032	0.038
	C	4.4	0.040	0.048
	D	4.6	0.048	0.058
	E	4.8	0.055	0.066
	F	5.0	0.062	0.075
2	A	3.7	0.022	0.027
	B	4.1	0.032	0.038
	C	4.4	0.042	0.050
	D	4.6	0.048	0.058
	E	4.8	0.055	0.066
	F	5.0	0.062	0.075

(1) For LACROSSE10 fuel assemblies, the enrichment shall be reduced by 0.1 wt. % U-235.

(2) For ABB-10x10-1 fuel assemblies with a pitch greater than 0.502 inches, the enrichment shall be reduced by 0.25 wt. % U-235.

Table A.1.4.8-5
BWR Fuel Assembly Lattice Average Initial Enrichment v/s Minimum B10 Requirements for the NUHOMS®-61BTH DSC Poison Plates (Damaged/Failed Fuel)

61BTH DSC Type	Basket Type	Maximum Lattice Average *Initial* Enrichment (wt. % U-235) (1)(5)(6)		Minimum B10 Areal Density, gram/cm²	
		Up to 4 Damaged Assemblies(2)(3)	Five or More Damaged Assemblies (16 Maximum)(2)	Borated Aluminum/MMC	Boral®
1	A	3.7	2.80	0.021	0.025
	B	4.1	3.10	0.032	0.038
	C	4.4	3.20	0.040	0.048
	D	4.6	3.40	0.048	0.058
	E	4.8	3.50	0.055	0.066
	F	5.0	3.60	0.062	0.075
2	A	3.7	2.80	0.022	0.027
	B	4.1	3.10	0.032	0.038
	C	4.4	3.20	0.042	0.050
	D	4.6	3.40	0.048	0.058
	E	4.8	3.50	0.055	0.066
	F	5.0	3.60	0.062	0.075
61BTH DSC Type	Basket Type	Maximum Lattice Average *Initial* Enrichment (wt. % U-235) (1)(5)(6)		Minimum B10 Areal Density, gram/cm²	
		Up to 4 Failed Assemblies (Corner Locations) (3)(4)	Up to 4 Failed Assemblies (Corner Locations) and up to 12 Damaged Assemblies (2)(4)	Borated Aluminum/MMC	Boral®
2	A	3.7	2.80	0.022	0.027
	B	4.0	3.10	0.032	0.038
	C	4.4	3.20	0.042	0.050
	D	4.6	3.40	0.048	0.058
	E	4.8	3.40	0.055	0.066
	F	5.0	3.50	0.062	0.075

Note

(1) For LACROSSE10 fuel assemblies, the enrichment shall be reduced by 0.1 wt. % U-235
(2) See Figure A.1.4.8-9 for the location of damaged assemblies within the 61BTH DSC.
(3) Maximum Pellet Enrichment 5.0 wt. % U-235
(4) Failed fuel assemblies are allowed only in the 61BTH Type 2 DSC. See Figure A.1.4.8-9 for the location of failed assemblies within the 61BTH Type 2 DSC.
(5) For ABB-10x10-1 fuel assemblies with a pitch greater than 0.502 inches, the enrichment shall be reduced by 0.25 wt. % U-235.
(6) Enrichments limits of the damaged fuel assemblies. The enrichment limits of the complementary intact fuels are shown in Table A.1.4.8-4.

Table A.1.4.8-6
BWR Fuel Qualification Table for NUHOMS®-61BTH Type 1 DSC
(Minimum required years of cooling time after reactor core discharge)

BU (GWd/MTU)	Assembly Average Initial Enrichment (wt.% U-235)																														
	0.9	1.2	1.5	2.0	2.4	2.5	2.6	2.7	2.8	2.9	3.0	3.1	3.2	3.3	3.4	3.5	3.6	3.7	3.8	3.9	4.0	4.1	4.2	4.3	4.4	4.5	4.6	4.7	4.8	4.9	5.0
10	7.0	7.0	7.0	7.0	7.0	7.0	7.0	7.0	7.0	7.0	7.0	7.0	7.0	7.0	7.0	7.0	7.0	7.0	7.0	7.0	7.0	7.0	7.0	7.0	7.0	7.0	7.0	7.0	7.0	7.0	7.0
15	7.0	7.0	7.0	7.0	7.0	7.0	7.0	7.0	7.0	7.0	7.0	7.0	7.0	7.0	7.0	7.0	7.0	7.0	7.0	7.0	7.0	7.0	7.0	7.0	7.0	7.0	7.0	7.0	7.0	7.0	7.0
20	7.0	7.0	7.0	7.0	7.0	7.0	7.0	7.0	7.0	7.0	7.0	7.0	7.0	7.0	7.0	7.0	7.0	7.0	7.0	7.0	7.0	7.0	7.0	7.0	7.0	7.0	7.0	7.0	7.0	7.0	7.0
25	7.0	7.0	7.0	7.0	7.0	7.0	7.0	7.0	7.0	7.0	7.0	7.0	7.0	7.0	7.0	7.0	7.0	7.0	7.0	7.0	7.0	7.0	7.0	7.0	7.0	7.0	7.0	7.0	7.0	7.0	7.0
30	7.0	7.0	7.0	7.0	7.0	7.0	7.0	7.0	7.0	7.0	7.0	7.0	7.0	7.0	7.0	7.0	7.0	7.0	7.0	7.0	7.0	7.0	7.0	7.0	7.0	7.0	7.0	7.0	7.0	7.0	7.0
32				7.0	7.0	7.0	7.0	7.0	7.0	7.0	7.0	7.0	7.0	7.0	7.0	7.0	7.0	7.0	7.0	7.0	7.0	7.0	7.0	7.0	7.0	7.0	7.0	7.0	7.0	7.0	7.0
36				7.0	7.0	7.0	7.0	7.0	7.0	7.0	7.0	7.0	7.0	7.0	7.0	7.0	7.0	7.0	7.0	7.0	7.0	7.0	7.0	7.0	7.0	7.0	7.0	7.0	7.0	7.0	7.0
38				7.0	7.0	7.0	7.0	7.0	7.0	7.0	7.0	7.0	7.0	7.0	7.0	7.0	7.0	7.0	7.0	7.0	7.0	7.0	7.0	7.0	7.0	7.0	7.0	7.0	7.0	7.0	7.0
39				7.0	7.0	7.0	7.0	7.0	7.0	7.0	7.0	7.0	7.0	7.0	7.0	7.0	7.0	7.0	7.0	7.0	7.0	7.0	7.0	7.0	7.0	7.0	7.0	7.0	7.0	7.0	7.0
40							7.0	7.0	7.0	7.0	7.0	7.0	7.0	7.0	7.0	7.0	7.0	7.0	7.0	7.0	7.0	7.0	7.0	7.0	7.0	7.0	7.0	7.0	7.0	7.0	7.0
44							7.0	7.0	7.0	7.0	7.0	7.0	7.0	7.0	7.0	7.0	7.0	7.0	7.0	7.0	7.0	7.0	7.0	7.0	7.0	7.0	7.0	7.0	7.0	7.0	7.0
45							7.5	7.0	7.0	7.0	7.0	7.0	7.0	7.0	7.0	7.0	7.0	7.0	7.0	7.0	7.0	7.0	7.0	7.0	7.0	7.0	7.0	7.0	7.0	7.0	7.0
46							8.0	7.5	7.0	7.0	7.0	7.0	7.0	7.0	7.0	7.0	7.0	7.0	7.0	7.0	7.0	7.0	7.0	7.0	7.0	7.0	7.0	7.0	7.0	7.0	7.0
47							9.0	8.5	8.0	7.5	7.0	7.0	7.0	7.0	7.0	7.0	7.0	7.0	7.0	7.0	7.0	7.0	7.0	7.0	7.0	7.0	7.0	7.0	7.0	7.0	7.0
48							10.0	9.5	8.5	8.0	7.5	7.5	7.0	7.0	7.0	7.0	7.0	7.0	7.0	7.0	7.0	7.0	7.0	7.0	7.0	7.0	7.0	7.0	7.0	7.0	7.0
49							11.5	10.5	10.0	9.0	8.5	8.0	7.5	7.0	7.0	7.0	7.0	7.0	7.0	7.0	7.0	7.0	7.0	7.0	7.0	7.0	7.0	7.0	7.0	7.0	7.0
50							12.5	12.0	11.0	10.0	9.5	9.0	8.5	8.0	7.5	7.0	7.0	7.0	7.0	7.0	7.0	7.0	7.0	7.0	7.0	7.0	7.0	7.0	7.0	7.0	7.0
51							14.0	13.0	12.0	11.5	10.5	10.0	9.5	8.5	8.5	7.5	7.5	7.0	7.0	7.0	7.0	7.0	7.0	7.0	7.0	7.0	7.0	7.0	7.0	7.0	7.0
52							15.5	14.5	13.5	12.5	12.0	11.0	10.5	9.5	9.0	8.5	8.0	7.5	7.5	7.0	7.0	7.0	7.0	7.0	7.0	7.0	7.0	7.0	7.0	7.0	7.0
53							16.5	15.5	15.0	14.0	13.0	12.5	11.5	10.5	10.0	9.5	9.0	8.5	8.0	7.5	7.5	7.0	7.0	7.0	7.0	7.0	7.0	7.0	7.0	7.0	7.0
54							18.0	17.0	16.0	15.0	14.5	13.5	12.5	12.0	11.0	10.5	10.0	9.0	9.0	8.5	8.0	7.5	7.0	7.0	7.0	7.0	7.0	7.0	7.0	7.0	7.0
55							19.5	18.5	17.5	16.5	15.5	15.0	14.0	13.0	12.5	11.5	11.0	10.5	9.5	9.0	8.5	8.5	8.0	7.5	7.5	7.0	7.0	7.0	7.0	7.0	7.0
56							21.0	20.0	19.0	18.0	17.0	16.0	15.5	14.5	13.5	13.0	12.0	11.5	10.5	10.0	9.5	9.0	8.5	8.0	7.5	7.5	7.0	7.0	7.0	7.0	7.0
57							22.5	21.5	20.5	19.5	18.5	17.5	16.5	15.5	15.0	14.0	13.5	12.5	11.5	11.0	10.5	10.0	9.5	9.0	8.5	8.0	7.5	7.5	7.0	7.0	7.0
58							23.5	22.5	21.5	21.0	20.0	19.0	18.0	17.0	16.5	15.5	14.5	13.5	13.0	12.5	11.5	11.0	10.5	9.5	9.5	8.5	8.5	8.0	7.5	7.5	7.0
59							25.0	24.0	23.0	22.0	21.0	20.0	19.5	18.5	17.5	16.5	16.0	15.0	14.0	13.5	12.5	12.0	11.5	11.0	10.0	9.5	9.0	9.0	8.5	8.0	7.5
60							26.5	25.5	24.5	23.5	22.5	21.5	21.0	20.0	19.0	18.0	17.0	16.0	15.5	14.5	14.0	13.0	12.5	12.0	11.0	10.5	10.0	9.5	9.0	8.5	8.5
61							28.0	27.0	26.0	25.0	24.0	23.0	22.0	21.5	20.5	19.5	18.5	17.5	17.0	16.0	15.0	14.5	13.5	13.0	12.5	11.5	11.0	10.5	10.0	9.5	9.0
62							29.5	28.5	27.5	26.5	25.5	24.5	23.5	22.5	21.5	21.0	20.0	19.0	18.0	17.5	16.5	15.5	15.0	14.5	13.5	13.0	12.0	11.5	11.0	10.5	10.0

Note: Explanatory notes and limitations regarding the use of this table follow Table A.1.4.8-7.

Table A.1.4.8-7
BWR Fuel Qualification Table for NUHOMS®-61BTH Type 2 DSC

(Minimum required years of cooling time after reactor core discharge)

BU (GWd/MTU)	Assembly Average Initial Enrichment (wt.% U-235)																													
	0.9	1.2	1.5	2.0	2.5	2.6	2.7	2.8	2.9	3.0	3.1	3.2	3.3	3.4	3.5	3.6	3.7	3.8	3.9	4.0	4.1	4.2	4.3	4.4	4.5	4.6	4.7	4.8	4.9	5.0
10	7.0	7.0	7.0	7.0	7.0	7.0	7.0	7.0	7.0	7.0	7.0	7.0	7.0	7.0	7.0	7.0	7.0	7.0	7.0	7.0	7.0	7.0	7.0	7.0	7.0	7.0	7.0	7.0	7.0	7.0
15	7.0	7.0	7.0	7.0	7.0	7.0	7.0	7.0	7.0	7.0	7.0	7.0	7.0	7.0	7.0	7.0	7.0	7.0	7.0	7.0	7.0	7.0	7.0	7.0	7.0	7.0	7.0	7.0	7.0	7.0
20	7.0	7.0	7.0	7.0	7.0	7.0	7.0	7.0	7.0	7.0	7.0	7.0	7.0	7.0	7.0	7.0	7.0	7.0	7.0	7.0	7.0	7.0	7.0	7.0	7.0	7.0	7.0	7.0	7.0	7.0
25	7.0	7.0	7.0	7.0	7.0	7.0	7.0	7.0	7.0	7.0	7.0	7.0	7.0	7.0	7.0	7.0	7.0	7.0	7.0	7.0	7.0	7.0	7.0	7.0	7.0	7.0	7.0	7.0	7.0	7.0
30	7.0	7.0	7.0	7.0	7.0	7.0	7.0	7.0	7.0	7.0	7.0	7.0	7.0	7.0	7.0	7.0	7.0	7.0	7.0	7.0	7.0	7.0	7.0	7.0	7.0	7.0	7.0	7.0	7.0	7.0
32				7.0	7.0	7.0	7.0	7.0	7.0	7.0	7.0	7.0	7.0	7.0	7.0	7.0	7.0	7.0	7.0	7.0	7.0	7.0	7.0	7.0	7.0	7.0	7.0	7.0	7.0	7.0
36				7.0	7.0	7.0	7.0	7.0	7.0	7.0	7.0	7.0	7.0	7.0	7.0	7.0	7.0	7.0	7.0	7.0	7.0	7.0	7.0	7.0	7.0	7.0	7.0	7.0	7.0	7.0
38				7.0	7.0	7.0	7.0	7.0	7.0	7.0	7.0	7.0	7.0	7.0	7.0	7.0	7.0	7.0	7.0	7.0	7.0	7.0	7.0	7.0	7.0	7.0	7.0	7.0	7.0	7.0
39				7.0	7.0	7.0	7.0	7.0	7.0	7.0	7.0	7.0	7.0	7.0	7.0	7.0	7.0	7.0	7.0	7.0	7.0	7.0	7.0	7.0	7.0	7.0	7.0	7.0	7.0	7.0
40						7.0	7.0	7.0	7.0	7.0	7.0	7.0	7.0	7.0	7.0	7.0	7.0	7.0	7.0	7.0	7.0	7.0	7.0	7.0	7.0	7.0	7.0	7.0	7.0	7.0
44						7.0	7.0	7.0	7.0	7.0	7.0	7.0	7.0	7.0	7.0	7.0	7.0	7.0	7.0	7.0	7.0	7.0	7.0	7.0	7.0	7.0	7.0	7.0	7.0	7.0
45						7.0	7.0	7.0	7.0	7.0	7.0	7.0	7.0	7.0	7.0	7.0	7.0	7.0	7.0	7.0	7.0	7.0	7.0	7.0	7.0	7.0	7.0	7.0	7.0	7.0
46						7.0	7.0	7.0	7.0	7.0	7.0	7.0	7.0	7.0	7.0	7.0	7.0	7.0	7.0	7.0	7.0	7.0	7.0	7.0	7.0	7.0	7.0	7.0	7.0	7.0
47						7.0	7.0	7.0	7.0	7.0	7.0	7.0	7.0	7.0	7.0	7.0	7.0	7.0	7.0	7.0	7.0	7.0	7.0	7.0	7.0	7.0	7.0	7.0	7.0	7.0
48						7.0	7.0	7.0	7.0	7.0	7.0	7.0	7.0	7.0	7.0	7.0	7.0	7.0	7.0	7.0	7.0	7.0	7.0	7.0	7.0	7.0	7.0	7.0	7.0	7.0
49						7.0	7.0	7.0	7.0	7.0	7.0	7.0	7.0	7.0	7.0	7.0	7.0	7.0	7.0	7.0	7.0	7.0	7.0	7.0	7.0	7.0	7.0	7.0	7.0	7.0
50						7.0	7.0	7.0	7.0	7.0	7.0	7.0	7.0	7.0	7.0	7.0	7.0	7.0	7.0	7.0	7.0	7.0	7.0	7.0	7.0	7.0	7.0	7.0	7.0	7.0
51						7.5	7.0	7.0	7.0	7.0	7.0	7.0	7.0	7.0	7.0	7.0	7.0	7.0	7.0	7.0	7.0	7.0	7.0	7.0	7.0	7.0	7.0	7.0	7.0	7.0
52						8.0	7.5	7.0	7.0	7.0	7.0	7.0	7.0	7.0	7.0	7.0	7.0	7.0	7.0	7.0	7.0	7.0	7.0	7.0	7.0	7.0	7.0	7.0	7.0	7.0
53						9.0	8.5	8.0	7.5	7.0	7.0	7.0	7.0	7.0	7.0	7.0	7.0	7.0	7.0	7.0	7.0	7.0	7.0	7.0	7.0	7.0	7.0	7.0	7.0	7.0
54						10.5	9.5	9.0	8.5	7.5	7.5	7.0	7.0	7.0	7.0	7.0	7.0	7.0	7.0	7.0	7.0	7.0	7.0	7.0	7.0	7.0	7.0	7.0	7.0	7.0
55						11.5	10.5	10.0	9.0	8.5	8.0	7.5	7.0	7.0	7.0	7.0	7.0	7.0	7.0	7.0	7.0	7.0	7.0	7.0	7.0	7.0	7.0	7.0	7.0	7.0
56						12.5	11.5	11.0	10.0	9.5	9.0	8.0	8.0	7.5	7.0	7.0	7.0	7.0	7.0	7.0	7.0	7.0	7.0	7.0	7.0	7.0	7.0	7.0	7.0	7.0
57						14.0	13.0	12.0	11.0	10.5	10.0	9.0	8.5	8.0	7.5	7.0	7.0	7.0	7.0	7.0	7.0	7.0	7.0	7.0	7.0	7.0	7.0	7.0	7.0	7.0
58						15.0	14.0	13.0	12.5	11.5	11.0	10.0	9.5	9.0	8.5	8.0	7.5	7.0	7.0	7.0	7.0	7.0	7.0	7.0	7.0	7.0	7.0	7.0	7.0	7.0
59						16.5	15.5	14.5	13.5	12.5	12.0	11.0	10.5	10.0	9.0	8.5	8.0	7.5	7.5	7.0	7.0	7.0	7.0	7.0	7.0	7.0	7.0	7.0	7.0	7.0
60						17.5	16.5	15.5	14.5	14.0	13.0	12.5	11.5	11.0	10.0	9.5	9.0	8.5	8.0	7.5	7.0	7.0	7.0	7.0	7.0	7.0	7.0	7.0	7.0	7.0
61						18.5	17.5	17.0	16.0	15.0	14.5	13.5	12.5	12.0	11.5	10.5	10.0	9.5	8.5	8.5	8.0	7.5	7.0	7.0	7.0	7.0	7.0	7.0	7.0	7.0
62						20.0	19.0	18.0	17.5	16.5	15.5	14.5	14.0	13.0	12.5	11.5	11.0	10.5	9.5	9.0	8.5	8.0	7.5	7.5	7.0	7.0	7.0	7.0	7.0	7.0

Note: Explanatory notes and limitations regarding the use of this table follow Table A.1.4.8-7.

Notes: Tables A.1.4.8-6 and Table A.1.4.8-7:

- BU = assembly average burnup
- For fuel assemblies with natural uranium blankets greater than 8 inches at the top and/or bottom end, BU=Maximum Planar Average Burnup.
- Use burnup and enrichment to lookup minimum cooling time in years. Licensee is responsible for ensuring that uncertainties in fuel enrichment and burnup are correctly accounted for during fuel qualification.
- Round burnup UP to next higher entry, round enrichments DOWN to next lower entry.
- Fuel with a lattice average initial enrichment less than 0.9 (or less than the minimum provided above for each burnup) or greater than 5.0 wt.% U-235 is unacceptable for transportation.
- Fuel with a burnup greater than 62 GWd/MTU is unacceptable for transportation.
- Fuel with a burnup less than 10 GWd/MTU is acceptable for transportation after 7-years cooling.
- For reconstituted fuel assemblies with irradiated stainless steel rods, increase the cooling time by 1 year for fuel assemblies in the 24 peripheral locations of the canister with cooling times less than 10 years. No adjustment of cooling time is required for fuel assemblies in other locations or for those that have cooled for more than 10 years.
- Example: An assembly with an initial enrichment of 4.85 wt. % U-235 and a burnup of 41.5 GWd/MTU is acceptable for transport after a 7-year year cooling time as defined by 4.8 wt. % U-235 (rounding down) and 42 GWd/MTU (rounding up) on the qualification table (other considerations not withstanding).
- *Fuel in the peripheral compartments may require additional cooling time per equation A.1.4.8-1.*

Table A.1.4.8-7a
"B" Parameters to Determine Additional Cooling Time for Fuel in Peripheral Compartments (years)

BU	***Assembly Average Initial Enrichment (wt.% U-235)***																								
GWd/MTU	***2.6***	***2.7***	***2.8***	***2.9***	***3.0***	***3.1***	***3.2***	***3.3***	***3.4***	***3.5***	***3.6***	***3.7***	***3.8***	***3.9***	***4.0***	***4.1***	***4.2***	***4.3***	***4.4***	***4.5***	***4.6***	***4.7***	***4.8***	***4.9***	***5.0***
49	*1.5*																								
50	*2.5*	*1.5*	*0.5*																						
51	*4.0*	*3.0*	*2.0*	*1.0*																					
52	*5.0*	*4.0*	*3.5*	*2.5*	*1.5*	*0.5*																			
53	*6.0*	*5.5*	*4.5*	*4.0*	*3.0*	*2.0*	*1.0*	*0.5*										*No Additional Cooling Required*							
54	*7.0*	*6.0*	*5.5*	*5.0*	*4.0*	*3.5*	*2.5*	*1.5*	*1.0*																
55	*7.5*	*7.0*	*6.5*	*6.0*	*5.0*	*4.5*	*3.5*	*3.0*	*2.0*	*1.0*	*0.5*														
56	*8.5*	*8.0*	*7.0*	*6.5*	*6.0*	*5.5*	*5.0*	*4.0*	*3.5*	*2.5*	*2.0*	*1.0*													
57	*9.0*	*8.5*	*8.0*	*7.5*	*7.0*	*6.5*	*6.0*	*5.0*	*4.5*	*3.5*	*3.0*	*2.0*	*1.0*	*0.5*											
58	*9.5*	*9.0*	*8.5*	*8.0*	*7.5*	*7.5*	*6.5*	*6.0*	*5.5*	*5.0*	*4.0*	*3.5*	*2.5*	*2.0*	*1.0*										
59	*9.5*	*9.5*	*9.0*	*8.5*	*8.5*	*8.0*	*7.5*	*7.0*	*6.5*	*6.0*	*5.0*	*4.5*	*4.0*	*3.0*	*2.5*	*1.5*	*0.5*								
60	*10.0*	*10.0*	*9.5*	*9.0*	*9.0*	*8.5*	*8.0*	*7.5*	*7.0*	*6.5*	*6.0*	*5.5*	*5.0*	*4.0*	*3.5*	*3.0*	*2.0*	*1.0*	*0.5*						
61	*10.5*	*10.0*	*10.0*	*9.5*	*9.5*	*9.0*	*8.5*	*8.5*	*7.5*	*7.5*	*7.0*	*6.5*	*6.0*	*5.0*	*4.5*	*4.0*	*3.0*	*2.5*	*2.0*	*1.0*					
62	*10.5*	*10.5*	*10.5*	*10.0*	*10.0*	*9.5*	*9.0*	*9.0*	*8.5*	*8.0*	*7.5*	*7.0*	*6.5*	*6.0*	*5.5*	*5.0*	*4.5*	*3.5*	*3.0*	*2.0*	*1.5*	*0.5*			
Enr. wt.%	***2.6***	***2.7***	***2.8***	***2.9***	***3.0***	***3.1***	***3.2***	***3.3***	***3.4***	***3.5***	***3.6***	***3.7***	***3.8***	***3.9***	***4.0***	***4.1***	***4.2***	***4.3***	***4.4***	***4.5***	***4.6***	***4.7***	***4.8***	***4.9***	***5.0***

Table A.1.4.8-8
BWR Assembly Decay Heat for Heat Load Configurations

The decay heat (DH) in watts is expressed as:

$$F1 = -59.1 + 23.4*X1 - 21.1*X2 + 0.280*X1^2 - 3.52*X1*X2 + 12.4*X2^2$$
$$DH = F1*Exp(\{[1-(1.2/X3)]* -0.720\}*[(X3-4.5)^{0.157}]*[(X2/X1)^{-0.132}]) + 10$$

where,

F1 Intermediate function
X1 Assembly burnup in GWD/MTU
X2 Initial enrichment in wt. % U-235
X3 Cooling time in years (minimum *5* years)

A uranium loading of 198 kg is employed in the calculation of the decay heat equation. Alternatively, the decay heat can be calculated without employing the decay heat equation, using an approved methodology with actual spent fuel parameters instead of bounding spent fuel parameters.

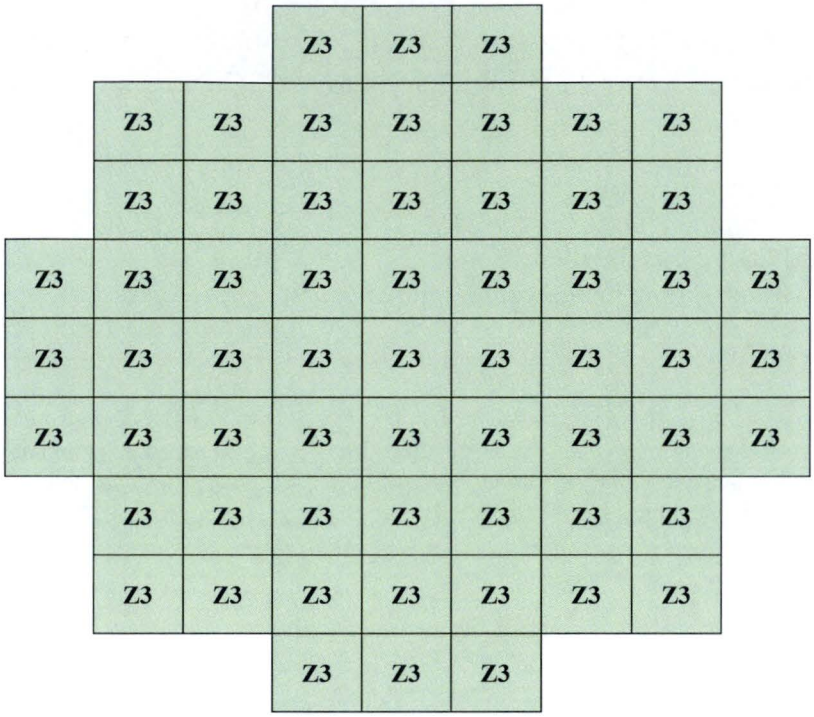

	Zone 1	Zone 2	Zone 3	Zone 4	Zone 5	Zone 6
Maximum Decay Heat (kW/FA)(1) (3)	NA	NA	0.393	NA	NA	NA
Maximum Decay Heat per Zone (kW)	NA	NA	22.0	NA	NA	NA
Maximum Decay Heat per DSC (kW)	22.0(3)					

(1) Decay heat per fuel assembly shall be determined per Table A.1.4.8-8.
(2) *Not used.*
(3) Reduce the maximum decay heat to 70% of the listed values for *LACROSSE10* fuel assembly. The total decay heat for *LACROSSE10* fuel assembly is 15.4 kW per DSC for HLZC No. 1.

Figure A.1.4.8-1
Heat Load Zoning Configuration No. 1 for Type 1 or Type 2 61BTH DSCs

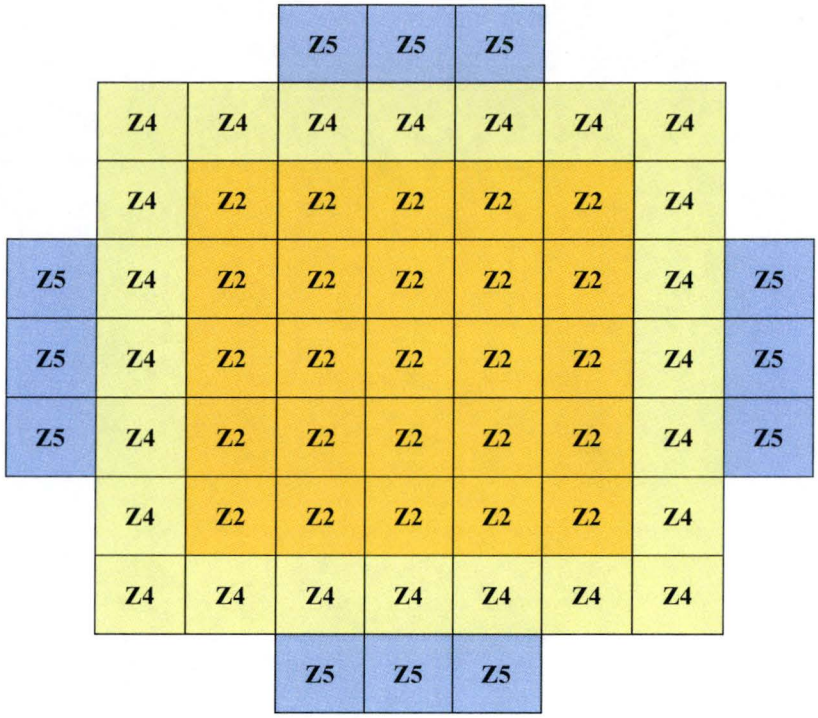

	Zone 1	Zone 2	Zone 3	Zone 4	Zone 5	Zone 6
Maximum Decay Heat (kW/FA)(1) (3)	NA	0.35	NA	0.48	0.54	NA
Maximum Decay Heat per Zone (kW)	NA	8.75	NA	11.52	6.48	NA
Maximum Decay Heat per DSC (kW)	22.0 (3)					

(1) Decay heat per fuel assembly shall be determined per Table A.1.4.8-8.
(2) *Not used.*
(3) Reduce the maximum decay heat to 70% of the listed values for *LACROSSE10* fuel assembly. The total decay heat for *LACROSSE10* fuel assembly is 15.4 kW per DSC for HLZC No. 2.

Figure A.1.4.8-2
Heat Load Zoning Configuration No. 2 for Type 1 or Type 2 61BTH DSCs

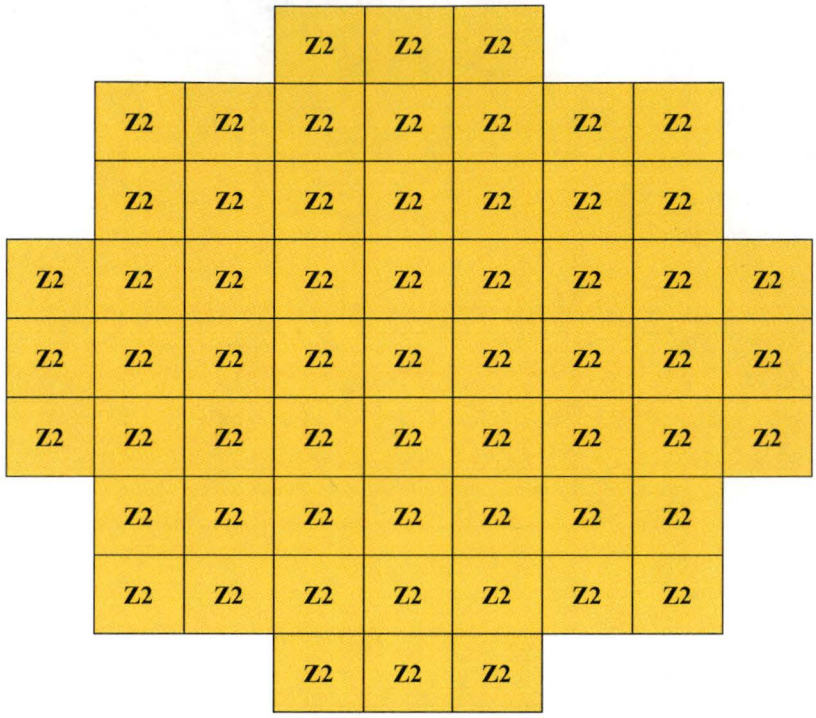

	Zone 1	Zone 2	Zone 3	Zone 4	Zone 5	Zone 6
Maximum Decay Heat (kW/FA)(1) (2)	NA	0.35	NA	NA	NA	NA
Maximum Decay Heat per Zone (kW)	NA	19.4	NA	NA	NA	NA
Maximum Decay Heat per DSC (kW)	19.4(2)					

(1) Decay heat per fuel assembly shall be determined per Table A.1.4.8-8.

(2) Reduce the maximum decay heat to 70% of the listed values for *LACROSSE10* fuel assembly. The total decay heat for *LACROSSE10* fuel assembly is 13.58 kW per DSC for HLZC No. 3.

Figure A.1.4.8-3
Heat Load Zoning Configuration No. 3 for Type 1 or Type 2 61BTH DSCs

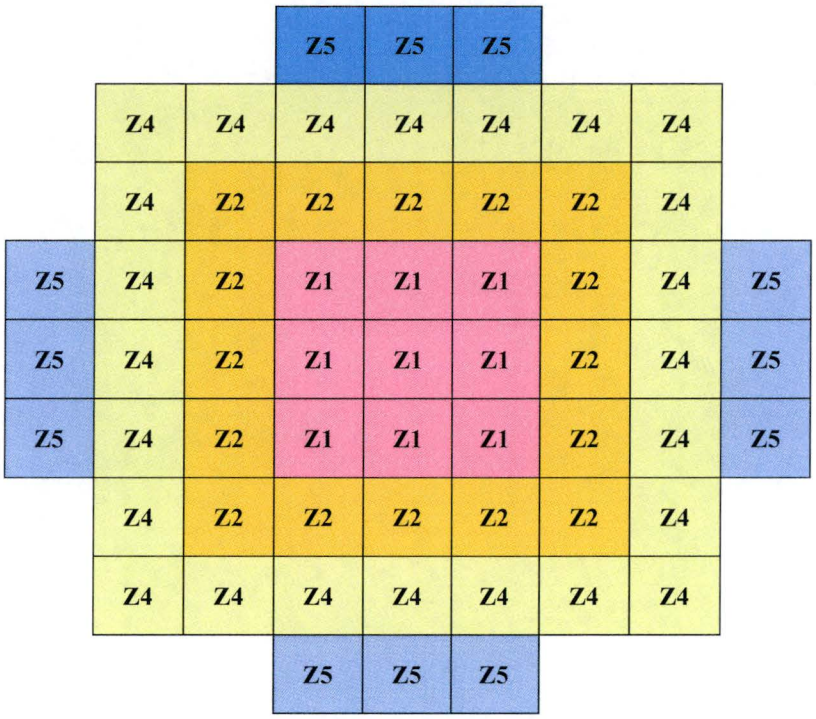

	Zone 1	Zone 2	Zone 3	Zone 4	Zone 5	Zone 6
Maximum Decay Heat (kW/FA)(1) (2)	0.22	0.35	NA	0.48	0.54	NA
Maximum Decay Heat per Zone (kW)	1.98	5.60	NA	11.52	6.48	NA
Maximum Decay Heat per DSC (kW)	19.4(2)					

(1) Decay heat per fuel assembly shall be determined per Table A.1.4.8-8.
(2) Reduce the maximum decay heat to 70% of the listed values for *LACROSSE10* fuel assembly. The total decay heat for *LACROSSE10* fuel assembly is 13.58 kW per DSC for HLZC No. 4.

Figure A.1.4.8-4
Heat Load Zoning Configuration No. 4 for Type 1 or Type 2 61BTH DSCs

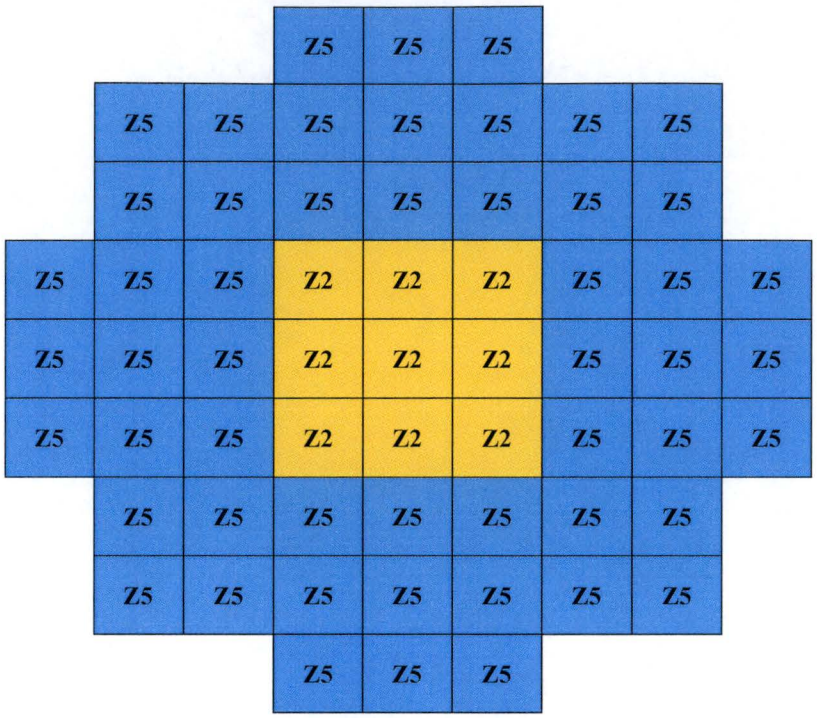

	Zone 1	Zone 2	Zone 3	Zone 4	Zone 5	Zone 6
Maximum Decay Heat (kW/FA)(1) (3)	NA	0.35	NA	NA	0.54	NA
Maximum Decay Heat per Zone (kW)	NA	3.15	NA	NA	24.0	NA
Maximum Decay Heat per DSC (kW)	24.0(3)					

(1) Decay heat per fuel assembly shall be determined per Table A.1.4.8-8.
(2) *Not Used.*
(3) Reduce the maximum decay heat to 70% of the listed values for *LACROSSE10* fuel assembly. The total decay heat for *LACROSSE10* fuel assembly is 16.8 kW per DSC for HLZC No. 5.

Figure A.1.4.8-5
Heat Load Zoning Configuration No. 5 for Type 2 61BTH DSC(2)

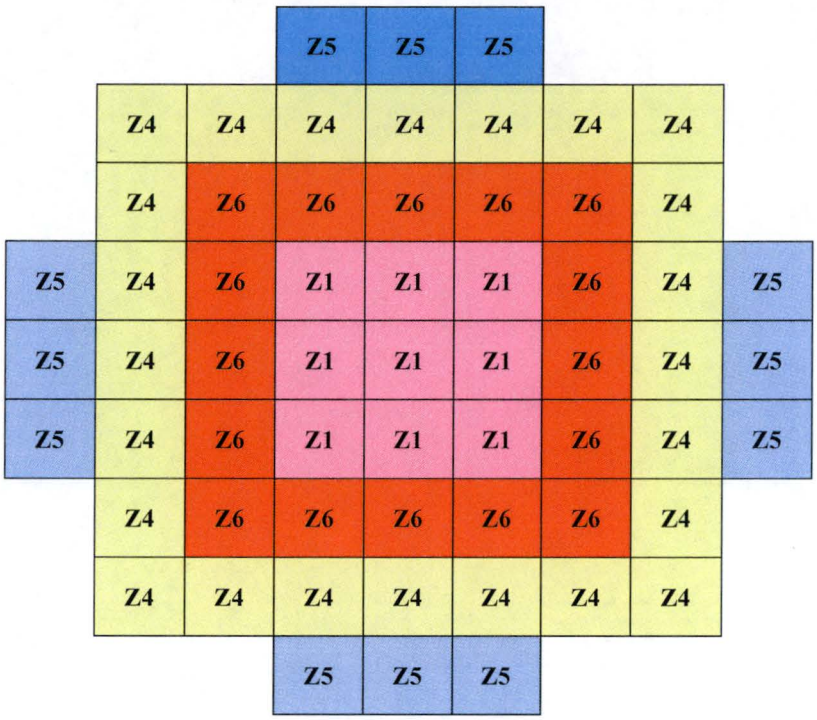

	Zone 1	Zone 2	Zone 3	Zone 4	Zone 5	Zone 6
Maximum Decay Heat (kW/FA)(1) (3)	0.22	NA	NA	0.48	0.54	0.70
Maximum Decay Heat per Zone (kW)	1.98	NA	NA	11.52	6.48	11.20
Maximum Decay Heat per DSC (kW)	24.0(3)					

(1) Decay heat per fuel assembly shall be determined per Table A.1.4.8-8.
(2) *Not used.*
(3) Reduce the maximum decay heat to 70% of the listed values for *LACROSSE10* fuel assembly. The total decay heat for *LACROSSE10* fuel assembly is 16.8 kW per DSC for HLZC No. 6.

Figure A.1.4.8-6
Heat Load Zoning Configuration No. 6 for Type 2 61BTH DSC

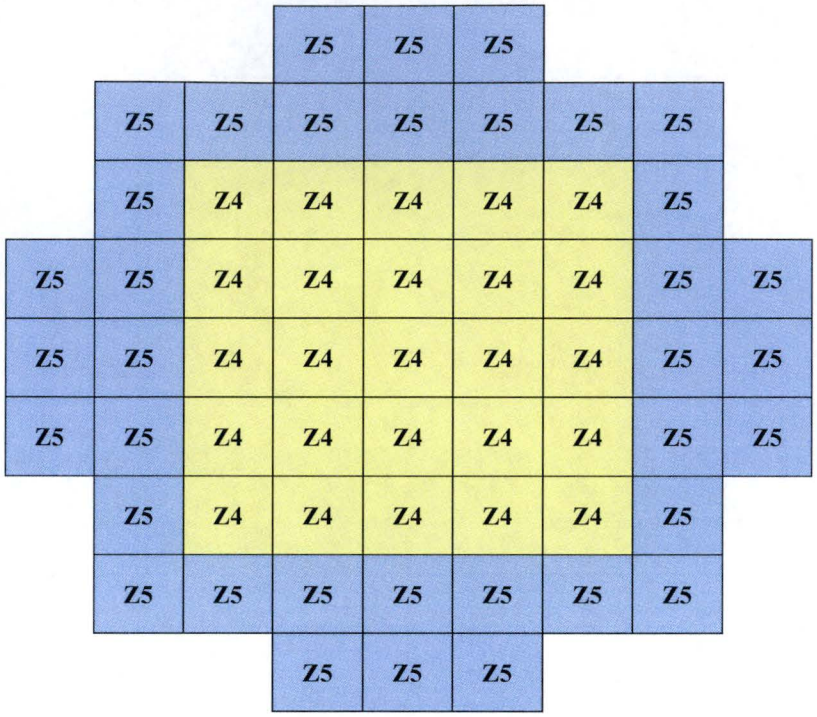

	Zone 1	Zone 2	Zone 3	Zone 4	Zone 5	Zone 6
Maximum Decay Heat (kW/FA)(1) (3)	NA	NA	NA	0.48	0.54	NA
Maximum Decay Heat per Zone (kW)	NA	NA	NA	12.00	19.44	NA
Maximum Decay Heat per DSC (kW)	24.0(3)					

(1) Decay heat per fuel assembly shall be determined per Table A.1.4.8-8.
(2) *Not used.*
(3) Reduce the maximum decay heat to 70% of the listed values for *LACROSSE10* fuel assembly. The total decay heat for *LACROSSE10* fuel assembly is 16.8 kW per DSC for HLZC No. 7.

Figure A.1.4.8-7
Heat Load Zoning Configuration No. 7 for Type 2 61BTH DSC

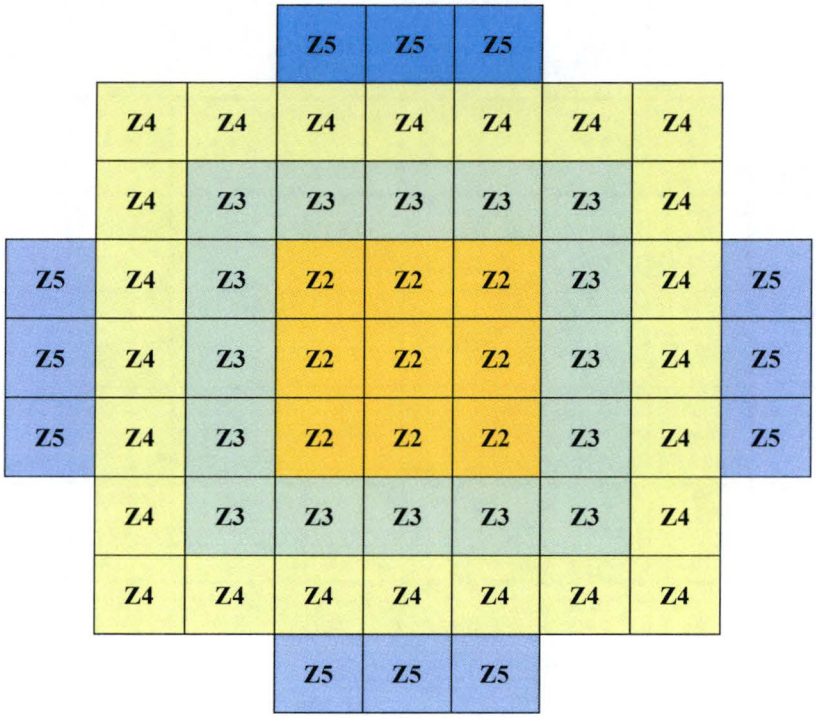

	Zone 1	Zone 2	Zone 3	Zone 4	Zone 5	Zone 6
Maximum Decay Heat (kW/FA)[(1) (2)]	NA	0.35	0.393	0.48	0.54	NA
Maximum Decay Heat per Zone (kW)	NA	3.15	6.288	11.52	6.48	NA
Maximum Decay Heat per DSC (kW)	24.0[(2)]					

(1) Decay heat per fuel assembly shall be determined per Table A.1.4.8-8.
(2) Reduce the maximum decay heat to 70% of the listed values for *LACROSSE10* fuel assembly. The total decay heat for *LACROSSE10* fuel assembly is 16.8 kW per DSC for HLZC No. 8.

Figure A.1.4.8-8
Heat Load Zoning Configuration No. 8 for Type 2 61BTH DSC

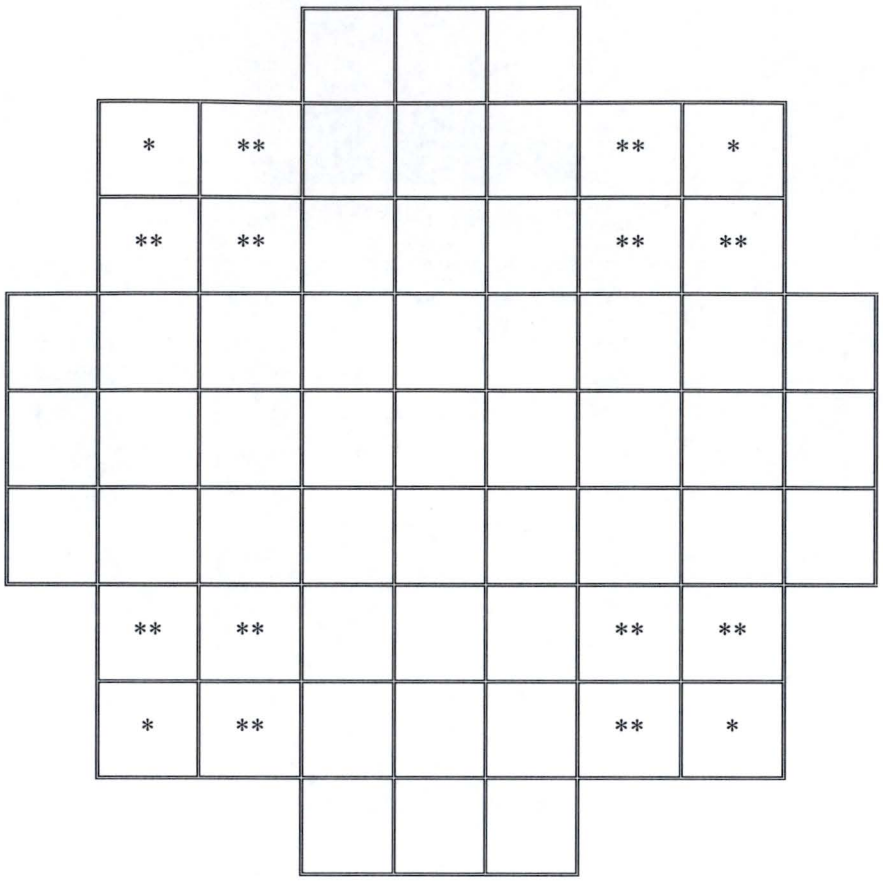

*	Corner Locations See Note 1

**	Interior Locations See Note 2

Note 1: These corner locations shall only be used to load up to four damaged or failed assemblies with the remaining intact in a 61BTH Basket. The maximum lattice average initial enrichment of assemblies (damaged or intact transported in the 2x2 compartment assemblies) is limited to the "Up to 4 Damaged Assemblies" column of Table A.1.4.8-5. For the Type 2 DSC containing failed fuel assemblies, this enrichment is limited to the "Up to 4 Failed Assemblies" column of Table A.1.4.8-5.

Note 2: If loading more than four damaged assemblies, place first four damaged assemblies in the corner locations per Note 1, and up to 12 additional damaged assemblies in these interior locations, with the remaining intact in a 61BTH Basket. The maximum lattice average initial enrichment of assemblies (damaged or intact transported in the 2x2 compartment assemblies) is limited to the "Five or More Damaged Assemblies" column of Table A.1.4.8-5. For the Type 2 DSC containing failed fuel assemblies, this enrichment is limited to the "and up to 12 Damaged Assemblies" column of Table A.1.4.8-5.

Figure A.1.4.8-9
Location of Damaged and Failed Fuel Assemblies Inside 61BTH DSC

			P	P	P			
	P	P	I	I	I	P	P	
	P	I	I	I	I	I	P	
P	I	I	I	I	I	I	I	P
P	I	I	I	I	I	I	I	P
P	I	I	I	I	I	I	I	P
	P	I	I	I	I	I	P	
	P	P	I	I	I	P	P	
			P	P	P			

Figure A.1.4.8-10
Peripheral and Inner Fuel Locations for the 61BTH DSC

Appendix A.1.4.9
NUHOMS®-69BTH DSC

TABLE OF CONTENTS

A.1.4.9.1 NUHOMS®-69BTH DSC Description A.1.4.9-1
A.1.4.9.2 NUHOMS®-69BTH Fuel Basket A.1.4.9-1
A.1.4.9.3 NUHOMS®-69BTH DSC Contents A.1.4.9-2
A.1.4.9.4 References A.1.4.9-2a

LIST OF TABLES

Table A.1.4.9-1 BWR Fuel Specification for the Fuel to be Transported in the NUHOMS®-69BTH DSC A.1.4.9-3
Table A.1.4.9-2 BWR Fuel Assembly Design Characteristics for the NUHOMS®-69BTH DSC A.1.4.9-4
Table A.1.4.9-3 BWR Fuel Assembly Lattice Average Initial Enrichment v/s Minimum B10 Requirements for the NUHOMS®-69BTH DSC Poison Plates A.1.4.9-6
Table A.1.4.9-4 BWR Fuel Qualification Table for the NUHOMS®-69BTH DSC (Uranium Loading ≤ 198 kg) A.1.4.9-7
Table A.1.4.9-5 BWR Fuel Qualification Table for the NUHOMS®-69BTH DSC (Uranium Loading ≤ 182 kg) A.1.4.9-8
Table A.1.4.9-5a "B" Parameters to Determine Additional Cooling Time for Fuel in Peripheral Compartments (years) A.1.4.9-9a
Table A.1.4.9-5b BWR Fuel Qualification Table for NUHOMS®-69BTH DSC using Type "F" Poison in HLZC 8: A.1.4.9-9b
Table A.1.4.9-6 BWR Assembly Decay Heat for Heat Load Configurations A.1.4.9-10

LIST OF FIGURES

Figure A.1.4.9-1 Location of Damaged Fuel Assemblies Inside 69BTH DSC A.1.4.9-11
Figure A.1.4.9-2 Heat Load Zoning Configuration No. 1 for 69BTH Basket A.1.4.9-12
Figure A.1.4.9-3 Heat Load Zoning Configuration No. 2 for 69BTH Basket A.1.4.9-13
Figure A.1.4.9-4 Heat Load Zoning Configuration No. 3 for 69BTH Basket A.1.4.9-14
Figure A.1.4.9-5 Heat Load Zoning Configuration No. 4 for 69BTH Basket A.1.4.9-15
Figure A.1.4.9-5a Heat Load Zoning Configuration No. 8 for 69BTH DSC Basket A.1.4.9-15a
Figure A.1.4.9-6 Peripheral and Inner Fuel Locations for the 69BTH DSC A.1.4.9-16

Appendix A.1.4.9
NUHOMS®-69BTH DSC

NOTE: References in this Appendix are shown as [1], [2], etc. and refer to the reference list in Section A.1.4.9.4.

A.1.4.9.1 NUHOMS®-69BTH DSC Description

Each NUHOMS®-69BTH DSC consists of a DSC shell assembly and a basket assembly. The shell assembly consists of a cylindrical shell, the inner cover plates of the top and bottom shield plug assemblies and outer top cover plate. The DSC shell assembly is designed, fabricated and inspected in accordance with ASME B&PV Code Subsection NB [1]. Alternatives to the code are provided in Chapter A.2, Appendix A.2.13.13. The maximum length and the outer diameter of the 69BTH DSC are approximately 197.0 inches and 69.8 inches, respectively. The shell assembly is a high integrity stainless steel welded pressure vessel that provides confinement of radioactive materials, encapsulates the fuel in an inert atmosphere (the canister is back-filled with helium before being seal welded closed) and provides biological shielding (in axial direction). The 69BTH DSC has double redundant seal welds that join the shell and the top and bottom cover plate assemblies to seal the canister. The bottom end assembly welds are made during fabrication of the 69BTH DSC. The top plug penetrations (siphon and vent ports) are redundantly sealed after the 69BTH DSC drying operations are complete.

The canister is designed to contain the fuel basket and fuel assemblies, and is completely supported by the transport cask. Under normal transport conditions, the canister rests on four canister rails attached to the inside surface of the transport cask.

A.1.4.9.2 NUHOMS®-69BTH Fuel Basket

The basket structure is designed, fabricated and inspected in accordance with ASME B&PV Code Subsection NG[1]. Alternatives to the code are provided in Chapter A.2, Appendix A.2.13.13. The overall length and outer diameter of the basket, including the hold down ring, are approximately 178.6 inches and 68.4 inches respectively. The details of the 69BTH fuel basket is shown in the drawings in Section A.1.4.10.10 of Appendix A.1.4.10. The 69BTH basket is designed to accommodate 69 intact, or up to 24 damaged with the remainder intact BWR fuel assemblies with or without fuel channels. The basket structure consists of a welded assembly of stainless steel tubes (fuel compartments) separated by poison plates and surrounded by larger stainless steel boxes and support rails.

The basket structure is open at each end. Therefore, longitudinal fuel assembly loads are applied directly to the canister/cask body and not the fuel basket structure. The fuel assemblies are laterally supported by the stainless steel structural boxes. The basket is laterally supported by the basket rails and the canister shell. The aluminum basket rails are oriented parallel to the axis of the canister, and are attached to the periphery of the basket to provide support, and to establish and maintain basket orientation.

Shear keys, welded to the inner wall of the DSC, mate with notches in the basket support rails to prevent the basket from rotating during normal operations. Also a hold down ring is installed above the basket to prevent the basket from moving axially during transport.

The NUHOMS®-69BTH DSC is designed with six alternate basket configurations based on the boron content in the poison plates as listed in Table A.1.4.9-3 (designated as "A" for the poison plates with the lowest B10 loading to "F" for the highest B10 loading). Three alternate poison materials are allowed: (a) Borated Aluminum alloy, (b) Boron Carbide/Aluminum Metal Matrix Composite (MMC), or (c) Boral®. The poison plates provide a heat conduction path from the fuel assemblies to the canister wall, as well as the necessary criticality control.

A.1.4.9.3 NUHOMS®-69BTH DSC Contents

The NUHOMS®-69BTH DSC is designed to transport 69 intact, or up to 24 damaged and the remainder intact, standard BWR fuel assemblies with or without fuel channels. The NUHOMS®-69BTH DSC can transport intact or damaged BWR fuel assemblies with the characteristics described in Table A.1.4.9-1. *The fuel to be transported is limited to a maximum lattice average initial enrichment of 5.0 wt. % U-235. The maximum allowable fuel assembly average burnup is limited to 70 GWd/MTU.* Damaged BWR fuel assemblies are fuel assemblies containing fuel rods with known or suspected cladding defects greater than hairline cracks or pinhole leaks. The extent of damage in the fuel assembly is to be limited such that the fuel assembly will still be able to be handled by normal means. Missing fuel rods are allowed.

The fuel assemblies considered are listed in Table A.1.4.9-2.

A.1.4.9.3.1 Heat Load Zone Configurations 1, 2, 3, and 4

The basket is divided into inner and peripheral zones, as shown in Figure A.1.4.9-6. Fuel in the inner zone is governed by the cooling times presented in Table A.1.4.9-4 and Table A.1.4.9-5 for fuel loadings ≤198 kgU and ≤182 kgU, respectively. These cooling times are determined to meet dose rate limits. For fuel in the peripheral zone, certain burnup and enrichment combinations require additional cooling time governed by the following equation:

Peripheral Compartment Cooling = Fuel Qualification Table Cooling + Δt

$$\Delta t = 26.13 \cdot \ln\left(\frac{m}{198}\right) + B \qquad \text{(A.1.4.9-1)}$$

Where,

Δt = cooling time to be added to the appropriate value in Table A.1.4.9-4 (years). (Do not add Δt to the values from Table A.1.4.9-5)
m = the uranium loading of the fuel assembly to be shipped (kg),
B = additional cooling time (years), obtain*ed* from Table A.1.4.9-5a

This equation applies only if the "B" value is defined in Table A.1.4.9-5a. Additional cooling is not required for burnup and enrichment combinations that fall in the zone labeled "no additional cooling time required." *No* additional cooling *time* is required for burnups < *49* GWd/MTU.

This equation can return a negative value for Δt, which indicates that no additional cooling is required. In such a scenario, $\Delta t \equiv 0$ years. Application of the method is illustrated in the following examples.

Example #1: Fuel with a burnup of 62 GWd/MTU, enrichment of 2.6 wt. % U-235, and uranium loading of 198 kgU is to be loaded in the peripheral zone. From Table A.1.4.9-4, the minimum cooling time is 18.5 years. From the equation above, $\Delta t = 26.13*\ln(1) + 10.5 = 10.5$ years. Therefore, the minimum required cooling time for this fuel assembly in the peripheral zone is $18.5+10.5 = 29.0$ years.

Example #2: Fuel with a burnup of *58* GWd/MTU, enrichment of 4.0 wt. % U-235, and uranium loading of 185 kgU is to be loaded in the peripheral zone. From Table A.1.4.9-4, the minimum cooling time is *7.5* years. From the equation above, $\Delta t = 26.13*\ln(185/198)+1.0$ years = -0.8 years $\equiv$ 0 years. Therefore, the minimum required cooling time for this fuel assembly in the peripheral zone is *7.5* years. No additional cooling time is required because the reduction in uranium loading is sufficient to reduce the dose rate to acceptable levels.

The cooling times determined by Table A.1.4.9-4 (as supplemented by equation A.1.4.9-1) or Table A.1.4.9-5 *(as supplemented by equation A.1.4.9-1)* are developed to meet dose rate limits only. The minimum cooling time for an assembly is the longer of that given by Table A.1.4.9-4 or Table A.1.4.9-5 *(as supplemented by equation A.1.4.9-1)* and the cooling time required to meet the decay heat restrictions provided in Figure A.1.4.9-2 through Figure A.1.4.9-5 for the heat load zoning configuration selected.

*Example #3: Fuel with a burnup of 70 GWd/MTU, enrichment of 3.7 wt. % U-235, and uranium loading of 180 kgU is acceptable for loading after 17.5-year cooling time, from Table A.1.4.9-5, when placed in inner positions. When placed in peripheral positions, the required cooling time is 27.5-year cooling time calculated as 19.5 (from Table A.1.4.9-4) + 26.13 * ln (180/198) (from Equation A.1.4.9-1) + 10.5 (from Table A.1.4.9-5a).*

A.1.4.9.3.2 Heat Load Zone Configuration 8

The Heat Load Zone Configuration 8 applies only to the 69 BTH DSC Type F, Table A.1.4.9-3. The 69BTH DSC basket using Heat Load Zone Configuration 8 is divided into five zones, as shown in Figure A.1.4.9-5a for fuel loadings ≤ 188 kgU. Fuel in zone 1 is governed by the cooling times presented in Table A.1.4.9-5b, Part 1. Fuel in zone 2 is governed by the cooling times presented in Table A.1.4.9-5b, Part 2. Fuel in zone 3 is governed by the cooling times presented in Table A.1.4.9-5b, Part 3. Fuel in zone 4 is governed by the cooling times presented in Table A.1.4.9-5b, Part 4. Fuel in zone 5 is governed by the cooling times presented in Table A.1.4.9-5b, Part 5. These cooling times are determined to meet dose rate limits in NCT and HAC. There are no supplemental cooling time tables generated for the 69BTH DSC basket using Heat Load Zone Configuration 8.

A.1.4.9.4 References

1. American Society of Mechanical Engineers, ASME Boiler And Pressure Vessel Code, Section III, Division 1 - Subsections NB, NG and NF, 2004 edition including 2006 Addenda.

Table A.1.4.9-1
BWR Fuel Specification for the Fuel to be Transported in the NUHOMS®-69BTH DSC

PHYSICAL PARAMETERS: Fuel Class	Intact or damaged 7x7, 8x8, 9x9 or 10x10 BWR assemblies manufactured by General Electric or Exxon/ANF or FANP or ABB or reload fuel manufactured by same or other vendors that are enveloped by the fuel assembly design characteristics listed in Table A.1.4.9-2. Damaged fuel assemblies beyond the definition contained below are not authorized for transport.
Damaged Fuel	Damaged BWR fuel assemblies are assemblies containing fuel rods with known or suspected cladding defects greater than hairline cracks or pinhole leaks. The extent of damage in the fuel assembly is to be limited such that the fuel assembly will still be able to be handled by normal means. Missing fuel rods are allowed. Damaged fuel assemblies shall also contain top and bottom end fittings or nozzles or tie plates depending on the fuel type.
RECONSTITUTED FUEL ASSEMBLIES[1]**:** • Maximum Number of Reconstituted Assemblies per DSC with Irradiated Stainless Steel Rods • Maximum Number of Irradiated Stainless Steel Rods per Reconstituted Fuel Assembly • Maximum Number of Reconstituted Assemblies per DSC with unlimited number of low enriched UO_2 rods or Zr Rods or Zr Pellets or Unirradiated Stainless Steel Rods	 4 4 69
Number of Intact Assemblies	≤69
Number and Location of Damaged Assemblies	Up to 24 damaged fuel assemblies, with balance intact or dummy assemblies, are authorized for transport in 69BTH DSC. Damaged fuel assemblies may only be transported in the four outer "6-compartment" arrays as shown in Figure A.1.4.9-1. The DSC basket cells which accommodate damaged fuel assemblies are provided with top and bottom end caps.
Channels	Fuel may be transported with or without channels, channel fasteners, or finger springs.
Maximum Assembly Weight with Channels	705 lbs
THERMAL/RADIOLOGICAL PARAMETERS: Maximum Lattice Average Initial Enrichment (wt. % U-235)	Per Table A.1.4.9-3.
Allowable Heat Load Zoning Configurations for each 69BTH DSC	Per Figure A.1.4.9-2 or Figure A.1.4.9-3 or Figure A.1.4.9-4 or Figure A.1.4.9-5 *or Figure A.1.4.9-5a.*
Fuel Assembly Average Burnup and minimum Cooling Time	Per Table A.1.4.9-4 (as supplemented by equation A.1.4.9-1 for peripheral compartments) or Table A.1.4.9-5 *or Table A.1.4.9-5b.*
Decay Heat per DSC	Per Figure A.1.4.9-2 or Figure A.1.4.9-3 or Figure A.1.4.9-4 or Figure A.1.4.9-5 *or Figure A.1.4.9-5a.*
Minimum B10 Content in Poison Plates	Per Table A.1.4.9-3.

[1] Reconstituted rods shall displace an amount of water equal to or greater than that displaced by the original fuel rods in the active fuel region of the fuel assembly.

Table A.1.4.9-2
BWR Fuel Assembly Design Characteristics for the NUHOMS®-69BTH DSC
(Part 1 of 2)

Transnuclear ID	**7x7-49/0**	**8x8-63/1**	**8x8-62/2**	**8x8-60/4**	**8x8-60/1**	**9x9-74/2**
Initial Design or Reload Fuel Designation	GE1	GE4	GE5	GE8 Type II	GE9	GE11
	GE2		GE6		GE10	GE13
	GE3		GE7			
			GE8 Type I			
			FANP 8x8-2			
Length (in) (Unirradiated)	≤ 176.6	≤ 176.6	≤ 176.6	≤ 176.6	≤ 176.6	≤ 176.6
Maximum Active-Fuel Length (in)	*144*	*146*	*150*	*150*	*150*	*146*
Fissile Material	UO_2	UO_2	UO_2	UO_2	UO_2	UO_2
Number of Fuel Rods	≤ 49	≤ 63	≤ 62	≤ 60	≤ 60	≤ 74
Initial Uranium Content (kg)	≤ 198	≤ 192	≤ 192	≤ 192	≤ 192	≤ 192
Rod Pitch (in)	≤ 0.738	≤ 0.640	≤ 0.640	≤ 0.640	≤ 0.640	≤ 0.566
Pellet Diameter (in)	≤ 0.487	≤ 0.416	≤ 0.411	≤ 0.411	≤ 0.411	≤ 0.376
Clad Outer Diameter (in)	≥ 0.563	≥ 0.493	≥ 0.483	≥ 0.483	≥ 0.483	≥ 0.440
Clad Thickness (in)	≥ 0.032	≥ 0.034	≥ 0.032	≥ 0.032	≥ 0.032	≥ 0.028

Transnuclear ID	**10x10-92/2**	**7x7-49/0Z**	**7x7-48/1Z**	**8x8-60/4Z**	**FANP 9x9**	**Siemens**
Initial Design or Reload Fuel Designation	GE12	ENC-IIIA	ENC-III	ENC Va	FANP 9x9-72	QFA 9x9
	GE14		ENC-IIIE	ENC Vb	FANP 9x9-79	
			ENC-IIIF		FANP 9x9-80	
					FANP 9x9-81	
Length (in) (Unirradiated)	≤ 176.6	≤ 176.6	≤ 176.6	≤ 176.6	≤ 176.6	≤ 176.6
Maximum Active-Fuel Length (in)	*150*	*144*	*144*	*144*	*150*	*145.24*
Fissile Material	UO_2	UO_2	UO_2	UO_2	UO_2	UO_2
Number of Fuel Rods	≤ 92	≤ 49	≤ 48	≤ 60	≤ 81	≤ 72
Initial Uranium Content (kg)	≤ 192	≤ 198	≤ 198	≤ 192	≤ 192	≤ 192
Rod Pitch (in)	≤ 0.510	≤ 0.738	≤ 0.738	≤ 0.642	≤ 0.572	≤ 0.570
Pellet Diameter (in)	≤ 0.345	≤ 0.491	≤ 0.491	≤ 0.420	≤ 0.357	≤ 0.374
Clad Outer Diameter (in)	≥ 0.404	≥ 0.570	≥ 0.570	≥ 0.501	≥ 0.424	≥ 0.433
Clad Thickness (in)	≥ 0.026	≥ 0.035	≥ 0.035	≥ 0.035	≥ 0.030	≥ 0.026

Table A.1.4.9-2
BWR Fuel Assembly Design Characteristics for the NUHOMS®-69BTH DSC
(Part 2 of 2)

Transnuclear ID	**10x10-91/1**	**LACROSSE10**	**ABB-8x8**	**ABB-10x10-1**	**ABB-10x10-2**
Initial Design or Reload Fuel Designation	ATRIUM-10	ALLIS CHALMERS	SVEA-64	SVEA-92	SVEA-100
	ATRIUM-10XM	EXXON/ANF		SVEA-96	
				SVEA-96 +/L	
				SVEA-OPTIMA	
				SVEA-OPTIMA 2	
Length (in) (Unirradiated)	≤ 176.6	≤ 130	≤ 176.6	≤ 176.6	≤ 176.6
Maximum Active-Fuel Length (in)	*150*	*100*	*151*	*151*	*151*
Fissile Material	UO_2	UO_2	UO_2	UO_2	UO_2
Number of Fuel Rods	≤ 91	≤ 100	≤ 64	≤ 96	≤ 100
Initial Uranium Content (kg)	≤ 192	≤ 150	≤ 192	≤ 192	≤ 192
Rod Pitch (in)	≤ 0.510	≤ 0.565	≤ 0.622	≤ 0.512	≤ 0.512
Pellet Diameter (in)	≤ 0.350	≤ 0.350	≤ 0.411	≤ 0.346	≤ 0.375
Clad Outer Diameter (in)	≥ 0.395	≥ 0.394	≥ 0.462	≥ 0.378	≥ 0.443
Clad Thickness (in)	≥ 0.023	≥ 0.020	≥ 0.027	≥ 0.022	≥ 0.024

Notes:
(1) The fuel assembly fabrication documentation may be used to demonstrate compliance with these fuel assembly parameters. The fuel assembly parameters are design nominal values. The maximum and minimum dimensions are specified to bound variations in design nominal values among fuel assemblies within a fuel assembly class (or an array type).
(2) Any fuel channel average thickness up to 0.120 inch is acceptable on any of the fuel designs. Fuel channels are required for loading intact fuel assemblies with an assembly average burnup greater than 45 GWd/MTU.

Table A.1.4.9-3
BWR Fuel Assembly Lattice Average Initial Enrichment v/s Minimum B10 Requirements for the NUHOMS®-69BTH DSC Poison Plates

Basket Type	Maximum Lattice Average Initial Enrichment[1] (wt. % U-235)	Minimum B10 Areal Density, gram/cm^2	
		Borated Aluminum/MMC	Boral®
A	3.7	0.021	0.025
B	4.1	0.031	0.037
C	4.4	0.039	0.047
D	4.6	0.046	0.055
E	4.8	0.053	0.064
F	5.0	0.061	0.073

	Maximum Lattice Average Initial Enrichment[1][3] (wt. % U-235)			
Basket Type	Intact Assemblies	Up to 4 Damaged Assemblies[2]	5 to 8 Damaged Assemblies[2]	9 to 24 Damaged Assemblies[2]
A	3.70	3.70	3.30	2.80
B	4.10	4.10	3.60	3.00
C	4.40	4.20	3.60	3.10
D	4.60	4.40	3.70	3.20
E	4.80	4.40	3.70	3.20
F	5.00	4.80	3.90	3.40

(1) For LACROSSE10 fuel assemblies, the enrichment shall be reduced by 0.1 wt. % U-235.
(2) Allowable locations in basket per Figure A.1.4.9-1. *Enrichment limits of the damaged fuel assemblies. The enrichment limits of the complementary intact fuel assemblies are shown in the second column.*
(3) For ABB-10x10-1 fuel assemblies with a pitch greater than 0.502 inches, the enrichment shall be reduced by 0.25 wt. % U-235.

Table A.1.4.9-4
BWR Fuel Qualification Table for the NUHOMS®-69BTH DSC *(Uranium Loading ≤ 198 kg)*

(Minimum required years of cooling time after reactor core discharge)

BU (GWd/ MTU)	Assembly Average Initial Enrichment (wt.% U-235)																												
	0.7	1.2	1.5	2.0	2.5	2.6	2.7	2.8	2.9	3.0	3.1	3.2	3.3	3.4	3.5	3.6	3.7	3.8	3.9	4.0	4.1	4.2	4.3	4.4	4.5	4.6	4.7	4.8	4.9	5.0
10	6.0	6.0	6.0	6.0	6.0	6.0	6.0	6.0	6.0	6.0	6.0	6.0	6.0	6.0	6.0	6.0	6.0	6.0	6.0	6.0	6.0	6.0	6.0	6.0	6.0	6.0	6.0	6.0	6.0	6.0
20	6.0	6.0	6.0	6.0	6.0	6.0	6.0	6.0	6.0	6.0	6.0	6.0	6.0	6.0	6.0	6.0	6.0	6.0	6.0	6.0	6.0	6.0	6.0	6.0	6.0	6.0	6.0	6.0	6.0	6.0
30	6.0	6.0	6.0	6.0	6.0	6.0	6.0	6.0	6.0	6.0	6.0	6.0	6.0	6.0	6.0	6.0	6.0	6.0	6.0	6.0	6.0	6.0	6.0	6.0	6.0	6.0	6.0	6.0	6.0	6.0
31				6.0	6.0	6.0	6.0	6.0	6.0	6.0	6.0	6.0	6.0	6.0	6.0	6.0	6.0	6.0	6.0	6.0	6.0	6.0	6.0	6.0	6.0	6.0	6.0	6.0	6.0	6.0
39				6.0	6.0	6.0	6.0	6.0	6.0	6.0	6.0	6.0	6.0	6.0	6.0	6.0	6.0	6.0	6.0	6.0	6.0	6.0	6.0	6.0	6.0	6.0	6.0	6.0	6.0	6.0
40						6.0	6.0	6.0	6.0	6.0	6.0	6.0	6.0	6.0	6.0	6.0	6.0	6.0	6.0	6.0	6.0	6.0	6.0	6.0	6.0	6.0	6.0	6.0	6.0	6.0
45						6.0	6.0	6.0	6.0	6.0	6.0	6.0	6.0	6.0	6.0	6.0	6.0	6.0	6.0	6.0	6.0	6.0	6.0	6.0	6.0	6.0	6.0	6.0	6.0	6.0
46						6.5	6.0	6.0	6.0	6.0	6.0	6.0	6.0	6.0	6.0	6.0	6.0	6.0	6.0	6.0	6.0	6.0	6.0	6.0	6.0	6.0	6.0	6.0	6.0	6.0
47						6.5	6.5	6.0	6.0	6.0	6.0	6.0	6.0	6.0	6.0	6.0	6.0	6.0	6.0	6.0	6.0	6.0	6.0	6.0	6.0	6.0	6.0	6.0	6.0	6.0
48						7.0	7.0	6.5	6.5	6.0	6.0	6.0	6.0	6.0	6.0	6.0	6.0	6.0	6.0	6.0	6.0	6.0	6.0	6.0	6.0	6.0	6.0	6.0	6.0	6.0
49						7.5	7.0	7.0	6.5	6.5	6.5	6.0	6.0	6.0	6.0	6.0	6.0	6.0	6.0	6.0	6.0	6.0	6.0	6.0	6.0	6.0	6.0	6.0	6.0	6.0
50						8.0	7.5	7.5	7.0	7.0	6.5	6.5	6.5	6.0	6.0	6.0	6.0	6.0	6.0	6.0	6.0	6.0	6.0	6.0	6.0	6.0	6.0	6.0	6.0	6.0
51						8.5	8.0	8.0	7.5	7.0	7.0	7.0	6.5	6.5	6.5	6.0	6.0	6.0	6.0	6.0	6.0	6.0	6.0	6.0	6.0	6.0	6.0	6.0	6.0	6.0
52						9.0	8.5	8.5	8.0	7.5	7.5	7.0	7.0	6.5	6.5	6.5	6.5	6.0	6.0	6.0	6.0	6.0	6.0	6.0	6.0	6.0	6.0	6.0	6.0	6.0
53						10.0	9.5	9.0	8.5	8.0	8.0	7.5	7.5	7.0	7.0	6.5	6.5	6.5	6.5	6.0	6.0	6.0	6.0	6.0	6.0	6.0	6.0	6.0	6.0	6.0
54						10.5	10.0	9.5	9.0	8.5	8.5	8.0	7.5	7.5	7.0	7.0	7.0	6.5	6.5	6.5	6.5	6.0	6.0	6.0	6.0	6.0	6.0	6.0	6.0	6.0
55						11.5	11.0	10.5	10.0	9.5	9.0	8.5	8.0	8.0	8.0	7.5	7.0	7.0	7.0	7.0	6.5	6.5	6.5	6.0	6.0	6.0	6.0	6.0	6.0	6.0
56						12.5	12.0	11.0	10.5	10.0	9.5	9.0	9.0	8.5	8.0	8.0	7.5	7.5	7.0	7.0	7.0	6.5	6.5	6.5	6.5	6.0	6.0	6.0	6.0	6.0
57						13.5	12.5	12.0	11.5	11.0	10.5	10.0	9.5	9.0	8.5	8.5	8.0	8.0	7.5	7.5	7.0	7.0	7.0	6.5	6.5	6.5	6.5	6.5	6.0	6.0
58						14.5	13.5	13.0	12.5	11.5	11.0	10.5	10.0	9.5	9.5	9.0	8.5	8.5	8.0	7.5	7.5	7.5	7.0	7.0	7.0	6.5	6.5	6.5	6.5	6.5
59						15.5	14.5	14.0	13.5	12.5	12.0	11.5	11.0	10.5	10.0	9.5	9.0	8.5	8.5	8.0	8.0	7.5	7.5	7.5	7.0	7.0	7.0	6.5	6.5	6.5
60						16.5	15.5	15.0	14.5	13.5	13.0	12.5	11.5	11.5	10.5	10.5	9.5	9.5	9.0	8.5	8.5	8.0	8.0	7.5	7.5	7.5	7.0	7.0	7.0	6.5
61						17.5	17.0	16.0	15.5	14.5	14.0	13.5	12.5	12.0	11.5	11.0	10.5	10.0	9.5	9.0	9.0	8.5	8.5	8.0	8.0	7.5	7.5	7.0	7.0	7.0
62						18.5	18.0	17.0	16.5	15.5	15.0	14.5	13.5	13.0	12.5	12.0	11.5	11.0	10.5	10.0	9.5	9.0	9.0	8.5	8.5	8.0	8.0	7.5	7.5	7.5
63																	12.5	11.5	11.0	10.5	10.5	10.0	9.5	9.0	9.0	8.5	8.5	8.0	8.0	7.5
64																	13.0	12.5	12.0	11.5	11.0	10.5	10.0	9.5	9.5	9.0	8.5	8.5	8.5	8.0
65																	14.0	13.5	13.0	12.5	12.0	11.5	11.0	10.5	10.0	9.5	9.5	9.0	8.5	8.5
66																	15.0	14.5	14.0	13.5	12.5	12.0	11.5	11.5	10.5	10.5	10.0	9.5	9.5	9.0
67																	16.0	15.5	15.0	14.5	13.5	13.0	12.5	12.0	11.5	11.0	10.5	10.5	10.0	9.5
68																	17.0	16.5	16.0	15.0	14.5	14.0	13.5	13.0	12.5	12.0	11.5	11.0	10.5	10.0
69																	18.5	17.5	17.0	16.5	15.5	15.0	14.5	14.0	13.5	12.5	12.5	12.0	11.5	11.0
70																	19.5	19.0	18.0	17.5	16.5	16.0	15.5	15.0	14.0	13.5	13.0	12.5	12.0	12.0

Note: Explanatory notes and limitations regarding the use of this table follow *Table A.1.4.9-5.*

Table A.1.4.9-5

BWR Fuel Qualification Table for the NUHOMS®-69BTH DSC (Uranium Loading ≤ 182 kg)

(Minimum required years of cooling time after reactor core discharge)

BU (GWd/MTU)	Assembly Average Initial Enrichment (wt.% U-235)																													
	0.7	1.2	1.5	2.0	2.5	2.6	2.7	2.8	2.9	3.0	3.1	3.2	3.3	3.4	3.5	3.6	3.7	3.8	3.9	4.0	4.1	4.2	4.3	4.4	4.5	4.6	4.7	4.8	4.9	5.0
10	6.0	6.0	6.0	6.0	6.0	6.0	6.0	6.0	6.0	6.0	6.0	6.0	6.0	6.0	6.0	6.0	6.0	6.0	6.0	6.0	6.0	6.0	6.0	6.0	6.0	6.0	6.0	6.0	6.0	6.0
20	6.0	6.0	6.0	6.0	6.0	6.0	6.0	6.0	6.0	6.0	6.0	6.0	6.0	6.0	6.0	6.0	6.0	6.0	6.0	6.0	6.0	6.0	6.0	6.0	6.0	6.0	6.0	6.0	6.0	6.0
30	6.0	6.0	6.0	6.0	6.0	6.0	6.0	6.0	6.0	6.0	6.0	6.0	6.0	6.0	6.0	6.0	6.0	6.0	6.0	6.0	6.0	6.0	6.0	6.0	6.0	6.0	6.0	6.0	6.0	6.0
31				6.0	6.0	6.0	6.0	6.0	6.0	6.0	6.0	6.0	6.0	6.0	6.0	6.0	6.0	6.0	6.0	6.0	6.0	6.0	6.0	6.0	6.0	6.0	6.0	6.0	6.0	6.0
39				6.0	6.0	6.0	6.0	6.0	6.0	6.0	6.0	6.0	6.0	6.0	6.0	6.0	6.0	6.0	6.0	6.0	6.0	6.0	6.0	6.0	6.0	6.0	6.0	6.0	6.0	6.0
40						6.0	6.0	6.0	6.0	6.0	6.0	6.0	6.0	6.0	6.0	6.0	6.0	6.0	6.0	6.0	6.0	6.0	6.0	6.0	6.0	6.0	6.0	6.0	6.0	6.0
45						6.0	6.0	6.0	6.0	6.0	6.0	6.0	6.0	6.0	6.0	6.0	6.0	6.0	6.0	6.0	6.0	6.0	6.0	6.0	6.0	6.0	6.0	6.0	6.0	6.0
46						6.0	6.0	6.0	6.0	6.0	6.0	6.0	6.0	6.0	6.0	6.0	6.0	6.0	6.0	6.0	6.0	6.0	6.0	6.0	6.0	6.0	6.0	6.0	6.0	6.0
47						6.0	6.0	6.0	6.0	6.0	6.0	6.0	6.0	6.0	6.0	6.0	6.0	6.0	6.0	6.0	6.0	6.0	6.0	6.0	6.0	6.0	6.0	6.0	6.0	6.0
48						6.5	6.0	6.0	6.0	6.0	6.0	6.0	6.0	6.0	6.0	6.0	6.0	6.0	6.0	6.0	6.0	6.0	6.0	6.0	6.0	6.0	6.0	6.0	6.0	6.0
49						6.5	6.5	6.5	6.0	6.0	6.0	6.0	6.0	6.0	6.0	6.0	6.0	6.0	6.0	6.0	6.0	6.0	6.0	6.0	6.0	6.0	6.0	6.0	6.0	6.0
50						7.0	7.0	6.5	6.5	6.0	6.0	6.0	6.0	6.0	6.0	6.0	6.0	6.0	6.0	6.0	6.0	6.0	6.0	6.0	6.0	6.0	6.0	6.0	6.0	6.0
51						7.5	7.0	7.0	6.5	6.5	6.5	6.0	6.0	6.0	6.0	6.0	6.0	6.0	6.0	6.0	6.0	6.0	6.0	6.0	6.0	6.0	6.0	6.0	6.0	6.0
52						8.0	7.5	7.5	7.0	7.0	6.5	6.5	6.5	6.0	6.0	6.0	6.0	6.0	6.0	6.0	6.0	6.0	6.0	6.0	6.0	6.0	6.0	6.0	6.0	6.0
53						8.5	8.0	8.0	7.5	7.5	7.0	7.0	6.5	6.5	6.5	6.0	6.0	6.0	6.0	6.0	6.0	6.0	6.0	6.0	6.0	6.0	6.0	6.0	6.0	6.0
54						9.5	9.0	8.5	8.0	7.5	7.5	7.0	7.0	7.0	6.5	6.5	6.5	6.0	6.0	6.0	6.0	6.0	6.0	6.0	6.0	6.0	6.0	6.0	6.0	6.0
55						10.0	9.5	9.0	8.5	8.0	8.0	7.5	7.5	7.0	7.0	6.5	6.5	6.5	6.5	6.0	6.0	6.0	6.0	6.0	6.0	6.0	6.0	6.0	6.0	6.0
56						11.0	10.0	9.5	9.0	9.0	8.5	8.0	8.0	7.5	7.5	7.0	7.0	6.5	6.5	6.5	6.0	6.0	6.0	6.0	6.0	6.0	6.0	6.0	6.0	6.0
57						12.0	11.0	10.5	10.0	9.5	9.0	8.5	8.5	8.0	8.0	7.5	7.0	7.0	7.0	7.0	6.5	6.5	6.0	6.0	6.0	6.0	6.0	6.0	6.0	6.0
58						12.5	12.0	11.5	11.0	10.5	9.5	9.5	9.0	8.5	8.5	8.0	7.5	7.5	7.5	7.0	7.0	6.5	6.5	6.5	6.5	6.0	6.0	6.0	6.0	6.0
59						13.5	13.0	12.0	11.5	11.0	10.5	10.0	9.5	9.0	9.0	8.5	8.0	8.0	7.5	7.5	7.0	7.0	7.0	6.5	6.5	6.5	6.0	6.0	6.0	6.0
60						14.5	14.0	13.0	12.5	12.0	11.5	11.0	10.0	10.0	9.5	9.0	8.5	8.5	8.0	8.0	7.5	7.5	7.0	7.0	7.0	6.5	6.5	6.5	6.0	6.0
61						15.5	15.0	14.5	13.5	13.0	12.5	11.5	11.0	10.5	10.0	9.5	9.5	9.0	8.5	8.5	8.0	7.5	7.5	7.5	7.0	7.0	6.5	6.5	6.5	6.5
62						16.5	16.0	15.5	14.5	14.0	13.5	12.5	12.0	11.5	11.0	10.5	10.0	9.5	9.0	8.5	8.5	8.0	8.0	7.5	7.5	7.5	7.0	7.0	7.0	6.5
63																	10.5	10.5	9.5	9.5	9.0	8.5	8.5	8.0	8.0	7.5	7.5	7.5	7.0	7.0
64																	11.5	11.0	10.5	10.0	9.5	9.5	9.0	8.5	8.5	8.0	8.0	7.5	7.5	7.5
65																	12.5	12.0	11.5	11.0	10.5	10.0	9.5	9.0	9.0	8.5	8.5	8.0	8.0	7.5
66																	13.5	12.5	12.0	11.5	11.0	10.5	10.5	10.0	9.5	9.0	9.0	8.5	8.5	8.0
67																	14.5	13.5	13.0	12.5	12.0	11.5	11.0	10.5	10.0	9.5	9.5	9.0	8.5	8.5
68																	15.5	14.5	14.0	13.5	13.0	12.5	12.0	11.5	11.0	10.5	10.0	9.5	9.5	9.0
69																	16.5	15.5	15.0	14.5	14.0	13.5	12.5	12.0	11.5	11.5	10.5	10.5	10.0	9.5
70																	17.5	17.0	16.0	15.5	15.0	14.0	13.5	13.0	12.5	12.0	11.5	11.0	10.5	10.0

Note: Explanatory notes and limitations regarding the use of this table follow Table A.1.4.9-5.

Notes, Table A.1.4.9-4 and Table A.1.4.9-5:

- BU = Assembly Average burnup.
- For fuel assemblies with natural uranium blankets greater than 8 inches at the top and/or bottom end, BU=Maximum Planar Average Burnup.
- Use burnup and enrichment to lookup minimum cooling time in years. Licensee is responsible for ensuring that uncertainties in fuel enrichment and burnup are correctly accounted for during fuel qualification.
- Round burnup UP to next higher entry, round enrichments DOWN to next lower entry.
- Fuel with a lattice average initial enrichment less than 0.7 (or less than the minimum provided above for each burnup) or greater than 5.0 wt. % U-235 is unacceptable for transportation.
- Fuel with an assembly average burnup greater than *70* GWd/MTU is unacceptable for transportation.
- Fuel with a burnup less than 10 GWd/MTU is acceptable for transportation after 6-years cooling.
- For reconstituted fuel assemblies with irradiated stainless steel rods, increase the cooling time by 1 for fuel assemblies in the 24 peripheral locations of the canister with cooling times less than 10 years. No adjustment of cooling time is required for fuel assemblies in other locations or for those that have cooled for more than 10 years.
- Example: An assembly with an initial enrichment of 4.85 wt. % U-235, a Uranium loading of 190 kg, and a burnup of 41.5 GWd/MTU is acceptable for transport after a 6-year cooling time as defined by 4.8 wt. % U-235 (rounding down) and 42 GWd/MTU (rounding up) on the qualification table (other considerations not withstanding).
- The minimum cooling times from Table A.1.4.9-4 shall be utilized for fuel assemblies with a Uranium loading greater than 182 kg.
- Fuel in the peripheral compartments may require additional cooling time per equation A.1.4.9-1*; the additional cooling is to be added to the minimum cooling time in Table A.1.4.9-4.*

Table A.1.4.9-5a
"B" Parameters to Determine Additional Cooling Time for Fuel in Peripheral Compartments (years)

BU	***Assembly Average Initial Enrichment (wt.% U-235)***																								
GWd/MTU	***2.6***	***2.7***	***2.8***	***2.9***	***3.0***	***3.1***	***3.2***	***3.3***	***3.4***	***3.5***	***3.6***	***3.7***	***3.8***	***3.9***	***4.0***	***4.1***	***4.2***	***4.3***	***4.4***	***4.5***	***4.6***	***4.7***	***4.8***	***4.9***	***5.0***
49	*1.5*																								
50	*2.5*	*1.5*	*0.5*																						
51	*4.0*	*3.0*	*2.0*	*1.0*																					
52	*5.0*	*4.0*	*3.5*	*2.5*	*1.5*	*0.5*																			
53	*6.0*	*5.5*	*4.5*	*4.0*	*3.0*	*2.0*	*1.0*	*0.5*																	
54	*7.0*	*6.0*	*5.5*	*5.0*	*4.0*	*3.5*	*2.5*	*1.5*	*1.0*																
55	*7.5*	*7.0*	*6.5*	*6.0*	*5.0*	*4.5*	*3.5*	*3.0*	*2.0*	*1.0*	*0.5*														
56	*8.5*	*8.0*	*7.0*	*6.5*	*6.0*	*5.5*	*5.0*	*4.0*	*3.5*	*2.5*	*2.0*	*1.0*													
57	*9.0*	*8.5*	*8.0*	*7.5*	*7.0*	*6.5*	*6.0*	*5.0*	*4.5*	*3.5*	*3.0*	*2.0*	*1.0*	*0.5*											
58	*9.5*	*9.0*	*8.5*	*8.0*	*7.5*	*7.5*	*6.5*	*6.0*	*5.5*	*5.0*	*4.0*	*3.5*	*2.5*	*2.0*	*1.0*										
59	*9.5*	*9.5*	*9.0*	*8.5*	*8.5*	*8.0*	*7.5*	*7.0*	*6.5*	*6.0*	*5.0*	*4.5*	*4.0*	*3.0*	*2.5*	*1.5*	*0.5*								
60	*10.0*	*10.0*	*9.5*	*9.0*	*9.0*	*8.5*	*8.0*	*7.5*	*7.0*	*6.5*	*6.0*	*5.5*	*5.0*	*4.0*	*3.5*	*3.0*	*2.0*	*1.0*	*0.5*						
61	*10.5*	*10.0*	*10.0*	*9.5*	*9.5*	*9.0*	*8.5*	*8.5*	*7.5*	*7.5*	*7.0*	*6.5*	*6.0*	*5.0*	*4.5*	*4.0*	*3.0*	*2.5*	*2.0*	*1.0*					
62	*10.5*	*10.5*	*10.5*	*10.0*	*10.0*	*9.5*	*9.0*	*9.0*	*8.5*	*8.0*	*7.5*	*7.0*	*6.5*	*6.0*	*5.5*	*5.0*	*4.5*	*3.5*	*3.0*	*2.0*	*1.5*	*0.5*			
63												*7.5*	*7.5*	*7.0*	*6.5*	*6.0*	*5.0*	*4.5*	*4.0*	*3.5*	*3.0*	*2.0*	*1.5*	*0.5*	
64												*8.5*	*8.0*	*7.5*	*7.0*	*6.5*	*6.5*	*5.5*	*5.0*	*4.5*	*4.0*	*3.5*	*2.5*	*2.0*	*1.0*
65												*9.0*	*8.5*	*8.5*	*8.0*	*7.5*	*7.0*	*6.5*	*6.0*	*5.5*	*5.0*	*4.5*	*3.5*	*3.0*	*2.5*
66												*9.5*	*9.0*	*9.0*	*8.5*	*8.0*	*8.0*	*7.0*	*6.5*	*6.5*	*6.0*	*5.5*	*4.5*	*4.0*	*3.5*
67												*10.0*	*9.5*	*9.0*	*9.0*	*8.5*	*8.5*	*8.0*	*7.5*	*7.0*	*6.5*	*6.0*	*5.5*	*5.0*	*4.5*
68												*10.0*	*10.0*	*9.5*	*9.5*	*9.0*	*9.0*	*8.5*	*8.0*	*8.0*	*7.5*	*7.0*	*6.5*	*6.0*	*5.5*
69												*10.5*	*10.0*	*10.0*	*10.0*	*9.5*	*9.0*	*9.0*	*8.5*	*8.5*	*8.0*	*7.5*	*7.0*	*7.0*	*6.5*
70												*10.5*	*10.5*	*10.5*	*10.0*	*10.0*	*10.0*	*9.5*	*9.0*	*9.0*	*8.5*	*8.0*	*8.0*	*7.5*	*7.0*
Enr. wt.%	***2.6***	***2.7***	***2.8***	***2.9***	***3.0***	***3.1***	***3.2***	***3.3***	***3.4***	***3.5***	***3.6***	***3.7***	***3.8***	***3.9***	***4.0***	***4.1***	***4.2***	***4.3***	***4.4***	***4.5***	***4.6***	***4.7***	***4.8***	***4.9***	***5.0***

No Additional Cooling Required

Not Analyzed

Table A.1.4.9-5b
BWR Fuel Qualification Table for NUHOMS®-69BTH DSC using Type "F" Poison in HLZC 8: Zone 1 with 188 kgU/FA
(Minimum required years of cooling time after reactor core discharge for fuel with 188 kgU per FA)
(Part 1 of 5)

BU, GWd/MTU	Assembly Average Initial Enrichment (wt.% U-235)																																		
	0.7	1.2	1.5	2.0	2.1	2.2	2.3	2.4	2.5	2.6	2.7	2.8	2.9	3.0	3.1	3.2	3.3	3.4	3.5	3.6	3.7	3.8	3.9	4.0	4.1	4.2	4.3	4.4	4.5	4.6	4.7	4.8	4.9	5.0
5	0.5	0.5	0.5	0.5	0.5	0.5	0.5	0.5	0.5	0.5	0.5	0.5	0.5	0.5	0.5	0.5	0.5	0.5	0.5	0.5	0.5	0.5	0.5	0.5	0.5	0.5	0.5	0.5	0.5	0.5	0.5	0.5	0.5	0.5
10	1.0	1.0	1.0	1.0	1.0	1.0	1.0	1.0	1.0	1.0	1.0	1.0	1.0	1.0	1.0	1.0	1.0	1.0	1.0	1.0	1.0	1.0	1.0	1.0	1.0	1.0	1.0	1.0	1.0	1.0	1.0	1.0	1.0	1.0
15	1.0	1.0	1.0	1.0	1.0	1.0	1.0	1.0	1.0	1.0	1.0	1.0	1.0	1.0	1.0	1.0	1.0	1.0	1.0	1.0	1.0	1.0	1.0	1.0	1.0	1.0	1.0	1.0	1.0	1.0	1.0	1.0	1.0	1.0
16	1.0	1.0	1.0	1.0	1.0	1.0	1.0	1.0	1.0	1.0	1.0	1.0	1.0	1.0	1.0	1.0	1.0	1.0	1.0	1.0	1.0	1.0	1.0	1.0	1.0	1.0	1.0	1.0	1.0	1.0	1.0	1.0	1.0	1.0
17	1.5	1.0	1.0	1.0	1.0	1.0	1.0	1.0	1.0	1.0	1.0	1.0	1.0	1.0	1.0	1.0	1.0	1.0	1.0	1.0	1.0	1.0	1.0	1.0	1.0	1.0	1.0	1.0	1.0	1.0	1.0	1.0	1.0	1.0
18	1.5	1.5	1.0	1.0	1.0	1.0	1.0	1.0	1.0	1.0	1.0	1.0	1.0	1.0	1.0	1.0	1.0	1.0	1.0	1.0	1.0	1.0	1.0	1.0	1.0	1.0	1.0	1.0	1.0	1.0	1.0	1.0	1.0	1.0
19	1.5	1.0	1.0	1.0	1.0	1.0	1.0	1.0	1.0	1.0	1.0	1.0	1.0	1.0	1.0	1.0	1.0	1.0	1.0	1.0	1.0	1.0	1.0	1.0	1.0	1.0	1.0	1.0	1.0	1.0	1.0	1.0	1.0	1.0
20	2.5	1.5	1.0	1.0	1.0	1.0	1.0	1.0	1.0	1.0	1.0	1.0	1.0	1.0	1.0	1.0	1.0	1.0	1.0	1.0	1.0	1.0	1.0	1.0	1.0	1.0	1.0	1.0	1.0	1.0	1.0	1.0	1.0	1.0
21	5.5	1.5	1.5	1.0	1.0	1.0	1.0	1.0	1.0	1.0	1.0	1.0	1.0	1.0	1.0	1.0	1.0	1.0	1.0	1.0	1.0	1.0	1.0	1.0	1.0	1.0	1.0	1.0	1.0	1.0	1.0	1.0	1.0	1.0
22	9.5	1.5	1.5	1.5	1.5	1.5	1.5	1.5	1.5	1.5	1.5	1.0	1.0	1.0	1.0	1.0	1.0	1.0	1.0	1.0	1.0	1.0	1.0	1.0	1.0	1.0	1.0	1.0	1.0	1.0	1.0	1.0	1.0	1.0
23	13.5	2.5	1.5	1.5	1.5	1.5	1.5	1.5	1.5	1.5	1.5	1.5	1.5	1.5	1.5	1.5	1.5	1.5	1.5	1.5	1.5	1.0	1.0	1.0	1.0	1.0	1.0	1.0	1.0	1.0	1.0	1.0	1.0	1.0
24	17.0	4.5	1.5	1.5	1.5	1.5	1.5	1.5	1.5	1.5	1.5	1.5	1.5	1.5	1.5	1.5	1.5	1.5	1.5	1.5	1.5	1.5	1.5	1.5	1.5	1.5	1.5	1.5	1.5	1.5	1.5	1.5	1.5	1.5
25	20.5	8.0	2.5	1.5	1.5	1.5	1.5	1.5	1.5	1.5	1.5	1.5	1.5	1.5	1.5	1.5	1.5	1.5	1.5	1.5	1.5	1.5	1.5	1.5	1.5	1.5	1.5	1.5	1.5	1.5	1.5	1.5	1.5	1.5
26	23.5	11.5	4.5	1.5	1.5	1.5	1.5	1.5	1.5	1.5	1.5	1.5	1.5	1.5	1.5	1.5	1.5	1.5	1.5	1.5	1.5	1.5	1.5	1.5	1.5	1.5	1.5	1.5	1.5	1.5	1.5	1.5	1.5	1.5
27	26.5	15.0	8.0	1.5	1.5	1.5	1.5	1.5	1.5	1.5	1.5	1.5	1.5	1.5	1.5	1.5	1.5	1.5	1.5	1.5	1.5	1.5	1.5	1.5	1.5	1.5	1.5	1.5	1.5	1.5	1.5	1.5	1.5	1.5
28	29.5	18.5	11.5	2.5	2.0	1.5	1.5	1.5	1.5	1.5	1.5	1.5	1.5	1.5	1.5	1.5	1.5	1.5	1.5	1.5	1.5	1.5	1.5	1.5	1.5	1.5	1.5	1.5	1.5	1.5	1.5	1.5	1.5	1.5
29	32.5	21.5	15.0	4.5	3.0	2.0	2.0	1.5	1.5	1.5	1.5	1.5	1.5	1.5	1.5	1.5	1.5	1.5	1.5	1.5	1.5	1.5	1.5	1.5	1.5	1.5	1.5	1.5	1.5	1.5	1.5	1.5	1.5	1.5
30	35.0	24.5	18.0	7.5	5.5	4.0	2.5	2.0	1.5	1.5	1.5	1.5	1.5	1.5	1.5	1.5	1.5	1.5	1.5	1.5	1.5	1.5	1.5	1.5	1.5	1.5	1.5	1.5	1.5	1.5	1.5	1.5	1.5	1.5
31				10.5	8.5	6.5	4.5	3.0	2.5	2.0	1.5	1.5	1.5	1.5	1.5	1.5	1.5	1.5	1.5	1.5	1.5	1.5	1.5	1.5	1.5	1.5	1.5	1.5	1.5	1.5	1.5	1.5	1.5	1.5
32				13.5	11.5	9.5	7.5	5.5	4.0	3.0	2.5	2.0	1.5	1.5	1.5	1.5	1.5	1.5	1.5	1.5	1.5	1.5	1.5	1.5	1.5	1.5	1.5	1.5	1.5	1.5	1.5	1.5	1.5	1.5
33				16.5	14.5	12.5	10.5	8.5	7.0	5.0	3.5	2.5	2.0	2.0	1.5	1.5	1.5	1.5	1.5	1.5	1.5	1.5	1.5	1.5	1.5	1.5	1.5	1.5	1.5	1.5	1.5	1.5	1.5	1.5
34				19.5	17.5	15.5	13.5	11.5	10.0	8.0	6.0	4.5	3.5	2.5	2.0	2.0	1.5	1.5	1.5	1.5	1.5	1.5	1.5	1.5	1.5	1.5	1.5	1.5	1.5	1.5	1.5	1.5	1.5	1.5
35				22.0	20.5	18.5	16.5	14.5	13.0	11.0	9.0	7.5	6.0	4.5	3.5	2.5	2.0	2.0	1.5	1.5	1.5	1.5	1.5	1.5	1.5	1.5	1.5	1.5	1.5	1.5	1.5	1.5	1.5	1.5
36				25.0	23.0	21.0	19.5	17.5	15.5	14.0	12.0	10.5	8.5	7.0	5.5	4.5	3.5	2.5	2.0	2.0	1.5	1.5	1.5	1.5	1.5	1.5	1.5	1.5	1.5	1.5	1.5	1.5	1.5	1.5
37				27.5	25.5	24.0	22.0	20.0	18.5	16.5	15.0	13.0	11.5	10.0	8.5	7.0	5.5	4.0	3.5	2.5	2.0	2.0	1.5	1.5	1.5	1.5	1.5	1.5	1.5	1.5	1.5	1.5	1.5	1.5
38				30.0	28.0	26.5	24.5	23.0	21.0	19.5	17.5	16.0	14.5	13.0	11.0	9.5	8.0	6.5	5.5	4.0	3.5	2.5	2.5	2.0	2.0	1.5	1.5	1.5	1.5	1.5	1.5	1.5	1.5	1.5
39				32.5	30.5	29.0	27.0	25.5	23.5	22.0	20.5	18.5	17.0	15.5	14.0	12.5	11.0	9.5	8.0	6.5	5.5	4.0	3.5	3.0	2.5	2.0	2.0	1.5	1.5	1.5	1.5	1.5	1.5	1.5
40										24.5	23.0	21.5	19.5	18.0	16.5	15.0	13.5	12.0	10.5	9.5	8.0	6.5	5.5	4.0	3.5	3.0	2.5	2.0	2.0	2.0	2.0	2.0	1.5	1.5
41										27.0	25.5	24.0	22.0	20.5	19.0	17.5	16.5	15.0	13.5	12.0	10.5	9.0	8.0	6.5	5.5	4.5	3.5	3.0	2.5	2.0	2.0	2.0	2.0	2.0
42										29.5	28.0	26.5	25.0	23.5	22.0	20.5	19.0	17.5	16.0	14.5	13.5	12.0	10.5	9.5	8.0	7.0	5.5	4.5	3.5	3.0	2.5	2.5	2.0	2.0
43										32.0	30.5	29.0	27.5	26.0	24.5	23.0	21.5	20.0	18.5	17.5	16.0	14.5	13.5	12.0	10.5	9.5	8.0	7.0	6.0	5.0	4.0	3.5	3.0	2.5
44										34.5	32.5	31.0	30.0	28.5	27.0	25.5	24.0	22.5	21.0	20.0	18.5	17.0	16.0	14.5	13.5	12.0	11.0	9.5	8.5	7.0	6.0	5.0	4.0	3.5
45										36.5	35.0	33.5	32.0	30.5	29.5	28.0	26.5	25.0	23.5	22.5	21.0	19.5	18.5	17.0	16.0	14.5	13.5	12.0	11.0	10.0	8.5	7.5	6.5	5.5
46																																		
70																																		
Enr. wt.%	0.7	1.2	1.5	2.0	2.1	2.2	2.3	2.4	2.5	2.6	2.7	2.8	2.9	3.0	3.1	3.2	3.3	3.4	3.5	3.6	3.7	3.8	3.9	4.0	4.1	4.2	4.3	4.4	4.5	4.6	4.7	4.8	4.9	5.0

Not Analyzed

Table A.1.4.9-5b
BWR Fuel Qualification Table for NUHOMS®-69BTH DSC using Type "F" Poison in HLZC 8: Zone 2 with 188 kgU/FA
(Minimum required years of cooling time after reactor core discharge for fuel with 188 kgU per FA)
(Part 2 of 5)

BU, GWd/MTU	Assembly Average Initial Enrichment (wt.% U-235)																																		
	0.7	1.2	1.5	2.0	2.1	2.2	2.3	2.4	2.5	2.6	2.7	2.8	2.9	3.0	3.1	3.2	3.3	3.4	3.5	3.6	3.7	3.8	3.9	4.0	4.1	4.2	4.3	4.4	4.5	4.6	4.7	4.8	4.9	5.0
10	0.5	0.5	0.5	0.5	0.5	0.5	0.5	0.5	0.5	0.5	0.5	0.5	0.5	0.5	0.5	0.5	0.5	0.5	0.5	0.5	0.5	0.5	0.5	0.5	0.5	0.5	0.5	0.5	0.5	0.5	0.5	0.5	0.5	0.5
20	1.0	1.0	1.0	1.0	1.0	1.0	1.0	1.0	1.0	1.0	1.0	1.0	1.0	1.0	1.0	1.0	1.0	1.0	1.0	1.0	1.0	1.0	1.0	1.0	1.0	1.0	1.0	1.0	1.0	1.0	1.0	1.0	1.0	1.0
30	3.5	2.0	2.0	1.5	1.5	1.5	1.5	1.5	1.5	1.5	1.5	1.5	1.5	1.5	1.5	1.5	1.5	1.5	1.5	1.0	1.0	1.0	1.0	1.0	1.0	1.0	1.0	1.0	1.0	1.0	1.0	1.0	1.0	1.0
31				1.5	1.5	1.5	1.5	1.5	1.5	1.5	1.5	1.5	1.0	1.0	1.0	1.0	1.0	1.0	1.0	1.0	1.0	1.0	1.0	1.0	1.0	1.0	1.0	1.0	1.0	1.0	1.0	1.0	1.0	1.0
35				2.0	2.0	2.0	1.5	1.5	1.5	1.5	1.5	1.5	1.5	1.5	1.5	1.5	1.5	1.5	1.5	1.5	1.5	1.5	1.5	1.5	1.5	1.5	1.5	1.5	1.5	1.5	1.5	1.5	1.5	1.0
39				3.0	2.5	2.5	2.5	2.0	2.0	2.0	2.0	2.0	2.0	2.0	2.0	1.5	1.5	1.5	1.5	1.5	1.5	1.5	1.5	1.5	1.5	1.5	1.5	1.5	1.5	1.5	1.5	1.5	1.5	1.5
40										2.0	2.0	2.0	2.0	2.0	2.0	2.0	2.0	1.5	1.5	1.5	1.5	1.5	1.5	1.5	1.5	1.5	1.5	1.5	1.5	1.5	1.5	1.5	1.5	1.5
42										2.5	2.5	2.5	2.5	2.0	2.0	2.0	2.0	2.0	2.0	2.0	2.0	2.0	1.5	1.5	1.5	1.5	1.5	1.5	1.5	1.5	1.5	1.5	1.5	1.5
44										3.5	3.0	3.0	2.5	2.5	2.5	2.5	2.0	2.0	2.0	2.0	2.0	2.0	2.0	2.0	2.0	2.0	2.0	2.0	1.5	1.5	1.5	1.5	1.5	1.5
45										4.0	3.5	3.0	3.0	3.0	2.5	2.5	2.5	2.5	2.5	2.0	2.0	2.0	2.0	2.0	2.0	2.0	2.0	2.0	2.0	2.0	2.0	2.0	2.0	1.5
46										8.0	7.0	6.0	5.0	4.5	4.0	3.5	3.0	3.0	3.0	2.5	2.5	2.5	2.5	2.0	2.0	2.0	2.0	2.0	2.0	2.0	2.0	2.0	2.0	2.0
47										10.0	8.5	7.5	6.5	5.5	4.5	4.0	3.5	3.5	3.0	3.0	3.0	2.5	2.5	2.5	2.5	2.5	2.0	2.0	2.0	2.0	2.0	2.0	2.0	2.0
48										12.0	10.5	9.5	8.0	7.0	6.0	5.0	4.5	4.0	3.5	3.5	3.0	3.0	3.0	2.5	2.5	2.5	2.5	2.5	2.0	2.0	2.0	2.0	2.0	2.0
49										14.0	12.5	11.5	10.0	9.0	7.5	6.5	5.5	5.0	4.5	4.0	3.5	3.5	3.0	3.0	3.0	2.5	2.5	2.5	2.5	2.5	2.0	2.0	2.0	2.0
50										16.0	14.5	13.0	12.0	10.5	9.5	8.5	7.0	6.0	5.5	4.5	4.0	4.0	3.5	3.0	3.0	3.0	3.0	2.5	2.5	2.5	2.5	2.5	2.5	2.0
51										17.5	16.5	15.0	14.0	12.5	11.5	10.0	9.0	8.0	7.0	6.0	5.0	4.5	4.0	3.5	3.5	3.0	3.0	3.0	3.0	2.5	2.5	2.5	2.5	2.5
52										19.5	18.0	17.0	15.5	14.5	13.5	12.0	11.0	9.5	8.5	7.5	6.5	5.5	5.0	4.5	4.0	3.5	3.5	3.0	3.0	3.0	3.0	2.5	2.5	2.5
53										21.0	20.0	18.5	17.5	16.5	15.0	14.0	13.0	11.5	10.5	9.5	8.0	7.0	6.0	5.5	5.0	4.5	4.0	3.5	3.5	3.0	3.0	3.0	3.0	2.5
54										23.0	21.5	20.5	19.5	18.0	17.0	16.0	14.5	13.5	12.5	11.0	10.0	9.0	8.0	7.0	6.0	5.5	4.5	4.5	4.0	3.5	3.5	3.0	3.0	3.0
55										24.5	23.5	22.0	21.0	20.0	18.5	17.5	16.5	15.0	14.0	13.0	12.0	10.5	9.5	8.5	7.5	6.5	6.0	5.0	4.5	4.0	4.0	3.5	3.5	3.0
56										26.0	25.0	24.0	22.5	21.5	20.5	19.5	18.0	17.0	16.0	14.5	13.5	12.5	11.5	10.5	9.5	8.0	7.5	6.5	5.5	5.0	4.5	4.0	4.0	3.5
57										28.0	26.5	25.5	24.5	23.0	22.0	21.0	20.0	18.5	17.5	16.5	15.5	14.5	13.0	12.0	11.0	10.0	9.0	8.0	7.0	6.0	5.5	5.0	4.5	4.0
58										29.5	28.0	27.0	26.0	25.0	23.5	22.5	21.5	20.5	19.5	18.0	17.0	16.0	15.0	14.0	13.0	11.5	10.5	9.5	8.5	7.5	7.0	6.0	5.5	5.0
59										31.0	29.5	28.5	27.5	26.5	25.5	24.0	23.0	22.0	21.0	20.0	19.0	17.5	16.5	15.5	14.5	13.5	12.5	11.5	10.5	9.5	8.5	7.5	6.5	6.0
60										32.5	31.0	30.0	29.0	28.0	27.0	26.0	24.5	23.5	22.5	21.5	20.5	19.5	18.5	17.0	16.0	15.0	14.0	13.0	12.0	11.0	10.0	9.0	8.0	7.5
61										34.0	32.5	31.5	30.5	29.5	28.5	27.5	26.5	25.5	24.0	23.0	22.0	21.0	20.0	19.0	18.0	17.0	16.0	15.0	14.0	13.0	12.0	11.0	10.0	9.0
62										35.5	34.0	33.0	32.0	31.0	30.0	29.0	28.0	27.0	26.0	25.0	24.0	22.5	21.5	20.5	19.5	18.5	17.5	16.5	15.5	14.5	13.5	12.5	11.5	10.5
63																					25.5	24.5	23.5	22.5	21.5	20.5	19.0	18.0	17.5	16.5	15.5	14.5	13.5	12.5
64																					27.0	26.0	25.0	24.0	23.0	22.0	21.0	20.0	19.0	18.0	17.0	16.0	15.0	14.0
65				Not Analyzed																	28.5	27.5	26.5	25.5	24.5	23.5	22.5	21.5	20.5	19.5	18.5	17.5	16.5	16.0
66																					30.0	29.0	28.0	27.0	26.0	25.0	24.0	23.0	22.0	21.0	20.5	19.5	18.5	17.5
67																					31.5	30.5	29.5	28.5	27.5	26.5	25.5	24.5	24.0	23.0	22.0	21.0	20.0	19.0
68																					33.0	32.0	31.0	30.0	29.0	28.0	27.0	26.5	25.5	24.5	23.5	22.5	21.5	20.5
69																					34.5	33.5	32.5	31.5	30.5	29.5	28.5	28.0	27.0	26.0	25.0	24.0	23.0	22.5
70																					36.0	35.0	34.0	33.0	32.0	31.0	30.0	29.5	28.5	27.5	26.5	25.5	24.5	24.0
Enr. wt.%	0.7	1.2	1.5	2.0	2.1	2.2	2.3	2.4	2.5	2.6	2.7	2.8	2.9	3.0	3.1	3.2	3.3	3.4	3.5	3.6	3.7	3.8	3.9	4.0	4.1	4.2	4.3	4.4	4.5	4.6	4.7	4.8	4.9	5.0

Table A.1.4.9-5b
BWR Fuel Qualification Table for NUHOMS®-69BTH DSC using Type "F" Poison in HLZC 8: Zone 3 with 188 kgU/FA
(Minimum required years of cooling time after reactor core discharge for fuel with 188 kgU per FA)
(Part 3 of 5)

BU, GWd/MTU	Assembly Average Initial Enrichment (wt.% U-235)																																	
	0.7	1.2	1.5	2.0	2.1	2.2	2.3	2.4	2.5	2.6	2.7	2.8	2.9	3.0	3.1	3.2	3.3	3.4	3.5	3.6	3.7	3.8	3.9	4.0	4.1	4.2	4.3	4.4	4.5	4.6	4.7	4.8	4.9	5.0
10	0.5	0.5	0.5	0.5	0.5	0.5	0.5	0.5	0.5	0.5	0.5	0.5	0.5	0.5	0.5	0.5	0.5	0.5	0.5	0.5	0.5	0.5	0.5	0.5	0.5	0.5	0.5	0.5	0.5	0.5	0.5	0.5	0.5	0.5
20	0.5	0.5	0.5	0.5	0.5	0.5	0.5	0.5	0.5	0.5	0.5	0.5	0.5	0.5	0.5	0.5	0.5	0.5	0.5	0.5	0.5	0.5	0.5	0.5	0.5	0.5	0.5	0.5	0.5	0.5	0.5	0.5	0.5	0.5
30	0.5	0.5	0.5	0.5	0.5	0.5	0.5	0.5	0.5	0.5	0.5	0.5	0.5	0.5	0.5	0.5	0.5	0.5	0.5	0.5	0.5	0.5	0.5	0.5	0.5	0.5	0.5	0.5	0.5	0.5	0.5	0.5	0.5	0.5
31				0.5	0.5	0.5	0.5	0.5	0.5	0.5	0.5	0.5	0.5	0.5	0.5	0.5	0.5	0.5	0.5	0.5	0.5	0.5	0.5	0.5	0.5	0.5	0.5	0.5	0.5	0.5	0.5	0.5	0.5	0.5
35				0.5	0.5	0.5	0.5	0.5	0.5	0.5	0.5	0.5	0.5	0.5	0.5	0.5	0.5	0.5	0.5	0.5	0.5	0.5	0.5	0.5	0.5	0.5	0.5	0.5	0.5	0.5	0.5	0.5	0.5	0.5
39				0.5	0.5	0.5	0.5	0.5	0.5	0.5	0.5	0.5	0.5	0.5	0.5	0.5	0.5	0.5	0.5	0.5	0.5	0.5	0.5	0.5	0.5	0.5	0.5	0.5	0.5	0.5	0.5	0.5	0.5	0.5
40										0.5	0.5	0.5	0.5	0.5	0.5	0.5	0.5	0.5	0.5	0.5	0.5	0.5	0.5	0.5	0.5	0.5	0.5	0.5	0.5	0.5	0.5	0.5	0.5	0.5
42										0.5	0.5	0.5	0.5	0.5	0.5	0.5	0.5	0.5	0.5	0.5	0.5	0.5	0.5	0.5	0.5	0.5	0.5	0.5	0.5	0.5	0.5	0.5	0.5	0.5
44										1.0	1.0	1.0	0.5	0.5	0.5	0.5	0.5	0.5	0.5	0.5	0.5	0.5	0.5	0.5	0.5	0.5	0.5	0.5	0.5	0.5	0.5	0.5	0.5	0.5
45										1.0	1.0	1.0	1.0	1.0	0.5	0.5	0.5	0.5	0.5	0.5	0.5	0.5	0.5	0.5	0.5	0.5	0.5	0.5	0.5	0.5	0.5	0.5	0.5	0.5
46										1.0	1.0	1.0	1.0	1.0	1.0	1.0	1.0	0.5	0.5	0.5	0.5	0.5	0.5	0.5	0.5	0.5	0.5	0.5	0.5	0.5	0.5	0.5	0.5	0.5
47										1.5	1.0	1.0	1.0	1.0	1.0	1.0	1.0	1.0	1.0	1.0	0.5	0.5	0.5	0.5	0.5	0.5	0.5	0.5	0.5	0.5	0.5	0.5	0.5	0.5
48										1.5	1.5	1.5	1.0	1.0	1.0	1.0	1.0	1.0	1.0	1.0	1.0	1.0	1.0	0.5	0.5	0.5	0.5	0.5	0.5	0.5	0.5	0.5	0.5	0.5
49										2.0	1.5	1.5	1.5	1.5	1.0	1.0	1.0	1.0	1.0	1.0	1.0	1.0	1.0	1.0	1.0	0.5	0.5	0.5	0.5	0.5	0.5	0.5	0.5	0.5
50										2.0	2.0	1.5	1.5	1.5	1.5	1.0	1.0	1.0	1.0	1.0	1.0	1.0	1.0	1.0	1.0	1.0	1.0	1.0	0.5	0.5	0.5	0.5	0.5	0.5
51										2.5	2.0	2.0	2.0	1.5	1.5	1.5	1.5	1.0	1.0	1.0	1.0	1.0	1.0	1.0	1.0	1.0	1.0	1.0	1.0	1.0	0.5	0.5	0.5	0.5
52										3.0	2.5	2.5	2.0	2.0	2.0	1.5	1.5	1.5	1.5	1.0	1.0	1.0	1.0	1.0	1.0	1.0	1.0	1.0	1.0	1.0	1.0	1.0	1.0	1.0
53										4.0	3.5	3.0	2.5	2.0	2.0	2.0	1.5	1.5	1.5	1.5	1.5	1.0	1.0	1.0	1.0	1.0	1.0	1.0	1.0	1.0	1.0	1.0	1.0	1.0
54										5.0	4.0	3.5	3.0	2.5	2.5	2.0	2.0	2.0	1.5	1.5	1.5	1.5	1.5	1.0	1.0	1.0	1.0	1.0	1.0	1.0	1.0	1.0	1.0	1.0
55										6.5	5.5	4.5	4.0	3.0	3.0	2.5	2.5	2.0	2.0	2.0	1.5	1.5	1.5	1.5	1.5	1.0	1.0	1.0	1.0	1.0	1.0	1.0	1.0	1.0
56										7.5	6.5	5.5	5.0	4.0	3.5	3.0	2.5	2.5	2.0	2.0	2.0	1.5	1.5	1.5	1.5	1.5	1.5	1.0	1.0	1.0	1.0	1.0	1.0	1.0
57										9.0	8.0	7.0	6.0	5.0	4.5	4.0	3.5	3.0	2.5	2.5	2.0	2.0	2.0	1.5	1.5	1.5	1.5	1.5	1.5	1.0	1.0	1.0	1.0	1.0
58										10.5	9.5	8.5	7.5	6.5	5.5	5.0	4.0	3.5	3.0	2.5	2.5	2.5	2.0	2.0	2.0	1.5	1.5	1.5	1.5	1.5	1.5	1.0	1.0	1.0
59										12.0	11.0	10.0	9.0	8.0	7.0	6.0	5.0	4.5	4.0	3.5	3.0	2.5	2.5	2.0	2.0	2.0	2.0	1.5	1.5	1.5	1.5	1.5	1.5	1.5
60										13.5	12.5	11.5	10.5	9.5	8.5	7.5	6.5	5.5	4.5	4.0	3.5	3.0	3.0	2.5	2.5	2.0	2.0	2.0	2.0	1.5	1.5	1.5	1.5	1.5
61										15.0	14.0	13.0	12.0	11.0	10.0	9.0	8.0	7.0	6.0	5.0	4.5	4.0	3.5	3.0	2.5	2.5	2.5	2.0	2.0	2.0	1.5	1.5	1.5	1.5
62										16.5	15.0	14.0	13.5	12.5	11.5	10.5	9.5	8.5	7.5	6.5	5.5	5.0	4.0	3.5	3.0	3.0	2.5	2.5	2.0	2.0	2.0	2.0	1.5	1.5
63																					7.0	6.0	5.5	4.5	4.0	3.5	3.0	3.0	2.5	2.5	2.0	2.0	2.0	2.0
64																					8.5	7.5	6.5	5.5	5.0	4.5	4.0	3.5	3.0	3.0	2.5	2.5	2.0	2.0
65				Not Analyzed																	10.0	9.0	8.0	7.0	6.0	5.5	4.5	4.0	3.5	3.0	3.0	2.5	2.5	2.5
66																					11.0	10.5	9.5	8.5	7.5	6.5	6.0	5.0	4.5	4.0	3.5	3.0	3.0	2.5
67																					12.5	11.5	11.0	10.0	9.0	8.0	7.0	6.5	5.5	5.0	4.5	4.0	3.5	3.0
68																					14.0	13.0	12.0	11.5	10.5	9.5	8.5	7.5	7.0	6.0	5.5	4.5	4.0	3.5
69																					15.5	14.5	13.5	12.5	12.0	11.0	10.0	9.0	8.5	7.5	6.5	6.0	5.0	4.5
70																					17.0	16.0	15.0	14.0	13.0	12.5	11.5	10.5	9.5	9.0	8.0	7.0	6.5	5.5
Enr. wt.%	0.7	1.2	1.5	2.0	2.1	2.2	2.3	2.4	2.5	2.6	2.7	2.8	2.9	3.0	3.1	3.2	3.3	3.4	3.5	3.6	3.7	3.8	3.9	4.0	4.1	4.2	4.3	4.4	4.5	4.6	4.7	4.8	4.9	5.0

Table A.1.4.9-5b
BWR Fuel Qualification Table for NUHOMS®-69BTH DSC using Type "F" Poison in HLZC 8: Zone 4 with 188 kgU/FA
(Minimum required years of cooling time after reactor core discharge for fuel with 188 kgU per FA)
(Part 4 of 5)

BU, GWd/MTU	Assembly Average Initial Enrichment (wt.% U-235)																																	
	0.7	1.2	1.5	2.0	2.1	2.2	2.3	2.4	2.5	2.6	2.7	2.8	2.9	3.0	3.1	3.2	3.3	3.4	3.5	3.6	3.7	3.8	3.9	4.0	4.1	4.2	4.3	4.4	4.5	4.6	4.7	4.8	4.9	5.0
10	0.5	0.5	0.5	0.5	0.5	0.5	0.5	0.5	0.5	0.5	0.5	0.5	0.5	0.5	0.5	0.5	0.5	0.5	0.5	0.5	0.5	0.5	0.5	0.5	0.5	0.5	0.5	0.5	0.5	0.5	0.5	0.5	0.5	0.5
20	0.5	0.5	0.5	0.5	0.5	0.5	0.5	0.5	0.5	0.5	0.5	0.5	0.5	0.5	0.5	0.5	0.5	0.5	0.5	0.5	0.5	0.5	0.5	0.5	0.5	0.5	0.5	0.5	0.5	0.5	0.5	0.5	0.5	0.5
30	0.5	0.5	0.5	0.5	0.5	0.5	0.5	0.5	0.5	0.5	0.5	0.5	0.5	0.5	0.5	0.5	0.5	0.5	0.5	0.5	0.5	0.5	0.5	0.5	0.5	0.5	0.5	0.5	0.5	0.5	0.5	0.5	0.5	0.5
31				0.5	0.5	0.5	0.5	0.5	0.5	0.5	0.5	0.5	0.5	0.5	0.5	0.5	0.5	0.5	0.5	0.5	0.5	0.5	0.5	0.5	0.5	0.5	0.5	0.5	0.5	0.5	0.5	0.5	0.5	0.5
35				0.5	0.5	0.5	0.5	0.5	0.5	0.5	0.5	0.5	0.5	0.5	0.5	0.5	0.5	0.5	0.5	0.5	0.5	0.5	0.5	0.5	0.5	0.5	0.5	0.5	0.5	0.5	0.5	0.5	0.5	0.5
39				1.0	0.5	0.5	0.5	0.5	0.5	0.5	0.5	0.5	0.5	0.5	0.5	0.5	0.5	0.5	0.5	0.5	0.5	0.5	0.5	0.5	0.5	0.5	0.5	0.5	0.5	0.5	0.5	0.5	0.5	0.5
40										0.5	0.5	0.5	0.5	0.5	0.5	0.5	0.5	0.5	0.5	0.5	0.5	0.5	0.5	0.5	0.5	0.5	0.5	0.5	0.5	0.5	0.5	0.5	0.5	0.5
42										1.0	1.0	0.5	0.5	0.5	0.5	0.5	0.5	0.5	0.5	0.5	0.5	0.5	0.5	0.5	0.5	0.5	0.5	0.5	0.5	0.5	0.5	0.5	0.5	0.5
44										1.0	1.0	1.0	1.0	1.0	1.0	1.0	0.5	0.5	0.5	0.5	0.5	0.5	0.5	0.5	0.5	0.5	0.5	0.5	0.5	0.5	0.5	0.5	0.5	0.5
45										1.0	1.0	1.0	1.0	1.0	1.0	1.0	1.0	1.0	1.0	0.5	0.5	0.5	0.5	0.5	0.5	0.5	0.5	0.5	0.5	0.5	0.5	0.5	0.5	0.5
46										1.0	1.0	1.0	1.0	1.0	1.0	1.0	1.0	1.0	1.0	1.0	1.0	1.0	1.0	0.5	0.5	0.5	0.5	0.5	0.5	0.5	0.5	0.5	0.5	0.5
47										1.5	1.0	1.0	1.0	1.0	1.0	1.0	1.0	1.0	1.0	1.0	1.0	1.0	1.0	1.0	1.0	1.0	1.0	0.5	0.5	0.5	0.5	0.5	0.5	0.5
48										1.5	1.5	1.5	1.0	1.0	1.0	1.0	1.0	1.0	1.0	1.0	1.0	1.0	1.0	1.0	1.0	1.0	1.0	1.0	1.0	1.0	1.0	0.5	0.5	0.5
49										1.5	1.5	1.5	1.5	1.5	1.0	1.0	1.0	1.0	1.0	1.0	1.0	1.0	1.0	1.0	1.0	1.0	1.0	1.0	1.0	1.0	1.0	1.0	1.0	1.0
50										2.0	1.5	1.5	1.5	1.5	1.5	1.5	1.0	1.0	1.0	1.0	1.0	1.0	1.0	1.0	1.0	1.0	1.0	1.0	1.0	1.0	1.0	1.0	1.0	1.0
51										2.0	2.0	1.5	1.5	1.5	1.5	1.5	1.5	1.5	1.0	1.0	1.0	1.0	1.0	1.0	1.0	1.0	1.0	1.0	1.0	1.0	1.0	1.0	1.0	1.0
52										2.5	2.0	2.0	2.0	1.5	1.5	1.5	1.5	1.5	1.5	1.0	1.0	1.0	1.0	1.0	1.0	1.0	1.0	1.0	1.0	1.0	1.0	1.0	1.0	1.0
53										2.5	2.5	2.0	2.0	2.0	2.0	1.5	1.5	1.5	1.5	1.5	1.5	1.5	1.0	1.0	1.0	1.0	1.0	1.0	1.0	1.0	1.0	1.0	1.0	1.0
54										3.0	2.5	2.5	2.5	2.0	2.0	2.0	2.0	1.5	1.5	1.5	1.5	1.5	1.5	1.5	1.0	1.0	1.0	1.0	1.0	1.0	1.0	1.0	1.0	1.0
55										3.5	3.0	3.0	2.5	2.5	2.0	2.0	2.0	2.0	1.5	1.5	1.5	1.5	1.5	1.5	1.5	1.5	1.5	1.0	1.0	1.0	1.0	1.0	1.0	1.0
56										4.0	3.5	3.0	3.0	2.5	2.5	2.5	2.0	2.0	2.0	2.0	1.5	1.5	1.5	1.5	1.5	1.5	1.5	1.5	1.5	1.0	1.0	1.0	1.0	1.0
57										5.0	4.5	4.0	3.5	3.0	3.0	2.5	2.5	2.0	2.0	2.0	2.0	2.0	1.5	1.5	1.5	1.5	1.5	1.5	1.5	1.5	1.0	1.0	1.0	1.0
58										6.0	5.5	4.5	4.0	3.5	3.0	3.0	2.5	2.5	2.5	2.0	2.0	2.0	2.0	2.0	1.5	1.5	1.5	1.5	1.5	1.5	1.5	1.5	1.5	1.5
59										7.5	6.5	5.5	5.0	4.5	4.0	3.5	3.0	3.0	2.5	2.5	2.5	2.0	2.0	2.0	2.0	2.0	1.5	1.5	1.5	1.5	1.5	1.5	1.5	1.5
60										8.5	7.5	7.0	6.0	5.0	4.5	4.0	3.5	3.0	3.0	2.5	2.5	2.5	2.0	2.0	2.0	2.0	2.0	2.0	1.5	1.5	1.5	1.5	1.5	1.5
61										10.0	9.0	8.0	7.0	6.5	5.5	5.0	4.5	4.0	3.5	3.0	3.0	2.5	2.5	2.5	2.0	2.0	2.0	2.0	2.0	1.5	1.5	1.5	1.5	1.5
62										11.5	10.5	9.5	8.5	7.5	6.5	6.0	5.0	4.5	4.0	3.5	3.5	3.0	3.0	2.5	2.5	2.5	2.0	2.0	2.0	2.0	2.0	2.0	1.5	1.5
63																					4.0	3.5	3.0	3.0	2.5	2.5	2.5	2.5	2.0	2.0	2.0	2.0	2.0	2.0
64																					4.5	4.0	3.5	3.5	3.0	3.0	2.5	2.5	2.5	2.5	2.0	2.0	2.0	2.0
65																					5.5	5.0	4.5	4.0	3.5	3.0	3.0	3.0	2.5	2.5	2.5	2.0	2.0	2.0
66																					6.5	6.0	5.0	4.5	4.0	4.0	3.5	3.0	3.0	3.0	2.5	2.5	2.5	2.0
67																					8.0	7.0	6.5	5.5	5.0	4.5	4.0	3.5	3.5	3.0	3.0	2.5	2.5	2.5
68																					9.0	8.5	7.5	6.5	6.0	5.5	4.5	4.5	4.0	3.5	3.5	3.0	3.0	2.5
69																					10.5	9.5	9.0	8.0	7.0	6.5	5.5	5.0	4.5	4.0	3.5	3.5	3.0	3.0
70																					12.0	11.0	10.0	9.0	8.5	7.5	7.0	6.0	5.5	5.0	4.5	4.0	3.5	3.5
Enr. wt.%	0.7	1.2	1.5	2.0	2.1	2.2	2.3	2.4	2.5	2.6	2.7	2.8	2.9	3.0	3.1	3.2	3.3	3.4	3.5	3.6	3.7	3.8	3.9	4.0	4.1	4.2	4.3	4.4	4.5	4.6	4.7	4.8	4.9	5.0

Not Analyzed

Table A.1.4.9-5b
BWR Fuel Qualification Table for NUHOMS®-69BTH DSC using Type "F" Poison in HLZC 8: Zone 5 with 188 kgU/FA
(Minimum required years of cooling time after reactor core discharge for fuel with 188 kgU per FA)
(Part 5 of 5)

BU, GWd/MTU	Assembly Average Initial Enrichment (wt.% U-235)																																			
	0.7	1.2	1.5	2.0	2.1	2.2	2.3	2.4	2.5	2.6	2.7	2.8	2.9	3.0	3.1	3.2	3.3	3.4	3.5	3.6	3.7	3.8	3.9	4.0	4.1	4.2	4.3	4.4	4.5	4.6	4.7	4.8	4.9	5.0
10	2.0	2.0	2.0	2.0	2.0	2.0	2.0	2.0	2.0	2.0	2.0	2.0	2.0	2.0	2.0	2.0	2.0	2.0	2.0	2.0	2.0	2.0	2.0	2.0	2.0	2.0	2.0	2.0	2.0	2.0	2.0	2.0	2.0	2.0
20	3.0	2.5	2.5	2.5	2.5	2.5	2.5	2.5	2.5	2.5	2.5	2.5	2.5	2.5	2.5	2.5	2.5	2.5	2.5	2.5	2.5	2.5	2.5	2.5	2.5	2.5	2.5	2.5	2.5	2.5	2.5	2.5	2.5	2.5
30	4.0	3.5	3.5	3.0	3.0	3.0	3.0	3.0	3.0	3.0	3.0	3.0	3.0	3.0	3.0	3.0	3.0	3.0	3.0	3.0	3.0	3.0	3.0	3.0	3.0	3.0	3.0	3.0	3.0	3.0	3.0	3.0	3.0	3.0
31				3.0	3.0	3.0	3.0	3.0	3.0	3.0	3.0	3.0	3.0	3.0	3.0	3.0	3.0	3.0	3.0	3.0	3.0	3.0	3.0	3.0	3.0	3.0	3.0	3.0	3.0	3.0	3.0	3.0	3.0	2.5
35				3.5	3.5	3.5	3.5	3.5	3.0	3.0	3.0	3.0	3.0	3.0	3.0	3.0	3.0	3.0	3.0	3.0	3.0	3.0	3.0	3.0	3.0	3.0	3.0	3.0	3.0	3.0	3.0	3.0	3.0	3.0
39				4.0	4.0	3.5	3.5	3.5	3.5	3.5	3.5	3.5	3.5	3.5	3.5	3.5	3.5	3.5	3.5	3.0	3.0	3.0	3.0	3.0	3.0	3.0	3.0	3.0	3.0	3.0	3.0	3.0	3.0	3.0
40										3.5	3.5	3.5	3.5	3.5	3.5	3.5	3.5	3.5	3.5	3.5	3.5	3.5	3.5	3.0	3.0	3.0	3.0	3.0	3.0	3.0	3.0	3.0	3.0	3.0
42										4.0	4.0	3.5	3.5	3.5	3.5	3.5	3.5	3.5	3.5	3.5	3.5	3.5	3.5	3.5	3.5	3.5	3.5	3.5	3.5	3.5	3.5	3.5	3.0	3.0
44										4.0	4.0	4.0	4.0	4.0	4.0	4.0	3.5	3.5	3.5	3.5	3.5	3.5	3.5	3.5	3.5	3.5	3.5	3.5	3.5	3.5	3.5	3.5	3.5	3.5
45										4.0	4.0	4.0	4.0	4.0	4.0	4.0	4.0	4.0	3.5	3.5	3.5	3.5	3.5	3.5	3.5	3.5	3.5	3.5	3.5	3.5	3.5	3.5	3.5	3.5
46										4.5	4.5	4.5	4.0	4.0	4.0	4.0	4.0	4.0	4.0	4.0	4.0	3.5	3.5	3.5	3.5	3.5	3.5	3.5	3.5	3.5	3.5	3.5	3.5	3.5
47										4.5	4.5	4.5	4.5	4.5	4.0	4.0	4.0	4.0	4.0	4.0	4.0	4.0	4.0	3.5	3.5	3.5	3.5	3.5	3.5	3.5	3.5	3.5	3.5	3.5
48										5.0	5.0	4.5	4.5	4.5	4.5	4.5	4.0	4.0	4.0	4.0	4.0	4.0	4.0	4.0	4.0	4.0	3.5	3.5	3.5	3.5	3.5	3.5	3.5	3.5
49										5.5	5.0	5.0	5.0	4.5	4.5	4.5	4.5	4.5	4.0	4.0	4.0	4.0	4.0	4.0	4.0	4.0	4.0	4.0	4.0	3.5	3.5	3.5	3.5	3.5
50										6.0	5.5	5.5	5.0	5.0	5.0	4.5	4.5	4.5	4.5	4.5	4.0	4.0	4.0	4.0	4.0	4.0	4.0	4.0	4.0	4.0	4.0	4.0	3.5	3.5
51										6.5	6.0	5.5	5.5	5.0	5.0	5.0	4.5	4.5	4.5	4.5	4.5	4.5	4.0	4.0	4.0	4.0	4.0	4.0	4.0	4.0	4.0	4.0	4.0	4.0
52										7.0	6.5	6.0	6.0	5.5	5.5	5.0	5.0	5.0	4.5	4.5	4.5	4.5	4.5	4.5	4.0	4.0	4.0	4.0	4.0	4.0	4.0	4.0	4.0	4.0
53										8.0	7.0	6.5	6.5	6.0	5.5	5.5	5.5	5.0	5.0	5.0	4.5	4.5	4.5	4.5	4.5	4.5	4.0	4.0	4.0	4.0	4.0	4.0	4.0	4.0
54										9.0	8.0	7.5	7.0	6.5	6.0	6.0	5.5	5.5	5.0	5.0	5.0	5.0	4.5	4.5	4.5	4.5	4.5	4.5	4.0	4.0	4.0	4.0	4.0	4.0
55										10.0	9.0	8.5	8.0	7.0	7.0	6.5	6.0	6.0	5.5	5.5	5.0	5.0	5.0	5.0	4.5	4.5	4.5	4.5	4.5	4.5	4.0	4.0	4.0	4.0
56										11.0	10.5	9.5	9.0	8.0	7.5	7.0	6.5	6.0	6.0	5.5	5.5	5.5	5.0	5.0	5.0	5.0	4.5	4.5	4.5	4.5	4.5	4.5	4.5	4.0
57										12.5	11.5	10.5	10.0	9.0	8.5	8.0	7.5	7.0	6.5	6.0	6.0	5.5	5.5	5.0	5.0	5.0	5.0	5.0	4.5	4.5	4.5	4.5	4.5	4.5
58										13.5	13.0	12.0	11.0	10.0	9.5	8.5	8.0	7.5	7.0	6.5	6.5	6.0	5.5	5.5	5.5	5.0	5.0	5.0	5.0	5.0	4.5	4.5	4.5	4.5
59										15.0	14.0	13.0	12.0	11.5	10.5	10.0	9.0	8.5	8.0	7.5	7.0	6.5	6.0	6.0	5.5	5.5	5.5	5.0	5.0	5.0	5.0	5.0	4.5	4.5
60										16.5	15.5	14.5	13.5	12.5	12.0	11.0	10.0	9.5	8.5	8.0	7.5	7.0	6.5	6.5	6.0	6.0	5.5	5.5	5.5	5.0	5.0	5.0	5.0	5.0
61										17.5	16.5	15.5	15.0	14.0	13.0	12.0	11.5	10.5	10.0	9.0	8.5	8.0	7.5	7.0	6.5	6.5	6.0	6.0	5.5	5.5	5.5	5.0	5.0	5.0
62										19.0	18.0	17.0	16.0	15.0	14.5	13.5	12.5	12.0	11.0	10.0	9.5	9.0	8.0	7.5	7.0	7.0	6.5	6.0	6.0	6.0	5.5	5.5	5.5	5.0
63																					10.5	10.0	9.0	8.5	8.0	7.5	7.0	6.5	6.5	6.0	6.0	5.5	5.5	5.5
64																					12.0	11.0	10.5	9.5	9.0	8.5	8.0	7.5	7.0	6.5	6.5	6.0	6.0	5.5
65																					13.0	12.5	11.5	10.5	10.0	9.5	9.0	8.0	7.5	7.5	7.0	6.5	6.5	6.0
66																					14.5	13.5	12.5	12.0	11.0	10.5	10.0	9.0	8.5	8.0	7.5	7.0	7.0	6.5
67																					15.5	15.0	14.0	13.0	12.5	11.5	11.0	10.0	9.5	9.0	8.5	8.0	7.5	7.0
68																					17.0	16.0	15.0	14.5	13.5	13.0	12.0	11.5	10.5	10.0	9.5	9.0	8.5	8.0
69																					18.0	17.5	16.5	15.5	15.0	14.0	13.5	12.5	12.0	11.0	10.5	10.0	9.0	8.5
70																					19.5	18.5	17.5	17.0	16.0	15.5	14.5	13.5	13.0	12.0	11.5	11.0	10.0	9.5
Enr. wt.%	0.7	1.2	1.5	2.0	2.1	2.2	2.3	2.4	2.5	2.6	2.7	2.8	2.9	3.0	3.1	3.2	3.3	3.4	3.5	3.6	3.7	3.8	3.9	4.0	4.1	4.2	4.3	4.4	4.5	4.6	4.7	4.8	4.9	5.0

Not Analyzed

Notes for using Table A.1.4.9-5b, parts 1 through 5:

- *BU = Assembly Average burnup.*
- *For fuel assemblies with natural uranium blankets greater than 8 inches at the top and/or bottom end, BU=Maximum Planar Average Burnup.*
- *Use burnup and enrichment to lookup minimum cooling time in years. Licensee is responsible for ensuring that uncertainties in fuel enrichment and burnup are correctly accounted for during fuel qualification.*
- *Round burnup UP to next higher entry, round enrichments DOWN to next lower entry.*
- *Fuel with a lattice average initial enrichment of less than 0.7 (or less than the minimum provided above for each burnup) or greater than 5.0 wt. % U-235 is unacceptable for transportation.*
- *Fuel with an assembly average burnup greater than 70 GWd/MTU is unacceptable for transportation.*
- *For reconstituted fuel assemblies with irradiated stainless steel rods, increase the cooling time by 1 for fuel assemblies in the 24 peripheral locations of the canister with cooling times less than 10 years. No adjustment of cooling time is required for fuel assemblies in other locations or for those that have cooled for more than 10 years.*
- *Example: An assembly is to be loaded into 69BTH using HLZC 8: The initial enrichment is 4.85 wt. % U-235, the Uranium loading is 188 kg, and the burnup is 41.5 GWD/MTU. Round 4.85 wt. % U-235 down to 4.8 wt. % U-235, round 41.5 GWD/MTU up to 42 GWD/MTU.*
    - *The FA is acceptable for transport in heat loading zone 1 according to Table A.1.4.9-5b, part 1 after 2.5 years of cooling time (other considerations not withstanding).*
    - *The FA is acceptable for transport in heat loading zone 2 according to Table A.1.4.9-5b, part 2 after 1.5 years of cooling time (other considerations not withstanding).*
    - *The FA is acceptable for transport in heat loading zone 3 according to Table A.1.4.9-5b, part 3 after 0.5 years of cooling time (other considerations not withstanding).*
    - *The FA is acceptable for transport in heat loading zone 4 according to Table A.1.4.9-5b, part 4 after 0.5 years of cooling time (other considerations not withstanding).*
    - *The FA is acceptable for transport in heat loading zone 5 according to Table A.1.4.9-5b, part 5 after 3.5 years of cooling time (other considerations not withstanding).*

Table A.1.4.9-6
BWR Assembly Decay Heat for Heat Load Configurations

The Decay Heat (DH) in watts is expressed as:

$$F1 = -59.1 + 23.4*X1 - 21.1*X2 + 0.280*X1^2 - 3.52*X1*X2 + 12.4*X2^2$$
$$DH = F1*Exp(\{[1-(1.2/X3)]* -0.720\}*[(X3-4.5)^{0.157}]*[(X2/X1)^{-0.132}]) + 10$$

where,

F1 Intermediate Function
X1 Assembly Burnup in GWD/MTU
X2 Initial Enrichment in wt. % U-235
X3 Cooling Time in Years (minimum *5* years)

A uranium loading of 198 kg is employed in the calculation of the decay heat equation. Alternatively, the decay heat can be calculated without employing the decay heat equation, using an approved methodology with actual spent fuel parameters instead of bounding spent fuel parameters.

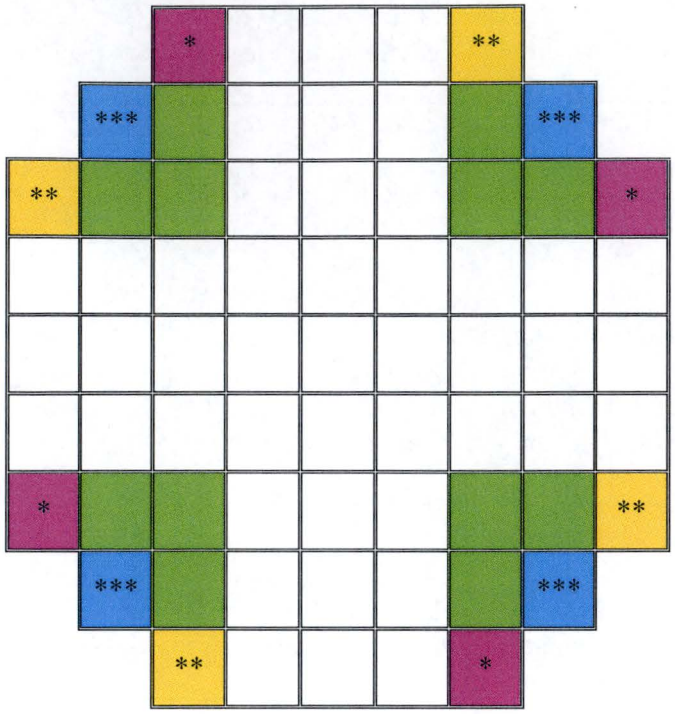

*	Configuration 1(1)	**	Configuration 2(1)	***	Configuration 3(1)

1	Either one of these three sets of corner locations shall only be utilized to load up to four damaged assemblies with the remaining intact in a 69BTH Basket. The maximum lattice average initial enrichment of fuel assemblies (damaged or intact transported in either magenta set of cells for configuration 1, gold set of cells for configuration 2, or blue set of cells for configuration 3) is limited to the "up to 4 damaged assemblies" column of Table A.1.4.9-3.
	Following the placement of damaged fuel assemblies in either configuration 1 or 2, the remaining gold or magenta locations shall be used to load up to 4 additional damaged assemblies, with the remaining intact in a 69BTH Basket. The maximum lattice average initial enrichment for these fuel assemblies (damaged or intact transported in gold or magenta cells available) is limited to the "5 to 8 damaged assemblies" column of Table A.1.4.9-3.
	Following the placement of eight damaged fuel assemblies in the set of corner locations marked with a "*" (shaded in magenta) and a "**" (shaded in gold), the locations shaded in green or blue in Figure shall be used to load up to sixteen additional damaged assemblies, with the remaining intact in a 69BTH Basket. The maximum lattice average initial enrichment for all 24 fuel assemblies (damaged or intact transported in these 24 locations) is limited to the "9 to 24 Damaged Assemblies" column of Table A.1.4.9-3.

Figure A.1.4.9-1
Location of Damaged Fuel Assemblies Inside 69BTH DSC

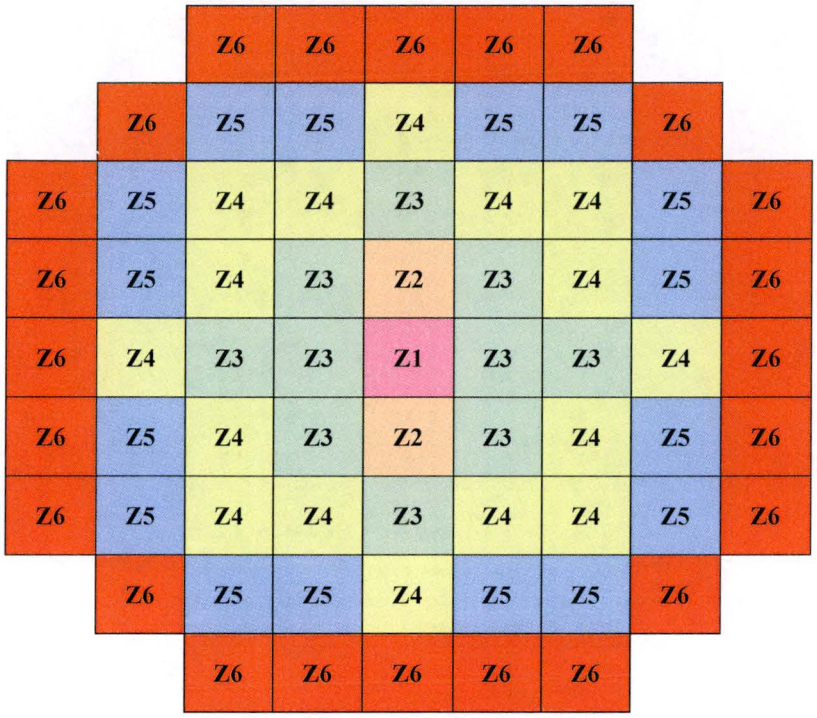

	Zone 1	Zone 2	Zone 3	Zone 4	Zone 5	Zone 6
Max. Decay Heat (kW/FA) (3)(4)	0.10	0.27	0.30	0.40	0.55	0.45
No. of Fuel Assemblies (1)	1	2	10	16	16	24
Max. Decay Heat per Zone (kW) (3)	0.10	0.54	3.0	6.4	8.8	10.8
Max. Decay Heat per DSC (kW)	26.0 (2) (3)					

Notes:
(1) Total number of fuel assemblies is 69 for HLZC # 1.
(2) Adjust payload to maintain the total DSC heat load within the specified limit.
(3) Reduce the maximum decay heat to 70% of the listed values for *LACROSSE10* fuel assembly. The total decay heat for *LACROSSE10* fuel assembly is 18.2 kW per DSC for HLZC No. 1.
(4) Decay heat per fuel assembly shall be determined per Table A.1.4.9-*6*.

Figure A.1.4.9-2
Heat Load Zoning Configuration No. 1 for 69BTH Basket

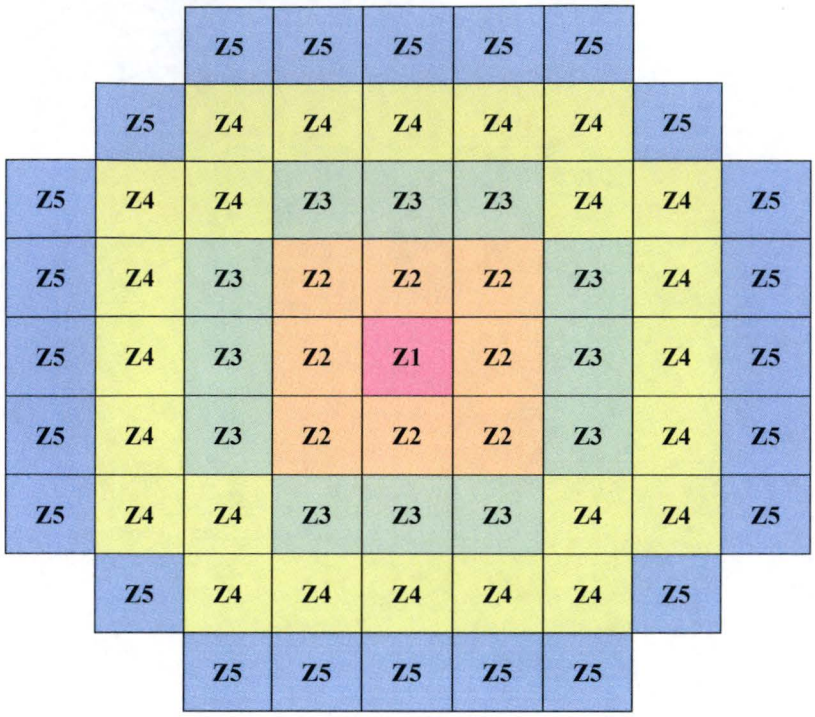

	Zone 1	Zone 2	Zone 3	Zone 4	Zone 5
Max. Decay Heat (kW/FA) (4)(5)	0.25	0.0 (1)	0.40	0.60	0.50
No. of Fuel Assemblies (2)	1	0	12	24	24
Max. Decay Heat per Zone (kW) (4)	0.25	0	4.8	14.4	12.0
Max. Decay Heat per DSC (kW)	26.0 (3) (4)				

Notes:
(1) Aluminum dummy assemblies replace the fuel assemblies in zone 2.
(2) Total number of fuel assemblies is 61 for HLZC # 2.
(3) Adjust payload to maintain the total DSC heat load within the specified limit.
(4) Reduce the maximum decay heat to 70% of the listed values for *LACROSSE10* Fuel assembly. The total decay heat for *LACROSSE10* fuel assembly is 18.2 kW per DSC for HLZC No. 2.
(5) Decay heat per fuel assembly shall be determined per Table A.1.4.9-*6*.

Figure A.1.4.9-3
Heat Load Zoning Configuration No. 2 for 69BTH Basket

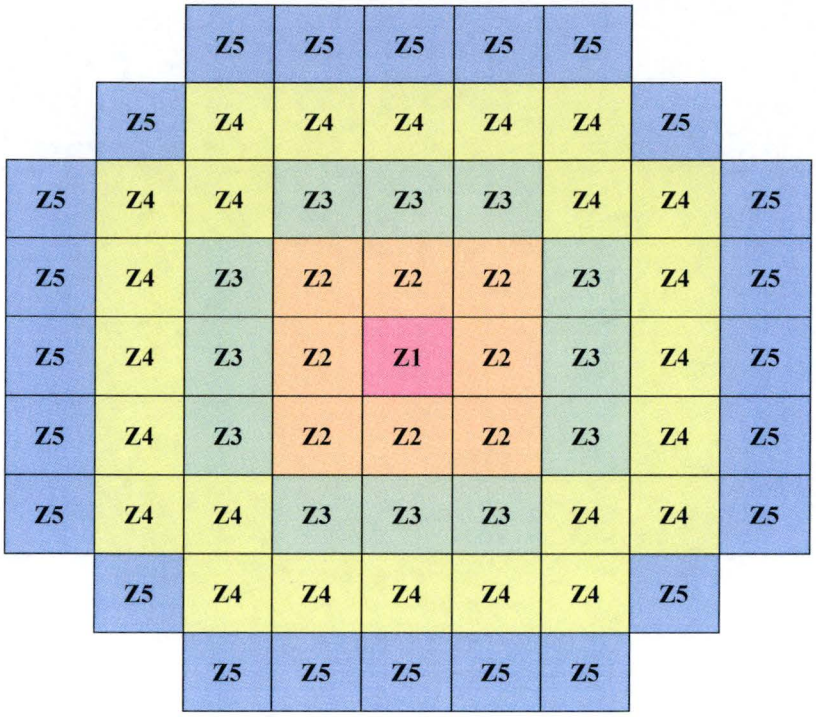

	Zone 1	Zone 2	Zone 3	Zone 4	Zone 5
Max. Decay Heat (kW/FA) (4)(5)	0.25	0.0 (1)	0.40	0.60	0.50
No. of Fuel Assemblies (2)	1	0	12	24	24
Max. Decay Heat per Zone (kW) (4)	0.25	0	4.8	14.4	12.0
Max. Decay Heat per DSC (kW)	29.2 (3) (4)				

Notes:
(1) Aluminum dummy assemblies replace the fuel assemblies in zone 2.
(2) Total number of fuel assemblies is 61 for HLZC # 3.
(3) Adjust payload to maintain the total DSC heat load within the specified limit.
(4) Reduce the maximum decay heat to 70% of the listed values for *LACROSSE10* Fuel assembly. The total decay heat for *LACROSSE10* fuel assembly is 20.4 kW per DSC for HLZC No. 3.
(5) Decay heat per fuel assembly shall be determined per Table A.1.4.9-*6*.

Figure A.1.4.9-4
Heat Load Zoning Configuration No. 3 for 69BTH Basket

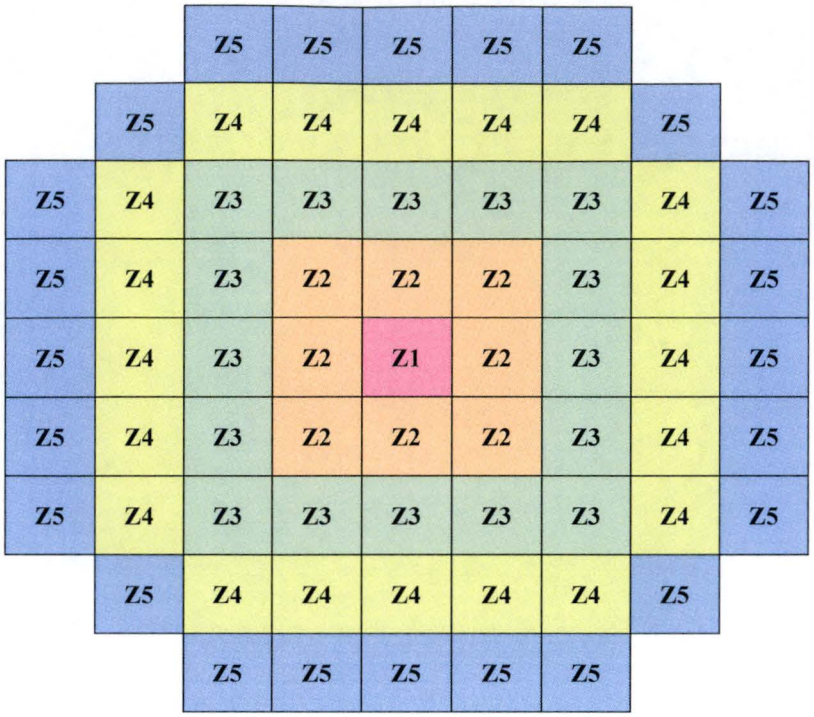

	Zone 1	Zone 2	Zone 3	Zone 4	Zone 5
Max. Decay Heat (kW/FA) (4)(5)	0.0 (1)	0.45	0.0 (2)	0.70	0.60
No. of Fuel Assemblies (3)	0	8	0	20	24
Max. Decay Heat per Zone (kW) (4)	0	3.6	0	14.0	14.4
Max. Decay Heat per DSC (kW)	32.0 (4)				

Notes:
(1) The fuel compartment in zone 1 remains empty.
(2) Aluminum dummy assemblies replace the fuel assemblies in zone 3.
(3) Total number of fuel assemblies is 52 for HLZC # 4.
(4) Reduce the maximum decay heat to 70% of the listed values for *LACROSSE10* Fuel assembly. The total decay heat for *LACROSSE10* fuel assembly is 22.4 kW per DSC for HLZC No. 4.
(5) Decay heat per fuel assembly shall be determined per Table A.1.4.9-*6*.
(6) Borated Aluminum is the only poison material allowed for HLZC #4.

Figure A.1.4.9-5
Heat Load Zoning Configuration No. 4 for 69BTH Basket

		Z5	Z5	Z5	Z5	Z5		
	Z5	- (1)	Z3	Z2	Z3	-	Z5	
Z5	-	Z4	Z3	-	Z3	Z4	-	Z5
Z5	Z3	Z3	-	Z1	-	Z3	Z3	Z5
Z5	Z2	-	Z1	-	Z1	-	Z2	Z5
Z5	Z3	Z3	-	Z1	-	Z3	Z3	Z5
Z5	-	Z4	Z3	-	Z3	Z4	-	Z5
	Z5	-	Z3	Z2	Z3	-	Z5	
		Z5	Z5	Z5	Z5	Z5		

	Z1 (Zone 1)	Z2 (Zone 2)	Z3 (Zone 3)	Z4 (Zone 4)	Z5 (Zone 5)
Max. Decay Heat (kW/FA) (4)(5)	0.13	0.31	0.76	0.95	0.52
No. of Fuel Assemblies(2)	4	4	16	4	24
Max. Decay Heat per DSC (kW)	30.20 (3)(4)				

Notes:
(1) *Aluminum dummy assembly (solid aluminum block) is required in the fuel compartments designated with a dash (-).*
(2) *Total number of fuel assemblies is 52 for HLZC No. 8.*
(3) *Adjust payload to maintain total DSC heat load within the specified limit.*
(4) *Reduce the maximum decay heat to 70% of the listed values for LACROSSE10 Fuel assembly. The total decay heat for LACROSSE10 fuel assembly is 21.1 kW per DSC for HLZC No. 8.*
(5) *Type "F" borated aluminum is the only poison material authorized to use with HLZC No. 8.*
(6) *This figure is also shown in Section A.3.3.1.4, titled "Heat Load Zoning Configuration No. 8 for 69BTH Basket."*
(7) *The decay heat per fuel assembly may be determined using an approved methodology (e.g., ORIGEN-ARP) with actual spent fuel parameters. Alternately, for cooling times > 5 years, the decay heat equation (Table A.1.4.9-6) may be used.*

Figure A.1.4.9-5a
Heat Load Zoning Configuration No. 8 for 69BTH DSC Basket

		P	*P*	*P*	*P*	*P*		
	P	*I*	*I*	*I*	*I*	*I*	*P*	
P	*I*	*I*	*I*	*I*	*I*	*I*	*I*	*P*
P	*I*	*I*	*I*	*I*	*I*	*I*	*I*	*P*
P	*I*	*I*	*I*	*I*	*I*	*I*	*I*	*P*
P	*I*	*I*	*I*	*I*	*I*	*I*	*I*	*P*
P	*I*	*I*	*I*	*I*	*I*	*I*	*I*	*P*
	P	*I*	*I*	*I*	*I*	*I*	*P*	
		P	*P*	*P*	*P*	*P*		

Figure A.1.4.9-6
Peripheral and Inner Fuel Locations for the 69BTH DSC

Pages A.2.13.11-i, A.2.13.11-ii, and A.2.13.11-1 through A.2.13.11-44 are proprietary information withheld pursuant to 10 CFR 2.390.

Chapter A.3
Thermal Evaluation

TABLE OF CONTENTS

A.3.1 Description of Thermal Design Criteria A.3-1a
A.3.1.1 Design Features A.3-3
A.3.1.2 Content's Decay Heat A.3-6
A.3.1.3 Summary Tables of Temperatures A.3-7
A.3.1.4 Summary Tables of Maximum Pressures A.3-8
A.3.2 Material Properties and Component Specifications A.3-8
A.3.2.1 Material Properties A.3-8
A.3.2.2 Component Specifications A.3-27
A.3.3 Thermal Evaluation under Normal Conditions of Transport A.3-29
A.3.3.1 Thermal Models A.3-29
A.3.3.2 Heat and Cold A.3-72
A.3.3.3 Maximum Normal Operating Pressure A.3-74
A.3.3.4 Thermal Evaluation for Loading/Unloading Operations A.3-84
A.3.4 Thermal Evaluation under Hypothetical Accident Conditions A.3-86
A.3.4.1 Initial Conditions A.3-86
A.3.4.2 Fire Test Conditions A.3-87
A.3.4.3 Maximum Temperatures and Pressure A.3-95
A.3.4.4 Maximum Thermal Stresses A.3-97
A.3.4.5 Accident Conditions for Fissile Material Packages for Air Transport A.3-97
A.3.5 References A.3-98
A.3.6 Appendices A.3-101
A.3.6.1 Thermal Evaluation of MP197HB TC and 69BTH DSC for HLZC # 8 for NCT and HAC A.3-102
A.3.6.2 Mesh Sensitivity A.3-103
A.3.6.3 Justification for Bounding Temperature Profiles A.3-104
A.3.6.4 Acceptance Criteria for Coating Damages for MP197HB TC A.3-106
A.3.6.5 Effective Thermal Properties of the Fuel Assemblies A.3-113
A.3.6.6 Thermal Analysis of 24PTHF and 61BTHF DSCs in the MP197HB TC A.3-120
A.3.6.7 Justification of Hot Gaps A.3-127
A.3.6.8 Sensitivity Study for Effects of Fire Emissivity A.3-140
A.3.6.9 Sensitivity Study for Effects of High Burnup Damaged Fuel Assemblies A.3-144
A.3.6.10 Sensitivity Analysis for HAC using Coupled Model A.3-145
A.3.6.11 Thermal Evaluation of MP197HB Transport Cask with High Burnup Fuel Assemblies A.3-147

LIST OF TABLES

Table A.3-1 DSC Shell Nominal Dimensions *A.3-152*
Table A.3-2 Peaking Factors for Fuel Assemblies in the 69BTH DSC Model *A.3-153*
Table A.3-3 Effective Density for the 69BTH Basket *A.3-154*
Table A.3-4 Effective Specific Heat for the 69BTH Basket *A.3-155*
Table A.3-5 Effective Axial Conductivity for the 69BTH Basket *A.3-156*
Table A.3-6 Effective Radial Conductivity for the 69BTH Basket *A.3-157*
Table A.3-7 Peaking Factors for Fuel Assemblies in the 37PTH DSC Model *A.3-158*
Table A.3-8 Maximum TC Component and DSC Shell Temperatures for NCT (100°F and Insolation), BWR DSCs *A.3-159*
Table A.3-9 Maximum TC Component and DSC Shell Temperatures for NCT (100°F and Insolation), PWR DSCs *A.3-160*
Table A.3-10 Maximum Fuel Cladding and Basket Component Temperatures for NCT *A.3-161*
Table A.3-11 Maximum/Minimum Component Temperatures for NCT *A.3-162*
Table A.3-12 Maximum TC Component and 69BTH DSC Temperatures for Cold NCT (32 kW, No insolation) *A.3-164*
Table A.3-13 Maximum TC Component and 37PTH DSC Temperatures for Cold NCT (22 kW, No insolation) *A.3-165*
Table A.3-14 Average Component Temperatures for NCT and HAC *A.3-166*
Table A.3-15 List of the Gaps and Thermal Properties for HAC Analysis *A.3-167*
Table A.3-16 Maximum Temperatures of TC Components / DSC Shell for HAC *A.3-168*
Table A.3-17 Maximum DSC Shell Temperatures for Steady-State Cool-Down *A.3-169*
Table A.3-18 Maximum Fuel Cladding and Basket Component Temperatures for HAC *A.3-170*
Table A.3-19 Summary of the Maximum Temperatures for HAC *A.3-171*
Table A.3-20 MP197HB TC Cavity Pressure for NCT *A.3-173*
Table A.3-21 Volume and Average Helium Temperatures in 69BTH and 37PTH DSCs for NCT and HAC *A.3-174*
Table A.3-22 Maximum Internal Pressures of 69BTH and 37PTH DSCs in MP197HB TC *A.3-175*
Table A.3-23 Maximum Internal Pressure in DSCs for Transport in MP197HB TC *A.3-176*
Table A.3-24 Comparison of Maximum DSC Shell Temperatures *A.3-177*
Table A.3-25 MP197HB Transport Cask Thermal Evaluation for Reconfigured Fuel Assemblies *A.3-178*
Table A.3-26 Maximum Temperatures of 69BTH DSC/ MP197HB Transport Cask Components (Reconfigured Fuel at Top, 32 kW with Fins, Load Case # F1O & F1A) *A.3-179*
Table A.3-27 Maximum Temperatures of 69BTH DSC/ MP197HB Transport Cask Components (Reconfigured Fuel at Bottom, 32 kW with Fins, Load Case # F2O & F2A) *A.3-180*
Table A.3-28 Maximum Temperatures of 69BTH DSC/ MP197HB Transport Cask Components (Reconfigured Fuel at Top, 26 kW, Load Case # U1O & U1A) *A.3-181*

Table A.3-29 Maximum Temperatures of 69BTH DSC/ MP197HB Transport Cask Components (Reconfigured Fuel at Bottom, 26 kW, Load Case # U2O & U2A).....*A.3-182*
Table A.3-30 Comparison of Maximum Seal Temperatures.....*A.3-182a*
Table A.3-31 Grid Sizes and Refinement Factors.....*A.3-182b*
Table A.3-32 Temperature of Neutron Shield Resin.....*A.3-182b*
Table A.3-33 Discretization Error of the Neutron Shield Resin within MP197HB TC.....*A.3-182c*

LIST OF FIGURES

Figure A.3-1 Location of DSC within the MP197HB TC *A.3-183*
Figure A.3-2 Finite Element Model of the MP197HB with the 69BTH DSC *A.3-184*
Figure A.3-3 Components of the MP197HB TC Model *A.3-185*
Figure A.3-4 Gaps in the MP197HB TC Model *A.3-186*
Figure A.3-5 Gaps in the MP197HB TC Cross Section *A.3-187*
Figure A.3-6 Typical Decay Heat and Insolance Boundary Conditions *A.3-188*
Figure A.3-7 Typical Convection and Radiation Boundary Conditions *A.3-189*
Figure A.3-8 Typical Convection and Radiation Boundary Conditions – Details *A.3-190*
Figure A.3-9 Schematic View of Cask and Personnel Barrier *A.3-191*
Figure A.3-10 Sub-Model of the External Fins for MP197HB TC *A.3-192*
Figure A.3-11 Sub-Model for Helium Gap Effective Conductivity Calculation *A.3-193*
Figure A.3-12 Assumed Geometry of Internal Sleeve in Thermal Model *A.3-194*
Figure A.3-13 Finite Element Model of 69BTH DSC/Basket *A.3-195*
Figure A.3-14 69BTH DSC/Basket – Cross Section *A.3-196*
Figure A.3-15 69BTH DSC/Basket – Gaps between Rail Sections at Cross Section *A.3-197*
Figure A.3-16 69BTH DSC/Basket – Gaps between Basket Plates at Cross Section *A.3-198*
Figure A.3-17 69BTH DSC/Basket – Axial Gaps *A.3-199*
Figure A.3-18 Typical Boundary Conditions for the 69BTH Basket *A.3-200*
Figure A.3-19 Thermal Resistances for Aluminum Dummy Assembly *A.3-201*
Figure A.3-20 Basket Slice Models *A.3-202*
Figure A.3-21 Typical Boundary Conditions for the Basket Slice Model *A.3-203*
Figure A.3-22 Schematic View of Top Grid Assembly (Hold-Down Ring) *A.3-204*
Figure A.3-23 Finite Element Model of the 37PTH DSC/Basket *A.3-205*
Figure A.3-24 37PTH DSC/Basket – Cross Section and Details *A.3-206*
Figure A.3-25 37PTH DSC/Basket – Gaps between Rail Sections *A.3-207*
Figure A.3-26 37PTH DSC/Basket – Gaps between Basket Plates at Cross Section *A.3-208*
Figure A.3-27 37PTH DSC/Basket – Axial Gaps *A.3-209*
Figure A.3-28 Typical Boundary Conditions for the 37PTH Basket *A.3-210*
Figure A.3-29 Temperature Profiles for MP197HB Transport Cask NCT, 100 °F, Insolation, 69BTH DSC, 32 kW *A.3-211*
Figure A.3-30 Temperature Profiles for MP197HB Transport Cask NCT, 100 °F, Insolation, 24PTH DSC, 26 kW *A.3-212*
Figure A.3-31 Typical Temperature Distributions for 69BTH Basket (NCT @ 100 °F, HLZC#1, 26kW) *A.3-213*
Figure A.3-32 Typical Temperature Distributions for 69BTH Basket (NCT @ 100 °F, HLZC#4, 32kW) *A.3-214*
Figure A.3-33 Temperature Distributions for Fuel Assemblies in 69BTH Basket (NCT @ 100 °F) *A.3-215*
Figure A.3-34 Typical Temperature Distributions for 37PTH Basket (NCT @ 100 °F, 22 kW) *A.3-216*

Figure A.3-35 Impact Limiter Crush Areas for MP197HB (Side, End, and Corner Drop) *A.3-217*
Figure A.3-36 Impact Limiter Crush Areas for MP197HB (Slap Down) *A.3-218*
Figure A.3-37 Finite Element Model of TC with Deformed Impact Limiters *A.3-219*
Figure A.3-38 Typical Boundary Conditions during Fire Conditions *A.3-220*
Figure A.3-39 Typical Boundary Conditions for Smoldering/Cool-Down Periods *A.3-221*
Figure A.3-40 Time-Temperature Histories for TC/DSC Shell HAC, with External Fins (Melted after Fire), 69BTH DSC, 32 kW *A.3-222*
Figure A.3-41 Time-Temperature Histories for TC/DSC Shell HAC, w/o Fins, 69BTH DSC, 26 kW *A.3-223*
Figure A.3-42 Time-Temperature Histories for TC/DSC Shell HAC, w/o Fins, 24PTH DSC, 26 kW *A.3-224*
Figure A.3-43 Temperature Profiles for MP197HB Transport Cask HAC, 69BTH DSC, 32 kW, with External Fins (Melted after Fire) *A.3-225*
Figure A.3-44 Temperature Profiles for MP197HB Transport Cask HAC, 24PTH DSC, 26 kW, without External Fins *A.3-226*
Figure A.3-45 Typical Temperature Distributions for 69BTH DSC (HAC Post Fire Cool-Down, HLZC#1, 26kW) *A.3-227*
Figure A.3-46 Typical Temperature Distributions for 69BTH DSC (HAC Post Fire Cool-Down, HLZC#4, 32kW) *A.3-228*
Figure A.3-47 Temperature Distributions for Fuel Assemblies in 69BTH DSC (HAC Post Fire Cool-Down) *A.3-229*
Figure A.3-48 Typical Temperature Distributions for 37PTH DSC (HAC Post Fire Cool-Down, 22 kW, Boral Plates) *A.3-230*
Figure A.3-49 Location of Damaged/Failed Fuel inside 24PTHF DSC *A.3-231*
Figure A.3-50 Location of Damaged/Failed Fuel inside 61BTHF DSC *A.3-232*
Figure A.3-51 Comparison of DSC Shell Temperature Profiles for 61BTH DSC *A.3-233*
Figure A.3-52 Comparison of DSC Shell Temperature Profiles for 24PTH DSC *A.3-234*
Figure A.3-53 Coupled Model of MP197HB TC and 69BTH DSC *A.3-235*
Figure A.3-54 Temperature Time Histories for Coupled Model, 69BTH DSC Components *A.3-236*
Figure A.3-55 Temperature Time Histories for Coupled Model, MP197HB TC Components *A.3-237*
Figure A.3-56 Temperature Time History for MP197HB Transport Cask HAC, 69BTH DSC, 32 kW, with External Fins (Load Case F1A) *A.3-238*
Figure A.3-57 Temperature Time History for MP197HB Transport Cask HAC, 69BTH DSC, 32 kW, with External Fins (Load Case F2A) *A.3-239*
Figure A.3-58 Temperature Time History for MP197HB Transport Cask HAC, 69BTH DSC, 26 kW, without External Fins (Load Case U1A) *A.3-240*
Figure A.3-59 Temperature Time History for MP197HB Transport Cask HAC, 69BTH DSC, 26 kW, without External Fins (Load Case U2A) *A.3-241*
Figure A.3-60 Temperature vs. Number of Elements *A.3-242*

Chapter A.3
Thermal Evaluation

NOTE: References in this Chapter are shown as [1], [2], etc. and refer to the reference list in Section A.3.5.

This chapter presents the thermal evaluations which demonstrate that the MP197HB transport cask (TC) meets thermal requirements of 10 CFR 71 [6] for transportation of BWR and PWR spent fuel assemblies (FA) within the following DSCs: 69BTH, 61BTH Type 1 and Type 2, 61BT, 37PTH, 32PTH, 32PTH Type 1, 32PTH1 Type 1 and Type 2, 32PT, 24PTH-S, 24PTH-L, 24PTH-S-LC, 24PT4, 61BTHF, and 24PTHF.

The maximum heat load per DSC allowed for transportation in MP197HB TC varies for different DSC types from 18.3 kW to 32 kW. The table below summarizes the maximum heat load per DSC for transportation in comparison with maximums allowed for storage.

Maximum Heat Load per DSC

DSC type	Max. Heat Load for Transport (kW)	Max. Heat Load for Storage (kW)
69BTH	26.0	*26.0 [3]*
	29.2	*29.2 [3]*
	30.2	*N/A*
	32.0	*32.0 [3]*
61BTH Type 1[(1)]	22.0	22.0 [3]
61BTH Type 2[(1)]	24.0	31.2 [3]
61BT	18.3	18.3 [1]
37PTH	22.0	N/A
32PTH/32PTH Type 1	26.0	34.8 [4]
32PTH1 Type 1	26.0	40.8 [3]
32PTH1 Type 2	24.0	31.2 [3]
32PT	24.0	24.0 [1]
24PTH-S or –L (w/ Al inserts)[(1)]	26.0	40.8 [1]
24PTH-S or –L (w/o Al inserts)[(1)]	26.0	31.2 [1]
24PTH-S-LC	24.0	24.0 [1]
24PT4	24.0	24.0 [2]

Note:
[(1)] See Section A.3.1.2 for heat loads of 61BTHF and 24PTHF DSCs.

For all DSC types, this evaluation demonstrates that DSC component temperatures are within material temperature limits and fuel cladding temperatures meet the thermal requirements of ISG-11 [7].

[

Proprietary Information Withheld Pursuant to 10 CFR 2.390

]

Proprietary Information Withheld Pursuant to 10 CFR 2.390

A.3.1 Description of Thermal Design Criteria

The MP197HB TC is designed to passively reject decay heat under Normal Conditions of Transport (NCT) and Hypothetical Accident Conditions (HAC) while maintaining packaging temperatures and pressures within specified limits. Objectives of the thermal analyses performed for this evaluation include:

a) Determination of maximum component temperatures with respect to cask materials limits to ensure components perform their intended safety functions,

b) Determination of temperature distributions to support the calculation of thermal stresses,

c) Determination of the TC cavity gas temperature to support containment pressure calculations, and

d) Determination of the maximum fuel cladding temperature.

Chapter A.1 presents the principal design bases for the MP197HB TC.

Several thermal design criteria are established for the MP197HB TC to ensure that the package meets all its functional and safety requirements. These are:

- Maximum fuel cladding temperature limits of 752°F (400°C) for NCT and 1,058°F (570°C) for HAC are considered for the fuel assemblies with an inert cover gas as concluded in ISG-11 [7].

- Containment of radioactive material and gases is a major design requirement. Seal temperatures must be maintained within specified limits to satisfy the leak tight containment requirement. A maximum temperature limit of 400°F (204°C) is considered for the Fluorocarbon seals (Viton O-rings) in the containment vessel ([18] and [19]) for NCT and HAC. *The maximum operating temperatures for the metallic seals in the ram plate and test/drain port seals are 644 °F (340 °C) [52] and 1100 °F (593 °C) [53], respectively. A maximum seal temperature of 644 °F (340 °C) is considered for all metallic seals for thermal evaluation for NCT and HAC.*

- To maintain the stability of the neutron shield resin, a maximum allowable temperature of 320°F (160°C) is considered for the neutron shield [17] for NCT.

- Based on [25], the onset of polypropylene thermal degradation associated with weight loss starts at 230°C to 250°C (446°F to 482°F). Although the breakdown of the polymer leading to volatile products begins above 300°C (572°F), no significant weight loss occurs below 350°C (662°F). A temperature limit of 445°F (229°C) is considered conservatively for polypropylene to prevent thermal degradation of resin in trunnion plugs.

- To prevent melting of the gamma shield (lead) under NCT, an allowable maximum temperature of 621°F (327.5°C – melting point of lead) is considered for the gamma shield [5].

- A temperature limit of 320°F (160°C) is considered for wood to prevent excessive reduction in structural properties at elevated temperatures [20].

- In accordance with 10 CFR 71.43(g) [6] the maximum temperature of the accessible packaging surfaces in the shade is limited to 185°F (85°C).

The NCT ambient temperature range is –20°F to 100°F (-29°C to 38°C) per 10 CFR 71.71(b) [6]. In general, all the thermal criteria are associated with maximum temperature limits and not minimum temperatures. All materials can be subjected to the minimum environment temperature of -40°F (-40°C) without adverse effects as required by 10 CFR 71.71 (c)(2) [6].

Thermal performance of MP197HB TC is evaluated based on finite element analyses using ANSYS computer code [27].

The following thermal design criteria are established for 69BTH and 37PTH DSCs to satisfy the functional and safety requirements.

- Maximum fuel cladding temperature limits of 752°F (400°C) for NCT and 1,058°F (570°C) for HAC are considered for the fuel assemblies with an inert cover gas as concluded in ISG-11 [7].
- Based on ISG-11 [7], the fuel cladding temperature is limited to 400°C (752°F) for short term operation such as vacuum drying.
- The maximum DSC cavity internal design pressures are summarized below:

Operating condition	69BTH DSC	37PTH DSC
Normal Conditions of Transport (NCT) (3% rods ruptured)	15 psig	15 psig
Hypothetical Accident Conditions (HAC) (100% rods ruptured)	*120* psig	140 psig

The thermal performance of 69BTH and 37PTH DSCs is evaluated based on finite element analyses using ANSYS computer code [27].

A.3.1.1 Design Features

A.3.1.1.1 MP197HB TC

The MP197HB transport cask includes optional features such as an aluminum internal sleeve to accommodate DSC types with outer diameters smaller than 69.75" and an aluminum shell with external circular fins. The external circular fins are used for heat loads greater than 26 kW. The TC design features for different DSC types considered for transportation in MP197HB TC are listed in the table below.

MP197HB TC Design Features

DSC Type	DSC OD (in.)	TC Sleeve	TC External Fins	Max. DSC Heat Load for Transport (kW)
69BTH	69.75	No	No	26.0
			Yes	29.2
			Yes	*30.2*
			Yes	32.0
61BTH Type 1 (1)	67.25	Yes	No	22.0
61BTH Type 2 (1)	67.25	Yes	No	24.0
61BT	67.25	Yes	No	18.3
37PTH	69.75	No	No	22.0
32PTH/32PTH Type 1	69.75	No	No	26.0
32PTH1 Type 1	69.75	No	No	26.0
32PTH1 Type 2	69.75	No	No	24.0
32PT	67.19	Yes	No	24.0
24PTH-S or -L (w/ Al inserts)(1)	67.19	Yes	No	26.0
24PTH-S or –L (w/o Al inserts)(1)	67.19	Yes	No	26.0
24PTH-S-LC (1)	67.19	Yes	No	24.0 (2)
24PT4	67.19	Yes	No	24.0

Notes:
(1) 61BTHF and 24PTHF DSCs have the same dimensions and use the same MP197HB features as DSC types 61BTH and 24PTH, respectively.
(2) The 24PTH-S-LC DSC is allowed for 24 kW heat load. The analyis assumes a heat load of 26 kW for conservatism.

The MP197HB TC consists of multiple shells which conduct the decay heat to the cask outer surface. The other thermal design feature of the cask is the conduction path created by the aluminum boxes that contain the neutron shielding material as described in Chapter A.5. The neutron shielding material is provided by a resin compound cast into long slender aluminum boxes placed around the gamma shield shell and enclosed within a steel shell (shield shell). The aluminum boxes are designed to fit tightly against the steel shell surfaces, thus improving the heat transfer across the neutron shield.

Heat dissipates from the packaging outer surfaces via natural convection and radiation. The outer surface of the shield shell is painted white to enhance the thermal radiation exchange with ambient.

The design of the steel-encased wood impact limiters is described in Chapter A.1, Section A.1.2. These components are included in the thermal analysis because of their contribution as a thermal insulator. The impact limiters provide protection to the lid and bottom regions from the external heat input due to fire during the HAC thermal event.

A personnel barrier prevents access to the outer surfaces of the cask body. The barrier, which consists of a stainless steel mesh attached to stainless steel tubing, encloses the cask body between the impact limiters, and have an open area fraction of approximately 80%.
The gaps considered in the thermal model of MP197HB TC are described in Section A.3.3.1.1.

A.3.1.1.2 69BTH DSC

The 69BTH DSC design is similar to the 61BTH DSC design documented in Appendix T, associated with Amendment 10 to Part 72 CoC 1004 for the Standardized NUHOMS® System [3], with the maximum decay heat load per canister of 32.0 kW for off-site transportation. The 69BTH DSC consists of a shell assembly, which provides confinement and shielding, and an internal basket assembly which locates and supports the fuel assemblies.

The basket structure consists of 9 and 6 compartment fuel cell subassemblies held in place by basket rails in combination with a holddown ring. The compartment subassemblies are held together by welded stainless plates wrapped around the fuel compartments, which also retain the aluminum and/or neutron absorbing plates sandwiched between the fuel compartments. The aluminum and neutron absorbing plates provide the necessary criticality control and heat conduction paths from the fuel cells to the perimeter of subassemblies. The aluminum plates retained between the subassemblies provide the heat conduction paths from the subassemblies to the perimeter of the basket. The space between the fuel compartments assembly and the DSC shell is bridged by solid aluminum transition rails.

No convection heat transfer is considered within the basket for conservatism. Radiation heat transfer is considered implicitly between the fuel rods and the fuel compartment in calculation of transverse effective fuel conductivity. No other radiation heat transfer is considered within the 69BTH DSC models.

The decay heat from the canister is carried to the inner shell of the MP197HB cask via conduction, convection, and radiation. Convection heat transfer in the annulus between the DSC outer shell and the cask inner shell is not considered in the thermal evaluation for conservatism.

A.3.1.1.3 37PTH DSC

The 37PTH DSC design is similar to the 32PT DSC design documented in [1], Appendix M with a maximum decay heat load per canister of 22.0 kW for off-site transportation. The 37PTH DSC consists of a shell assembly, which provides confinement and shielding, and an internal basket assembly which locates and supports the fuel assemblies.

The basket is an assembly of welded stainless steel plates that make up a grid for 37 fuel compartments. Each fuel compartment accommodates aluminum and/or neutron absorbing plates that provide the necessary criticality control and heat conduction paths from the fuel assemblies to the basket grid. The space between the fuel compartments grid assembly and the perimeter of the DSC shell is bridged by solid aluminum transition rails.

There are two 37PTH canister types: A short canister type designated as the 37PTH-S and a medium canister type designated as the 37PTH-M. Use of spacers may be required to accommodate short fuel assemblies.

No convection heat transfer is considered within the basket for conservatism. Radiation heat transfer is considered implicitly between the fuel rods and the fuel compartment in calculation of transverse effective fuel conductivity. No other radiation heat transfer is considered within the 37PTH DSC models.

The decay heat from the canister is carried to the inner shell of the MP197HB cask via conduction, convection, and radiation. Convection heat transfer in the annulus between the DSC outer shell and the cask inner shell is not considered in the thermal evaluation for conservatism.

A.3.1.1.4 Other DSC Types

The design features of DSC types 61BT, 32PT, and 24PTH are described in [1], Appendices K, M, and P, respectively. The design features of 24PT4 DSC are described in [2], Appendix A. The design features of DSC types 61BTH and 32PTH1 are described in Appendices T and U, respectively, associated with Amendment 10 to Part 72 CoC 1004 for the Standardized NUHOMS® System [3]. The design features of 32PTH and 32PTH Type 1 DSCs are described in [4].

A.3.1.2 Content's Decay Heat

The thermal analysis for MP197HB TC loaded with existing DSCs currently qualified for storage along with 69BTH and 37PTH DSCs is based on a range of maximum total heat load of 18.3 kW to 32 kW per DSC.

The maximum decay heat loads of 26.0, 29.2, and 32.0 kW are considered for transport of 69BTH DSC in combination with various design features of MP197HB TC listed in Section A.3.1.1.1.

The maximum decay heat loads for transport of DSC types 61BTH Type 1, 61BT, 32PT, and 24PT4 are equal to the maximum heat loads for storage conditions i.e., 22.0 kW, 18.3 kW, 24.0 kW, and 24.0 kW, respectively as shown in Section A.3.1.1.1 based on [3], [1], and [2].

The maximum decay heat load for transport of DSC types 32PTH, 32PTH Type 1, 32PTH1 Type 1, 24PTH-S, and 24PTH-L are considered equal to 26.0 kW.

The maximum decay heat load for 24PTH-S-LC is 24 kW [1]. Therefore, the results of 24PTH-S or -L (without aluminum inserts) DSC shell temperatures with 26 kW heat load is bounding for use with the 24PTH-S-LC DSC with 24 kW heat load.

The maximum decay heat load for transport of DSC types 61BTH Type 2 and 32PTH1 Type 2 are considered equal to 24.0 kW in order to maintain the maximum DSC shell temperature below the values reported for normal transfer conditions in Appendix T.4 and Appendix U.4 of the SAR associated with Amendment 10 to Part 72 CoC 1004 for the Standardized NUHOMS® System [3].

The maximum decay heat load for 37PTH DSC is equal to 22.0 kW for transport operations.

61BTHF and 24PTHF DSCs contain failed fuel and have lower heat loads than 61BTH and 24PTH DSCs, respectively. Nevertheless, it is considered in the thermal analysis that the heat loads for 61BTHF and 24PTHF DSCs are the same as those for 61BTH and 24PTH DSCs, respectively.

The MP197HB TC is designed to transport a payload of up to 56.0 tons of dry irradiated and/or contaminated non-fuel bearing solid materials in secondary containers. The decay heat load of the radioactive material is limited to 5 kW, which is well below the heat loads specified for the cask loaded with DSCs.

The permitted heat load zoning configurations (HLZC) for all DSCs are listed in Chapter A.1, Appendix 1.4.1 through Appendix 1.4.9. These design basis HLZCs are symmetrical and show maximum allowable heat load per FA and per DSC, which result in bounding maximum fuel cladding and DSC component temperatures. Possible asymmetry in HLZC (within specified FA and DSC limits) means reduction of heat load in a particular FA resulting in reduction of local and maximum temperatures of fuel cladding and DSC components.

A peaking factor is considered along the active fuel length for calculation of the decay heat profile of the fuel assemblies as described in Section A.3.3.1.4 and Section A.3.3.1.6 for 69BTH and 37PTH DSCs, respectively.

Proprietary Information Withheld Pursuant to 10 CFR 2.390

A description of the detailed analyses of MP197HB TC, 69BTH and 37PTH DSCs for NCT an HAC is provided in Section A.3.3 and Section A.3.4, respectively. These analyses demonstrate that the maximum temperatures and pressures for other DSC types under transport conditions of 10 CFR 71 are bounded by the evaluations provided in [1], [2], [3], and [4] under storage/transfer conditions of 10 CFR 72.

Summaries of the maximum temperatures and pressures are provided in Section A.3.1.3 and Section A.3.1.4, respectively. The thermal evaluation concludes that for the maximum heat loads listed in Section A.3.1.1.1 all design criteria listed in Section A.3.1 are satisfied.

A.3.1.3 Summary Tables of Temperatures

The maximum and minimum MP197HB TC and DSC component temperatures for NCT are summarized in Table A.3–11. The component temperatures remain within the allowable range for NCT.

The maximum MP197HB TC and DSC component temperatures for cold conditions at -20°F and -40°F ambient without insolance are presented in Table A.3–12 and Table A.3–13. These temperatures are used for the structural evaluation of 69BTH and 37PTH DSCs.

The maximum accessible surface temperatures under shade are 121°F and *152*°F for impact limiter shell and personnel barrier as calculated in Section A.3.3.1.2.

The maximum transient temperatures of the MP197HB TC and DSC components and the time at which they occur are summarized in Table A.3–19 for HAC. The resins and wood are assumed to be decomposed or charred after fire accident. Therefore, the maximum temperatures for these components are irrelevant for HAC. The maximum fuel cladding, gamma shield and seal temperatures remain below the allowable limits and ensure the integrity of the fuel cladding and the containment boundary for HAC.

A.3.1.4 Summary Tables of Maximum Pressures

The maximum internal pressures inside MP197HB TC cavity are calculated in Section A.3.3.3 for NCT and Section A.3.4.3 for HAC. The maximum internal pressures of the MP197HB TC cavity are summarized in Table A.3–20. The maximum pressures inside canister cavities of 69BTH and 37PTH DSCs are listed in Table A.3–22. The maximum internal pressures for all DSCs proposed for transport in MP197HB TC are summarized in Table A.3–23. These pressures remain below the design pressures for NCT and HAC considered for the structural evaluation.

A.3.2 Material Properties and Component Specifications

A.3.2.1 Material Properties

The following tables provide the thermal properties of materials used in the analysis of the MP197HB TC with DSCs. Each table is valid for all the models unless it is specifically noted in the title of the table.

1. Bounding PWR Fuel Assembly for 37PTH DSC

Calculation of the effective properties for homogenized PWR fuel assemblies in a 37PTH DSC are discussed in Section A.3.6.5.1. The bounding effective properties for PWR fuel assemblies in 37PTH DSC are listed below.

Homogenized PWR Fuel Assemblies in Four Corner Fuel Compartments in 37PTH DSC

Temp (°F)	Transverse Conductivity (Btu/hr-in-°F)	Temp (°F)	Axial Conductivity (Btu/hr-in-°F)	Temp (°F)	Specific Heat (Btu/lbm-°F)	Density (lbm/in^3)
178	0.0168	200	0.0456	80	0.05924	0.1114
267	0.0195	300	0.0481	260	0.06538	
357	0.0230	400	0.0506	692	0.07255	
448	0.0273	500	0.0527	1502	0.07779	
541	0.0323	600	0.0548			
635	0.0380	800	0.0594			
730	0.0444					
826	0.0513					

Homogenized PWR Fuel Assemblies in Other Fuel Compartments in 37PTH DSC

Temp (°F)	Transverse Conductivity (Btu/hr-in-°F)	Temp (°F)	Axial Conductivity (Btu/hr-in-°F)	Bounding effective specific heat and density are the same as those for corner fuel assemblies.
138	0.0174	200	0.0454	
233	0.0199	300	0.0478	
328	0.0238	400	0.0503	
423	0.0285	500	0.0524	
519	0.0340	600	0.0545	
616	0.0403	800	0.0591	
714	0.0473			
812	0.0552			

Note:
(1) Only 95% of the axial effective conductivity calculated in [1, Appendix M, Section M.4.8] for 32PT DSC is considered in the 37PTH DSC model for conservatism.

2. Bounding BWR Fuel Assembly for 69BTH DSC

Calculation of the effective properties for homogenized BWR fuel assemblies in 69BTH DSC are discussed in Section A.3.6.5.2. The bounding effective properties for BWR fuel assemblies in 69BTH DSC are listed below.

Homogenized BWR Fuel Assemblies in 69BTH DSC

Temperature (°F)	k, Transverse (Btu/hr-in-°F)	k, Axial (Btu/hr-in-°F)	ρ (lb_m/in^3)	C_p (Btu/lb_m-°F)
200	0.0157	0.0402	0.103	0.0575
300	0.0181			
400	0.0211			
500	0.0246			
600	0.0285			
700	0.0328			
800	0.0375			

3. SA-240, Type 304 Stainless Steel [10]

Temperature (°F)	k (Btu/hr-in-°F)	ρ (lbm/in^3)	C_p (Btu/lb_m-°F)
70	0.717	0.284	0.116
100	0.725		0.117
200	0.775		0.122
300	0.817		0.125
400	0.867		0.129
500	0.908		0.131
600	0.942		0.133
700	0.983		0.135
800	1.025		0.136
900	1.058		0.137
1000	1.092		0.138

4. SA-240 Type 316 [2, Section 4.2.c]

Temperature (°F)	k (Btu/hr-in-°F)	ρ (lbm/in^3)	C_p (Btu/lb$_m$-°F)
70	0.642	0.285	0.117
100	0.658		0.118
200	0.700		0.121
300	0.750		0.126
400	0.792		0.126
500	0.833		0.130
600	0.875		0.132
700	0.917		0.134
800	0.958		0.135
900	1.000		0.137
1000	1.033		0.137

5. SA-182-F6NM [10]

Temperature (°F)	k (Btu/hr-in-°F)	ρ (lbm/in^3)	C_p (Btu/lb$_m$-°F)
70	1.183	0.284	0.105
100	1.183		0.107
200	1.192		0.112
300	1.200		0.117
400	1.208		0.122
500	1.208		0.128
600	1.217		0.135
700	1.217		0.142
800	1.225		0.150
900	1.225		0.157
1000	1.225		0.166

6. SA-516-70 or A36 [10]

Temperature (°F)	k (Btu/hr-in-°F)	ρ (lbm/in^3)	C_p (Btu/lb$_m$-°F)
70	2.275	0.284	0.105
100	2.300		0.108
200	2.317		0.116
300	2.275		0.122
400	2.208		0.127
500	2.142		0.131
600	2.075		0.136
700	2.008		0.142
800	1.933		0.148
900	1.858		0.156
1000	1.758		0.163

7. SA-203, Gr. E or SA-350-LF3 [10]

Temperature (°F)	k (Btu/hr-in-°F)	ρ (lbm/in^3)	C_p (Btu/lb$_m$-°F)
70	1.975	0.284	0.105
100	1.967		0.107
200	1.958		0.113
300	1.950		0.119
400	1.925		0.124
500	1.892		0.130
600	1.850		0.135
700	1.800		0.140
800	1.750		0.147
900	1.692		0.154
1000	1.642		0.163

8. Aluminum, Type 1100 [10]

Temperature (°F)	k (Btu/hr-in-°F)	ρ (lb$_m$/in^3)	C_p (Btu/lb$_m$-°F)
70	11.092	0.098	0.214
100	10.983[(1)]		0.216
150	10.833		0.219
200	10.708		0.222
250	10.608		0.224
300	10.517		0.227
350	10.442		0.229
400	10.375		0.232

Note: [(1)] The input files of the ANSYS models for the baskets contain a thermal conductivity of 11.150 Btu/hr-in-°F (133.8 Btu/hr-ft-°F) instead of 10.983 Btu/hr-in-°F. Since this value is used only at 100°F and since the basket temperature is over 150°F for all analyzed cases, this value does not affect the results in this SAR.

9. Aluminum, Type 6063 [10]

Temperature (°F)	k (Btu/hr-in-°F)	ρ (lb$_m$/in^3)	C_p (Btu/lb$_m$-°F)
70	10.067	0.098	0.213
100	10.025		0.215
150	9.975		0.218
200	9.917		0.221
250	9.875		0.223
300	9.842		0.226
350	9.833		0.228
400	9.800		0.230

10. Aluminum, Type 6061 [10]

Temperature (°F)	k (Btu/hr-in-°F)	ρ (lb_m/in^3)	C_p (Btu/lb_m-°F)
70	8.008	0.098	0.213
100	8.075		0.215
150	8.167		0.218
200	8.250		0.221
250	8.317		0.223
300	8.383		0.226
350	8.442		0.228
400	8.492		0.230

11. Gamma Shield, ASTM B29 Lead [24]

Temperature (°F)	k (Btu/hr-in-°F)	ρ (lb_m/in^3)	C_p (Btu/lb_m-°F)
-100	1.767	0.413	0.030
-10	1.733	0.411	0.030
80	1.700	0.409	0.031
260	1.637	0.406	0.032
440	1.579	0.402	0.033
620	1.512	0.398	0.034

12. Neutron Shield Resin (Vyal B) [17]

Temperature (°F)	k (Btu/hr-in-°F)	ρ (lb_m/in^3)	C_p (Btu/lb_m-°F)
104	0.039	0.06	0.256
140			0.260
176			0.282
212			0.301
284			0.358
320			0.380

13. Trunnion Plug Resin (Polypropylene) [5]

Temperature (°F)	k (Btu/hr-in-°F)	ρ (lb_m/in^3)	C_p (Btu/lb_m-°F)
All temperatures	0.0067	0.032	0.46

14. Wood [20]

Minimum conductivity, k_{min} = 0.0019 Btu/hr-in-°F for NCT and cool-down period, see MP197 SAR, Section 3.2, Item 8		
Maximum conductivity, k_{max} = 0.0378 Btu/hr-in-°F during fire period, see MP197 SAR, Section 3.2, Item 8		
Temperature (°F)	**ρ (lb_m/in^3) (1)**	**C_p (Btu/lb_m-°F)**
100	0.007	0.312
200	0.006	0.363
300	0.005	0.414
400	0.005	0.466
500	0.004	0.517
600	0.004	0.568

Note: (1) The wood density is calculated based on thermal diffusivity using $\alpha = \frac{k}{\rho c_P}$ with

α = 0.00025 in^2/s (0.9 in^2/hr) based on Wood Handbook [20],
k = conductivity =0.0019 (Btu/hr-in-°F),
ρ = density (lbm/in^3), and
c_P = specific heat (Btu/lbm-°F).

15. Helium [21]

Temperature (K)	k (W/m-K)	Temperature (°F)	k (Btu/hr-in-°F)
300	0.1499	80	0.0072
400	0.1795	260	0.0086
500	0.2115	440	0.0102
600	0.2466	620	0.0119
800	0.3073	980	0.0148
1000	0.3622	1340	0.0174
1050	0.3757	1430	0.0181

The above data are calculated base on the following polynomial function from [21]

$k = \sum C_i \, T_i$ for conductivity in(W/m-K) and T in (K)

For 300 < T < 500 K		for 500< T < 1050 K	
C0	-7.761491E-03	C0	-9.0656E-02
C1	8.66192033E-04	C1	9.37593087E-04
C2	-1.5559338E-06	C2	-9.13347535E-07
C3	1.40150565E-09	C3	5.55037072E-10
C4	0.0E+00	C4	-1.26457196E-13

No density or specific heat is considered for helium for conservatism.

16. Air [21]

Temperature (K)	k (W/m-K)	Temperature (°F)	k (Btu/hr-in-°F)
250	0.02228	-10	0.0011
300	0.02607	80	0.0013
400	0.03304	260	0.0016
500	0.03948	440	0.0019
600	0.04557	620	0.0022
800	0.05698	980	0.0027
1000	0.06721	1340	0.0032

The above data are calculated base on the following polynomial function from [21]

$k = \sum C_i T_i$ for conductivity in(W/m-K) and T in (K)

For 250 < T < 1050 K	
C0	-2.2765010E-03
C1	1.2598485E-04
C2	-1.4815235E-07
C3	1.7355064E-10
C4	-1.0666570E-13
C5	2.4766304E-17

No density or specific heat is considered for air in the thermal models for conservatism. Specific heat, viscosity, density and Prandtl number of air are used to calculate heat transfer coefficients described in Section A.3.3.1.1 based on the following data from [21].

$c_p = \sum A_i T_i$ for specific heat in (kJ/kg-K) and T in (K)

For 250 < T < 1050 K	
A0	0.103409E+1
A1	-0.2848870E-3
A2	0.7816818E-6
A3	-0.4970786E-9
A4	0.1077024E-12

$\mu = \sum B_i T_i$ for viscosity (N-/m^2)×10^6 and T in (K)

For 250 < T < 600 K		For 600 < T < 1050 K	
B0	-9.8601E-1	B0	4.8856745
B1	9.080125E-2	B1	5.43232E-2
B2	-1.17635575E-4	B2	-2.4261775E-5
B3	1.2349703E-7	B3	7.9306E-9
B4	-5.7971299E-11	B4	-1.10398E-12

$\rho = P / RT$ for density (kg/m^3) with P=101.3 kPa; R = 0.287040 kJ/kg-K; T = air temp in (K)

$\mathrm{Pr} = c_p \mu / k$ Prandtl number

17. Effective Conductivity for Paired Aluminum and Boral in 69BTH DSC
(See Section A.3.3.1.5 for calculation of effective properties)

Conductivity of Boral Core Material		
Temp	k_c (1)	$k_{c,90\%}$
(°F)	(Btu/hr-in-°F)	(Btu/hr-in-°F)
100	4.136	3.723
500	3.698	3.328

t_{total} = 0.25" total thickness for paired Al/Poison t_{model} = 0.21" total thickness for paired Al/Poison as modeled t_{core} = 0.16" Boral core thickness t_{Al} = 0.09" Aluminum thickness				t_{total} = 0.375" total thickness for paired Al/Poison t_{model} = 0.375" total thickness for paired Al/Poison as modeled t_{core} = 0.16" Boral core thickness t_{Al} = 0.215" Aluminum thickness			
Temp	k_{Al} [10]	k_{core} (3)	$k_{eff,across}$	Temp	k_{Al} [10]	k_{core} (3)	$k_{eff,across}$
(°F)	(Btu/hr-in-°F)	(Btu/hr-in-°F)	(Btu/hr-in-°F)	(°F)	(Btu/hr-in-°F)	(Btu/hr-in-°F)	(Btu/hr-in-°F)
70	11.092	3.752	4.137	70	11.092	3.752	6.046
100	10.983 (4)	3.723	4.104 (4)	100	10.983 (4)	3.723	5.995 (4)
200	10.708	3.624	3.996	200	10.708	3.624	5.839
300	10.517	3.525	3.893	300	10.517	3.525	5.697
400	10.375	3.427	3.793	400	10.375	3.427	5.563
650	10.042 (2)	3.180	3.543	650	10.042 (2)	3.180	5.229
Temp	k_{Al} [10]	k_{core} (3)	$k_{eff,along}$	Temp	k_{Al} [10]	k_{core} (3)	$k_{eff,along}$
(°F)	(Btu/hr-in-°F)	(Btu/hr-in-°F)	(Btu/hr-in-°F)	(°F)	(Btu/hr-in-°F)	(Btu/hr-in-°F)	(Btu/hr-in-°F)
70	11.092	3.752	7.612	70	11.092	3.752	7.960
100	10.983 (4)	3.723	7.543 (4)	100	10.983 (4)	3.723	7.885 (4)
200	10.708	3.624	7.350	200	10.708	3.624	7.686
300	10.517	3.525	7.193	300	10.517	3.525	7.534
400	10.375	3.427	7.057	400	10.375	3.427	7.410
650	10.042 (2)	3.180	6.727	650	10.042 (2)	3.180	7.114

Notes:
(1) Taken from data in [26]
(2) Extrapolated from data in [10]
(3) Inter- and extrapolated from data of 90% Boral core conductivity
(4) A conductivity value of 11.150 Btu/hr-in-°F is used instead of 10.983 Btu/hr-in-°F for k_{Al} at 100°F. This increases the effective conductivity by approximately 1% for paired aluminum and Boral plates in the ANSYS model. Since the calculated basket temperature is over 100°F for all analyzed cases, use of this higher value does not affect the results in this SAR.

18. Effective Conductivity for Paired Aluminum and MMC in 69BTH DSC
(See Section A.3.3.1.5 for calculation of effective properties)

t_{total} = 0.25" total thickness for paired Al/Poison t_{model} = 0.21" total thickness for paired Al/Poison as modeled t_{core} = 0.175" MMC thickness t_{Al} = 0.075" Aluminum thickness				t_{total} = 0.375" total thickness for paired Al/Poison t_{model} = 0.375" total thickness for paired Al/Poison as modeled t_{core} = 0.175" MMC thickness t_{Al} = 0.200" Aluminum thickness			
Temp	k_{Al} [10]	k_{MMC} (1)	$k_{eff,across}$	Temp	k_{Al} [10]	k_{MMC} (1)	$k_{eff,across}$
(°F)	(Btu/hr-in-°F)	(Btu/hr-in-°F)	(Btu/hr-in-°F)	(°F)	(Btu/hr-in-°F)	(Btu/hr-in-°F)	(Btu/hr-in-°F)
70	11.092	5.78	5.673	70	11.092	5.78	7.766
100	10.983	5.78	5.663	100	10.983	5.78	7.737
200	10.708	5.78	5.636	200	10.708	5.78	7.664
300	10.517	5.78	5.617	300	10.517	5.78	7.611
400	10.375	5.78	5.602	400	10.375	5.78	7.571
650	10.042 (2)	5.78	5.567	650	10.042 (2)	5.78	7.474
Temp	k_{Al} [10]	k_{MMC} (1)	$k_{eff,along}$	Temp	k_{Al} [10]	k_{MMC} (1)	$k_{eff,along}$
(°F)	(Btu/hr-in-°F)	(Btu/hr-in-°F)	(Btu/hr-in-°F)	(°F)	(Btu/hr-in-°F)	(Btu/hr-in-°F)	(Btu/hr-in-°F)
70	11.092	5.78	8.781	70	11.092	5.78	8.615
100	10.983	5.78	8.743	100	10.983	5.78	8.557
200	10.708	5.78	8.644	200	10.708	5.78	8.410
300	10.517	5.78	8.576	300	10.517	5.78	8.308
400	10.375	5.78	8.525	400	10.375	5.78	8.233
650	10.042 (2)	5.78	8.406	650	10.042 (2)	5.78	8.055

Notes:
(1) The lowest conductivity is taken from data in [3]
(2) Extrapolated from data in [10]

19. Effective Conductivity for Paired Aluminum and Borated Aluminum in 69BTH DSC (See Section A.3.3.1.5 for calculation of effective properties)

t_{total} = 0.25" total thickness for paired Al/Poison t_{model} = 0.21" total thickness for paired Al/Poison as modeled t_{core} = 0.175" Borated Aluminum thickness t_{Al} = 0.075" Aluminum thickness				t_{total} = 0.375" total thickness for paired Al/Poison t_{model} = 0.375" total thickness for paired Al/Poison as modeled t_{core} = 0.175" Borated Aluminum thickness t_{Al} = 0.200" Aluminum thickness			
Temp	k_{Al} [10]	k_{BAl} (1)	$k_{eff,across}$	Temp	k_{Al} [10]	k_{BAl} (1)	$k_{eff,across}$
(°F)	(Btu/hr-in-°F)	(Btu/hr-in-°F)	(Btu/hr-in-°F)	(°F)	(Btu/hr-in-°F)	(Btu/hr-in-°F)	(Btu/hr-in-°F)
70	11.092	7.39	6.896	70	11.092	7.39	8.988
100	10.983 (3)	7.50	6.962 (3)	100	10.983 (3)	7.50	9.027 (3)
200	10.708	7.88	7.185	200	10.708	7.88	9.169
300	10.517	8.18	7.365	300	10.517	8.18	9.282
400	10.375	8.48	7.537	400	10.375	8.48	9.396
650	10.042 (2)	9.15	7.895	650	10.042 (2)	9.15	9.604
Temp	k_{Al} [10]	k_{BAl} (1)	$k_{eff,along}$	Temp	k_{Al} [10]	k_{BAl} (1)	$k_{eff,along}$
(°F)	(Btu/hr-in-°F)	(Btu/hr-in-°F)	(Btu/hr-in-°F)	(°F)	(Btu/hr-in-°F)	(Btu/hr-in-°F)	(Btu/hr-in-°F)
70	11.092	7.39	10.118	70	11.092	7.39	9.363
100	10.983 (3)	7.50	10.173 (3)	100	10.983 (3)	7.50	9.358 (3)
200	10.708	7.88	10.387	200	10.708	7.88	9.386
300	10.517	8.18	10.576	300	10.517	8.18	9.428
400	10.375	8.48	10.773	400	10.375	8.48	9.491
650	10.042 (2)	9.15	11.210	650	10.042 (2)	9.15	9.625

Notes:

(1) Inter- and extrapolated from data in [3]

(2) Extrapolated from data in [10]

(3) A conductivity value of 11.150 Btu/hr-in-°F is used instead of 10.983 Btu/hr-in-°F for k_{Al} at 100°F. This increases the effective conductivity by approximately 1% for paired aluminum and Boral plates in the ANSYS model. Since the calculated basket temperature is over 100°F for all analyzed cases, use of this higher value does not affect the results in this SAR.

20. Effective Conductivity for Dummy Aluminum Assemblies in 69BTH DSC
(See Section A.3.3.1.5 for calculation of effective properties)

a_{dummy} =	5.875	in
t_{gap} =	0.0625	in
w_{comp} =	6	in

Temp	k_{Al6061} [10]
(°F)	(Btu/hr-in-°F)
70	8.008
100	8.075
200	8.250
300	8.383
400	8.492
650	8.492 (1)

Temp	k_{He} (2)	Temp	k_{He}
(°F)	(Btu/hr-in-°F)	(°F)	(Btu/hr-in-°F)
-10	0.0064	70	0.0071
80	0.0072	100	0.0074
260	0.0086	200	0.0081
440	0.0102	300	0.0090
620	0.0119	400	0.0098
980	0.0148	650	0.0121
1340	0.0174		

Temp	$R_{th\ He1}$	$R_{th\ Al6061}$	$R_{th\ He2}$	$R_{th,tr,dummy}$	$k_{eff,tr,dummy}$	$k_{eff,ax,dummy}$
(°F)	(Btu/hr-in-°F)	(Btu/hr-in-°F)	(Btu/hr-in-°F)	(Btu/hr-in-°F)	(Btu/hr-in-°F)	(Btu/hr-in-°F)
70	1.4648	0.1249	13218.8	3.0546	0.327	7.678
100	1.4162	0.1238	12779.5	2.9562	0.338	7.742
200	1.2807	0.1212	11557.4	2.6827	0.373	7.910
300	1.1632	0.1193	10496.3	2.4456	0.409	8.037
400	1.0581	0.1178	9548.5	2.2340	0.448	8.142
650	0.8579	0.1178	7741.9	1.8336	0.545	8.142

Notes:
(1) Al6061 conductivity increases at higher temperatures. Increasing of the Al6061 conductivity is conservatively ignored for calculation of effective conductivity of aluminum dummy assembly.
(2) See Section A.3.2.1, material # 15 for helium properties.

21. Effective Conductivity for Boral Plates in 37PTH DSC
(See Section A.3.3.1.7 for calculation of effective properties)

Conductivity of Boral Core Material		
Temp	k_c (1)	$k_{c\ 90\%}$
(°F)	(Btu/hr-in-°F)	(Btu/hr-in-°F)
100	4.136	3.723
500	3.698	3.328

t_{total} = 0.075" total thickness for Boral plate t_{model} = 0.075" total thickness for Boral plate as modeled t_{core} = 0.06" Boral core thickness t_{Al} = 0.015" Aluminum clad thickness			
Temp	k_{Al} [10]	k_{core}	$k_{eff,across}$
(°F)	(Btu/hr-in-°F)	(Btu/hr-in-°F)	(Btu/hr-in-°F)
100	10.983	3.723	4.290
500	10.242 (2)	3.328	3.848
Temp	k_{Al} [10]	k_{core}	$k_{eff,along}$
(°F)	(Btu/hr-in-°F)	(Btu/hr-in-°F)	(Btu/hr-in-°F)
100	10.983	3.723	5.175
500	10.242 (2)	3.328	4.711

Notes:
(1) Taken from data in [26]
(2) Extrapolated from data in [10]

22. Effective Heat Transfer Coefficients for External Fins @ 100°F Ambient
(See Section A.3.3.1.3 for calculation of effective properties)

fin_h =	3.0	fin height (in)
fin_p =	1.0	fin pitch (in)
fin_t =	0.156	fin thickness (in)
fin_n =	3	No. of fins in model
D_o =	98.25	cask diameter (in)
D_f =	104.25	fin diameter (in)
D_f/D_o =	1.061	
A_eff =	77.2	area of un-finned surface (in^2)

From Rohsenow Handbook [21]

D_f/D_o	c	b
1.36	0.62	0.29
1.14	0.59	0.27
Extrapolated for this calculation based on above data		
1.061	0.579	0.263

T_s (°F)	T_{amb} (°F)	Q_{react} (Btu/hr)	A_{eff} (in^2)	h_{eff} (Btu/hr-in^2-°F)
120	100	31.295	77.2	0.0203
140	100	71.639	77.2	0.0232
160	100	116.59	77.2	0.0252
180	100	165.15	77.2	0.0268
200	100	216.89	77.2	0.0281
220	100	271.55	77.2	0.0293
240	100	329.01	77.2	0.0305
260	100	388.75	77.2	0.0315
280	100	452.15	77.2	0.0326
300	100	518.00	77.2	0.0336
320	100	586.59	77.2	0.0346
340	100	658.05	77.2	0.0355

23. Effective Heat Transfer Coefficients for External Fins @ -20°F Ambient
(See Section A.3.3.1.3 for calculation of effective properties)

T_s (°F)	T_{amb} (°F)	Q_{react} (Btu/hr)	A_{eff} (in^2)	h_{eff} (Btu/hr-in^2-°F)
0	-20	26.511	77.2	0.0172
20	-20	61.325	77.2	0.0199
40	-20	99.88	77.2	0.0216
60	-20	141.15	77.2	0.0229
80	-20	184.56	77.2	0.0239
100	-20	229.46	77.2	0.0248
120	-20	278.04	77.2	0.0257
140	-20	329.65	77.2	0.0267
160	-20	382.98	77.2	0.0276
180	-20	437.79	77.2	0.0284
200	-20	494.84	77.2	0.0291
220	-20	553.94	77.2	0.0299

24. Effective Heat Transfer Coefficients for External Fins @ -40°F Ambient
(See Section A.3.3.1.3 for calculation of effective properties)

T_s (°F)	T_{amb} (°F)	Q_{react} (Btu/hr)	A_{eff} (in^2)	h_{eff} (Btu/hr-in^2-°F)
-20	-40	26.044	77.2	0.0169
0	-40	60.344	77.2	0.0196
20	-40	98.33	77.2	0.0212
40	-40	139.00	77.2	0.0225
60	-40	181.83	77.2	0.0236
80	-40	226.42	77.2	0.0245
100	-40	272.53	77.2	0.0252
120	-40	321.95	77.2	0.0261
140	-40	374.39	77.2	0.0270
160	-40	427.93	77.2	0.0277
180	-40	483.57	77.2	0.0285
200	-40	541.13	77.2	0.0292

25. Radial Effective Conductivity for Helium in DSC Shell/TC Inner Shell Gap (See Section A.3.3.1.3 for calculation of effective properties

$D_{o,DSC}$ =	69.75	DSC OD (in)
$D_{i,TC}$ =	70.50	Cask ID (in)
L =	10	Model height (in)

T_{DSC}	T_{TC}	q_{react}	T_{avg}	k_{eff}
(°F)	(°F)	(Btu/hr)	(°F)	(Btu/hr-in-°F)
110	-20	506	45	0.0080
153	30	506	92	0.0084
195	80	506	138	0.0090
237	130	506	183	0.0097
279	180	506	230	0.0104
296	200	506	248	0.0108
339	250	506	294	0.0116
382	300	506	341	0.0126
426	350	506	388	0.0136
470	400	506	435	0.0148
515	450	506	482	0.0160
560	500	506	530	0.0173
606	550	506	578	0.0187
652	600	506	626	0.0202
698	650	506	674	0.0217
745	700	506	722	0.0233
791	750	506	771	0.0251

26. Radial Effective Conductivity for Helium in DSC Shell/TC Internal Sleeve Gap (See Section A.3.3.1.3 for calculation of effective properties)

$D_{o,DSC}$ =	67.19	DSC OD (in)
$D_{i,Sleeve}$ =	68.00	Cask ID (in)
L =	10	Model height (in)

T_{DSC}	T_{Sleeve}	q_{react}	T_{avg}	k_{eff}	k_{eff} in Model [1]
(°F)	(°F)	(Btu/hr)	(°F)	(Btu/hr-in-°F)	(Btu/hr-in-°F)
297	200	487	249	0.0115	0.0102
339	250	487	295	0.0125	0.0111
382	300	487	341	0.0136	0.0121
425	350	487	388	0.0148	0.0132
469	400	487	435	0.0161	0.0144
514	450	487	482	0.0175	0.0156
559	500	487	529	0.0191	0.0170
604	550	487	577	0.0207	0.0185
650	600	487	625	0.0225	0.0201
696	650	487	673	0.0244	0.0217
742	700	487	721	0.0263	0.0235
789	750	487	770	0.0285	0.0254

Note:
[1] For conservatism, approximately 90% of the calculated effective conductivity values are considered in the model.

27. Axial Effective Conductivities for Bottom Shield Plug and Top Inner Cover Plate (See Section A.3.3.1.3 for calculation of effective properties)

Top inner cover plate for all DSC types except 24PT4
Plate thickness = 0.75 in
Gap thickness = 0.0625 in
Two axial gaps

Temp (°F)	k_SS304 (Btu/hr-in-°F)	Temp (K)	k_air (W/m-K)	k_air (Btu/hr-in-°F)	k_eff (Btu/hr-in-°F)
70	0.717	294.4	0.0257	0.0012	0.0086
100	0.725	311.1	0.0269	0.0013	0.0090
200	0.775	366.7	0.0308	0.0015	0.0103
300	0.817	422.2	0.0345	0.0017	0.0115
400	0.867	477.8	0.0381	0.0018	0.0127
500	0.908	533.3	0.0415	0.0020	0.0138
600	0.942	588.9	0.0449	0.0022	0.0149
700	0.983	644.4	0.0482	0.0023	0.0160
800	1.025	700.0	0.0514	0.0025	0.0171
900	1.058	755.6	0.0545	0.0026	0.0181
1,000	1.092	811.1	0.0576	0.0028	0.0191

Bottom shield plug for all DSC types except 24PT4
Plate thickness = 3 in
Gap thickness = 0.0625 in
Two axial gaps

Temp (°F)	k_A36 (Btu/hr-in-°F)	Temp (K)	k_air (W/m-K)	k_air (Btu/hr-in-°F)	k_eff (Btu/hr-in-°F)
70	2.275	294.4	0.0257	0.0012	0.030
100	2.300	311.1	0.0269	0.0013	0.032
200	2.317	366.7	0.0308	0.0015	0.037
300	2.275	422.2	0.0345	0.0017	0.041
400	2.208	477.8	0.0381	0.0018	0.045
500	2.142	533.3	0.0415	0.0020	0.049
600	2.075	588.9	0.0449	0.0022	0.053
700	2.008	644.4	0.0482	0.0023	0.056
800	1.933	700.0	0.0514	0.0025	0.060
900	1.858	755.6	0.0545	0.0026	0.063
1,000	1.758	811.1	0.0576	0.0028	0.067

28. Axial Effective Conductivities for Cover Plates of 24PT4 DSC
(See Section A.3.3.1.3 for calculation of effective properties)

Top outer cover plate for 24PT4 DSC
Plate thickness = 1.25 in
Gap thickness = 0.0625 in
One axial gap

Temp (°F)	k_SS316 (Btu/hr-in-°F)	Temp (K)	k_air (W/m-K)	k_air (Btu/hr-in-°F)	k_eff (Btu/hr-in-°F)
70	0.642	294.4	0.0257	0.0012	0.025
100	0.658	311.1	0.0269	0.0013	0.026
200	0.700	366.7	0.0308	0.0015	0.030
300	0.750	422.2	0.0345	0.0017	0.033
400	0.792	477.8	0.0381	0.0018	0.037
500	0.833	533.3	0.0415	0.0020	0.040
600	0.875	588.9	0.0449	0.0022	0.043
700	0.917	644.4	0.0482	0.0023	0.046
800	0.958	700.0	0.0514	0.0025	0.049

Bottom inner cover plate for 24PT4 DSC
Plate thickness = 2 in
Gap thickness = 0.0625 in [1]
One axial gap

Temp (°F)	k_SS316 (Btu/hr-in-°F)	Temp (K)	k_air (W/m-K)	k_air (Btu/hr-in-°F)	k_eff (Btu/hr-in-°F)
70	0.642	294.4	0.0257	0.0012	0.038
100	0.658	311.1	0.0269	0.0013	0.040
200	0.700	366.7	0.0308	0.0015	0.046
300	0.750	422.2	0.0345	0.0017	0.051
400	0.792	477.8	0.0381	0.0018	0.056
500	0.833	533.3	0.0415	0.0020	0.061
600	0.875	588.9	0.0449	0.0022	0.066
700	0.917	644.4	0.0482	0.0023	0.071
800	0.958	700.0	0.0514	0.0025	0.075

Note: [1] The axial gap between the bottom inner cover plate and the bottom shield plug is integrated in the axial effective conductivity for bottom shield plug as well. Considering this additional gap for the bottom inner cover maximizes the DSC shell temperature in the radial direction and is therefore conservative for steady state analysis.

29. Axial Effective Conductivities for Lead Shield Plugs of 24PT4 DSC
(See Section A.3.3.1.3 for calculation of effective properties)

Top shield plug for 24PT4 DSC
Plate thickness = 3.38 in
Gap thickness = 0.025 in
Two axial gaps

Temp (°F)	k_lead (Btu/hr-in-°F)	Temp (K)	k_air (W/m-K)	k_air (Btu/hr-in-°F)	k_eff (Btu/hr-in-°F)
-100	1.767	200	0.0182	0.0009	0.0582
-10	1.733	250	0.0223	0.0011	0.0706
80	1.700	300	0.0261	0.0013	0.0820
260	1.637	400	0.0330	0.0016	0.1024
440	1.579	500	0.0395	0.0019	0.1206
620	1.512	600	0.0456	0.0022	0.1371

Bottom shield plug for 24PT4 DSC
Plate thickness = 2.88 in
Gap thickness = 0.025 in
Two axial gaps

Temp (°F)	k_lead (Btu/hr-in-°F)	Temp (K)	k_air (W/m-K)	k_air (Btu/hr-in-°F)	k_eff (Btu/hr-in-°F)
-100	1.767	200	0.0182	0.0009	0.0500
-10	1.733	250	0.0223	0.0011	0.0607
80	1.700	300	0.0261	0.0013	0.0706
260	1.637	400	0.0330	0.0016	0.0883
440	1.579	500	0.0395	0.0019	0.1042
620	1.512	600	0.0456	0.0022	0.1187

30. Effective Conductivities for TC Slide Rail
(See Section A.3.3.1.3 for calculation of effective properties)

Slide rail thickness = 0.12 in
Gap thickness = 0.01 in

Temp (°F)	k_SS304 (Btu/hr-in-°F)	Temp (K)	k_He (W/m-K)	k_He (Btu/hr-in-°F)	k_eff (Btu/hr-in-°F)
70	0.717	294.4	0.1482	0.0071	0.076
100	0.725	311.1	0.1533	0.0074	0.079
200	0.775	366.7	0.1697	0.0082	0.087
300	0.817	422.2	0.1861	0.0090	0.095
400	0.867	477.8	0.2038	0.0098	0.104
500	0.908	533.3	0.2236	0.0108	0.113
600	0.942	588.9	0.2429	0.0117	0.122
700	0.983	644.4	0.2610	0.0126	0.131
800	1.025	700.0	0.2781	0.0134	0.139
900	1.058	755.6	0.2945	0.0142	0.147
1,000	1.092	811.1	0.3104	0.0149	0.154

31. Effective Conductivity of Internal Sleeve
(See Section A.3.3.1.3 for calculation of effective properties)

Temperature	k_{Al} (1)	k_{He} (2)	$k_{eff,axl,1}$	$k_{eff,axl}$	$k_{eff,rad}$
(°F)	(Btu/hr-in-°F)	(Btu/hr-in-°F)	(Btu/hr-in-°F)	(Btu/hr-in-°F)	(Btu/hr-in-°F)
70	8.008	0.0071	1.894	1.808	7.646
100	8.075	0.0074	1.947	1.859	7.710
150	8.167	0.0077	2.030	1.938	7.798
200	8.250	0.0081	2.111	2.016	7.878
250	8.317	0.0085	2.190	2.091	7.941
300	8.383	0.0090	2.276	2.173	8.005
350	8.442	0.0094	2.362	2.255	8.061
400	8.492	0.0098	2.445	2.335	8.109

Notes:
(1) See Section A.3.2.1 material # 10 for the lowest aluminum properties.
(2) Interpolated / extrapolated between data in Section A.3.2.1 material # 15 for helium.

Thermal radiation at the external surfaces of the packaging is considered for thermal analysis. The outer surface of the cask shield shell is painted white. Reference [22] gives an emissivity between 0.92 and 0.96 and a solar absorptivity between 0.09 and 0.23 for white paints. To account for dust and dirt and to bound the problem, the thermal analysis uses a solar absorptivity of 0.3 and an emissivity of 0.9 for the white painted surfaces.

The outer surfaces of the impact limiter shells are uncoated stainless steel. An emissivity of 0.587 is considered for these surfaces based on [15]. Solar absorptance values of 0.39 and 0.47 are given in [34] for rolled and machined stainless steel plates. For conservatism, it is assumed that the solar absorptivity of stainless steel is equal to emissivity.

The emissivity of rolled stainless steel plates is 0.578 as considered in [15]. The emissivity for rolled steel sheets is 0.657 as reported in [5], Table 10-17. The transport cask inner shell is stainless steel clad. The emissivity value of 0.587 is considered for both the DSC shell (stainless steel) and the transport cask inner shell (stainless steel clad) in the calculation of thermal radiation exchange between these shells.

The emissivity of anodized aluminum is between 0.84 and 0.72 for temperatures between 296K and 484K (between 73°F and 411°F) and its solar absorptivity is between 0.12 and 0.16 ([21], Table A.7.2). An emissivity of 0.70 and a solar absorptivity of 0.16 are considered for the finned aluminum shell of MP197HB cask in this analysis.

After a fire, the cask outer surfaces will be partially covered in soot. Based on [22], emissivity and solar absorptivity of soot are 0.95. The HAC thermal analysis conservatively assumes an absorptivity of 1.0 and an emissivity of 0.9 for the post fire, cool-down period.

Various ASME code years are called for various DSCs in the MP197HB TC. Except for 24PT4, the other DSC types are covered by ASME code from 1998 to 2006 as shown in the following table.

Applicable Code Years for Each Canister Design

Canister Design	Applicable Storage License	ASME B&PV Code Year
NUHOMS® 32PTH	1030	1998 w/ 2000 Addenda
NUHOMS® 32PTH1	1004	1998 w/ 2000 Addenda
NUHOMS® 37PTH	Note (1)	2004 w/2006 Addenda
NUHOMS® 69BTH	Note (1)	2004 w/2006 Addenda
NUHOMS® 24PT4	1029	1992 thru1994 Addenda
NUHOMS® 24PTH	1004	1998 w/ 2000 Addenda
NUHOMS® 32PT	1004	1998 w/ 2000 Addenda
NUHOMS® 61BT	1004	1998 w/ 1999 Addenda
NUHOMS® 61BTH	1004	1998 w/ 2000 Addenda
NUHOMS® 61BTH with failed fuel (61BTHF)	Note (1)	2004 w/2006 Addenda
NUHOMS® 24PTH with failed fuel (24PTHF)	Note (1)	2004 w/2006 Addenda

Note (1): These DSCs are currently not a part of CoC 1004 but will be added at a later date via amendment.

The shell and cover plates of all DSC types except for 24PT4 consist of stainless steel SA-240, type 304 (SS304). There are no changes in thermal conductivity of SS304 in ASME 1998 to 2006 in temperature range from 70 to 700°F. This range properly covers the DSC shell temperature for all DSC types in this calculation.

The shield plugs of all DSC types except for 24PT4 consist of carbon steel A36. The changes in the A36 conductivity between ASME code years 1998 to 2006 are limited to ±0.9%. This small change has no significant effect on the thermal evaluation.

The thermal properties for 24PT4 DSC are taken from UFSAR for standardized advanced NUHOMS® system [2]. These properties are based on ASME code 1992 through 1994 addenda and used in this calculation without any changes.

A.3.2.2 Component Specifications

The components for which thermal technical specification are necessary are the MP197HB containment seals and poison plates used in DSC basket.

A.3.2.2.1 MP197HB TC

The seals used in the packaging are the Fluorocarbon seals (Viton O-rings *and metallic seals*). The *Fluorocarbon* seals will have a minimum and maximum temperature rating of -40°F and 400°F, respectively.

The metallic seals will have a minimum and maximum temperature rating of -40°F and 644°F, respectively.

A.3.2.2.2 69BTH DSC

The 69BTH DSC design allows the use of different neutron absorber materials based on the heat load zoning configuration (HLZC). Boral, Metal Matrix Composite (MMC), or Borated Aluminum can be used as poison materials for HLZC # 1, # 2 and # 3 in 69BTH basket. For

69BTH basket with HLZC # 4 *and HLZC # 8*, only borated aluminum can be used as poison material. The HLZCs for 69BTH are described in Section A.3.3.1.4. *Sections A.3.3 and A.3.4 present the thermal evaluation of the 69BTH DSC for HLZC # 1 through 4. Section A.3.6.1 presents the thermal evaluation of the 69BTH DSC for HLZC # 8.*

A.3.2.2.3 37PTH DSC

The 37PTH DSC design allows the use of different neutron absorber materials. Boral plates paired with Al1100 plates or single plates of metal matrix composite (MMC) or borated aluminum can be used as poison materials in 37PTH basket with 22 kW heat load.

The following table summarizes the poison material configuration allowed for 69BTH and 37PTH basket designs:

Heat Load Zoning Configurations for 69BTH and 37PTH DSCs in MP197HB

	DSC type	HLZC	Poison Material	Max. Heat Load (kW)
1	69BTH	1 or 2	Boral/MMC/ Borated Aluminum	26.0
2	69BTH	3	Boral/MMC/ Borated Aluminum	29.2
3	69BTH	4	Borated Aluminum	32.0
4	*69BTH*	*8*	*Borated Aluminum*	*30.2*
5	37PTH	---	Boral Paired Al/ Single MMC/Borated Al	22

The neutron absorber materials in 69BTH and 37PTH baskets are subjected to the following minimum thermal conductivity, which are used in the canister thermal analyses.

Minimum Conductivity of Poison Material

Boral Core Matrix			
Temperature (°F)	Conductivity (W/cm-K) [26]	Conductivity (Btu/hr-in-°F)	90% Conductivity(1) (Btu/hr-in-°F)
100	0.859	4.136	3.723
500	0.768	3.698	3.328
Metal Matrix Composite (MMC)			
Temperature (°F)	Conductivity (Btu/min-in-°F),	Conductivity (Btu/hr-in-°F)	
All temperatures	0.0964 [3]	5.78	
Borated Aluminum			
Temperature (°F)	Conductivity (Btu/min-in-°F) [3]	Conductivity (Btu/hr-in-°F)	
68	0.123	7.38	
212	0.132	7.92	
392	0.141	8.46	
482	0.145	8.70	

Note: (1) The conductivity of Boral core is reduced by 10% and used in thermal analysis

A.3.3 Thermal Evaluation under Normal Conditions of Transport

The NCT ambient conditions are used for the determination of the maximum fuel cladding temperature, the maximum MP197HB TC and DSC temperatures, the containment pressure, and the thermal stresses. These steady state environmental conditions correspond to maximum daily averaged ambient temperature of 100°F and to 10 CFR 71.71(c)(1) [6] insolation averaged over a 24 hour period.

Ambient conditions for NCT are taken from 10 CFR 71 [6] and applied to the boundaries of the cask model. These conditions are listed in the following table.

Normal Conditions of Transport

Case #	Ambient temperature (°F)	Insolance	Purpose
1	100	Yes	Maximum Component Temperatures
2	-20	No	Cold conditions for Structural Analysis
3	-40	No	Maximum Thermal Stress
4	100	No	Maximum Accessible Surface Temperature

Except for DSC types 69BTH and 37PTH, all other DSC types considered for transport in MP197HB TC are analyzed for storage/transfer conditions under 10 CFR 72 [8]. The safety analysis reports (SAR) for these DSC types under storage/transfer conditions are presented in [1], [2], [3], and [4].

A.3.3.1 Thermal Models

The MP197HB TC loaded with a DSC is analyzed based on finite element models developed using the ANSYS computer code [27]. ANSYS is a comprehensive thermal, structural and fluid flow analysis package. ANSYS is capable of solving steady state and transient thermal analysis problems in one, two, or three dimensions. Heat transfer via a combination of conduction, radiation, and convection can be modeled by ANSYS.

The evaluations are presented in Section A.3.6.11 for the case that the physical integrity of the fuel assemblies may not be guaranteed. For the case that the physical configuration of the fuel assemblies is not altered, the thermal evaluations are presented below for NCT.

Three finite element models are developed for analyses of the MP197HB TC loaded with DSC.

a) A half-symmetric, three-dimensional finite element model of the MP197HB TC is developed using ANSYS [27], version 8.1. The model contains the cask shells, cask bottom plate, cask lid, impact limiters, DSC shell, and DSC end plates without the basket. The DSC dimensions correspond to nominal DSC dimensions listed in Table A.3–1 for variations of the MP197HB model. SOLID70 elements are used to model the components including the gaseous gaps. Impact limiter gussets, cask slide rails, and trunnion plug plates are modeled using SHELL57 elements. Surface elements SURF152 are used for applying the insolation boundary conditions.

b) A half-symmetric, three-dimensional finite element model of the 69BTH basket and DSC is developed using ANSYS [27], version 8.1. The model contains the DSC shell, the DSC cover plates, shield plugs, aluminum rails, basket plates, and homogenized fuel assemblies. Only SOLID70 elements are used in the 69BTH DSC/basket model.

c) A three-dimensional finite element model of the 37PTH DSC/basket model is developed using ANSYS [27], version 8.1. The model contains the DSC shell, the DSC cover plates, shield plugs, aluminum rails, basket plates, and homogenized fuel assemblies. Only SOLID70 elements are used in the 37PTH DSC/basket model.

The DSC shell temperatures for NCT are retrieved from the MP197HB transport cask model and transferred to the DSC/basket models to evaluate the maximum fuel cladding and basket component temperatures. The models are run with steady state conditions for NCT evaluations.

The nominal dimensions with the following gaps are used to develop the finite element models.

A.3.3.1.1 MP197HB TC Model

The following assumptions are considered in the MP197HB TC model:

- DSC types without spacer are centered axially in the transport cask. For DSC types with the spacer, a 0.5" gap is considered between the DSC outer top cover plate and the cask lid. These assumptions reduce the axial heat transfer and maximize the DSC shell temperatures, which in turn result in higher fuel cladding temperatures.

- Heat load is simulated by heat flux distributed uniformly over the basket length on the radial inner surface of the DSC shell.

- Since the transfer operation occurs in horizontal position, the lower halves of the cask cylindrical surfaces are not exposed to insolance. No solar heat flux is considered over these surfaces. To remove any uncertainty about the solar impact on the vertical surfaces, the entire surface areas of vertical surfaces are considered for application of the solar heat flux.

- For the cask with external fins, insolance is applied only over the radial surfaces of the shield shell and fins. Insolance over the vertical surfaces of the fins is ignored. This approach is justified since the shadow of the exposed fins covers most of the other fins and the cask outer surface.

- No convection is considered within the cask cavity.

- No convection is considered between the cask ends and the thermal shields.

- No heat transfer is considered within the bearing block.

- No heat transfer is considered through spacers used at the bottom of TC for short DSC types.

- Heat dissipations from lateral surfaces of the skid straps, inner radial surface of impact limiter recess, thermal shield outer rings, and neutron shield end caps are conservatively neglected.

- No thermal radiation to ambient is considered for the cask surfaces in contact with the transport skid saddles.

- Radiation heat exchange is considered between the DSC and the cask inner shell/internal sleeve by calculating effective conductivities for helium in this region.

The following gaps are considered in the MP197HB TC model:

a) 0.0625" axial gap between thermal shield and impact limiter shell,
b) 0.0625" axial gap between thermal shield standoffs and the cask top or bottom end surfaces,
c) 0.10" diametrical gap between cask lid and cask inner shell,
d) 0.01" axial gap between cask lid and cask flange,
e) 0.01" axial gap between ram closure plate and cask bottom plate,
f) 0.01" radial gaps between neutron shield boxes and surrounding shells,
g) 0.025" radial gap between gamma shield and cask outer shell,
h) 0.01" radial gaps between the cask inner shell and aluminum sleeve,
i) 0.01" radial gap between the finned aluminum shell and the cask shield shell,
j) 0.0625" axial gaps between the DSC bottom shield plug and bottom cover plates,
k) 0.0625" axial gaps between the DSC top inner cover and the adjacent top shield plug and top outer cover plate,
l) 0.025" axial gaps between the lead shield plugs and encapsulating plates for 24PT4 DSC,
m) 0.01" gaps between trunnion replacement plugs and the trunnion attachment blocks.

The 0.0625" gaps between thermal shield, impact limiter shell, and cask top or bottom end surfaces are based on the main SAR, Section 3.4.1.1 assumptions and account for the 0.06" thick weld overlay conservatively.

The 0.01" gap between cask lid/ cask flange and ram closure plate/cask bottom plate account for thermal resistance between bolted components. The 0.01" radial gaps between the neutron shield boxes and the surrounding shells is also based on main SAR, Section 3.4.1.1 assumptions.

The gap of 0.025" assumed between gamma shield and cask outer shell is justified in Section A.3.6.7.1.

The radial gap of 0.01" assumed between the finned aluminum shell and the cask shield shell is justified in Section A.3.6.7.2.

The 0.0625" and 0.025" axial gaps between DSC end plates maximize the radial heat transfer through DSC shell toward the cask to bound the maximum component temperatures conservatively.

The width of TC slide rail is 3". For conservatism, a gap of 0.01" with a contact width of 0.12" is considered between the TC slide rails and the DSC shell at 168° and 192° orientations. The 0° orientation is located at the top of the horizontal TC as shown in Chapter A.1, the drawings in Appendix A.1.4.10.

The finned shell is divided into three axial sections with one inch distance between adjacent sections. No finned shell is considered over the trunnion plugs in the model. Since the finned shell is designed as a continuous shell which covers the trunnion plugs, the model which has fewer fins is conservative for thermal analysis of transport cask under NCT.

The nominal dimensions considered for DSCs in MP197HB model are listed in Table A.3–1. For each basket type, the shortest cavity length is considered for the analysis to bound the maximum decay heat flux.

To provide thermal input for structural evaluation, a heat load of 23.2 kW (along with 22.0 kW) is considered for the 37PTH DSC. Since the heat load of 23.3 kW is higher than the design heat load of 22.0 kW, this assumption is conservative for the structural evaluation of the 37PTH DSC.

Decay heat load is applied as a uniform heat flux over the inner surface of the DSC shell covering the basket length. The decay heat flux applied in the TC model is calculated as follows.

$$q'' = \frac{Q}{\pi D_i L_b}$$

q" = decay heat flux (Btu/hr-in^2)
Q = decay heat load (Btu/hr) (to convert from kW multiply by 3412.3)
D_i = DSC inner diameter (in)
L_b = Basket length (in)

The applied decay heat values in the model are listed below.

DSC Decay Heat Flux

DSC Type	Heat Load (kW)	(Btu/hr)	D_i (in)	L_b (in)	Decay heat flux (Btu/hr-in^2)
69BTH	26.0	88,720	68.75	164	2.505
	29.2	99,639			2.813
	32.0	109,194			3.083
61BTH Type 1 (1)	22.0	75,071	66.25	164	2.199
61BTH Type 2 (1)	24.0	81,895	66.25	164	2.399
61BT	18.3	62,445	66.25	164	1.829
37PTH	22.0	75,071	68.75	162	2.146
32PTH/32PTH Type 1	26.0	88,720	68.75	162	2.536
32PTH1 Type 1	26.0	88,720	68.75	162	2.536
32PTH1 Type 2	24.0	81,895	68.75	162	2.341
32PT	24.0	81,895	66.19	166.10	2.371
24PTH (all types)(1)(2)	26.0	88,720	66.19	168.60	2.531
24PT4	24.0	81,895	66.19	179.13	2.199

Notes:
(1) DSC types 61BTHF and 24PTHF has the same dimensions and heat loads as DSC types 61BTH and 24PTH, respectively.
(2) The allowable heat load for 24PTH-S-LC DSC is 24 kW. A heat load of 26 kW is assumed conservatively in the analysis for 24PTH-S-LC.

Radiation and conduction between the DSC and the TC inner shell / internal sleeve is considered by calculating effective conductivities for helium gaps between the components listed above. Calculation of the helium effective conductivity within this gap is described in Section A.3.3.1.3. Insolance is applied as a heat flux over the TC outer surfaces using average insolence values from 10 CFR 71 [6]. The insolance values are averaged over 24 hours and multiplied by the surface absorptivity factor to calculate the solar heat flux. The solar heat flux values used in the MP197HB TC model are summarized below.

Solar Heat Flux

Surface Material	Shape	Insolance over 12 hrs[6] (gcal/cm^2)	Solar Absorptivity	Total solar heat flux averaged over 24 hrs (Btu/hr-in^2)
Stainless Steel	Curved	400	0.587 (1)	0.2505
	Flat vertical	200	0.587 (1)	0.1252
White Paint (shield shell)	Curved	400	0.30	0.1280
Anodized Aluminum	Curved	400	0.16	0.0683
Plain aluminum	Flat vertical	200	0.10	0.0213

Note: (1) Solar absorptivity of stainless steel is taken equal to its emissivity. See Section A.3.2.1 for justification.

The cask external fins are not considered explicitly in the TC model. Instead, an effective heat transfer coefficient is applied over the outer surface of the un-finned aluminum shell to simulate the heat dissipation from this area. The methodology to calculate the effective heat transfer coefficient for external fins is described in Section A.3.3.1.3.

Convection and radiation heat transfer from the un-finned cask surfaces are combined together as total heat transfer coefficients. The total heat transfer coefficients are calculated using free convection correlations from Rohsenow Handbook [21] and are incorporated in the model using ANSYS macros.

The total heat transfer coefficient, ht, is used to combine the convection and radiation heat transfer together.

$$h_t = h_r + h_c$$

Where,

h_r = radiation heat transfer coefficient (Btu/hr-in^2-°F)

h_c = free convection heat transfer coefficient (Btu/hr-in^2-°F)

The radiation heat transfer coefficient, hr, is given by the equation:

$$h_r = \varepsilon F_{w\infty} \left[\frac{\sigma(T_w^{\,4} - T_{amb}^{\,4})}{T_w - T_{amb}} \right] \quad \text{Btu/hr-in}^2\text{-°F}$$

Where,

ε	= surface emissivity
F_{12}	= view factor from surface 1 to ambient = 1
σ	= 0.1714×10^{-8} Btu/hr-ft^2-°R^4
T_w	= surface temperature (°R)
T_{amb}	= ambient temperature (°R)

Surface emissivity values are discussed in Section A.3.2.1.

The natural convection coefficients are calculated using handbook correlations [21] and are incorporated in the model using ANSYS macros. These correlations are described below.

For horizontal cylinders:

$$Ra = Gr\,\mathrm{Pr} \quad ; \quad Gr = \frac{g\,\beta\,(T_w - T_\infty)\,D^3}{\nu^2}$$

$$Nu_l = \frac{2f}{\ln(1 + 2f / Nu^T)} \text{ with}$$

$$Nu^T = 0.772\,\overline{C}_l\,Ra^{1/4} \quad ; f = 1 - \frac{0.13}{(Nu^T)^{0.16}}; \ \overline{C}_l = 0.515 \text{ for gases [21]}$$

$$Nu_t = \overline{C}_t\,Ra^{1/3}$$

$$\overline{C}_t = 0.103 \text{ for air with Pr} \approx 0.71 \text{ [21]}$$

$$Nu = \left[(Nu_l)^m + (Nu_t)^m\right]^{1/m} \qquad with \quad m = 10 \quad for \ \ 10^{-10} < Ra < 10^7$$

$$h_c = \frac{Nu\,k}{D}$$

The above correlations are incorporated in ANSYS model via macro "HTOT_HCL.mac".

For vertical flat surfaces:

$$Ra = Gr\,\mathrm{Pr} \quad ; \quad Gr = \frac{g\,\beta\,(T_w - T_\infty)\,L^3}{\nu^2}$$

$$Nu_l = \frac{2.0}{\ln(1 + 2.0 / Nu^T)} \text{ with}$$

$$Nu^T = \overline{C}_l\,Ra^{1/4} \ ; \ \overline{C}_l = 0.515 \text{ for gases [21]}$$

$$Nu_t = C_t^V\,f\,Ra^{1/3} / \left(1 + 1.4 \times 10^9\,\mathrm{Pr}/Ra\right) \qquad \text{with}$$

$$C_t^V = \frac{0.13\,\mathrm{Pr}^{0.22}}{(1 + 0.61\,\mathrm{Pr}^{0.81})^{0.42}} \qquad f = 1.0 + 0.078\left(\frac{T_w}{T_\infty} - 1\right)$$

$$Nu = \left[(Nu_l)^m + (Nu_t)^m\right]^{1/m} \qquad with \quad m = 6 \quad for \;\; 1 < Ra < 10^{12}$$

$$h_c = \frac{Nu\,k}{L}$$

The above correlations are incorporated in ANSYS model via macro "HTOT_VPL.mac".

For horizontal flat surfaces facing downwards:

The following correlations are used only for the outer surface of the bearing block at the lower half of the TC.

$$Ra = Gr\,\mathrm{Pr} \quad ; \quad Gr = \frac{g\,\beta(T_w - T_\infty)(L^*)^3}{\nu^2}$$

$$Nu_l = \frac{2.5}{\ln(1 + 2.5/Nu^T)} \qquad \text{with}$$

$$Nu^T = \frac{0.527}{\left(1 + (1.9/\mathrm{Pr})^{9/10}\right)^{2/9}}\; Ra^{1/5}$$

$$Nu = Nu_l \qquad for \;\; 10^3 < Ra < 10^{10}$$

$$h_c = \frac{Nu\,k}{L^*}$$

The above correlations are incorporated in ANSYS model via macro "HTOT_HPD.mac".

The following parameters are used in the above correlations.

g = gravitational constant = 9.81 (m/s^2)
β = expansion coefficient = 1/T (1/K)
T = absolute temperature (K)
ν = kinematic viscosity (m^2/s)
L = height of the vertical surface (in)

D = diameter of the horizontal cylinder (in)

$L^* = \frac{A}{p} = \frac{heated\ area}{heated\ perimeter}$ =1.2" (shortest surface of bearing block)

k = air conductivity (W/m-K)

During transportation, the DSC shell rests on four slide rails in the TC. These rails are Nitronic 60 stainless steel plates welded to the inner shell of the TC. The thickness of the slide rail is 0.12" when no internal sleeve is used. The slide rail at the 180° orientation is 0.06" thick and is not in contact with the DSC shell. The same configuration is considered for the small diameter DSC and the internal sleeve.

The angle between the lower rail and the vertical plane is 12 degree. Considering this configuration as shown in Figure A.3–1, the distance between the centerline of the DSC and the centerline of the cask is calculated as follows.

$$R_2^{\ 2} = R_1^{\ 2} + x^2 - 2\,R_1\,x\,Cos(\alpha)$$

With,

$R_1 = D_{i,\,TC}/2 - t_{rail}$
$R_2 = D_{o,\,DSC}/2$
$\alpha = 12°$
x = Distance between the DSC and TC centerlines
$D_{i,\,TC}$ = Inner diameter of TC or internal sleeve
$D_{o,\,DSC}$ = DSC outer diameter
t_{rail} = cask slide rail thickness = 0.12"

The calculated values for x are listed in the following table. In the ANSYS model, the DSC is shifted down by the amount of x in the Cartesian y-direction within the TC cavity.

Distance between DSC and TC Centerlines

DSC Type	$D_{i,TC}$ (in)	$D_{o,DSC}$ (in)	R_1 (in)	R_2 (in)	α (degree)	x (in)
69BTH 37PTH 32PTH 32PTH1	70.5	69.75	35.130	34.875	12	0.261
61BT 61BTH 61BTHF	68	67.25	33.880	33.625	12	0.261
32PT 24PTH 24PTHF 24PT4	68	67.19	33.880	33.595	12	0.291

To simplify the model, the lower cask slide rails at 168° and 192° orientations are modeled using shell elements with the conductivity of Nitronic 60 and a helium gap of 0.01". The effects of the other cask slide rails are conservatively omitted. The slide rail width is 3". For conservatism, a contact width of 0.12" is considered between the lower rails and the DSC shell.

The axial gaps considered between DSC cover plates and shield plugs are integrated into bottom shield plug and top inner cover plates. The axial gaps considered for the lead shield plugs of 24PT4 are also integrated into the shield plug material. The axial effective conductivities are calculated for these components in Section A.3.3.1.3. The conductivity in radial direction remained unchanged and equal to the conductivity of the corresponding material.

To reduce the complexity of the model, effective conductivities are calculated for the internal sleeve in axial and radial directions. The methodology to calculate the effective conductivity of the internal sleeve is described in Section A.3.3.1.3. These effective conductivities are

conservative since the number and the assumed gaps between the internal sleeve pieces are larger than those considered for the proposed internal sleeve.

The material properties used in the MP197HB model are listed in Section A.3.2.1.

The seal o-rings are not explicitly considered in the models. The maximum seal temperatures are retrieved from the models by selecting the nodes at the locations of the corresponding seal o-rings.

The geometry of the TC model and the gaps are shown in Figure A.3–2 through Figure A.3–5. Mesh sensitivity of the MP197HB model is discussed in Appendix A.3.6.2.1.

Typical boundary conditions for TC model under NCT are shown in Figure A.3–6 through Figure A.3–8.

A.3.3.1.2 Calculation of Maximum Accessible Surface Temperature

A personnel barrier installed on the transport skid between the two impact limiters of MP197HB TC limits the accessible packaging surfaces to the impact limiter and barrier outer surfaces. The personnel barrier has an open area of at least 80%. Radiation heat transfer between the cask and the barrier will be minimal due to the small radiation view factor between the cask and the barrier. Due to large distance between the barrier and cask outer surface, the free convection heat transfer around TC remains undisturbed. The transport configuration is shown in the drawings in Chapter A.1, Appendix A.1.4.10.

The TC model described in Section A.3.3.1.1 is run without insolance to determine the accessible surface temperature of the impact limiters in the shade. A heat load of 32 kW and boundary conditions at 100°F and no insolance are considered in the cask model to bound the maximum accessible surface temperature under shade.

The maximum accessible surface temperature of impact limiters under these conditions is 121°F. The maximum temperature of the cask outer surface is 302°F and belongs to a part of shield shell uncovered by the external fins in the model. The maximum temperature of the personnel barrier is calculated based on the maximum temperature of the cask outer surface using the following methodology.

The personnel barrier is exposed to thermal radiation from the cask shield shell / finned shell and dissipates heat via thermal radiation and natural convection to ambient. Since the personnel barrier is far apart from the cask shield shell, it is not exposed to the hot air streams from the cask. This assumption is justified in Section A.3.3.1.2.1.

The heat balance for the personnel barrier is shown schematically in Figure A.3–9. The following conservative assumptions are considered to simplify the heat balance.

- Convection heat dissipation from the barrier is omitted completely.
- Radiation heat dissipation to ambient from barrier surfaces facing the cask is omitted.
- The maximum cask outer surface temperature is considered for the cask entire outer surface facing the barrier.

- An emissivity of 0.9 is considered for the cask outer surface. Based on discussion in Section A.3.2.1, the emissivities for shield shell and finned shell are 0.9 and 0.7, respectively. The assumed emissivity of 0.9 maximizes the radiation heat from the cask toward the personnel barrier conservatively.

The simplified heat balance for the personnel barrier is as follows.

$$q_{in,rad} = q_{out,rad}$$

$$q_{in,rad} = \frac{\sigma\left(T_{shell}^{\ 4} - T_{PB}^{\ 4}\right)}{\dfrac{1-\varepsilon_{shell}}{\varepsilon_{shell}\,A_{shell}} + \dfrac{1}{F_{PB-shell}\,A_{PB}} + \dfrac{1-\varepsilon_{PB}}{\varepsilon_{PB}\,A_{PB}}}$$

$q_{out,rad} = q_{1,rad,amb} + q_{2,rad,amb}$, $q_{1,rad,amb} = 0$ (conservatively, omitted in this analysis)

$$q_{2,rad,amb} = \frac{\sigma\left(T_{PB}^{\ 4} - T_{\infty}^{\ 4}\right)}{\dfrac{1-\varepsilon_{PB}}{\varepsilon_{PB}\,A_{PB}} + \dfrac{1}{F_{PB-\infty}\,A_{PB}}}$$

σ = Stefan-Boltzmann constant = 0.119E-10 (Btu/hr-in^2-°R^4)
T_{shell} = maximum cask shield shell temperature (°R)
T_{PB} = maximum personnel barrier temperature (°R)
T_{∞} = ambient temperature = 100 °F = 560 °R
ε_{shell} = emissivity of TC outer surface = 0.9
ε_{PB} = emissivity of personnel barrier SS304 = 0.587 (see discussion in Section A.3.2.1)
$F_{PB\text{-}shell}$ = view factor from personnel barrier to cask shield shell
$F_{PB\text{-}\infty}$ = view factor from personnel barrier (not facing cask) to ambient = 1.0
A_{PB} = surface area of personnel barrier (in^2)
A_{shell} = surface area of cask shield shell (in^2)

The dimensions of the cask shield shell (Dshell) and personnel barrier (lPB) are 97.75" and 52.38", respectively as shown in the drawings in Chapter A.1, Appendix A.1.4.10.

$$\frac{A_{shell}}{A_{PB}} = \frac{\pi D_{shell}/2}{l_{PB}} = \frac{\pi \times 97.75/2}{52.38} = 2.931$$

The view factor of a long strip element to a parallel cylinder is given in [21], Chapter7, Appendix B, Page 7.80 as follows. The dimensions are defined in Figure A.3–9.

$$F_{d1-2} = \frac{Y}{X^2 + Y^2}$$

With
Y = y/r, X = x/r
y = 58" (See the drawings in Appendix A.1.4.10)
r = 97.75/2 = 48.875" (See the drawings in Appendix A.1.4.10)

Integration of the above incremental view factor over the length of the strip barrier gives the view factor of the strip to the cask.

$$F_{1-2} = \frac{1}{l_{PB}} \int_0^{l_{PB}} \left(\frac{Y}{X^2 + Y^2} \right) dx$$

Considering L=lPB/r and dX=dx/r, gives the view factor of the personnel barrier to the cask.

$$F_{1-2} = \frac{1}{L} \int_0^{L} \left(\frac{Y}{X^2 + Y^2} \right) dX = \frac{1}{L} \left(\tan^{-1} \frac{L}{Y} \right) = \frac{r}{l_{PB}} \tan^{-1} \left(\frac{l_{PB}}{y} \right) = 0.685$$

Since the personnel barrier has an open area of 80%, a factor of 0.2 should be considered to calculate the view factor of the personnel barrier mesh to the cask.

$$F_{PB-shell} = F_{1-2} \times 0.2 = 0.137$$

The substitution of the above values in the heat balance of the personnel barrier gives the maximum temperature of the personnel barrier as *152*°F.

A.3.3.1.2.1 Personnel Barrier and Hot Stream from Cask

The assumption that the personnel barrier is not exposed to hot air stream from the cask shield shell can be justified by calculation of the thermal boundary layer thickness around the lower half of the cask. This calculation demonstrates that the thermal boundary layer thickness is smaller than the shortest distance between the personnel barrier and the cask and therefore the personnel barrier remains out of the hot air stream from the cask.

The large diameter of the cask and the relative large temperature difference between the cask outer surface and ambient temperature suggest that the free convection over the cylinder is a turbulent flow.

The theoretical and experimental studies of the free convection and its related thermal boundary layer thickness are widely available and well documented ([43], [45], [46], and [47]). These correlations can be used to determine the free convection thermal boundary layer thickness over the horizontal MP197HB cask. These studies show that the thickness of the free convection thermal boundary layer is inversely proportional to a power of the local Nusselt number for laminar or turbulent flows.

$$\frac{\delta}{x} = \frac{C f(Pr)}{Nu_x^{\ m}} \qquad (1)$$

δ = local thermal boundary layer thickness
x = local position
f(Pr) = a function of Prandtl number
Nu_x = local Nusselt number
m and c = constant values

For instance, the theoretical calculation in reference [46] determines the following equation for a free convection laminar flow over flat vertical plates.

$$\frac{\delta}{x} = \frac{2}{Nu_x}$$

This equation means that c = 2, f(Pr) =1, and m = 1 in equation (1).

The correlations to determine the free convection thermal boundary layer thickness and local Nusselt number over a vertical flat plate in turbulent flow are documented in references [44] and [45]. These correlations are shown below.

$$\frac{\delta_x}{x} = 0.565\, Gr_x^{-0.1}\, Pr^{-8/15} \left(1 + 0.494\, Pr^{2/3}\right)^{0.1} \qquad [44] \qquad (2)$$

$$Gr_x = \frac{g\beta\Delta T\, x^3}{\upsilon^2}$$

$$Nu_x = 0.0295 \left[\frac{Pr^7}{\left(1 + 0.494\, Pr^{2/3}\right)^6}\right]^{1/15} Gr_x^{2/5} \qquad [45]$$

$$Nu_L = 0.834\, Nu_x \qquad [45] \qquad (3)$$

An examination of the above equations shows that the thermal boundary layer thickness is reversely proportional to the $Nu_x^{0.25}$ for turbulent free convection over a vertical flat plate.

Considering the relationship between the thermal boundary layer thickness and the local Nusselt number, the boundary layer thickness over a horizontal cylinder in free convection turbulent flow can be determined using the correlations over a vertical flat plate and the inverse ratio of the local Nusselt numbers. Since the correlations for the average Nusselt numbers of free convection for vertical flat plates and horizontal cylinders are known better than the local Nusselt numbers, the ratio of the local Nusselt numbers are extended to include the average Nusselt numbers and avoid elimination of any functions related to Prandtl number.

$$\frac{\delta_{D0}}{\delta_x} = \frac{\delta_L}{\delta_x} \cdot \frac{\delta_D}{\delta_L} \cdot \frac{\delta_{D0}}{\delta_D}$$

$$\frac{\delta_{D0}}{\delta_x} = \left(\frac{Nu_x}{Nu_L}\right)^p \left(\frac{Nu_L}{Nu_D}\right)^q \left(\frac{Nu_D}{Nu_{D0}}\right)^r \qquad (4)$$

δ_{D0} = thermal boundary layer thickness at midsection of a horizontal cylinder ($\alpha = 0$)
δ_x = thermal boundary layer thickness at height of x for a vertical flat plate
Nu_x = local Nusselt number for a vertical flat plate at height x
Nu_L = average Nusselt number for a vertical flat plate at height L
Nu_{D0} = local Nusselt number at midsection of a horizontal cylinder ($\alpha = 0$)
Nu_D = average Nusselt number for a horizontal cylinder with outer diameter of D
p, q, and r = constant parameters

Based on the discussion for the thermal boundary layer thickness over a vertical flat plate above, the constant parameter p in equation (4) is 0.25.

An extensive study on free convection over large diameter, horizontal cylinders conducted in reference [48] shows that the onset of turbulent transition occurs at a point passing the midsection of the cylinder by five degree even for large Rayleigh numbers so that the free convection over the lower half of the cylinder remains laminar.

Since the personnel barrier designed for MP197HB cask is extended only to the midsection of the cask, the correlations for free convection laminar flow over horizontal cylinders can be used to determine the thermal boundary layer thickness at this location.

The free convection local Nusselt number over a horizontal cylinder in laminar flow in air is given in reference [47] as follows.

$$Nu_{D\alpha} = 0.604\, Gr_D^{1/4}\, \phi(\alpha) \qquad [47]$$

$$Gr_D = \frac{g\beta\Delta T\, D^3}{\upsilon^2}$$

α	-90°	-60°	-30°	0°	30°	60°	75°	90°
$\phi(\alpha)$	0.76	0.75	0.72	0.66	0.58	0.46	0.36	0
	Bottom half			Top half				

The local Nusselt number at the midsection of the cylinder at $\alpha = 0$ is:

$$Nu_{D0} = 0.604\, Gr_D^{1/4} \times 0.66$$

Based on the above correlation, the average Nusselt number over the horizontal cylinder is:

$$Nu_D = \frac{1}{180}\int_{-90}^{90} Nu_{D\alpha}\, d\alpha = 0.604\, Gr_D^{1/4} \times \frac{1}{180}\int_{-90}^{90} \phi(\alpha)\, d\alpha$$

The integration of $\phi(\alpha)$ over the range of -90° to 90° performed using the data in the above table gives:

$$Nu_D = 0.604\, Gr_D^{1/4} \times 0.6025$$

Comparison of the correlations for NuD0 and NuD gives:

$$Nu_D = \frac{0.6025}{0.66} Nu_{D0} = 0.913\, Nu_{D0} \qquad (5)$$

Since the equation (5) is based on free convection laminar flow, the constant parameter r in equation (4) is equal to 1.

The ratio of the average Nusselt numbers for vertical flat plate and horizontal cylinder can be determined using the corresponding correlations shown in Section A.3.3.1.1.

The thickness of the boundary layer at the midsection of the cask can be determined by substitution of the correlations for the local and average Nusselt numbers into equation (4). The height (L) of the vertical flat plate can be set equal to the outer diameter of the cask (D) for this

evaluation. Average of the cask outer surface and ambient temperatures are considered in calculation of the Nusselt numbers.

As seen above, the correlations for the local and average Nusselt numbers depend on the Grashof and Prandtl numbers, which in turn depend on the cask outer surface temperature. A sensitivity analysis is performed to cover the effects of a wide range of cask temperatures from 200°F to 500°F on the thickness of free convection thermal boundary layer at the midsection of the cask. This sensitivity analysis starts with variation of Grashof and Prandtl numbers as summarized in the following table.

Variation of Grashof, Prandtl, and Rayleigh Numbers

T_∞ =100°F
For L=D

T_{cask}	T_{cask}	T_∞	T_{avg}	β	ν	Gr	Pr	Ra
(F)	(K)	(K)	(K)	(1/K)	(m^2/s)	(---)	(---)	(---)
200	367	311	339	2.95E-03	2.235E-05	4.931E+10	0.71	3.490E+10
300	422	311	367	2.73E-03	2.849E-05	5.609E+10	0.70	3.948E+10
400	478	311	394	2.54E-03	3.516E-05	5.135E+10	0.70	3.602E+10
500	533	311	422	2.37E-03	4.232E-05	4.415E+10	0.70	3.091E+10

The values in the above table are calculated based on air properties shown in Section A.3.2.1, Item 16, at the average air temperature. As seen in the above table, the Grashof number varies between 5.6E10 and 4.4E10, the Prandtl number varies between 0.70 and 0.71, and the Rayleigh number varies between 3.1E10 and 4.0E10 for the cask outer surface temperatures between 200°F and 500°F. Since the variation of Prandtl is relative small, an average Prandtl number of 0.70 is considered in the sensitivity analysis to calculate the average Nusselt numbers for a vertical flat plate (NuL) and a horizontal cylinder (NuD). To bound the variation of the Rayleigh number conservatively, the average Nusselt numbers NuL and NuD are evaluated for a wider range between 1E10 and 1E11.

As shown in Section A.3.3.1.1, the correlation for NuL depends on C_t^v and f factors, which in turn depend on Prandtl number and surface temperature, respectively. C_t^v is a weak function of Prandtl number. The variation of the f factor is determined for a cask outer surface temperature from 200°F to 500°F. The variations of these values are summarized in the following table.

Variation of C_t^v and f in Calculation of Nu_L

T_∞ =100°F

Pr	C_t^v	T_{cask}	f
(---)	(---)	(°F)	(---)
0.70	0.103	200	1.014
0.71	0.103	300	1.028
Average	0.103	400	1.042
		500	1.056
		Average	1.035

The average values of C_t^v and f from the above table are considered in calculation of NuL. The variation of the average Nusselt numbers NuL and NuD and their ratios summarized in the table below.

Variation of Nu_L/Nu_D

Vertical Flat Plate
Pr = 0.70

Ra	Nu^T	Nu_l	C_t^v	f	Nu_t	Nu_L
(---)	(---)	(---)	(---)	(---)	(---)	
1.00E+10	162.86	163.9	0.103	1.035	208.5	216.0
2.00E+10	193.67	194.7	0.103	1.035	275.0	280.5
5.00E+10	243.53	244.5	0.103	1.035	384.0	388.1
8.00E+10	273.89	274.9	0.103	1.035	452.4	456.1
1.00E+11	289.61	290.6	0.103	1.035	488.5	492.0

Horizontal Cylinder
Pr = 0.70

Ra	Nu^T	F	Nu_l	$\overline{C}_t$	Nu_t	Nu_D	Nu_L/Nu_D
(---)	(---)	(---)	(---)	(---)	(---)	(---)	(---)
1.00E+10	125.73	0.940	126.7	0.103	221.9	222.0	0.973
2.00E+10	149.51	0.942	150.5	0.103	279.6	279.6	1.003
5.00E+10	188.00	0.944	188.9	0.103	379.5	379.5	1.023
8.00E+10	211.44	0.945	212.4	0.103	443.8	443.8	1.028
1.00E+11	223.58	0.945	224.5	0.103	478.1	478.1	1.029
						Average	1.011

As shown in the above table, the ratio of NuL to NuD varies between 0.973 and 1.029 for the range of considered Rayleigh numbers. An average value of 1.011 is considered for this ratio to use in equation (4). Since this ratio is close to one, the constant parameter q in equation (4) does not have any significant effect and can be omitted.

Substitution of the local and average Nusselt number ratios from equation (3), equation (5), and the table of NuL/NuD variations into equation (4) gives:

$$\delta_{D0} = (1/0.834)^{0.25} \times 1.011 \times 0.913\ \delta_x$$

Using δx from equation (2) in the above equation determines the range of boundary layer thickness at the midsection of the cask as summarized in the following table.

Thickness of the Thermal Boundary Layer

T_∞=100°F
L = D = 97.75"

T_{cask}	T_{cask}	T_∞	T_{avg}	Gr	Pr	δ_x/L	δ_x	δ_{D0}
(°F)	(K)	(K)	(K)	(---)	(---)	(---)	(in)	(in)
200	367	311	339	4.931E+10	0.71	0.060	5.9	**5.7**
300	422	311	367	5.609E+10	0.70	0.059	5.8	**5.6**
400	478	311	394	5.135E+10	0.70	0.060	5.9	**5.7**
500	533	311	422	4.415E+10	0.70	0.061	6.0	**5.7**

As seen in the above table, the variation of the thermal boundary layer thickness is small and its maximum value at the midsection of the cask is 5.7" for a uniform cask surface temperature of 500°F. Based on data shown in Section A.3.3.1.2, the shortest distance between the outer surface of the cask and the personnel barrier is over 9".

Shortest distance = distance to cask centerline – cask OD/2 = 58 – 97.75 / 2 = 9.125"

The conservatively evaluated boundary layer thickness of 5.7" is much smaller than shortest distance between the outer surface of the cask and the personnel barrier. Therefore, the personnel barrier remains out of the hot air streams flowing around the cask outer surface.

A.3.3.1.3 Effective Thermal Properties in MP197HB TC Model

1) Effective Heat Transfer Coefficient for External Fins

To reduce the complexity of the TC model, an effective heat transfer coefficient is calculated for the external fins based on the geometry shown in the drawings in Chapter A.1, Appendix A.1.4.10. Circular external fins are welded to an aluminum shell which will be installed over the outer surface of the TC shield shell to enhance heat dissipation for heat loads over 26 kW. An effective heat transfer coefficient is calculated for the external fins which includes the convection and radiation heat transfer to ambient. The following dimensions are considered for the fins.

- Fin height = 3.0"
- Fin thickness = 0.156"
- Fin pitch = 1.0"

A sub-model of the TC outer surface is developed for this purpose using ANSYS [27].

This sub-model considers a 30 degree segment of the aluminum shell with three circular external fins. Figure A.3–10 shows the sub-model of the finned shell.

Convection boundary conditions are applied over the outer surfaces of the fins in the model using surface load (SF) commands in ANSYS [27]. SHELL57 elements are overlaid on the external surfaces of the fins to create radiation super-element. The radiation shell elements are shown in Figure A.3–10. Thermal radiation from the outer surfaces is modeled using /AUX12 processor. Ambient temperatures of 100°F, -20°F, and -40°F are considered for convection and radiation.

An emissivity of 0.70 is considered for the anodized aluminum for exposed finned surfaces as shown in Section A.3.2.1.

Fixed temperature boundary conditions are applied over the inner surface of the aluminum shell. The amount of heat dissipation is retrieved from the model using reaction solution command (PRRSOL) in ANSYS [27]. The effective heat transfer coefficient is calculated as follows.

$$h_{eff} = \frac{Q_{react}}{A_{eff}(T_s - T_{amb})}$$

h_{eff} = effective heat transfer coefficient over finned surface (Btu/hr-in^2)
Q_{react} = heat input entering the cask shield shell (reaction solution) retrieved from model (Btu/hr)
T_s = shield shell inner surface temperature (fixed temperature boundary conditions) (°F)
T_{amb} = ambient temperature (°F) = 100°F, -20°F, and -40°F
A_{eff} = outer surface area of the un-finned shield shell (in^2).

Since the h_{eff} will be applied over the un-finned surface of the aluminum shell, A_{eff} is the area of the un-finned surface.

$$A_{eff} = \pi D_o (3 \times fin\ pitch)(30/360) = \pi \times 98.25 \times 3 \times 1.0 \times (30/360) = 77.2 \text{ in}^2$$

Convection heat transfer coefficients are calculated using correlations from Rohsenow Handbook [21], page 4.39 and 4.40, equations 4.68 to 4.70b. The correlations used for convection coefficients are:

$$Nu = \frac{h\,S}{k}; \qquad \zeta = \frac{D_o}{D_f}; \qquad Ra = \frac{g\beta(T_w - T_{amb})S^3}{\nu\alpha}\frac{S}{D_f}; \ \mathrm{Pr} = \frac{\nu}{\alpha}$$

D_o = outer diameter of un-finned surface = 98.25"
D_f = outer diameter of circular fins = (98.25 + 2×3.0) = 104.25"
S = fin pitch = 1.0"
g = gravitational constant =9.81 (m/s^2)
β = expansion coefficient = 1/T (1/K)
T = absolute temperature (K)
ν = kinematic viscosity (m^2/s)
α = thermal diffusivity (m^2/s)
k = air conductivity (W/m-K)

On fin tips:

$Nu = c\ Ra^b$ for $2 \le Ra \le 10^4$ with c and b defined in Section A.3.2.1 material #. 22.

On fin lateral surfaces together with the supporting shell:

$$Nu = C_0\, Ra_0^{\,p}\left\{1 - \exp\left[-\left(\frac{C_1}{Ra_0}\right)^{C_2}\right]\right\}^{C_3} \qquad \text{for } 1.0 \le \frac{D_f}{D_o} \le 1.67$$

where $C_0 = -0.15 + 0.3\zeta + 0.32\zeta^{16}$ $\qquad C_1 = -180 + 480\zeta - 1.4\,\zeta^{-8}$
$C_2 = 0.04 + 0.9\zeta$ $\qquad C_3 = 1.3\,(1 - \zeta) + 0.0017\,\zeta^{-12}$
$p = 0.25 + C_2\,C_3$ $\qquad Ra_0 = Ra/\zeta$

Properties are evaluated at wall temperature as required in [21]. Air properties used for these correlations are listed in Section A.3.2.1, material # 16.

The results for the effective heat transfer coefficient are summarized in Section A.3.2.1 material # 22, 23, and 24 for ambient temperatures of 100°F, -20°F, and -40°F, respectively.

2) Effective Conductivity for Helium Gap between DSC and TC/Sleeve

Effective conductivities are calculated for helium between the DSC and the TC inner shell / internal sleeve to account for conduction and radiation between these components. Based on discussion in Section A.3.2.1, a conservative emissivity of 0.587 is considered for the DSC shell and TC inner shell.

The inner surface of the internal sleeve is anodized. Based on discussion in Section A.3.2.1, a conservative emissivity of 0.7 is considered for the anodized/painted surface of the internal sleeve.

The effective conductivity of helium within the gap between the DSC shell and TC inner shell is calculated based on a detailed sub-model of this region. This sub-model considers a 10" high, 30 degree segment of the shells. Conductivity of helium is considered for the gap between the shells. Radiation between surfaces is modeled using /AUX12 processor. Figure A.3–11 shows the sub-model of the DSC shell and the TC inner shell.

In the DSC/TC sub-model, a heat flux of 2.813 Btu/hr-in^2 equivalent to 29.2 kW (see Section A.3.3.1.1) is applied on the radial surface of the innermost shell (DSC shell) and fixed temperature boundary conditions are applied over the radial surface of the outermost shell (TC inner shell).

The nodes of the gap between the DSC shell and TC inner shell build up the radiation super element (MATRIX50). To avoid convergence problems, the heat flux or fixed temperature boundary conditions are not applied directly on the nodes of the radiation super element. Instead the heat flux is applied on the innermost nodes of the DSC shell and the fixed temperatures are applied on the outermost nodes of the TC shell.

The effective conductivity is calculated as follows.

$$k_{eff} = \frac{(q_{react} \times 360/30)\ \ln(D_{i,TC}/D_{o,DSC})}{2\pi \times 10 \times (T_{DSC} - T_{TC})}$$

Where,
q_{react} = reaction solution retrieved from the model (Btu/hr)
$D_{i,TC}$ = inner diameter of TC inner shell = 70.5"
$D_{o,DSC}$ = outer diameter of DSC for 69BTH, 37PTH, 32PTH, and 32PTH1 = 69.75"
T_{TC} = temperature of the TC inner shell innermost nodes (°F)
T_{DSC} = average temperature of DSC shell (°F)

The conductivity of SA-240, type 304 is considered for the TC inner shell in this sub-model. Since the TC inner shell material is SA-203 and has higher conductivity than SA-240, type 304, this approach is conservative.

Due to high conductivity of the metallic shells, the temperature gradient across the shells is very small (< 1°F). Therefore the actual temperature gradient across the gap is slightly lower than the temperature gradient between the shells ($T_{DSC} - T_{TC}$) considered in the above equation. This results in a slightly underestimated effective conductivity across the gap, which is conservative for the purpose of this calculation.

The average temperature of the DSC shell is retrieved from the model using "ETABLE" commands in ANSYS [27]. The fixed temperature boundary condition applied on the outermost node of TC shell is considered as TC temperature.

The q_{react} depends on the applied heat flux. Since the effect of q_{react} is accounted for in the equation for k_{eff}, the calculated k_{eff} values can be used for other heat loads considered in this analysis.

The effective conductivity values for the helium within the gap between the DSC shell and the TC inner shell are summarized in Section A.3.2.1, material # 25.

The calculated effective conductivity in Section A.3.2.1, material # 25 is applied only in radial direction for the gap between the DSC shell and the TC inner shell. The conductivity in axial direction is set equal to helium conductivity for conservatism.

As shown in Section A.3.3.1.1, the gap size between the 61BTH or 61BT DSC shell and the internal sleeve is equal to the gap size between the large diameter DSC shells (69BTH, 37PTH, 32PTH, and 32PTH1) and the TC inner shell. Since the assumed emissivity of 0.587 for TC inner shell is lower than the emissivity of anodized aluminum, the above effective conductivity calculated for the gap between the large diameter DSC and TC inner shell can be used conservatively for the gap between the DSC and the internal sleeve for DSC types 61BTH and 61BT.

For small diameter DSC types, 32PT, 24PTH, and 24PT4, an effective conductivity is calculated for the gap between the DSC shell and TC internal sleeve using the same methodology described above with the following data.

$D_{i,sleeve}$ = inner diameter of TC internal sleeve = 68.0"
$D_{o,DSC}$ = outer diameter of small diameter DSC types = 67.19"
ε_{DSC} = 0.587 (emissivity of steel or stainless steel, see Section A.3.2.1)
ε_{sleeve} = 0.7 (emissivity of anodized aluminum, see Section A.3.2.1)

The effective conductivity values for the helium within the gap between the small DSC shell and the TC internal sleeve are listed in Section A.3.2.1, material # 26.

This analysis uses the effective conductivity values from Section A.3.2.1, material # 26 for the gaps between the DSC shell and TC internal sleeve for 32PT, 24PTH, and 24PT4 DSC types only in radial direction. The conductivity in axial direction is set equal to helium conductivity for conservatism.

3) Effective Conductivity for DSC Top and Bottom Cover Plates

Axial air gaps of 0.0625" are considered between the carbon steel/stainless steel shield plugs and cover plates for all DSC types. These gaps account for contact resistance and fabrication imperfections between these components and adjacent plates. In addition, axial gaps of 0.025" are considered on both sides of lead shield plugs for 24PT4 DSC.

For simplification of the model, the axial air gaps of 0.0625" are integrated into DSC bottom shield plug and DSC top inner cover plate for all DSC types except for 24PT4.

Single axial air gaps of 0.0625" are integrated into DSC bottom inner cover plate and DSC top outer cover plate for 24PT4 DSC. The axial gaps of 0.025" are also integrated into the lead shield plugs of 24PT4 DSC.

An effective conductivity in the axial direction is calculated for these components. The conductivities of these components remain unchanged in the radial direction.

The gaps and the plates build up serial thermal resistances in the axial direction. The effective conductivity through these serial pieces is:

$$k_{eff} = \frac{t_{plate} + n \cdot t_{gap}}{\frac{t_{plate}}{k_{plate}} + \frac{n \cdot t_{gap}}{k_{air}}}$$

Where,
k_{eff} = effective conductivity in axial direction (Btu/hr-in-°F)
t_{plate} = thickness of targeted plate
(bottom shield plug and top inner cover plate for all DSC types except 24PT4)
(bottom inner cover plate, top outer cover plate, and lead shield plugs for 24PT4 DSC)
t_{gap} = 0.0625" between steel shield plugs and stainless steel plates
0.025" between lead shield plugs and stainless steel plates
k_{plate} = conductivity of A36 steel for bottom shield plug (all DSC except 24PT4)
conductivity of SS304 steel for top cover plate (all DSC except 24PT4)
conductivity of SS316 steel for top outer cover and bottom inner cover plates for 24PT4
conductivity of lead for lead shield plugs of 24PT4 DSC (Btu/hr-in-°F)
k_{air} = conductivity of air (Btu/hr-in-°F)
n = number of gaps
= 2 for gaps between shield plugs and cover plates for all DSC types except 24PT4
=1 for gap between top shield plug and outer cover plate for 24PT4
=1 for gap between bottom shield plug and outer cover plate for 24PT4
=2 for gaps between lead shield plugs and encapsulating stainless steel plates for 24PT4

The conductivity values are taken from Section A.3.2.1.

Based on data in Table A.3–1, the smallest DSC shield plug thickness is 3" and the smallest DSC top cover plate thickness is 0.75". These values are considered to calculate the axial effective

conductivities conservatively for all DSC types except for 24PT4. The thicknesses of cover plates for 24PT4 are as follows.

24PT4 DSC top outer cover plate =1.25"
24PT4 DSC bottom inner cover plate =2.0"
24PT4 DSC top lead shield plug = 3.38"
24PT4 DSC bottom lead shield plug = 2.88"

The axial effective conductivities for bottom shield plug and top inner cover plates of all DSC types except 24PT4 are listed in Section A.3.2.1, material # 27.

The axial effective conductivities calculated for top/bottom inner cover plates and lead shield plugs of 24PT4 DSC are listed in Section A.3.2.1, material # 28 and 29, respectively.

4) Effective Conductivity for TC Slide Rails

A helium gap of 0.01" is considered between the slide rail and DSC shell to account for the contact resistance. For simplification of the model, this gap is integrated into the slide rail model and an effective conductivity is calculated for this component. The calculated effective conductivity for the slide rail is applied conservatively in all directions.

The gap and the slide rail built up serial thermal resistances along the rail height. The effective conductivity through these serial pieces is:

$$k_{eff} = \frac{t_{rail} + t_{gap}}{\frac{t_{rail}}{k_{rail}} + \frac{t_{gap}}{k_{He}}}$$

Where,
k_{eff} = effective conductivity (Btu/hr-in-°F)
t_{rail} = thickness of TC slide rail = 0.12"
t_{gap} = thickness of gap = 0.01"
k_{rail} = conductivity of TC slide rails (Nitronic 60)
k_{He} = conductivity of helium (Btu/hr-in-°F)

The conductivity values are taken from Section A.3.2.1. The effective conductivities for the TC slide rail are listed in Section A.3.2.1, material # 30.

5) Effective Conductivity for Internal Sleeve

The designed shape of the aluminum internal sleeve is shown in the drawings in Chapter A.1, Appendix A.1.4.10. As seen in this drawing, there is virtually no gap between the segments of the internal sleeve. A different shape is considered for the internal sleeve in the TC model. The assumed shape includes 120 individual aluminum pieces with 39 radial gaps and three axial gaps. The thicknesses of the radial and axial gaps are respectively 0.25" and 0.188" as shown in Figure A.3–12. In addition, the material properties of the inner shell elements in contact with the cask slide rails are changed to those of helium to avoid any direct conduction between these two

components. Since the considered shape of the internal sleeve in the TC model includes more gaps, it is conservative to use it for thermal analysis of the transport cask under NCT.

To reduce the complexity of the TC model, an effective conductivity is calculated for the assumed shape of the internal sleeve shown in Figure A.3–12. The following dimensions are considered for the internal sleeve in the thermal model.

Sleeve ID =	68 in.
Sleeve OD =	70.5 in.
Total length =	196 in.
No. of pieces in axial direction =	4 in.
No. of segments in radial direction =	40 in.
Axial gap =	0.188 in.
Radial gap =	0.25 in.

Axial Effective Conductivity

Along one segment of the sleeve, there are four sections of aluminum pieces with 0.1875" gaps between them in the axial direction (see Figure A.3–12, at bottom). The thermal resistance through these serial pieces is:

$$R_{axl,1} = 4\,R_{Al} + 3\,R_{gap}$$

$$R_{axl,1} = \frac{L_t}{k_{eff}.A}; \qquad R_{Al} = \frac{L_{Al}}{k_{Al}.A}; \qquad R_{gap} = \frac{L_{gap}}{k_{He}.A}$$

$L_t = 196$"
$L_{gap} = 0.1875$"
$L_{Al} = (196 - 3\times0.1875) / 4 = 48.86$"
k_{eff} = effective conductivity of one axial segment (Btu/hr-in-°F)
k_{Al} = conductivity of aluminum (Btu/hr-in-°F)
k_{He} = conductivity of helium (Btu/hr-in-°F)
A = surface area of one segment (in^2)

Rearranging the above equations gives:

$$k_{eff,axl,1} = \frac{L_t}{\left(\frac{4\,L_{Al}}{k_{Al}} + \frac{3\,L_{gap}}{k_{He}}\right)}$$

The axial segments are parallel to each other. Due to low conductivity of helium in comparison to aluminum, helium conductivity can be conservatively ignored. The total axial effective conductivity is then proportional to the ratio of the surface area for the aluminum segments in cross section to the total cross-sectional area of the internal sleeve, which is equivalent to the ratio of aluminum segment angle to the nominal angle (see Figure A.3–12).

$$k_{eff,axl} = k_{eff,axl,1} \times \frac{\theta_{Al}}{\theta_{nom}}$$

with $\theta_{nom} = \frac{360}{40} = 9°$

$$\theta_{Al} = \theta_{nom} - \frac{gap_{rad}}{D_{o,sleeve}/2} \times \frac{180}{\pi} = 8.6°$$

gap_{rad} = radial gap =0.25"
$D_{o,sleeve}$ = 70.5"

Radial Effective Conductivity

Forty aluminum segments in the radial direction build up parallel resistances perpendicular to the direction of heat flow from the center to the periphery. Again, the total radial effective conductivity can be set proportional to the ratio of the angle for one aluminum segment (θ_{Al}) to the nominal angle of each segment (θ_{nom}).

$$k_{eff,rad} = k_{Al} \times \frac{\theta_{Al}}{\theta_{nom}}$$

The effective conductivity values calculated for the sleeve are summarized in Section A.3.2.1, material # 31.

A.3.3.1.4 69BTH DSC Model

The following assumptions and conservatism are considered for the 69BTH DSC model:

The fuel assemblies contained in the DSC basket are intact fuel assemblies. Since the damaged fuel assemblies are loaded in the outermost fuel compartment cells, they do not affect the maximum temperatures or the maximum temperature gradients in this evaluation. A sensitivity analysis is conducted to bound the effects of the damaged fuel assemblies on the thermal performance of the MP197HB cask considering the worst case condition, in which the high burnup damaged fuel assemblies becomes rubble. This sensitivity analysis is discussed in Section A.3.6.9.

No convection is considered within the canister cavity.

Only helium conduction is considered from the basket upper surface to the canister top shield plug.

Radiation is considered only implicitly between the fuel rods and the fuel compartment walls in the calculation of effective fuel conductivity. No other radiation heat exchange is considered within the basket model.

Active fuel length for BWR fuel assemblies is 144" [11] and starts about 7.5" from the bottom of the basket [11]. The total length of the basket assembly is 176.5".

The following gaps are considered in the DSC canister/basket model at thermal equilibrium:

a) 0.30" diametrical hot gap between the basket outer surface and the canister inner surface. This gap is justified in Section A.3.6.7.3.

b) 0.125" axial gap between the bottom of the basket and the DSC bottom inner cover plate

c) 0.01" gap between any two adjacent plates or components in the cross section of the basket.

d) 0.125" gap in axial direction between the aluminum rail pieces.

e) 0.01" gap between the sections of the paired aluminum and poison plates in axial direction.

f) 0.1" gap between the two small aluminum rails at the basket corners.

g) 0.1" gap between the two pieces of large aluminum rails at 0° -180° and 90° -270° orientations.

h) 0.0625" gap between DSC shield plugs and DSC cover plates for calculation of effective conductivities in axial direction.

No gap is considered between the paired poison and aluminum plates. The 0.01" gaps considered on either side of the paired plates account for the thermal resistance between the multiple plates. This assumption is justified in Section A.3.6.7.4.

The gaps considered between the aluminum rail segments are larger than the nominal cold gaps and are therefore conservative. The axial gaps considered between the aluminum rail pieces in the axial direction are larger than the tolerances considered for the rails and are therefore conservative.

The benchmarking of finite element models against test data in [35] shows that the 0.01" gaps considered between adjacent plates or components in the cross section of the basket account conservatively for the tolerances and contact resistances.

In the fabrication, the diametrical gap between the basket and canister shell assigned as gap "a" above is controlled by dimensional inspections of the diameters of the basket and canister shell.

The structure of the 69BTH basket is similar to the 61BT and 61BTH baskets approved in accordance with 10 CFR 72 regulations. The uniform gap of 0.01" assigned as gap "c" above considered in the thermal model between any two adjacent components in the cross section of the 69BTH basket has the same size as the corresponding gaps considered in the 61BT and 61BTH baskets. In practical terms, fabrication of the 69BTH basket requires very tightly compressed assembly in order to fit the basket into the shell. Interfaces are formed as components and parts are assembled. The fit between mating components, for example between fuel compartment tubes and adjacent sheets, cannot practically be measured. Fabrication methods provide for the tightest practical assembly of these parts.

The gaps between adjacent components are related only to the flatness and roughness tolerances of the plates. The micro gaps related to these tolerances are non-uniform and provide

interference contact at some areas and gaps on the other areas as shown schematically in the figure in Section A.3.6.7.2. For the purpose of thermal evaluation, surfaces of intermittent contact between adjacent components are conservatively modeled as a uniform gap of 0.01". As shown in SAR Section A.3.6.7.4, the assumed gap size of 0.01" is approximately two times larger than the contact resistances between the adjacent components. It should be noted that for conservatism no contact pressure was considered between the components. This assumption implies that no friction exists between the components within the basket, which adds to the conservatism considered in the size of this uniform gap. In reality, there is sufficient friction that 61BT baskets have been lifted during fabrication using only the friction on the perimeter of the four-compartment subassemblies.

The 0.01" axial gaps between the sections of the paired aluminum and poison sheets assigned as gap "e" above are shown in SAR Figure A.3-17. The 0.1" gaps between the rail segments assigned as gaps "f" and "g" above are shown in SAR Figure A.3-15. These gaps are not located in the primary heat flow paths. A sensitivity analysis is performed to determine the effect of these gaps on the thermal performance. The results of this sensitivity analysis show that doubling the size of these gaps increases the maximum temperatures by less than 1 °F. Therefore, the effects of these gaps on the thermal performance are insignificant.

The thickness of paired aluminum and poison plates within the wrapped compartment blocks of 69BTH basket is 0.25". This thickness is reduced to 0.21" to accommodate for the size of the gaps and maintain the outer basket diameter contained within the DSC inner diameter. An effective conductivity is calculated for these plates in Section A.3.3.1.5 to maintain the conductivity of plates within the basket. All other dimensions are based on nominal dimensions for 69BTH basket.

Paired aluminum and poison plates are considered as one homogenized material in the 69BTH basket model. The effective conductivities for paired aluminum poison plates are calculated in Section A.3.3.1.5.

To reduce the complexity of the 69BTH basket model, the contact resistances between the DSC shield plugs and DSC cover plates are integrated into the bottom shield plug and top inner cover plate. Axial effective conductivities are calculated for top and bottom shield plugs of DSC in Section A.3.3.1.3 and listed in Section A.3.2.1. The conductivities of these components remain unchanged in the radial direction.

Decay heat load is applied as heat generation boundary conditions over the elements representing homogenized fuel assemblies. The base heat generation rate is multiplied by peaking factors along the axial fuel length to represent the axial decay heat profile. A correction factor is used to avoid degradation of decay heat load due to imperfections in application of peaking factors. The heat generation rates used in this analysis is calculated as follows.

$$\dot{q}''' = \left(\frac{q}{a^2 L_a} \times PF \right) \times CF$$

where,
q = Decay heat load per assembly defined for each loading zone
a = Width of the homogenized fuel assembly = 6.0"
L_a =Active fuel length = 144"
PF = Peaking Factor
CF = correction factor = 1.00697 for 69BTH

The base heat generation rates used in 69BTH basket model are listed in the following table.

Base Heat Generation Rates for 69BTH

Heat Load in the Model (KW)	$\dot{q}'''$ value without PF (Btu/hr-in^3)	Heat Load in the Model (KW)	$\dot{q}'''$ value without PF (Btu/hr-in^3)
0.10	0.0663	0.50	0.3314
0.25	0.1657	0.55	0.3646
0.30	0.1988	0.60	0.3977
0.40	0.2651	0.70	0.4640
0.45	0.2983		

The active fuel length for fuel assembly LaCrosse is only 85", which is significantly shorter than the other fuel assemblies considered for transport in the 69BTH DSC. The heat load of this fuel assembly fuel should be lower than the longer fuel assemblies to maintain the same temperature distribution in 69BTH DSC.

Since conduction and effective conductivities are the only heat transfer paths considered in the 69BTH DSC, the temperatures are directly proportional to the fuel assembly heat load and reversely proportional to the active fuel length and effective fuel conductivity. Therefore, the following equations determine the reduction in heat load for fuel assembly LaCrosse to maintain the 69BTH temperatures at the same level as those determined for the bounding fuel assembly.

$$\left(\frac{q}{L_a\, k_{eff}}\right)_{LaCrosse} = \left(\frac{q}{L_a\, k_{eff}}\right)_{BoundingFA}$$

$$q_{LaCrosse} = q_{boundingFA}\,\frac{L_{a,LaCrosse}}{L_{a,BoundingFA}}\cdot\frac{k_{eff,LaCrosse}}{k_{eff,boundingFA}}$$

With,
k_{eff} = effective fuel assembly conductivity (Btu/hr-in-°F)
q = Decay heat load per assembly defined for each loading zone (Btu/hr)
L_a =Active fuel length (in)
= 144 " for bounding fuel assembly
= 85" for LaCrosse fuel assembly

Based on calculations described in Section A.3.6.5.2, the transverse and axial effective conductivities of fuel assembly LaCrosse are at least 19.9% higher than those for the bounding

fuel assembly. Substitution of these values in the above equation gives the reduction of the heat load for fuel assembly LaCrosse.

$$q_{LaCrosse} = q_{boundingFA} \frac{85}{144} \times 1.199 = 0.708\ q_{bundingFA}$$

The heat load for LaCrosse fuel assembly should be reduced to 70% of the heat load for bounding fuel assembly to maintain the 69BTH DSC temperatures at the same level calculated for the bounding fuel assembly.

Axial Heat Flux Profile

In-core data from an operating BWR facility forms the basis for the evaluation. The data provides the burnup and moderator density for 25 axial locations along the length of a fuel assembly. Five fuel assemblies at different locations in the reactor core are utilized to generate a burnup (peaking factor) distribution for the assembly. The resulting axial heat flux profile is shown in Figure T.4-37 associated with Amendment 10 to Part 72 CoC 1004 for the Standardized NUHOMS® System [3].

The heat flux profile shown in Figure T.4-37 [3] is used in the thermal model of the Transnuclear, Inc. TN-68 dry transport/storage cask [36], which can accommodate BWR spent fuel with a maximum bundle average burnup of 45,000 MWd/MTU. The maximum assembly average burnup allowed in 69BTH DSCs is *70*,000 MWd/MTU, which is considerably higher than 45,000 MWd/MTU for TN-68. Reference [12] shows that at a higher burnup, the heat flux shape tends to flatten with a reduction in the maximum axial peaking factor in the middle region, and the flux shape becomes more pronounced in the fuel end regions. The reduction of the maximum axial peaking factor in a more flattened heat flux shape will result in lower fuel cladding temperatures. Therefore, the application of a heat flux shape for a lower burnup spent fuel (45,000 MWd/MTU) on a higher burnup spent fuel (*70*,000 MWd/MTD) is conservative.

Axial decay heat profile for BWR fuel assemblies is the same as the one described in Appendix T, Section T.4.6.4 associated with Amendment 10 to Part 72 CoC 1004 for the Standardized NUHOMS® System [3]. The peaking factors from Appendix T, Section T.4.6.4 [3] are converted to match the regions defined for the fuel assemblies in 69BTH DSC/basket model. These peaking factors are listed in Table A.3–2 and are shown in the following figure.

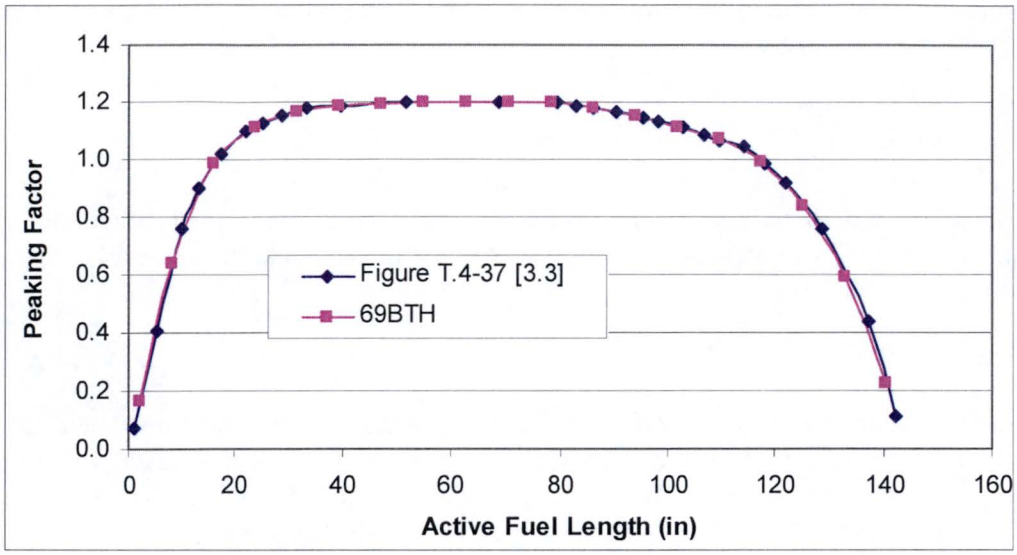

Peaking Factor Curve for BWR Fuels

As seen in Table A.3–2, the normalized area under peaking factor curve is smaller than 1.0. To avoid any degradation of decay heat load, a correction factor of 1.00697 calculated as follows is used when applying the peaking factors.

$$Nomalized\ Area\ under\ Curve = \frac{\text{Area under Axial Heat Profile}}{\text{Active Fuel Length}} = 0.99308$$

Active fuel length = 144"

$$Correction\ Factor = \frac{1}{Normalized\ Area\ under\ Curve} = 1.00697$$

The heat generating rates for the elements representing the active fuel are calculated based on the HLZCs for each basket type. The HLZCs and their restrictions for 69BTH basket are shown in the following figures.

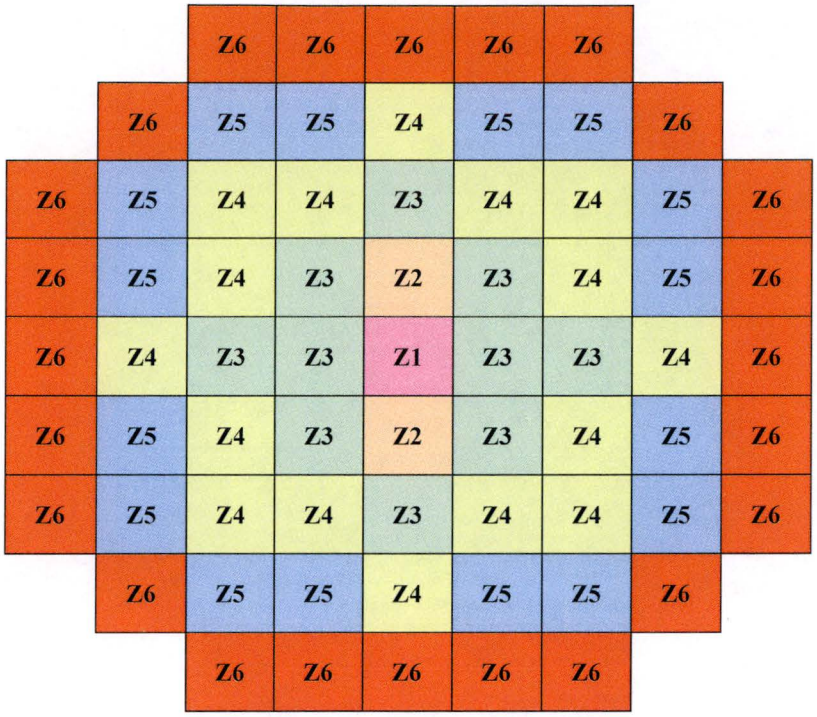

	Zone 1	Zone 2	Zone 3	Zone 4	Zone 5	Zone 6
Max. Decay Heat (kW/FA) (3)	0.10	0.27	0.30	0.40	0.55	0.45
No. of Fuel Assemblies (1)	1	2	10	16	16	24
Max. Decay Heat per Zone (kW) (3)	0.10	0.54	3.0	6.4	8.8	10.8
Max. Decay Heat per DSC (kW)	26.0 (2) (3)					

Notes: (1) Total number of fuel assemblies is 69 for HLZC # 1.
(2) Adjust payload to maintain the total DSC heat load within the specified limit.
(3) Reduce the maximum decay heat to 70% of the listed values for LaCrosse Fuel assembly. The total decay heat for LaCrosse fuel assembly is 18.2 kW per DSC for HLZC No. 1.

Heat Load Zoning Configuration No. 1 for 69BTH Basket

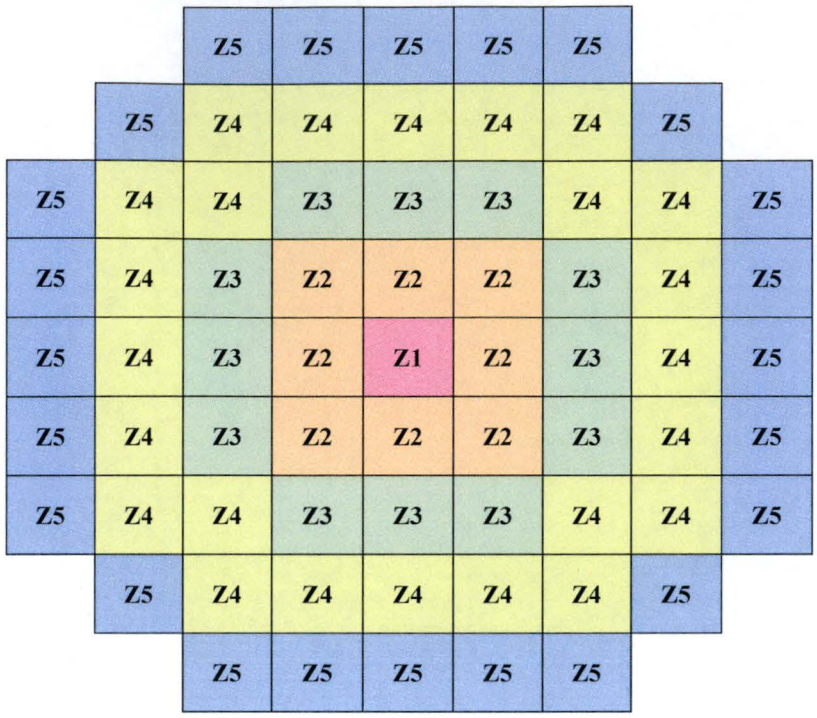

	Zone 1	Zone 2	Zone 3	Zone 4	Zone 5
Max. Decay Heat (kW/FA) (4)	0.25	0.0 (1)	0.40	0.60	0.50
No. of Fuel Assemblies (2)	1	0	12	24	24
Max. Decay Heat per Zone (kW) (4)	0.25	0	4.8	14.4	12.0
Max. Decay Heat per DSC (kW)	26.0 (3) (4)				

Notes: (1) Aluminum dummy assemblies replace the fuel assemblies in zone 2
(2) Total number of fuel assemblies is 61 for HLZC # 2
(3) Adjust payload to maintain the total DSC heat load within the specified limit
(4) Reduce the maximum decay heat to 70% of the listed values for LaCrosse Fuel assembly. The total decay heat for LaCrosse fuel assembly is 18.2 kW per DSC for HLZC No. 2.

Heat Load Zoning Configuration No. 2 for 69BTH Basket

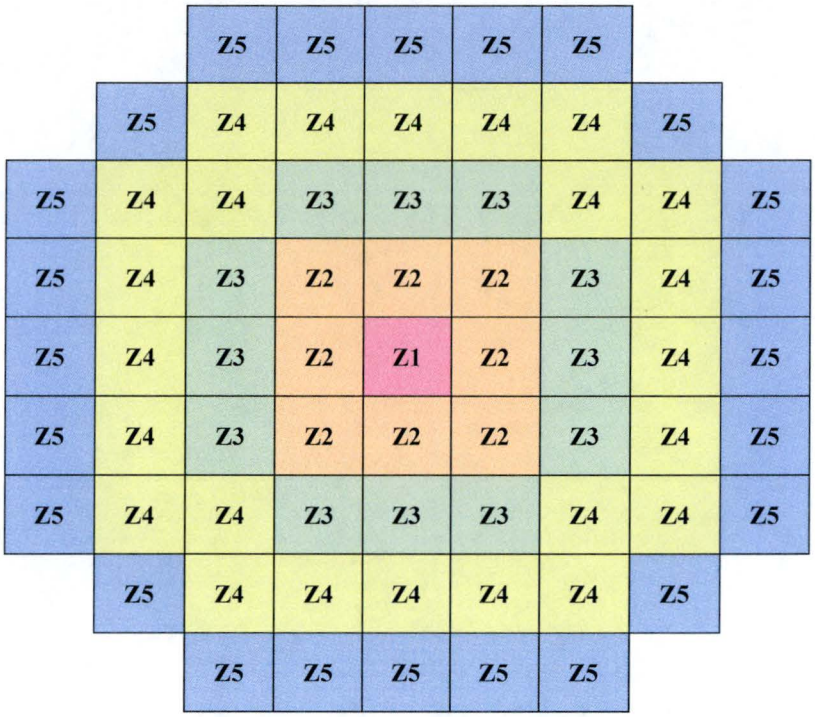

	Zone 1	Zone 2	Zone 3	Zone 4	Zone 5
Max. Decay Heat (kW/FA) (4)	0.25	0.0 (1)	0.40	0.60	0.50
No. of Fuel Assemblies (2)	1	0	12	24	24
Max. Decay Heat per Zone (kW) (4)	0.25	0	4.8	14.4	12.0
Max. Decay Heat per DSC (kW)	29.2 (3) (4)				

Notes: (1) Aluminum dummy assemblies replace the fuel assemblies in zone 2.
(2) Total number of fuel assemblies is 61 for HLZC # 3.
(3) Adjust payload to maintain the total DSC heat load within the specified limit.
(4) Reduce the maximum decay heat to 70% of the listed values for LaCrosse Fuel assembly. The total decay heat for LaCrosse fuel assembly is 20.4 kW per DSC for HLZC No. 3.

Heat Load Zoning Configuration No. 3 for 69BTH Basket

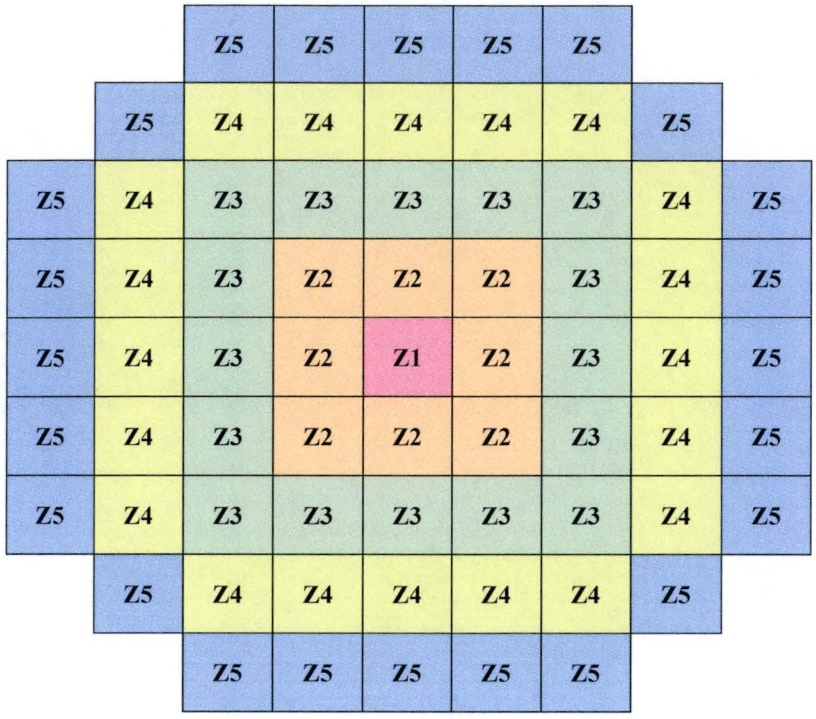

	Zone 1	Zone 2	Zone 3	Zone 4	Zone 5
Max. Decay Heat (kW/FA) (4)	0.0 (1)	0.45	0.0 (2)	0.70	0.60
No. of Fuel Assemblies (3)	0	8	0	20	24
Max. Decay Heat per Zone (kW) (4)	0	3.6	0	14.0	14.4
Max. Decay Heat per DSC (kW)	32.0 (4)				

Notes: (1) The fuel compartment in zone 1 remains empty
(2) Aluminum dummy assemblies replace the fuel assemblies in zone 3
(3) Total number of fuel assemblies is 52.
(4) Reduce the maximum decay heat to 70% of the listed values for LaCrosse Fuel assembly. The total decay heat for LaCrosse fuel assembly is 22.4 kW per DSC.
(5) Borated Aluminum is the only poison material allowed for HLZC #4.

Heat Load Zoning Configuration No. 4 for 69BTH Basket

		Z5	Z5	Z5	Z5	Z5		
	Z5	- (1)	Z3	Z2	Z3	-	Z5	
Z5	-	Z4	Z3	-	Z3	Z4	-	Z5
Z5	Z3	Z3	-	Z1	-	Z3	Z3	Z5
Z5	Z2	-	Z1	-	Z1	-	Z2	Z5
Z5	Z3	Z3	-	Z1	-	Z3	Z3	Z5
Z5	-	Z4	Z3	-	Z3	Z4	-	Z5
	Z5	-	Z3	Z2	Z3	-	Z5	
		Z5	Z5	Z5	Z5	Z5		

	Z1 (Zone 1)	Z2 (Zone 2)	Z3 (Zone 3)	Z4 (Zone 4)	Z5 (Zone 5)
Max. Decay Heat (kW/FA) (4)(5)	0.13	0.31	0.76	0.95	0.52
No. of Fuel Assemblies(2)	4	4	16	4	24
Max. Decay Heat per DSC (kW)	30.20 (3)(4)				

Notes:
(1) Aluminum dummy assembly (solid aluminum block) is required in the fuel compartments designated with a dash (-).
(2) Total number of fuel assemblies is 52 for HLZC No. 8.
(3) Adjust payload to maintain total DSC heat load within the specified limit.
(4) Reduce the maximum decay heat to 70% of the listed values for LACROSSE10 Fuel assembly. The total decay heat for LACROSSE10 fuel assembly is 21.1 kW per DSC for HLZC No. 8.
(5) Type "F" borated aluminum is the only poison material authorized to use with HLZC No. 8.
(6) This figure is also shown as Figure A.1.4.9-5a, "Heat Load Zoning Configuration No. 8 for 69BTH Basket."

Heat Load Zoning Configuration No. 8 for 69BTH Basket

The DSC shell temperatures for NCT at 100°F, -20°F and -40°F are retrieved from the MP197HB transport cask model described in Section A.3.3.1.1 and transferred to the basket models.

The material properties used in the 69BTH DSC/basket model are listed in Section A.3.2.1

The effective thermal conductivities for paired aluminum/poison plates and for dummy aluminum assemblies are calculated in Section A.3.3.1.5.

The geometry of the DSC model and the gaps are shown in Figure A.3–13 through Figure A.3–17. Mesh sensitivity of the model is discussed in Appendix A.3.6.2.2.

Typical boundary conditions for the DSC basket model are shown in Figure A.3–18.

A.3.3.1.5 Effective Thermal Properties in 69BTH DSC Basket

1) Effective Conductivity for Paired Aluminum and Poison Plates in 69BTH DSC

Paired aluminum and poison plates are considered as one homogenized material in the 69BTH basket model. The possible combinations for paired aluminum and poison plates are summarized in the following table.

Combinations for Paired Al/Poison Plates in 69BTH Basket

		Paired Plated within Compartment Blocks	Paired Plated between Compartment Blocks
	Total Thickness	0.25"	0.375"
Al/Boral	Boral Plate Thickness	0.25"	0.25"
	Boral Core Thickness	0.16"	0.16"
	Al Plate Thickness	0	0.125"
Al/Borated Al or Al/MMC	Total Thickness	0.25"	0.375"
	Poison Plate Thickness	0.175"	0.175"
	Al Plate Thickness	0.075"	0.200"

The paired plates built up parallel thermal resistances along their length and serial thermal resistances across their thickness. The gaps considered between the paired plates and their adjacent basket plates at the cross section account for the contact resistance between the plates.

The effective conductivities of the paired plates are calculated as follows:

$$k_{eff,along} = \frac{k_{poison} \times t_{poison} + k_{Al} \times t_{Al}}{t_{model}}$$ along the length (parallel resistances)

$$k_{eff,across} = \frac{t_{model}}{\frac{t_{poison}}{k_{poison}} + \frac{t_{Al}}{k_{Al}}}$$ across the thickness (serial resistances)

where,
k_{poison} = conductivity of poison plate or conductivity of core material for Boral (Btu/hr-in-°F)
t_{poison} = thickness of poison plate or thickness of core material for Boral (in)
k_{Al} = conductivity of Al 1100 (Btu/hr-in-°F)
t_{Al} = thickness of aluminum plate or aluminum clad for Boral (in)
t_{model} = thickness paired Al/Poison plates in the model (in)

For conservatism, the conductivity of Boral core is reduced by 10% for calculation of effective conductivities.

The calculated effective conductivity values for paired aluminum and poison plates are listed in Section A.3.2.1 material # 17 to 19.

Borated aluminum plates can be used for all HLZCs in 69BTH basket. Boral or MMC plates paired with aluminum 1100 plates can be used for HLZC # 1, # 2, and # 3 but shall not be used for HLZC # 4 *and # 8*.

A comparison between material # 17 and 18 in Section A.3.2.1 shows that the effective conductivities for paired aluminum and MMC plates are higher than those for paired aluminum and Boral plates for the entire temperature range. Therefore, the effective conductivities of paired aluminum and Boral plates are considered to bound the maximum component temperatures for HLZC # 1, # 2, and # 3.

The effective conductivities for paired aluminum and borated aluminum plates are used for HLZC # 4 *and # 8*.

2) Effective Conductivity for Dummy Aluminum Assemblies

Aluminum dummy assemblies replace the fuel assemblies in assigned compartments defined in the 69BTH basket for HLZC # 2 through # 4, *and # 8* as shown in Section A.3.3.1.4.

The dummy assemblies are considered as aluminum blocks with a cross section of 5.875" × 5.875" and a length equal to BWR fuel assemblies. A uniform gap of 0.0625" is considered around the cross section of the dummy assembly within the fuel compartment.

The effective conductivity in transverse direction is a combination of serial and parallel thermal resistances shown in the following Figure A.3–19. The transverse effective conductivity for dummy assembly is calculated as follows.

$$k_{eff,tr,dummy} = \frac{1}{R_{eff,tr,dummy}}$$

with

$$R_{eff,tr,dummy} = 2R_{th,He1} + \frac{1}{\left(\frac{2}{R_{th,He2}} + \frac{1}{R_{th,Al}}\right)}$$

where

$$R_{th,He1} = \frac{t_{gap}}{k_{He}\ w_{comp}}; \qquad R_{th,He2} = \frac{a_{dummy}}{k_{He}\ t_{gap}}; \qquad R_{th,Al} = \frac{a_{dummy}}{k_{Al6061}\ a_{dummy}} = \frac{1}{k_{Al6061}}$$

a_{dummy} = width of dummy assembly = 5.875"
w_{comp} = inner width of fuel compartment = 6.0"
t_{gap} = thickness of gap between dummy assembly and fuel compartment =0.0625"
k_{Al6061} = conductivity of Al 6061 (Btu/hr-in-°F)
k_{He} = conductivity of Helium (Btu/hr-in-°F)

The conductivity of helium is conservatively ignored in the axial direction. The axial transverse effective conductivity for dummy assemblies is calculated as follows.

$$k_{eff,ax,dummy} = \frac{a_{dummy}^{2}}{W_{comp}^{2}} k_{Al6061}$$

The calculated effective conductivities for dummy assembly are listed in Section A.3.2.1 material # 20.

3) Effective Thermal Properties of 69BTH DSC Basket

The DSC basket effective density, thermal conductivity and specific heat are calculated for use in the transient analyses of the MP197HB under HAC.

Dimensions of the Homogenized 69BTH DSC Basket

DSC Type	69BTH
Basket OD (in)	68.75
Basket length (in)	164
Top grid assembly OD (in)	68.75
Top grid assembly length (in)	14.4

The basket effective density $\rho_{eff\,basket}$, and specific heat $c_{p\,eff\,basket}$ are calculated as volumetric and weight average, respectively using the following equations.

$$\rho_{eff\,basket} = \frac{\sum W_i}{V_{basket}} = \frac{W_{steel} + W_{Al} + W_{poison} + W_{fuel}}{L_{basket} \cdot \pi \cdot D_{basket}^{2} / 4}$$

$$c_{p\,eff\,basket} = \frac{\sum W_i \cdot c_{pi}}{\sum W_i} = \frac{W_{steel} \cdot c_{p\,steel} + W_{Al} \cdot c_{p\,Al} + W_{poison} \cdot c_{p\,poison} + W_{fuel} \cdot c_{pfuel}}{W_{steel} + W_{Al} + W_{poison} + W_{fuel}}$$

Where: W_i = weight of basket components
V_{model} = total volume of basket in FE model
L_{basket} = basket length = 164 in.
D_{basket} = basket OD = 68.75 in.
$c_{p\,i}$ = specific heat of basket materials.

The specific heat and density values used in the above equations are listed in Section A.3.2.1. The following assumptions are used in the calculation of the basket effective density and specific heat calculation:

- Specific heat of SA 240, type 304 and Al 6061 are considered for stainless steel and aluminum components, respectively.
- For poison material c_p values are conservatively assumed equal to those for 6061 aluminum.
- For aluminum at T > 400°F c_p value is conservatively assumed equal to its value at 400°F.
- Conservatively, Helium is not included in density and specific heat calculation.

The same approach as described above for the basket is used to calculate the effective density $\rho_{eff\ top\ grid}$, for top grid assembly (hold-down ring) of 69BTH DSC.

$$\rho_{eff\ topgrid} = \frac{\sum W_i}{V_{topgrid}} = \frac{W_{steel}}{L_{topgrid} \cdot \pi \cdot D_{topgrid}^{\ 2} / 4}$$

Where: W_{steel} = weight of steel in top grid assembly
$V_{topgrid}$ = total volume of top grid assembly in FE model
$L_{topgrid}$ = top grid assembly length in FE model = 14.4"
$D_{topgrid}$ = top grid assembly OD in FE model = 68.75"

Since no density and specific heat are considered for the helium, the specific heat of the top grid assembly is equal to the specific heat of steel.

The calculation of the effective density and effective specific heat for the 69BTH basket are summarized in Table A.3–3 and Table A.3–4, respectively.

To calculate the effective thermal conductivities, the 69BTH basket with Boral poison plates is chosen. A 26" long slice of 69BTH basket is created by selecting the nodes and elements of the basket from the finite element model described in Section A.3.3.1.4. The length of the slice model is twice the length of the aluminum plates and the axial gaps between them. The slice model is shown in Figure A.3–20.

To calculate the axial effective conductivity of the baskets, constant temperature boundary conditions are applied at the top and bottom of the slice models. No heat generation is considered for the fuel elements in these cases. The axial effective conductivity is calculated using the following equation.

$$k_{basket,axl} = \frac{Q_{axl} \times L}{A_{slice} \times \Delta T} \times 0.95$$

Where:
Q_{axl} = Amount of heat leaving the upper face of the slice model – reaction solution of the uppermost nodes (Btu/hr)

L = Length of the model = 26" for 69BTH
A_{slice} = Surface area of the upper (or bottom) face of the basket slice model
= 1856 in^2 for 69BTH (=$\pi/8 \times D_{basket}^2$)
$\Delta T = (T_2 - T_1)$ =Temperature difference between upper and lower faces of the model (°F)
T_2 = Constant temperature applied on the upper face of the model (°F)
T_1 = Constant temperature applied on the lower face of the model (°F)

Only 95% of the estimated axial effective conductivity is considered for conservatism.

Typical applied boundary conditions are shown in Figure A.3–21.

In determining the temperature dependent axial effective conductivities an average temperature equal to $(T_1 + T_2)/2$, is used for the basket temperature. The axial effective conductivities for 69BTH basket are listed in Table A.3–5.

The axial effective conductivity for the top grid assembly of 69BTH basket is calculated considering only the 14.4" high plates. The effects of the extension, base plate, and short plates are conservatively ignored. The assumed geometry of the top grid assembly is shown in Figure A.3–22. The following equation is used to calculate the axial effective conductivity for the top grid assembly.

$$k_{topgrid,axl} = k_{SS304} \frac{A_{plates}}{A_{model}}$$

Where: k_{SS304} = conductivity of stainless steel, see Section A.3.2.1 (Btu/hr-in-°F)
A_{plates} = Surface area of the 14.4" high plates, see Figure A.3–22 (in^2)
A_{model} = Surface area of the homogenized top grid assembly model
= $\pi/4 \times D_{basket}^2 = 3712$ in^2

The axial effective conductivities for the top grid assembly are listed in Table A.3–5.

The basket slice models are also used to calculate the transverse effective conductivity of the basket. For this purpose, constant temperature boundary conditions are applied on the outermost nodes of the slice model and heat generating conditions are applied over the fuel elements.

The heat generation rates for the slice model of 69BTH basket are calculated based on the HLZC # 1 shown in Section A.3.3.1.4 with a total heat load of 26 kW and a peaking factor of 1.2 for BWR assemblies.

The following equation is given in [23] for long solid cylinders with uniformly distributed heat sources.

$$T = T_o + \frac{\dot{q}\, r_o^2}{4k}\left[1 - \left(\frac{r}{r_o}\right)^2\right]$$

With T_o = Temperature at the outer surface of the cylinder (°F)
T = Maximum temperature of cylinder (°F)
$\dot{q}$ = Heat generation rate (Btu/hr-in^3)
r_o = Outer radius = D_{basket} /2 = 34.375" for 69BTH basket
r = Inner radius = 0 for slice model
k = Conductivity (Btu/hr-in-°F)

The above equation is rearranged to calculate the transverse effective conductivity of the basket as follows. Only 95% of the estimated radial effective conductivity is considered for conservatism.

$$\dot{q} = \frac{Q_{rad}}{V}$$

$$k_{basket,rad} = \frac{Q_{rad} \cdot r_0^2}{4 \cdot V \cdot \Delta T} \times 0.95 = \frac{0.95\, Q_{rad}}{2\pi \cdot L \cdot \Delta T} \text{ for 69BTH}$$

With Q_{rad} = Amount of heat leaving the periphery of the slice model – Reaction solution of the outermost nodes (Btu/hr)

L = Length of the slice model = 26" for 69BTH
V = Volume of the slice model = $(\pi r_0^2 L)/2$ for 69BTH
$\Delta T = (T_{max} - T_o)$ = Difference between maximum and the outer surface temperatures in (°F)

Since the surface area of the fuel assemblies at the basket cross section is much larger than the other components, assuming a uniform heat generation is a reasonable approximation to calculate the radial effective conductivity.

Typical applied boundary conditions are shown in Figure A.3–21.

In determining the temperature dependent transverse effective conductivities an average temperature equal to $(T_{max} + T_o)/2$, is used for the basket temperature.

The transverse (radial) effective conductivities of the 69BTH basket are listed in Table A.3–6.

The effect of stainless steel in the top grid assembly is ignored conservatively in the radial direction. The effective conductivity of the top grid assembly is set equal to helium conductivity in the radial direction.

A.3.3.1.6 37PTH DSC Model

The following assumptions and conservatism are considered for the 37PTH DSC model:

The fuel assemblies contained in the 37PTH basket are intact fuel assemblies. Since the damaged fuel assemblies are loaded in the outermost fuel compartment cells, they do not affect the maximum temperatures or the maximum temperature gradients in this evaluation.

No convection is considered within the DSC cavity.

Radiation is considered only implicitly between the fuel rods and the fuel compartment walls in the calculation of effective fuel conductivity. No other radiation heat exchange is considered within the basket model.

The modeled active fuel length for PWR fuel assemblies is 144" with the length of the bottom fitting about 4" based on WE 14x14 PWR fuel assembly [37]. The total length of the basket assembly is 162".

The following gaps are considered in the 37PTH basket/DSC model at thermal equilibrium:

a) 0.45" diametrical hot gap between the basket outer surface and the canister inner surface. This assumed gap is larger than the nominal cold gap and is therefore conservative.

b) 0.45" diametrical hot gap between the shield plugs and the canister shell inner surface. The maximum diametrical cold gaps between the top and bottom shield plugs and the canister shell inner surface are 0.18" and 0.25", respectively. The assumed hot gap is therefore conservative.

c) 0.01" gap between the basket rails and compartment plates.

d) 0.0075" gap between any two adjacent plates or components within the cross section of fuel compartments.

e) 0.125" gap in axial direction between the aluminum rail pieces. This gap is larger than the axial tolerances considered for rail aluminum pieces and therefore conservative.

f) Two pieces of MMC plates with 0.0075" contact gap as shown in Figure A.3–26 are conservatively assumed to model single MMC plate in the model.

g) 0.01" gap between any two adjacent plates between shield plugs and canister cover plates.

h) 0.1" axial gap between the canister inner bottom plate and bottom basket assembly.

It has been shown in [1], Appendix M, Section M.4.4.1.1, that the 0.01" and 0.0075" gaps considered in the basket cross section account adequately for tolerances and contact resistances in a similar basket design.

Fourteen single aluminum plates with 0.125" nominal thickness are considered in the fuel compartments. The thickness of single aluminum plate is modeled as 0.1325". To account for this thickness change, an effective conductivity is estimated by a conservative reduction factor of 0.926 (=0.125"/0.135") to maintain the conductivity of aluminum plates within the basket. All other dimensions are based on nominal dimensions for the 37PTH basket/DSC model.

A total thickness of 0.075" is considered for Boral plates with a maximum core thickness of 0.06". It is considered that the single MMC or borated aluminum plates have a thickness of 0.125".

The nominal widths of fuel compartments are 9" for four corner compartments and 8.725" for all other compartments. The corresponding nominal compartment opening sizes are 8.875" for fuel assemblies in the corner compartments and 8.6" for the other fuel assemblies. The widths of all compartments are reduced to 8.6" in 37PTH DSC model to accommodate for the size of the gaps and maintain the outer basket diameter contained within the canister inner diameter. Due to reduced size of the compartments, the compartment opening widths are 8.46" for all the fuel assemblies in the 37PTH DSC model.

Due to the reduced compartment opening in 37PTH DSC model, the related heat generation rates are increased by 10.0% ($=8.875^2 / 8.46^2$) for corner fuel assemblies and 3.3% ($=8.6^2 / 8.46^2$) for all other fuel assemblies. The transverse effective fuel conductivity is calculated using the following equation from Appendix T, Section T.4.8.1.4 associated with Amendment 10 to Part 72 CoC 1004 for the Standardized NUHOMS® System [3].

$$k_{eff} = \frac{q''' a^2}{(T_c - T_o)}(0.29468)$$

With

k_{eff} = transverse effective fuel conductivity (Btu/hr-in-°F)

q''' = volumetric heat generation rate (Btu/hr-in^3)

$$q''' = \frac{Q}{4a^2 L_a}$$

Q = decay heat load (Btu/hr)

a= half of the compartment width (in.)

L_a = Active fuel length (in.)

T_c = maximum temperature of fuel assembly (°F)

T_o = compartment wall temperature (°F)

Since the increase of the heat generation rate and the decrease of the compartment opening size cancel each other out in the above equation, the transverse effective fuel conductivity calculated for compartment openings of 8.875" and 8.6" can be used in the 37PTH DSC model with compartment openings of 8.46" without affecting the maximum fuel cladding temperature.

Except for the four corner compartments, 32PT and 37PTH baskets have similar fuel compartment material and configuration. Since the opening size of these compartments in the 37PTH DSC (8.6") is smaller than the compartment opening size of the 32PT DSC (8.7"), the bounding (lowest) effective properties for homogenized PWR fuel assemblies in 32PT basket taken from [1], Appendix M, Section M.4.2 can be used conservatively for the 37PTH DSC model for all fuel assemblies except the ones located in the four corner compartments. The bounding fuel assembly is WE 14x14 PWR fuel assembly.

Only 95% of the axial effective fuel conductivity calculated for 32PT DSC in [1], Appendix M, Section M.4.2 is considered for use in the 37PTH DSC model for conservatism. This value is utilized in 37PTH DSC model for all fuel assemblies except the ones located in the four corner compartments.

Based on [1], Drawing NUH24PTH-1003 SAR, sheet 2 of 7, Rev. 1, the compartment opening size for 24PTH DSC is 8.9" and the material of the compartments for 24PTH DSC is stainless steel SA 240, type 304. Since the compartment opening size for the four corner compartments in the 37PTH DSC (8.875") is smaller than the compartment opening size of the 24PTH DSC (8.9") and the emissivity of anodized aluminum used in the four corner compartments of 37PTH is higher than the emissivity of stainless steel, the bounding (lowest) effective fuel properties calculated for 24PTH DSC in [1], Appendix P, Section P.4.2 can be used conservatively for the fuel assemblies located in the four corner compartments in the 37PTH DSC model. The bounding effective fuel conductivity used for the four corner fuel assemblies in the 37PTH DSC model belongs to WE 14x14 PWR fuel assembly taken from [1], Appendix P, Section P.4.2.

Decay heat load is applied as heat generation boundary conditions over the elements representing homogenized fuel assemblies. The base heat generation rate is multiplied by peaking factors along the axial fuel length to represent the axial decay heat profile. A correction factor is used to avoid degradation of decay heat load due to imperfections in application of peaking factors. The heat generation rates used in this analysis is calculated as follows.

$$\dot{q}''' = \left(\frac{q}{a^2 L_a} \times PF \right) \times CF$$

where,
q = Decay heat load per assembly defined for each loading zone
a = Width of the homogenized fuel assembly in model = 8.46"
L_a =Active fuel length = 144"
PF = Peaking Factor
CF = correction factor = 1.002 for 37PTH

The base heat generation rates used in the 37PTH basket model are listed in the following table.

Base Heat Generation Rates for 37PTH

Heat Load in the Model (KW)	$\dot{q}'''$ value without PF (Btu/hr-in^3)
0.40	0.1327
0.60	0.1991
0.70	0.2322

Axial Heat Flux Profile

The normalized axial burnup profile for typical PWR fuels with burnup higher than 30 GWd/MTU is taken from DOE/RW0472 [12]. The peaking factors from [12] are converted to match the regions defined for the fuel assembly in the 37PTH finite element model.

The maximum *assembly* average burnup allowed in 37PTH DSCs is *62,000* MWD/MTU, which is considerably higher than 30,000 MWD/MTU referenced in the report. Research [12] shows that at a higher burnup, the heat flux shape tends to flatten with a reduction in the maximum axial peaking factor in the middle region, and the flux shape becomes more pronounced in the

fuel end regions. The reduction of maximum axial peaking factor in a more flattened heat flux shape will result in lower fuel cladding temperatures. Therefore, the application of heat flux shape for a lower burnup spent fuel (30,000 MWD/MTU) on a higher burnup spent fuel (*62,000* MWD/MTD) is conservative.

These peaking factors are listed in Table A.3–7 and are shown in the following figure.

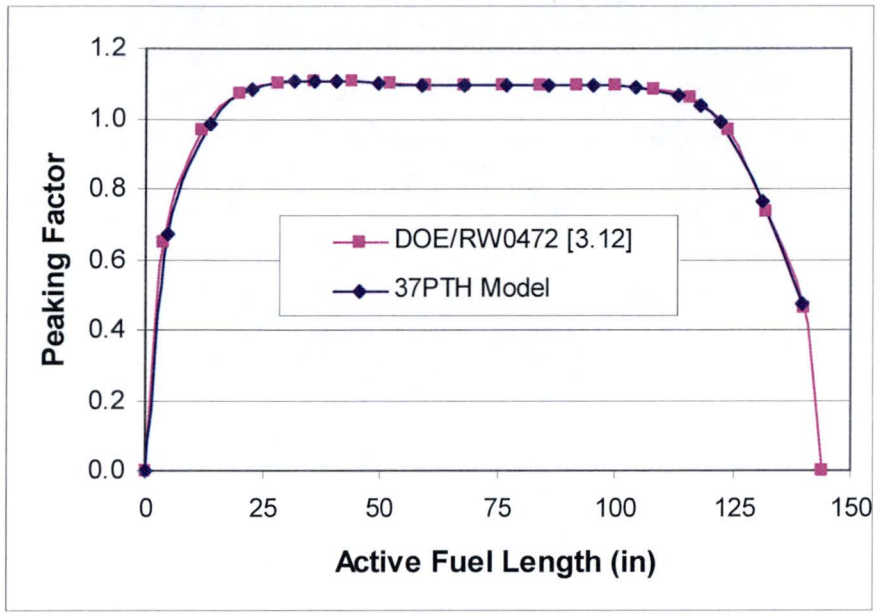

Peaking Factor Curve for PWR Fuels

As seen in Table A.3–7, the normalized area under the peaking factor curve is smaller than 1.0. To avoid any degradation of decay heat load, a correction factor of 1.002 calculated as follows is used when applying the peaking factors.

$$Nomalized\ Area\ under\ Curve = \frac{\text{Area under Axial Heat Profile}}{\text{Active Fuel Length}} = 0.998$$

Active fuel length = 144"

$$Correction\ Factor = \frac{1}{Normalized\ Area\ under\ Curve} = 1.002$$

The heat generating rates for the elements representing the active fuel are calculated based on the HLZC for 37PTH DSC. The HLZC and its restrictions for 37PTH basket are shown in the following figure.

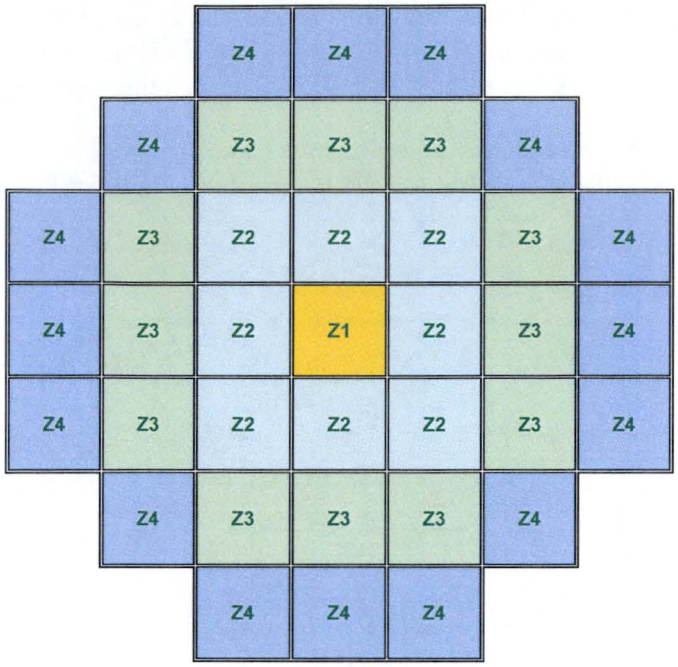

	Zone 1	Zone 2	Zone 3	Zone 4
Max. Decay Heat (kW/FA)	0.40	0.40	0.60	0.70
No. of Fuel Assemblies	1	8	12	16
Max. Decay Heat per Zone (kW)	0.4	3.2	7.2	11.2
Max. Decay Heat per DSC (kW)	22.0			

Heat Load Zoning Configuration for 37PTH Basket

The DSC shell temperatures for NCT at 100°F, -20°F and -40°F are retrieved from the MP197HB transport cask model described in Section A.3.3.1.1 and transferred to the basket models.

The material properties used in the 37PTH basket/DSC model are listed in Section A.3.2.1.

Section A.3.2.2.3 shows that the conductivity of MMC plate is lower than those of borated aluminum plate. Therefore, the conductivity of MMC plate is considered for single poison plates in the 37PTH basket model to bound the maximum component temperatures.

The effective thermal conductivities for Boral plates are calculated in Section A.3.3.1.7.

The geometry of the DSC model and the gaps are shown in Figure A.3–23 through Figure A.3-27.

Mesh sensitivity of the model is discussed in Appendix A.3.6.2.3.

Typical boundary conditions for DSC basket model are shown in Figure A.3–28.

A.3.3.1.7 Effective Thermal Properties of 37PTH DSC Basket

1) Effective Conductivity for Boral Plates in 37PTH DSC

Boral plates are considered as one homogenized material in the 37PTH basket model. The total thickness of the Boral plate is 0.075" with a core thickness of 0.06" in the 37PTH basket.

The Boral core and its aluminum claddings built up parallel thermal resistances along their length and serial thermal resistances across their thickness. The effective conductivities of the Boral plate are calculated using equations for $k_{eff,along}$ and $k_{eff,across}$ described in Section A.3.3.1.4 with the following parameters.

k_{poison} = conductivity of core material for Boral (Btu/hr-in-°F)
t_{poison} = thickness of core material for Boral = 0.06 in
k_{Al} = conductivity of Al 1100 (Btu/hr-in-°F)
t_{Al} = thickness of aluminum clad for Boral = 0.015 in
t_{model} = thickness of Boral plates in the model =0.075 in

For conservatism, the conductivity of Boral core is reduced by 10% for calculation of effective conductivities.

The calculated effective conductivity values for Boral plates in 37PTH basket model are listed in Section A.3.2.1 material # 21.

A.3.3.2 Heat and Cold

Table A.3–8 and Table A.3–9 present the maximum temperatures for TC components and DSC Shells.

The DSC types 61BTH, 61BT, 32PTH, 32PTH1, 32PT, 24PTH, and 24PT4 are evaluated previously for normal transfer conditions under 10 CFR 72 requirements. The DSC shell temperature profiles of these DSCs in MP197HB model are compared with the corresponding profiles from 10 CFR 72 SARs in Section A.3.6.3. It is shown that the fuel cladding and the basket component temperatures in 10 CFR 72 SARs represent the bounding values for these DSCs under transport conditions.

Therefore, no additional analysis is performed for the DSCs previously evaluated under 10 CFR 72 conditions. The maximum fuel cladding and the basket component temperatures for these DSCs are taken from 10 CR 72 SARs and reported as the bounding values for transport conditions.

The maximum temperatures for DSC contents for all DSCs to be transported in MP197HB TC for NCT are listed in Table A.3–10.

The heat load of the secondary containers is limited to 5 kW and is bounded by the DSC heat loads of 18.3 kW to 32 kW. The maximum component temperatures of the MP197HB TC loaded

with a secondary container are therefore bounded by those evaluated for TC loaded with DSCs. The content of the secondary containers are irradiated and/or contaminated non-fuel bearing solid materials, which have temperature limits significantly higher than the fuel cladding. Due to the lower heat load of secondary container, the maximum temperature of the content will be less than the basket and fuel cladding temperatures loaded in the DSCs. Therefore, no additional analysis is required for the secondary containers.

As calculated in Section A.3.3.1.2, the maximum accessible surface temperatures for impact limiter and personnel barrier are 121 °F and 152 °F, respectively. These temperatures are well below the limit of 185 °F defined in Section A.3.1.

The thermal analysis of NCT demonstrates that the MP197HB TC with up to 32 kW heat load meets all applicable requirements. The highest maximum temperatures are summarized in Table A.3–11.

The maximum temperatures calculated using conservative assumptions are well below specified limits. The seal O-rings are not explicitly considered in the models. The maximum seal temperatures are retrieved from the models by selecting the nodes at the locations of the corresponding seal O-rings. The maximum Fluorocarbon seal temperature (341 °F, 172 °C) for NCT is below the long-term limit of 400 °F (204 °C) specified for continued seal function. The maximum metallic seal temperature (402 °F, 206 °C) for NCT is below the long-term limit of 644 °F (340 °C) specified for continued seal function.

The maximum neutron shield temperature is 316 °F (158 °C) for NCT *belonging to the case in which the fuel assembly configuration is assumed to be altered. This temperature* is below the long term limit of 320 °F (160 °C). *A grid convergence study is performed in Section A.3.6.11.6. This study shows that the neutron shield temperature determined using the grid density in the model described in Section A.3.6.11.1 is adequate in evaluating the thermal performance and the neutron shield temperature including the computational uncertainties remains below the long-term limit of 320 °F. Therefore, no* degradation of the neutron shielding is expected.

The maximum temperature of gamma shield is 410°F (210 °C) for NCT, which is well below the melting point of lead (621 °F, 327 °C).

If the fuel assembly configuration is not altered, the predicted maximum fuel cladding temperature of 560 °F (343 °C) for the maximum heat load of 32kW is well within the allowable fuel temperature limit of 752 °F (400 °C) for NCT.

The temperature distributions for NCT with 100 °F ambient and insolation are shown in Figure A.3–29 to Figure A.3–34.

Under the minimum ambient temperature of -40 °F (-40 °C), the resulting packaging component temperatures will approach -40 °F if no credit is taken for the decay heat load. Since the package materials, including containment structures and the seals, continue to function at this temperature, the minimum temperature condition has no adverse effect on the performance of the MP197HB TC.

The maximum component temperatures for ambient temperatures of -40 °F and -20 °F with maximum decay heat and no insulation are calculated for 69BTH DSC and 37PTH DSC to use for structural evaluations. These temperatures are listed in Table A.3–12 and Table A.3–13.

The average temperatures of helium gas in TC cavity, and the average temperatures of fuel assemblies and helium within 37PTH and 69BTH DSC cavities for NCT are listed in Table A.3-14. These temperatures are used to evaluate the maximum internal pressures within TC and DSC cavities.

Thermal stresses for the MP197HB TC loaded with DSC are discussed in Chapter A.2. The maximum normal operating pressure for the MP197HB TC is discussed in Section A.3.3.3. The performance of the MP197HB TC loaded with DSCs for HAC is discussed in Section A.3.4.

A.3.3.3 Maximum Normal Operating Pressure

A.3.3.3.1 MP197HB TC Operating Pressure

The following assumptions are considered to determine the maximum pressures within the MP197HB TC cavity during NCT when the TC is loaded with DSCs.

- All dimensions used in calculation of the maximum pressures are nominal.
- Length of the DSCs and the spacer in the axial direction are selected to minimize TC cavity volume and increase pressure.
- Length of the sleeve is conservatively assumed equal to the length of the TC cavity.
- The spacer is considered as a solid cylinder in this calculation.
- *Ninety-eight percent* of the TC cavity free volume is conservatively used in calculating the maximum pressures.
- The initial temperature of helium backfill in the cask cavity is assumed to be 70 °F.
- The maximum initial pressure of the helium backfill in the cask cavity is 3.5 (2.5 $\pm$ 1) psig.
- For HAC, the highest average temperature of helium in the cask cavity in the transient run is considered for calculation of the maximum pressure.

The average helium temperatures in the cask cavity are retrieved from the MP197HB model described in Section A.3.3.1.1. The data used in calculating the pressures in the MP197HB TC cavity during NCT and HAC are listed below.

Data used in Calculation of Maximum Pressures in TC Cavity

DSC Type	Heat Load kW	OD_{DSC} in	L_{DSC} in	$T_{avg, he,NCT}$ °F	$T_{avg, he,HAC}$ °F	ID_{Shell} in	L_{TC} in
69BTH	32	69.75	196.04	339	387	70.5	199.25
37PTH	22	69.75	189.25	269	N/A		
32PTH	26	69.75 [4]	185.75 [4]	301			
32PTH, Type 1	26	69.75 [4]	193.00 [4]				
32PTH1, Type 1	26	69.75 [3]	198.50 [3]				
32PTH1, Type 2	24	69.75 [3]	198.50 [3]	288			
DSC Type		OD_{DSC}	L_{DSC}	$T_{avg, he,NCT}$	$T_{avg, he,HAC}$	ID_{Sleeve}	
61BTH, Type 1 (1)	22	67.25 [3]	196.04 [3]	301	N/A	68	
61BTH, Type 2 (1)	24	67.25 [3]	196.04 [3]	316			
61BT	18	67.25 [1]	196.04 [1]	273			
32PT	24	67.19 [1]	192.55 [1]	281			
24PTH, (all types) (1)	26	67.19 [1]	186.67 [1]	297	333		
24PT4	24	67.19 [2]	196.30 [2]	313	N/A		

Note:
(1) DSCs 61BTHF and 24PTHF have the same dimensions and use the same MP197HB features as DSCs 61BTH and 24PTH, respectively. The thermal expansion of 61BTHF and 24PTHF DSCs is bounded by values for 61BTH and 24PTH DSCs and is not analyzed separately.

Where,

OD_{DSC} = Outer Diameter of the DSC, *in*

L_{DSC} = Length of the DSC, *in*

$T_{avg,he,NCT}$ = Average Temperature of helium for NCT

$T_{avg,he,HAC}$ = Average Temperature of helium for HAC

ID_{Shell} = Inner diameter of TC inner shell, in

ID_{Sleeve} = Inner diameter of sleeve, in

L_{TC} = MP197HB Cavity Length, in

The spacer data used in calculating the pressures in the MP197HB TC cavity during NCT and HAC are listed below.

Spacer Data used in Calculating Maximum Pressures

DSC Type	L_{Spacer} (in)	OD_{Spacer} (in)
69BTH	2.2	69.75
61BT/61BTH Type 1 and 2	2.2	67.25
37PTH	9	69.75
32PTH	12.5	69.75
32PTH Type 1	5.25	69.75
32PTH1 Type 1 and Type 2	N/A (1)	N/A (1)
32PT	5.7	67.25
24PTH (all types)	11.7	67.25
24PT4	2.2	67.25

Note: (1) 32PTH1-L is used in calculating the cask cavity pressures.

where,

L_{Spacer} = Length of the spacer, in

OD_{Spacer} = Outer Diameter of the Spacer Disc, in

The free volume of the MP197HB cask cavity is determined based on the dimensions presented in the above tables. The free volume of the MP197HB cask cavity is calculated as:

$$V_{free,cc} = \frac{\pi}{4} * \left[(ID_{Cask}^2 * L_{TC}) - (OD_{DSC}^2 * L_{DSC} + OD_{Spacer}^2 * L_{Spacer}) \right]$$

where,

ID_{Cask} = ID_{Shell}, Inner diameter of the cask inner shell for DSCs without sleeve, in

= ID_{Sleeve}, Inner diameter of the cask sleeve for DSCs with sleeve, in

The number of moles of helium in the cask cavity is calculated using the ideal gas law and is as follows:

$$n_{he,Initial} = \frac{P_{initial} * (6894.8 Pa / psi) * V_{free,cc} * (1.6387 * 10^{-5} m^3 / in^3)}{R * T_{avg,He} (5/9 K/^oR)}$$

The maximum pressure in the cask cavity for NCT is calculated as:

$$P_{NCT} = \frac{\left(1.4504 * 10^{-4} \frac{psia}{Pa}\right) * (n_{he,initial}) * R * T_{avg,he,NCT} * (5/9 K/^oR)}{0.98 * V_{free,cc} * (1.6387 * 10^{-5} m^3 / in^3)}$$

where,

$T_{avg,He}$ = Initial Average Temperature of helium

R = Universal gas constant, $8.314 J/(mol - K)$

$n_{he,initial}$ = number of moles of helium in MP197HB cask cavity, $g - moles$

$P_{initial}$ = Initial pressure in the MP197HB cask cavity, $psia$

P_{NCT} = Pressure in the MP197HB cask cavity during NCT, $psia$

$V_{free,cc}$ = Free volume of MP197HB cask cavity, in^3

The maximum pressures in the cask cavity calculated for loaded MP197HB TC are presented in Table A.3–20. The case of the 69BTH DSC in MP197HB TC with 32 kW heat load is bounding for the maximum TC cavity pressure for all DSCs. The maximum pressure in the cask cavity of the MP197HB TC for NCT is 12.7 psig.

Due to low heat load of the secondary containers and expected low amount of fission gas release, the internal pressure of the cask loaded with the DSCs is bounding for the cask loaded with the secondary containers.

A.3.3.3.2 69BTH DSC Operating Pressure

The maximum internal pressure for the 69BTH DSC within MP197HB TC for NCT is determined based on the maximum allowable heat load for each HLZC discussed in Section A.3.3.1.4 and maximum assembly average burnup of *70* GWD/MTU. The limiting fuel assembly type considered in this evaluation is the FANP 9x9-2 assembly.

The calculations account for the canister free volume, the quantities of canister backfill gas, fuel rod fill gas, and fission products and the average canister cavity gas temperature. The internal canister pressures are then calculated using ideal gas law.

$$P_{can} = \frac{n_{total}\, R\, T_{avg,can}}{V_{free,can}}$$

Where:
n_{total} = Total number of moles of gases within canister cavity (lb-moles),
R = Universal gas constant (10.73 psia-ft^3/lb-moles-°R),
$T_{avg,can}$ = DSC cavity average temperature (°R),
$V_{free,can}$ = DSC free volume (ft^3), and
P_{can} = DSC internal pressure (psia).

The following assumptions and conservatisms are considered in calculating the maximum internal pressures within the 69BTH DSC:

- The DSC internal pressure is calculated below for the most limiting normal and accident cases for the 69BTH DSC. For these cases, 3% and 100% of the fuel rods are assumed to rupture, 100% of the fuel rod helium fill gas and 30% of the fission gases are assumed to be released into the DSC cavity [9]. The methodology for DSC internal pressure calculations is in accordance with the methodology used for the 61BTH DSC associated with Amendment 10 to Part 72 CoC 1004 for the Standardized NUHOMS® System [3].

- *The amount of fission gases produced by the "generic" BWR fuel assembly (FA) is calculated in Section A.5.5.4.*

- The DSC cavity average helium temperatures calculated *for* 69BTH DSC in Sections A.3.3.*2* and A.3.4 for limiting FANP 9x9-2 fuel assembly, are assumed to bound average helium temperatures for the rest of 69BTH fuel assemblies (FA).

- Similar to the 61BTH DSC, the 69BTH DSC is assumed to be backfilled with helium to a pressure of 3.5 (2.5 ± 1.0) psig after vacuum drying [3].

- An average temperature of 212°F equal to water boiling temperature is considered for the DSC shell during backfill operation.

- The initial temperature of fuel rod plenum fill gas is assumed to be at room temperature (70°F or 530°R). This is a reasonable assumption since the process takes place in a controlled environment.
- The highest assembly average burnup of *70* GWD/MTU proposed for the 69BTH DSC is assumed for the pressure calculation. Maximum burnup creates a bounding case for the amount of fission gases produced in the fuel rod during reactor operation.
- The highest weight and volume of fuel assembly was conservatively used because it displaces the most of free DSC cavity volume.
- The bounding (maximum) plenum volume among all fuel assemblies V_{pl}=2.136 in^3 (For SVEA FAs) is conservatively used in this calculation.
- The bounding (maximum) initial rod pressure ($p_{initial}$) of 160 psia (For SVEA FAs) is used.
- Only 98% of the DSC free cavity volume is used for pressure calculation.

1) Free DSC Cavity Volume

The volume of helium in the DSC cavity is calculated based on 69BTH weight calculations provided in Chapter A.2. The 69BTH DSC cavity free volume is calculated as DSC cavity volume minus basket, dummy assemblies (DA) and fuel assemblies' volume. The free volume for helium in the DSC is calculated as,

$$V_{He_DSC} = V_{He_DSC_w/o_FA} - V_{FAs} - V_{DAs}$$

Where,

V_{He_DSC} = Free helium volume in DSC

$V_{He_DSC_w/o_FA}$ = Helium volume outside fuel compartments in DSC cavity

V_{FAs} = Helium volume within compartment containing fuel assemblies

V_{DAs} = Helium volume within compartment containing dummy assemblies

The 69BTH DSC free helium volume and DSC cavity volumes used for pressure calculations are summarized in Table A.3–21 and Table A.3–22, respectively.

2) Average Helium Temperature

The average helium temperature in the DSC cavity is calculated based on DSC thermal analysis presented in Section A.3.3.1.4 and weight data provided in Chapter A.2 as volumetric average:

$$T_{He_DSC} = (V_{He_in_FA_act_fuel} \cdot T_{He_in_FA_act_fuel} + V_{He_in_DA_act_fuel} \cdot T_{He_in_DA_act_fuel} + V_{He_DSC_out_FA/DA_act_fuel} \cdot T_{He_DSC_out_FA/DA_act_fuel}) / V_{He_DSC}.$$

where,

T_{He_DSC} = Temperature of helium in DSC
$V_{He_in_FA_act_fuel}$ = Volume of helium in FAs along active fuel
$T_{He_in_FA_act_fuel}$ = Temperature of FAs along active fuel
$V_{He_in_DA_act_fuel}$ = Volume of helium outside DAs along active fuel
$T_{He_in_DA_act_fuel}$ = Temperature of DAs along active fuel
$V_{He_DSC_out_FA/DA_act_fuel}$ = Rest of helium volume in DSC outside FAs and DAs along active fuel
$T_{He_DSC_out_FA/DA_act_fuel}$ = Temperature of helium in cavity outside FAs and DAs along active fuel

Calculation of the average temperature of helium in 69BTH and 37PTH DSCs cavity for NCT and HAC is summarized in Table A.3–21.

3) Quantity of Helium Fill Gas in DSC

The 69BTH DSC free volume is assumed to be filled with 3.5 psig (18.2 psia) of helium. The average temperature of helium during backfill is evaluated based on linear extrapolation of helium average temperatures versus DSC shell temperatures for cold and hot NCT. A DSC shell temperature equal to water boiling temperature of 212°F is assumed during backfill operation. The average helium temperatures for 69BTH DSC in MP197HB at ambient temperature of -40°F and 100°F are calculated using the method described above. The evaluation of average helium backfill temperature for 69BTH and 37PTH DSCs is shown in the following table.

Evaluation of Helium Backfill Temperature

	69BTH	DSC		37PTH	DSC	
Operation	Transport T_{amb}=100°F	Transport T_{amb}=-40°F	He backfill	Transport T_{amb}=100°F	Transport T_{amb}=-40°F	He backfill
$T_{DSC\ shell\ av}$, °F	420	288	212	357	259	212
$T_{he\ av}$, °F	538	448	**396**	500	413	**371**
$T_{he\ av}$, °R	-	-	**856**	-	-	**831**

These average helium temperatures are used to estimate the number of moles of helium backfill in the DSC in accordance with the methodology of [1], Appendix P, Section P.4.6.5.4 for 24PTH DSC.

Using the ideal gas law,

$$PV = nRT,$$

$$n = PV / RT,$$

$$R = 8.314\, J/(mol \cdot K).$$

The quantity of helium in the DSC for the 69BTH DSC for HLZC #1 is:

$$n_{he,std} = \frac{(18.2\, psia)(6894.8\, Pa/psi)(258413\, in^3)(1.6387 \cdot 10^{-5}\, m^3/in^3)}{(8.314\, J/(mol \cdot K))(856\, °R)(5/9\, K/°R)},$$

$$n_{he,std} = 134.39\ g-moles.$$

The initial 69BTH DSC helium fill gas quantities are listed in Table A.3–22.

4) Quantity of Fill Gas in Fuel Rod

The volume of the helium fill gas in a fuel rod for the limiting (by number of fuel rods) SVEA fuel assemblies, at cold, unirradiated conditions is assumed to be 2.136 in^3 (maximum among all 69BTH fuels). There are at most 100 fuel rods in an SVEA fuel assembly with a maximum fill pressure of 145.3 psig (160 psia).

The fill gas is assumed to be at room temperature (70°F or 530°R). Per the ideal gas law, the quantity of fuel rod fill gas in 69 assemblies is:

$$n_{he} = \frac{(160\,psia)(6894.8\,Pa/psi)(69 \cdot 100 \cdot 2.136\,in^3)(1.6387 \cdot 10^{-5}\,m^3/in^3)}{(8.314\,J/(mol \cdot K))(530\,°R)(5/9\,K/°R)},$$

$$n_{he} = 108.91\,g-moles.$$

Based on 10 CFR 71 [6], the maximum fraction of the fuel pins that are assumed to rupture and release their charge gas for normal and accident conditions is 3% and 100%, respectively. Table A.3–22 summarizes the amount of helium fill gas released for the 69BTH DSC for NCT and HAC.

5) Quantity of Gases released as a Result of Irradiation

For the 69BTH DSC, the amount of fission gases produced by the "generic" BWR fuel assembly (FA) is 23.0 g-moles calculated in Section A.5.5.4. The total gas moles (per fuel assembly) are then multiplied by the 30% release fraction to obtain the number of moles contributing to 69BTH DSC cavity gas pressure.

The amount of gas released from one assembly due to irradiation is:

$n_{ig\,1\,FA}$ = *23.0 g-moles * 0.3 = 6.9 g-moles*

Table A.3–22 presents the amount of gas released into the DSC cavity by fuel assemblies n_{ig} for normal and accident conditions assuming a 30% gas release from the fuel pellets [9] and a 3% and 100% rod rupture percentage, respectively.

6) Maximum Normal Operating Pressure Calculation

Calculation of the maximum pressure in the 69BTH DSC HLZC #1 for normal conditions of transport is shown below. In accordance with [9], 3% of the fuel rods are assumed to be ruptured. The total amount of gas in the DSC cavity is therefore:

$$n_{DSC-NCT} = n_{he\ initial} + n_{he\ fuel\ rod\ release} + n_{ig},$$

$$n_{DSC-NCT} = 134.39 + 3.27 + 14.28 = 151.94\,g-moles$$

Ruptured pins will vent plenum gas until it comes into equilibrium with the DSC pressure; therefore, the plenum volume within the ruptured pins can be included in the total DSC internal volume. For a 3% pin rupture the additional volume is therefore:

$$V_{pin\ plenum} = 100\, pins/assy \cdot 2.136\, in^3/pin \cdot 69\, assy/basket \cdot 0.03 = 442.15\ \ in^3.$$

The maximum normal operating pressure (MNOP) for this configuration is then,

$$P_{DSC-NCT} = \frac{\left(1.4504 \cdot 10^{-4}\, \frac{psia}{Pa}\right)(151.94\, g-moles)(8.314\, J/(mol \cdot K))(984\, °R)(5/9\, K/°R)}{(258413\, in^3 + 442.15\, in^3)(1.6387 \cdot 10^{-5}\, m^3/in^3)},$$

$$P_{DSC-NCT} = 23.61\, psia\, (8.91\, psig).$$

The maximum pressures are summarized in Table A.3–22. As seen from Table A.3–22, the maximum internal pressures in the 69BTH DSC calculated based on thermal conditions are lower than the design pressures considered for the structural evaluation.

A.3.3.3.3 37PTH DSC Operating Pressure

The maximum internal pressure for the 37PTH DSC within the MP197HB TC for NCT is determined based on the maximum allowable heat load of 22 kW discussed in Section A.3.3.1.6 and maximum assembly average burnup of 62 GWD/MTU. Although BW 15x15 fuel assembly is not allowed for transport in the 37PTH DSC, it is considered as the limiting fuel assembly type in this evaluation for conservatism.

Calculation of Maximum Normal Operating Pressure inside the 37PTH DSC follows the same methodology as described for 69BTH DSC in Section A.3.3.3.2.

The following assumptions and conservatisms are considered in calculating the maximum internal pressures within the 37PTH DSC:

a) The DSC internal pressure is calculated for the most limiting normal, and accident cases. For these cases, 3% and 100% of the fuel rods are assumed to rupture, 100% of the fuel rod helium fill gas and 30% of the fission gases are assumed to be released into the DSC cavity [9]. The methodology for DSC internal pressure calculations is in accordance with the methodology used for the 32PTH1 associated with Amendment 10 to Part 72 CoC 1004 for the Standardized NUHOMS® System [3].

b) The following fuel assemblies are considered bounding for internal DSC pressure analyses performed for 32PTH1, 32PTH, 24PTH, and 24PT4 DSCs:
WE 15x15 - for 32PTH DSC [4],
BW 15x15 - for 24PTH DSC [1],
CE 16x16 – for 24PT4 DSC [2].
Since BW15x15 is bounding by amount of irradiation gases [30], it is selected for this analysis.

c) The 37PTH DSC is assumed to be backfilled with helium to a pressure of 2.5 ± 1.0 psig after vacuum drying similar to the 32PTH1 DSC [3].

d) The fuel rod plenum fill temperature is assumed to be room temperature (70°F or 530°R). This is a reasonable assumption since the process takes place in a controlled environment.

e) The BW 15x15 fuel assembly used in the pressure calculation is assumed to be burned to *62* GWD/MTU, which is the highest *assembly average* burnup proposed for the 37PTH DSC configuration. Assuming maximum burnup creates a bounding case for the amount of fission gases produced in the fuel rod during reactor operation.

f) The average helium temperatures used in this calculation for 37PTH DSC configuration are obtained from the thermal analysis of 37PTH DSC short length configuration. The medium length 37PTH DSC results are bounded by the short length 37PTH DSC results, and hence, it is conservative to use the short cavity results.

g) Data of bounding BW15x15 fuels assembly with control components (CC) is conservatively used for calculating internal pressure for 37PTH DSC.

h) The short length 37PTH DSC design with lowest free volume and fill gas amount is conservatively used in this calculation.

i) Only 98% of DSC free cavity volume is used for pressure calculation.

1) Free DSC Cavity Volume

Free DSC Cavity volume for the 37PTH DSC is calculated using the same methodology used for the 69BTH in Section A.3.3.3.2.

The 37PTH DSC free helium volume and conservative DSC cavity volumes used for pressure calculations are summarized in Table A.3–21 and Table A.3–22, respectively.

2) Average Helium Temperature

Average Helium Temperature for the 37PTH DSC is calculated using the same methodology used for 69BTH in Section A.3.3.3.2.

The 37PTH DSC average helium temperature used for pressure calculations are calculated and summarized in Table A.3–21 and Table A.3–22, respectively.

3) Quantity of Helium Fill Gas in DSC

Helium Fill Gas in DSC for the 37PTH DSC is calculated using the same methodology used for 69BTH in Section A.3.3.3.2.

The initial 37PTH DSC helium fill gas quantities are listed in Table A.3–22.

4) Quantity of Fill Gas in Fuel Rod and Gases released as a Result of Irradiation

The total free gas in fuel rod, which includes fuel rod fill gas and gases released because of irradiation for bounding BW15x15 FA is provided in Table 7-14 of [30] for maximum burnup of 55000 MWD/MTU and extrapolated linearly for 65000 MWD/MTU as shown in the following table *for conservatism, although only a maximum average assembly burnup of 62,000 MWd/MTU is allowed for fuel assemblies in the 37PTH DSC.*

Amount of Gas released from Fuel Rods (BW15x15 FA)

Burnup, MWD/MTU	**Total Free Gas at STP,** (cm^3)
55,000	1400
65,000	1665 [(1)]

Note:
[(1)] Extrapolated value.

For 37PTH DSC, the amount of fill gas in fuel rods and fission gases released as results of irradiation are combined and the total is shown in Table A.3–22.

5) Quantity of Gas in Control Components

The 37PTH DSC PWR fuel assembly may include control components (CCs). The evaluation of gas quantities for CCs is based on the BW15x15 CCs documented in [1] Appendix J, Section J.4. For the controlling BW 15x15 assembly, up to 37 CCs may be present. These CCs are assumed to have an initial helium fill of 14.7 psia, and if 100% of the boron is consumed, and 30% released into the DSC, a total of 82.94 g-moles of gas could be released to the DSC assuming 100% cladding rupture (based on 53.8 g-mol for 24 BPRA in the 24P DSC, from [1] Appendix J, Section J.4).

The percentage of CCs rods ruptured during normal and accident conditions is assumed to be 3% and 100%, respectively, similar to the assumptions for the fuel rod rupturing. The maximum amount of gas released to the DSC cavity from the CCs n_{CC} for normal and accident conditions is given in Table A.3–22.

6) Maximum Normal Operating Pressure Calculation

Calculation of the maximum pressure in 37PTH DSC follows the same methodology as used for 69BTH DSC in Section A.3.3.3.2.

The maximum pressures for 37PTH DSC are summarized in Table A.3–22. As seen from Table A.3-22, the maximum internal pressures in 37PTH DSC calculated based on thermal conditions are lower than the design pressures considered for the structural evaluation.

A.3.3.3.4 Internal Pressure for DSCs analyzed for Storage/Transfer

The maximum internal pressures for 61BTH, 61BT, 32PTH, 32PTH1, 32PT, 24PTH, and 24PT4 DSCs for storage and transfer conditions under 10 CFR 72 requirements are determined in [1], [2], [3], and [4].

Based on discussions in Section A.3.3.2 the maximum fuel cladding and basket component temperatures for 61BTH, 61BT, 32PTH, 32PTH1, 32PT, 24PTH, and 24PT4 DSC in MP197HB TC for transport conditions (10 CFR 71) are bounded by temperatures for storage and transfer conditions (10 CFR 72) and no DSC thermal analysis is required. It is also applicable to the average gas temperatures in DSC cavity. Therefore, the internal pressure in a DSC for NCT with 3% ruptured fuel rods can be evaluated interpolating between the internal pressures calculated for normal storage/transfer conditions with 1% ruptured fuel rods and off-normal storage/transfer conditions with 10% ruptured fuel rods. Higher average helium temperatures for accident storage

and transfer conditions compared to normal temperatures provide additional conservatism in the internal pressure calculation for NCT.

Since 100% percent of ruptured fuel rods is assumed for both transfer accident conditions and transport HAC and maximum DSC shell temperatures for transfer accident conditions bound those for transport HAC as noted in Section A.3.4 (which results in lower average DSC helium temperature), the internal pressures calculated for storage licensed DSCs for transfer accident conditions bound the internal pressures for transport in MP197HB TC during HAC.

As seen from Table A.3-23, the maximum internal pressures in storage licensed DSCs calculated based on thermal conditions are lower than the design pressures considered for the structural evaluation.

A.3.3.3.5 Operating Pressures for 61BTHF and 24PTHF DSCs

As shown in Chapter 4, Table 4-28 of [4] for 32PTH DSC, a loading configuration with 50% intact and 50% damaged fuel assemblies results in negligible increase (~0.1 psi) in maximum internal pressure for bounding accident conditions.

The number of failed and damaged fuel assemblies for 61BTHF and 24PTHF DSCs is 16 and 12, respectively. Therefore, the maximum pressures calculated for 61BTH DSC and 24PTH DSC reported in Table A.3–23 can be used for 61BTHF and 24PTHF DSCs. As seen from Table A.3–23, the maximum internal pressures in storage licensed DSCs calculated based on thermal conditions are lower than the design pressures considered for the structural evaluation.

A.3.3.4 Thermal Evaluation for Loading/Unloading Operations

Vacuum drying is considered as a normal condition for wet loading operations. The fuel transfer operations for wet loading occur when the MP197HB and the loaded DSC are in the spent fuel pool. The fuel is always submerged in free-flowing pool water permitting heat dissipation. After completion of fuel loading, the TC and DSC are removed from the pool and the DSC is drained, dried, sealed and backfilled with helium. These operations occur when the annulus between the TC and DSC remains filled with water.

The water in the annulus is replenished with fresh water to prevent boiling and maintain the water level if excessive evaporation occurs. Presence of water within the annulus maintains the maximum DSC shell temperature below the boiling temperature of water in open atmosphere (212°F).

Water in the DSC cavity is forced out of the cavity (blowdown operation) before the start of vacuum drying. Helium is used as the medium to remove water and subsequent vacuum drying occurs with a helium environment in the DSC cavity. The vacuum drying operation does not reduce the pressure sufficiently to reduce the thermal conductivity of the helium in the canister cavity ([3], Appendix T, Section T.4 based on [5], [32], and [33]).

With helium being present during vacuum drying operations, the maximum temperatures including the maximum fuel cladding temperature are bounded by those calculated for transport operation if the DSC shell temperature under NCT is higher than the DSC shell temperature of

212 °F maintained during vacuum drying. As shown in Table A.3–8 and Table A.3–9 for all DSCs in MP197HB TC, all DSC shell minimum temperatures are higher than 212 °F. *Considering free convection in water in the cask/DSC annulus, evaporation cooling, and replenishing water in the annulus, which maintains cooling during vacuum dry operation, the DSC shell temperature remains below the local boiling temperature of water in the annulus. The effect of local boiling temperature of water in the annulus on thermal evaluation for loading/unloading operations is bounded by the margins provided for NCT and is, therefore, insignificant.* Therefore, no additional thermal evaluation is needed.

Presence of helium during blowdown and vacuum drying operations eliminates the thermal cycling of fuel cladding during helium backfilling of the DSCs subsequent to vacuum drying. Therefore, the thermal cycling limit of 65 °C (117 °F) for short-term operations set by ISG-11 [7] is satisfied for vacuum drying operation in MP197HB.

The bounding unloading operation considered is the reflood of the DSCs with water. For unloading operations, the DSC is filled with the spent fuel pool water through its siphon port. During this filling operation, the DSC vent port is maintained open with effluents routed to the plant's off-gas monitoring system.

The maximum fuel cladding temperature during *the* reflooding event is significantly less than the vacuum drying condition owing to the presence of water/steam in the canister cavity. Based on the above rational, the maximum cladding temperature during unloading operation is bounded by the maximum fuel cladding temperature for vacuum drying operation.

Initially, the pool water is added to the canister cavity containing hot fuel and basket components. *S*ome of the water will flash to steam causing *the* internal cavity pressure to rise. This steam pressure is released through the vent port. The procedures specify that the flow rate of the reflood water be controlled such that the internal pressure in the canister cavity does not exceed the maximum pressure specified for reflooding operations as noted in Chapter A.7, Appendices A.7.7.1 through A.7.7.9. This is assured by monitoring the maximum internal pressure in the canister cavity during the reflood event. The reflood for the DSC is considered as a Service Level D event and the design pressures of the DSCs are well above 15 psig for the 32PTH DSC and 20 psig for the other DSCs (see Chapter A.7, Appendices A.7.7.1 through A.7.7.9). Therefore, there is sufficient margin in the DSC internal pressure during the reflooding event to assure that the canister will not be over pressurized.

The effects of the thermal loads on the fuel cladding during reflooding operations are evaluated in Appendix T, Section T.4.7.3 and Appendix U, Section U.4.7.3 for BWR and PWR fuel assemblies respectively, associated with Amendment 10 to Part 72 CoC 1004 for the Standardized NUHOMS® System [3]. Since the same fuel assemblies are handled in the DSCs contained in MP197HB, these evaluations remain valid for this calculation.

A.3.4 Thermal Evaluation under Hypothetical Accident Conditions

The thermal performance of the MP197HB TC loaded with DSCs with heat load up to 32 kW is evaluated in this section under the HAC described in 10 CFR 71.73 [6]. This evaluation is performed primarily to demonstrate the containment integrity of the MP197HB TC for HAC. This is assured as long as the *seal temperatures* remain below *the long-term temperature limits presented in Section A.3.1.* 400°F (204°C) and the cask cavity pressure is less than the design pressure as specified in Section A.3.1.

The evaluations are presented in Section A.3.6.11 for the case that the physical integrity of the fuel assemblies may not be guaranteed. For the case that the physical configuration of the fuel assemblies is not altered, the thermal evaluations are presented in below for HAC.

The finite element model of the MP197HB TC developed in Section A.3.3.1.1 is modified in this evaluation to determine the maximum component temperatures for HAC. For the transient runs considering HAC conditions, the basket and hold-down ring (if applicable) are homogenized. SOLID70 elements are used to model the homogenized basket and hold-down ring. The elements for other components are the same as those described in Section A.3.3.1.1.

Ambient conditions for HAC are based on 10 CFR 71 [6] requirements and are applied on the boundaries of the cask model. These conditions are listed below.

Hypothetical Accident Conditions for MP197HB

Period	Ambient temperature (°F)	Insolance	Duration (hr)
Initial Conditions	100	Yes	N/A
Fire	1475	No	0.5
Wood Smoldering	100	Yes	0.5
Cool-Down	100	Yes	N/A

The assumptions and conservatism considered in evaluation for HAC are described in Sections A.3.4.1 and A.3.4.2.

A.3.4.1 Initial Conditions

The initial temperatures for the MP197HB TC transient model before the fire accident are determined using the same boundary conditions for NCT (100°F ambient with insolation) described in Section A.3.3.1.1 except that the decay heat load is applied as a uniform heat generation rate over the homogenized basket for the transient runs.

$$q''' = \frac{Q}{(\pi/4)\, D_i^2\, L_b}$$

q''' = decay heat generation rate (Btu/hr-in^3)
Q = decay heat load (Btu/hr) (to convert from kW multiply by 3412.3)
D_i = DSC inner diameter (in)
L_b = Basket length (in)
The decay heat generation rates used in the transient model are listed below.

Decay Heat Generation Rate

DSC Type	Heat Load (kW)	Heat Load (Btu/hr)	D_i (in)	L_b (in)	Decay heat Generation Rate (Btu/hr-in^3)
69BTH	26.0	88,720	68.75	164	0.1457
	32.0	109,194	68.75	164	0.1794
24PTH	26.0	88,720	66.19	168.60	0.1529

All the assumptions and conservatism described in Section A.3.3.1.1 for the MP197HB model are valid for determination of initial conditions.

A.3.4.2 Fire Test Conditions

No fire test is performed. Instead, the fire conditions are simulated using the finite element model of the MP197HB TC.

Based on the requirements in 10 CFR 71, part 73 [6], a fire temperature of 1475 °F, fire emissivity of 0.9 and a period of 30 minutes are considered for the fire conditions. A bounding forced convection coefficient of 4.5 Btu/hr-ft^2-°F is considered during burning period based on data from reference [13]. Surface emissivity of 0.8 is considered for the packaging surfaces exposed to fire based on 10 CFR 71, part 73 [6].

The total heat transfer coefficient during fire is determined using the following equations.

$$h_{t,fire} = h_{r,fire} + h_{c,fire}$$

Where,

$h_{r,fire}$ = fire radiation heat transfer coefficient (Btu/hr-in^2-°F)

$h_{c,fire}$ = forced convection heat transfer coefficient during fire = 4.5 Btu/hr-in^2-°F

The radiation heat transfer coefficient, $h_{r,fire}$, is given by the equation:

$$h_{r,fire} = \varepsilon_w F_{wf} \left[\frac{\sigma(\varepsilon_f T_f^4 - T_w^4)}{T_f - T_w} \right] \quad \text{Btu/hr-in}^2\text{-°F}$$

where,

ε_w = TC outer surface emissivity = 0.8 [6]

ε_f = fire emissivity = 0.9 [6]

F_{wf} = view factor from TC surface to fire = 1.0

$\sigma = 0.1714 \times 10^{-8}$ Btu/hr-ft^2-°R^4

T_w = surface temperature (°R)

T_f = fire temperature = 1475°F = 1,935°R

The sensitivity study that documents the effects of fire emissivity of 1.0 on the thermal performance of the MP197HB TC is documented in Appendix A.3.6.8.

The following gaps are reduced from 0.0625" under NCT to 0.01" under HAC to maximize the heat input from the fire toward the cask after free drop:

a) 0.01" axial gap between thermal shield and impact limiter case

b) 0.01" axial gap between thermal shields and cask top or bottom end surface

The following modifications are considered for the MP197HB TC model to maximize the heat input from the fire toward the cask during fire period and bound the maximum temperatures during the cool-down period.

a) The thermal properties of the gaps considered for initial conditions are changed to the properties for one of the adjacent components. The thermal properties of these gaps are restored after the fire during cool-down period. These gaps are listed in Table A.3–15.

b) Based on the cask slide rail thickness and orientation shown in Figure A.3–1, the gap between the lowest point of the DSC shell and the cask inner shell is maximized when the DSC centerlines are shifted by x" calculated in Section A.3.3.1.1. For the HAC analysis, the DSC centerlines are considered to be shifted by the same amount as described in Section A.3.3.1.1 to maximize the initial and the cool-down temperatures for TC and DSC components.

c) As noted in Section A.3.3.1.1, axial and radial gaps are considered for internal sleeve. These gaps are removed during the fire period by changing the material properties of internal sleeve to those of aluminum 6061. The assumed gaps within the internal sleeve are restored for the cool-down period by changing its material properties to the effective values calculated in Section A.3.4.2.1.

d) The cask slide rails are assumed to be in contact with DSC shell during the fire period. The properties of the cask slide rail are changed to helium or a dummy material with a conductivity of 1×10-8 Btu/hr-in-°F for cool-down period.

e) It is assumed that the cask is equipped with external fins for 32 kW head load and the external fins maintain their shape during the fire and completely melt away after the fire. The finned shell and the gap between the finned shell and the shield shell outer surface remain in place after the fire.

f) The neutron shield resin and the trunnion plug resin assumed to remain intact during the fire period and disintegrate completely after the fire. Air with conduction only properties replaces these resins during the cool-down period.

g) Based on structural evaluation in Chapter A.2, the aluminum blocks of thermal shield will be crushed due to end drop accident. This crush causes also local deformation of impact limiter at the location of the aluminum blocks, which creates a relative large gap between the thermal shield and the impact limiter plates at these locations. The magnitude of deformation is larger at the lateral segments and smaller at the central segment of the impact limiter. A uniform height of 0.25" is considered for aluminum blocks after the drop accident. This value is smaller than the average block heights shown in Chapter A.2. This assumption bounds conservatively the heights of the aluminum blocks to maximize the heat input from the fire toward the seals, particularly for the port seals and ram closure plate seal located beneath the central segment of the impact limiter.

h) No heat dissipation is considered for the impact limiter outer surfaces to evaluate the maximum canister shell temperatures under steady state cool-down conditions.

In order to maximize the heat input from the fire toward the TC, the impact limiters of the MP197HB TC model are modified to reflect deformation due to drop accidents. The crush depths of impact limiters are determined in Chapter A.2 based on end, side, corner, and slap down accident drops. The minimum distances between the TC and the surface of the damaged impact limiters are recalculated based on the crush depths given in Chapter A.2 and depicted in Figure A.3–35 and Figure A.3–36. For conservatism, the maximum crush depth experienced by the impact limiter in a given direction is assumed to occur everywhere on the impact limiter.

Comparison between Figure A.3–35 and Figure A.3–36 shows that the maximum deformation is caused by the side and corner drop accidents. The shortest distances between the TC and the surface of the damaged impact limiter are 9.25" and 8" in the radial and axial directions, respectively.

To bound the shortest distances conservatively in the model, the shortest distances between the TC and the surface of the damaged impact limiter are reduced to 8.25" and 7" in the radial and axial directions, respectively. To implement this, the cask the impact limiters outer diameter is reduced from 126" to 101" and the length of the impact limiter is reduced from 58" to 34.5". The shortest distances between the TC and the surface of the damaged impact limiters in the model are calculated as follows.

Shortest distance for radial direction: $(OD_{IL,crush} - OD_{TO}) / 2 = (101 - 84.5) / 2 = 8.25$"

Impact limiter height after drop ($H_{IL,crush}$) = 34.5"
Length of Impact limiter above the cask bottom plate / lid ($h_{1,IL}$) = 27.5" (see Figure A.3–35 for end drop)
Shortest distance for axial direction: $(H_{IL,crush} - h_{1,IL}) = (34.5 - 27.5) = 7.0$"

Since the shortest distances between the cask and the deformed impact limiters are considered uniformly in all directions, the thermal model bounds conservatively the deformations determined in Section A.2. The geometry of the TC model with deformed impact limiters is shown in Figure A.3–37.

Although the impact limiters are locally deformed during the drop accident, they remain attached to the cask. Since the welds of the impact limiter shell do not break, the wood within the impact limiter shell cannot access air and would char but not burn during the hypothetical fire accident. Hence, the steel encased wood impact limiters still protect the bottom plate and the lid of the cask from direct exposure to fire.

Although unlikely, the worst-case damage due to a hypothetical puncture condition based on 10 CFR 71.73 [6] may result in tearing off the outer steel skin of the impact limiter, crushing the wood out of the damaged area, and exposing the partially contained wood to the hypothetical fire conditions.

A study of fire performance of wood at elevated temperatures and heat fluxes [14] shows that the surface temperature for the rapid spontaneous ignition of wood is between 330 °C and 600 °C (626 °F and 1,112 °F). Based on standard fire test (ASTM E119, 1988) reported in [14], if a thick piece of wood is exposed to fire temperatures between 815 °C and 1,038 °C (1,500 °F and

1,900 °F), the outermost layer of wood is charred. At a depth of 13mm (~0.5") from the active char zone, the wood is only 105 °C (220 °F). This behavior is due to the low conductivity of wood and fire retardant characteristics of char.

It is also shown that the char forming rate under high temperature fire conditions is between 37 mm/hr for soft woods and 55 mm/hr for hard woods. Redwood has a char rate of 46 mm/hr [14].

Based on the shortest distance considered between the TC and impact limiter in the axial direction, the thickness of Redwood at the central segment of the impact limiter is approximately 6" (152 mm) in the model. Assuming the redwood is compressed after drop accident, a char rate of 55 mm/hr can be considered for the wood in the central segment of the impact limiter. The time interval for the charring until the active char zone reaches 13 mm above the inner surface of the center cover plate can be calculated as follows.

$$\text{(Redwood thickness -13) / char rate} = \frac{(152-13)}{55} = 2.5 \text{ hr}$$

After this moment, the temperature of active char would be gradually imposed at the impact limiter inner surface. It takes another 14 minutes until the last 13 mm of Redwood is charred as shown below.

$$\text{(Thickness of last portion of hot Redwood) / char rate} = \frac{13}{55} = 0.24 \text{ hr} = 14.2 \text{ min}$$

During the last 14 minutes the inner surface of the impact limiter is exposed to the high temperature of the active char.

The impact of charring wood on the cask is maximized if the inner surface of the impact limiter is exposed to active char immediately after fire for 14 minutes.

To bound the problem and remain conservative, it is considered in the finite element model that the inner surface of the impact limiter inner cover is exposed to the char wood temperature for 30 minutes immediately after the end of fire. A char wood temperature of 900°F is considered for these conditions, which is approximately the average of the maximum and minimum char wood temperatures given in [14].

No heat dissipation is considered for the open surface of the torn segment after this period, assuming conservatively that this surface is entirely covered with a thin layer of low conductivity wood char.

For the MP197HB TC containing a BWR DSC, the heat load is closer to the rear impact limiter. The ram closure plate and the test *seals* are located within a radius of 18.5" from the TC centerline in the cask bottom plate. Considering the locations of the seals and the impact limiter segments, the worst case condition occurs for MP197HB TC containing a BWR DSC when the center segment of the rear impact limiter (from centerline to OD 40") is punctured.

For the MP197HB TC containing a PWR DSC, the heat load is closer to the front impact limiter due to the use of cask spacers at the bottom of the cask. The cask lid O-ring and the vent and test O-rings are located outside the radius of 32.25". Therefore, the worst case condition occurs for the MP197HB TC containing a PWR DSC when a lateral segment of the front impact limiter (from ID 40" OD 126") is punctured.

Based on thermal analysis presented in Section A.3.3.1.1 and results shown in Table A.3–8 and Table A.3–9 for NCT, the maximum seal temperatures of MP197HB TC are bounded by

69BTH DSC with 32 kW heat load in TC with external fins,
69BTH DSC with 26 kW heat load in TC without internal sleeve, and
24PTH DSC with 26 kW heat load in TC with an internal sleeve and without external fins.

To determine the peak seal temperatures for HAC, a series of transient runs with the above bounding maximum heat loads are performed. The transient runs are listed in the following table.

List of Transient Runs

Case No.	DSC Type	Fuel Type	Heat Load (kW)	External Fins	Internal Sleeve
1	69BTH	BWR	32	Yes	No
2	69BTH	BWR	26	No	No
3	24PTH	PWR	26	No	Yes

As noted previously, the basket and hold-down ring are homogenized for the transient runs considering HAC conditions. The properties for homogenized baskets and hold-down ring are calculated in Section A.3.3.1.5 for 69BTH DSC and in [1], Appendix P, Section P.4 for 24PTH DSC.

Transient runs are performed for 20 hours after the fire. The results of the transient runs discussed in Section A.3.4.3 show that the maximum temperatures of cask components are declining so that the maximum cask component temperatures at 20 hours after the fire accident bound the maximum temperatures for the steady state conditions.

Due to large thermal mass of the basket, the maximum basket component temperatures will be achieved under steady state conditions after the fire accident. The results of transient runs discussed in Section A.3.4.3 verify this conclusion. Steady state runs are performed for all DSC types in this calculation.

The DSC shell temperature profiles from steady state runs are used to determine the maximum basket component temperatures including the maximum fuel cladding temperature during HAC.

The steady state runs performed in this calculation are listed below.

List of Steady State Runs for Cool-Down Period

Case No.	DSC Type	Heat Load (kW)	External Fins	Internal Sleeve
1	69BTH	32.0	Yes, Melted	No
2	69BTH	29.2	Yes, Melted	No
3	69BTH	26.0	No	No
4	24PTH	26.0	No	Yes
5	61BTH Type 1	22.0	No	Yes
6	61BTH Type 2	24.0	No	Yes
7	61BT	18.3	No	Yes
8	37PTH	22.0	No	No
9	32PTH / 32PTH Type 1	26.0	No	No
10	32PTH1 Type 1	26.0	No	No
11	32PTH1 Type 2	24.0	No	No
12	32PT	24.0	No	Yes
13	24PT4	24.0	No	Yes

For the post fire conditions, it is assumed that all external surfaces are covered with soot. The solar absorptivity of soot is 0.95 [22]. To bound the problem, the thermal analysis uses a solar absorptivity of 1.0 and an emissivity of 0.9 for the packaging outer surfaces during the cool-down period.

Insolance during the post fire, cool-down conditions is applied as a heat flux over the TC outer surfaces using average insolence values from 10 CFR 71 [6]. The insolance values are averaged over 24 hours and multiplied by the surface absorptivity factor to calculate the solar heat flux. The solar heat flux values used in MP197HB TC model for cool-down conditions are summarized below.

Solar Heat Flux for Cool-Down Period

Surface Material	Shape	Insolance over 12 hrs [6] (gcal/cm^2)	Solar Absorptivity	Total solar heat flux averaged over 24 hrs (Btu/hr-in^2)
All materials	Curved	400	1.0	0.4267
	Flat vertical	200	1.0	0.2133

For cool-down conditions, convection and radiation heat transfer from the TC outer surfaces are combined together as total heat transfer coefficients using the same methodology described in Section A.3.3.1.1 with an emissivity of 0.9 representing the soot covered external surfaces.

The finite element models described in Section A.3.3.1.1 are used for the steady state runs considering cool-down conditions. These models are modified to consider the deformed shape of the impact limiters. In addition, the material properties of neutron shield resin and trunnion plug resin are changed to air (conduction only) to conservatively bound the conductivity of charred or decomposed resins after fire.

The following modifications are considered for the steady state runs to maximize the DSC shell temperatures conservatively.

a) Homogenized baskets are not considered in the steady state runs for the cool-down period. Instead decay heat fluxes are applied on the inner surface of the DSC shells using the same methodology and values described in Section A.3.3.1.1 for NCT.

b) Adiabatic boundary conditions are imposed on the impact limiter outer surfaces for steady state runs under cool-down conditions.

The other boundary conditions and the surface properties for steady state runs are the same as those considered for cool-down period in transient runs.

The material properties used in the MP197HB model are listed in Section A.3.2.1.

The geometry of the TC model with deformed impact limiters is shown in Figure A.3–37.

Typical boundary conditions for HAC are shown in Figure A.3–38 and Figure A.3–39.

For the 69BTH and 37PTH DSCs, the DSC shell temperature profiles retrieved form the post fire steady state runs are applied to the DSC/basket finite element models to determine the maximum fuel cladding and basket component temperatures during HAC. For all other DSC types, comparison between the maximum DSC shell temperatures for HAC and accident transfer conditions is used to bound the maximum fuel cladding and basket component temperatures.

The finite element models of 69BTH DSC and 37PTH DSC described in Section A.3.3.1.4 and Section A.3.3.1.6, respectively are used for HAC thermal analysis calculation without any modifications. The methodology and the heat generation boundary conditions for these models are the same as those described in Section A.3.3.1.4 and Section A.3.3.1.6. The DSC shell temperatures for post fire, cool-down conditions are retrieved from the MP197HB transport cask models and transferred to the DSC/basket models. All other boundary conditions for 69BTH DSC and 37PTH DSC models remain the same as those described in Section A.3.3.1.4 and Section A.3.3.1.6 without any modification.

A.3.4.2.1 Effective Properties in the MP197HB TC HAC Model

The effective properties for 69BTH basket, 69BTH top grid assembly are calculated in Section A.3.3.1.5 and are used in HAC analysis.

The effective properties for 24PTH basket are based on data for 24PTH-S or –L without inserts from [1], Appendix P, Section P.4.2, Item 13 and are used in HAC analysis.

Effective Density for the Cask Internal Sleeve

The effective conductivities for the cask internal sleeve were calculated in Section A.3.3.1.3. Since no density and no specific heat is considered for helium, the specific heat for the internal sleeve is equal to specific heat of aluminum.

$m_{He} = \rho_{He} \times V_{gaps} = 0$
$c_{P,He} = 0$

$$C_{p,eff} = \frac{m_{Al} \cdot C_{P,Al} + m_{He} \cdot C_{P,He}}{m_{Al} + m_{He}} = C_{p,Al}$$

The effective density of the cask internal sleeve is calculated as follow.

Vol_1 = Volume of one piece as shown in Figure A.3–12.

$$= \frac{\pi}{4}\left(D_o^{\,2} - D_i^{\,2}\right) \cdot \frac{\theta_{Al}}{360} \cdot L_{Al} = 317.4 \text{ in}^3$$

D_o = OD of internal sleeve = 70.5" (Section A.3.3.1.5)
D_i = ID of internal sleeve =68" (Section A.3.3.1.5)
θ_{Al} = angel of one internal sleeve piece = 8.6° (Section A.3.3.1.5)
L_{Al} = length of one internal sleeve piece = 48.86" (Section A.3.3.1.5)

V_{Sleeve} =Volume of internal sleeve = No. of pieces × Vol_1 = 4 × 40 × 317.4 = 50,784 in^3

V_{Total} = Volume occupied by internal sleeve = $\frac{\pi}{4}\left(D_o^{\,2} - D_i^{\,2}\right) \cdot L_{Sleeve}$ = 53,301 in^3

L_{Sleeve} = 196" (Section A.3.3.1.5)

$$\rho_{eff,Sleeve} = \rho_{Al} \cdot \frac{V_{Sleeve}}{V_{Total}} = 0.098 \times \frac{50{,}784}{53{,}301} = 0.098 \times 0.95 = 0.093 \text{ lbm/in}^3$$

Effective Heat Transfer Coefficient for Cask External Fins

Since the cask external fins are not considered explicitly in the TC model, an effective total heat transfer coefficient is calculated for finned shell based on the area ratio of the finned surface to the un-finned base.

$$\text{Fin factor} = \frac{A_{finned}}{A_{base}} = 7.193$$

$$A_{finned} = \frac{\pi}{4}\left[(98.25 + 2 \times 3)^2 - (98.25)^2\right] \times 2 + \pi(1 - 0.156) \times 98.25 + \pi(0.156)(98.25 + 2 \times 3)$$

A_{finned} = 2220.1 in^2

$A_{base} = \pi(98.25)(1)$ = 308.7 in^2

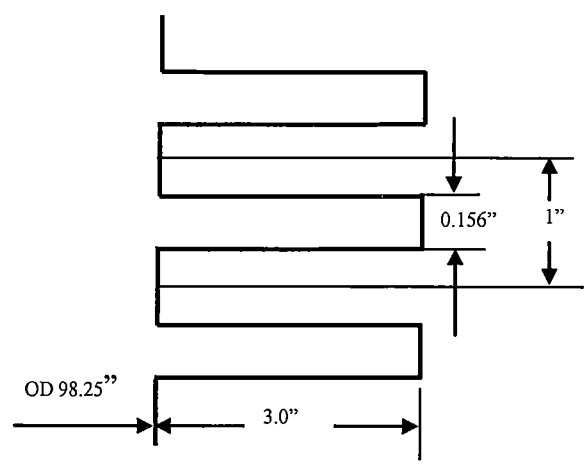

As noted, the finned shell in the thermal model is shorter and has fewer fins than the designed finned shell. To be conservative for the fire simulation, the effective total heat transfer coefficient for the finned shell is applied on the entire radial outer surface of the TC located between the two impact limiters.

It is assumed that the fins melt away after the fire *and* the shell and the gap between the finned shell and the shield shell remains in place. Therefore, the convection coefficient over the cask outer surface is determined using the correlations for horizontal cylinder described in Section A.3.3.1.1.

A.3.4.3 Maximum Temperatures and Pressure

The maximum component temperatures for transient runs are listed in Table A.3–16.

The seal*s* are not explicitly considered in the models. The maximum seal temperatures are retrieved from the models by selecting the nodes at the locations of the corresponding seal.

The time temperature histories for the TC components, DSC shell, and homogenized basket are shown in Figure A.3–40 through Figure A.3–42. As seen in time temperature histories, the basket temperature increases steadily during *the* cool-down period. It indicates that the maximum basket component temperatures will be reached for steady state conditions after fire. This behavior was expected due to *the* large thermal mass of the basket and the relative large gap between the DSC shell and the cask inner shell.

The maximum DSC shell temperatures for steady state runs are listed in Table A.3–17.

The DSC types 61BTH, 61BT, 32PTH, 32PTH1, 32PT, 24PTH, and 24PT4 are evaluated previously for accident transfer conditions under 10 CFR *Part* 72 requirements. The DSC shell temperature profiles of these DSCs in MP197HB model are compared with the corresponding profiles from 10 CFR *Part* 72 SARs in Appendix A.3.6.3. Based on discussions in Appendix A.3.6.3, the fuel cladding and the basket component temperatures for accident transfer conditions under 10 CFR *Part* 72 represent the bounding values for these DSCs for HAC under 10 CFR *Part* 72 requirements.

Therefore, no additional analysis is performed for the DSCs previously evaluated under 10 CFR *Part* 72 conditions. The maximum fuel cladding and the basket component temperatures for these DSCs are taken from 10 CFR *Part* 72 SARs and reported as the bounding values for HAC.

The maximum temperatures for DSC contents for all DSCs to be transported in MP197HB TC for HAC are listed in Table A.3–18.

The maximum TC and DSC component temperatures for HAC are summarized in Table A.3–19. Table A.3–19 shows that the maximum temperatures of the MP197HB components calculated for HAC are lower than the allowable limits.

The maximum seal temperature for fluorocarbon seals is 394 °F at cask lid for 32 kW heat load in 69BTH DSC when TC is equipped with external fins. This *short-term* temperature is below the long-term limit of 400 °F specified for continued seal function. *The short-term temperature limit for fluorocarbon seals is 482 °F as shown in [18].*

The maximum seal temperature for metallic seals is 434 °F at drain port for 32 kW heat load in 69BTH DSC when TC is equipped with external fins. This temperature is below the long-term limit of 644 °F specified for continued seal function.

The maximum temperature of gamma shield (lead) is *574*°F, which is well below the lead melting point of 621°F.

If the fuel assembly configuration is not altered, the maximum fuel cladding temperature is between 668°F and 693°F for 69BTH DSC with 26 kW to 32 kW heat loads. For 37PTH DSC, the bounding maximum fuel cladding temperature is 671°F with 22 kW heat load. These temperatures are well below the limit of 1,058°F (570°C) established in [7].

The maximum fuel cladding temperature for the DSC types evaluated at higher heat loads for transfer conditions under 10 CFR 72 remain below the allowable limit of 1,058°F (570°C).

The resins and wood are assumed to be decomposed or charred after fire accident. Therefore, the maximum temperatures for these components are irrelevant for HAC.

Typical temperature distributions for the MP197HB TC under HAC are shown in Figure A.3–43 and Figure A.3–44.

Typical temperature distributions for the 69BTH and 37PTH DSC under HAC are shown in Figure A.3–45 through Figure A.3–48.

The maximum pressures in the cask and canister cavities for HAC are calculated using the same methodology described in Section A.3.3.3.

1) MP197HB TC Cask Cavity HAC Pressure

The maximum cask cavity pressure in the MP197HB TC for HAC is calculated using the same methodology and assumptions as described for NCT in Section A.3.3.3. The nomenclature used is defined in Section A.3.3.3.

The maximum pressure in the cask cavity for HAC is calculated as:

$$P_{HAC} = \frac{\left(1.4504*10^{-4}\frac{psia}{Pa}\right)*(n_{he,initial})*R*T_{avg,he,HAC}*(5/9K/^{o}R)}{0.98*V_{free,cc}*(1.6387*10^{-5}m^{3}/in^{3})}$$

As seen from Table A.3–20 for NCT the case of 69BTH DSC in MP197HB with 32 heat load is bounding for the maximum TC cavity pressure for all DSCs. Therefore, the 69BTH DSC in MP197HB provides bounding cavity pressure for HAC as well. Based on $T_{avg,he,HAC}$ of 387°F for 69BTH DSC with 32 kW heat load shown in Table A.3–14 and the methodology presented in Section A.3.3.3, the maximum pressure in the cask cavity of MP197HB TC for HAC is calculated as 14.4 psig.

2) Internal Pressure for 69BTH and 37PTH DSCs under HAC

The maximum pressures in the 69BTH and 37PTH DSCs for HAC are calculated using the same methodology described in Section A.3.3.3. Per 10 CFR 71 [6], the percentage of fuel rods

ruptured for accident cases is 100%. The total quantity of moles released to 69BTH DSC cavity is, therefore,

$$n_{DSC-HAC} = n_{he\ initial} + n_{he\ fuel\ rod\ release,HAC} + n_{ig,HAC}$$

$$n_{DSC-HAC} = 134.39 + 108.91 + 476.10 = 719.40\, g - moles$$

The maximum accident operating pressure for this configuration is then,

$$P_{DSC-HAC} = \frac{\left(1.4504 \cdot 10^{-4}\ \frac{psia}{Pa}\right)(719.40\, g - moles)(8.314\, J/(mol \cdot K))(992\,°R)(5/9\, K/°R)}{(258415\, in^3 + 14738.40\, in^3)(1.6387 \cdot 10^{-5}\ m^3/in^3)}$$

$$P_{DSC-HAC} = 106.77\, psia\ (92.07\, psig).$$

The maximum internal pressures inside 37PTH and 69BTH DSCs are summarized in Table A.3–22. The maximum internal pressures are 102.64 psig and *96.16* psig for the 37PTH DSC and 69BTH DSC under HAC, respectively. These maximum calculated internal DSC pressures are below the design pressure*s* of *120 psig and* 140 psig specified in Section A.3.1 for HAC *for* the 69BTH and 37PTH DSCs*, respectively.*

Based on discussions in Section A.3.3.3.4, the maximum internal pressures for DSCs analyzed for accident storage/transfer conditions under 10 CFR 72 requirements remain bounding for transport conditions under HAC. The evaluated DSC internal pressures for DSCs to be transported within MP197HB TC are summarized in Table A.3–23. As seen in Table A.3–23, the maximum calculated internal pressures under HAC remains below the corresponding design pressures considered for the structural evaluations for HAC for all DSC types.

A.3.4.4 Maximum Thermal Stresses

Thermal stresses for the MP197HB TC loaded with DSCs are discussed in Chapter A.2.

A.3.4.5 Accident Conditions for Fissile Material Packages for Air Transport

The MP197HB TC is not designed for air transportation. Therefore, the accident conditions for air transport are irrelevant.

A.3.5 References

1. Updated Final Safety Analysis Report for the Standardized NUHOMS® Horizontal Modular Storage System for Irradiated Nuclear Fuel, NUH-003, Rev. *14*.
2. Updated Final Safety Analysis Report for the Standardized Advanced NUHOMS® Horizontal Modular Storage System for Irradiated Nuclear Fuel, ANUH-01.0150, Rev. *6*.
3. Same as Reference 1.
4. *Updated* Final Safety Analysis Report for NUHOMS® HD Horizontal Modular Storage System for Irradiated Nuclear Fuel, Rev. *5*.
5. Perry, Chilton, Chemical Engineers' Handbook, 5th Edition, 1973.
6. U.S. Code of Federal Regulations, Part 71, Title 10, "Packaging and Transportation of Radioactive Material."
7. U.S. NRC, Spent Fuel Project Office, Interim Staff Guidance, ISG-11, Rev 3, Cladding Considerations for the Transportation and Storage of Spent Fuel.
8. U.S. Code of Federal Regulations, Part 72, Title 10, Licensing Requirements for the Independent Storage of Spent Nuclear Fuel and High-Level Radioactive Waste.
9. U.S. Nuclear Regulatory Commission, Standard Review Plan for Transportation Packages for Spent Nuclear Fuel, Final Report, NUREG-1617, January 2000.
10. ASME Boiler and Pressure Vessel Code, Section II, Part D, Material Properties, 2004.
11. Moore, R. S., Notz, K. J., Physical Characteristics of GE BWR Fuel Assemblies, Oak Ridge National Laboratory, Report No. ORNL/TM-10902, June 1989.
12. Report, Topical Report on Actinide-Only Burnup Credit for PWR Spent Nuclear Fuel Packages, Office of Civilian Radioactive Waste Management, DOE/RW-0472, Revision 2, September 1998.
13. Gregory, et al., Thermal Measurements in a Series of Long Pool Fires, SANDIA Report, SAND 85-0196, TTC-0659, 1987.
14. Mitchell S. Sweet, Fire Performance of Wood: Test Methods and Fire Retardant Treatments, Fire Safety of Wood Products, USDA Forest Service, http://www.fpl.fs.fed.us/documnts/pdf1993/sweet93a.pdf
15. Bucholz, J. A., Scoping Design Analysis for Optimized Shipping Casks Containing 1-, 2-, 3-, 5-, 7-, or 10-Year old PWR Spent Fuel, Oak Ridge National Laboratory, January, 1983, ORNL/CSD/TM-149.
16. NOT USED
17. Test Report, Properties to be Considered for Safety for Resin Vyal B, Transnuclear International, Report No. DI/RI-A-1-5-02, Rev. 1, 2006.
18. Parker O-ring Handbook 5700, Y2000 Edition, 1999.
19. Parker O-ring Division, Material Report Number KJ0835, 1989.

20. U.S. Department of Agriculture, Forest Service, Wood Handbook: Wood as an Engineering Material, March 1999.

21. Rohsenow, Hartnett, Cho, Handbook of Heat Transfer, 3rd Edition, 1998.

22. Siegel, Howell, Thermal Radiation Heat Transfer, 4th Edition, 2002.

23. Kreith, Frank, Principles of Heat Transfer, 3rd Edition, 1973.

24. Rohsenow, Hartnett, Handbook of Heat Transfer Fundamentals, 2nd Edition, 1985.

25. Kumar, Madras, Thermal Degradation Kinetics of Isotatic and Atactic Polypropylene, Journal of Applied Polymer Science, Vol. 90, 2206-2213, 2003.

26. AAR Brooks & Perkins, Advanced Structural Division, "Boral® The Neutron Absorber," Product Performance Report 624.

27. ANSYS computer code and On-Line User's Manuals, Version 8.1 and 10.0.

28. NOT USED

29. NOT USED

30. Plannel, et al., "Topical Report, Extended Fuel Burnup Demonstration Program. Transport Considerations for Transnuclear Casks," Project 1014, DOE/ET 34014-11, TN-E-4226.Transnuclear Inc., 1983.

31. Nylund, O., Hjarne, L., "The SVEA BWR Fuel, Eight Years of Further development," ABB atom AB, Fuel Division, Vaesteras, Sweden.

32. Roth, A., "Vacuum Technology," 2nd Edition, 1982.

33. Lide, David, R., "CRC Handbook of Chemistry and Physics," 83rd edition, 2002-2003, CRC Press.

34. Henninger, J. H., "Solar Absorptance and Thermal Emittance of Some Common Spacecraft Thermal-Control Coatings," NASA Scientific and Technical Information Branch, NASA Reference Publication 1121, 1984.

35. Calculation, "TN-24P Benchmarking Analysis Using ANSYS," Transnuclear, Inc., Calculation No. NUH32PT.0408, Revision 0, provided to USNRC in TN Letter NUH03-03-04, Dated January 24, 2003, "Response to Request for Additional Information (RAI) and Submittal of Revision 4 of Application for Amendment No. 5 to the NUHOMS® Certificate of Compliance No. 1004 (TAC NO. L23343), Docket No. 72-1004."

36. Updated Final Safety Analysis Report for TN-68 Dry Storage Cask, Revision *8*. Certificate of Compliance No. 1027, Amendment 1.

37. U.S. Department of Energy, "Characteristics of Spent Nuclear Fuel, High- Level Waste, and Other Radioactive Wastes Which May Require Long-Term Isolation, Appendix 2A," U.S Department of Energy, Office of Civilian Radioactive Waste Management, DOE/RW-0184, Volume 3 of 6, December, 1987.

38. M. M. Yovanovich, J. R. Culham, P. Teertstra, "Calculating Interface Resistance," Electronics Cooling, Vol. 3, No. 2, May 1997.

39. Amiss, J. M., et al., "Machinery's Handbook," 24th Edition, Industrial Press, 1992 - Fig. 5, pg 672.

40. Aluminum Association, Inc., "Aluminum Standards and Data," 10th Edition, 1990 - Table 2.1, pg 33.

41. ASME Boiler and Pressure Vessel Code, Section II, Part A, "Ferrous Material Specification," 1998 and 2000 addenda - Table 2.

42. Gordon England Company, "Microhardness Test," http://www.gordonengland.co.uk/hardness/microhardness.htm

43. Eckert, "Introduction to the Transfer of Heat and Mass," 1st Edition, 1950.

44. Eckert and Jackson, "Analysis of Turbulent Free-Convection Boundary Layer on Flat Plate," NASA Technical Reports, Report Number NACA-TN-2207, 1950.

45. Kays, Crawford, and Weigand, "Convective Heat and Mass Transfer," 4th Edition, 2005.

46. Holman, "Heat Transfer," 8th Edition, 1997.

47. Kreith, "Principles of Heat Transfer," 3rd Edition, 1973.

48. Misumi, Suzuki, and Kitamura, "Fluid Flow and Heat Transfer of Natural Convection around Large Horizontal Cylinders: Experiments with Air," Heat *Transfer --Asian Research*, 32 (4), 2003.

49. T. Eric Skidmore, "Performance Evaluation of O-Ring Seals in Model 9975 Packaging Assemblies (U)," Savannah River Technology Center, WSRC-TR-98-00439, December 1998.

50. Oak Ridge National Laboratory, "Effect of Fuel Failure on Criticality Safety and Radiation Dose for Spent Fuel Casks," by K.R. Elam, J.C. Wagner and C.V. Parks, NUREG/CR-6835 (ORNL/TM-2002/255), September 2003.

51. H. J. Rack, G. A. Knorovsky, "An Assessment of Stress-Strain Data Suitable for Finite-Element Elastic-Plastic Analysis of Shipping Containers," Sandia Laboratories, NUREG/CR-0481, SAND77-1872 R-7, 1978.

52. Garlock Sealing Technologies, Inc., LLC; Catalogue: HELICOFLEX® Spring Energized Seals http://pdf.directindustry.com/pdf/garlock-sealing-technologies-inc-llc/helicoflex-spring-energized-seals/5615-10918.html

53. Parker Hannifen Corporation, Composite Sealing Systems Division, "Metal Seal Design Guide, High Performance Engineered Seals and Sealing Systems. http://www.parker.com/literature/Seal%20Group/CSS%205129.pdf

54. Domestic Light Water Reactor Fuel design, Volume III, DOE/ET/47912-3, September 1981

55. *American Society of Mechanical Engineers, "Standard for Verification and Validation in Computational Fluid Dynamics and Heat Transfer," ASME V&V 20-2009, November 30, 2009.*

56. *Fundamental FEA Concepts and Applications, ANSYS Inc.*

A.3.6 Appendices

A.3.6.1 Thermal Evaluation of MP197HB TC and 69BTH DSC for HLZC # 8 for NCT and HAC

This section presents the thermal evaluation of the 69BTH DSC with HLZC # 8 during the transport in the MP197HB TC. As shown in Figure A.1.4.9-5a, the maximum allowable heat load for HLZC # 8 is 30.2 kW and is bounded by the maximum heat load of 32 kW for HLZC # 4 shown in Figure A.1.4.9-5. Therefore, the thermal evaluation is limited to a sensitivity evaluation of the 69BTH DSC in MP197HB TC for the hot NCT.

The sensitivity study of the MP197HB TC loaded with the 69BTH DSC with HLZC # 8 for hot NCT is based on the methodology and thermal models presented in Section A.3.3. For the MP197HB TC, the thermal model described in Section A.3.3.1.1 with external fins is re-evaluated by modifying the heat load to 30.2 kW. Similarly, the thermal model for the 69BTH DSC in Section A.3.3.1.4 for HLZC # 4 is re-evaluated by modifying the heat generation rates for HLZC # 8 and the DSC shell temperature profile from the MP197HB TC thermal model with 30.2 kW heat load. No other changes are considered in these thermal models.

Normal Conditions of Transport

The maximum component temperatures for the MP197HB TC model with 30.2 kW heat load (HLZC # 8) during hot NCT are listed in table below.

Maximum Component Temperatures of MP197HB TC / 69BTH DSC Shell for Hot NCT (100 °F and Insolation)

	HLZC # 4 (1)	HLZC # 8
Heat Load	32 kW	30.2 kW
Component	T_{max} (°F)	
DSC shell	484	467
DSC shell @ mid-length (2)	470	454
Cask inner shell	367	354
Gamma shield	366	352
Outer shell	352	339
Shield shell	305	295
Finned Shell	229	223
Cask lid	267	259
Cask bottom plate	353	341
Neutron Shield Resin (3)	290	281
Trunnion Plug Resin (3)	277	268
Cask lid seal	268	260
Ram plate seal	352	339
Drain port seal @ bottom	351	339
Test seal @ bottom	349	337
Vent & test seal @ top	267	259
Wood in Impact limiter	302	292

(1) *The temperature data are from Table A.3-8 for HLZC # 4.*

(2) *This value is the maximum DSC shell temperature in the region where the fuel assemblies have the maximum peaking factor.*

(3) *This temperature is the volumetric, average temperature of the elements located at hottest cross section of the neutron shield resin / the trunnion plug resin.*

The average temperature of helium within the MP197HB TC cavity for hot NCT is listed in the table below.

Average Helium Temperatures of MP197HB TC for Hot NCT (100 °F and Insolation)

	HLZC # 4 (1)	HLZC # 8
Heat Load	32 kW	30.2 kW
Component	T_{avg} (°F)	
Helium in TC cavity	339	328

(1) *The temperature is from Table A.3-14 for HLZC # 4.*

Based on the comparisons in the above two tables, both the maximum and average temperatures of the MP197HB TC components for HLZC # 8 are bounded by those for HLZC # 4. Therefore, the MP197HB TC components are within temperature limits for their respective materials, and perform their intended safety function within the operating range for hot NCT of the 69BTH DSC with HLZC # 8.

The maximum fuel cladding and component temperatures for the 69BTH basket with HLZC # 8 are compared with those for HLZC # 4 for hot NCT in the table below.

Maximum Fuel Assemblies and 69BTH Basket Component Temperatures for Hot NCT

	HLZC # 4 (1)	HLZC # 8
Heat Load	32 kW	30.2 kW
Component	T_{max} (°F)	
Fuel Cladding	650	642
Basket (compartment)	612	594
Al / Poison Plate	612	593
Basket Rails	507	489

(1) *The temperature data are from Table A.3-10 for HLZC # 4.*

As shown in the table above, the maximum fuel cladding and 69BTH DSC component temperatures for HLZC # 8 are bounded by those for the HLZC # 4.

The average temperatures of fuel assemblies and helium within the DSC cavities are listed in the table below.

Average Fuel/Dummy Assemblies and 69BTH DSC Helium Temperatures for Hot NCT

HLZC	HLZC # 4 (1)	HLZC # 8
Heat Load	32 kW	30.2 kW
Component	T_{avg} (°F)	
Fuel Assemblies	547	533
Dummy Assemblies	558	534
Helium Elements (2)	432	413

(1) *The temperature data are from Table A.3-14 and Table A.3-21 for HLZC # 4.*

(2) *This value is the volumetric, average temperature of the elements with helium properties in the basket model. In addition to the gaps, helium properties are considered for the elements within the fuel compartments located beyond the active fuel length and for the empty compartments*

Based on the comparisons in the above two tables, both the maximum and average temperatures of fuel cladding and 69BTH DSC components for HLZC # 8 are bounded by those for HLZC # 4. Therefore, the 69BTH DSC components are within temperature limits for their respective materials, and perform their intended safety function within the operating range for hot NCT of the 69BTH DSC in the MP197HB TC with HLZC # 8.

Hypothetical Accident Conditions

As concluded above, all the temperatures of the 69BTH DSC with HLZC # 8 during hot NCT in the MP197HB TC are bounded by those computed for HLZC # 4. A similar behavior will also be observed during HAC since the thermal model of the 69BTH DSC with HLZC # 8 during HAC in the MP197HB TC is identical to that for HLZC # 4, except for the heat load in each zone. Therefore, the maximum temperatures of the 69BTH DSC with HLZC # 4 (32 kW) during HAC in the MP197HB TC remain bounding for HLZC # 8.

Internal Pressure in 69BTH DSC

As shown in the last table above, all the average temperatures within the 69BTH DSC with HLZC # 8 are lower than those computed for HLZC # 4. Therefore, the average helium temperature within the 69BTH DSC for HLZC # 4 remains bounding.

In addition to the average temperatures in the 69BTH DSC, a review of the HLZC # 4 and 8 in Figures A.1.4.9-5 and A.1.4.9-5a, respectively, shows that both configurations allow for the same number of fuel assemblies, i.e., 52. This ensures that the quantities of fill gases in fuel rods and fission gases for HLZC # 8 are the same as those for HLZC # 4. However, HLZC # 8 has one additional dummy fuel assembly in the center compartment; whereas, it remains empty in HLZC # 4 (identified as Zone 1 in Figure A.1.4.9-5). This small change does not have any significant impact on the internal pressure for HLZC # 8, as the small reduction in the DSC free volume due to the addition of one dummy fuel assembly will be offset by the lower initial helium back fill gas and the lower average temperatures discussed above.

Therefore, the internal pressures for the 69BTH DSC with HLZC # 4 for NCT and HAC in the MP197HB transport cask are still applicable for HLZC # 8.

A.3.6.2 Mesh Sensitivity

A.3.6.2.1 MP197HB TC Model Mesh Sensitivity

A slice of the MP197HB TC model containing 69BTH DSC shell is recreated for mesh sensitivity analysis. The length of the TC slice model is 24" and includes the DSC shell and cask shells. The mesh density of this model is the same as the mesh density of the geometry model used in Section A.3.3.1.1 from z=30.5" to z=60.34" except that the element size is decreased from 3.73" to 3.0" in the axial direction. The slice model contains 26,744 elements and 29,574 nodes.

For the purpose of mesh sensitivity analysis, the mesh density of the slice model is increased to more than five folds of its original value so that the number of elements and nodes are increased to 147,376 and 154,564, respectively.

Ambient temperature of 100°F with insolation and a decay heat of 26 kW are considered as boundary conditions for both TC slice models with coarse and fine meshes. The boundary conditions are applied using the same methodology as described in Section A.3.3.1.1.

The differences between the maximum temperature for coarse and fine mesh models are less than 1°F. It concludes that the TC model described in Section A.3.3.1.1 is mesh insensitive and the results are adequately accurate for evaluation.

A.3.6.2.2 Mesh Sensitivity for the 69BTH DSC Model

The mesh sensitivity analysis for the 69BTH DSC described in Section A.3.3.1.4 is performed based on a slice model of 69BTH DSC with Boral poison plates. The slice model is 26" long and is recreated by selecting the nodes and elements of the 69BTH DSC model from z=50.8" to z=76.8". The length of the slice model is twice the length of the aluminum plates and the axial gaps between them. This model contains 124,968 elements and 137,423 nodes.

A fine mesh model for the same slice is recreated. The number of elements and nodes in the fine meshed model are almost tripled to 391,644 and 414,874, respectively.

A fixed temperature of 400°F on the outer surface of the DSC shell and a decay heat of 26 kW with HLZC # 1 is selected as boundary conditions for the mesh sensitivity analysis of 69BTH DSC. A peaking factor of 1.2 is considered to apply the heat generation rate on the homogenized fuel assemblies. The heat generation boundary conditions are applied using the same methodology as described in Section A.3.3.1.4.

The differences between the maximum temperature for coarse and fine mesh models are approximately 1.0°F. It concludes that the 69BTH DSC model described in Section A.3.3.1.4 is mesh insensitive and the results reported are adequately accurate for evaluation.

A.3.6.2.3 Mesh Sensitivity for the 37PTH DSC Model

The 37PTH DSC model described in Section A.3.3.1.6 containing paired Boral and aluminum plates is selected for mesh sensitivity analysis. The homogenized fuel assemblies in this model

are modeled using a 10x10 mesh at the cross section with the largest mesh size of 0.95"×0.95". This model contains 385,933 elements and 409,836 nodes.

A fine mesh model is created for the 37PTH DSC in which the mesh density of the fuel assembly is increased to 12x12 with the largest mesh size of 0.76" ×0.76". The number of elements and nodes in the fine mesh model are increased to 508,605 and 536,592, respectively.

The DSC shell temperature profile retrieved from MP197HB transport cask model for NCT at ambient temperature of 100°F with insolation and a decay heat of 22 kW are selected as boundary conditions for the sensitivity analysis of 37PTH DSC. The boundary conditions are applied using the same methodology as described in Section A.3.3.1.6. The differences between the maximum temperature for coarse and fine mesh models are less than 1.5°F. It concludes that the 37PTH DSC model described in Section A.3.3.1.6 is mesh insensitive and the results reported are adequately accurate for evaluation.

A.3.6.3 Justification for Bounding Temperature Profiles

DSC types 61BTH Type 1 and 2, 61BT, 32PTH, 32PTH Type 1, 32PTH1 Type 1 and 2, 32PT, 24PTH, and 24PT4 are evaluated in [1], [2], [3], and [4] for storage/transfer conditions under 10 CFR 72 requirements. For these DSCs, the DSC shell temperature profile is retrieved from the transfer cask model and applied as boundary conditions to the DSC/basket model. The DSC shell temperatures and the heat generation rates within the homogenized fuel assemblies are the only boundary conditions used for each DSC/basket model. The same approach is used in this evaluation to determine the maximum fuel cladding and basket component temperatures for transportation in MP197HB TC. In this approach for each DSC type, a lower DSC shell temperature at the hottest cross section of the basket model, where the peaking factors are at their highest level, results in lower fuel cladding and basket component temperature provided that the heat load remain unchanged. In the case of a lower heat load, the fuel cladding and basket component temperature decease, even when the DSC shell temperature remain unchanged.

The maximum DSC shell temperature for normal transfer conditions under 10 CFR 72 (without air circulation) occurs generally in the mid section of the DSC where the fuel assembly has its highest peaking factor while the maximum DSC shell temperature for NCT under 10 CFR 71 occurs toward the ends of the DSC shell where it is covered by impact limiters. To illustrate this fact, the DSC shell temperature profiles for 61BTH DSC and 24PTH DSC under NCT and normal transfer conditions at 100°F ambient are compared in Figure A.3–51 and Figure A.3–52.

Based on peaking factor profiles discussed in Sections A.3.3.1.4 and A.3.3.1.6, the maximum peaking factor region is located between ~36.1" and ~84.9" for BWR and between ~28.0" to ~100.0" for PWR fuel assemblies. These locations are measured from the bottom of active fuel length. The active fuel length starts approximately 7.5" and 4.0" measured from the bottom of the fuel assembly for BWR and PWR fuel assemblies, respectively.

To quantify the differences between the DSC shell temperatures under NCT and normal transfer conditions, the maximum DSC shell temperature for each DSC type under NCT is retrieved at the above locations from the MP197HB TC model and shown in Table A.3–8 and Table A.3–9.

These temperatures give the maximum DSC shell temperature in the region of highest peaking factors, where the maximum fuel cladding temperatures are expected

The maximum DSC shell temperatures for NCT under 10 CFR 71 requirements are compared to the corresponding data for transfer conditions under 10 CFR 72 requirements in Table A.3–24.

As shown in Table A.3–24, the maximum DSC shell temperature for NCT at the mid section, where the highest peaking factors are located, is 7 to 17°F lower than the absolute maximum DSC shell temperature for the NCT. Both of these values are lower than the maximum DSC shell temperature for normal transfer conditions.

Since the DSC shell temperatures for NCT at the ends and at mid section are lower than those for the normal transfer conditions, the DSC shell temperature profile for normal transfer conditions gives the bounding values for the basket and fuel cladding temperatures.

For DSC types, 61BTH Type 2, 32PTH, 32PTH Type 1, 32PTH Type 1 and 2, 24PTH-S, and 24PTH-L the maximum heat loads for transport conditions are lower than the maximum heat loads for transfer conditions. Therefore for these DSC types, even lower basket and fuel cladding temperatures are expected for NCT.

Based on this discussion, the thermal analysis results for DSCs in 10 CFR 72 SARs ([1], [2], [3] and [4]) under normal transfer conditions are applicable for NCT and represent the bounding fuel cladding and basket component temperatures.

Based on the comparison shown in the lower half of Table A.3–24, the maximum DSC shell temperatures for HAC under 10 CFR 71 requirements are also lower than the corresponding ones for accident transfer conditions under 10 CFR 72 requirements. The same arguments as above are therefore valid for HAC of transport as well. Therefore, the thermal analysis results for DSCs in 10 CFR 72 SARs ([1], [2], [3] and [4]) under accident transfer conditions are bounding for HAC and no further thermal analyses are required for these DSC types.

To provide additional assurance that the above arguments are valid and the fuel cladding and the basket component temperatures in 10 CFR Part 72 SARs represent the bounding values for transport conditions, the DSC type 24PTH-S (without Al inserts) is selected for evaluation under NCT.

Among the DSC types previously evaluated for storage applications and proposed for transport in MP197HB, DSC type 24PTH-S (without Al inserts) has the smallest margin (19°F) for the maximum fuel cladding temperature under storage conditions and has the second highest heat load for transportation conditions (26 kW) after the 69BTH DSC.

Consistent with the approach described in Section A.3.3.1.4, the DSC shell temperature profile for 24PTH DSC is retrieved from the cask model and applied as boundary conditions to the detailed model of the 24PTH-S DSC/basket. The DSC/basket model of 24PTH-S is identical to the model previously used for storage conditions in 10 CFR 72 UFSAR [1], Appendix P. A uniform heat load zone configuration with the maximum heat load of 26 kW is applied in the DSC model. The results of this case are compared with the results used in the SAR to demonstrate the conservative nature of the approach.

Comparisons of the maximum DSC component temperatures are listed in the following table.

Comparison of the Maximum Temperatures for 24PTH-S DSC

DSC Type	**24PTH-S (w/o Al inserts)**		
HLZC	Uniform (1.3 kW/FA)	Uniform (1.08 kW/FA)	Additional Thermal Margin
Operating Condition	Normal Transfer 31.2 kW UFSAR [1], Tables P.4-10, -14 and -16	NCT 26 kW	
	$T_{Transfer}$ (°F)	T_{NCT} (°F)	($T_{Transfer} - T_{NCT}$) (°F)
Fuel Cladding	733	664	+69
Fuel Compartment	682	616	+66
Al/Poison	681	615	+66
DSC Shell	475	463	+12

As seen in the above table, the maximum fuel cladding and basket component temperatures for the DSC type 24PTH-S (without Al inserts) under NCT are more than 60°F lower than the bounding values listed in the UFSAR [1]. This large difference demonstrates that the comparison of the DSC shell temperatures as discussed above is a conservative approach to bound the maximum fuel cladding and basket component temperatures for transport conditions.

A.3.6.4 Acceptance Criteria for Coating Damages for MP197HB TC

During handling and operation of MP197HB transport cask (TC), the painted surfaces of the shield shell for the un-finned cask or the anodized/painted surfaces of the finned aluminum shell for the finned cask can be scratched, peeled off, or physically damaged. The emissivity and solar absorptivity of the painted and anodized surfaces are considered as inputs for the thermal evaluation. Physical damages on the coating change the emissivity and absorptivity values of the surface, which affect the thermal performance of the cask.

This section determines acceptance criteria for the surface area of the damaged coating below which the effects on the thermal performance of the cask are insignificant.

The following assumptions and conservatism are considered in this section in addition to those described in Section A.3.3.1.1 for thermal evaluation of MP197HB TC with damaged surfaces.

- When the paint on the shield shell is damaged, the steel surface of the shield shell is exposed to ambient. In this case, emissivity and absorptivity of steel are considered for the area of damaged paint.
- An emissivity of 0.657 is reported in [5], Table 10-17 for rolled steel sheets. For conservatism, and emissivity of 0.587 is considered for steel in this section.
- When the coated surface (anodized or painted) on the external fins is damaged, the aluminum surface of these components is exposed to ambient. In this case, emissivity and absorptivity of plain, polished aluminum are considered for the damaged area.

- For polished, plain aluminum, an emissivity between 0.102 and 0.113, and a solar absorptivity between 0.09 and 0.10 are reported in [21], Table A.7.2. To bound the problem, emissivity and solar absorptivity of 0.1 are considered for the scratched surfaces of the external fins. All other material properties used in this analysis are presented in Section A.3.2.1.

Physical damages such as surface scratches or paint peel-offs expose the material beneath the coating to ambient and change the emissivity and absorptivity of the damaged area. To provide practical criteria for the coating damages, a temperature rise of approximately 1°F is considered for the maximum DSC shell temperature. Based on the thermal analysis presented in Section A.3.3, the increase in the maximum fuel cladding temperature is less than 1°F if the temperature rise of the maximum DSC shell temperature is limited to 1°F.

Considering the large margins to the temperature limits reported in Section A.3.3 for TC/DSC component and fuel cladding temperatures, this amount of rise for the maximum DSC shell and fuel cladding temperatures has insignificant effect on the thermal and structural performance of MP197HB and the DSCs loaded in it.

The finite element models of the MP197HB TC described in Section A.3.3.1.1 containing 69BTH DSC are used in this evaluation for cases when no internal sleeve is used. The un-finned MP197HB TC model is used with the maximum heat load of 26 kW and the MP19HB TC model with external fins is used with the maximum heat load of 32 kW. These models represent the maximum heat loads when no inner sleeve is used in MP197HB TC

The finite element model of the MP197HB TC described in Section A.3.3.1.1 with 24PTH DSC is used for the case that an internal sleeve is used to load a small diameter DSC. This model with the maximum heat load of 26 kW represents the maximum heat load when an internal sleeve is used in MP197HB TC.

As noted in Section A.3.3.1.1, the external finned shell considered for the thermal model of MP197HB has a different length than the designed shell. Since this calculation is a comparative analysis for damaged and undamaged coatings, the conclusion remains valid, although the assumed and designed external fin shells have different lengths.

Normal conditions of transport (NCT) at 100°F ambient with insolation are described in Section A.3.3.1.1 considered for the analyses. The analyses are performed using ANSYS, version 8.1 [27].

Two cases can be considered to develop acceptance criteria for coating damages:

1. Removal of a large portion of coating concentrated in one location
2. Multiple scratches and small peel-off spots scattered around the shield shell or finned shell

These two cases are discussed in the following sections.

Large Areal Damage – Case 1

The location and the size of a large damaged coating area affect the temperature profile on the cask surface. To bound the problem, it is considered that the large damaged coating area is located at the mid-length of the cask where the fuel assembly has its highest peaking factor. Based on discussions in Section A.3.6.3, the maximum peaking factor region is located between ~43.6" and ~92.4" for BWR fuel assemblies and between ~32" and ~104" for PWR fuel assemblies. The distances are measured in both cases from the bottom of the fuel assemblies. The maximum peaking factor region covers the z coordinates from z=31.3" to z=80.1" in the MP197HB TC model with 69BTH DSC and coordinates from z=30.65" to z=102.65" in the MP197HB TC model with 24PTH DSC considered in this analysis.

It is considered that the area of the damaged anodized coating is 250 in^2 for the anodized surface of the internal sleeve, 500 in^2 for the painted shield shell, and 2,000 in^2 for the coated surface of the external fins. The damaged coating area is located at the top of the cask in the middle of the maximum peaking factor region to maximize its effect on the DSC shell and fuel cladding temperatures.

The location of the damaged anodized coating on the internal sleeve is from z=58.75" to z=74.55" in the MP197HB TC model with 24PTH DSC which is 28.1" from each ends of the maximum peaking factor region. This length is selected so that the arc length of the curved surface is approximately equal to the length of the damaged area. The surface area of the damaged internal sleeve coat in this model is:

$$A_c = \frac{\theta_c}{360} \times \pi \times ID_{sleeve} \times L_c = 250 \text{ in}^2$$

A_c = Surface area of damaged internal sleeve anodized coat (in^2)

$\frac{\theta_c}{360} \times \pi \times ID_{sleeve}$ = arc length of the curved surface (in.)

θ_c = angle of damaged internal sleeve anodized coat ≈ 26.6°

ID_{sleeve} = inner diameter of internal sleeve= 68"

L_c = length of damaged internal sleeve anodized coat = 74.55 – 58.75 = 15.8"

Since the model is half-symmetric, only half of the above damaged area (approximately 125 in^2) is considered in the model. This area covers approximately 13.3° of the inner surface of the sleeve. The nodes located in the annulus between the internal sleeve and the DSC shell are adjusted in the cask model, to represent this area.

The emissivity of anodized coating was considered for the internal sleeve in the model of the MP197HB TC with 24PTH DSC described in Section A.3.3.1.1. Since the emissivity of painted coat is higher than the emissivity of anodized coat as shown in Section A.3.2.1, the model with anodized coated internal sleeve represents the bounding case. The emissivity of the damaged anodized area is changed to emissivity of polished aluminum (0.1) as discussed previously. This change affects the effective conductivity calculated for the gap between the internal sleeve and 24PTH DSC shell.

To calculate the effect of damaged anodized coating on the effective conductivity for the gap between the internal sleeve and DSC shell, the TC sub-model discussed in Section A.3.3.1.3 and shown in Figure A.3–11 is rerun with surface emissivity of 0.1 for internal sleeve. No other changes are considered for this sub-model. The results for the effective conductivity are summarized in the following table. These effective conductivities are used in the MP197HB TC model with 24PTH DSC for the area of the damaged anodized coating of internal sleeve.

All other material properties and boundary conditions are identical to those used in Section A.3.3.1.1 and remain unchanged in this calculation.

Radial Effective Conductivity for Helium in Gap between DSC Shell and Internal Sleeve with Damaged Anodized Coating

Between DSC Shell and Cask Internal Sleeve
(Mat # 39 in the ANSYS model)

$D_{o,DSC}$ =	67.19	DSC OD (in)
$D_{i,Sleeve}$ =	68.00	Cask ID (in)
L =	10	Model height (in)

T_{DSC} (°F)	T_{Sleeve} (°F)	q_{react} (Btu/hr)	T_{avg} (°F)	k_{eff} (Btu/hr-in-°F)
321	200	487	261	0.0092
365	250	487	307	0.0097
408	300	487	354	0.0103
453	350	487	401	0.0109
497	400	487	449	0.0115
542	450	487	496	0.0121
587	500	487	543	0.0128
632	550	487	591	0.0135
678	600	487	639	0.0142
725	650	487	687	0.0149
771	700	487	736	0.0157
818	750	488	784	0.0164

The location of the damaged paint on shield shell is from z=44.5" to z=66.9" in the un-finned cask model, which is 13.2" from each ends of the maximum peaking factor region in the MP197HB TC with 69BTH DSC. This length is selected so that the arc length of the curved surface is approximately equal to the length of the damaged area. The surface area of damaged paint in this model is:

$$A_P = \frac{\theta_P}{360} \times \pi \times OD_{shield} \times L_p = 500 \text{ in}^2$$

A_P = Surface area of damaged paint (in^2)

$\frac{\theta_P}{360} \times \pi \times OD_{shield}$ = arc length of the curved surface (in.)

θ_P = angle of damaged paint area ≈ 26.16°

OD_{shield} = shield shell outer diameter = 97.75"

L_P = length of damaged paint area = 66.9 – 44.5 = 22.4"

Since the model is half-symmetric, only half of the above damaged area (approximately 250 in^2) is considered in the model. This area covers approximately 13.1° of the shield shell outer surface. The nodes located on the shield shell in the un-finned cask model for MP197HB TC with 69BTH DSC, are adjusted to represent this area.

The emissivity and solar absorptivity of the damaged paint area are changed to emissivity and solar absorptivity of steel (0.587 in this analysis), which affects the solar heat flux and the total heat transfer coefficient calculated for the shield shell in the model.

Based on Section A.3.3.1.1, the solar heat flux over curved, steel surfaces is 0.2505 Btu/hr-in^2. This solar heat flux is used in the un-finned cask model for the damaged paint areas of the shield shell.

The macro "HTOT_HCL.mac" described in Section A.3.3.1.1 is used to calculate the total heat transfer coefficient for the shield shell. The same macro is used in this calculation with a surface emissivity value of 0.587 for the damaged paint areas of the shield shell.

The boundary conditions on the other surfaces are identical to those described in Section A.3.3.1.1 and remain unchanged in this calculation.

The external fins are not explicitly considered in the finned TC model as described in Section A.3.3.1.1. Instead, an effective heat transfer coefficient is applied over the outer surface of the un-finned aluminum shell to simulate the heat dissipation from this area. Due to this methodology, an effective surface area is calculated as follows to represent the damaged anodized coating of 2000 in^2.

$$A_{eff,A} = A_A \times \frac{A_{\text{footprint}}}{A_{\text{finned}}}$$

$A_{eff,A}$ = effective surface area of damaged anodized coating (in^2)
A_A = surface area of damaged anodized coating = 2000 in^2
$A_{footprint}$ = surface area of the footprint for finned shell for one fin (in^2)
A_{finned} = total surface area of the fins and finned shell for one fin (in^2)

$$A_{\text{footprint}} = \pi \times OD_{shell} \times P_{fin} = 308.7 \text{ in}^2$$

$$A_{\text{finned}} = \pi \times OD_{shell} \times (P_{fin} - t_{fin}) + 2 \times \frac{\pi}{4}\left(OD_{fin}{}^2 - OD_{shell}{}^2\right) + \pi \times OD_{fin} \times t_{fin} = 2{,}220.1 \text{ in}^2$$

OD_{shell} = finned aluminum shell outer diameter = 98.25"
P_{fin} = Fin pitch =1"
t_{fin} = fin thickness = 0.156"
OD_{fin} = fin outer diameter =104.25"

The effective surface area for the damaged anodized coating ($A_{eff,A}$) is 278 in^2. For conservatism, an effective surface area of 295 in^2 is considered in the model.

The location of the damaged coating for external fins is from z=47.1" to z=64.3" in the finned cask model, which is 15.8" from each ends of the maximum peaking factor region. This length is selected so that the arc length of the curved surface is approximately equal to the length of the damaged area. The effective surface area of damaged external fins coating in this model is:

$$A_{eff,A} = \frac{\theta_A}{360} \times \pi \times OD_{shell} \times L_A = 295 \text{ in}^2$$

θ_A = angle of damaged external fins coating area = 20.0°

$\frac{\theta_A}{360} \times \pi \times OD_{shell}$ = arc length of the curved surface (in)

OD_{shell} = external aluminum shell outer diameter = 98.25"

L_A = length of damaged external fins coating area = 64.3 – 47.1 = 17.2"

Since the model is half-symmetric, only half of the effective damaged area (approximately 147 in^2) is considered in the model. This area covers approximately 10.0° of the shield shell outer surface. The nodes located on the finned shell in the finned cask model, are adjusted to represent this area.

The emissivity and solar absorptivity of anodized coating were considered for the external fins in the original model of the finned cask. Since the emissivity of painted coat is higher than the emissivity of anodized coat as shown in Section A.3.2.1, the model with anodized coated external fins represents the bounding case. The emissivity and solar absorptivity of the damaged anodized area are changed to 0.1 which is the emissivity and solar absorptivity of polished aluminum in this analysis. This change affects solar heat flux and the effective heat transfer coefficient for the external fins with damaged anodized coating.

Based on the methodology described in Section A.3.3.1.1, the insolance value for a curved surface (400 $gcal/cm^2$) is averaged over 24 hours and multiplied by the surface absorptivity of polished aluminum to calculate the solar heat flux over fin areas with damaged anodized coating. The resultant solar heat flux is 0.0427 $Btu/hr\text{-}in^2$. This solar heat flux is used in the finned cask model for the effective surface area of the damaged anodized coating.

To calculate the effect of damaged anodized coating on the effective heat transfer coefficient for the external fins, the TC sub-model discussed in Section A.3.3.1.3 and shown in Figure A.3–10 is rerun with surface emissivity of 0.1. No other changes are considered for this sub-model. The results for the effective heat transfer coefficients are summarized in the following table. The effective heat transfer coefficients listed in the following table are used in the finned cask model for the effective surface area of the damaged anodized coating.

All other material properties and boundary conditions are identical to those in the used in Section A.3.3.1.1 and remain unchanged in this calculation.

Effective Heat Transfer Coefficients for External Fins @ 100°F Ambient

fin_h =	3.0	fin height (in)
fin_p =	1.0	fin pitch (in)
fin_t =	0.156	fin thickness (in)
fin_n =	3	No. of fins in model
D_o =	98.25	cask diameter (in)
D_f =	104.25	fin diameter (in)
D_f/D_o =	1.061	
A_eff =	77.2	area of un-finned surface (in^2)

From Rohsenow Handbook [21]

D_f/D_o	c	b
1.36	0.62	0.29
1.14	0.59	0.27
Extrapolated for this calculation based on above data		
1.061	0.579	0.263

T_s (°F)	T_{amb} (°F)	Q_{react} (Btu/hr)	A_{eff} (in^2)	h_{eff} (Btu/hr-in^2-°F)
120	100	22.760	77.2	0.0147
140	100	53.748	77.2	0.0174
160	100	88.42	77.2	0.0191
180	100	125.73	77.2	0.0204
200	100	165.16	77.2	0.0214
220	100	206.40	77.2	0.0223
240	100	248.94	77.2	0.0230
260	100	293.54	77.2	0.0238
280	100	339.55	77.2	0.0244
300	100	386.94	77.2	0.0251
320	100	435.62	77.2	0.0257
340	100	485.80	77.2	0.0262

Scattered Multiple Scratches and Small Peel-off Spots – Case 2

If the accumulated surface area of the multiple coating damages is smaller than the concentrated large damaged area considered in Case 1, the effects of the multiple damages are bounded by Case 1. Therefore, this calculation focuses on Case 1 for determination of the acceptance criteria for damaged coatings.

The maximum component temperatures for TC with damaged coatings under hot NCT with ambient temperature of 100°F and insolation are listed in the following table.

Maximum Temperatures of TC/DSC Shell with Damaged and Undamaged Coatings

TC type DSC type / Heat load Conditions	TC with External Fins and No Internal Sleeve 69BTH DSC / 32 kW NCT @ 100°F with Insolation			TC with No Fins/ No Internal Sleeve 69BTH DSC / 26 kW NCT @ 100°F with Insolation			TC with Internal Sleeve and No Fins 24PTH DSC / 26 kW NCT @ 100°F with Insolation		
Damaged Coat on External Fins 2000 in^2	Yes	No	---	N/A	N/A	---	N/A	N/A	---
Damaged Paint over Shield Shell 500 in^2	N/A	N/A	---	Yes	No	---	No	No	---
Damaged Coat on Internal Sleeve 250 in^2	N/A	N/A	---	N/A	N/A	---	Yes	No	---
Component	T_{max} (°F)	T_{max} (°F)	ΔT (°F)	T_{max} (°F)	T_{max} (°F)	ΔT (°F)	T_{max} (°F)	T_{max} (°F)	ΔT (°F)
DSC shell	484.0	483.8	0.2	451.6	451.1	0.5	464.0	464.0	0.0
Cask internal sleeve	N/A	N/A	N/A	N/A	N/A	N/A	346.7	346.7	0.0
Cask inner shell	367.4	367.3	0.1	350.9	350.7	0.2	343.0	343.0	0.0
Gamma shield	365.7	365.6	0.1	349.6	349.4	0.2	335.0	335.0	0.0
Outer shell	351.9	351.8	0.1	337.5	337.2	0.3	294.9	294.9	0.0
Shield shell	305.1	305.0	0.1	299.1	299.0	0.1	464.0	464.0	0.0
Finned Shell	229.4	229.4	0.0	N/A	N/A	N/A	N/A	N/A	N/A
Cask lid	266.9	266.9	0.0	265.4	265.3	0.1	336.0	336.0	0.0
Cask bottom plate	353.3	353.2	0.1	338.6	338.4	0.2	281.9	281.9	0.0
Cask lid seal	268.1	268.1	0.0	266.4	266.4	0.0	335.6	335.6	0.0
Ram plate seal	351.8	351.7	0.1	337.3	337.1	0.2	280.4	280.4	0.0
Drain port seal @ bottom	351.4	351.3	0.1	337.1	336.9	0.2	281.2	281.2	0.0
Test seal @ bottom	349.4	349.3	0.1	335.5	335.2	0.3	278.9	278.9	0.0
Vent & test seal @ top	266.7	266.6	0.1	265.2	265.1	0.1	335.9	335.9	0.0
Wood in Impact limiter	302.5	302.5	0.0	291.5	291.3	0.2	289.1	289.1	0.0

Note: (1) This value is the maximum DSC shell temperature in the region where the fuel assemblies have the maximum peaking factor.

As seen, the maximum DSC shell temperatures increase by 0.2°F for coating damages on external fins, 0.5°F for coating damages on shield shell, and 0.0°F for coating damages on inner sleeve. As noted previously, the rise in the maximum fuel cladding temperatures are lower than the above values and are therefore limited to less than 1°F.

A rise of less than 1°F for the maximum fuel cladding temperature is insignificant for the thermal performance of MP197HB.

Since the temperature rises are limited to 1°F, the effects of the coating damages on the thermal and structural performance of MP197HB are insignificant, if the accumulated coating damages are limited to:

- 2,000 in^2 for coating on external fins,
- 500 in^2 for paint on shield shell, and
- 250 in^2 for coating on internal sleeve.

A.3.6.5 Effective Thermal Properties of the Fuel Assemblies

This section presents the methodology and determines the bounding effective thermal conductivity, specific heat and density for the fuel assemblies to be transported within the

MP197HB TC for use in the analysis of the thermal performance. The types of fuel assemblies to be transported in MP197HB TC are listed in Chapter A.1, Section A.1.4.

A.3.6.5.1 Effective Thermal Properties for PWR Fuel Assemblies

The PWR fuel assemblies proposed for transportation in the MP197HB TC are listed in Chapter A.1, Section A.1.4. All of these PWR fuel assemblies are studied in [1] through [4]. There are minor deviations between the dimensions of the fuel assemblies listed in Chapter A.1, Section A.1.4 and those studied in [1] through [4], which have no effect on the bounding effective PWR fuel properties.

For PWR FAs, the effective fuel properties of FA WE14x14 are the bounding minimum values for all PWR FAs based on the SARS ([1] to [4]).

For the same FAs in the identical fuel compartment material and configuration, effective fuel properties for the large nominal opening sizes are lower than those for small nominal opening sizes.

For the 37PTH DSC, there are two kinds of nominal opening sizes for fuel compartments: 8.875" for four corner fuel compartments and 8.6" for the other fuel compartments. In addition, two of the compartment walls are covered with anodized aluminum/poison plates. Since the emissivity of the anodized plates is higher than the emissivity of stainless steel and the compartment opening size is smaller than 9" for the corner compartments, the effective fuel properties calculated in [1], Appendix P, Section P.4.2 based on 9.0" nominal opening size with WE14x14 FA for 24PTH DSC represent the bounding values for the fuel assemblies in the corner compartments in the 37PTH DSC.

The configuration of the other fuel compartments in the 37PTH DSC are identical to those in the 32PT DSC described in [1], Appendix M. Since the compartment opening in the 37PTH DSC (8.6") is smaller than the compartment opening in the 32PT DSC (8.7") and the compartment configurations are identical, the effective fuel properties calculated in [1], Appendix M, Section M.4.2 based on 8.7" nominal opening size with WE14x14 FA for the 32PT DSC represent the bounding values for the fuel assemblies in the compartments other than the four corner ones in the 37PTH DSC.

Based on the above discussion, no further analysis is required for PWR fuel assemblies for the 37PTH DSC model. The bounding effective properties for PWR fuel assemblies to use in the MP197HB thermal analysis are listed in Section A.3.2.1 material # 1

A.3.6.5.2 Effective Thermal Properties for BWR Fuel Assemblies

The BWR fuel assemblies proposed for transportation in the MP197HB TC are listed in Chapter A.1, Section A.1.4. Most of the proposed BWR fuel assemblies are studied in [3], Appendix T. The characteristics of the BWR fuel assemblies listed in Chapter A.1, Section A.1.4 are identical to those studied in [3], Appendix T.

Based on the study in [3], Appendix T, Section T.4.8, fuel assembly FANP 9x9-2 has the bounding transverse effective conductivity and fuel assembly Siemens QFA has the bounding axial effective conductivity, bounding effective density, and bounding effective specific heat.

BWR fuel assemblies listed in Chapter A.1, Section A.1.4 for transportation in the MP197HB TC, but not studied in [3], Appendix T, Section T.4.8 are:

- FANP 9x9, TN ID 9x9-81,
- LaCrosse, TN ID 10x10-100, and
- SVEA fuel assemblies.

The effective properties for these fuel assemblies are evaluated in this section to determine the bounding effective properties to use in the MP197HB TC and 69BTH DSC thermal analysis. The effective properties in [3], Appendix T, Section T.4.8 are calculated for stainless steel fuel compartments with a nominal opening size of 6". The same compartment material and size are considered in evaluation of the effective properties.

Effective properties for the above three BWR FAs are calculated using the methodologies and material properties approved in UFSAR for NUHOMS® system ([1], Appendices M and P) and associated with Amendment 10 to Part 72 CoC 1004 for the Standardized NUHOMS® System [3]. For the LaCrosse fuel assembly, a stainless steel cladding emissivity of 0.70 is considered in this evaluation. Perry in [5], Table 10-17, gives an emissivity between 0.62 and 0.82 for steel/stainless steel sheets heated or covered with shiny oxide layer. The assumed emissivity for the stainless steel cladding of the LaCrosse fuel assembly remain with this range and is therefore acceptable.

Effective Properties for Fuel Assembly FANP 9x9

The characteristics of fuel assembly FANP 9x9 (TN ID 9x9-81) shown in Chapter A.1, Section A.1.4 are identical to those for fuel assembly FANP 9x9-2 (TN ID 9x9-79/2) except for the number of fuel rods. The number of fuel rods for fuel assembly FANP 9x9 varies between 72 and 81 while fuel assembly FANP 9x9-2 has 79 fuel rods.

Due to the steel/stainless steel sheets steel/stainless steel sheets increased number of fuel rods in FANP 9x9 in comparison to FANP 9x9-2, the effective axial conductivity, density, and specific heat for FANP 9x9 is higher than those for FANP 9x9-2 and does not represent the bounding minimum values.

The two-dimensional finite element model used to determine the transverse effective conductivity of the fuel assembly FANP 9x9 is shown in the following figure. A correction factor of 1.0262 is used to increase the heat generation rate in the 2D model. This correction factor compensates the imperfection of the pellet cross section area in the model.

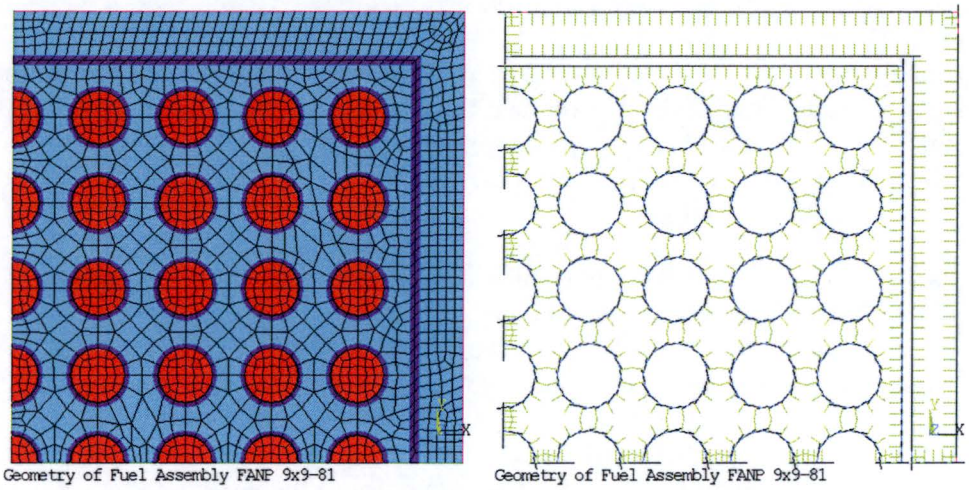

Quarter Symmetric FE Model for Fuel Assembly FANP 9x9

Effective Properties for Fuel Assembly LaCrosse

Fuel assembly LaCrosse consists of stainless steel cladding as indicated in Section A.1.4. This evaluation assumes a fuel cladding temperature limit of 752 °F (400 °C) for stainless steel cladding, which is identical to the limit for the Zircaloy cladding.

The two-dimensional finite element model used to determine the transverse effective conductivity of the fuel assembly LaCrosse is shown in the following figure. A correction factor of 1.0262 is used to increase the heat generation rate in the 2D model. This correction factor compensates the imperfection of the pellet cross section area in the model.

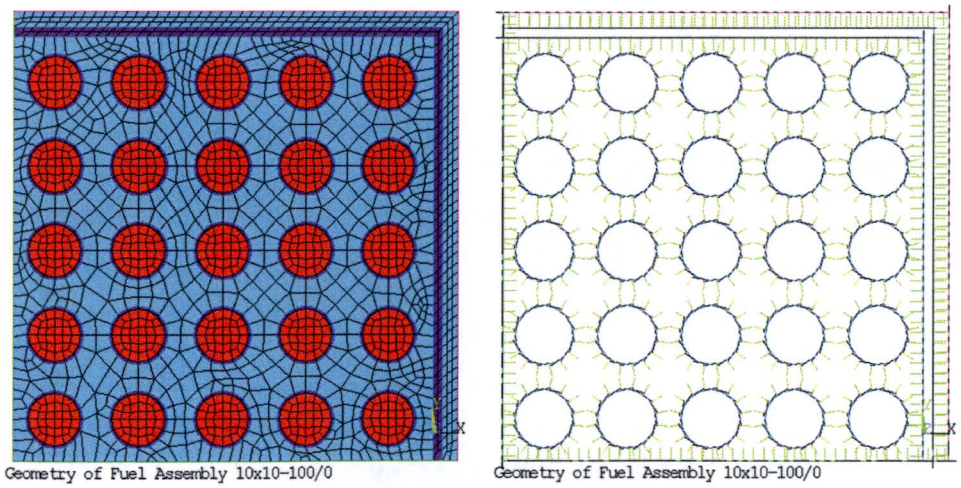

Quarter Symmetric FE Model for Fuel Assembly LaCrosse

Effective Properties for SVEA Fuel Assemblies

SVEA fuel assemblies are described in detail in [31]. Based on [31], the SVEA fuel assemblies provide larger heat transfer areas and lower heat fluxes in comparison to conventional BWR fuel assemblies with similar fuel rod arrays. In addition, the SVEA fuel assemblies consist of sub-channels which arrange the fuel rods closer to the periphery of the assembly. These factors result in higher transverse effective conductivity for these fuel types.

The sub-channels in SVEA fuel assemblies provide also more Zircaloy in comparison to conventional BWR fuel assemblies with similar fuel rod arrays. Therefore, the axial effective conductivity, effective density, and effective specific heat of the SVEA fuel assemblies are higher than those for comparable conventional BWR fuel assemblies.

To verify that the effective properties of SVEA fuel assemblies are bounded by comparable conventional BWR fuel assemblies, the effective properties of fuel assembly SVEA-92 (TN ID ABB-10-2) with four 5x5 sub-bundles are evaluated in this section.

The two-dimensional finite element model of the fuel assembly SVEA-92 used to determine the transverse effective conductivity is shown in the following figure. A correction factor of 1.0262 is used to increase the heat generation rate in the 2D model. This correction factor compensates the imperfection of the pellet cross section area in the model.

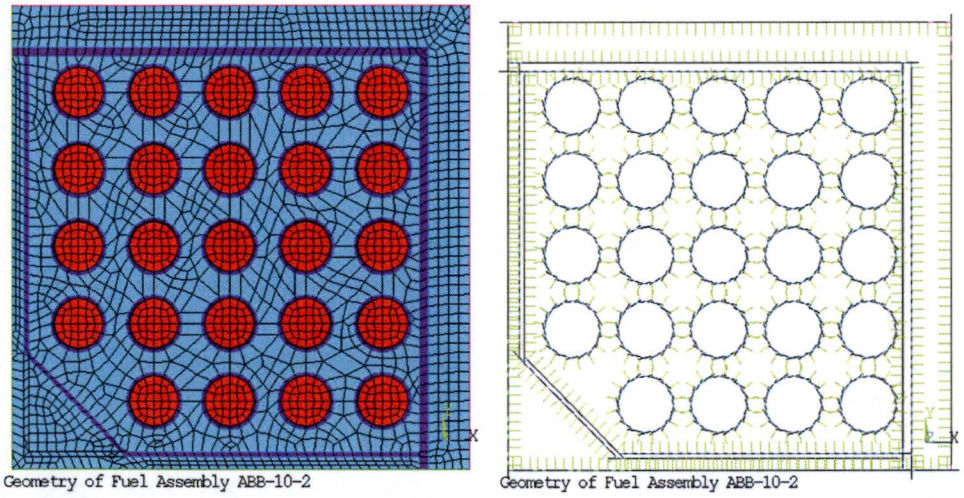

Quarter Symmetric FE Model for Fuel Assembly SVEA-92

Transverse Effective Conductivity

The results of the two-dimensional models for fuel assemblies FANP 9x9, LaCrosse, and SVEA-92 are summarized in the following table.

Fuel Assembly Transverse Effective Conductivity

FANP 9x9 (9x9-81)			
Fuel Compartment Wall Temperature (°F)	Maximum Fuel Temperature (°F)	Average Fuel Temperature (°F)	Transverse Conductivity $K_{eff,\ FANP9x9}$ (Btu/hr-in-°F)
200	228	214	0.0156
300	324	312	0.0184
400	420	410	0.0217
500	517	509	0.0255
600	615	607	0.0299
700	713	706	0.0348
800	811	805	0.0402
LaCrosse (10x10-100/0)			
Fuel Compartment Wall Temperature (°F)	Maximum Fuel Temperature (°F)	Average Fuel Temperature (°F)	Transverse Conductivity $K_{eff,\ LaCrosse}$ (Btu/hr-in-°F)
200	240	220	0.0194
300	334	317	0.0228
400	429	415	0.0267
500	525	512	0.0313
600	621	611	0.0365
700	719	709	0.0421
800	816	808	0.0483
SVEA-92 (ABB-10-2)			
Fuel Compartment Wall Temperature (°F)	Maximum Fuel Temperature (°F)	Average Fuel Temperature (°F)	Transverse Conductivity $K_{eff,\ SVEA-92}$ (Btu/hr-in-°F)
100	122	111	0.0199
200	220	210	0.0226
300	317	309	0.0255
400	415	408	0.0289
500	513	507	0.0327
600	612	606	0.0370

As seen, transverse effective conductivities for FANP 9x9 FA present the lowest conductivity values. The transverse effective conductivities for fuel assembly FANP 9x9 are compared to the bounding values from [3], Appendix T, Section T.4.8 and listed in the following table.

Transverse K_{eff} for FANP 9x9 and Bounding Values

Average Fuel Temperature (°F)	Transverse Conductivity $K_{eff, FANP9x9}$ (Btu/hr-in-°F)	Transverse Conductivity $K_{eff, bounding}$ [1] (Btu/hr-in-°F)	$\frac{K_{eff,FANP9x9} - K_{eff,bounding}}{K_{eff,bounding}}$ (---)
214	0.0156	0.0160	-2.5%
312	0.0184	0.0185	-0.1%
410	0.0217	0.0215	1.0%
509	0.0255	0.0249	2.3%
607	0.0299	0.0288	3.9%
706	0.0348	0.0331	5.1%
805	0.0402	0.0378	6.6%

Note: [1] Bounding values from [3], Appendix T, Section T.4.8

As seen, the transverse effective fuel conductivities from [3], Appendix T, Section T.4.8 remain the bounding values except for low operating temperatures below ~315°F (~157°C). For all practical purposes, the operating temperature of fuel assemblies within the 69BTH DSC is above 315°F. Therefore, the values from [3], Appendix T, Section T.4.8 remains the bounding values to be used in the thermal analysis.

Axial Effective Conductivity

The axial effective conductivities calculated for fuel assemblies FANP 9x9, LaCrosse, and SVEA-92 are compared to the bounding values from [3], Appendix T, Section T.4.8 in the following table.

Fuel Assembly Axial Effective Conductivity

	FANP 9x9 (9x9-81)	LaCrosse (10x10-100/0)	SVEA-92 (ABB-10-2)	
No of fuel rods	81	100	96	
OD fuel rod (in)	0.424	0.395	0.378	
Clad thickness (in)	0.03	0.0210	0.0243	
Sub-channel Area (in^2) [1]	N/A	N/A	0.59	
Cladding area (in^2)	3.01	2.47	3.18	
Compartment area (in^2)	36.0	36.0	36.0	
Temp (°F)	$K_{eff,axial}$ (Btu/hr-in-°F)	$K_{eff,axial}$ (Btu/hr-in-°F)	$K_{eff,axial}$ (Btu/hr-in-°F)	Bounding Value [2] $K_{eff,axial}$ (Btu/hr-in-°F)
70	0.0503	0.0491	0.0532	0.0402
100		0.0497		
200		0.0531		
300		0.0560		
700		0.0674		
1000		0.0748		

Notes:
[1] The area of sub-channel is determined using the FE model of SVEA-92.
[2] Bounding values are from [3], Appendix T, Section T.4.8

As seen, the axial effective fuel conductivity from [3], Appendix T, Section T.4.8 remains the bounding value to be used in the thermal analysis.

Effective Density and Specific Heat

The effective density (ρ_{eff}) and specific heat ($c_{P,\ eff}$) calculated for fuel assemblies FANP 9x9, LaCrosse, and SVEA-92 are compared to the bounding values from [3], Appendix T, Section T.4.8 in the following table.

Fuel Assembly Effective Density and Specific Heat

	FANP 9x9 (9x9-81)	LaCrosse (10x10-100/0)	SVEA-92 (ABB-10-2)	
No of fuel rods	96 (1)	81	96	Bounding Values (2)
OD fuel rod (in)	0.395	0.424	0.378	
Clad thickness (in)	0.0210	0.03	0.0243	
No of water tubes	4 (1)	0	0.59	
Pellet OD (in)	0.3465	0.3565	0.3224	
Fuel length (in)	85	150	150.59	
Cladding area (in^2)	2.47	3.01	3.18	
UO_2 area (in^2)	9.05	8.09	7.84	
Compartment area (in^2)	36.0	36.0	36.0	
Cladding volume (in^3)	210	451	479	
UO_2 volume (in^3)	769	1213	1180	
Compartment volume (in^3)	3060	5400	5421	
$Density_{eff}$ (lbm/in^3)	0.119	0.109	0.107	0.103
$c_{P,\ eff}$ (Btu/lbm-°F)	0.0658	0.0578	0.0579	0.0575

Notes:
(1) Fuel assembly FANP 9x9 can optionally contain up to four water rods. To determine the lowest possible density and specific heat, four water rods are considered for fuel assembly FA FANP 9x9.
(2) Bounding values are from [3], Appendix T, Section T.4.8

As seen, the effective density and specific heat from [3], Appendix T, Section T.4.8 remain the bounding values to be used in the thermal analysis.

The effective conductivities along with specific heat and density used for BWR fuel assemblies are summarized in Section A.3.2.1 material # 2.

A.3.6.6 Thermal Analysis of 24PTHF and 61BTHF DSCs in the MP197HB TC

The 24PTHF and 61BTHF DSCs are proposed for transportation of damaged and failed fuel assemblies in the MP197HB. The failed fuel assemblies are to be encapsulated in individual failed fuel cans (FFCs) that are designed to fit into the 61BTHF and 24PTHF basket fuel compartments. The 24PTHF and 61BTHF DSCs have the same basket configurations as those for 24PTH and 61BTH DSCs except for additional FFCs to store failed fuel assemblies.

Damaged FAs are assemblies containing missing or partial fuel rods or fuel rods with known or suspected cladding defects greater than hairline cracks or pinhole leaks. Damaged FA may be stored in the certain basket locations and does not require a separate FFC.

Failed FA is defined as any fuel assembly damage exceeding above damaged FA such as ruptured fuel rod, severed fuel rod, loose fuel pellets or fuel assemblies that cannot be handled by normal means. Failed FAs may contain breached rods, grossly breached rods, and other defects such as missing or partial rods. Failed FA can not be handled by normal means and requires a separate FFC to store.

The 24PTHF DSC can accommodate up to a maximum of 12 damaged fuel assemblies or up to eight failed FAs placed in the outermost fuel compartments as shown in Figure A.3–49. It is assumed in this evaluation that the 24PTHF DSC is loaded with four damaged FAs and eight failed FAs to bound the maximum temperatures.

The 61BTHF DSC can accommodate up to a maximum of 16 damaged fuel assemblies or up to four failed FAs placed in corner 2x2 fuel compartment assemblies as shown in Figure A.3–50. It is assumed in this evaluation that 61BTHF DSC is loaded with 12 damaged FAs and four failed FAs to bound the maximum temperatures.

The following assignments are used in the section for 24PTHF and 61BTHF DSCs.

	With Al inserts/ Aluminum Rails	**Without Al inserts /Aluminum Rails**
24PTH	Type 1	Type 2
61BTH	Type 2	Type 1

A.3.6.6.1 Effective Thermal Conductivity of Damaged Fuel

For PWR FAs, damaged WEO 17x17 PWR FA with minimum conductivity pitch size provides the minimum effective transverse conductivity for a damaged FA in the 32PTH DSC as discussed in [4], Section 4.14.3. For BWR FAs, damaged GE-2 BWR FA with a pitch of 0.607" provides the minimum and bounding effective transverse conductivity for a damaged FA in 61BT DSC as discussed in [1], Appendix K, Section K.4.8.1.

As listed in [4], Section 4.14.3 and [1], Appendix K, Section K.4.8.1, the damaged FA thermal conductivities in transverse direction are about 69% to 71% of the intact PWR FA thermal conductivity and about 82% to 85% of the intact BWR FA thermal conductivity. To bound the reduction in transverse thermal conductivity of damaged FAs in 24PTHF and 61BTHF DSCs, the effective transverse conductivities for intact FAs in 24PTH DSC and 61BTH DSC are reduced by 65% and 80% to use for the damaged PWR and BWR FAs, respectively.

Reconfiguration of fuel rods as a consequence of damaged grids doesn't have any impact on axial thermal conductivity of the damaged fuel. To bound the reduction in axial thermal conductivity due to the cladding defects, the axial effective conductivities for the intact FAs in 24PTH DSC and 61BTH DSC are reduced by 90% for the damaged PWR and BWR FAs.

The following tables summarize the bounding fuel thermal properties for 24PTHF and 61BTHFdamaged/intact FAs.

Bounding Damaged Fuel Thermal Conductivities for 24PTHF FAs

Keff_rad			Keff_axl		
Temp	Intact Fuel (1)	Damaged Fuel (2)	Temp	Intact Fuel (1)	Damaged Fuel (3)
°F	Btu/min-in-°F	Btu/min-in-°F	°F	Btu/min-in-°F	Btu/min-in-°F
178	2.798E-04	1.819E-04	200	7.596E-04	6.836E-04
267	3.257E-04	2.117E-04	300	8.014E-04	7.213E-04
357	3.829E-04	2.489E-04	400	8.432E-04	7.589E-04
448	4.547E-04	2.956E-04	500	8.781E-04	7.903E-04
541	5.389E-04	3.503E-04	600	9.129E-04	8.216E-04
635	6.326E-04	4.112E-04	800	9.896E-04	8.906E-04
730	7.398E-04	4.809E-04			
826	8.558E-04	5.563E-04			

Notes:
(1) Bounding thermal conductivities for 24PTH intact FA listed in [1] Appendix P, Section P.4.2.1.
(2) Based on 65% of bounding intact fuel thermal conductivities for transverse direction.
(3) Based on 90% of bounding intact fuel thermal conductivities for axial direction.

Bounding Damaged Fuel Thermal Conductivities for 61BTHF FAs

	$K_{eff\ rad}$		$K_{eff\ axl}$	
Temp	Intact Fuel (1)	Damaged Fuel (2)	Intact Fuel (1)	Damaged Fuel (3)
°F	Btu/min-in-°F	Btu/min-in-°F	Btu/min-in-°F	Btu/min-in-°F
200	2.618E-04	2.094E-04	6.720E-04	6.048E-04
300	3.021E-04	2.417E-04		
400	3.520E-04	2.816E-04		
500	4.104E-04	3.283E-04		
600	4.756E-04	3.805E-04		
700	5.468E-04	4.374E-04		
800	6.250E-04	5.000E-04		

Notes:
(1) Bounding thermal conductivities for 61BTH intact FA listed in [3] Appendix T, Section T.4.2.1.
(2) Based on 80% of bounding intact fuel thermal conductivities for transverse direction.
(3) Based on 90% of bounding intact fuel thermal conductivities for axial direction.

The FFC is required to encapsulate failed FA before loading it into the fuel compartment. To bound effective thermal conductivity of the FFC containing failed FAs, helium thermal conductivity is conservatively assumed for the space within a compartment loaded with a FFC.

A.3.6.6.2 Heat Generation Rates

The base heat generation rates are calculated assuming uniform heat loads for fuel assemblies loaded in 24PTHF and 61BTHF DSCs. The nominal fuel cell openings are 8.9 in^2 for 24PTHF DSC and 6.0 in^2 for 61BTHF DSC.

The conditions of failed FAs are unknown under NCT. The worse case condition occurs when the heat load from a failed FA is concentrated in the region where the intact FAs have the maximum peaking factor. Based on the decay heat profiles discussed in Sections A.3.3.1.4 and A.3.3.1.6, the maximum peaking factor region is located between 36.1" to 84.9" for BWR FAs and between 28.0" to 100.0" for PWR FA. These locations are measured from the bottom of the

active fuel length. This gives minimum heat load lengths of 48.8" (=84.9"-36.1") and 72.0" (=100.0"-28.0") for failed BWR and PWR FAs in 61BTHF and 24PTHF DSCs, respectively.

An unlikely hypothetical accident case is postulated in which the defected cladding of damaged FAs might break entirely in consequence of a drop accident and fuel pellets could be released in the compartment space. The concentration of the decay heat for the fuel rubble is maximized when all the rubble are compressed to a minimum length at one end of the fuel compartment.

The minimum length of the fuel rubble is calculated using equation (3) in [1] Appendix K, Section K.4.8.1.2. The shortest fuel rubble heights of 54" for a PWR FA and 50" for a BWR FA are calculated based on minimum fuel assembly volumes for WE14x14 and Siemens QFA 9x9 in this evaluation.

The following assumptions are considered for calculation of heat generation rates for failed FAs under NCT and HAC:

a) Active fuel length of 72" with uniform peaking factor of 1.11 for failed FA in 24PTHF under NCT. The heat load is concentrated in the region of the maximum peaking factors for intact fuel assemblies.

b) Minimum rubble length of 54" with peaking factor of 1.0 for failed and damaged FAs in 24PTHF under HAC. Fuel rubbles are collected at the top end of the fuel compartment (hot end).

c) Active fuel length of 48.8" with uniform peaking factor of 1.20 for failed FA in 61BTHF under NCT. The heat load is concentrated in the region of the maximum peaking factors for intact fuel assemblies

d) Minimum rubble length of 50" with peaking factor of 1.0 for failed and damaged FAs in 61BTHF under HAC. Fuel rubbles are collected at the bottom end of the fuel compartment (hot end).

The following equations calculate the base heat generation rates for the maximum allowable heat loads of 26 kW and 24 KW defined in Section A.3.1 for 24PTHF and 61BTHF DSCs in MP197HB TC under NCT and HAC, respectively:

For 1.083 kW/FA (26 kW / 24 FA) heat load in 24PTHF Intact/Damaged FAs under NCT

$$\ddot{q} = \frac{1.11 \cdot (1.083)\,kW \cdot 3412.3 \frac{Btu/hr}{kW} \cdot \frac{1\,hr}{60\,\min}}{(8.9\,in)^2 \cdot 140.6\,in} = 6.14e-3 \frac{Btu}{\min \cdot in^3},$$

For 1.083 kW/FA (26 kW / 24 FA) heat load in 24PTHF Failed FAs under NCT

$$\ddot{q} = \frac{1.11 \cdot (1.083)\,kW \cdot 3412.3 \frac{Btu/hr}{kW} \cdot \frac{1\,hr}{60\,\min}}{(8.9\,in)^2 \cdot 72\,in} = 1.20e-2 \frac{Btu}{\min \cdot in^3},$$

Note the above heat generation rate calculated for 72" for failed FAs is applied over 73.37" (from z-coordinates 48.18" to 120.55") in the model which is conservative.

For 1.083 kW/FA (26 kW / 24 FA) heat load in 24PTHF Intact under HAC

$$\dddot{q} = \frac{1.11 \cdot (1.083)\,kW \cdot 3412.3 \frac{Btu/hr}{kW} \cdot \frac{1\,hr}{60\,\min}}{(8.9\,in)^2 \cdot 140.6\,in} = 6.14e-3 \frac{Btu}{\min \cdot in^3},$$

For 1.083 kW/FA (26 kW / 24 FA) heat load in 24PTHF Failed/Damaged FAs under HAC

$$\dddot{q} = \frac{1.00 \cdot (1.083)\,kW \cdot 3412.3 \frac{Btu/hr}{kW} \cdot \frac{1\,hr}{60\,\min}}{(8.9\,in)^2 \cdot 54\,in} = 1.44e-2 \frac{Btu}{\min \cdot in^3},$$

Note the above heat generation rate calculated for 54" for failed/damaged FAs is applied over 55.93" (from z-coordinates 120.55" to 176.48") in the model which is conservative.

For 0.393 kW/FA (24 kW/61 FA) heat load in 61BTHF Intact/Damaged FAs under NCT

$$\dddot{q} = \frac{1.00 \cdot (0.393\,kW) \cdot 3412.3 \frac{Btu/hr}{kW} \cdot \frac{1\,hr}{60\,\min}}{(6.0\,in)^2 \cdot 144.0\,in} \cdot = 4.31e-3 \frac{Btu}{\min \cdot in^3},$$

For 0.393 kW/FA (24 kW/61 FA) heat load in 61BTHF Failed FAs under NCT

$$\dddot{q} = \frac{1.20 \cdot (0.393\,kW) \cdot 3412.3 \frac{Btu/hr}{kW} \cdot \frac{1\,hr}{60\,\min}}{(6.0\,in)^2 \cdot 48.8\,in} = 1.53e-2 \frac{Btu}{\min \cdot in^3},$$

For 0.393 kW/FA (24 kW/61 FA) heat load in 61BTHF Intact FAs under HAC

$$\dddot{q} = \frac{1.00 \cdot (0.393\,kW) \cdot 3412.3 \frac{Btu/hr}{kW} \cdot \frac{1\,hr}{60\,\min}}{(6.0\,in)^2 \cdot 144.0\,in} \cdot = 4.31e-3 \frac{Btu}{\min \cdot in^3},$$

For 0.393 kW/FA (24 kW/61 FA) heat load in 61BTHF Failed/Damaged FAs under HAC

$$\dddot{q} = \frac{1.00 \cdot (0.393\,kW) \cdot 3412.3 \frac{Btu/hr}{kW} \cdot \frac{1\,hr}{60\,\min}}{(6.0\,in)^2 \cdot 50.0\,in} = 1.24e-2 \frac{Btu}{\min \cdot in^3}.$$

Note the above heat generation rate calculated for 50" for failed/damaged FAs is applied over 50.89" (from z-coordinates 7.9" to 58.79") in the model which is conservative.

A.3.6.6.3 Calculation of Thermal Performance of the 24PTHF and 61BTHF DSC with Damaged/Failed Fuel

The maximum fuel cladding and basket component temperatures for the 24PTHF DSC are determined using the finite element models for the 24PTH-S DSC (w/o Al insert) described in [1] and the 61BTH Type 1 DSC (w/o Al R90 rail) in [3] without any geometrical modifications in this evaluation.

The DSC shell temperatures for hot normal and accident hypothetical accident conditions of transport are taken from the MP197HB TC models described in Section A.3.3.1.1 and Section A.3.4 and transferred to the above DSC/basket models.

A.3.6.6.4 Maximum Temperature of Failed Fuel Canister Wall

The maximum temperature of failed fuel canister wall is calculated using conduction through helium as follows.

$$T_{FFC} - T_{comp} = \frac{q'' \cdot d_{gap}}{K_{He}}$$

T_{FFC} = maximum temperature of failed fuel canister wall (°F)
T_{comp} = maximum temperature of fuel compartment containing failed fuel canister (°F) (retrieved from FE model)
d_{gap} = gap size between the fuel compartments and failed fuel canister
= 0.05" for 24PTHF DSC and 0.08" for 61BTHF DSC.
k_{He} = helium conductivity at T_{comp} (Btu/min-in-°F)

The heat flux from failed fuel canister is calculated as follows

$$q'' = \frac{q}{4w \cdot h} \cdot PF$$

q = heat load of failed fuel (Btu/min-in^2)
w = fuel compartment opening width (in)
h = assumed height of failed fuel (in)
PF = peaking factor

A.3.6.6.5 Evaluation of 61BTHF and 24PTHF DSCs for NCT and HAC

The maximum fuel cladding and basket component temperatures for 24PTHF Type 2 and 61BTHF Type 1 DSCs are collected in the following tables.

For NCT conditions, the maximum fuel cladding temperature is 674°F for the 24PTHF DSC with a maximum heat load of 26 kW and 711°F for the 61BTHF DSC with a maximum heat load of 24 kW.

For HAC conditions, the maximum fuel cladding temperature is 705°F for the 24PTHF DSC with a maximum heat load of 26 kW and 719°F for the 61BTHF DSC with a maximum heat load of 24 kW.

The maximum fuel cladding and basket temperatures for the 24PTHF Type 1 DSC with aluminum inserts and the 61BTHF Type 2 DSC with aluminum rails are bounded by the 24PTHF Type 2 DSC without aluminum insets and the 61BTHF Type 1 DSC without aluminum rails.

As seen in the following table, the maximum fuel cladding temperatures calculated for NCT and HAC conditions are well below the allowable limits for 24PTHF/61BTHF DSCs. All design criteria specified in Section A.3.1 are herein satisfied.

61BTHF and 24PTHF Maximum Temperatures for NCT and HAC

Transport Condition	Heat Load (kW)	$T_{max, Fuel}$ (°F)	$T_{max, Comp}$ (°F)	$T_{max, Al/Poison}$ (°F)	$T_{max, Rail}$ (°F)	Fuel Cladding Limit (°F)
24PTHF Type 1@ NCT (w/ Al inserts) (1)	26.0	<674	<628	<627	<485	
24PTHF Type 2 @ NCT (w/o Al inserts)	26.0	674	628	627	485	752 [7]
24PTHF Type 2 @ NCT (w/o Al inserts) (1)	24.0	<674	<628	<627	<485	
24PTHF Type 1@ HAC (w/ Al inserts) (1)	26.0	<705	<658	<657	<521	
24PTHF Type 2@ HAC (w/o Al inserts)	26.0	705	658	657	521	1,058 [7]
24PTHF Type 2@ HAC (w/o Al inserts) (1)	24.0	<705	<658	<657	<521	
61BHF Type 1 @ NCT (w/o Al R90 Rail)	22.0	<711 (3) (4)	<688 (3) (4)	<687 (3) (4)	<575 (3) (4)	752 [7]
61BTHF Type 2 @ NCT (w/ Al R90 Rail) (2)	24.0	<711	<688 (5)	<687 (5)	<575 (5)	
61BHF Type 1 @ HAC (w/o Al R90 Rail)	22.0	<719 (3)	<696 (3)	<696 (3)	<605 (3)	1,058 [7]
61BTHF Type 2 @ HAC (w/ Al R90 Rail) (2)	24.0	<719	<696	<696	<605	

Notes:
(1) Bounded by 24PTHF Type 2 (w/o Al insert) DSC with 26 kW heat load under transport conditions.
(2) Bounded by 61BTHF Type 1 (w/o Al R90 rail) DSC with 24 kW heat load under transport conditions.
(3) This temperature is calculated for 24 kW heat load instead of 22 kW heat load for conservatism.
(4) The small difference between this temperature and the one estimated in Table A.3–10 is due to the conservatism in note (3).
(5) Effect of aluminum inserts are omitted in calculation of this temperature for conservatism. The slight difference between this temperature and the one evaluated in Table A.3–10 has insignificant effect on thermal/structural performance.

The maximum temperatures for Failed Fuel Canisters

Transport Condition	Normal Condition of Transport (NCT)		Accident Condition of Transport (HAC)	
DSC Type	24PTHF	61BTHF	24PTHF	61BTHF
Heat Load	26 kW	24 kW	26 kW	24 kW
Component	T_{max} (°F)	T_{max} (°F)	T_{max} (°F)	T_{max} (°F)
Failed Fuel Compartment	601	606	645	645
Failed Fuel Canister	608	615	653	652

A.3.6.7 Justification of Hot Gaps

The following hot gaps assumed in the MP197HB TC, 69BTH DSC, and 37PTH DSC models are justified in this section.

a) The radial gap of 0.025" assumed between the gamma shield and the cask outer shell in MP197HB TC model.

b) The radial gap of 0.01" assumed between the finned aluminum shell and the cask shield shell in MP197HB TC model.

c) The diametrical hot gap of 0.30" between the basket outer surface and the DSC shell inner surface in 69BTH DSC model.

d) The 0.01" gaps considered on either side of the paired poison and aluminum plates in 69BTH DSC/basket model.

A.3.6.7.1 Gap between Gamma Shield and Cask Outer Shell

A radial air gap of 0.025" is assumed between the gamma shield (lead) and the TC outer shell within the finite element model of MP197HB described in Section A.3.3.1.1. This air gap is due to the differential thermal expansion of the cask body and the gamma shield.

The following assumptions are made for the verification of the gap:

- The cask body nominal dimensions *are taken* at 70°F.
- During the lead pour the cask body and lead *temperatures* are held above the melting point of lead at 620°F.
- *Because of the controlled cooling process used after lead pour is completed, the lead solidifies from the bottom upward and thus is always covered with molten lead. Any void volume or gap due to contraction of the solidifying lead is filled with molten lead which then solidifies.*
- The inner diameter of the gamma shell (lead) is equal to the outer diameter of the inner cask shell at thermal equilibrium.

The average coefficients of thermal expansion for SA-203, Gr. E and lead are listed in the following table.

Thermal Expansion Coefficients

Temperature (°F)	SA203, Gr. E α (in/in-°F) [10]
70	6.40E-06
200	6.70E-06
300	6.90E-06
400	7.10E-06
500	7.30E-06
600	7.40E-06
650	7.60E-06

Temperature (°F)	Lead α (in/in-°F) [51]
70	16.07 E-6
100	16.21 E-6
175	16.58 E-6
250	16.95 E-6
325	17.54 E-6
440	18.50 E-6
620	20.39 E-6

The density of lead as a function of temperature is listed below.

Density of Lead

Temperature (K)	Density [24] (kg/m3)	Temperature (°F)	Density (lbm/in^3)
50	11,570	-370	0.4180
100	11,520	-280	0.4162
150	11,470	-190	0.4144
200	11,430	-100	0.4129
250	11,380	-10	0.4111
300	11,330	80	0.4093
400	11,230	260	0.4057
500	11,130	440	0.4021
600	11,010	620	0.3978

The volume within the "lead cavity" is calculated by determining the cask body dimensions at 620°F. As no gaps will be present between the lead and the cask body, this volume is also equal to the volume of lead at 620°F. The mass of the lead *in the* lead cavity at 620°F is then determined.

The dimensions of the "lead cavity" for operating conditions are calculated based on cask body temperature at NCT. A temperature of 360°F is considered for the cask body. This temperature is lower than the maximum cask inner shell temperature shown in Table A.3–11 for 32 kW heat load. Since the gap size increases at lower temperatures, the above chosen value is conservative. From the mass of the lead and its density at 360°F, the lead volume at NCT is determined.

The length of the gamma shield at the cask body temperature is calculated based on thermal expansion coefficients listed in the above table. The lead volume is used to determine the maximum size of the air gap adjacent to the lead.

Determination of Lead Mass

$\alpha_{CS} = 7.44 \times 10^{-6}$ in/in-°F @ 620°F (via linear interpolation from expansion coefficients table, above)

$\rho_{lead} = 0.3978$ lbm/in^3 @ 620°F (from lead density table, above)

R_{in} = inner radius of lead cavity @ 70°F= 36.50"
R_{out} = outer radius of lead cavity @ 70°F = 39.75"
L_{cavity} = length of lead cavity @ 70°F = 195.75"

$R_{in,\,620} = (R_{in})(1+(\alpha_{CS})(\Delta T)) = (36.50)[1+(7.44E\text{-}6)(550)] = 36.6494$"

$R_{out,\,620} = (R_{out})(1+(\alpha_{CS})(\Delta T)) = (39.75)[1+(7.44E\text{-}6)(550)] = 39.9127$"

$L_{cavity,\,620} = (L_{cavity})(1+(\alpha_{CS})(\Delta T)) = (195.75)[1+(7.44E\text{-}6)(550)] = 196.5510$"

$V_{cavity} = V_{lead} = (\pi)(R_{out,620}^2 - R_{in,620}^2)(L_{cavity,\,620}) = 154{,}274.9$ in^3

$M_{lead} = (V_{lead})(\rho_{lead}) = (154{,}274.9 \text{ in}^3)(0.3978 \text{ lbm/in}^3) = 61{,}363.6$ lbm

Determination of Lead Gap

α_{CS} = 7.02 x 10^{-6} in/in-°F @ 360°F (via linear interpolation from expansion coefficients table, above)

$\alpha_{lead,\,620}$ = 20.39 x 10^{-6} in/in-°F @ 620°F (from expansion coefficients table, above)

$\alpha_{lead,\,360}$ = 17.83 x 10^{-6} in/in-°F @ 360°F (via linear interpolation from expansion coefficients table, above)

ρ_{lead} = 0.4037 lbm/in^3 at 360°F, via linear interpolation from lead density table, above)

$R_{in,\,cs,\,360} = (R_{in})(1+(\alpha_{CS})(\Delta T)) = (36.50)[1+(7.02E\text{-}6)(290)] = 36.5743"$

$R_{out,\,cs,\,360} = (R_{out})(1+(\alpha_{CS})(\Delta T)) = (39.75)[1+(7.02E\text{-}6)(290)] = 39.8309"$

$L_{lead,\,360} = (L_{cavity,\,620})/(1+(\alpha_{lead,620})(620-70))*(1+(\alpha_{lead,620})(360-70)) =$

$(196.5510) / [1+(20.39E\text{-}6)(550)] * [1+(17.83E\text{-}6)(290)] = 195.3764"$

$V_{lead,\,360} = M_{lead} / \rho_{lead} = 61{,}363.6 / 0.4037 = 152{,}004.6$ in^3

Since $R_{in,cs,360} = R_{in,lead,360}$, then :

$V_{lead,360} = (\pi)(R_{out,\,lead,360}^2 - R_{in,\,ss,\,360}^2)(L_{lead,\,360})$

It gives:

$R_{out,lead,360} = 39.8162"$

Air gap = $R_{out,cs,360} - R_{out,\,lead,360} = 39.8309 - 39.8162 = 0.0147"$

The assumed air gap of 0.025" is larger than the above calculated gap. Therefore, using a gap of 0.025" is conservative to maximize the DSC shell temperature.

A.3.6.7.2 Gap between Finned Aluminum Shell and Cask Shield Shell

An air gap of 0.01" is considered in the model between the cask shield shell (SA-516-70) and the finned aluminum shell (Al 6061) for the MP197HB cask with over 26 kW heat load. The following calculation shows that the modeled gap of 0.01" is adequate to bound the existing contact resistance between these two shells.

Yovanovich suggests the following approach in [38] to calculate the thermal contact conductance.

$$h_j = h_c + h_g \qquad \text{(A.1)}$$

h_j = total thermal contact conductance (m^2-K/W)

h_c = contact conductance (m^2-K/W)
h_g = gap conductance (m^2-K/W)

The thermal contact resistance is:

$$R_j = 1/h_j \qquad \text{(A.2)}$$

The contact conductance, h_c, is given in [38] by:

$$h_c = 1.25\, k_s \frac{m}{\sigma}\left(\frac{P}{H_c}\right)^{0.95} \qquad \text{(A.3)}$$

Where

$k_s = 2\,k_1\,k_2\,/(k_1 + k_2)$ Harmonic mean thermal conductivity of interface (W/m-K)

$m = \sqrt{m_1^2 + m_2^2}$ Effective mean absolute asperity slope of interface

$\sigma = \sqrt{\sigma_1^2 + \sigma_2^2}$ Effective RMS surface roughness of contacting asperities (m)

P = Contact pressure (MPa)
H_c = Microhardness of the softer of the two contacting solids (MPa) = $H_{C,Al}$ in this evaluation

The mean absolute asperity slope for each plate can be approximated by the following correlation from [38]:

$$m_i = 0.125\left(\sigma_i \times 10^{-6}\right)^{0.402} \quad \text{for } 0.216\,\mu m \le \sigma \le 9.6\,\mu m \qquad \text{(A.4)}$$

As seen in equation (A.3), the contact conductance, h_c, depends heavily on the contact pressure, P. Assuming a very small contact pressure of 10^{-6} psi, gives a negligible contact conductance, h_c and eliminates this term in calculation of the total thermal contact conductance in equation (A.1).

A contact pressure of 10^{-6} psi is equivalent to having no friction between the two shells, which is very conservative.

Due to elimination of h_c in equation (A.1), the conductivities of the contacting plates are not required for this calculation.

The gap conductance, h_g, is given in [38] by:

$$h_g = k_g\,/(Y + M) \qquad \text{(A.5)}$$

Where
k_g = thermal conductivity of the gap substance (W/m-K)
Y = effective gap thickness (m)
M = gas parameter (m)

Based on [38], the effective gap thickness, Y, shown in the figure below, can be calculated as follows:

$$Y = 1.53\,\sigma\,(P / H_c)^{-0.097} \qquad \text{for } 10^{-5} < P/H_c < 2\text{x}10^{-2} \qquad \text{(A.6)}$$

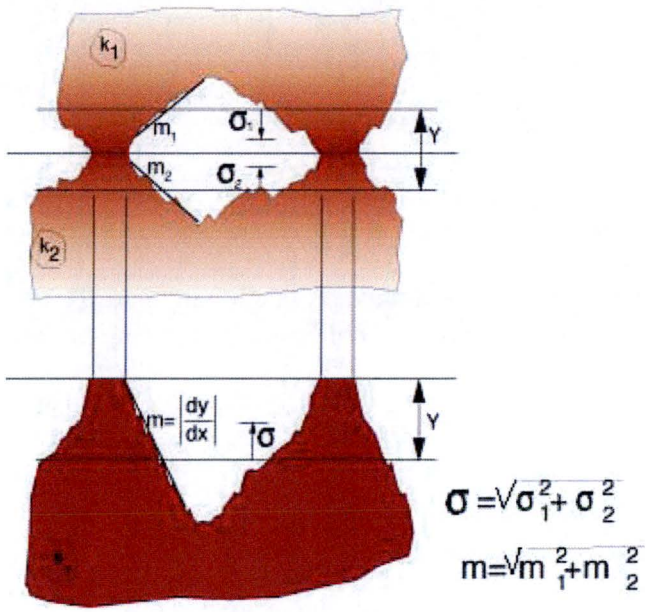

Conforming Rough Surfaces [38]

The gas parameter M accounts for the rarefaction effects at high temperatures and low gas pressure. This gas-surface parameter depends on the thermal accommodation coefficients, the ratio of specific heats, the Prandtl number, and the molecular mean free-path of the gas. This complex gas-surface parameter depends on gas pressure and temperature according to the following relationship:

$$M = M_0 \frac{T}{T_0} \frac{P_{g,0}}{P_g} \qquad \text{(A.7)}$$

Where M_0 denotes the gas parameter value at the reference values of gas temperature and pressure, T_0 and $P_{g,0}$, respectively. T and P_g are temperature and pressure of the contact gas. The gas parameter for air is 0.373x10-6 m at 50°C and 1 atm, as reported in [38].

An operating temperature of 200°F (378K) is considered for T and k_g in equations (A.5) and (A.7). The assumed operating temperature is well below the cask shield shell and the finned aluminum shell temperatures in Table A.3–11 and is therefore conservative.

A pressure of 1 atm is considered for air between the two shells.

Based on data in Section A.3.2.1, material # 16, the air conductivity is 0.0015 Btu/hr-in-°F or 0.031 W/m-K at 200°F.

The following data is considered for roughness and hardness of the shells.

Surface Properties for Aluminum and Stainless Steel Plates

Material	Roughness (μm)	Hardness	Microhardness [(1)] (MPa)
Aluminum	0.2 to 6.3 [39]	25 to 95 Brinell 500kg [40]	440 to 1079
SA 203, Gr. E	0.2 to 6.3 [39]	[(2)]	---

Notes:
[(1)] For conversion of roughness units see reference [42]
[(2)] Based on [38], the hardness of the softer plate, aluminum here, is taken for evaluation.

Surface roughness is mainly determined by the production method. The roughness values in the above table correspond to average values for cold rolling / drawing process.

The contact resistances are calculated based on the average roughness and hardness are listed below.

$\sigma_{Al} = 3.25\ \mu m, H_{c,Al} = 760$ MPa
$\sigma_{CS} = 3.25\ \mu m$

The calculated contact resistance between cask shield shell and finned aluminum shell is 2.7E-3 m^2-K/W as listed in the following table.

Contact Resistances between Shield Shell and Finned Aluminum Shell

Contact Type	Al / SA203
σ (μm)	4.60E-06
P (MPa)	6.891E-09
H_c (MPa)	760
P_g (atm)	1.0
T (K)	378
k_g (W/m-K)	0.031
P/H_c	9.073E-12
Y (μm)	8.283E-05
M (μm)	4.361E-07
h_c (W/m^2-K)	0.00
h_g (W/m^2-K)	374
h_i (W/m^2-K)	374
R_i (m^2-K/W)	2.7E-03

The equivalent thermal resistance for the air gaps across the shells considered in the MP197HB is:

$$R_{j,model} = \frac{\Delta x_{gap}}{k_g} \qquad \text{(A.8)}$$

Δx_{gap} = 0.01" = 2.54E-4 m

$$R_{j,model} = \frac{2.54E-4}{0.031} = 8.2E-3 \text{ m}^2\text{-K/W}$$

The above thermal resistance considered in the model ($R_{j,model}$) is about three times larger than the calculated contact resistances ($R_{j,}$) between cask shield shell and finned aluminum shell. This indicates that the air gap of 0.01" considered in the model is more than adequate to bound the contact resistance between the cask shield shell and the finned aluminum shell.

A.3.6.7.3 Gap between Basket Outer Surface and DSC Shell Inner Surface in the 69BTH DSC Model

Based on the drawings in Chapter A.1, Appendix A.1.4.10, a nominal diametrical cold gap of 0.40" is considered between the basket and the canister shell for the 69BTH DSC. The nominal canister inner diameter (ID) of the 69BTH DSC is 68.75". The nominal basket outer diameter (OD) is then 68.35".

To calculate the minimum gap, the average temperatures for the basket, aluminum rails, and DSC shell at the hottest cross section for NCT at 100°F ambient are required to calculate the thermal expansion at thermal equilibrium. These temperatures are retrieved from the 69BTH DSC/basket model described in Section A.3.3.1.4. These average temperatures are listed in the following table.

Average Temperatures at Hottest Cross Section for 69BTH Basket

Component	**HLZC#1, 26kW NCT at 100°F T_{avg} (°F)**	**HLZC#4, 32kW NCT at 100°F T_{avg} (°F)**
Basket (compartments & wrap plates only)	547	547
Al Rail @ 0 degree	472	504
Al Rail @ 180 degree	398	421
DSC Shell	388	408

The hot dimensions of the basket OD and DSC ID are calculated as follows.

The outer diameter of the hot basket is:

$$OD_{B,hot} = OD_B + [L_{SS,B} \times \alpha_{SS,B} (T_{avg,B} - T_{ref})] + L_{Rail} \times [\alpha_{Al,0} (T_{avg,R0} - T_{ref}) + \alpha_{Al,180} (T_{avg,R180} - T_{ref})]$$

Where:

$OD_{B,hot}$ = hot OD of the basket

OD_B = nominal cold OD of the basket

= 68.75" – 0.40" = 68.35"

$L_{SS,B}$ = width of basket at 0-180 direction

= 9 × compartment width +

9 × 2 × compartment plate +

6 × Al/Poison within nine-compartment blocks +

2 × Al/Poison between nine-compartment blocks +

$6 \times$ wrap plate

$= \quad 9 \times 6 + 9 \times 2 \times 0.165 + 6 \times 0.25 + 2 \times 0.375 + 6 \times 0.105 = 59.85$"

L_{Al} = width of aluminum rail = $(OD_B - L_{SS,B})/2 = 4.25$"

$\alpha_{SS,B}$ = Average stainless steel axial coefficient of thermal expansion (interpolated using data in [10], in/in-°F)

α_{Al} = Average aluminum coefficient of thermal expansion (interpolated using data in [10], in/in-°F)

$T_{avg,B}$ = Average basket temperature at the hottest cross section, see table above, (°F)

$T_{avg,R0}$ = Average Al rail temperature at the hottest cross section at 0 degree orientation, see table above, (°F)

$T_{avg,R180}$ = Average Al rail temperature at the hottest cross section at 180 degree orientation, see table above, (°F)

T_{ref} = reference temperature for stainless steel and aluminum alloys = 70°F [10]

The inner diameter of the hot DSC shell is:

$ID_{DSC,hot} = ID_{DSC} [1 + \alpha_{SS,DSC} (T_{avg,DSC} - T_{ref})]$

Where:

$ID_{DSC,hot}$ = Hot ID of DSC shell

ID_{DSC} = Cold ID of DSC shell = 68.75"

$\alpha_{SS,DSC}$ = Average stainless steel axial coefficient of thermal expansion (interpolated using data in [10], in/in-°F)

$T_{avg,DSC}$ = Average DSC shell temperature at hottest cross section, see above table, (°F)

T_{ref} = Reference temperature for low alloy steel = 70°F [10]

The diametrical hot gap between the basket and cask inner shell is:

$G_{hot} = ID_{DSC,hot} - OD_{B,hot}$

The diametrical hot gap at the hottest cross section is calculated for 26kW (HLZC#1) and 32 kW ((HLZC#4) heat loads in the 69BTH basket to bound the problem. The calculated hot gaps are listed below.

Diametrical Hot Gaps for 69BTH Basket

26kW, HLZC # 1					
	Cold dimension	Temp	$\alpha x10^{-6}$ (1)	ΔL	Hot dimension
	(in)	(°F)	(in/in/°F)	(in)	(in)
Basket width	59.85	547	9.747	0.278	60.128
Large rail @ 0°	4.25	472	13.844	0.024	4.274
Large rail @ 180°	4.25	398	13.592	0.019	4.269
Basket OD	68.35				68.671
DSC ID	68.75	388	9.464	0.207	68.957
Gap	0.4				**0.286**

32kW, HLZC # 4					
	Cold dimension	Temp	$\alpha x10^{-6}$ (1)	ΔL	Hot dimension
	(in)	(°F)	(in/in/°F)	(in)	(in)
Basket width	59.85	547	9.747	0.278	60.128
Large rail @ 0°	4.25	504	13.916	0.026	4.276
Large rail @ 180°	4.25	421	13.684	0.020	4.270
Basket OD	68.35				68.674
DSC ID	68.75	408	9.516	0.221	68.971
Gap	0.4				**0.297**

Note:
(1) The average thermal expansion coefficient is calculated by interpolation using data in [10].

A uniform diametrical hot gap of 0.30" is considered in the model between the basket and the DSC shell for the 69BTH DSC. This assumption is conservative since the hot gaps shown in the above table are smaller than the assumed gap of 0.3".

A.3.6.7.4 Contact Resistance across Paired Aluminum and Poison Plates in 69BTH Basket

The 0.01" gaps considered on both sides of the paired aluminum and poison plates account for all the thermal resistance across the paired plates. Dividing the thermal resistance into three separate resistances would only change the temperature distribution between the two paired plates without changing the overall thermal resistance. The temperature distribution among the paired aluminum and poison plates are of no particular significance.

The following calculation shows that the modeled gaps (0.01") on both sides of the paired aluminum and poison plates are adequate to bound the existing contact resistances.

According to the basket configuration, three contact resistances are recognizable for the paired aluminum/poison plates sandwiched between the fuel compartments or wrap plates:

a) contact resistance between the aluminum plate and the stainless steel fuel compartment or wrap plates
b) contact resistance between the aluminum plate and the poison plate
c) contact resistance between the poison plate and the stainless steel fuel compartment or wrap plate

These contact resistances are shown schematically in the following figure.

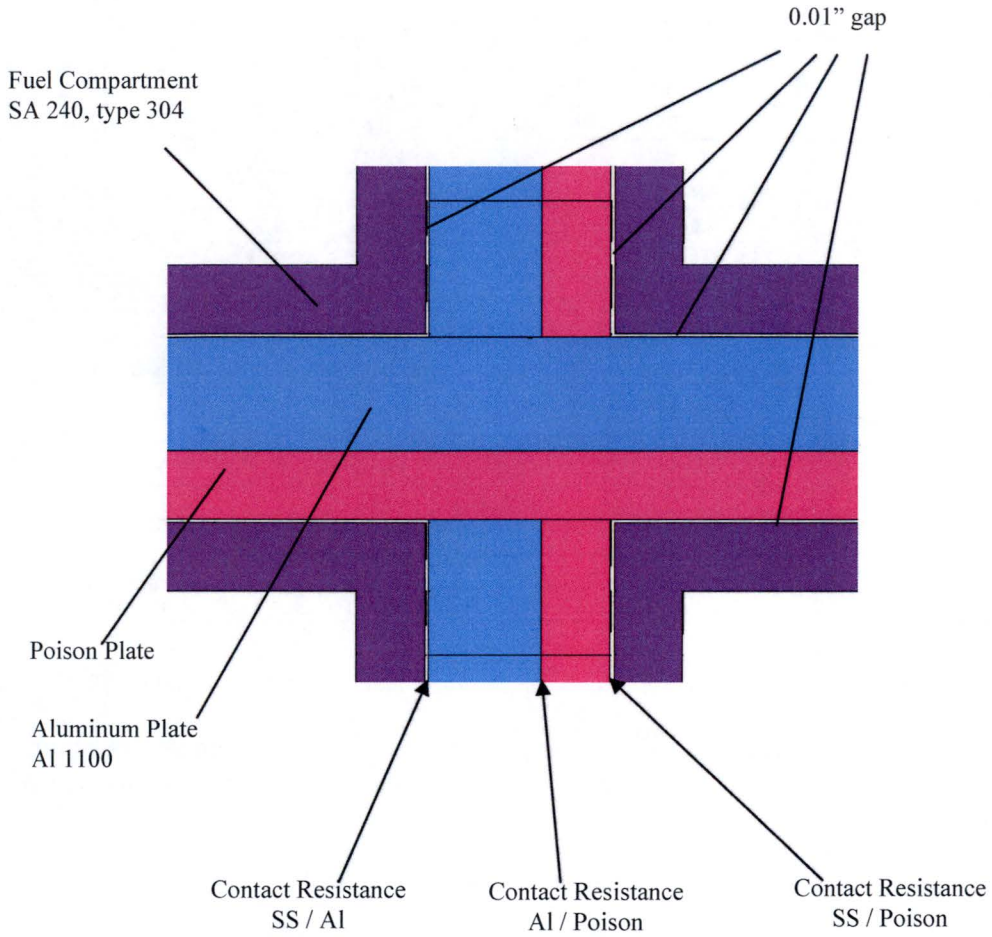

Location of Contact Resistances

The contact resistances between the components shown in the above figure are calculated using the same methodology as the one described in Section A.3.6.7.2.

The gas parameter for helium is 2.05×10^{-6} m at 50°C and 1 atm, as reported in reference [38].

The thermal contact resistance is:

$$R_j = 1/h_j$$

Based on the location of the contact resistances shown in the above figure, the total thermal contact resistance for the paired plates is:

$$R_{j,plates} = R_{j,SS-Al} + R_{j,Al-Poison} + R_{j,poison-SS}$$

$R_{j,ss\text{-}Al}$ = contact resistance between stainless steel and aluminum plates
$R_{j,Al\text{-}Poison}$ = contact resistance between aluminum and poison plates
$R_{j,Poison\text{-}SSl}$ = contact resistance between poison and stainless steel plates

An operating temperature of 400°F (204°C) is considered for conductivity of helium. The assumed operating temperature is well below the average basket temperature at the hottest cross section shown in Section A.3.6.7.3 and is therefore conservative.

A moderate gas pressure (Pg) of 5 psig (1.34 abs atm), lower than the normal operating pressures listed in Table A.3–23, is considered to evaluate the contact resistances.

Based on data in Section A.3.2.1, material # 15, the helium conductivity is 9.84E-3 Btu/hr-in-°F or 0.204 W/m-K at 400°F. The following data is considered for roughness and hardness of the plates.

Surface Properties for Aluminum and Stainless Steel Plates

Material	Roughness (μm)	Hardness	Microhardness [(1)] (MPa)
Aluminum 1100/ Poison Plate	0.2 to 6.3 [39]	25 to 95 Brinell 500kg [40]	440 to 1079
SA 240, type 304	0.2 to 6.3 [39]	92 Rockwell B [41], Table 2	1960 to 2000

Note: [(1)] For conversion of roughness units see reference [42]

Surface roughness is mainly determined by the production method. The roughness values in the above table correspond to average values for cold rolling / drawing process. The hardness values are collected for aluminum alloys 6063 and 6061, which are the closest to aluminum alloy 1100.

The contact resistances calculated based on the average roughness and hardness are:

σ_{Al} = 3.25 μm, $H_{c,Al}$ = 760 MPa
σ_{poison} = 3.25 μm, $H_{c,poison}$ = 760 MPa
σ_{SS} = 3.25 μm, $H_{c,SS}$ = 1980 MPa

The calculated contact resistances are listed in the following table.

Contact Resistances between Plates in 69BTH Basket

Contact Type	Al / Poison	SS / Al or SS/ Poison
σ (m)	4.60E-06	4.60E-06
P (MPa)	6.891E-09	6.891E-09
H_c (MPa)	760	760
P_g (atm)	1.34	1.34
T (K)	478	478
k_g (W/m-K)	0.204	0.204
P/H_c	9.073E-12	9.073E-12
Y (m)	8.283E-05	8.283E-05
M (m)	2.262E-06	2.262E-06
h_c (W/m^2-K)	0.00	0.00
h_g (W/m^2-K)	2402	2402
h_j (W/m^2-K)	2402	2402
R_j (m^2-K/W)	4.164E-04	4.164E-04

The total thermal contact resistance across the plates is:

$$R_{j,total} = 3 \times 4.164E-4 = 1.249E-3 \text{ m}^2\text{-K/W}$$

The equivalent thermal resistance for the helium gaps across the plates considered in the 69BTH basket model is:

Δx_{He} = 2 × 0.01" = 0.02" = 5.08E-4 m (total gap thickness across plates)

$$R_{j,\text{model}} = \frac{\Delta x_{He}}{k_g}$$

$$R_{j,\text{model}} = \frac{5.08E-4}{0.204} = 2.486E-3 \text{ m}^2\text{-K/W}$$

The total thermal resistance considered in the model ($R_{j,model}$) is about two times larger than the calculated contact resistances for the paired plates ($R_{j,total}$). This shows that the gaps considered in the model are more than adequate to bound the contact resistances and the other uncertainties, such as thickness tolerances, surface finishing, etc., involved in fabrication of the basket.

If the poison plate is paired with multiple aluminum plates, the total thermal contact resistance across the plates depends on the number of aluminum plates as follows.

$$R_{j,multiple} = R_{j,SS-Al} + (m-1)R_{j,Al-Al} + R_{j,Al-Poison} + R_{j,poison-SS}$$

m = number of aluminum plates used to pair with poison plate

According to the table of the contact resistances, the contact resistances between Al/SS, Al/Al, and Al/poison plates are equal if the contact pressure nears zero. The total thermal resistance for multiple aluminum plates is therefore:

$$R_{j,multiple} = (n+1)R_{j,Al-Al}$$

n = number of multiple aluminum plates including poison plate

The maximum number of multiple aluminum plates that can be used in 69BTH basket can be calculated by setting $R_{j,multiple}$ in the above equation equal to the total thermal resistance considered in the model, $R_{j,model}$.

$$n_{max} = \frac{R_{j,model}}{R_{j,Al-Al}} - 1$$

$$n_{max} = \frac{2.486E-3}{4.164E-4} - 1 = 4.97$$

This shows that at least four plates, three aluminum plates and one poison plate can be paired together in 69BTH basket without affecting the thermal performance evaluated in this calculation.

A.3.6.8 Sensitivity Study for Effects of Fire Emissivity

A fire emissivity (ε_f) of 0.9 was considered in Section A.3.4.2 to calculate the fire radiation heat transfer coefficient ($h_{r,fire}$). Assuming conservatively, the fire as a black body, an emissivity of 1.0 can be considered for the fire. The effect of this assumption is enveloped for the MP197HB TC in a sensitivity analysis in this section considering the maximum heat load of 32 kW with the external fins installed on the shield shell. The only change is the increase of the fire emissivity (ε_f) from 0.9 to 1.0 in the input file for running the finned TC under HAC. The maximum component temperatures from the sensitivity run with ε_f=1.0 are shown in the following table.

Maximum Component Temperatures for $\varepsilon_f = 1.0$

DSC type	69BTH DSC, with 32 kW heat load, Finned MP197HB TC, $\varepsilon_f = 1.0$			
Component	**Time (hr)**	T_{max} (°F)	T_∞ (°F)[2]	**Limit (°F)**
DSC shell	7.0	512	[3]	---
DSC shell at mid-length[1]	7.0	512	[3]	---
Cask inner shell	1.9	497	400	---
Gamma shield	0.5	571	399	621 [5]
Outer shell	0.5	720	382	---
Shield shell	0.5	1440	335	---
Cask lid	13.0	315	309	---
Cask bottom plate	1.0	416	383	---
Cask lid seal	10.0	323	314	400 [18, 19]
Vent & test seal at top	13.0	313	308	400 [18, 19]
Ram plate seal	1.9	380	377	*644 [52, 53]*
Test seal at bottom	13.0	382	377	*644 [52, 53]*
Drain port seal at bottom	10.0	388	381	*644 [52, 53]*
Helium in TC cavity	4.0	389	380	---

Notes:
(1) This value is the maximum DSC shell temperature in the region where the fuel assemblies have the maximum peaking factor.
(2) These values are retrieved from the transient model at 27.0 hrs after the end of the fire accident. Based on the time-temperature histories for the original TC model shown in Figure A.3-40 through Figure A.3-42, the steady state temperatures are bounded by these temperatures.
(3) Due to the adiabatic boundary conditions considered conservatively for the steady state cool-down runs (described in Section A.3.4.2), the maximum DSC shell temperature at the end of the transient run remains bounded by the steady state temperature of 537°F reported for the 69BTH DSC with 32kW heat load in Table A.3-17.

Since the fire emissivity does not have any effect on the steady state temperatures after cool-down, the maximum DSC shell temperature for the 69BTH with 32 kW heat load remains bounded by 537°F as reported in Table A.3-17.

A comparison of the maximum TC component temperatures for ε_f of 1.0 to those for ε_f of 0.9 are shown in the following table.

Comparison of the Maximum TC Component Temperatures for ε_f of 1.0 and 0.9

	Transient Temperature			Steady State Temperature		
	ε_f =1.0	ε_f = 0.9		ε_f =1.0	ε_f = 0.9	
Component	T_{max} (°F)	T_{max} (°F)	ΔT_{max} (°F)	T_∞ (°F)(2)	T_∞ (°F)(3)	ΔT_∞ (°F)
DSC shell	512	509	+3	(4)	(4)	0
DSC shell at mid-length(1)	512	509	+3	---	---	N/A
Cask inner shell	497	487	+10	400	403	-3
Gamma shield	571	552	+21	399	401	-2
Outer shell	720	690	+30	382	383	-1
Shield shell	1440	1393	+47	335	337	-2
Cask lid	315	314	+1	309	311	-2
Cask bottom plate	416	416	0	383	384	-1
Cask lid seal	323	321	+2	314	316	-2
Vent & test seal at top	313	311	+2	308	310	-2
Ram plate seal	380	380	0	377	378	-1
Test seal at bottom	382	380	+2	377	379	-2
Drain port seal at bottom	388	386	+2	381	383	-2
Helium in TC cavity	389	387	+2	380	380	0

Notes:
(1) This value is the maximum DSC shell temperature in the region where the fuel assemblies have the maximum peaking factor.
(2) These values are retrieved from the transient model at 27.0 hrs after the end of the fire accident.
(3) These values are retrieved from the transient model at 20.0 hrs after the end of the fire accident.
(4) Due to the adiabatic boundary conditions considered conservatively for the steady state cool-down runs (described in Section A.3.4.2), the maximum DSC shell temperature at the end of the transient run remains bounded by the steady state temperature of 537°F reported for the 69BTH DSC with 32kW heat load in Table A.3-17.

As seen in the above table, the largest effect of increasing the fire emissivity from 0.9 to 1.0 occurs during the short period of the fire at the shield shell, which is directly exposed to the fire. The other components remain shielded from the fire effect so that the cask inner shell temperature increases by only 10°F and the DSC shell temperature increases only by 3°F during the transient run.

These temperature increases are relatively small and occur for a short period of time and therefore do not affect the thermal and structural performance of the MP197HB TC.

The containment seals are protected from direct fire exposure by the impact limiters. The effect of increasing the fire emissivity from 0.9 to 1.0 on the maximum seal temperatures is limited to 2°F for a short period of time after the fire. The transient and the steady state temperatures of the containment seals remain well below the temperature limit of 400°F [18, 19] *for fluorocarbon seals and 644°F [52, 53] for metallic seals*. Therefore the containment function of the seals remains unaffected by the increase of the fire emissivity from 0.9 to 1.0.

The time temperature histories for the TC shield shell and DSC shell from the sensitivity study with ε_f of 1.0 are compared to those from the original model with ε_f of 0.9 in the following figures, respectively.

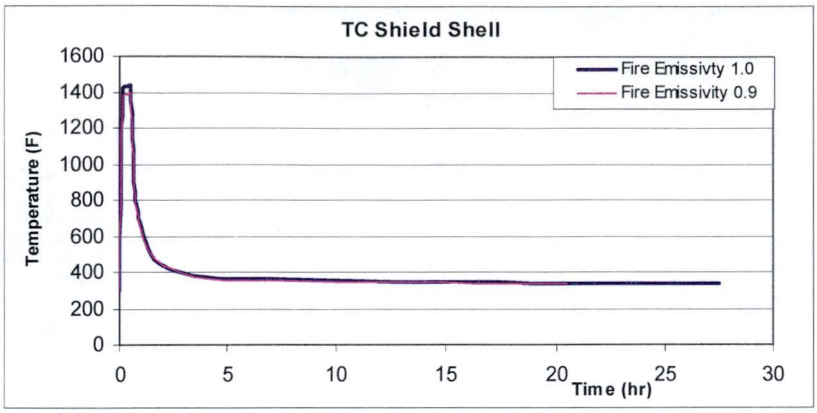

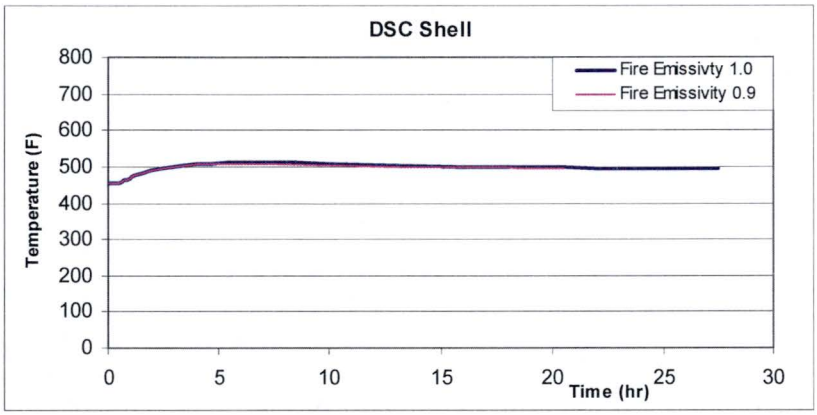

Results of the Sensitivity Study

As seen in Figure A.3-40 through Figure A.3-42, all the TC component temperatures decrease through the cool-down period. The small differences seen in the comparison table between the steady state temperatures are caused by the fact that the transient temperatures at different hours (27.0 hours for sensitivity run and 20.0 hours for the original run) are used to bound the steady state temperatures. Since the TC component temperatures are decreasing, the values at 27.0 hours for the sensitivity run are lower than those for the original run. It is expected that the actual steady state temperatures in both runs achieve the same values and are independent of the fire emissivity.

It is evident from the first table in this section that the maximum TC component temperatures remain well below the allowable limits.

In conclusion, the effect of increasing the fire emissivity from 0.9 to 1.0 occurs only for a short period of time on the outermost components of the TC exposed to the fire. The function of these TC components remains unaffected by this change in the fire emmissivity.

A.3.6.9 Sensitivity Study for Effects of High Burnup Damaged Fuel Assemblies

The cladding of high burnup damaged fuel assemblies can experience further damages during NCT. To bound the effect of these damages, a sensitivity analysis is conducted considering the worst case condition, in which the high burnup damaged fuel assemblies become rubbles. Following the rationale in NUREG/CR-6835 [50], it is assumed that the fuel rods do not shatter into very small pieces and the fuel rubble is not in a tightly compacted mass. Instead, the fuel rubble is assumed to be 50% void by volume. Since the end drop is the most critical condition under NCT and the end caps and the fuel compartment walls constrain the damaged fuel assembly, the fuel rubble is assumed to be contained within the original active fuel volume, albeit in the lower portion of the original volume. Consistent with NUREG/CR-6835, the axial-burnup variation in the rubble is also assumed to be uniform.

The height of the fuel rubbles with the assumption of 50% void by volume is determined based on the volume of the fuel rods. The bounding fuel rubble height is 108" for the fuel assemblies.

The 69BTH DSC with the bounding heat load of 32 kW is considered for this sensitivity analysis. In the sensitivity run, the heat generation rate corresponding to the damaged fuel assemblies is applied uniformly over the fuel rubble height of 108" concentrated at the rear bottom of the 69BTH DSC with a peaking factor of one.

Conductivity of helium is considered for the fuel rubble for conservatism.

The DSC shell temperature retrieved from the cask model described in Section A.3.3.1.1 is applied as boundary conditions for the 69BTH DSC model, which is consistent with the approach described in Section A.3.3.1.4.

The maximum component temperatures resulting from the sensitivity analysis are compared to the corresponding values for 69BTH with intact fuel assemblies in the following table.

Comparison of the Maximum Fuel Temperatures for 69BTH DSC with Intact and Damaged Fuel Assemblies under NCT

DSC Type	$T_{max, Fuel}$* (°F)	$T_{max, Comp}$ (°F)	$T_{max, Al/Poison}$ (°F)	$T_{max, Rail}$ (°F)
69BTH, 32 kW w/ intact FAs (see Table A.3-10)	674.3	638.3	621.8	534.3
69BTH, 32 kW w/ intact and damaged FAs	679.6	644.3	628.0	537.1
Difference	+ 5.3	+ 6.0	+ 6.2	+ 2.8

* Fuel cladding temperature limit is 752°F

As seen in the above table, the maximum fuel cladding temperature changes approximately by 5°F. Considering the large margin of 78°F for the fuel cladding temperature, this small change does not have any significant effect on the thermal performance of the cask and DSC.

A.3.6.10 Sensitivity Analysis for HAC using Coupled Model

The analysis for HAC described in Section A.3.4 is based on a combination of transient calculations of the MP197HB TC (including a homogenized basket) and steady state calculations of the DSC including basket components described in Section A.3.3.1 as separate thermal analyses. These models are used to calculate the component maximum temperatures (including cladding temperatures). To justify the approach considered in the HAC analysis, a coupled transient model is prepared to include the TC, DSC, and basket in one single model assigned here as coupled model.

The coupled model is created by introducing the elements and nodes from the 69BTH basket model described in Section A.3.3.1.4 into the TC model with crushed impact limiters described in Section A.3.4. The 69BTH basket and the MP197HB TC thermal models have dissimilar meshes since the mesh density of the 69BTH basket model is much finer than the mesh density of the TC model. The mesh density of the DSC shell is refined to provide adequate interfaces between the TC and the basket meshes. These two dissimilarly meshed models of the TC and 69BTH basket are tied together using the DSC shell nodes and constraint equations via the "CEINTF" command in ANSYS.

To ensure the correct application of the constraint equations, the same fine meshed DSC shell used in the coupled model described above was introduced into the coarser meshed model of TC described in Section A.3.3.1.1 and the constrained equations were applied at the intersection of the fine/coarse meshes. The results of this model were compared to the result of the TC model for NCT. The comparison showed that the maximum temperatures of the TC components remain virtually unchanged (the changes are within ±0.1°F) and the maximum DSC shell temperature changes by approximately by 1°F.

The coupled model of the TC, DSC, and basket includes the MP197HB TC and the bounding DSC (69BTH with 32 kW heat load) and considers the homogenized fuel assemblies within compartments. All the basket components (including back-filled gas and aluminum transition rails) are explicitly modeled in the coupled model considering the same assumption described in Section A.3.3.1.4 for 69BTH basket. The geometry of the coupled model is shown in Figure A.3-53.

Decay heat load is applied as heat generation boundary conditions over the elements representing homogenized fuel assemblies. The base heat generation rate is multiplied by peaking factors along the axial fuel length to represent the axial decay heat profile consistent with the approach described in Section A.3.3.1.4. The peaking factors remain identical to those shown in Table A.3-2.

The ambient boundary conditions for the coupled model are identical to those described in Section A.3.4 for the TC model under HAC.

The time temperature histories resulting from the coupled model are shown in Figure A.3-54 and Figure A.3-55. The maximum component temperatures from the coupled HAC thermal analysis are compared with the corresponding temperatures from the decoupled HAC analysis described in Sections A.3.4 in the following table.

Comparison of Maximum Temperatures of MP197HB TC for HAC with Coupled/Decoupled Models

DSC type	69BTH			
Heat Load	32 kW			
Inner sleeve	No			
External fins	Yes (Melted)			
Component	$T_{max, coupled}$ (°F)	$T_{max, decoupled}$ [(1)] (°F)	ΔT (°F)	Limit (°F)
Fuel Cladding	680	693	-13	1058 [7]
Fuel Compartment	650	658	-8	---
Aluminum / Poison Plates	649	657	-8	---
Basket Rails	548	557	-9	---
DSC shell	521	537	-16	---
Cask inner shell	499	497	2	---
Gamma shield	567	571	-4	621 [5]
Outer shell	716	720	-4	---
Shield shell	1440	1440	0	---
Cask lid	306	315	-9	---
Cask bottom plate	419	416	3	---
Cask lid seal	314	323	-9	*400 [18], [19]*
Vent & test seal @ top	304	313	-9	
Ram plate seal	387	380	7	*644 [52, 53]*
Test seal @ bottom	388	382	6	
Drain port seal @ bottom	392	388	4	
Helium in TC Cavity	387	389	-2	---

[(1)] For the maximum temperatures of the decoupled HAC analysis fire emissivity of 1.0, see Table A.3-17 and Table A.3-18 for 69BTH DSC (32 kW heat load) and Section A.3.6.8 for MP197HB TC.

As seen in the above table, all the maximum temperatures remain below the allowable limits in the coupled model.

The fuel cladding temperature resulting from the coupled model is 680°F and is lower by 13°F compared to the results from the decoupled models and is well below the accident temperature limit of 1058°F.

The maximum seal temperature is 392°F at drain port resulting from the coupled model. Although the maximum seal temperature increases by 4°F compared to the results from the decoupled models, the maximum seal temperature remains below the long-term limits specified for continued seal function. Parker O-ring [18] gives a short term temperature limit of 482°F for fluorocarbon seals. The short term temperature limit was verified in [49] for this seal compound. The maximum seal temperatures resulting from the coupled or decoupled models remain well below the short term limit.

The maximum temperature of gamma shield (lead) is 567°F in the coupled model, which is 4°F lower than the corresponding value from the decoupled model and remains well below the lead melting point of 621°F.

Based on the above discussion, the differences between the maximum temperatures of critical components resulting from the coupled and decoupled models are limited to a few degrees. This

comparison shows that although the decoupled models do not include the axial profile of the decay heat load directly, the approach followed in the decoupled models captures the transient behavior of the TC and DSC during the fire and cool-down stages with adequate accuracy.

Proprietary Information Withheld Pursuant to 10 CFR 2.390

Proprietary Information Withheld Pursuant to 10 CFR 2.390

Proprietary Information Withheld Pursuant to 10 CFR 2.390

Proprietary Information Withheld Pursuant to 10 CFR 2.390

Proprietary Information Withheld Pursuant to 10 CFR 2.390

Proprietary Information Withheld Pursuant to 10 CFR 2.390

Proprietary Information Withheld Pursuant to 10 CFR 2.390

A.3.6.11.6 Grid Sensitivity Study for the Neutron Shield Resin during NCT

The thermal evaluation of the MP197HB cask with high burnup fuel assemblies described in Section A.3.6.11 shows that among all the components, the neutron shield resin has the lowest margin to its temperature limit based on the results presented in Section A.3.6.11.4 and Table A.3-29 for NCT, Load Case UO2. Therefore, to provide further assurance that this component does not exceed its temperature limit, a grid convergence study of the coupled model of the MP197HB cask with 69BTH DSC is performed to determine the discretization error.

In addition to the discretization error, this section computes the observed order of accuracy (p) and compares it to the theoretical order of accuracy of the ANSYS solution. Four grids are considered for the study of the ANSYS model. The uncertainty and the GCI are computed using the five steps specified in Section 2-4.1 of ASME V&V 20-2009 [55].

A.3.6.11.6.1 Methodology of the Grid Convergence Study

The thermal model developed for the evaluation of Load Case U2O described in Section A.3.6.11.2 uses constraint equations to simulate the heat transfer between the dissimilar meshes at the interface between the inner shell of the cask and the DSC shell, between the DSC shell and the basket and also at the interfaces between the basket and the DSC end plates. The use of constraint equations requires manually modifying and verifying the mesh densities on both sides of the meshes such that a proper interface is formed for heat transfer.

Since performing the grid convergence study requires generation of multiple grids with similar refinement in the x, y and z directions, these manual operations are not possible on varying mesh densities. Therefore, the constraint equations are replaced by the contacts and target elements (CONTA173 and TARGE170). The use of contact elements eliminates the need to manually adjust the mesh densities, ensures proper refinement, and also ensures heat transfer through dissimilar meshes. The difference for the neutron shield resin temperature between the two models using constraint equations and contact elements is evaluated and is less than 0.6 °F and therefore remains virtually unchanged.

Using the models with contact elements as described above, the grid convergence study is performed based on the five steps specified in Section 2-4.1 of ASME V&V 20-2009 [55] to determine the discretization error as described below.

Step 1

The representative grid size (h) based on equation 2-4-2 of ASME V&V 20-2009 [55] is calculated as:

$$h = \left(\frac{\sum_{i=1}^{N} \Delta V_i}{N} \right)^{1/3}$$

Where,

N= Number of elements

$\sum_{i=1}^{N} \Delta V_i$ = *Volume of the half-symmetric model*

Based on the above equation, four grids with increasing numbers of elements are considered to determine the discretization error in this study. The refinement of the grids is performed in such a way that the refinement factor ($r \doteq h_{coarse}/h_{fine}$) is approximately 1.3. The sizes of the grids considered for this evaluation are noted in Table A.3-31.

Using the four grids, two sets of calculations are performed to determine the discretization error. Each set is comprised of three grids based on the guidelines noted in Step 2 of Section 2-4.1 of ASME V&V 20-2009 [55]. In Set # 1, Grids # 1, 2 and 3 are considered. In Set # 2, Grids # 2, 3 and 4 are considered. In each set, the lowest number refers to the fine grid and the largest number refers to the coarse grid.

For each set, the representative cell sizes h_1, h_2 and h_3 correspond to the fine, intermediate and coarse meshes of that set. Further, for each set, the refinement factors for the intermediate mesh to fine mesh and for the coarse mesh to intermediate mesh are defined as:

$r_{21} = h_2/h_1 = (N_1/N_2)^{1/3}$

$r_{32} = h_3/h_2 = (N_2/N_3)^{1/3}$

Step 2

Using the four grids described in Step 1, the bounding thermal condition, Load Case U2O, is re-evaluated for the grid convergence study. For this evaluation, the temperature of neutron shield resin is considered as the key simulation variable (Φ) to determine the discretization error. For each set, the temperatures of neutron shield resin (i.e., the key simulation variable, Φ_1, Φ_2 and Φ_3 corresponds to fine intermediate and coarse meshes of the set).

Step 3

Based on the refinement factors (r) and simulation variables (Φ) determined in Steps 1 and 2, the observed order of accuracy (p) of the solution is computed based on equations 2-4-5 through 2-4-7 of ASME V&V 20-2009 [55]. The observed order of accuracy (p) is defined as:

$$p = \left[\frac{1}{\ln(r_{21})}\right]\left[\ln\left|\frac{\varepsilon_{32}}{\varepsilon_{21}}\right| + q(p)\right]$$

Where,

$$q(p) = \ln\left(\frac{r_{21}{}^{p} - s}{r_{32}{}^{p} - s}\right)$$

$$s = 1 * sign\left(\frac{\varepsilon_{32}}{\varepsilon_{21}}\right)$$

$$\varepsilon_{32} = \phi_3 - \phi_2$$

$$\varepsilon_{21} = \phi_2 - \phi_1$$

ϕ_i = Average neutron shield temperature of the ith grid in each set (°F)

Based on the equations listed above, the observed order of accuracy (p) is computed iteratively. The observed order of accuracy (p) of the ANSYS model will be compared to the theoretical order of the ANSYS solution in Section A.3.6.11.6.2.

ANSYS uses the Newton-Raphson method to solve the non-linear problems [27], which is second order convergent as noted on Page 34 of [56]. Thermal evaluations with temperature dependent thermal conductivities are considered as nonlinear. This shows that all simulations for the coupled model of the MP197HB cask with 69BTH DSC are nonlinear in nature. Therefore, an order of accuracy (p_{method}) of 2 is expected for the ANSYS solution.

Step 4

Using the values determined in Steps 2 and 3, the extrapolated value, based on equation 2-4-8 of ASME V&V 20-2009 [55] is calculated as:

$$\phi_{ext}^{21} = (r_{21}^{p} * \phi_1 - \phi_2) / \left| r_{21}^{p} - 1 \right|$$

The discretization error for the fine grid in each set is computed in Step 5 based on the relative error and the grid convergence index (GCI) between the fine and intermediate meshes in each set.

Step 5

The relative error based on equation 2-4-9 of ASME V&V 20-2009 [55] is computed as:

$$e_a^{21} = \left| \phi_1 - \phi_2 \right|$$

Using the relative error, the GCI for the fine grid based on equation 2-4-12 of ASME V&V 20-2009 [55] as:

$$GCI_{fine}^{21} = \frac{F_s * e_a^{21}}{r_{21}^{p} - 1}$$

Since three grids are used in each set, a factor of safety (F_s) equal to 1.25 is used as noted in Step 5, Section 2-4-1 of [55]. The discretization error is considered equal to the GCI without any error distribution based on page 14 of ASME V&V 20-2009 [55] and is computed as:

$$U_{num} = GCI_{fine}^{21}$$

A.3.6.11.6.2 Computations for the Grid Convergence Study

As noted in Steps 1 and 2 of the methodology described in Section A.3.6.11.6.1, Load Case # U2O shown in Table A.3-29 is re-evaluated using the four grids listed in Table A.3-31 in two sets of calculations. As shown in Table A.3-32, the maximum number of elements for the coupled model of the MP197HB cask with 69BTH DSC used in this study ranges from 390,823 elements to 3,120,975 elements. Out of the four grids considered, Grid # 3 with 1,402,184 is identical to the thermal model used for the thermal analysis in Section A.3.6.11.2. However, for the grid convergence study, the neutron shield resin temperature determined using contact elements is used for Grid # 3. The use of contact elements does not alter the existing mesh, rather the contact elements are overlaid over the surfaces that are non-conformal.

For the remaining three grids, the ANSYS models developed for this evaluation are used to determine the neutron shield resin temperature using the methodology described in A.3.6.11.2. Since the axial mesh density is altered for these grids, the peaking factors are updated based on the updated axial segments using the same methodology described in Section A.3.6.11.3. The peaking factors for Grid # 4 are not changed since it adds axial segments without altering the existing ones used in Section A.3.6.11.3.

The temperature of neutron shield resin resulting for each grid size is summarized in Table A.3-32. Using the temperature of neutron shield resin listed in Table A.3-32, the discretization error and the observed order of accuracy are computed using the Steps 3 through 5 listed in Section A.3.6.11.6.1.

A.3.6.11.6.3 Results and Discussion of the Grid Convergence Study

Using the methodology specified in Section A.3.6.11.6.1 and the computations in Section A.3.6.11.6.2, the grid convergence study is performed for the coupled model of the MP197HB cask with 69BTH DSC. The results of the grid convergence study are listed in Table A.3-33. As seen from Table A.3-33, the discretization error (U_{num}) is 0.319 °F for the fine grid among Set# 1 with Grids # 1, 2 and 3. Therefore, the temperature of neutron shield resin for the fine grid within Set # 1 including the discretization error is 316.859 °F (Φ_1+ U_{num}= 316.540 + 0.319).

Similarly as shown in Table A.3-33, the discretization error (U_{num}) is 1.854 °F for the fine grid among Set# 2 with Grids#2, 3 and 4. Therefore, the neutron shield resin temperature for the fine grid within Set# 2 including the discretization error is 315.175 °F (Φ_1+ U_{num}= 313.321+1.854).

Therefore, for both Set# 1 and Set# 2, the neutron shield resin temperature including the discretization error, remains below the allowable limit of 320 °F [17].

Figure A.3-60 shows the neutron shield resin temperature as a function of the number of elements. As seen from the Figure A.3-60, the variation of the neutron shield resin temperature for Grid #1, 2 and 3 is within ±0.7 °F. However, with further refinement, the temperature of neutron shield resin for Grid# 4 is reduced by 3.22 °F compared to Grid# 3. Further, as seen from Table A.3-31 and Table A.3-33, an increase of 7.98 times in the element count from Grid # 1 with approximately 0.39 million elements to Grid # 4 with approximately 3.12 million elements resulted in a decrease of 2.488 °F in temperature of neutron shield resin. This shows that the neutron shield temperature determined using Grid # 3 is adequate in evaluating the thermal performance.

The observed order of accuracy (p) computed for both Set# 1 and Set# 2 is 5.7 and 4.4, respectively. The difference in the observed order of accuracy (p) between the two sets could be due to the difference in the refinement factors between the two sets.

The difference between the theoretical order of accuracy and the observed order could be due to the different refinement factors as shown in Table A.3-33. For this evaluation, since the DSC and the MP197HB cask were initially developed as separate models and then combined using contact elements, a difference exists in the refinement factors of the DSC and the MP197HB cask leading to a difference in the combined refinement ratio. Further, the geometry of the basket, due to the location of the axial plates and the gaps between the plates in both axial and radial directions, limits the ability to generate a coarse mesh, which in turn affects the achievement of a refinement ratio of 1.3 between the coarser grids. Instead of using coarser grids, additional refinement of the grids might successfully improve the order of accuracy. However, the finest grid (Grid# 4) currently used has slightly greater than 3 million elements and further refining to achieve a minimum refinement factor (h) of 1.3 will cause the next grid to have at least 7 million elements. This level of refinement is computationally prohibitive and is not needed since the temperature of neutron shield resin decreases slightly with increasing refinement. Overall, it can be observed the change in the neutron shield resin temperature is insignificant with the increase in refinement of the grid.

Table A.3-1
DSC Shell Nominal Dimensions

Parameter [1]	69BTH	61BT / 61BTH Type 1	61BTH Type 2	37PTH[2]	32PTH / 32PTH1[3]	32PT[4]	24PTH[5]	24PT4
Outer Top Cover	2.00	1.25	1.50	2.00	2.00	1.50	1.50	1.25
Inner Top Cover	2.00	0.75	1.25	2.00	2.00	1.25	1.25	6.75 [6]
Top Shield Plug	5.75	7.00	6.25	5.75	8.00	7.50	6.25	
Total Top End	9.75	9.00	9.00	9.75	12.00	10.25	9.00	8.00
Inner Bottom Cover	2.25 [8]	0.75	1.75	2.25 [8]	2.25	1.75	1.75	2.00
Bottom Shield Plug	3.00 [8]	5.00	4.00	3.00 [8]	4.50	5.25	4.00	4.75 [6]
Outer Bottom Cover	2.00	1.75	1.75	2.00	2.00	1.75	1.75	
Total Bottom End	7.25	7.50	7.50	7.25	8.75	8.75	7.50	6.75
Cavity Length	178.41	179.50	179.50	164.38	164.38	167.10	169.60	180.20
DSC Length (w/o grapple) [7]	195.41	196.00	196.00	181.38	185.13	186.10	186.10	194.95
Basket height	164	164	164	162	162.00	166.10	168.60	179.13

Note:
[1] 61BTHF and 24PTHF DSCs have the same dimensions as DSC types 61BTH and 24PTH, respectively.
[2] The shortest cavity length for 37PTH baskets belongs to 37PTH-S.
[3] The shortest cavity length for 32PTH, 32PTH, type 1 and 32PTH1 Type 1 & 2 baskets belongs to 32PTH1-S.
[4] The shortest cavity length for 32PT baskets belongs to 32PT-S125.
[5] The shortest cavity length for 24PTH baskets belongs to 24PTH-S.
[6] Shield plugs of the 24PT4 DSC are lead encapsulated in plates of stainless steel 316, see [2].
[7] The canister length in the model is the sum of total top end, total bottom end, and cavity length.
[8] The thicknesses of inner bottom cover plate and bottom shield plug for 69BTH and 37PTH DSCs are designed as 1.75" and 3.5", respectively. Since the bottom shield plug (carbon steel) has a higher conductivity than the inner bottom cover plate (stainless steel), considering a smaller thickness of 3" for bottom shield plug and higher thickness of 2.25" for inner bottom cover plate is conservative which increases the thermal resistance across these two plates.

Table A.3-2
Peaking Factors for Fuel Assemblies in the 69BTH DSC Model

Region #	Fuel Model Z-Coord (in) from	to	Average Height from Bottom (in)	Peaking Factor	Area under Curve
1	7.375	11.80	2.213	0.166	0.733
2	11.80	19.60	8.325	0.641	5.001
3	19.60	27.40	16.125	0.984	7.678
4	27.40	35.20	23.925	1.115	8.700
5	35.20	43.00	31.725	1.168	9.114
6	43.00	50.80	39.525	1.188	9.266
7	50.80	58.60	47.325	1.196	9.326
8	58.60	66.40	55.125	1.200	9.360
9	66.40	74.20	62.925	1.200	9.360
10	74.20	82.00	70.725	1.199	9.356
11	82.00	89.80	78.525	1.197	9.339
12	89.80	97.60	86.325	1.178	9.186
13	97.60	105.40	94.125	1.151	8.981
14	105.40	113.20	101.925	1.116	8.704
15	113.20	121.00	109.725	1.070	8.348
16	121.00	128.80	117.525	0.994	7.752
17	128.80	136.60	125.325	0.840	6.548
18	136.60	144.40	133.125	0.596	4.646
19	144.40	151.375	140.513	0.230	1.604
				Sum	143.003
				Normalized	0.99308
				Corr. Factor	1.00697

Table A.3-3
Effective Density for the 69BTH Basket

Basket		
Components	Material	Total Weight (lbm)
Fuel Assembly		48,645
Fuel Compartment	SS304	13,174
Poison Plate + Alum	Aluminum	2,169
Sub-Assy. Wrap	SS304	3,484
Aluminum Plates	Aluminum	1,434
Rail 90	Aluminum	6,204
Rail 45	Aluminum	3,508
Total		78,618
D_{basket}	68.75	in
L_{basket}	164.0	in
V_{basket}	608,806	in^3
$\rho_{eff\ basket}$	0.129	lbm/in^3

Top Grid Assembly		
Components	Material	Total Weight (lbm)
Plates	SA182	2,123
$D_{topgrid}$	68.75	in
$L_{topgrid}$	14.4	in
$V_{topgrid}$	53,493	in^3
$\rho_{eff\ topgrid}$	0.040	lbm/in^3

Table A.3-4
Effective Specific Heat for the 69BTH Basket

69BTH Basket									
Components	Fuel Assembly	Fuel compartments	Poison Plates	Sub-Assy. Wrap	Aluminum Plates	Rail 90	Rail 45	Total	
Material	---	Stainless Steel	Al	St. Steel	Al	Al	Al	---	
Weight (lbm)	48,645	13,174	2,169	3,484	1,434	6,204	3,508	78,618	
Temperature	m.Cp	m.Cp	m.Cp	m.Cp	m.Cp	m.Cp	m.Cp	Σ m.Cp	Cp_{eff}
(°F)	(Btu/°F)	(Btu/°F)	(Btu/°F)	(Btu/°F)	(Btu/°F)	(Btu/°F)	(Btu/°F)	(Btu/°F)	(Btu/lbm-°F)
70	2,797	1,529	462	404	305	1,322	747	7,566	0.096
100	2,797	1,536	466	406	308	1,334	754	7,603	0.097
200	2,797	1,600	479	423	317	1,371	775	7,763	0.099
300	2,797	1,644	490	435	324	1,402	793	7,885	0.100
400	2,797	1,692	499	447	330	1,427	807	7,999	0.102
500	2,797	1,731	499	458	330	1,427	807	8,049	0.102
600	2,797	1,743	499	461	330	1,427	807	8,064	0.103
700	2,797	1,770	499	468	330	1,427	807	8,097	0.103
800	2,797	1,794	499	475	330	1,427	807	8,129	0.103
900	2,797	1,804	499	477	330	1,427	807	8,140	0.104
1000	2,797	1,813	499	479	330	1,427	807	8,152	0.104
1100	2,797	1,844	499	488	330	1,427	807	8,192	0.104

Top Grid Assembly (SA 240, Type 304)			
Temp	Cp_{eff}	Temp	Cp_{eff}
(°F)	(Btu/lbm-°F)	(°F)	(Btu/lbm-°F)
70	0.116	600	0.132
100	0.117	700	0.134
200	0.121	800	0.136
300	0.125	900	0.137
400	0.128	1000	0.138
500	0.131	1100	0.140

Table A.3-5
Effective Axial Conductivity for the 69BTH Basket

Basket				
T2 (T_{top})	T1 (T_{bottom})	Q_{axl}	T_{avg}	$k_{basket, axl}$
(°F)	(°F)	(Btu/hr)	(°F)	(Btu/hr-in-°F)
50	0	6319.4	25	1.682
150	100	6389.7	125	1.701
250	200	6479.2	225	1.724
350	300	6559.4	325	1.746
450	400	6613.1	425	1.760
550	500	6615.9	525	1.761
650	600	6615.7	625	1.761
750	700	6630.8	725	1.765
850	800	6649.5	825	1.770
950	900	6665.5	925	1.774
1050	1000	6681.8	1025	1.778
1150	1100	6698.7	1125	1.783

Top Grid Assembly			
D_topgrid	68.5	in	
L_topgrid	14.4	in	
Plate Thickness	0.25	in	
	Length (in)	No. of Plates	Area (in^2)
L1	44.17	16	176.7
L2	18.71	4	18.7
L3	6.25	16	25.0
Total			220.4
A_model	3712	in^2	
A_plates	220.4	in^2	
Temp	k_{SS304}	$k_{topgrid, axl}$	
(°F)	(Btu/hr-in-°F)	(Btu/hr-in-°F)	
70	0.717	0.043	
100	0.725	0.043	
200	0.775	0.046	
300	0.817	0.048	
400	0.867	0.051	
500	0.908	0.054	
600	0.942	0.056	
700	0.983	0.058	
800	1.025	0.061	
900	1.058	0.063	
1000	1.092	0.065	
1100	1.133	0.067	

Table A.3-6
Effective Radial Conductivity for the 69BTH Basket

69BTH Basket				
T_{max} (°F)	T_o (°F)	Q_{rad} (Btu/hr)	T_{avg} (°F)	k_{basket_rad} (Btu/hr-in-°F)
336	0	9678	168	0.167
429	100	9678	264	0.171
519	200	9678	360	0.176
603	300	9678	451	0.186
688	400	9678	544	0.195
776	500	9678	638	0.204
866	600	9678	733	0.211
959	700	9678	830	0.217
1054	800	9678	927	0.222
1148	900	9678	1024	0.227
1243	1000	9678	1122	0.231
1339	1100	9678	1219	0.236

Table A.3-7
Peaking Factors for Fuel Assemblies in the 37PTH DSC Model

Region #	Fuel Model Z-Coord (in) from	to	Average Height from Bottom (in)	Peaking Factor	Area under Curve
1	11.350	20.350	4.500	0.672	6.044
2	20.350	29.350	13.500	0.987	8.884
3	29.350	38.350	22.500	1.083	9.748
4	38.350	47.350	31.500	1.105	9.947
5	47.350	47.475	36.063	1.108	0.138
6	47.475	56.558	40.667	1.108	10.061
7	56.558	65.642	49.750	1.103	10.021
8	65.642	74.725	58.834	1.098	9.971
9	74.725	83.808	67.917	1.094	9.937
10	83.808	92.892	77.000	1.094	9.939
11	92.892	101.970	86.081	1.095	9.943
12	101.970	111.060	95.165	1.096	9.959
13	111.060	120.140	104.250	1.090	9.899
14	120.140	129.220	113.330	1.068	9.698
15	129.220	129.350	117.935	1.038	0.135
16	129.350	138.020	122.335	0.989	8.577
17	138.020	146.680	131.000	0.767	6.644
18	146.680	155.350	139.665	0.473	4.105
				Sum	143.650
				Normalized	0.998
				Corr. Factor	1.002

Table A.3-8
Maximum TC Component and DSC Shell Temperatures for NCT
(100°F and Insolation), BWR DSCs

DSC type	69BTH			61BTH/61BTHF Type 1	61BTH/61BTHF Type 2	61BT	
Heat Load	32 kW	29.2 kW	26 kW	22 kW	24 kW	18.3 kW	
Internal sleeve	No	No	No	Yes	Yes	Yes	
External fins	Yes	Yes	No	No	No	No	
Component	T_{max} (°F)	T_{max} (°F)	T_{max} (°F)	T_{max} (°F)	T_{max} (°F)	T_{max} (°F)	Limit (°F)
DSC shell (T_{Max}/T_{Min})	484/266	458/255	451/266	414/250	435/260	372/229	---
DSC shell @ mid-length[1]	470	445	440	406	427	365	---
Internal sleeve	N/A	N/A	N/A	317	333	286	---
Cask inner shell	367	347	351	315	331	284	---
Gamma shield	366	345	349	314	330	283	621 [5]
Outer shell	352	332	337	306	321	276	---
Shield shell	305	289	299	272	285	248	---
Finned Shell	229	220	N/A	N/A	N/A	N/A	---
Cask lid	267	254	265	248	259	228	---
Cask bottom plate	353	334	338	307	322	277	---
Neutron Shield Resin[2]	290	276	288	264	276	241	320 [17]
Trunnion Plug Resin[2]	277	263	272	249	260	229	445 [25]
Cask lid seal	268	256	266	249	260	229	400 [18, 19]
Ram plate seal	352	332	337	306	321	277	*644 [52, 53]*
Drain port seal @ bottom	351	332	337	306	321	276	*644 [52, 53]*
Test seal @ bottom	349	330	335	305	320	276	*644 [52, 53]*
Vent & test seal @ top	267	254	265	248	259	228	400 [18, 19]
Wood in Impact limiter	302	287	291	265	278	242	320

Notes
(1) This value is the maximum DSC shell temperature in the region where the fuel assemblies have the maximum peaking factor.
(2) This temperature is the volumetric, average temperature of the elements located at hottest cross section of the neutron shield resin/the trunnion plug resin.

Table A.3-9
Maximum TC Component and DSC Shell Temperatures for NCT
(100°F and Insolation), PWR DSCs

DSC type	37PTH	32PTH / 32PTH Type1 / 32PTH1 Type 1	32PTH1 Type 2	32PT	24PTH or 24PTHF (all types)	24PT4	
Heat Load	22.0 kW	26 kW	24 kW	24 kW	26 kW	24 kW	
Internal sleeve	No	No	No	Yes	Yes	Yes	
External fins	No	No	No	No	No	No	
Component	T_{max} (°F)	T_{max} (°F)	T_{max} (°F)	T_{max} (°F)	T_{max} (°F)	T_{max} (°F)	Limit (°F)
DSC shell (T_{Max}/T_{Min})	408/261	444/289	423/278	443/283	464/299	428/313	---
DSC shell @ mid-length[(1)]	395	434	414	430	447	421	
Internal sleeve	N/A	N/A	N/A	329	347	319	---
Cask inner shell	314	337	322	326	344	317	---
Gamma shield	313	336	321	325	343	316	621 [5]
Outer shell	301	320	306	316	335	308	---
Shield shell	271	290	278	281	295	274	---
Cask lid	301	319	305	318	336	306	---
Cask bottom plate	246	276	265	268	282	309	---
Neutron Shield Resin[(2)]	263	280	268	273	285	265	320 [17]
Trunnion Plug Resin[(2)]	249	264	254	257	268	250	445 [25]
Cask lid seal	301	319	305	317	336	307	400 [18, 19]
Ram plate seal	244	274	263	267	280	308	*644 [52, 53]*
Drain port seal @ bottom	245	275	264	267	281	308	*644 [52, 53]*
Test seal @ bottom	243	272	262	265	279	307	*644 [52, 53]*
Vent & test seal @ top	300	318	305	317	336	306	400 [18, 19]
Wood in Impact limiter	262	278	266	274	289	267	320 [20]

Notes
(1) This value is the maximum DSC shell temperature in the region where the fuel assemblies have the maximum peaking factor.
(2) This temperature is the volumetric, average temperature of the elements located at hottest cross section of the neutron shield resin / the trunnion plug resin.

Table A.3-10
Maximum Fuel Cladding and Basket Component Temperatures for NCT

DSC Type	$T_{max,\ Fuel}$ (°F)	Reference for bounding fuel cladding temperature	$T_{max,\ Comp}$ (°F)	$T_{max,\ Al/Poison}$ (°F)	$T_{max,\ Rail}$ (°F)	Reference for bounding basket component temperatures
69BTH, 32 kW	650	–	612	612	507	–
69BTH, 29.2 kW	651	–	622	621	481	–
69BTH, 26 kW	658	–	643	643	475	–
61BTH Type 1	< 706	[3], Table T.4-12	< 683	< 682	< 565	[3], Table T.4-13
61BTH Type 2	< 721	[3], Table T.4-12(4)	< 692	< 692	< 549	[3], Table T.4-14(4)
61BT	< 638	[1], Table K.4-2	< 615	< 615	< 493	[1], Table K.4-2
37PTH	660	–	649	648	443	–
32PTH, 32PTH Type 1	< 723	[4], Table 4-1	< 697	< 696	< 561	[4], Table 4-1
32PTH1 Type 1	< 713	[3], Table U.4-15	< 677	< 676	< 520	[3], Table U.4-16
32PTH1 Type 2	< 728	[3], Table U.4-15	< 648	< 648	< 529	[3], Table U.4-17
32PT	< 720	[1], Table M.4-2	< 705	< 705	< 471	[1], Table M.4-3
24PTH-S or –L w/ Al Inserts	< 733	[1], Table P.4-14	< 680	< 679	< 576 (1)	[1], Table P.4-16
24PTH-S or –L w/o Al Inserts	< 733	[1], Table P.4-14	< 682	< 681	< 576 (1)	[1], Table P.4-16
24PTH-S-LC	< 714	[1], Table P.4-14	< 674	< 673	< 500 (1)	[1], Table P.4-17
24PT4	< 707	[2], Table A4.4-7	< 670	< 670	(2)	[2], Table A4.4-6

Notes:
(1) This value is the maximum rail temperature for rail R90 taken from evaluations of 24PTH DSC under normal transfer conditions.
(2) Based on [2], Table A.4.4-6, the maximum spacer disc and support rod temperatures for 24PT4 DSC under normal transfer conditions are 663°F and 574°F. These temperatures are the bounding values for NCT.
(3) *Not used.*
(4) The maximum temperatures for 61BTH Type 2 DSC are increased from values in [3] due to allowance of six shims between the basket and the rails per note 5 of Drawing NUH61BTH-71-1102 in Appendix A.1.4.10.9.

Table A.3-11
Maximum/Minimum Component Temperatures for NCT

(Part 1 of 2)

Conditions	**100°F with Insolation** (1)			**-40°F No Insolation** (2)	
Heat load	26 < Q ≤ 32 kW	Q ≤ 26 kW		0	
Inner sleeve	No	No	Yes	N/A	
External fins	Yes	No	No	N/A	
Component	T_{max} (°F)	T_{max} (°F)	T_{max} (°F)	T_{min} (°F)	Allowable Range (°F)
Fuel Cladding	651	< 728	< 733	-40	752 max. [7]
Fuel Compartment	622	< 697	< 692	-40	(4)
Al/Poison Plates	621	< 696	< 692	-40	(4)
Basket Rails	507	< 561	< 576	-40	(4)
DSC shell	484	451	464	-40	(4)
Inner sleeve	N/A	N/A	347	-40	(4)
Cask inner shell	367	351	344	-40	(4)
Gamma shield	366	349	343	-40	621 max. [5]
Outer shell	352	337	335	-40	(4)
Shield shell	305	299	295	-40	(4)
Finned Shell	229	N/A	N/A	-40	(4)
Cask lid (5)	267	319	336	-40	(4)
Cask bottom plate	353	338	322	-40	(4)
Neutron Shield Resin(3)	290	288	285	-40	320 max. [17]
Trunnion Plug Resin(3)	277	272	268	-40	445 max. [25]
Seals *at TC Lid*	*268*	*319*	*336*	-40	400 max. [18, 19]
Seals at Bottom Plate	*352*	*337*	*321*	*644 [52, 53]*	
Wood in Impact limiter	302	291	289	-40	320 max. [20]

Notes:

(1) These temperatures are the highest values taken from Table A.3–8, Table A.3–9, and Table A.3–10 *for the case that the physical configuration of the fuel assemblies is not altered.*

(2) These temperatures are based on assuming no credit for decay heat and a daily average ambient temperature of -40°F.

(3) The resin temperature is the volumetric, average temperature at the hottest cross section.

(4) The components perform their intended safety function within the operating range.

(5) The maximum cask lid temperatures for 26 kW < Q ≤ 32 kW and Q ≤ 26 kW belong to DSCs loaded with BWR and PWR fuel assemblies, respectively. Since a spacer is used for PWR DSCs, the heat load of the PWR fuel assemblies is closer to the cask lid. Due to this configuration, the maximum cask lid temperature for Q ≤ 26 kW is higher than for 26 kW < Q ≤ 32 kW. See Table A.3-8 and Table A.3-9 for details.

Proprietary Information Withheld Pursuant to 10 CFR 2.390

Table A.3-12
Maximum TC Component and 69BTH DSC Temperatures for Cold NCT
(32 kW, No insolation)

Ambient Temperature	-20°F	-40°F
Component	T_{max} (°F)	T_{max} (°F)
Fuel Cladding	582	570
Basket (compartment)	537	524
Al / Poison Plate	536	524
Basket Rails	431	419
DSC shell	405	392
Cask inner shell	267	250
Gamma shield	265	248
Outer shell	250	233
Shield shell	202	184
Finned Shell	124	105
Cask lid	162	145
Cask bottom plate	252	235
Neutron Shield Resin (1)	187	169
Trunnion Plug Resin (1)	169	151
Wood in Impact limiter	193	175

Note: (1) This temperature is the volumetric, average temperature of the elements located at hottest cross section of the neutron shield resin/the trunnion plug resin.

Table A.3-13
Maximum TC Component and 37PTH DSC Temperatures for Cold NCT
(22 kW, No insolation)

Ambient Temperature	-20°F	-40°F
Component	T_{max} (°F)	T_{max} (°F)
Fuel Cladding	593	582
Basket (compartment)	580	569
Al / Poison Plate	580	569
Basket Rails	365	353
DSC shell	328	315
Cask inner shell	219	203
Gamma shield	217	202
Outer shell	204	188
Shield shell	173	157
Cask lid	204	188
Cask bottom plate	146	130
Neutron Shield Resin (1)	164	148
Trunnion Plug Resin (1)	145	128
Wood in Impact limiter	157	140

Note: (1) This temperature is the volumetric, average temperature of the elements located at hottest cross section of the neutron shield resin/the trunnion plug resin.

Table A.3-14
Average Component Temperatures for NCT and HAC

DSC Type	69BTH	61BTH/ 61BTHF Type 1	61BTH/ 61BTHF Type 2	61BT	37PTH
Heat load	32 kW	22 kW	24 kW	18.3 kW	22.0 kW
Component	T_{avg} (°F)	T_{avg} (°F)	T_{avg} (°F)	T_{avg} (°F)	T_{avg} (°F)
Helium in TC cavity @ NCT	339	301	316	273	269
Helium in TC cavity @ HAC(1)	387	(2)	(2)	(2)	(2)

DSC Type	32PTH / 32PTH Type1 / 32PTH1 Type 1	32PTH1 Type 2	32PT	24PTH/ 24PTHF (all types)	24PT4
Heat load	26 kW	24 kW	24 kW	26 kW	24 kW
Component	T_{avg} (°F)	T_{avg} (°F)	T_{avg} (°F)	T_{avg} (°F)	T_{avg} (°F)
Helium in TC cavity @ NCT	301	288	281	297	313
Helium in TC cavity @ HAC(1)	(2)	(2)	(2)	333	(2)

Basket Type	69BTH	69BTH	69BTH	69BTH	37PTH
Heat Load	26 KW	26 kW	29.2 kW	32 kW	22 kW
Configuration	HLZC # 1	HLZC # 2	HLZC # 3	HLZC # 4	HLZC # 1
Component	T_{avg} (°F)	T_{avg} (°F)	T_{avg} (°F)	T_{avg} (°F)	T_{avg} (°F)
Normal Conditions of Transport					
Fuel Assemblies	534	525	535	547	517
Helium Elements(3)	398	404	404	432	406
Aluminum Rail	457	457	464	490	436
Hypothetical Accident Conditions					
Fuel Assemblies	544	535	579	592	530
Helium Elements(3)	411	417	453	482	426
Aluminum Rail	470	470	511	538	454

Note:
(1) This value is the highest average helium temperature for the transient run.
(2) The average helium temperature for this case is bounded by 69BTH or 24PTH cases.
(3) This value is the volumetric, average temperature of the elements with helium properties in the basket model. In addition to the gaps, helium properties are considered for the elements within the fuel compartments located beyond the active fuel length and for the empty compartments.

Table A.3-15
List of the Gaps and Thermal Properties for HAC Analysis

	Gap Size (in)	Location	Initial / Cool-down Properties	Properties during Fire
1	0.01[1]	Axial gap between aluminum blocks of thermal shield and impact limiter case	Air	SA-240, type 304 (Impact Limiter Shell)
2	0.01[1]	Axial gap between thermal shield plates and cask top or bottom end surfaces	Air	Al 6061 (Thermal shield)
3	0.01	Axial gap between cask lid and cask flange	Helium	SA-350-LF3/SA-203, Gr. E (Cask lid)
4	0.01	Axial gap between ram closure plate and cask bottom plate	Helium	SA-240, type 304 (Ram Closure Plate) [2]
5	0.01	Radial gaps between neutron shield boxes and surrounding shells	Air	Al 6063 (Neutron shield boxes)
6	0.01	Gaps between trunnion replacement plugs and the trunnion attachment blocks	Air	SA-182-F6NM (Trunnion block)
7	0.025	Radial gap between gamma shield and cask outer shell	Air	ASTM B-29 (Gamma shield)
8	0.01	Radial gaps between the cask inner shell and aluminum sleeve	Helium	Al 6061 (Inner sleeve w/o gaps)
9	0.01	Radial gap between the finned aluminum shell and the cask shield shell	Air	Al 6061 (Finned shell)
10	0.0625	Axial gaps between the DSC bottom shield plug and bottom cover plates	Air[3]	A36 (DSC bottom shield plug)
11	0.0625	Axial gaps between the DSC top inner cover and the adjacent plates	Air[3]	SA-240, type 304 (DSC top inner cover plate)

Notes:
[1] The size of this axial gap is 0.0625" for initial conditions.
[2] A stainless steel weld is overlaid on the ram closure surfaces in contact with the cask bottom plate. For conservatism, ram closure plate is considered as SA-240, type 304 in this analysis.
[3] These gaps are incorporated into corresponding plates as effective conductivities in Section A.3.3.1.3

Table A.3-16
Maximum Temperatures of TC Components / DSC Shell for HAC

DSC type	69BTH			69BTH			24PTH			
Heat Load	32 kW			26 kW			26 kW			
Internal sleeve	No			No			Yes			
External fins	Yes (Melted)			No			No			
Component	Time (hr)	T_{max} (°F)	T_{∞} (°F) (2)	Time (hr)	T_{max} (°F)	T_{∞} (°F) (2)	Time (hr)	T_{max} (°F)	T_{∞} (°F) (2)	Limit (°F)
DSC shell	7.2	509	496	4.7	451	443	7.6	473	467	---
DSC shell @ mid-length (1)	7.2	509	496	4.7	451	442	7.6	464	453	---
Internal sleeve	N/A	N/A	N/A	N/A	N/A	N/A	2.3	409	366	---
Cask inner shell	2.0	487	403	0.5	441	363	0.5	413	363	---
Gamma shield	0.5	552	401	0.5	521	362	0.5	508	361	621 [5]
Outer shell	0.5	690	383	0.5	651	352	0.5	645	352	---
Shield shell	0.5	1393	337	0.5	1072	306	0.5	1071	303	---
Cask lid	13.2	314	311	10.7	299	292	4.6	367	352	---
Cask bottom plate	1.0	416	384	1.0	404	353	7.6	309	300	---
Cask lid seal	10.2	321	316	7.7	304	295	4.6	373	351	400 [18, 19]
Vent & test seal @ top	13.2	311	310	10.7	298	291	4.6	366	351	400 [18, 19]
Ram plate seal	2.0	380	378	2.3	366	350	10.6	302	297	*644 [52, 53]*
Test seal @ bottom	13.2	380	379	1.3	364	350	10.6	303	297	*644 [52, 53]*
Drain port seal @ bottom	10.2	386	383	7.7	362	352	7.6	308	299	*644 [52, 53]*
Helium in TC Cavity	4.2	387	380	4.7	356	347	7.6	333	327	---

Notes:
(1) This value is the maximum DSC shell temperature in the region where the fuel assemblies have the maximum peaking factor. See Appendix A.3.6.3 for discussion.
(2) These values are retrieved from the transient model at 20 hrs after fire accident. Based on the time-temperature histories shown in Figure A.3–40 through Figure A.3–42, the steady state temperatures are bounded by the temperatures at 20 hr transient.

Table A.3-17
Maximum DSC Shell Temperatures for Steady State Cool-Down

DSC type	69BTH	69BTH	69BTH	61BTH/ 61BTHF Type 1	61BTH/ 61BTHF Type 2	61BT
Heat Load	32 kW	29.2 kW	26 kW	22 kW	24 kW	18.3 kW
Internal sleeve	No	No	No	Yes	Yes	Yes
External fins	Yes (Melted)	Yes (Melted)	No	No	No	No
T_{max} DSC shell (°F)	537	509	469	441	464	397

DSC type	37PTH	32PTH/ 32PTH Type1/ 32PTH1 Type 1	32PTH1 Type 2	32PT	24PTH / 24PTHF (all types)	24PT4
Heat Load	22.0 kW	26 kW	24 kW	24 kW	26 kW	24 kW
Inner sleeve	No	No	No	Yes	Yes	Yes
External fins	No	No	No	No	No	No
T_{max} DSC shell (°F)	438	473	452	470	480	454

Table A.3-18
Maximum Fuel Cladding and Basket Component Temperatures for HAC

DSC Type	$T_{max, Fuel}$ (°F)	Reference for bounding fuel cladding temperature	$T_{max, Comp}$ (°F)	$T_{max, Al/Poison}$ (°F)	$T_{max, Rail}$ (°F)	Reference for bounding basket component temperatures
69BTH, 32 kW	693	–	658	657	557	–
69BTH, 29.2 kW	693	–	667	666	529	–
69BTH, 26 kW	668	–	653	653	487	–
61BTH Type 1	< 749	[3], Table T.4-21	< 727	< 727	< 609	[3], Table T.4-22
61BTH Type 2	< 830	[3], Table T.4-21(6)	< 805	< 804	< 650	[3], Table T.4-23(6)
61BT	< 809	[1], Section K.4.6.4	< 787	< 787	< 772	[1], Table K.4-1(3)
37PTH	671	–	661	660	459	–
32PTH, 32PTH Type 1	< 1036	[4], Table 4-5	< 1021	< 1021	< 878	[4], Table 4-5
32PTH1 Type 1(1)	< 796	[3], Table U.4-24	< 766	< 766	< 609	[3], Table U.4-25
32PTH1 Type 2(2)	< 858	[3], Table U.4-24	< 831	< 830	<689	[3], Table U.4-26
32PT	< 863	[1], Table M.4-13	< 852	< 852	< 631	[1], Table M.4-14
24PTH-S or –L w/ Al inserts	< 843	[1], Table P.4-25	< 802	< 801	< 716(4)	[1], Table P.4-27
24PTH-S or –L w/o Al inserts	< 843	[1], Table P.4-25	< 802	< 801	< 716(4)	[1], Table P.4-27
24PTH-S-LC	< 747	[1], Table P.4-25	< 709	< 708	< 716(4)	[1], Table P.4-28
24PT4	< 805	[2], Table A4.4-7	< 768	< 768	(5)	[2], Table A4.4-6

Notes:
(1) This value is the maximum fuel cladding temperature for 32PTH1 Type 1 DSC with 31.2 kW heat load under transfer accident conditions.
(2) This value is the maximum fuel cladding temperature for 32PTH1 Type 2 DSC with 31.2 kW heat load under transfer accident condition.
(3) Based on discussion in [1], Appendix K, Section K.4.6.5, the maximum temperatures for transfer accident conditions are bounded by the maximum temperatures for blocked vent accident conditions.
(4) This value is the maximum rail, R90, temperature for transfer accident conditions with 40.8 kW heat load.
(5) Based on [2], Table A.4.4-6, the maximum spacer disc and support rod temperatures for 24PT4 DSC under accident transfer conditions (loss of sunshade and neutron shield) are 761°F and 673°F. These temperatures are the bounding values for transport HAC.
(6) The maximum temperatures for 61BTH Type 2 DSC are increased from values in [3] due to allowance of six shims between the basket and the rails per note 5 of Drawing NUH61BTH-71-1102 in Appendix A.1.4.10.9.

Table A.3-19
Summary of the Maximum Temperatures for HAC

(Part 1 of 2)

Heat load	26 < Q ≤ 32 kW (2)			Q ≤ 26 kW (2)						
Internal sleeve	No			No			Yes			
External fins	Yes (Melted)			No			No			
Component(1)	Time (hr)	T_{max} (°F)	T_{∞} (°F)	Time (hr)	T_{max} (°F)	T_{∞} (°F)	Time (hr)	T_{max} (°F)	T_{∞} (°F)	Limit (°F)
Fuel Cladding	∞	693	693	∞	<1036	<1036	∞	<863	<863	1058 [7]
Fuel Compartment	∞	667	667	∞	<1021	<1021	∞	<852	<852	---
Al/Poison Plates	∞	666	666	∞	<1021	<1021	∞	<852	<852	---
Basket Rails	∞	557	557	∞	<878	<878	∞	<772	<772	---
DSC shell	∞	537	537	∞	469	469	∞	480	480	---
Internal sleeve	N/A	N/A	N/A	N/A	N/A	N/A	2.3	409	366	---
Cask inner shell	2.0	487	403	0.5	441	363	0.5	413	363	---
Gamma shield	0.5	552	401	0.5	521	362	0.5	508	361	621 [5]
Outer shell	0.5	690	383	0.5	651	352	0.5	645	352	---
Shield shell	0.5	1393	337	0.5	1072	306	0.5	1071	303	---
Cask lid	13.2	314	311	10.7	299	292	4.6	367	352	---
Cask bottom plate	1.0	416	384	1.0	404	353	7.6	309	300	---
Seals at TC Lid	10.2	321	316	7.7	304	295	4.6	373	351	400 [18], [19]
Seals at TC Bottom Plate	10.2	386	383	2.3	366	352	7.6	308	299	*644 [52], [53]*

Notes:

(1) The maximum fuel cladding, basket component, and DSC shell temperatures are based on the conservative steady state cool-down period runs.

(2) These values are the highest temperatures taken from Table A.3–16 through Table A.3–18 *for the case that the physical configuration of the fuel assemblies is not altered.*

Proprietary Information Withheld Pursuant to 10 CFR 2.390

Table A.3-20
MP197HB TC Cavity Pressure for NCT

	Heat Load	$V_{free,cc}$ (1)	$n_{he\text{-}initial}$	$T_{avg,\ he,NCT}$	P_{NCT}
	kW	in^3	g-moles	°F	psig
69BTH	32	19914	16.73	339	12.7
37PTH	22	19876	16.70	269	10.3
32PTH	26	19876	16.70	301	11.4
32PTH, Type 1	26	19876	16.70	301	11.4
32PTH1, Type 1	26	18940	15.91	301	11.4
32PTH1, Type 2	24	18940	15.91	288	11.0
61BTH, Type 1	22	19072	16.02	301	11.4
61BTH, Type 2	24	19072	16.02	316	11.9
61BT	18.3	19072	16.02	273	10.5
32PT	24	20233	17.00	281	10.7
24PTH (all types)	26	19779	16.61	297	11.3
24PT4	24	19386	16.28	313	11.8

Note: (1) 98% of the TC cavity free volume is conservatively used in calculating the maximum pressures.

Table A.3-21
Volume and Average Helium Temperatures in 69BTH and 37PTH DSCs for NCT and HAC

Normal Conditions of Transport						
DSC		69BTH				37PTH
Thermally bounding FA		FANP9x9				BW15x15[5]
Heat Loading Zoning Configuration (HLZC)		#1	#2	#3	#4	---
Number of FAs		69	61	61	52	37
Temperature of Fas along active fuel [Table A.3–21]	°F	534	525	535	547	517
Volume of helium in Fas along active fuel [1]	in^3	244059	215763	215763	183929	231507
Number of dummy fuel assemblies (DA)		0	8	8	16	0
Temperature of Das along active fuel [Table A.3–21]	°F	n/a	559	568	558	n/a
Volume of helium outside Das along active fuel[2]	in^3	n/a	1710	1710	3420	n/a
Free helium volume in DSC[3]	in^3	263687	232756	232756	204051	273058
Temperature of helium in cavity outside Fas and Das along active fuel [Table A.3–21]	°F	398	404	404	432	406
Rest of helium volume in DSC outside Fas and Das along active fuel[4]	in^3	19628	15283	15283	16702	41551
Temperature of helium in DSC	°F	524	517	527	538	500
Hypothetical Accident Conditions						
DSC		69BTH				37PTH
Thermally bounding FA		FANP9x9				BW15x15[5]
HLZC		#1	#2	#3	#4	---
Number of FAs		69	61	61	52	37
Temperature of FAs along active fuel [Table A.3–21]	°F	541	532	576	589	530
Volume of helium in FAs along active fuel[1]	in^3	244059	215763	215763	183929	231507
Number of dummy FAs		0	8	8	16	0
Temperature of DAs along active fuel [Table A.3–21]	°F	0	567	610	601	0
Volume of helium outside DAs along active fuel[2]	in^3	0	1710	1710	3420	0
Free Helium volume in DSC[3]	in^3	263687	232756	232756	204051	273058
Temperature of helium in cavity outside FAs, DAs along active fuel [Table A.3–21]	°F	415	421	457	486	426
Rest of helium volume in DSC outside FAs and DAs along active fuel[4]	in^3	19628	15283	15283	16702	41551
Temperature of helium in DSC	°F	532	525	568	581	514

Notes:
(1) Calculated based on compartment dimensions and total fuel rods' volume along active fuel,
(2) Calculated based on compartment and assumed dummy fuel assembly dimensions along active fuel,
(3) Calculated using weight calculation results for DSC cavity helium volume without 69 FAs volume from Chapter A.2. FAs volume from Chapter A.2, dummy FAs volume as $V_{He_DSC} = V_{He_DSC_w/o_FA} - V_{FAs} - V_{DAs}$,
(4) Calculated as $V_{He_DSC_out_FA/DA_act_fuel} = V_{He_DSC} - V_{He_in_FA_act_fuel} - V_{He_in_DA_act_fuel}$.
(5) BW 15x15 is not allowed in the 37PTH DSC but is used in this analysis for conservatism.

Table A.3-22
Maximum Internal Pressures of 69BTH and 37PTH DSCs in MP197HB TC

Maximum Pressures for Normal Conditions of Transport

DSC	HLZC #	DSC cavity volume	Helium fill amount	Plenum volume	Plenum helium amount	CC gas amount	Fission products amount	Total gas amount	$T_{av\,He}$	Calculated Pressure	Design Pressure
		in^3	g-moles	in^3	g-moles	g-moles	g-moles	g-moles	°F	psig	psig
69BTH	1	258,413	134.4	*442*	3.3	0.0	*14.28*	*151.94*	524	*8.91*	15
	2	228,101	118.6	*391*	2.9	0.0	*12.63*	*134.14*	517	*8.76*	
	3	228,101	118.6	*391*	2.9	0.0	*12.63*	*134.14*	527	*8.98*	
	4	199,970	104.0	*333*	2.5	0.0	10.67	*117.22*	538	***9.17***	
37PTH	37 FAs w/CC	257,646	138.1	*306*	17.0	2.5	0.0	157.6	500	9.28	15

Maximum Pressures for Hypothetical Accident Conditions

DSC	HLZC #	DSC cavity volume	Helium fill amount	Plenum volume	Plenum helium amount	CC gas amount	Fission products amount	Total gas amount	$T_{av\,He}$	Calculated Pressure	Design Pressure
		in^3	g-moles	in^3	g-moles	g-moles	g-moles	g-moles	°F	psig	psig
69BTH	1	258,413	134.4	*14,738*	108.9	0.0	*476.40*	*719.40*	532	*92.07*	*120*
	2	228,101	118.6	*13,030*	96.3	0.0	*420.90*	*635.80*	525	*91.47*	
	3	228,101	118.6	*13,030*	96.3	0.0	*420.90*	*635.80*	568	***96.16***	
	4	199,970	104.0	*11,107*	82.1	0.0	*358.80*	*544.87*	581	*95.13*	
37PTH	37 FAs w/CC	257,646	138.1	*10,205*	568.1	82.9	0.0	789.2	514	102.64	140

Table A.3-23
Maximum Internal Pressure in DSCs for Transport in MP197HB TC

DSC	Operating conditions	Design Pressure psig	Calculated Pressure psig
69BTH	NCT	15	*9.17*
	HAC	*120*	*96.16*
61BTH/61BTHF Type 1	NCT	10	8.10
	HAC	65	56.10
61BTH Type 2	NCT	15	8.60
	HAC	120	68.70
61BT	NCT	10	9.56
	HAC	65	46.00
37PTH	NCT	15	9.28
	HAC	140	102.64
32PTH/32PTH Type 1	NCT	15	7.47
	HAC	120	91.00
32PTH1 Type 1/Type 2	NCT	15	10.74
	HAC	140	126.34
32PT	NCT	15	*8.09*
	HAC	*125*	*113.20*
24PTH/24PTHF (all types)	NCT	15	*8.66*
	HAC	120	*102.10*
24PT4	NCT	20	18.57
	HAC	100	*80.80*

Table A.3-24
Comparison of Maximum DSC Shell Temperatures

For Normal Conditions of Transport					
DSC type	10 CFR 71 DSC Shell Temp [1] (°F)	10 CFR 71 Heat Load (kW)	10 CFR 72 Bounding DSC Shell Temp [2] (°F)	10 CFR 72 Model Reference	10 CFR 72 Heat Load (kW)
61BTH Type 1	414/406	22.0	418 [3], Table T.4-7 [3]	[3], Section T.4.5.1	22.0
61BTH Type 2	435/427	24.0	441 [3], Table T.4-8 [3]	[3], Section T.4.5.1	31.2
61BT	372/365	18.3	378 [1], Table K.4-2	[1], Section K.4.4.1	18.3
32PTH / 32PTH Type 1	444/436	26.0	475 [4], Table 4-1	[4], Section 4.3.1.1	34.8
32PTH1 Type 1	444/436	26.0	485 [3], Table U.4-11	[3], Section U.4.5.2	40.8
32PTH1 Type 2	423/416	24.0	485 [3], Table U.4-11	[3], Section U.4.5.2	31.2
32PT	443/432	24.0	445 [1], Table M.4-3	[1], Section M.4.4.1.6	24.0
24PTH-S or –L w/ Al inserts	464/449	26.0	551 [1], Table P.4-11 [3]	[1], Section P.4.5.2	40.8
24PTH-S or –L w/o Al inserts	464/449	26.0	475 [1], Table P.4-10 [3]	[1], Section P.4.5.2	31.2
24PTH-S-LC	464/449 [4]	24.0	475 [1], Table P.4-10 [4]	[1], Section P.4.5.2	24.0
24PT4	428/424	24.0	439 [2], Table A.4.4-4	[2], Section 4.4.3.1	24.0

For Hypothetical Accident Conditions					
DSC type	10 CFR 71 DSC Shell Temp [5] (°F)	10 CFR 71 Heat Load (kW)	10 CFR 72 Bounding DSC Shell Temp [2] (°F)	10 CFR 72 Model Reference	10 CFR 72 Heat Load (kW)
61BTH Type 1	441	22.0	484 [3], Table T.4-10	[3], Section T.4.5.3.3	22.0
61BTH Type 2	464	24.0	544 [3], Table T.4-10	[3], Section T.4.5.3.3	31.2
61BT	397	18.3	499 [1], Table K.4-6	[1], Section K.4.6.5	18.3
32PTH / 32PTH Type 1	473	26.0	790 [4], Table 4-5	[4], Section 4.4.1.1	34.8
32PTH1 Type 1	473	26.0	578 [3], Table U.4-14	[3], Section U.4.5.4.2	40.8
32PTH1 Type 2	452	24.0	578 [3], Table U.4-14	[3], Section U.4.5.4.2	31.2
32PT	470	24.0	600 [1], Table M.4-14	[1], Section M.4.6.2	24.0
24PTH-S or –L w/ Al inserts	480	26.0	685 [1], Table P.4-26	[1], Section P.4.5.5.3	40.8
24PTH-S or –L w/o Al inserts	480	26.0	610 [1], Table P.4-27	[1], Section P.4.5.5.3	31.2
24PTH-S-LC	480 [4]	24.0	487 [1], Table P.4-28	[1], Section P.4.5.5.3	24.0
24PT4	454	24.0	536 [2], Table A.4.4-5	[2], Section 4.4.3.1	24.0

Notes:

[1] The first value is the absolute maximum DSC shell temperature and the second value is the maximum DSC shell temperature where the fuel has the maximum peaking factor. These values are taken fromTable A.3–8 and Table A.3–9.

[2] These values are the maximum DSC shell temperatures taken from evaluations under 10 CFR 72.

[3] The small differences between the maximum DSC shell temperatures in this table and those shown in Figure A.3-51 and Figure A.3-52 are caused by imperfections in the nodal temperature transfer from TC to DSC models for 61BTH and 24PTH DSCs in [3] and [1].

[4] The maximum DSC shell temperature for 24PTH-S or -L DSC (without aluminum inserts) with 26 kW heat load is bounding for use with the 24PTH-S-LC with 24 kW heat load.

[5] These values are taken from Table A.3–17.

Proprietary Information Withheld Pursuant to 10 CFR 2.390

Proprietary Information Withheld Pursuant to 10 CFR 2.390

Proprietary Information Withheld Pursuant to 10 CFR 2.390

Proprietary Information Withheld Pursuant to 10 CFR 2.390

Proprietary Information Withheld Pursuant to 10 CFR 2.390

Proprietary Information Withheld Pursuant to 10 CFR 2.390

Table A.3-31
Grid Sizes and Refinement Factors

	Set # 1 (Grid # 1,2,3)	*Set # 2 (Grid # 2,3,4)*
N_1	*1402464 (Grid # 3)*	*3120975 (Grid #4)*
N_2	*681269 (Grid # 2)*	*1402184 (Grid #3)*
N_3	*390823 (Grid # 1)*	*681269 (Grid #2)*
r_{21}	*1.272*	*1.306*
r_{32}	*1.204*	*1.272*

Table A.3-32
Temperature of Neutron Shield Resin

	Set # 1 (Grid # 1,2,3)	*Set # 2 (Grid # 2,3,4)*
Φ_1 (°F)	*316.540*	*313.321*
Φ_2 (°F)	*315.798*	*316.540*
Φ_3 (°F)	*315.808*	*315.798*
Φ_{avg} (°F)	*316.049*	*315.219*
$\varepsilon_{21} = \Phi_2 - \Phi_1$ (°F)	*-0.743*	*3.220*
$\varepsilon_{32} = \Phi_3 - \Phi_2$ (°F)	*0.011*	*-0.743*

Table A.3-33
Discretization Error of the Neutron Shield Resin within MP197HB TC

	Set # 1	***Set # 2***
	Grid # 1, 2,3	***Grid # 2,3,4***
N_1	*1402464*	*3120975*
N_2	*681269*	*1402464*
N_3	*390823*	*681269*
r_{21}	*1.272*	*1.306*
r_{32}	*1.204*	*1.272*
Φ_1 (°F)	*316.540*	*313.321*
Φ_2 (°F)	*315.798*	*316.540*
Φ_3 (°F)	*315.808*	*315.798*
Φ_{avg} (°F)	*316.049*	*315.219*
$\varepsilon_{21} = \Phi_2 - \Phi_1$	*-0.743*	*3.220*
$\varepsilon_{32} = \Phi_3 - \Phi_2$	*0.011*	*-0.743*
p	*5.669*	*4.326*
Φ^{21}_{ext} (°F)	*316.796*	*311.837*
e^{21}_{a}	*0.743*	*3.220*
F_s	*1.25*	*1.25*
GCI^{21}_{Fine}	*0.319*	*1.854*
U_{num} (°F)	*0.319*	*1.854*

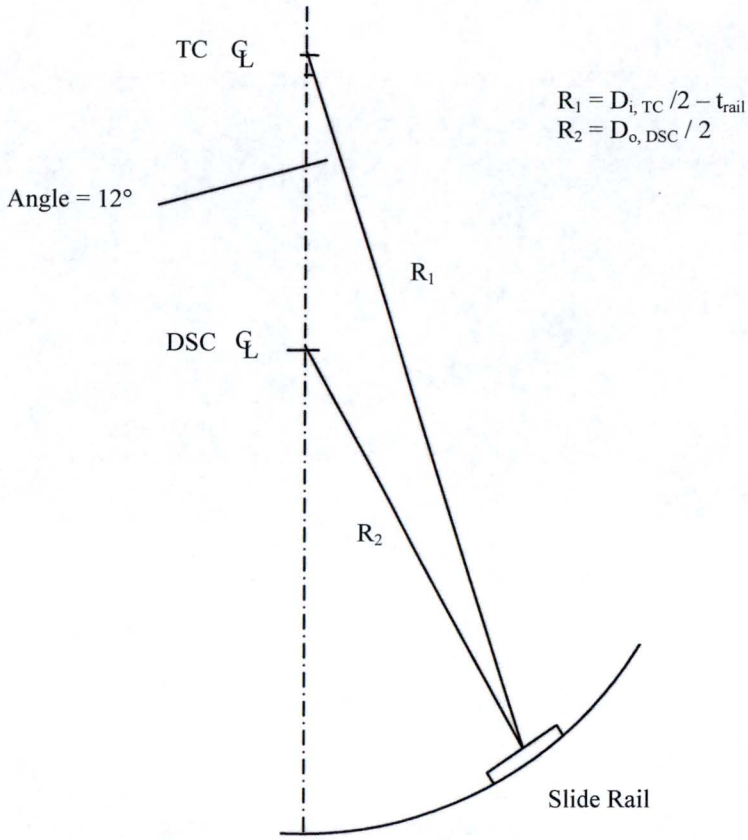

Figure A.3-1
Location of DSC within the MP197HB TC

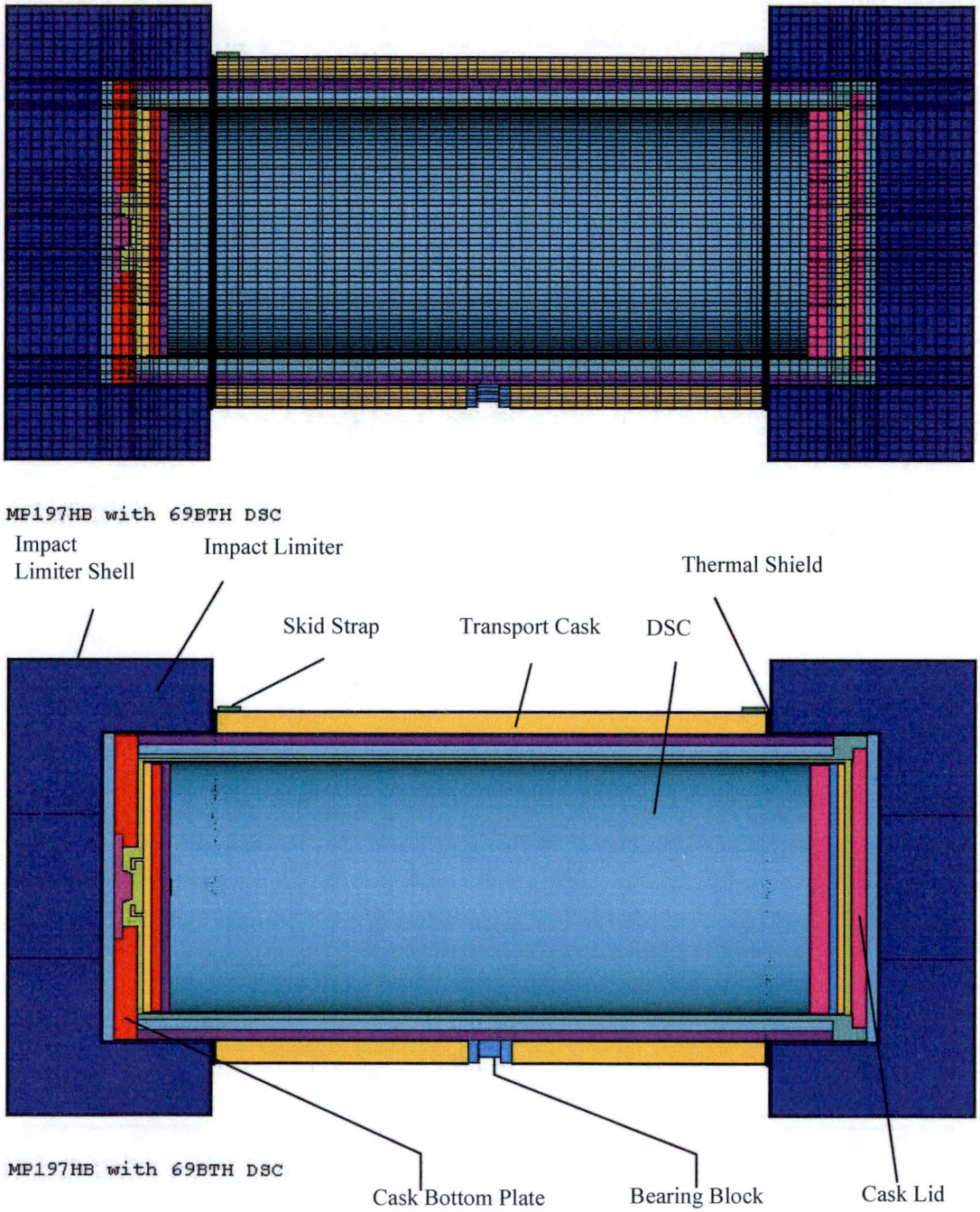

Figure A.3-2
Finite Element Model of the MP197HB with the 69BTH DSC

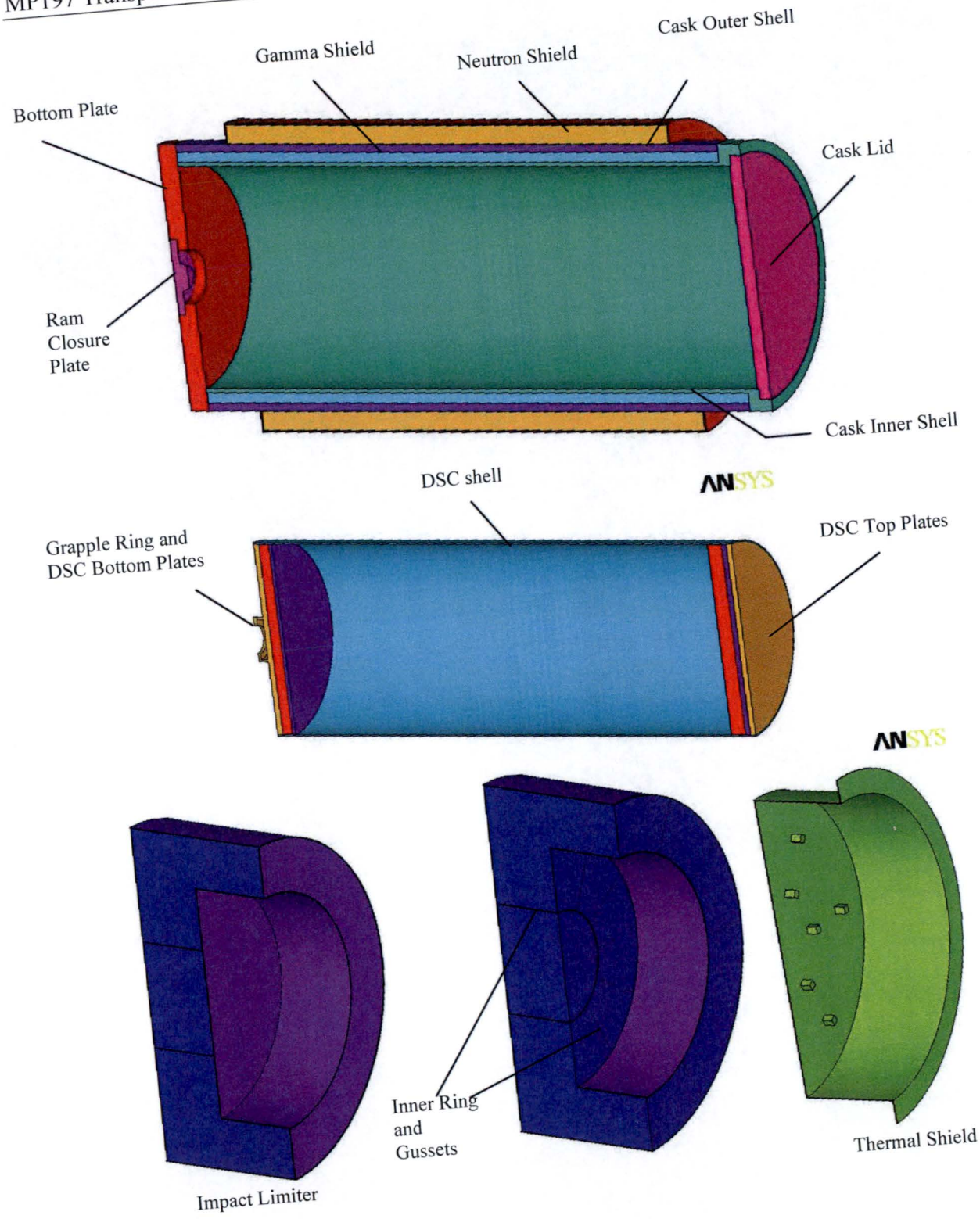

Figure A.3-3
Components of the MP197HB TC Model

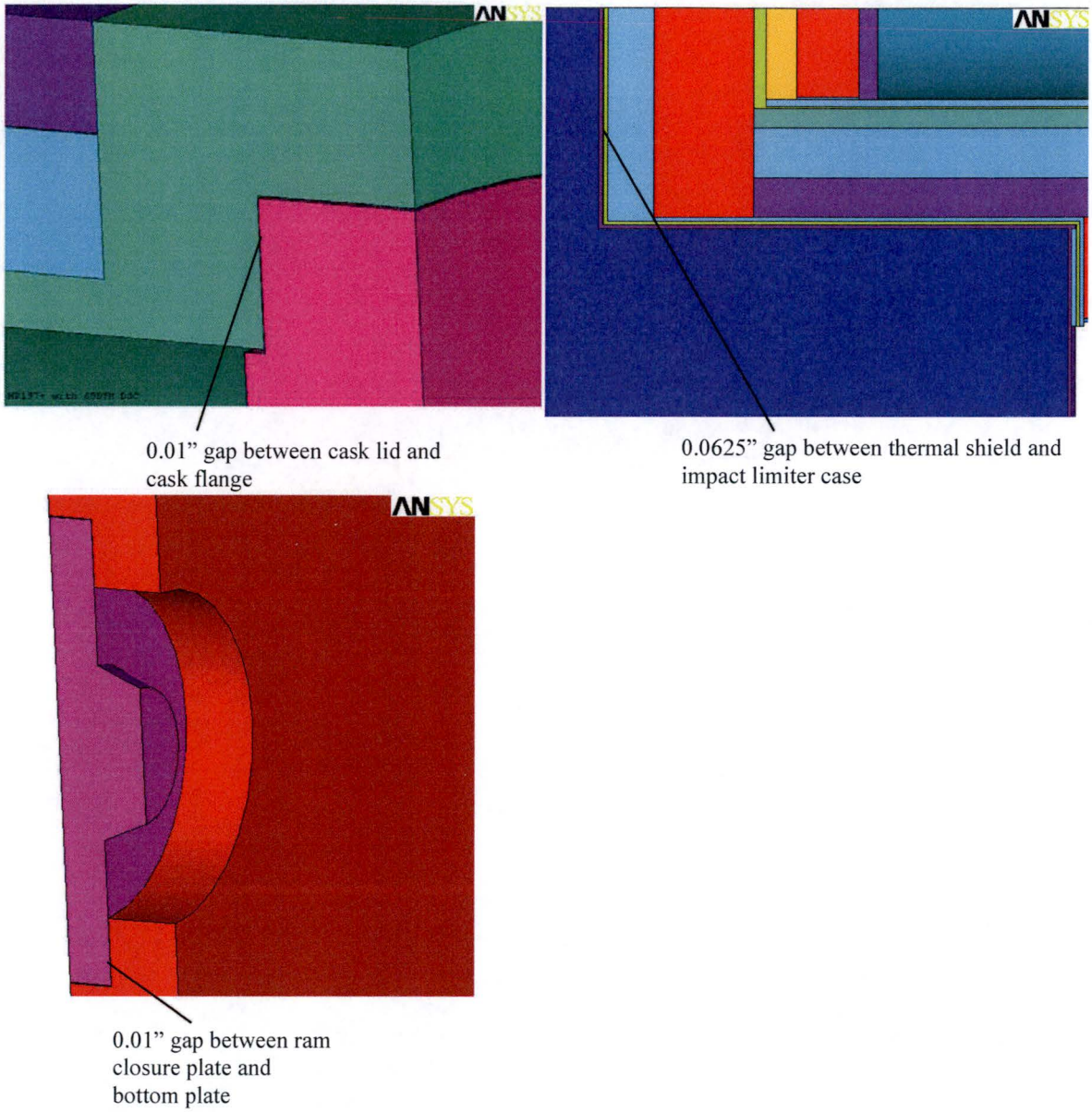

Figure A.3-4
Gaps in the MP197HB TC Model

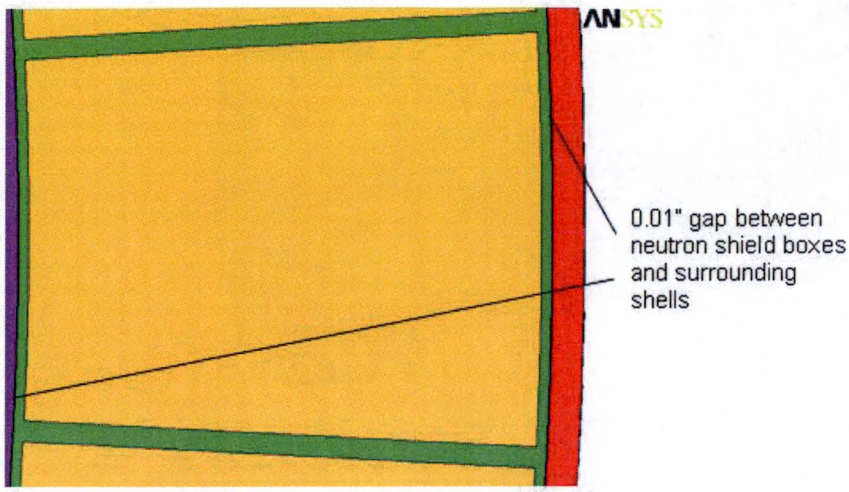

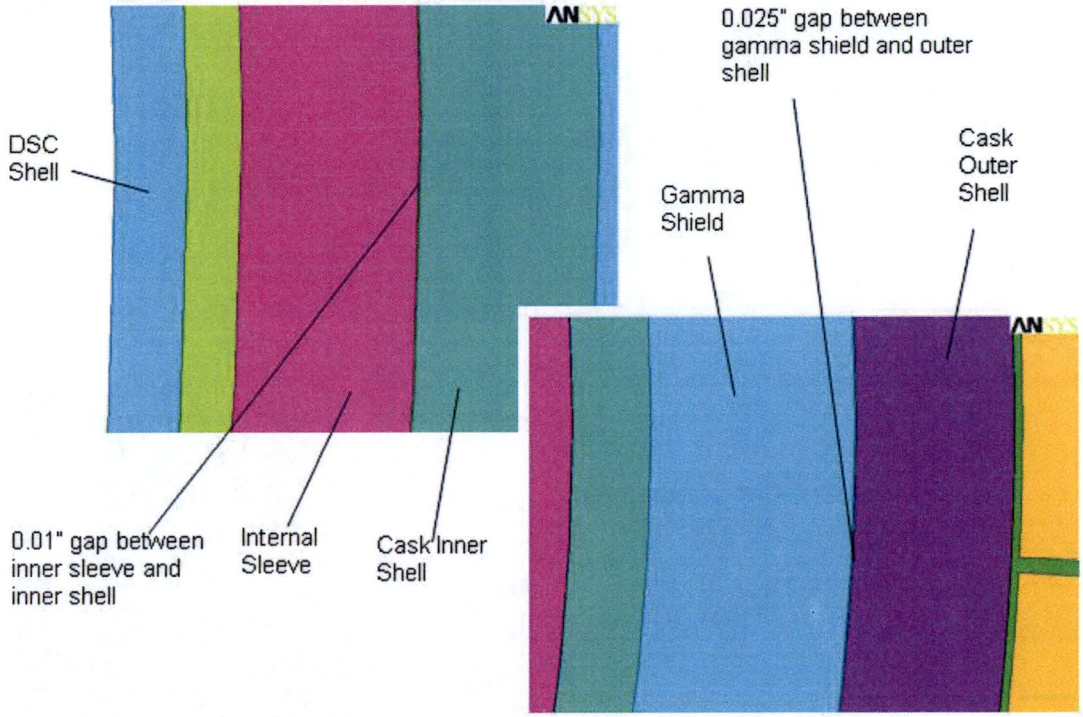

Figure A.3-5
Gaps in the MP197HB TC Cross Section

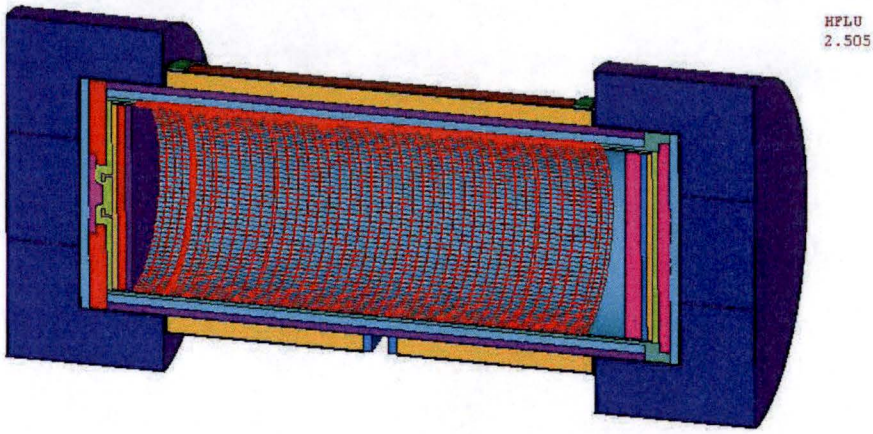

Decay Heat Boundary Conditions for 69BTH DSC, 26 kW

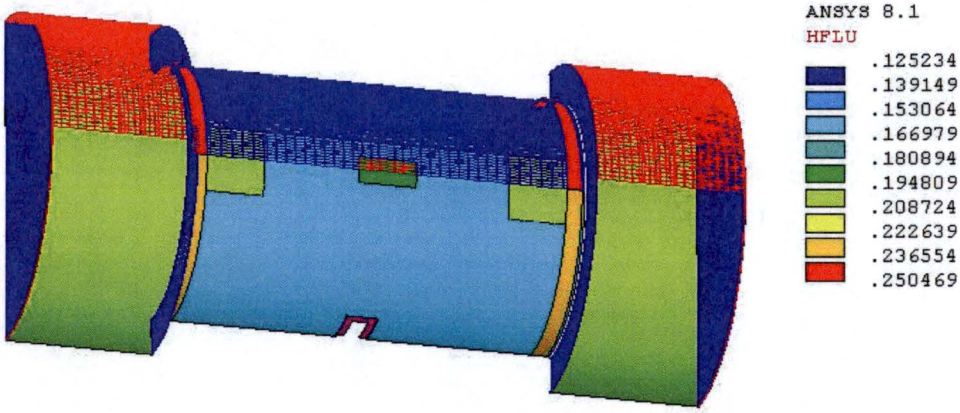

Insolance Boundary Conditions

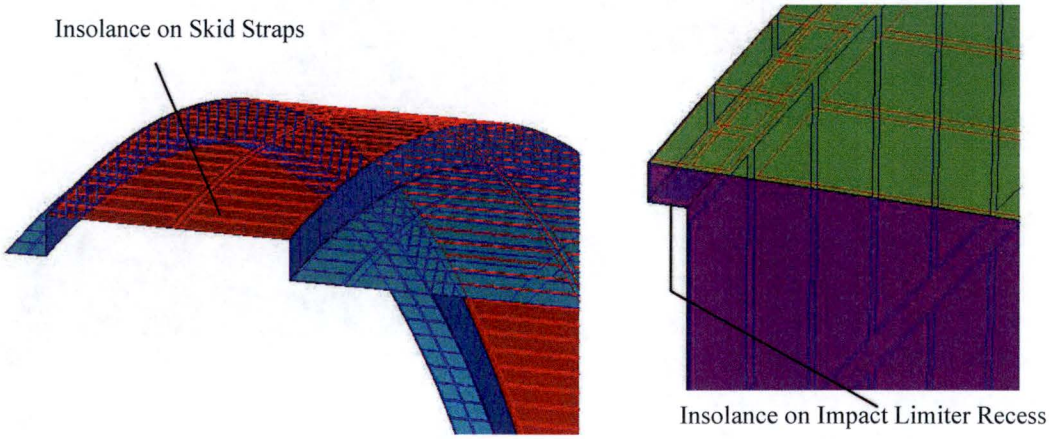

Figure A.3-6
Typical Decay Heat and Insolance Boundary Conditions

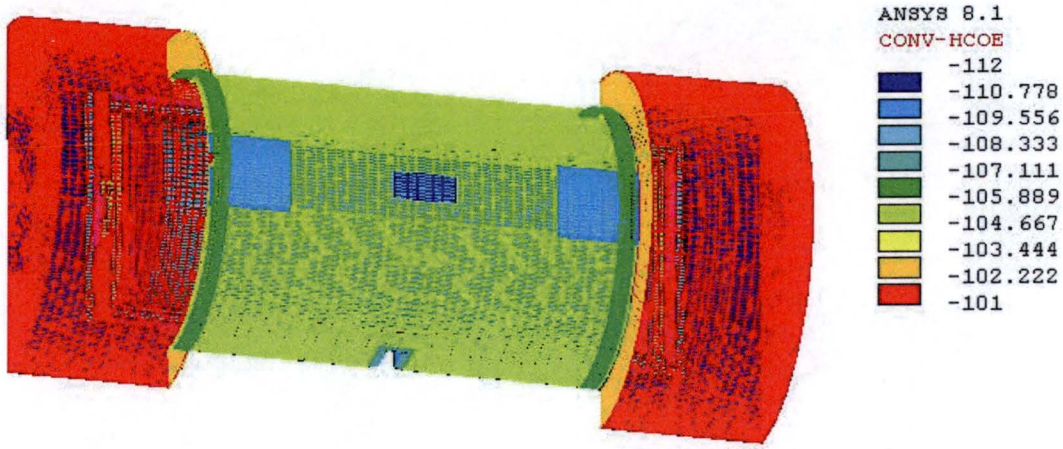

Convection and Radiation Boundary Conditions for MP197HB w/o External Fins

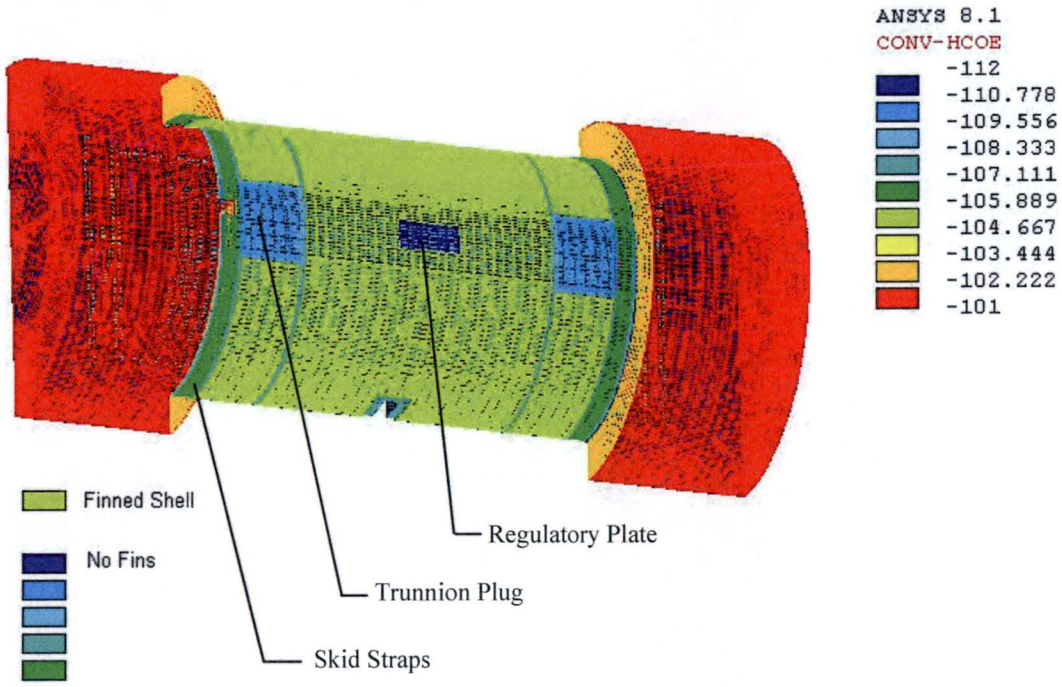

Convection and Radiation Boundary Conditions for MP197HB with External Fins

Figure A.3-7
Typical Convection and Radiation Boundary Conditions

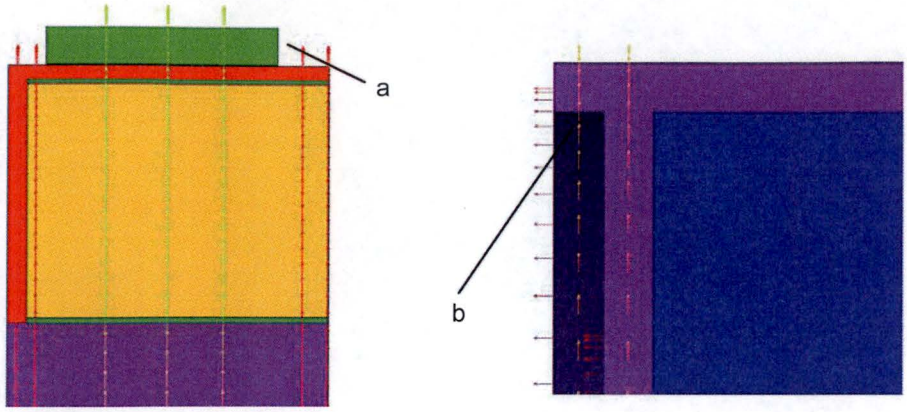

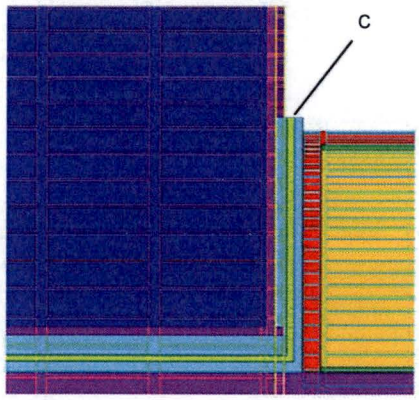

No heat dissipation is considered over marked areas, a, b, and c:

- a Lateral surface of skid straps
- b Inner radial surface of impact limiter recess
- c Thermal shield outer ring and neutron shield end caps

No thermal radiation exchange is considered on area d.

- d Cask area in contact with transport skid saddles

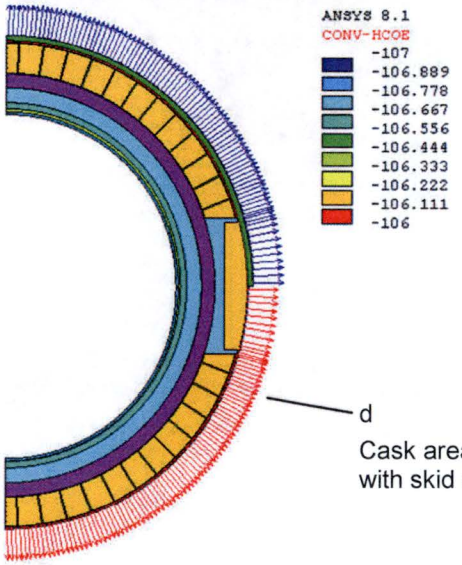

Figure A.3-8
Typical Convection and Radiation Boundary Conditions – Details

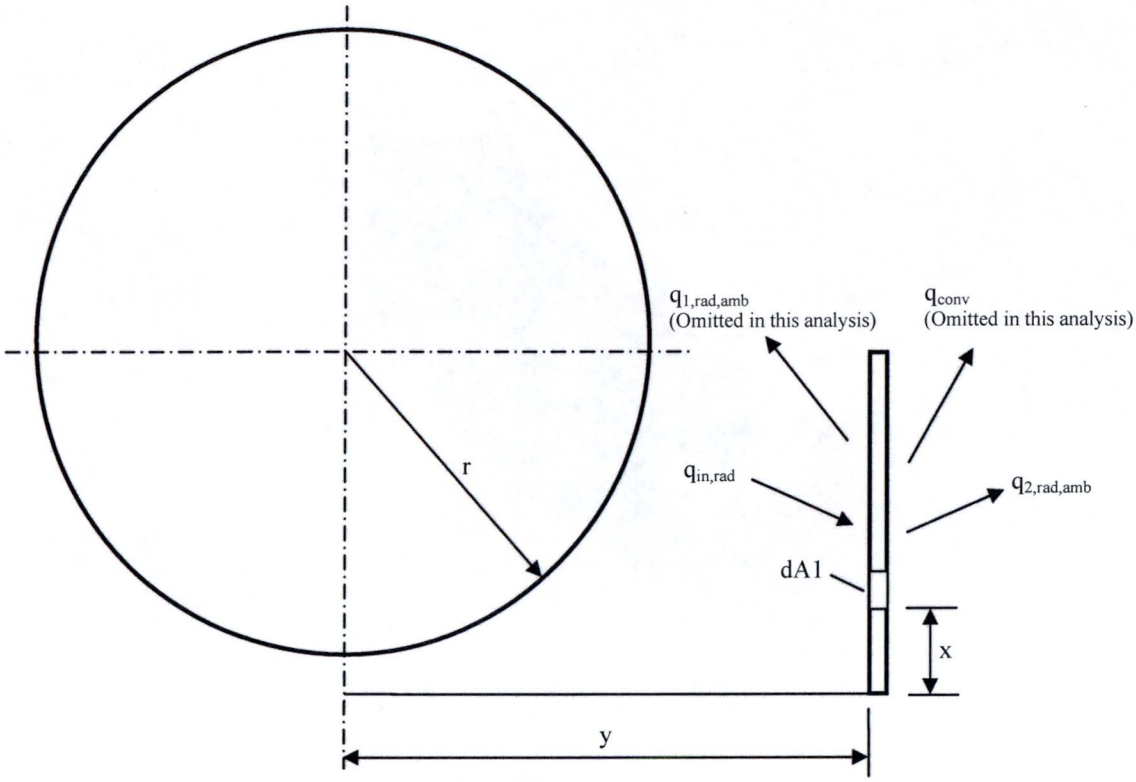

Figure A.3-9
Schematic View of Cask and Personnel Barrier

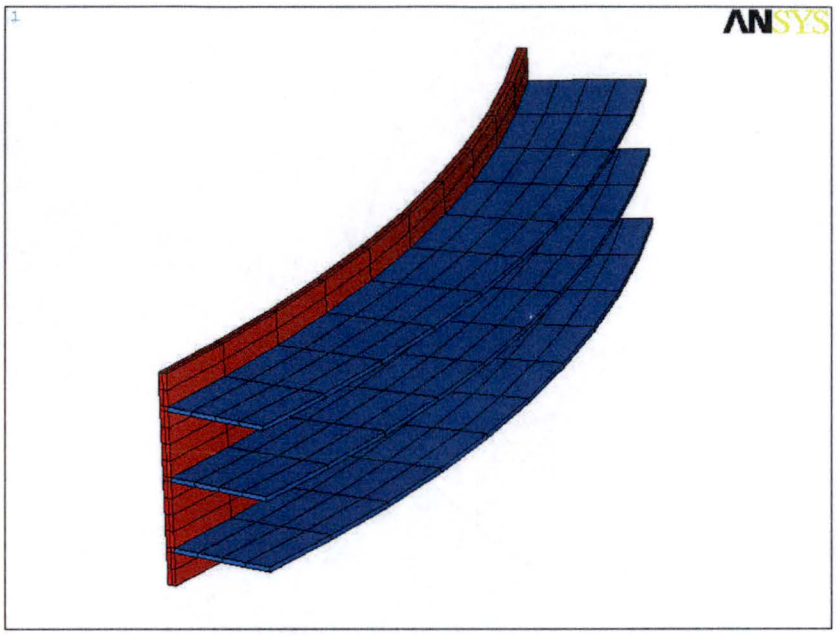

Solid Elements

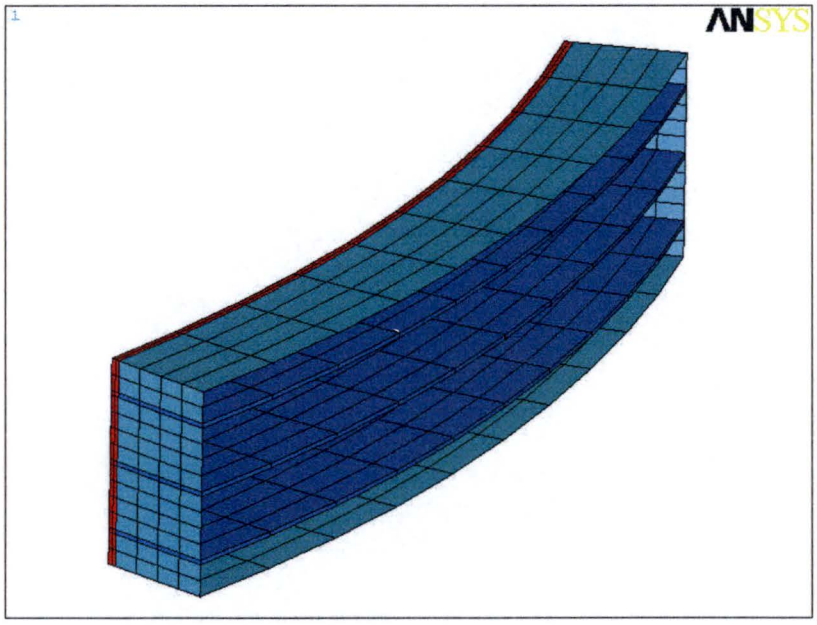

Shell Elements for Radiation

Figure A.3-10
Sub-Model of the External Fins for MP197HB TC

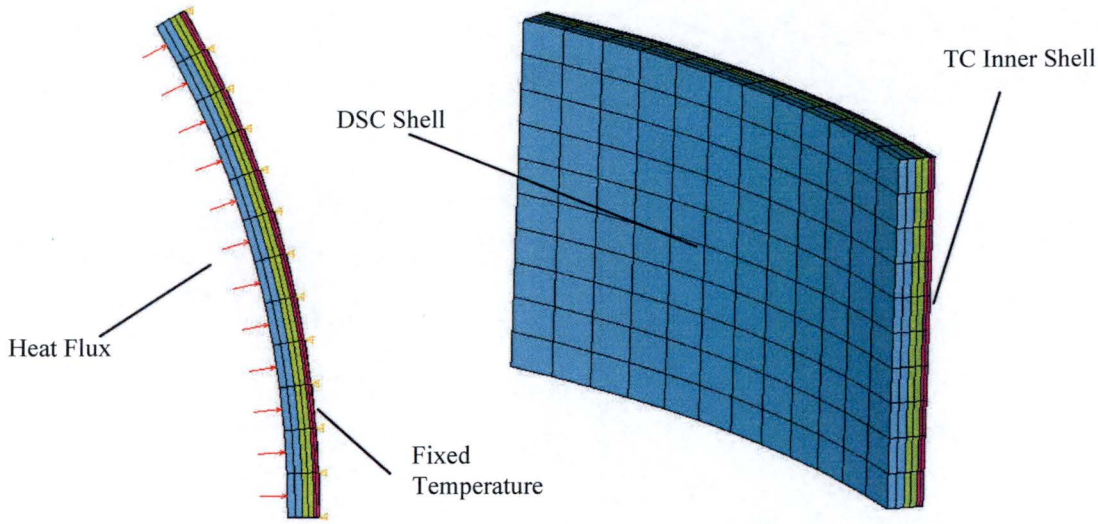

Figure A.3-11
Sub-Model for Helium Gap Effective Conductivity Calculation

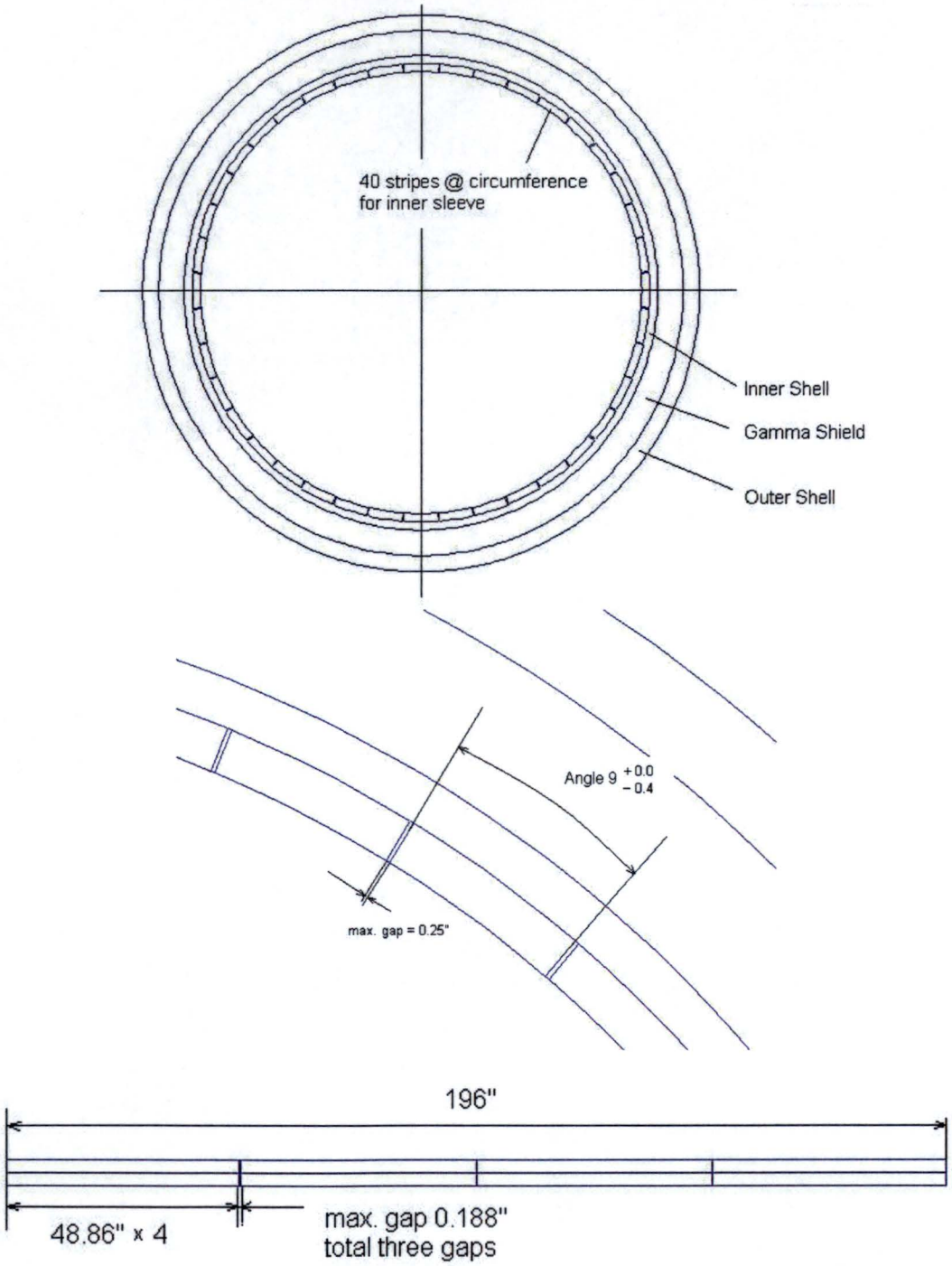

Figure A.3-12
Assumed Geometry of Internal Sleeve in Thermal Model

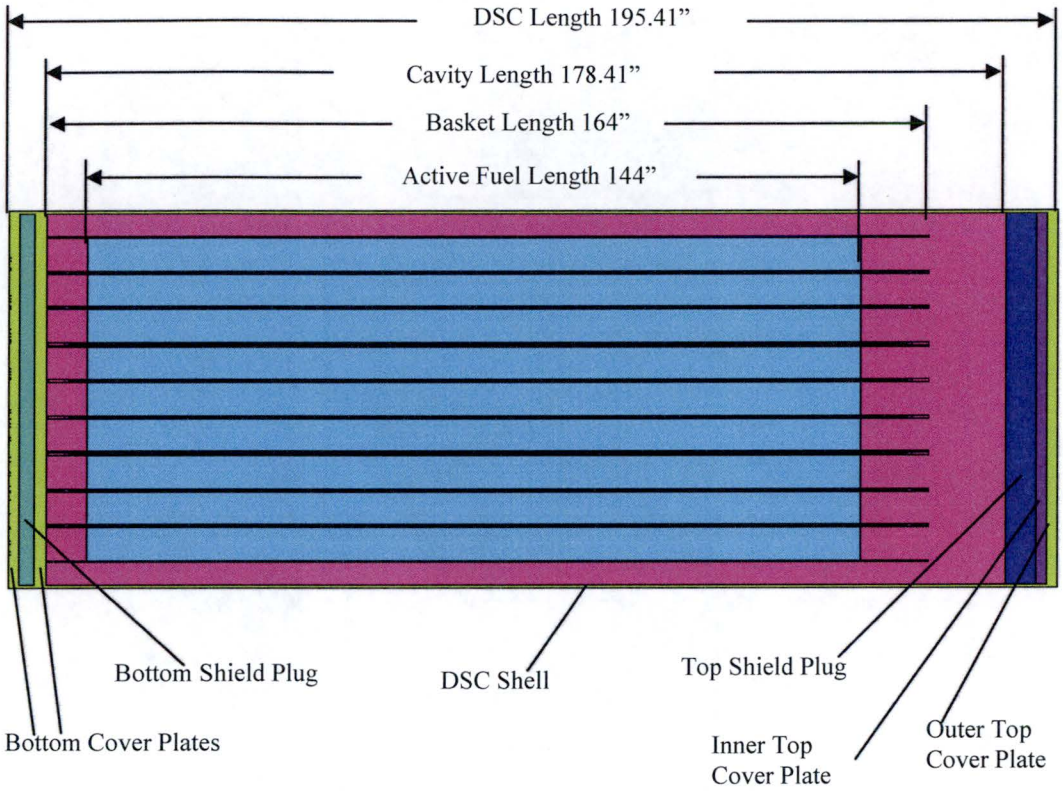

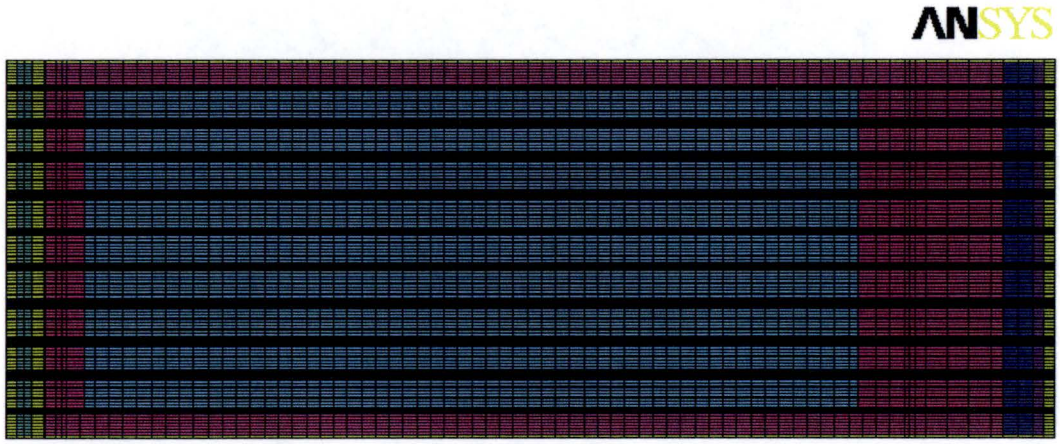

NUH69BTH DSC / Basket

Mesh Density

Figure A.3-13
Finite Element Model of 69BTH DSC/Basket

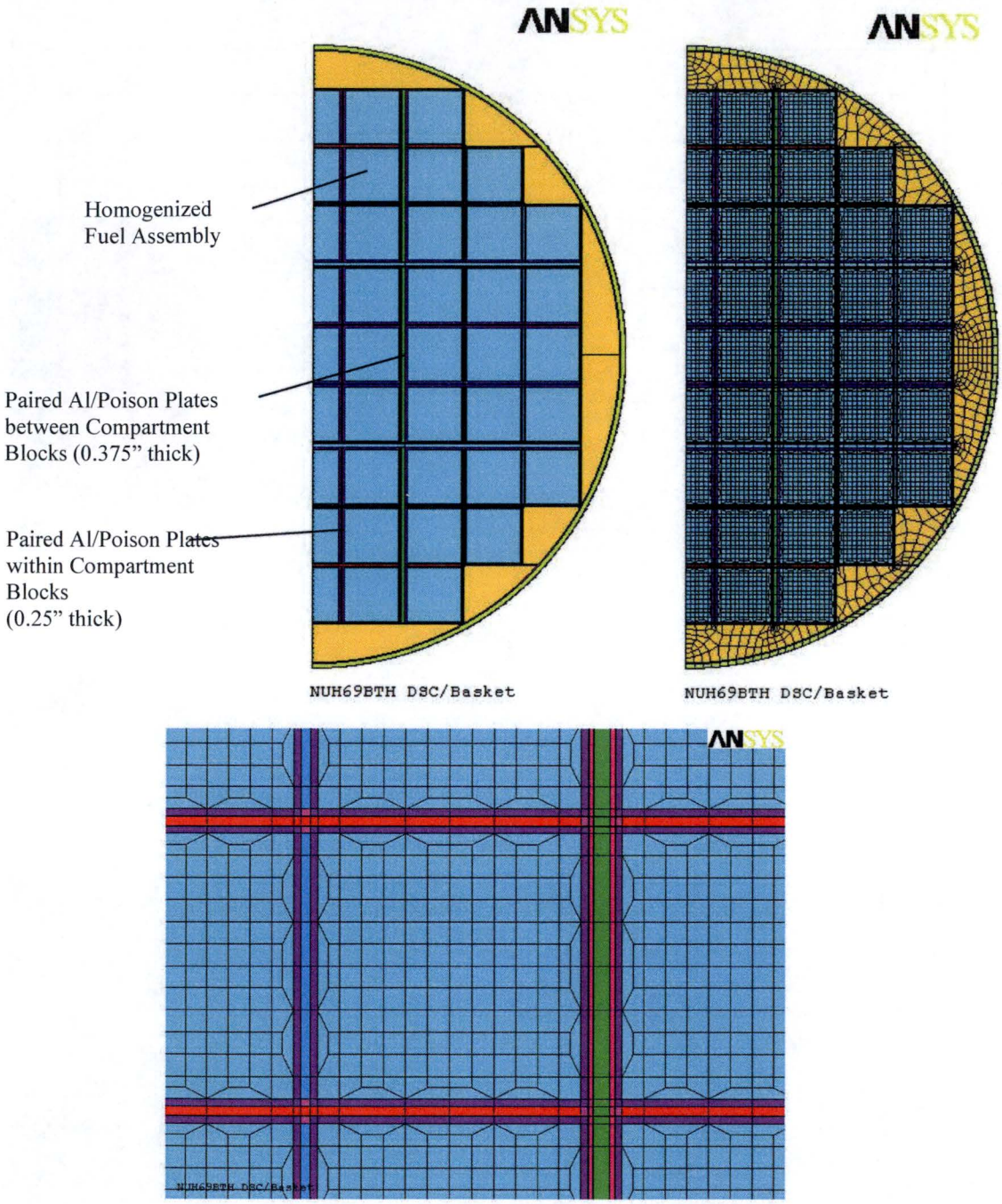

Mesh Density

Figure A.3-14
69BTH DSC/Basket – Cross Section

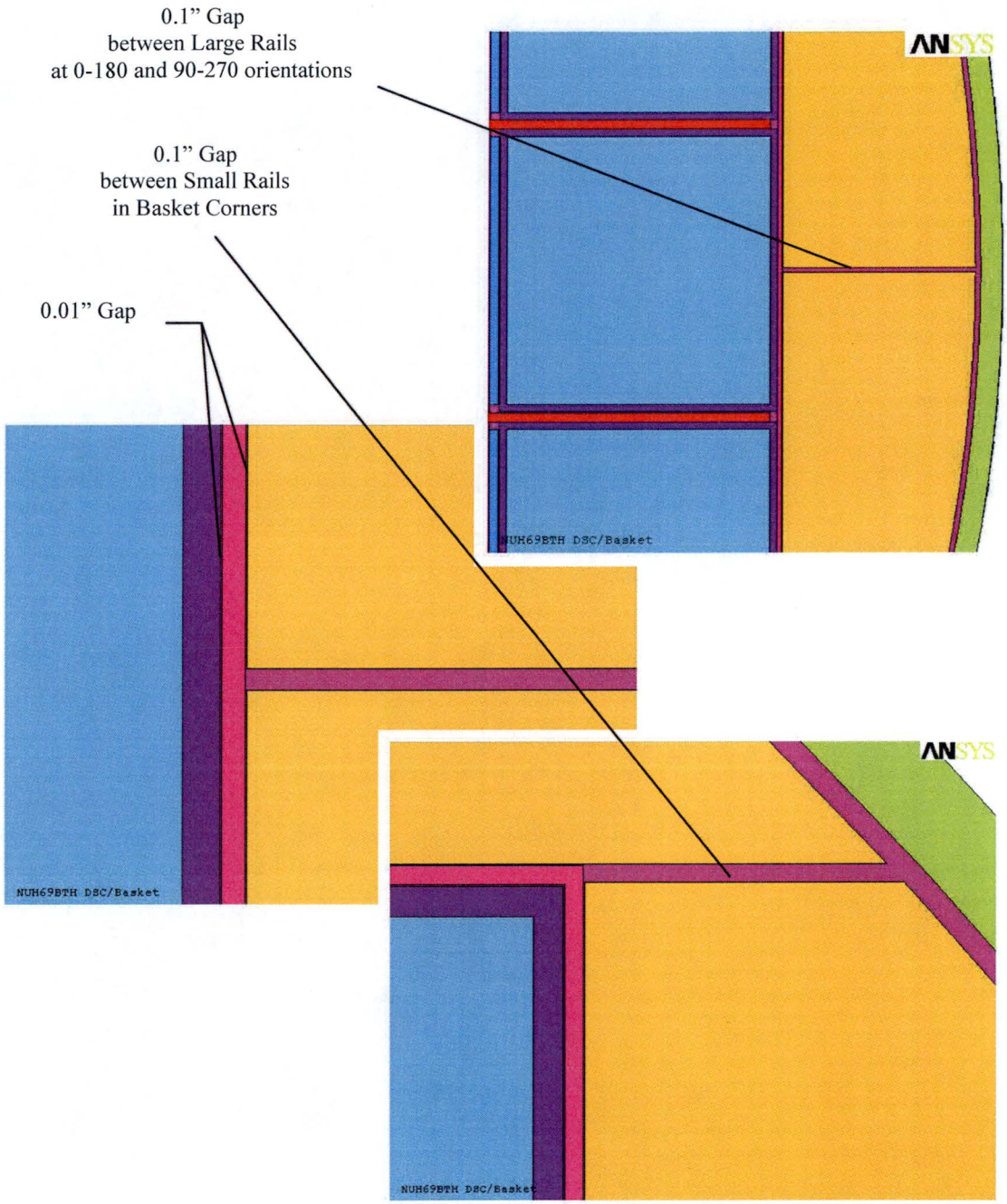

Figure A.3-15
69BTH DSC/Basket – Gaps between Rail Sections at Cross Section

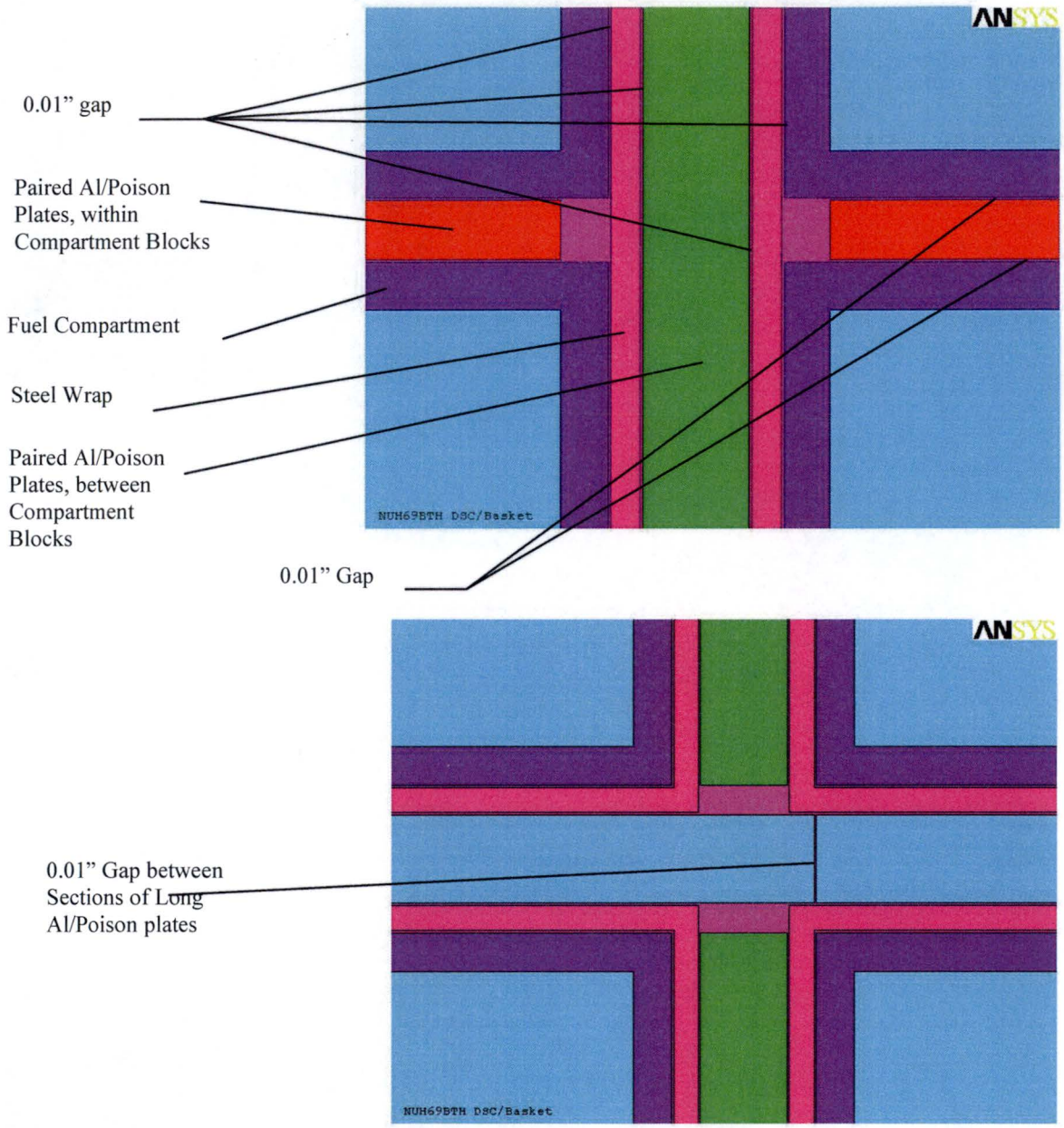

Figure A.3-16
69BTH DSC/Basket – Gaps between Basket Plates at Cross Section

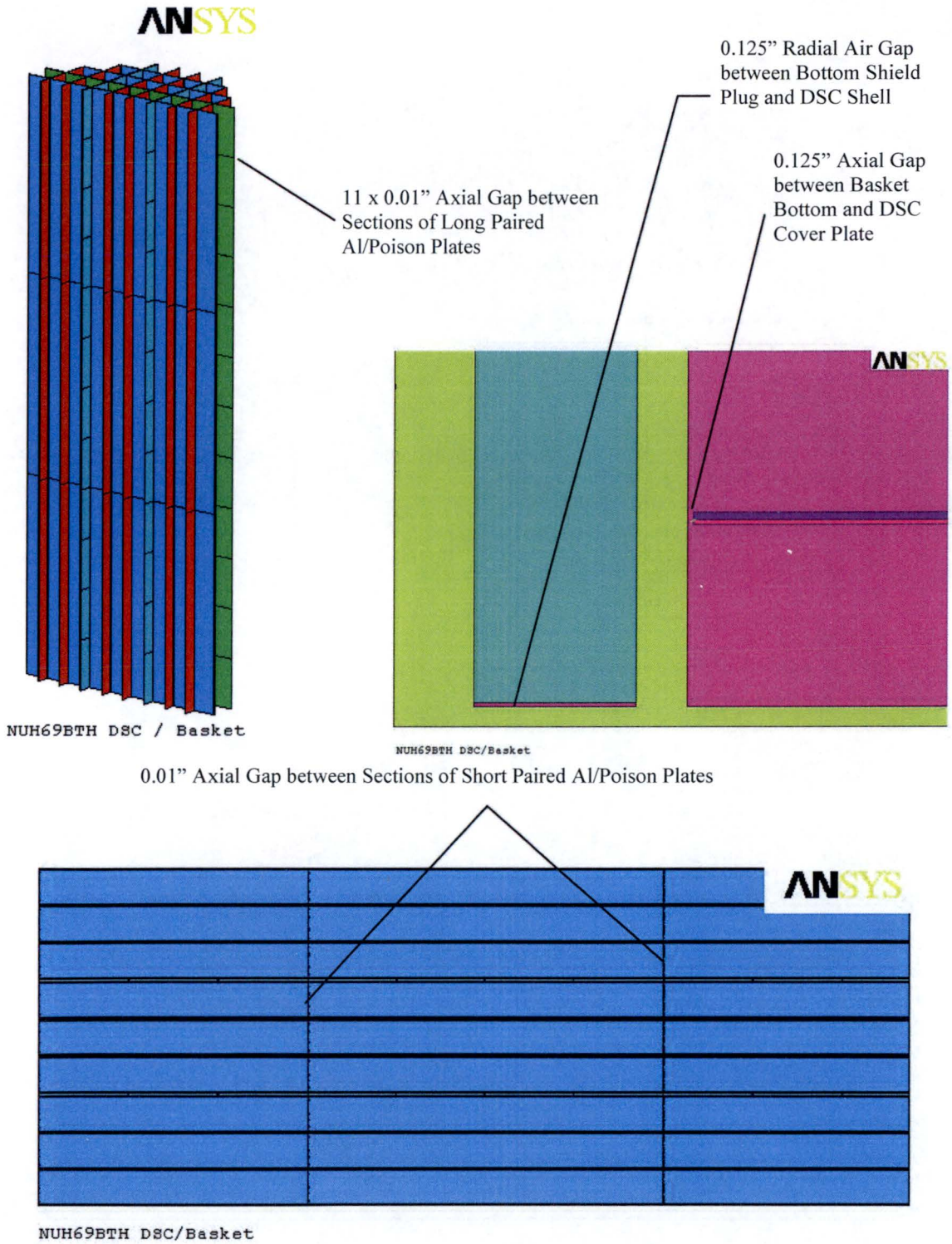

Figure A.3-17
69BTH DSC/Basket – Axial Gaps

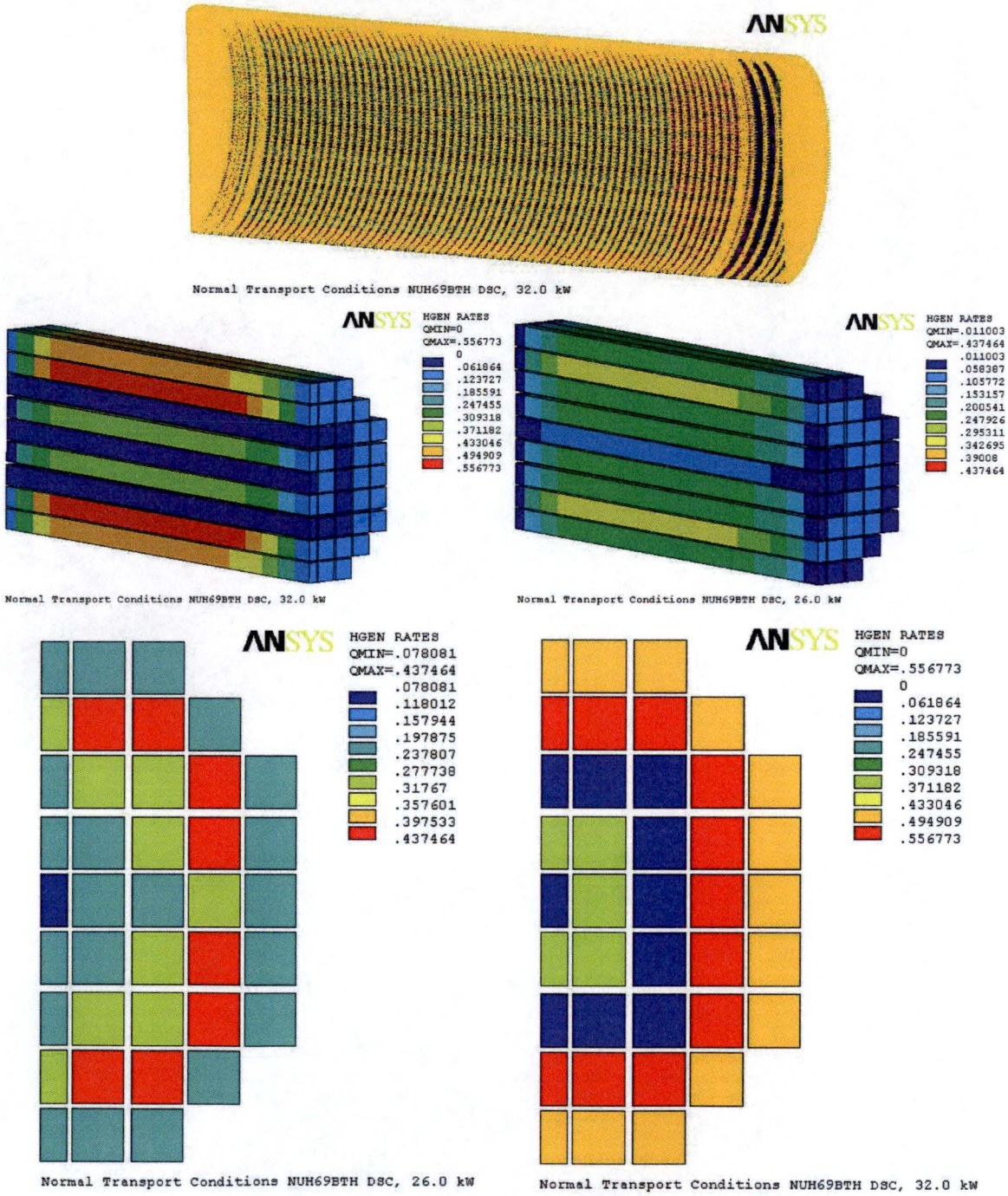

Figure A.3-18
Typical Boundary Conditions for the 69BTH Basket

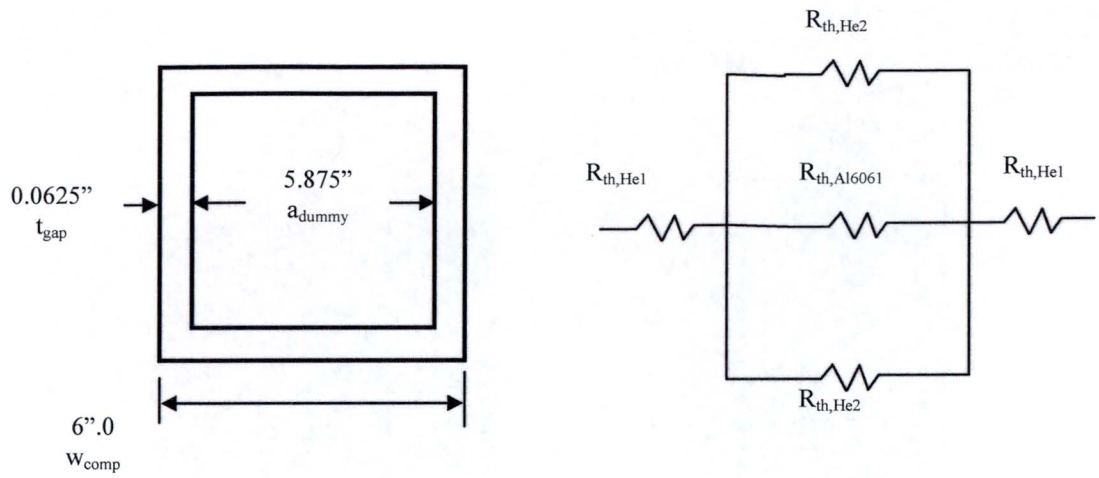

Figure A.3-19
Thermal Resistances for Aluminum Dummy Assembly

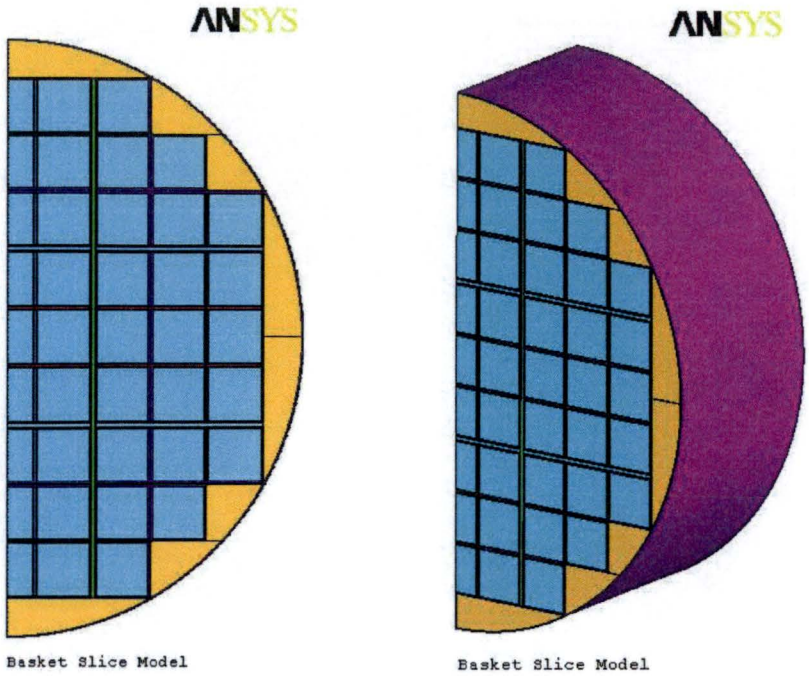

For 69BTH DSC

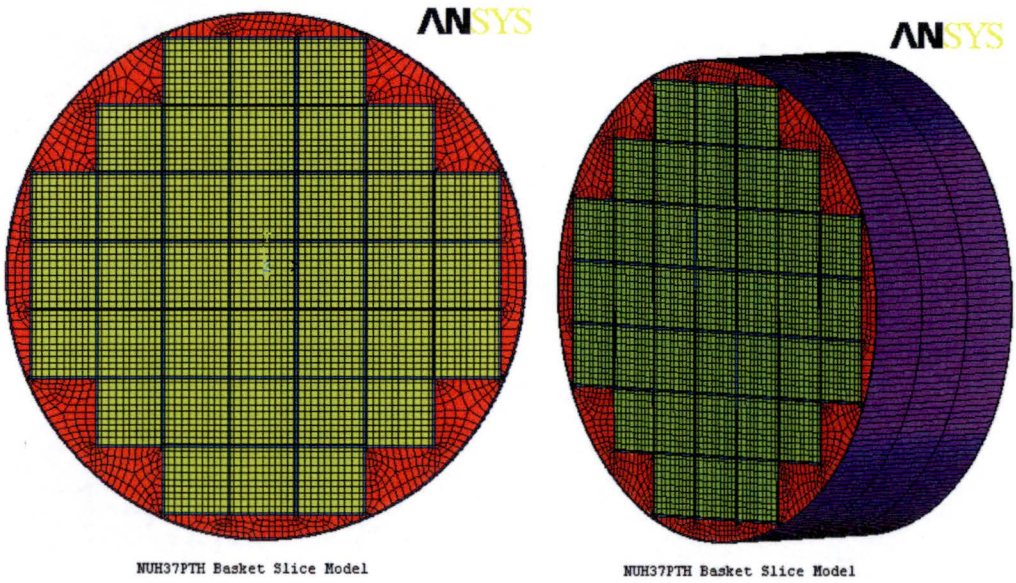

For 37PTH DSC

Figure A.3-20
Basket Slice Models

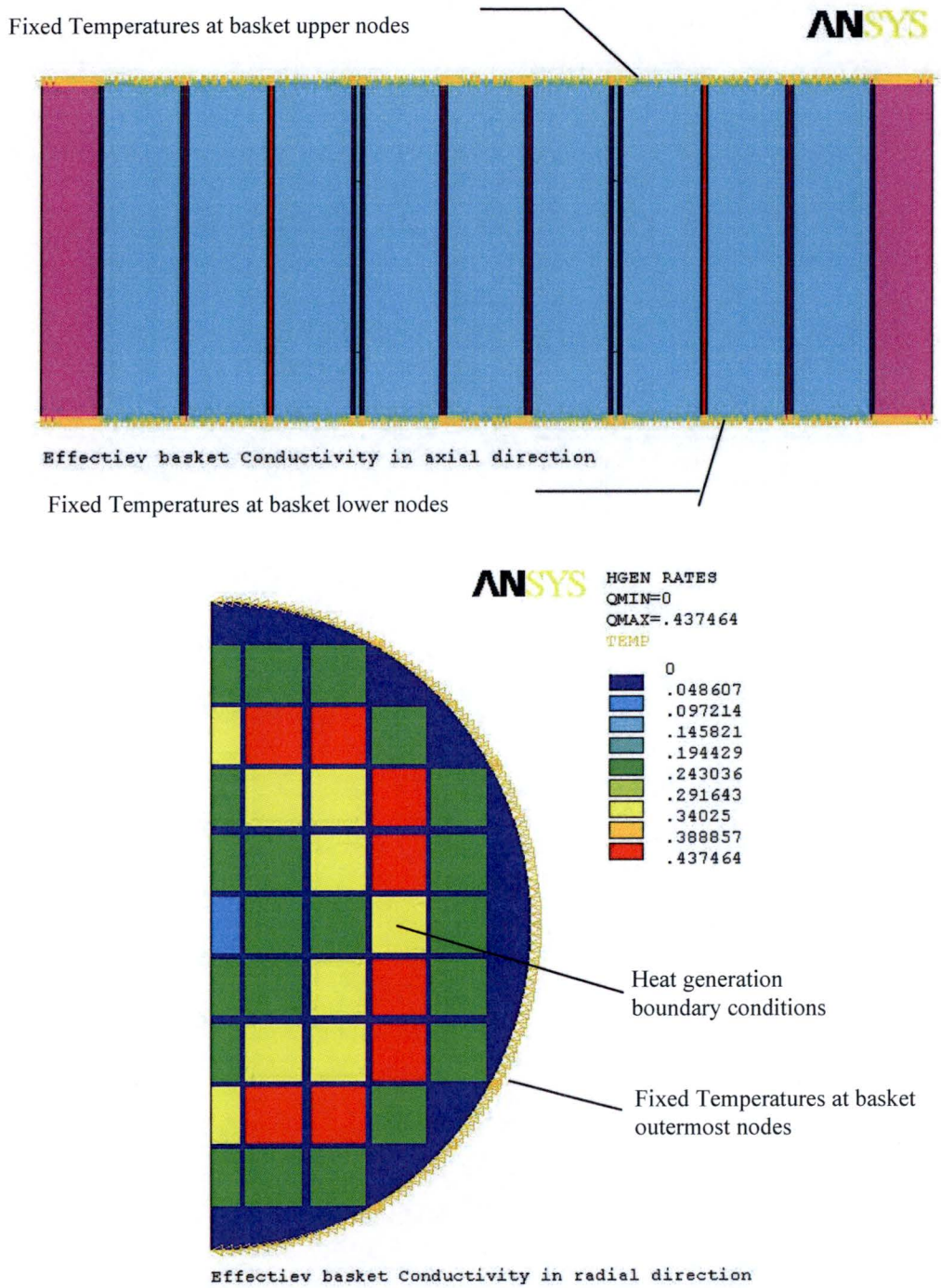

Figure A.3-21
Typical Boundary Conditions for the Basket Slice Model

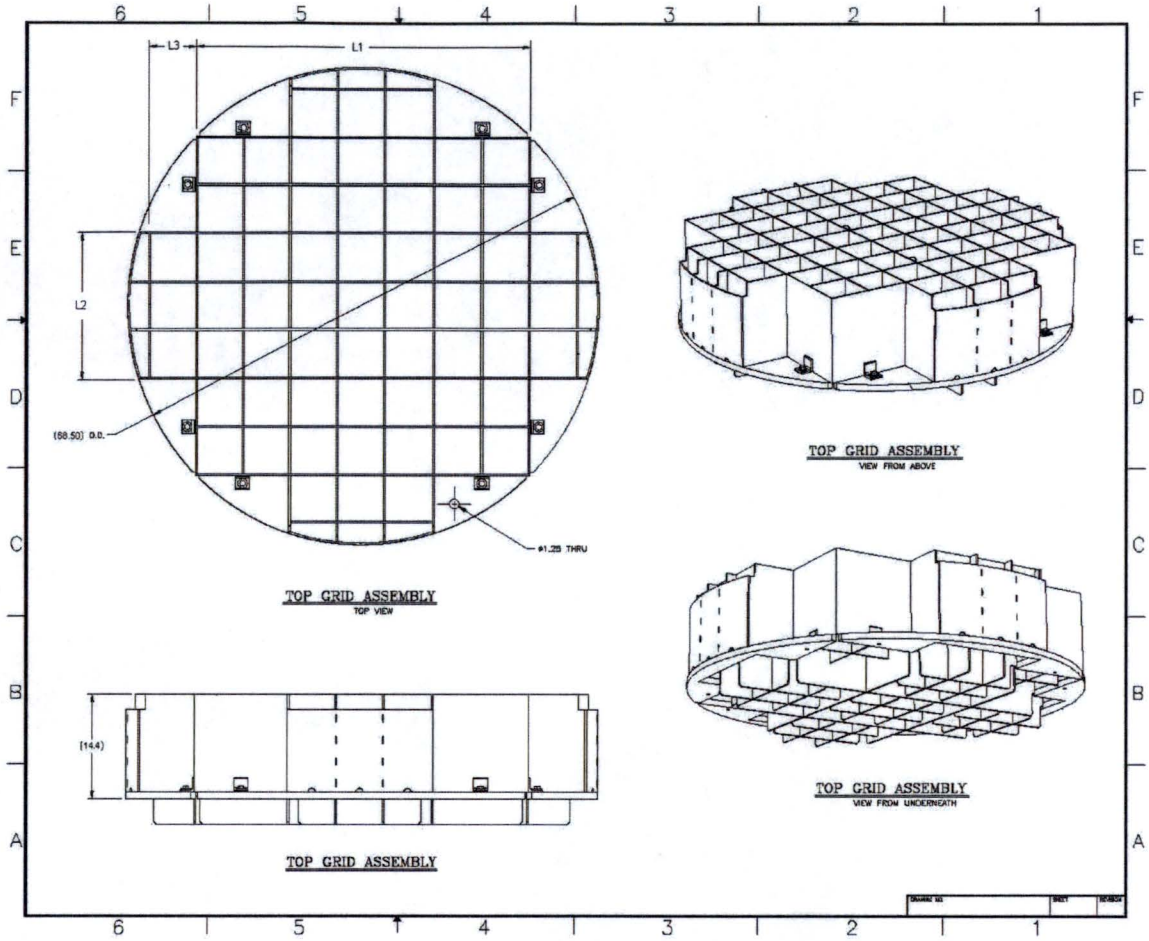

Figure A.3-22
Schematic View of Top Grid Assembly (Hold-Down Ring)

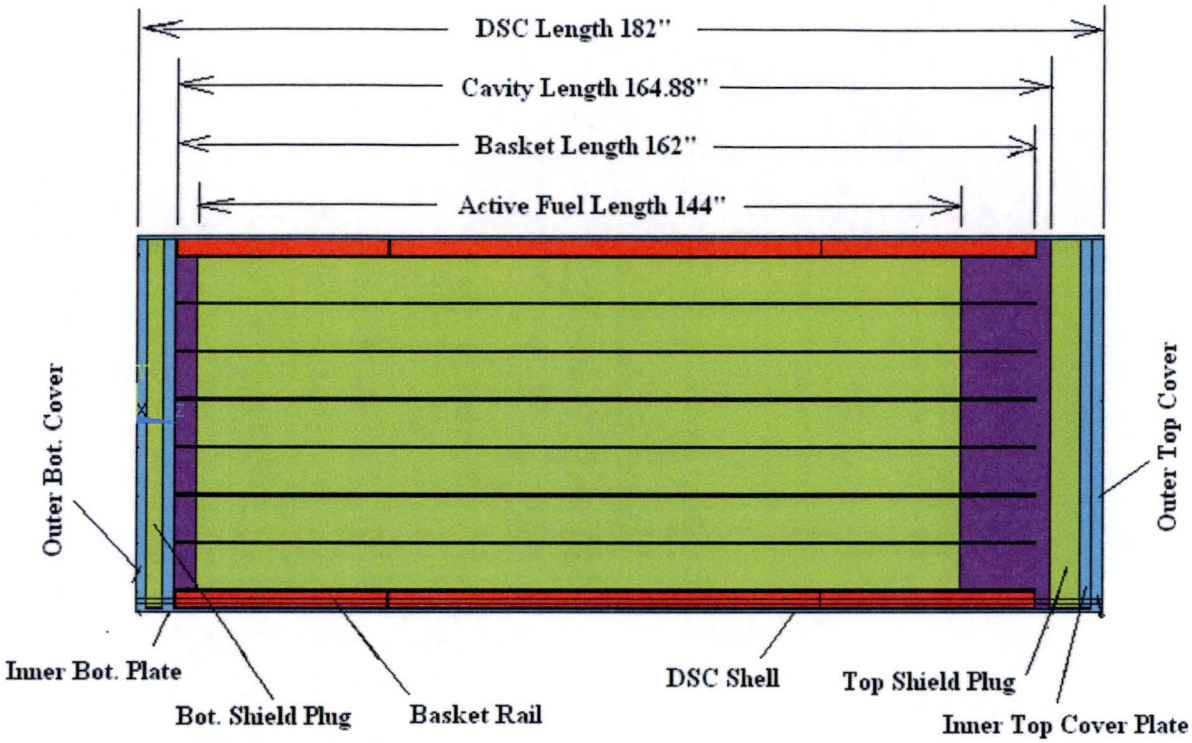

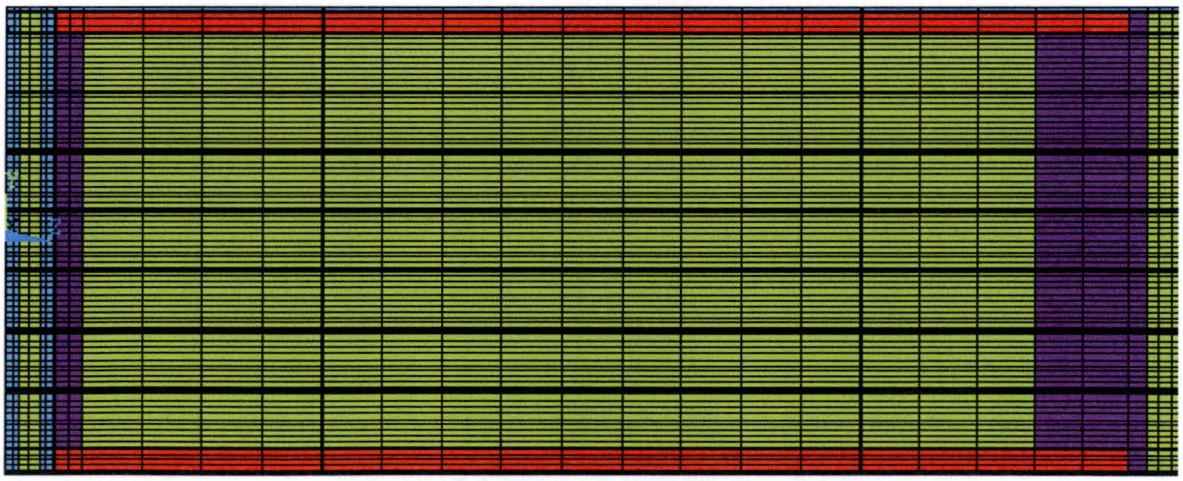

NUH37PTH DSC/Basket

Mesh Density

Figure A.3-23
Finite Element Model of the 37PTH DSC/Basket

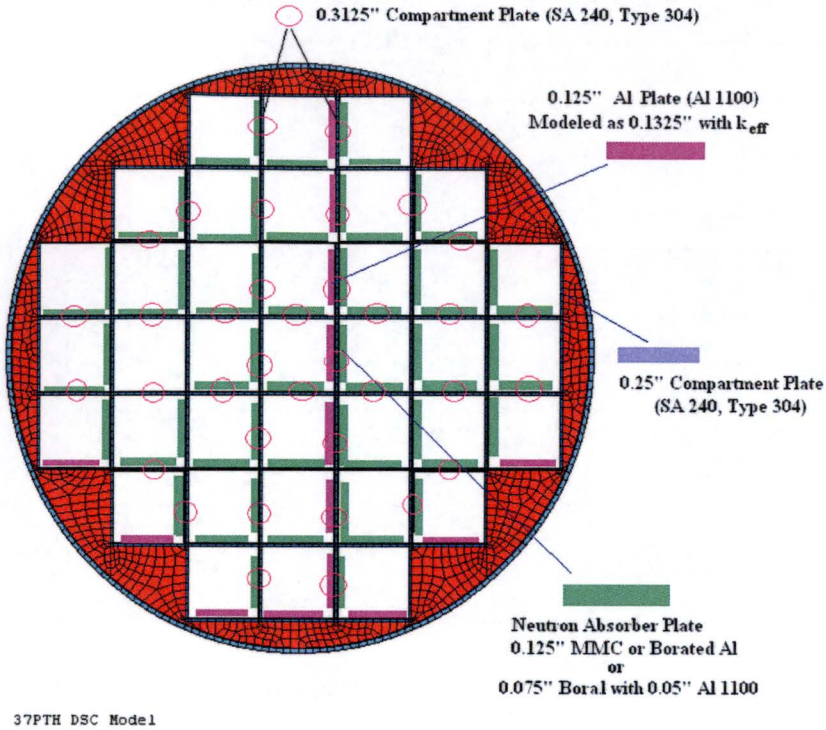

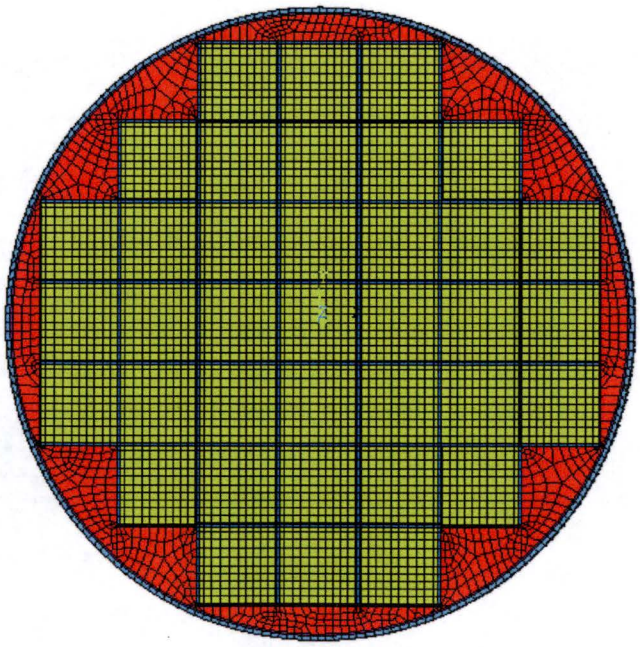

Mesh Density

Figure A.3-24
37PTH DSC/Basket – Cross Section and Details

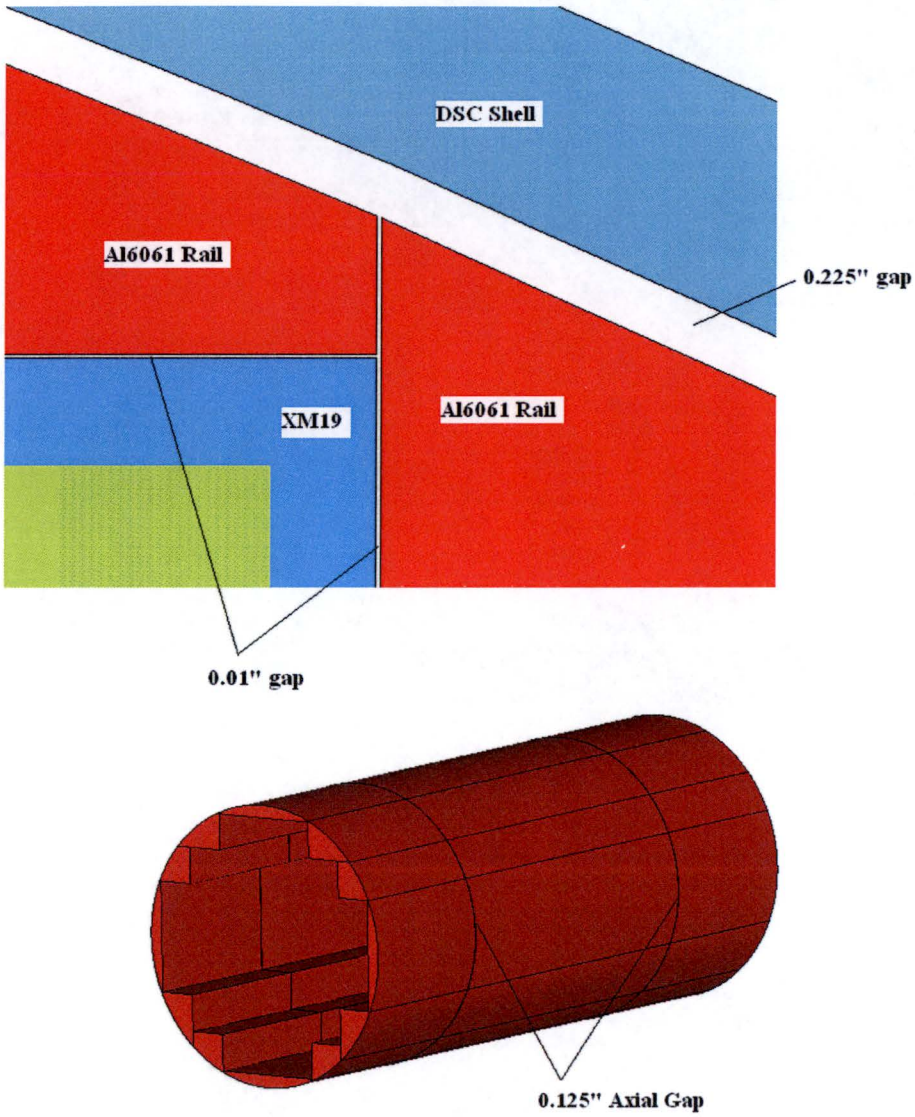

Figure A.3-25
37PTH DSC/Basket – Gaps between Rail Sections

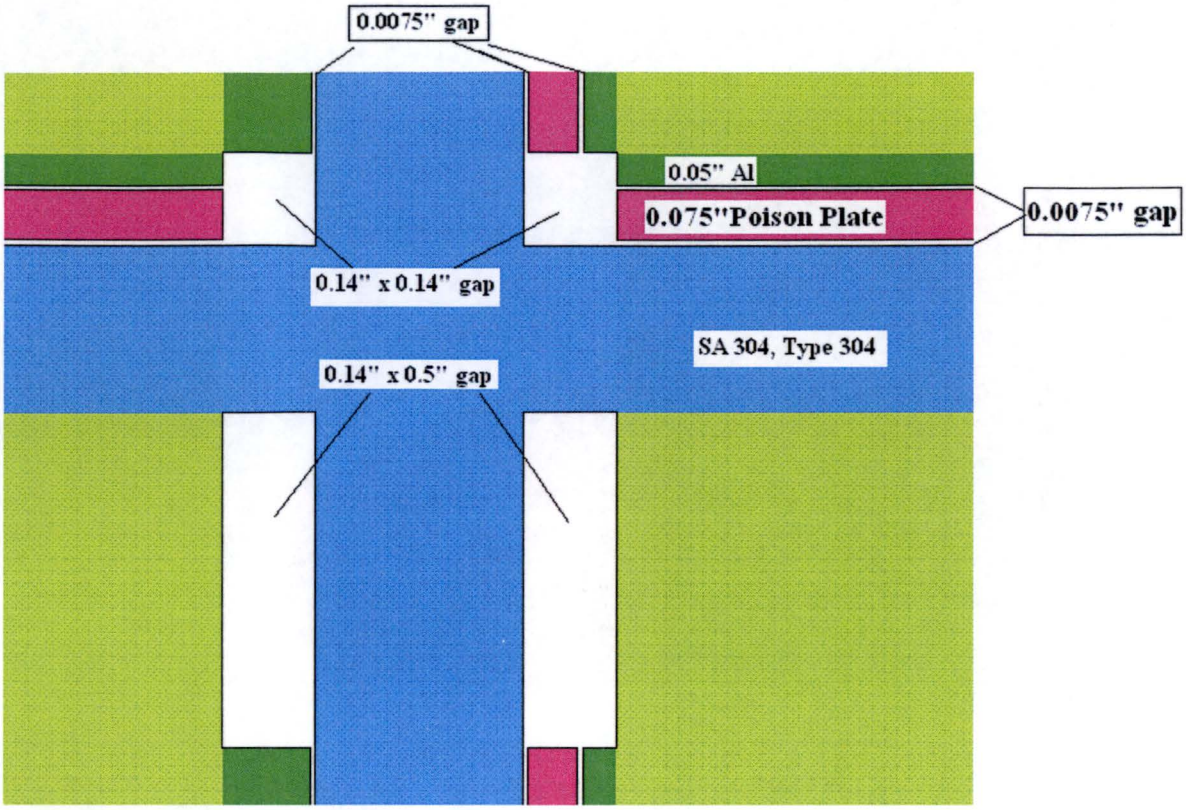

Figure A.3-26
37PTH DSC/Basket – Gaps between Basket Plates at Cross Section

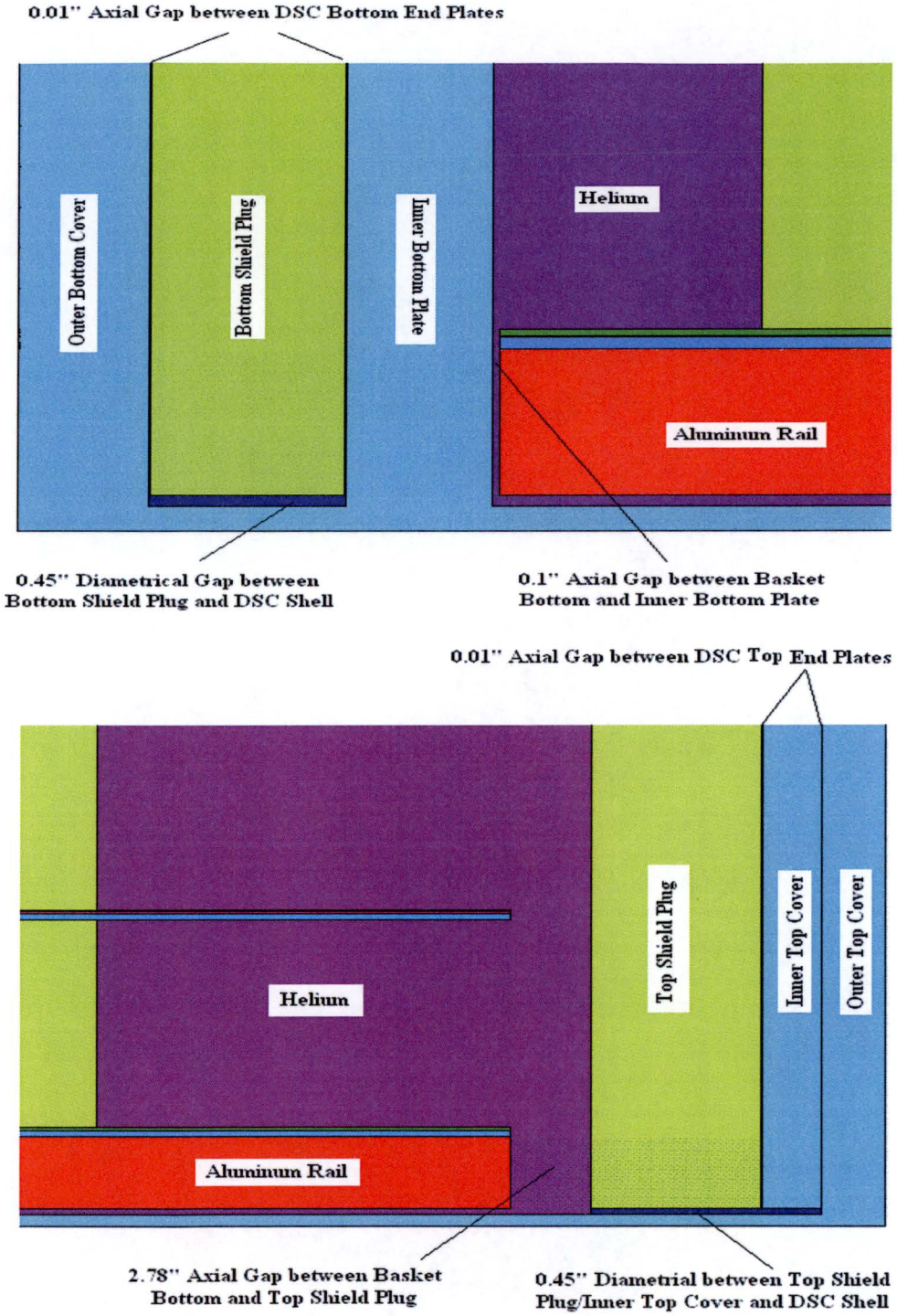

Figure A.3-27
37PTH DSC/Basket – Axial Gaps

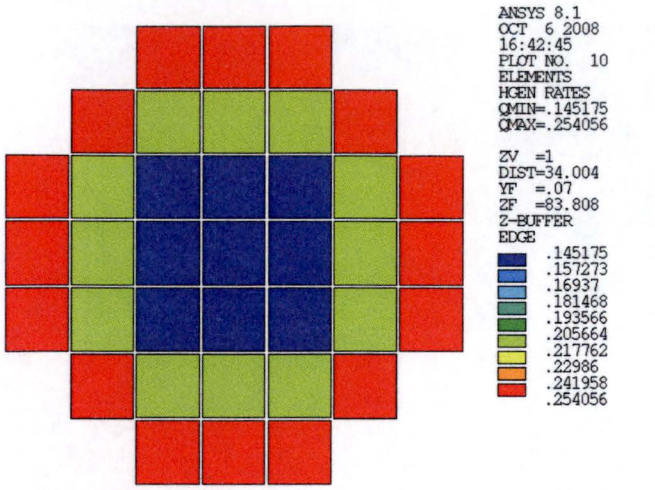

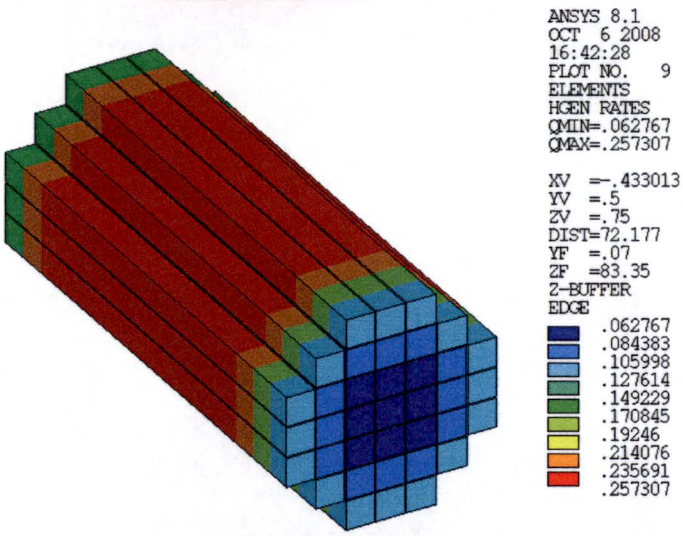

Heat Generation Boundary Conditions, 37PTH DSC, 22.0 kW

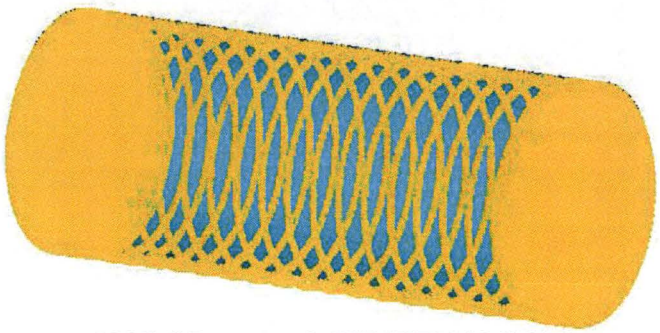

DSC Shell Temperatures for NCT, 37PTH DSC, 22.0 kW

Figure A.3-28
Typical Boundary Conditions for the 37PTH Basket

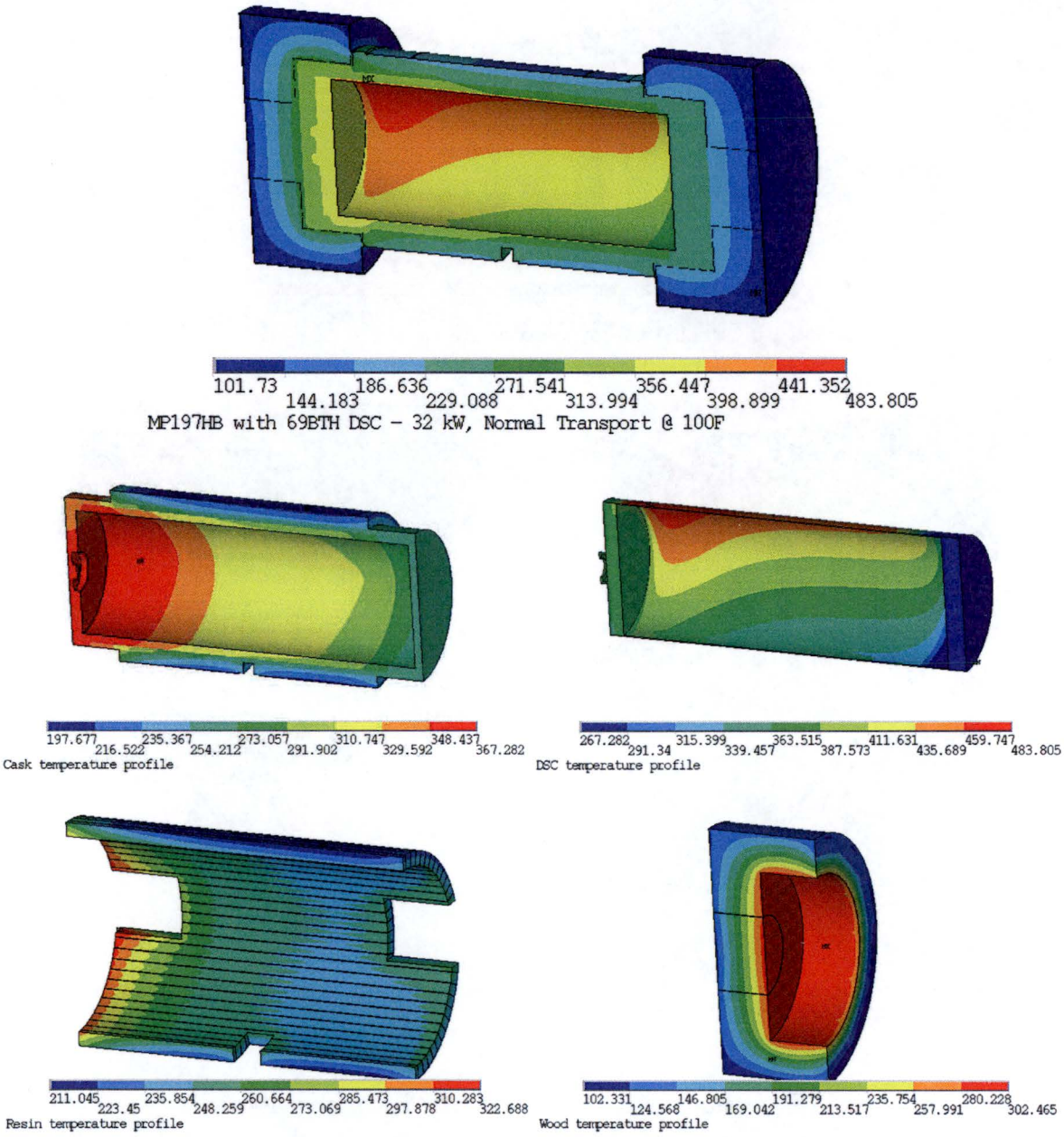

Figure A.3-29
Temperature Profiles for MP197HB Transport Cask
NCT, 100°F, Insolation, 69BTH DSC, 32 kW

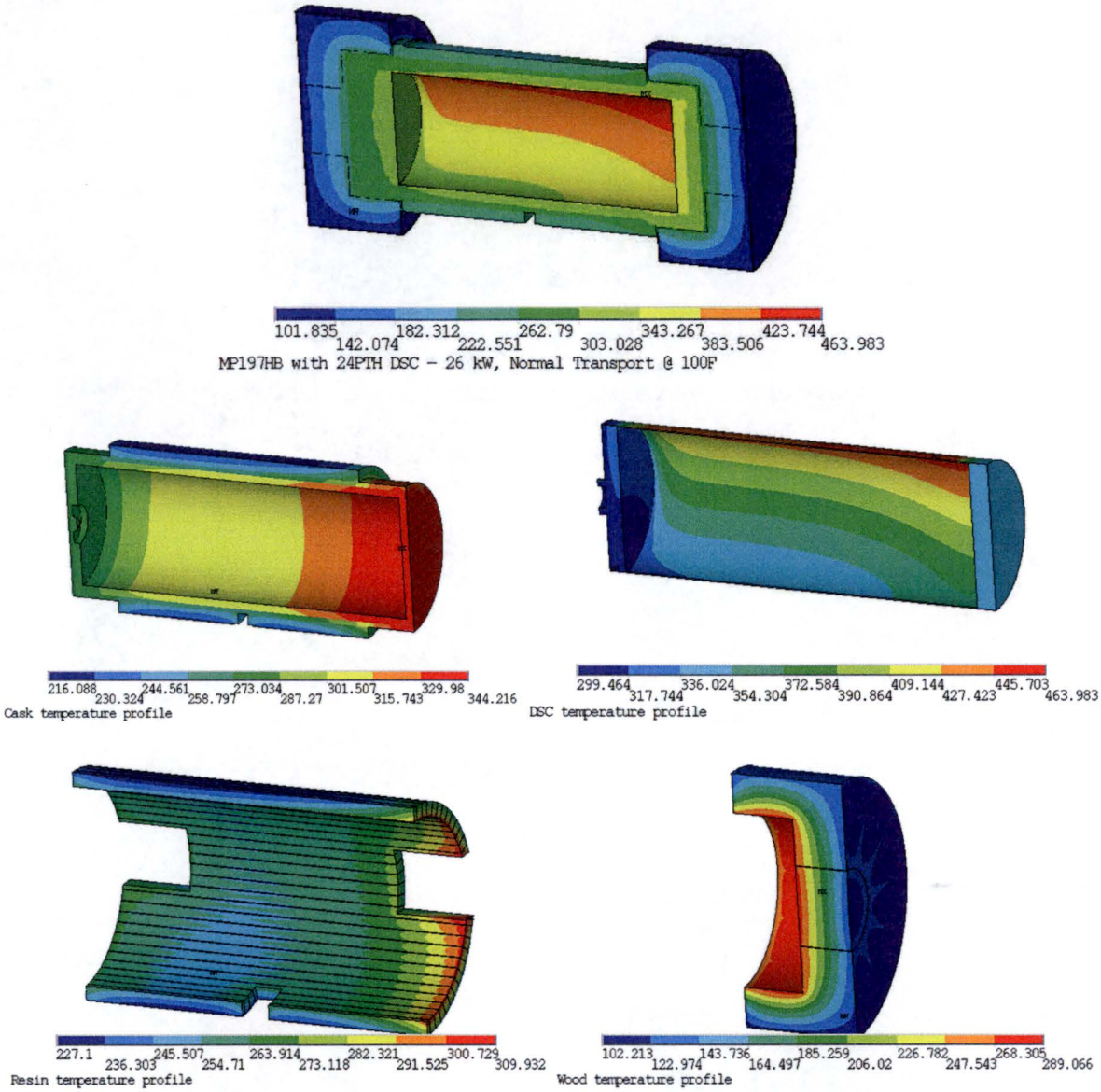

Figure A.3-30
Temperature Profiles for MP197HB Transport Cask
NCT, 100°F, Insolation, 24PTH DSC, 26 kW

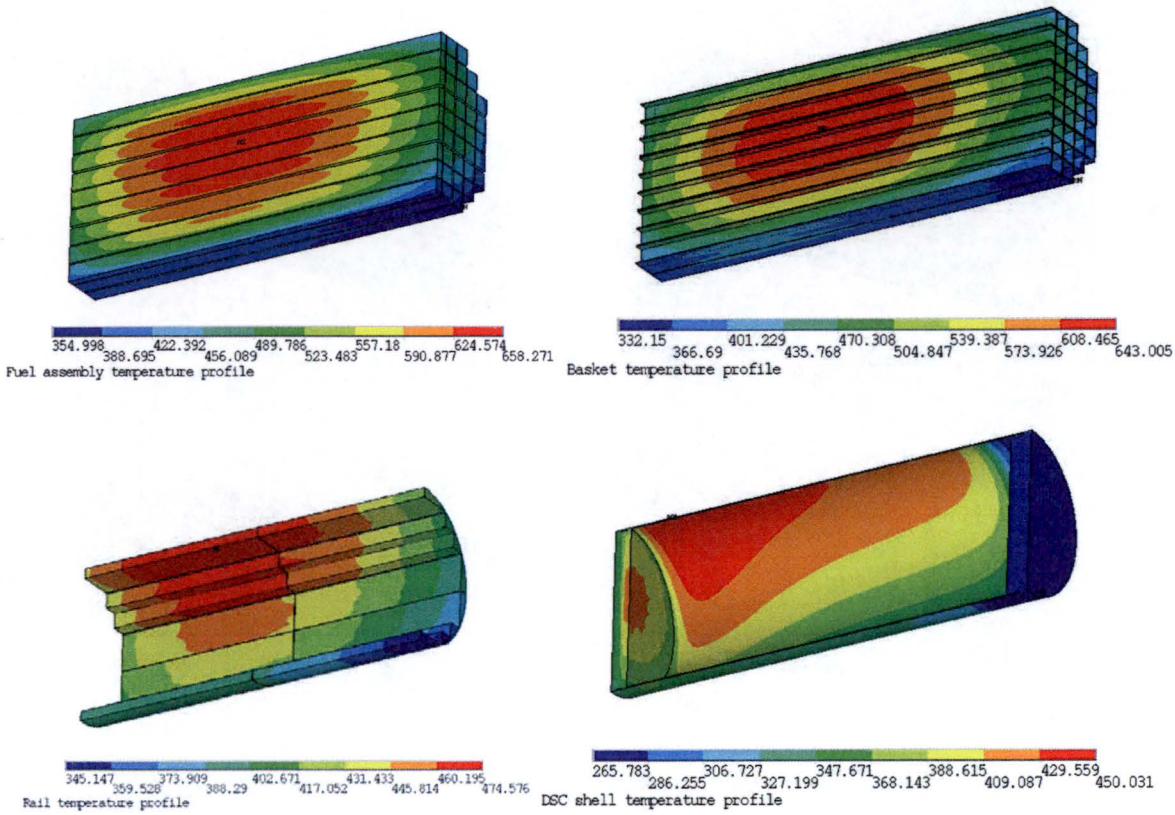

Figure A.3-31
Typical Temperature Distributions for 69BTH Basket
(NCT @ 100°F, HLZC#1, 26kW)

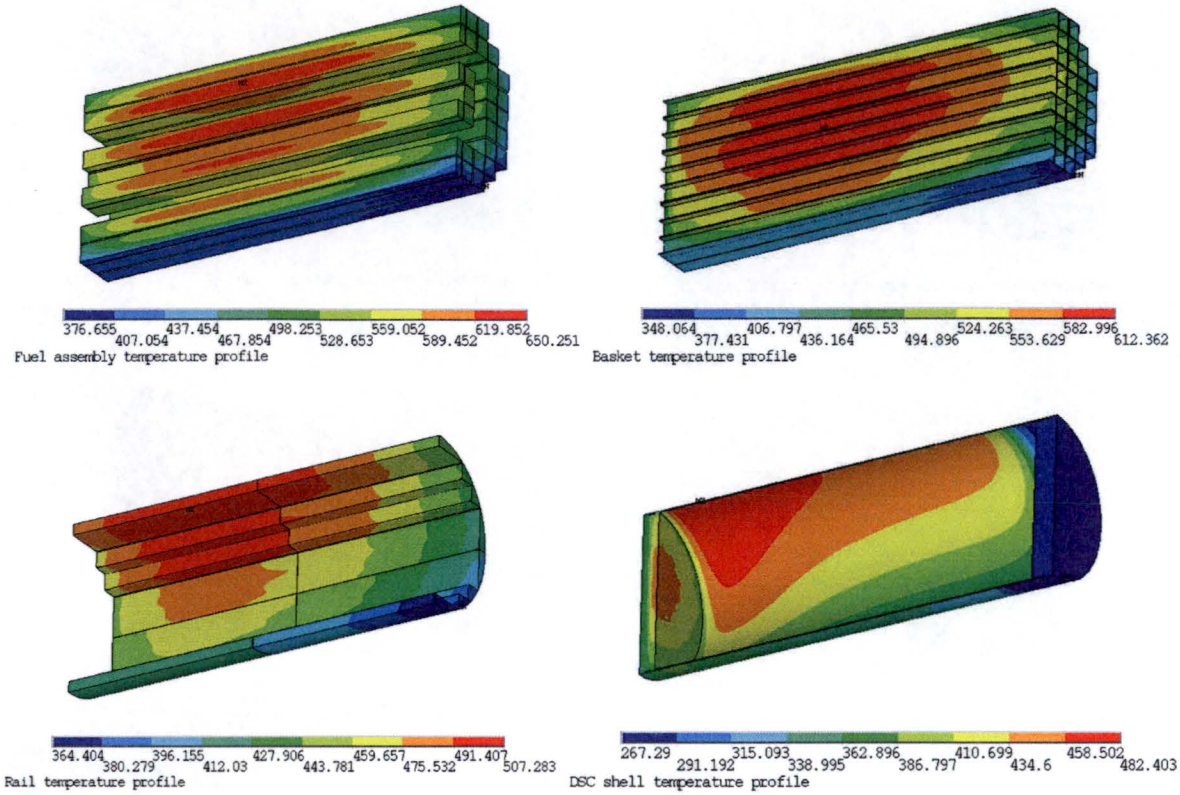

Figure A.3-32
Typical Temperature Distributions for 69BTH Basket
(NCT @ 100°F, HLZC#4, 32kW)

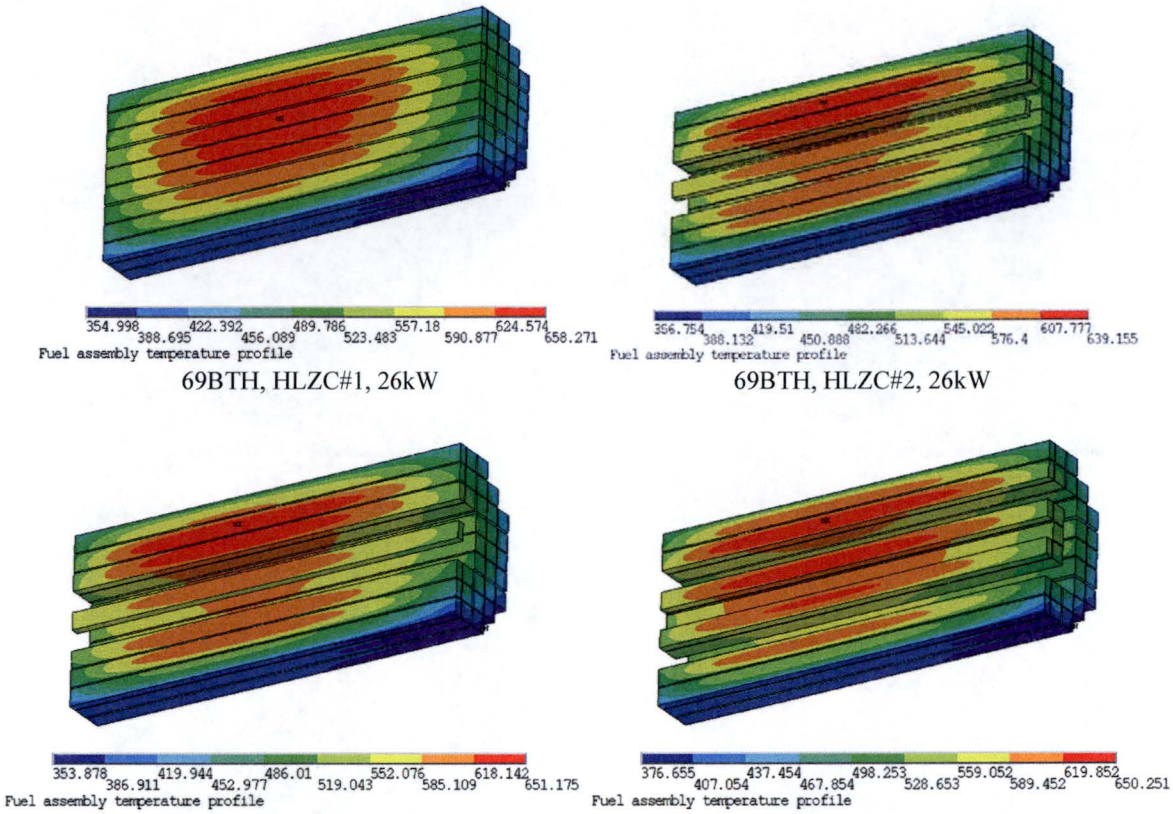

69BTH, HLZC#1, 26kW

69BTH, HLZC#2, 26kW

69BTH, HLZC#3, 29.2kW

69BTH, HLZC#4, 32kW

Figure A.3-33
Temperature Distributions for Fuel Assemblies in 69BTH Basket
(NCT @ 100°F)

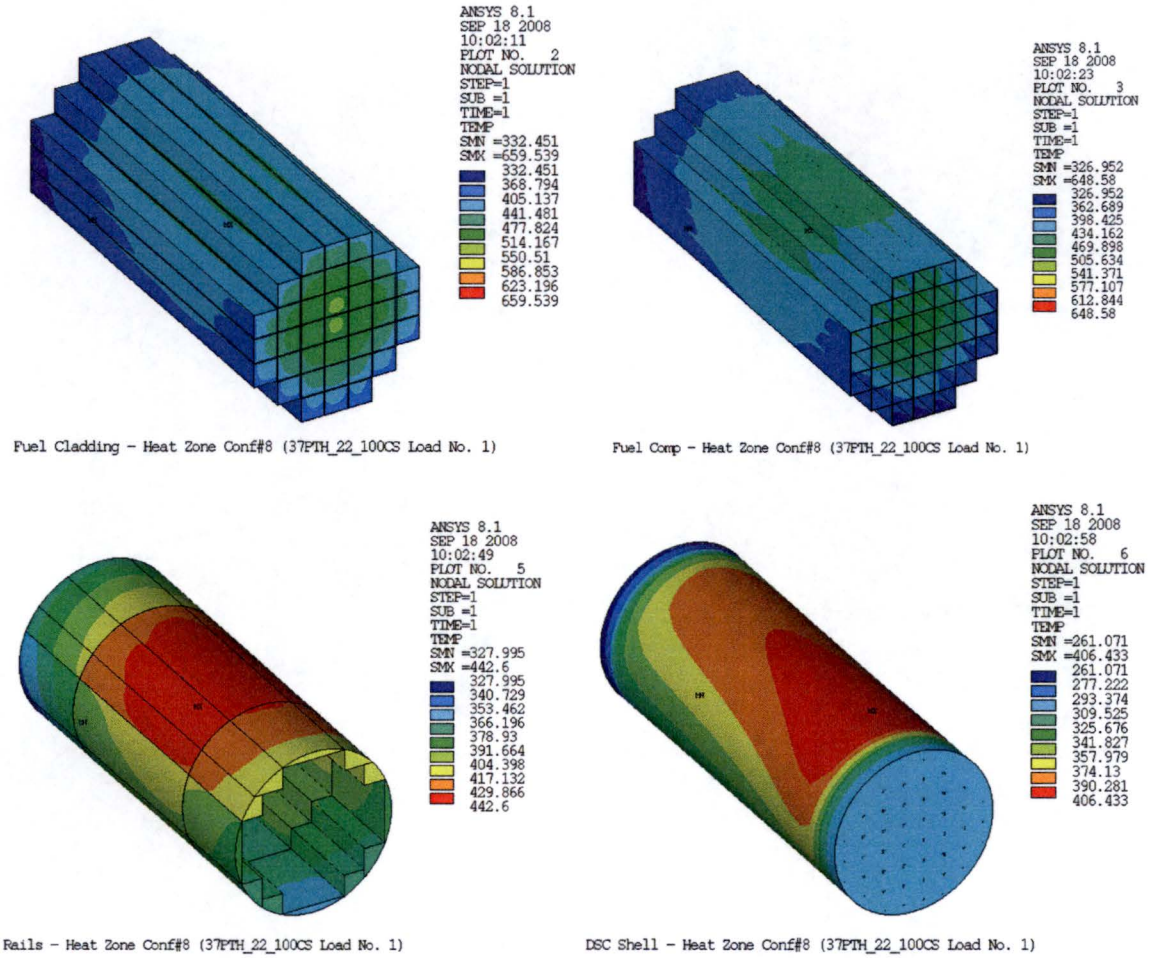

Figure A.3-34
Typical Temperature Distributions for 37PTH Basket
(NCT @ 100°F, 22 kW)

The shortest distance between TC and crushed impact limiter for end drop is 20.3".

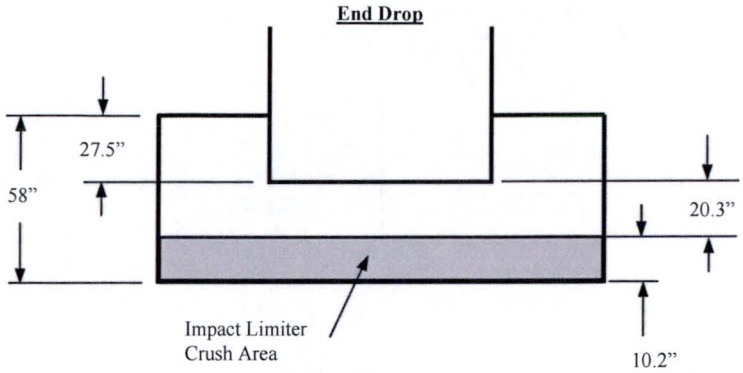

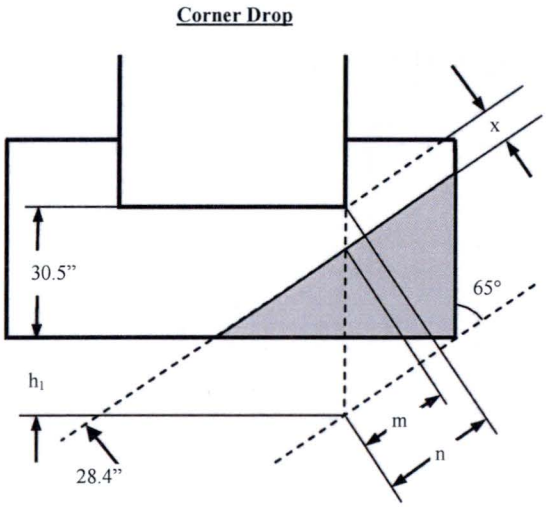

OD_{IL} = Impact limiter OD = 126"

OD_{TC} = Cask OD = 84.5"

$h_1 = [(OD_{IL}-OD_{TC}) / 2] / \tan 65 = 9.7$"

$n = (30.5 + h_1) \cos 65 = 17.0$"

$m = 28.4 / \tan 65 = 13.2$"

The shortest distance between TC and crushed impact limiter for corner drop is:

$x = (n - m) \tan 65 = 8.0$"

Figure A.3-35
Impact Limiter Crush Areas for MP197HB
(Side, End, and Corner Drop)

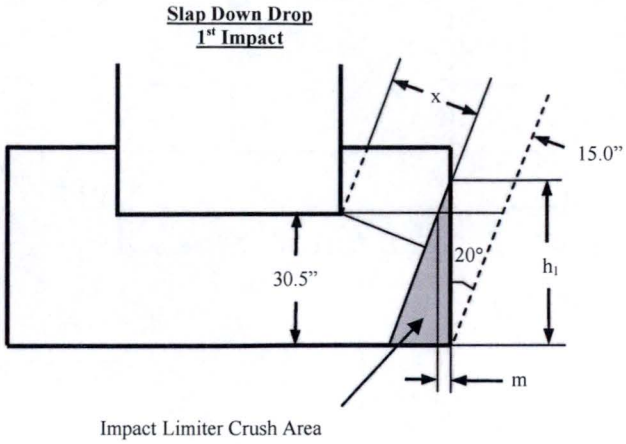

OD_{IL} = Impact limiter OD = 126"

OD_{TC} = Cask OD = 84.5"

$h_1 = 15 / \sin 20 = 43.9$"

$m = (h_1 - 30.5) \tan 20 = 4.9$"

The shortest distance between TC and crushed impact limiter for slap down drop, 1st impact is:

$x = [(OD_{IL} - OD_{TC}) /2 - m] \cos 20 = 14.9$"

The shortest distance between TC and crushed impact limiter for slap down drop, 2nd impact is 9.45"

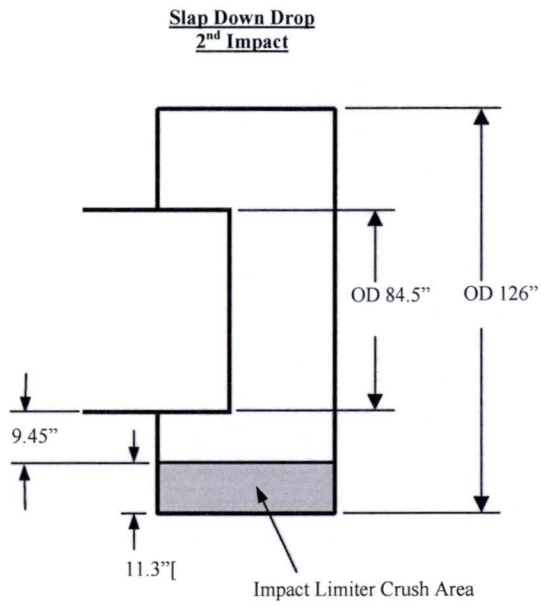

Figure A.3-36
Impact Limiter Crush Areas for MP197HB
(Slap Down)

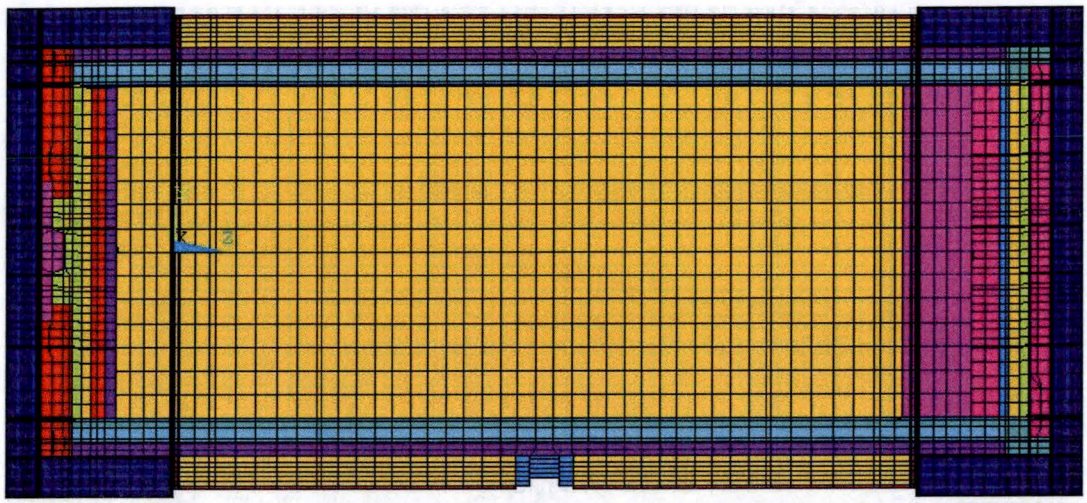

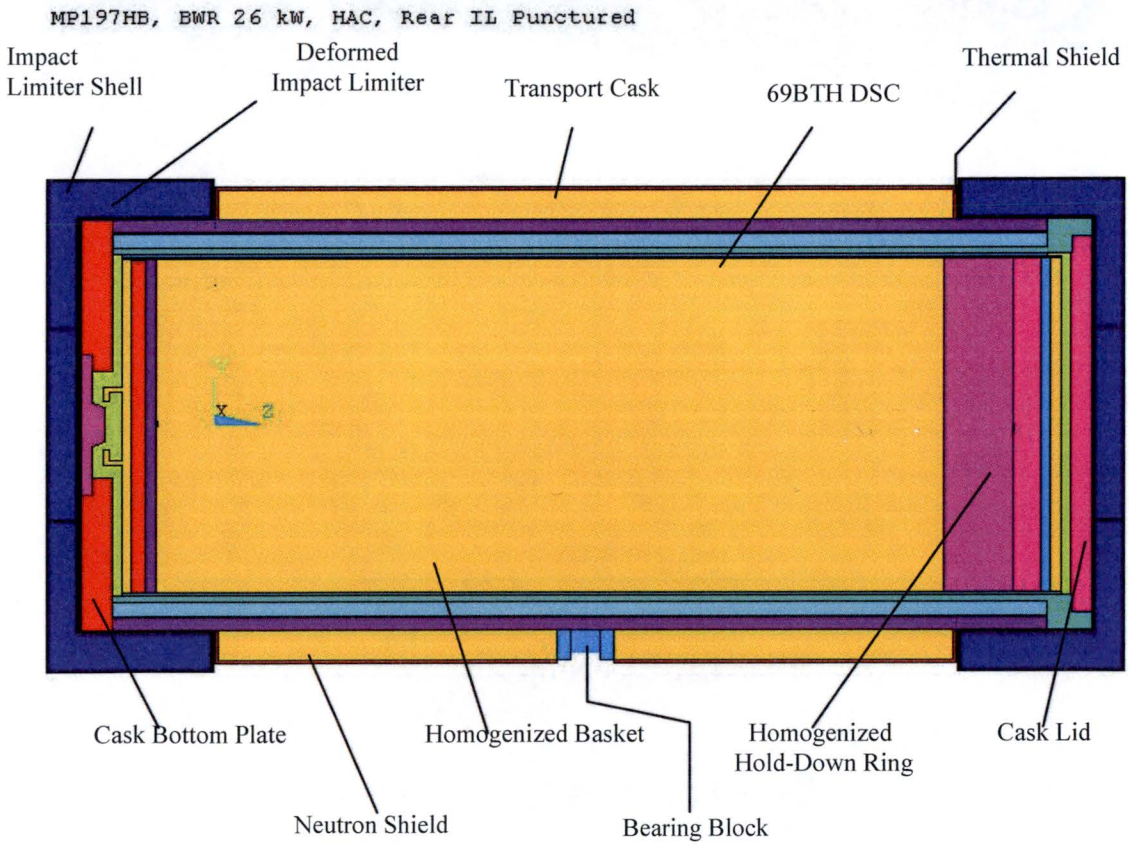

Figure A.3-37
Finite Element Model of TC with Deformed Impact Limiters

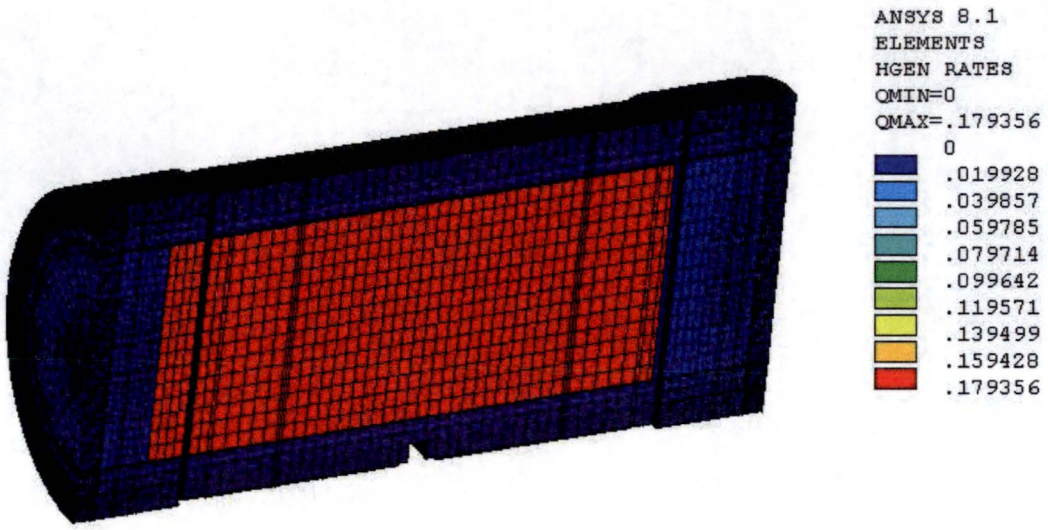

Heat Generation Boundary Conditions for MP197HB + 69BTH DSC, 32 kW, HAC

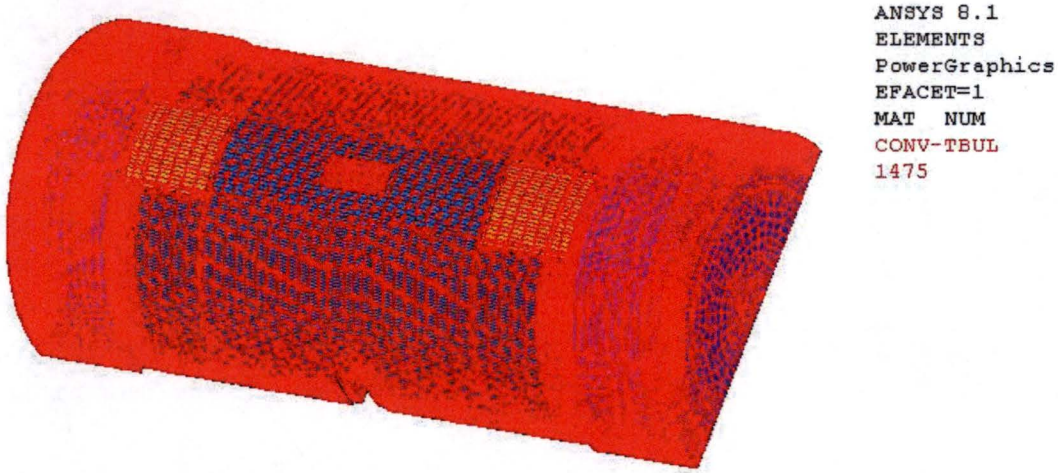

Convection & Radiation from Fire to MP197HB + 69BTH DSC, 32 kW

Figure A.3-38
Typical Boundary Conditions during Fire Conditions

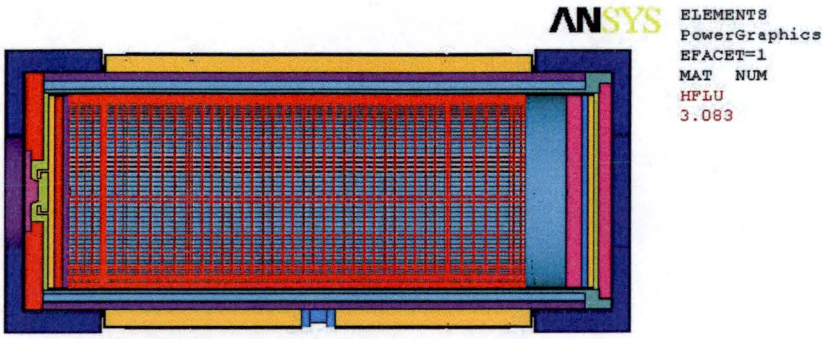

Decay Heat Flux for Cool-Down Conditions

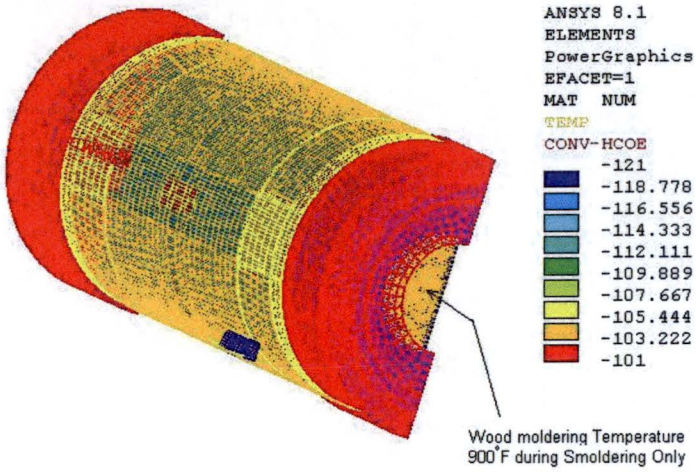

Convection & Radiation to Ambient, MP197HB + 69BTH DSC, 32 kW, Smoldering/Cool-Down

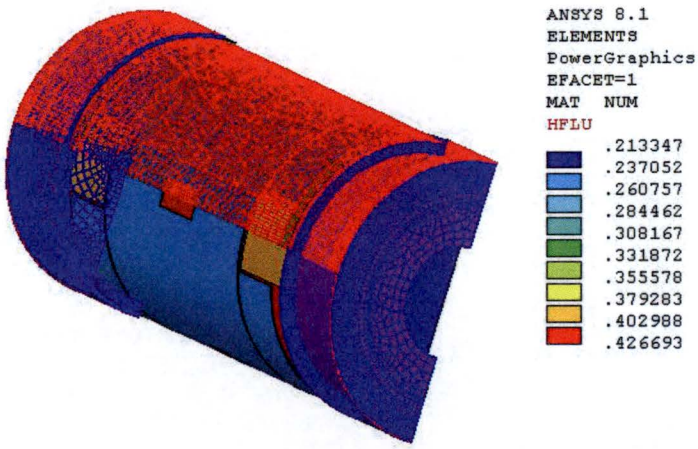

Insolance, MP197HB + 69BTH DSC, 32 kW, Smoldering/Cool-Down

Figure A.3-39
Typical Boundary Conditions for Smoldering/Cool-Down Periods

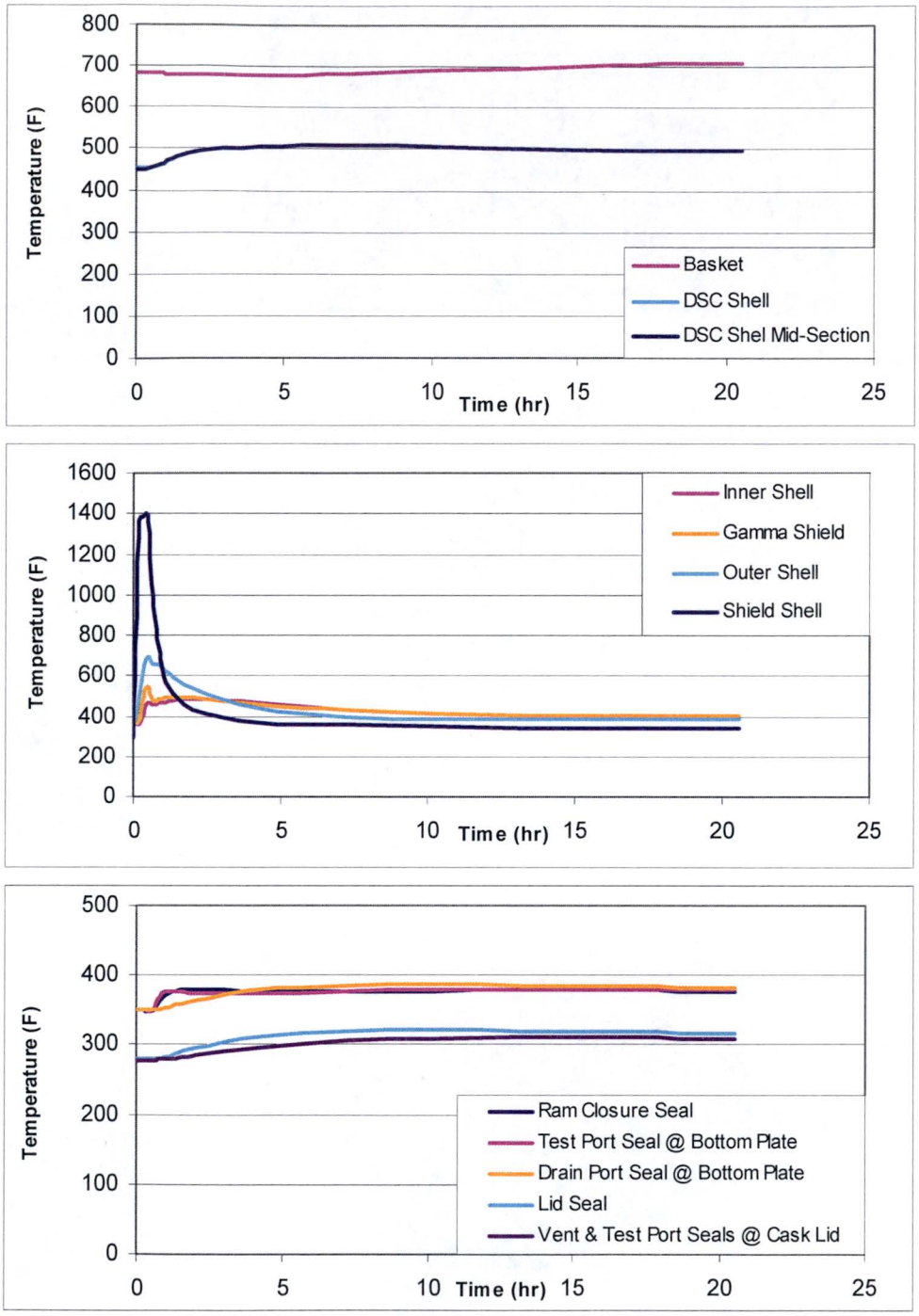

Figure A.3-40
Time-Temperature Histories for TC/DSC Shell
HAC, with External Fins (Melted after Fire), 69BTH DSC, 32 kW

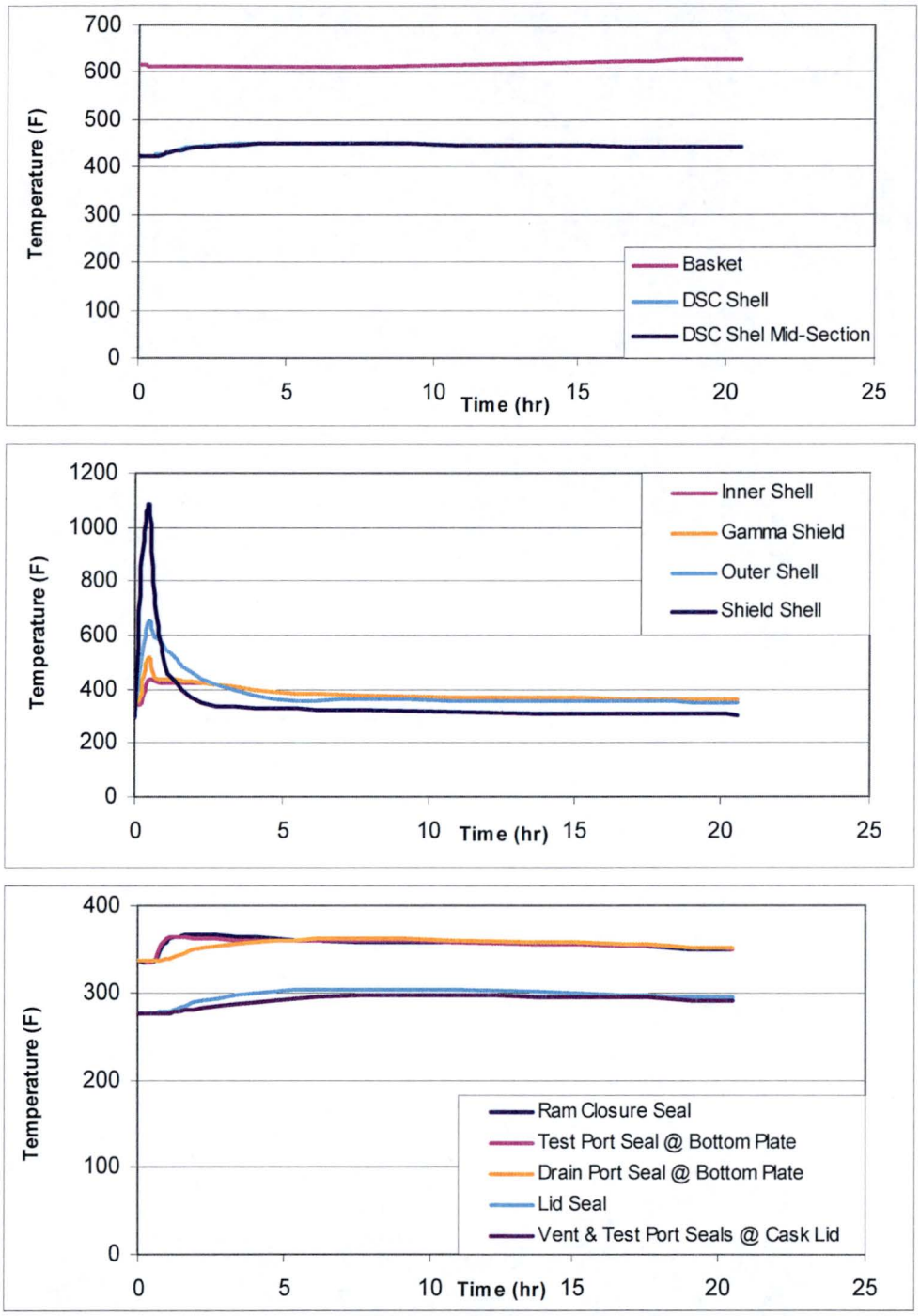

Figure A.3-41
Time-Temperature Histories for TC/DSC Shell
HAC, w/o Fins, 69BTH DSC, 26 kW

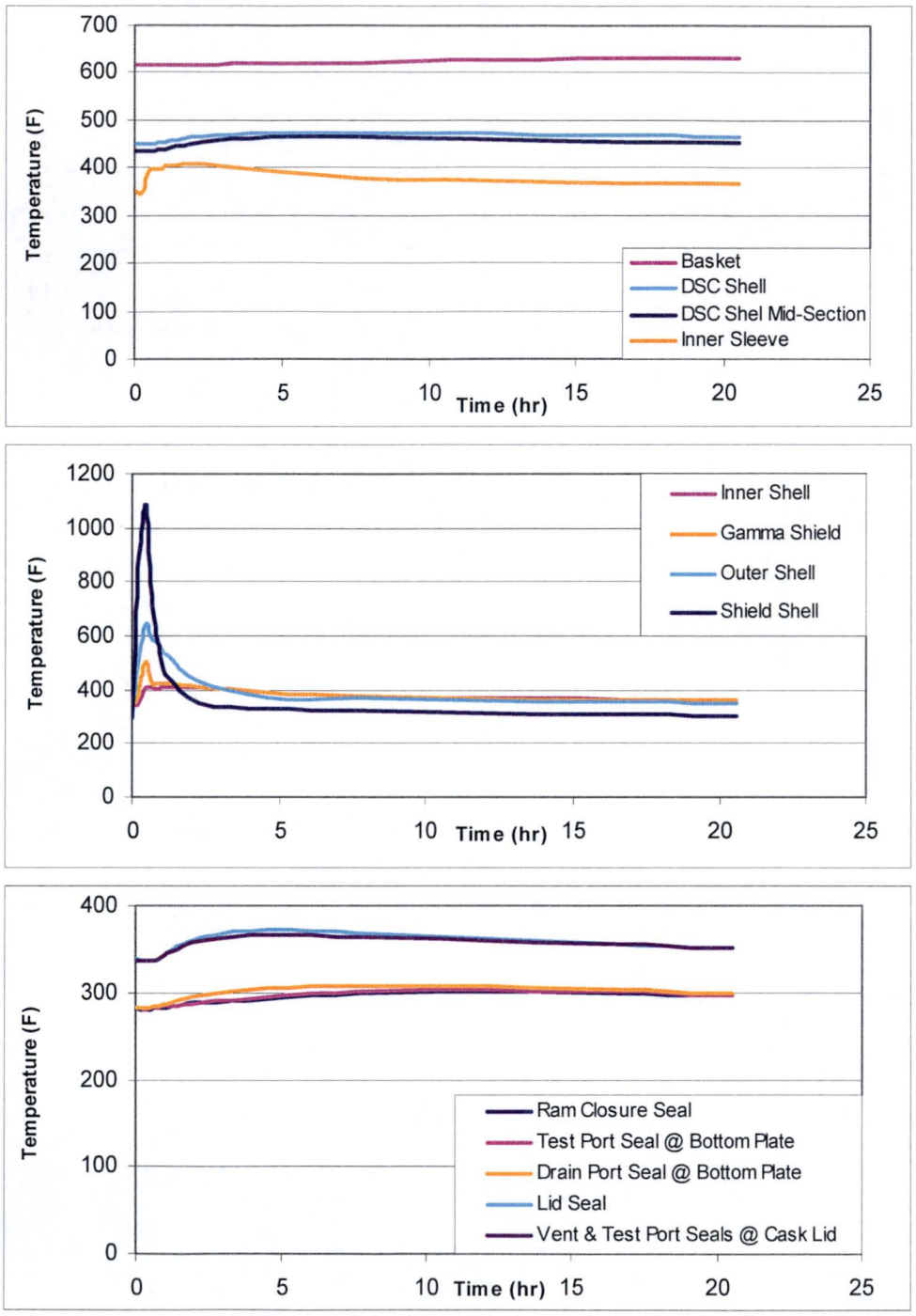

Figure A.3-42
Time-Temperature Histories for TC/DSC Shell
HAC, w/o Fins, 24PTH DSC, 26 kW

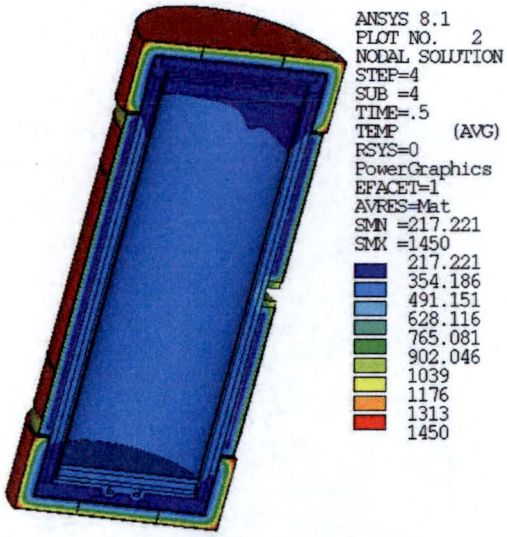

MP197HB w/ Fins, BWR 32 kW, End of Fire

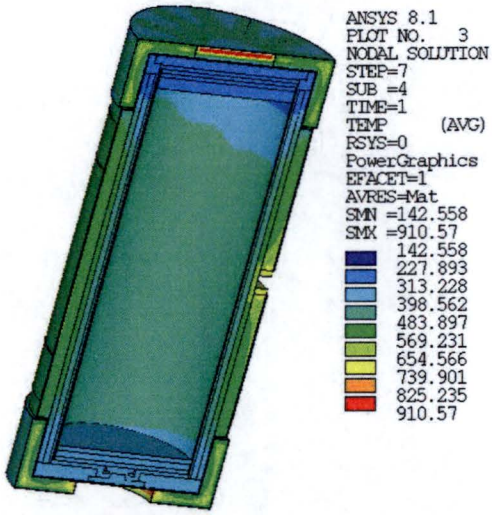

MP197HB w/ Fins, BWR 32 kW, Smoldering Wood after Fire

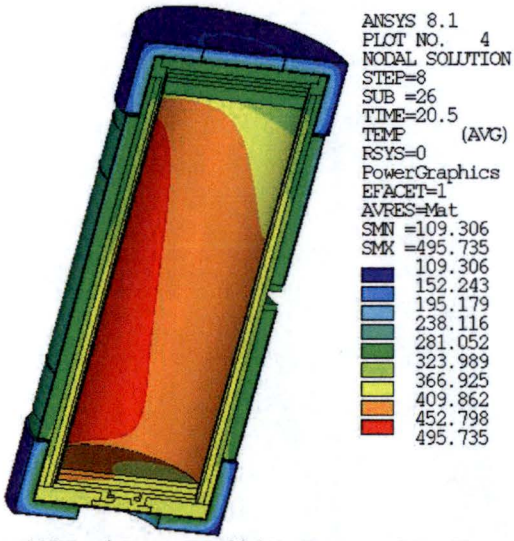

MP197HB w/ Fins, BWR 32 kW, Puncture Rear IL, 20 hrs after Fire

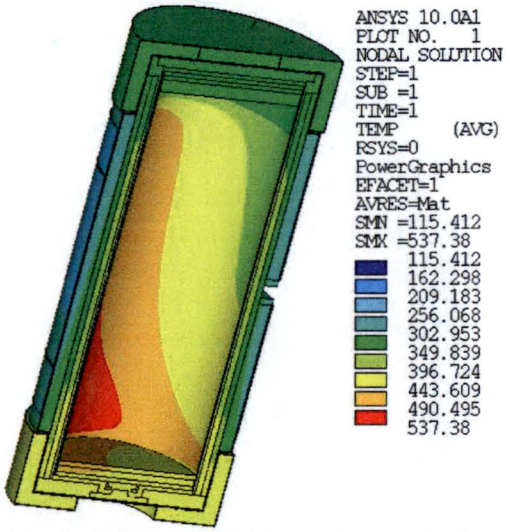

Finned MP197HB, BWR 32 kW, CD, Rear IL Punctured

Figure A.3-43
Temperature Profiles for MP197HB Transport Cask
HAC, 69BTH DSC, 32 kW, with External Fins
(Melted after Fire)

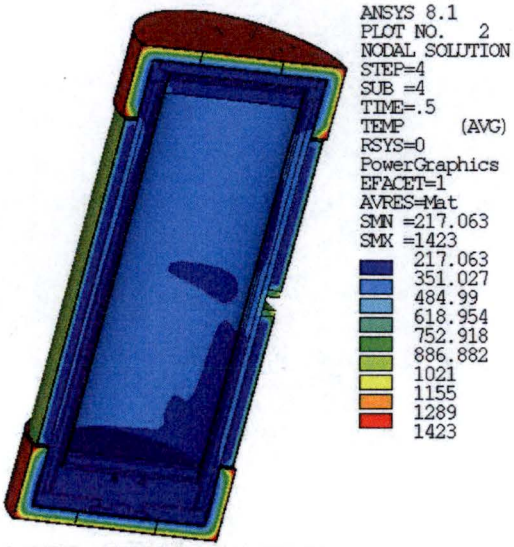

MP197HB, PWR 26 kW, End of Fire

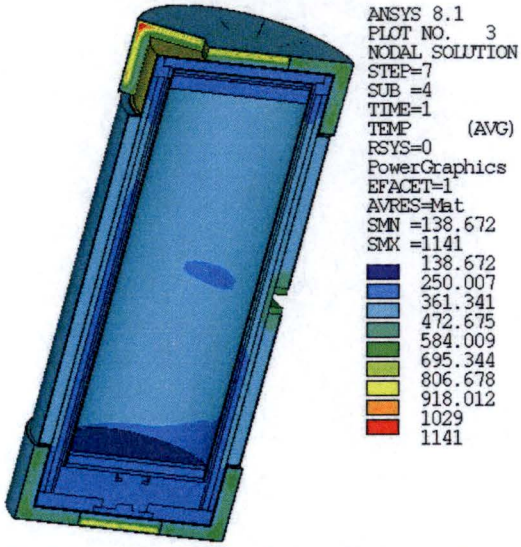

MP197HB, PWR 26 kW, Smoldering Wood after Fire

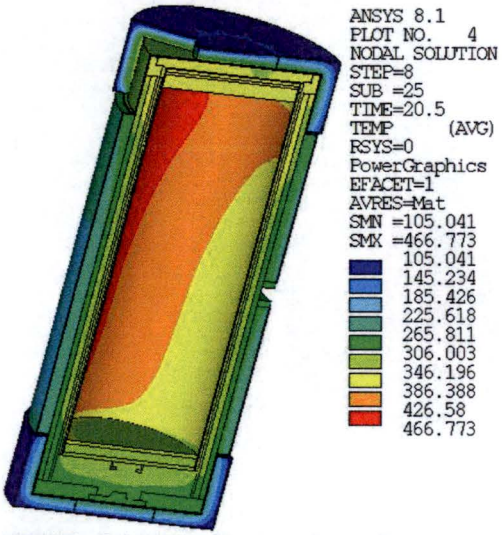

MP197HB, PWR 26 kW, Puncture Front IL,
20 hrs after Fire

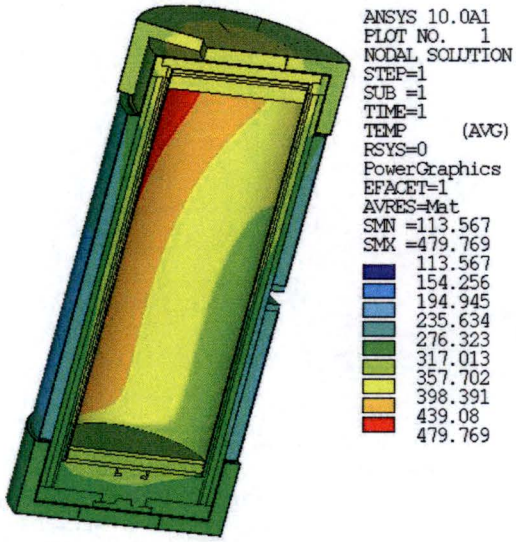

MP197HB, PWR 26 kW, CD, Front IL Punctured

Figure A.3-44
Temperature Profiles for MP197HB Transport Cask
HAC, 24PTH DSC, 26 kW, without External Fins

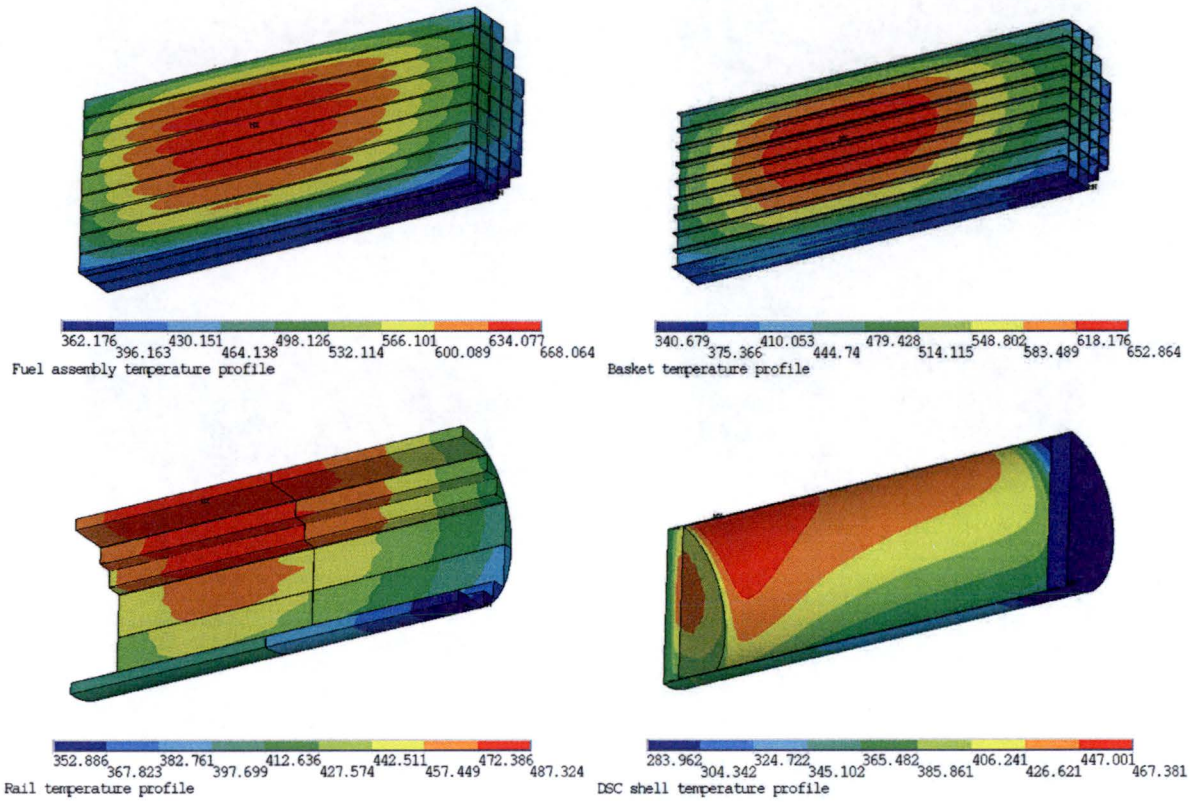

Figure A.3-45
Typical Temperature Distributions for 69BTH DSC
(HAC Post Fire Cool-Down, HLZC#1, 26kW)

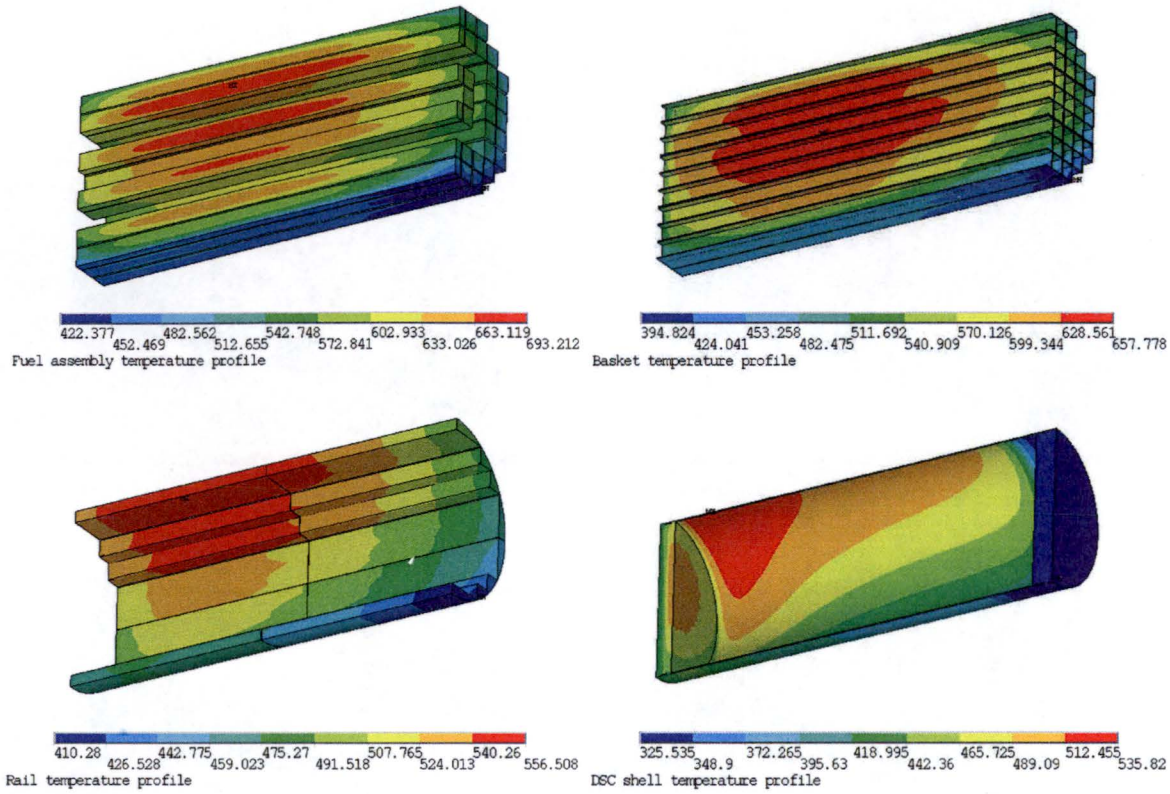

Figure A.3-46
Typical Temperature Distributions for 69BTH DSC
(HAC Post Fire Cool-Down, HLZC#4, 32kW)

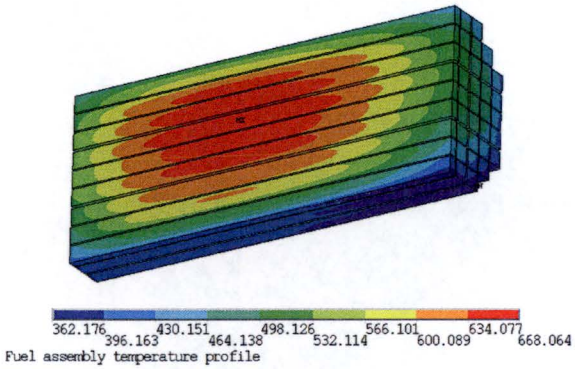

69BTH, HLZC#1, 26kW

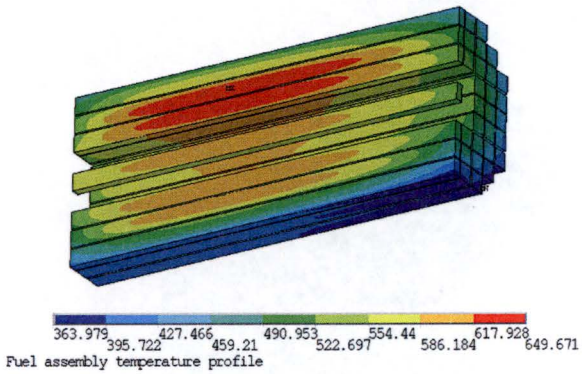

69BTH, HLZC#2, 26kW

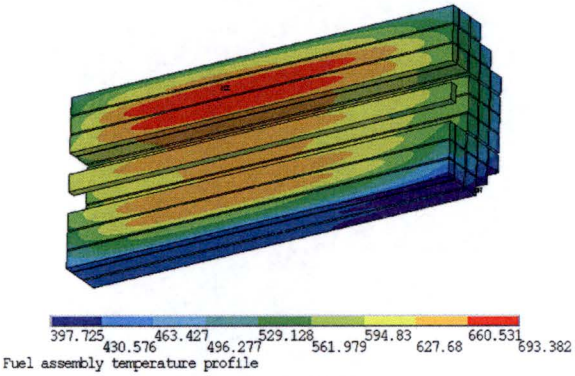

69BTH, HLZC#3, 29.2kW

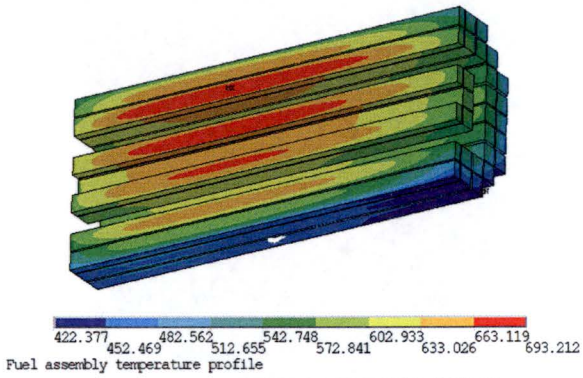

69BTH, HLZC#4, 32kW

Figure A.3-47
Temperature Distributions for Fuel Assemblies in 69BTH DSC
(HAC Post Fire Cool-Down)

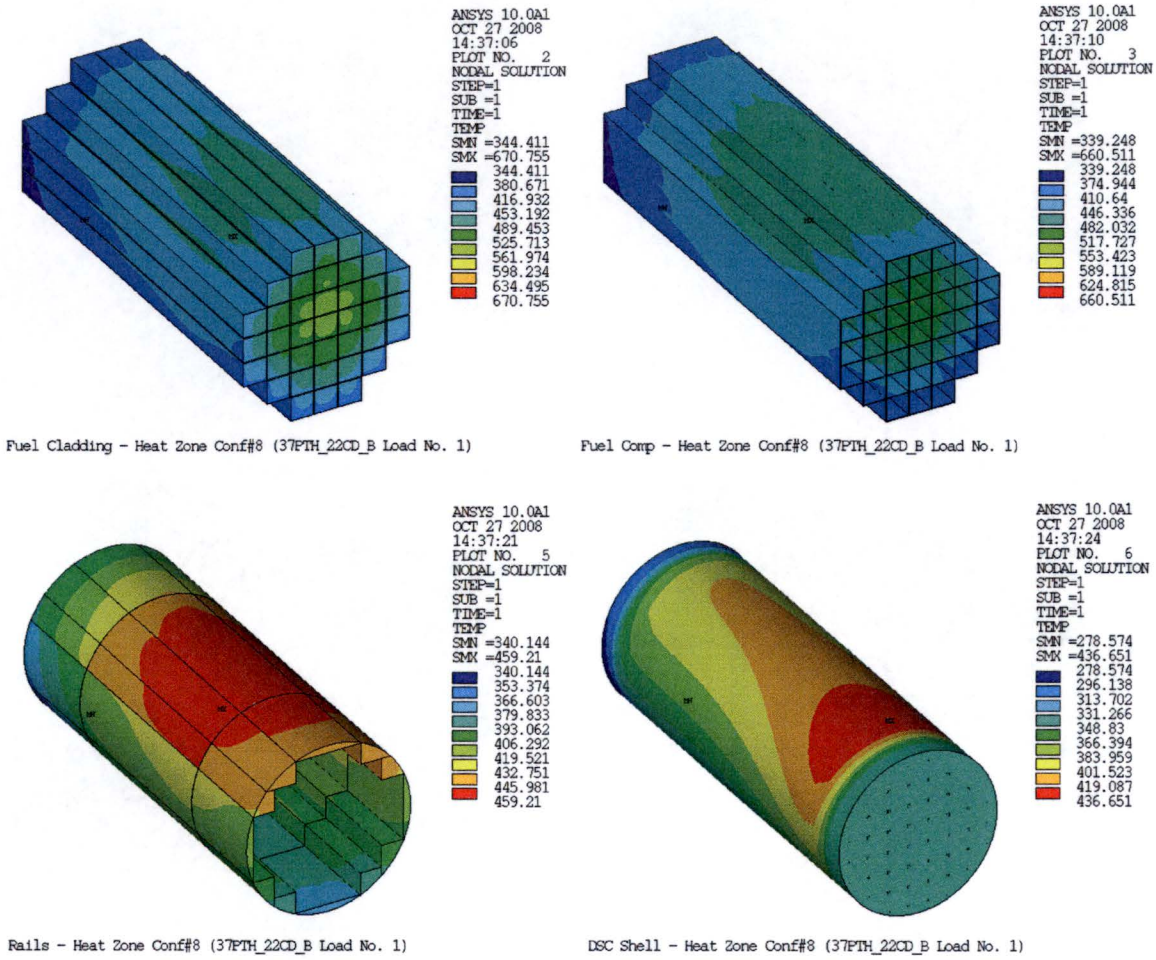

Figure A.3-48
Typical Temperature Distributions for 37PTH DSC
(HAC Post Fire Cool-Down, 22 kW, Boral Plates)

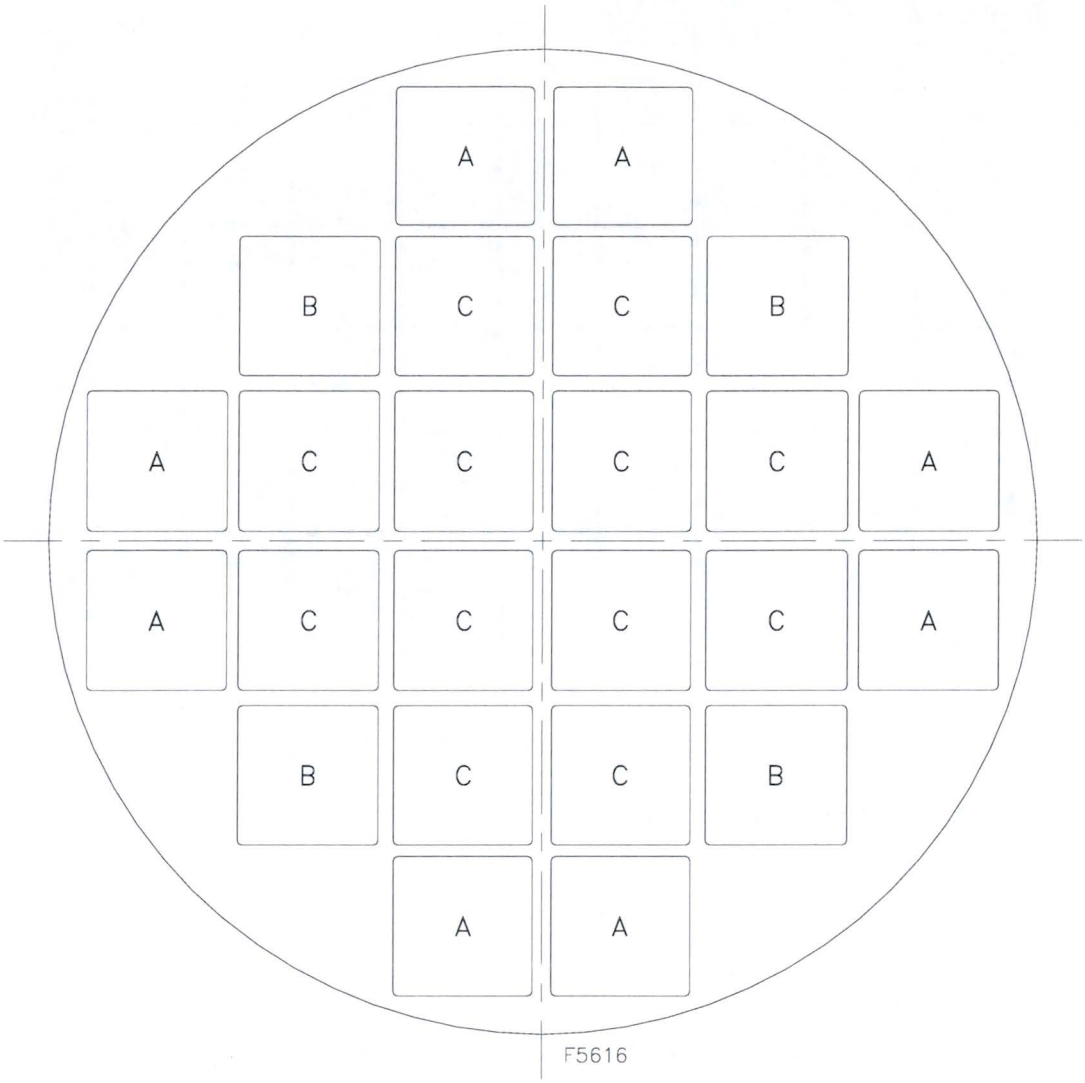

Notes:

1. Locations identified as "A" are for placement of up to 8 damaged or failed fuel assemblies (balance intact).
2. Locations identified as "B" are for placement of up to 4 additional damaged fuel assemblies (Maximum of 12 damaged fuel assemblies allowed, Locations "A" and "B" combined) (balance intact).
3. Locations identified as "C" are for placement of up to 12 intact fuel assemblies, including 4 empty slots in the center as shown in Chapter A.1, Appendix A.1.4.3, Figure A.1.4.3-2.

Figure A.3-49
Location of Damaged/Failed Fuel inside 24PTHF DSC

			C	C	C			
	A	B	C	C	C	B	A	
	B	B	C	C	C	B	B	
C	C	C	C	C	C	C	C	C
C	C	C	C	C	C	C	C	C
C	C	C	C	C	C	C	C	C
	B	B	C	C	C	B	B	
	A	B	C	C	C	B	A	
			C	C	C			

Notes:

1. Corner locations identified as "A" are for placement of up to 4 failed or damaged fuel assemblies with balance intact.
2. Locations identified as "B" are for placement of up to 12 additional damaged fuel assemblies (Maximum of 16 damaged fuel assemblies allowed in locations "A" and "B" combined with balance intact)
3. Locations identified as "C" are only for placement of additional 45 intact fuel assemblies.

Figure A.3-50
Location of Damaged/Failed Fuel inside 61BTHF DSC

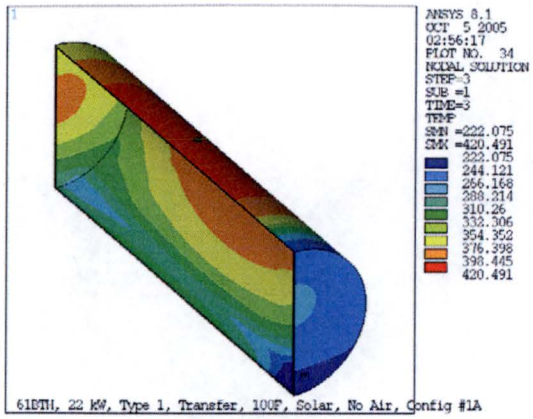

Transfer Conditions
61BTH Type 1, 22.0 kW, 100°F

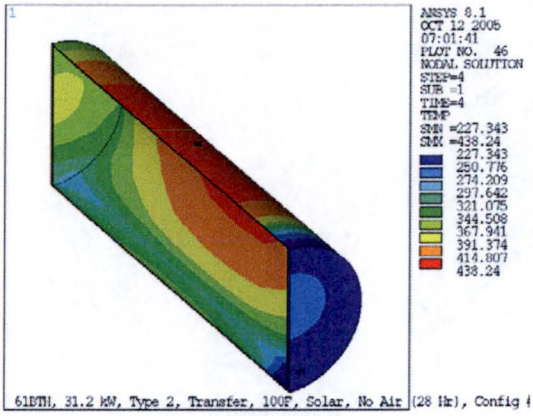

Transfer Conditions
61BTH Type 2, 31.2 kW, 100°F

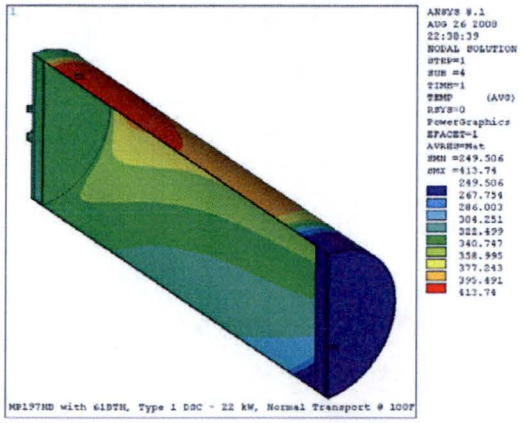

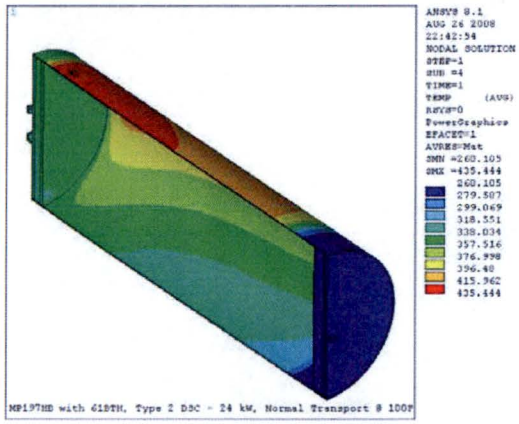

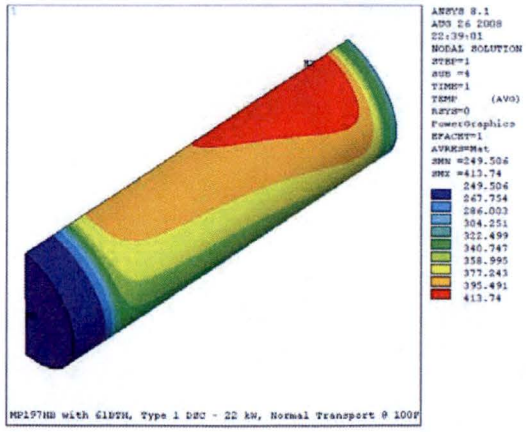

NCT, 61BTH Type 1, 22.0 kW, 100°F

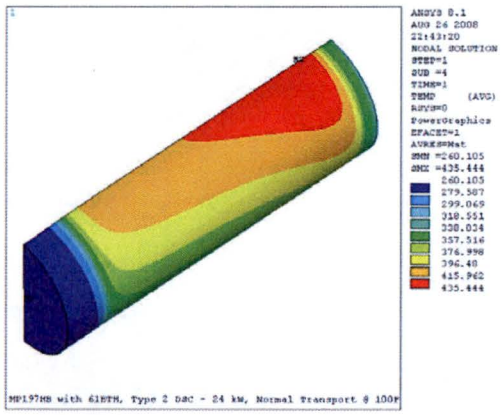

NCT, 61BTH Type 2, 24.0 kW, 100°F

Figure A.3-51
Comparison of DSC Shell Temperature Profiles for 61BTH DSC

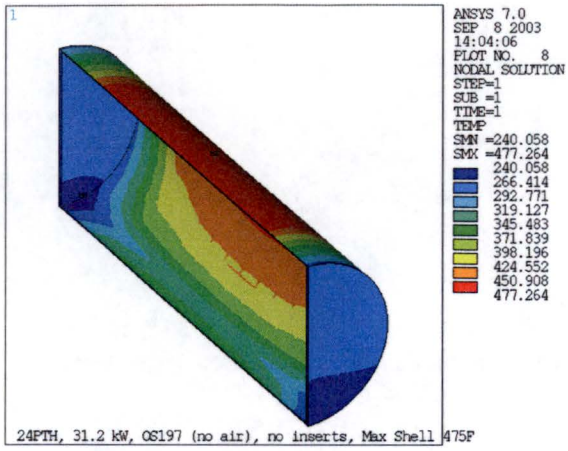

Transfer Conditions
24PTH-S or -L (w/o Al inserts), 31.2 kW, 100°F

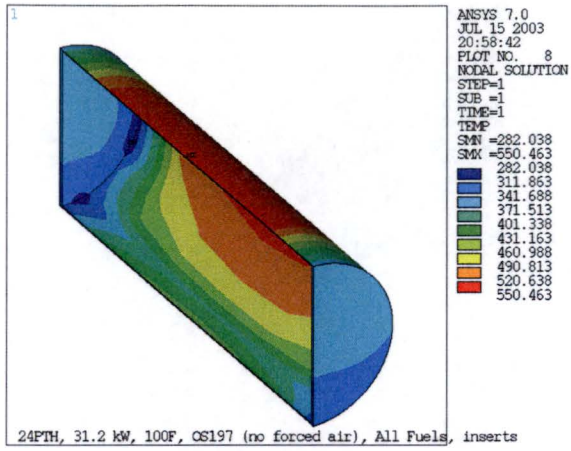

Transfer Conditions
24PTH-S or -L (w/ Al inserts), 31.2 kW, 100°F

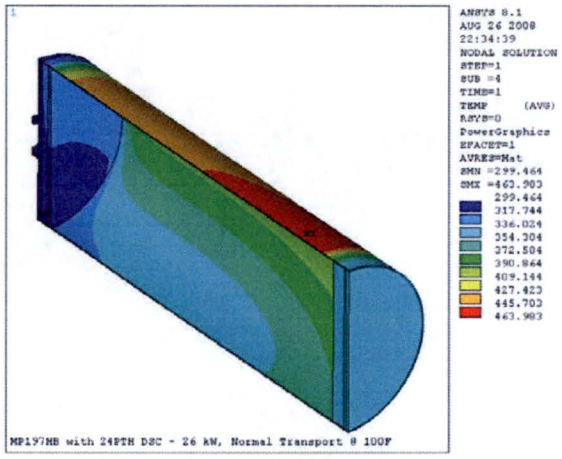

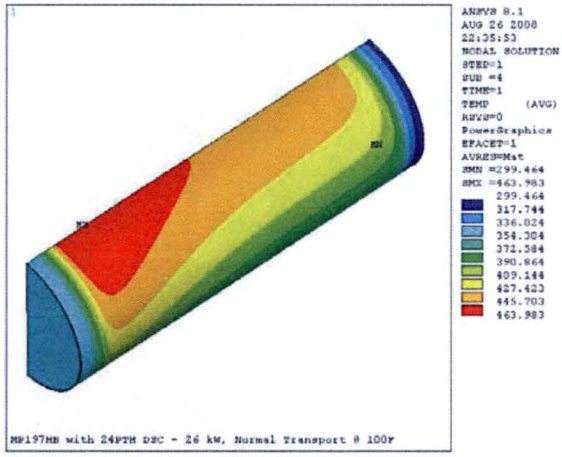

NCT, 24PTH, 26.0 kW, 100°F

Figure A.3-52
Comparison of DSC Shell Temperature Profiles for 24PTH DSC

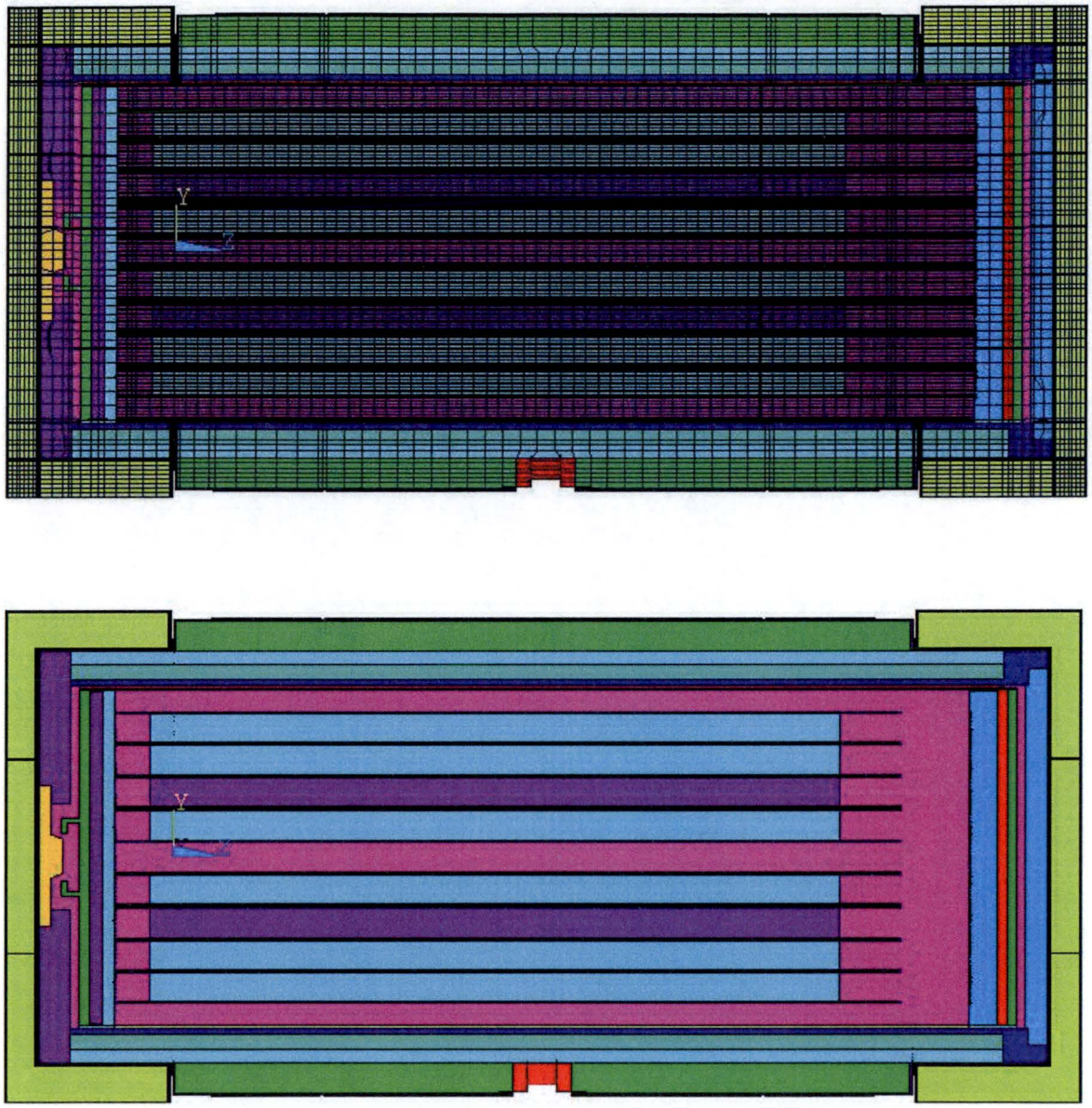

Figure A.3-53
Coupled Model of MP197HB TC and 69BTH DSC

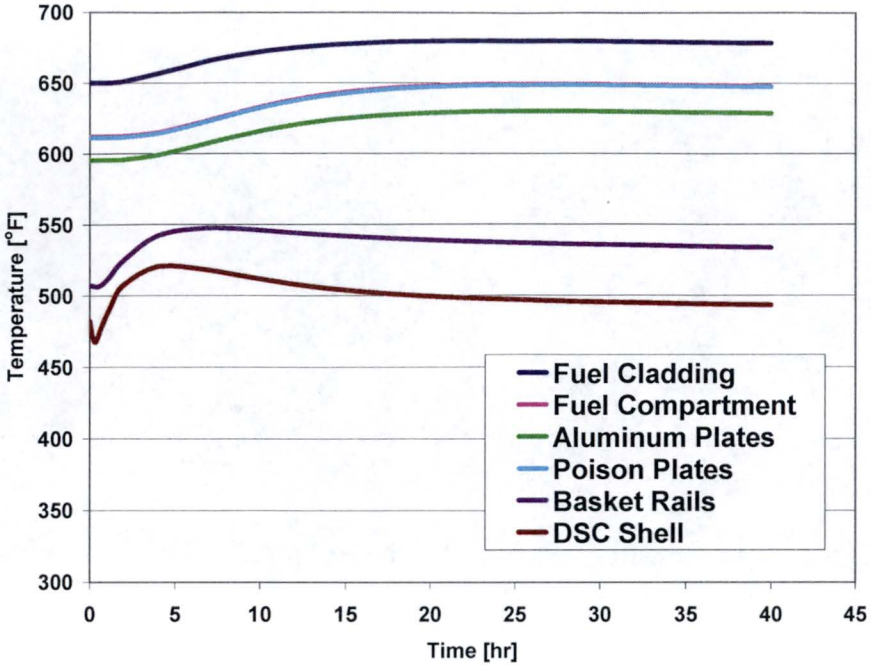

Figure A.3-54
Temperature Time Histories for Coupled Model, 69BTH DSC Components

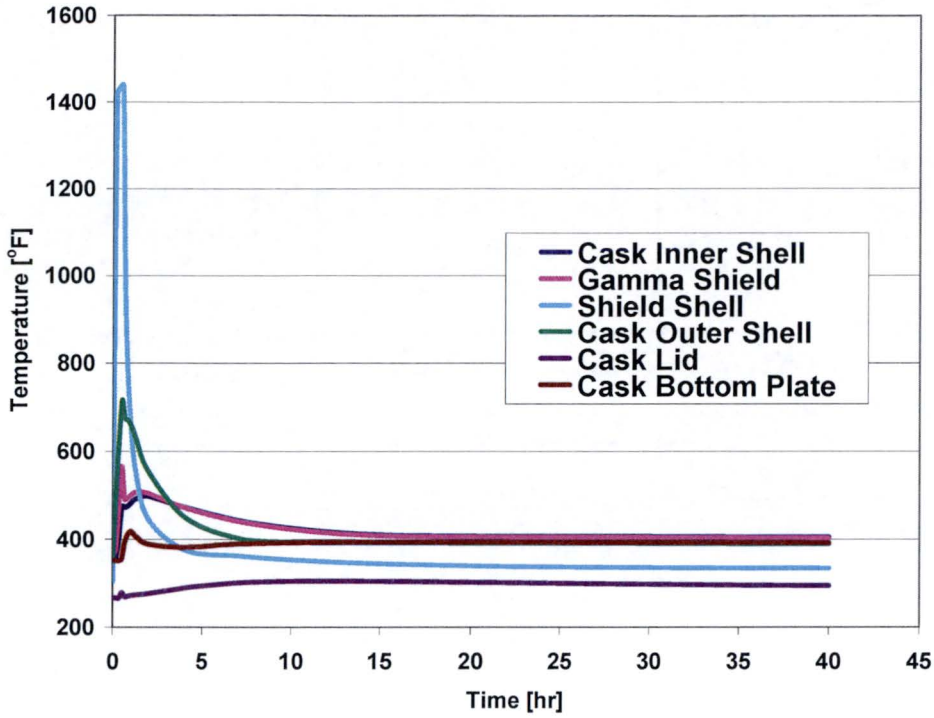

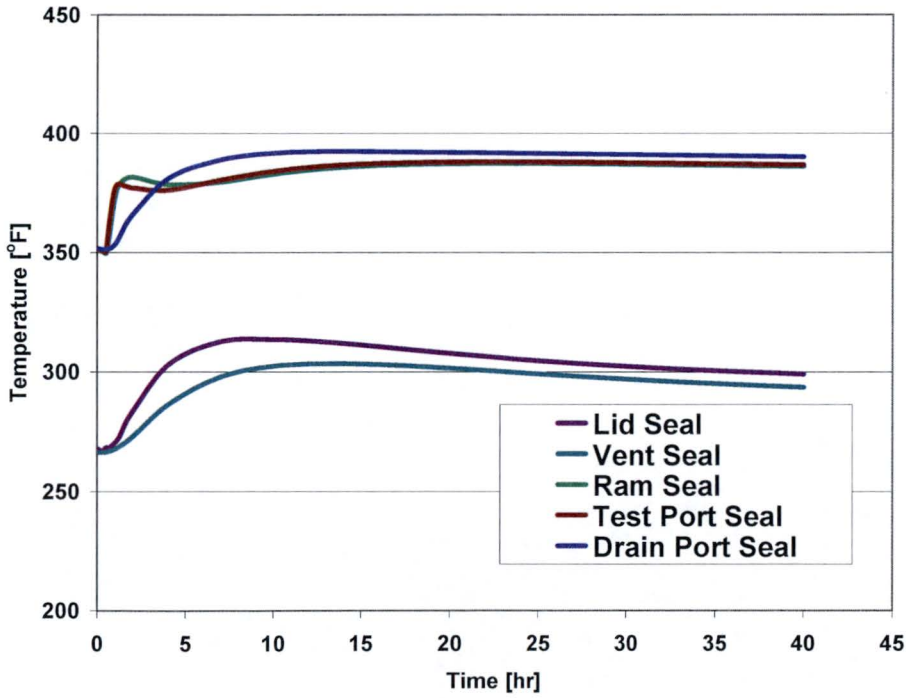

Figure A.3-55
Temperature Time Histories for Coupled Model, MP197HB TC Components

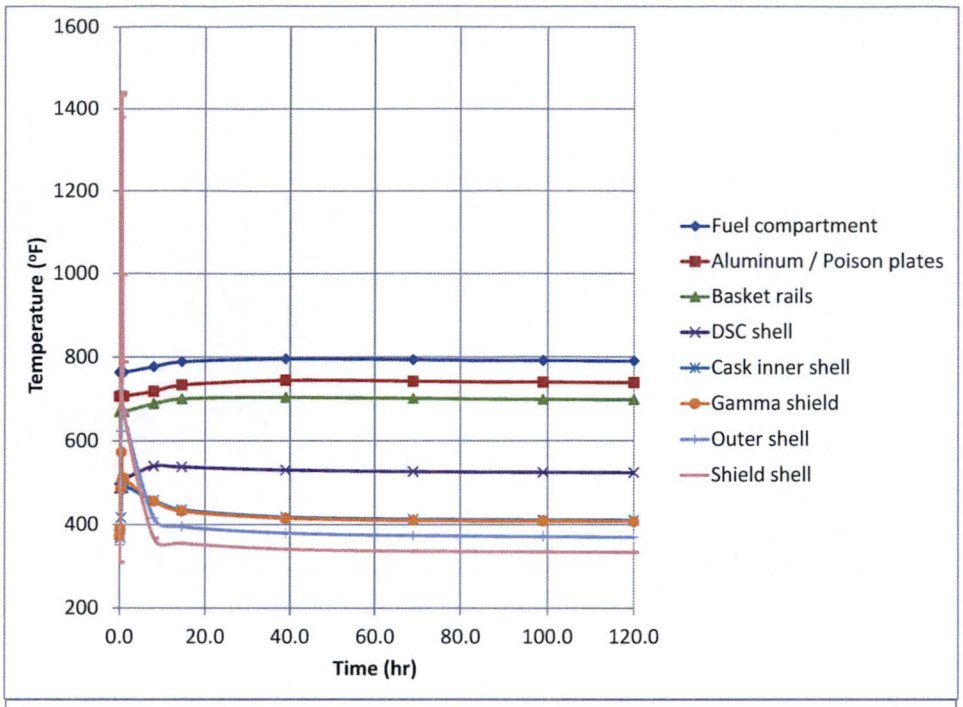

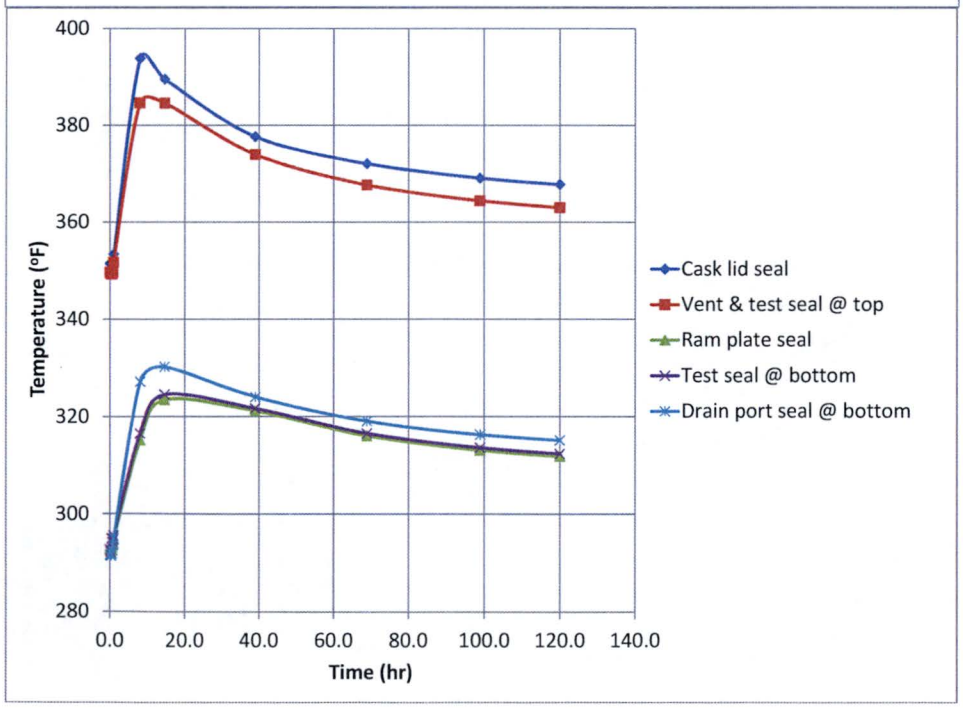

Figure A.3-56
Temperature Time History for MP197HB Transport Cask
HAC, 69BTH DSC, 32 kW, with External Fins (Load Case F1A)

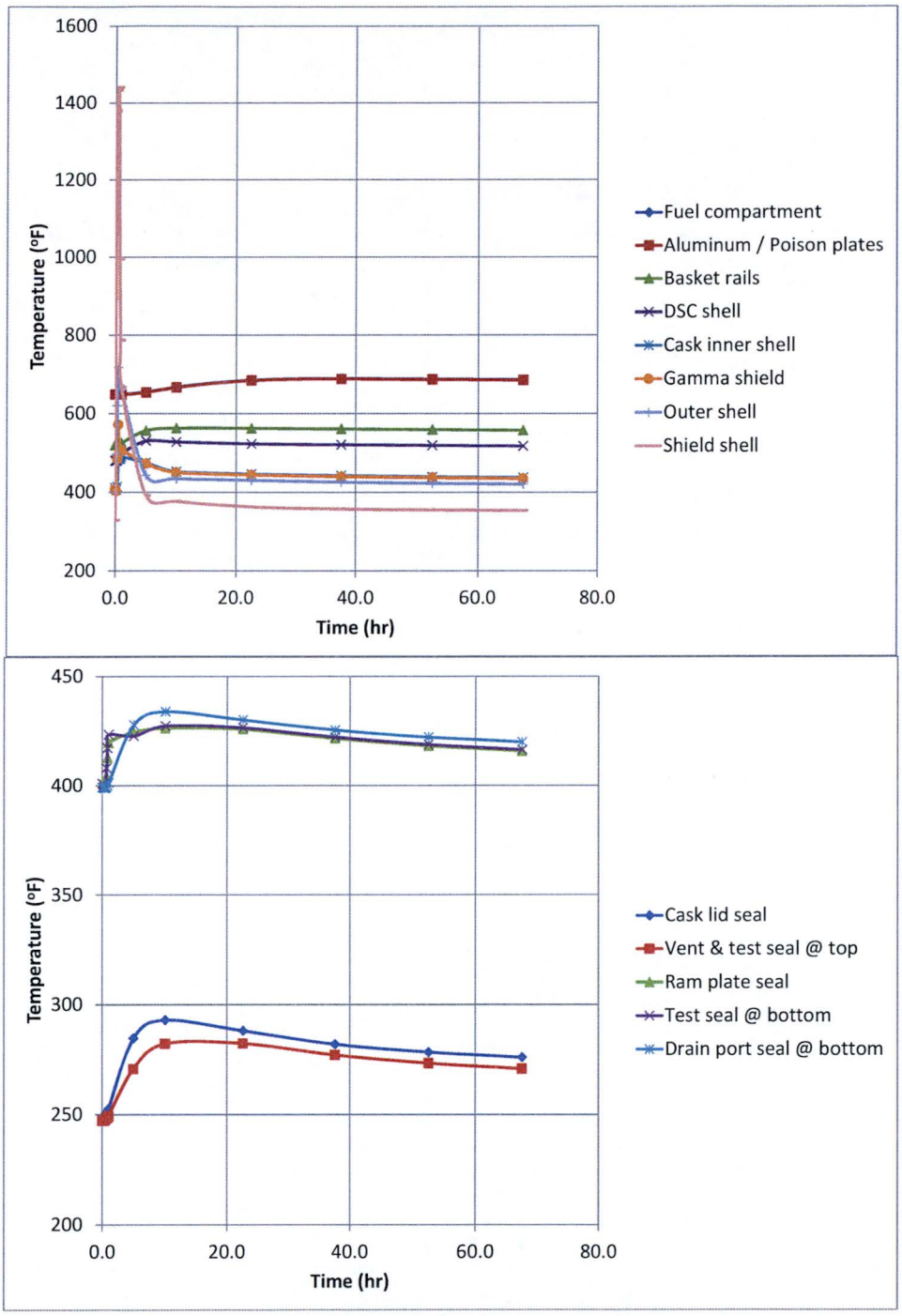

Figure A.3-57
Temperature Time History for MP197HB Transport Cask
HAC, 69BTH DSC, 32 kW, with External Fins (Load Case F2A)

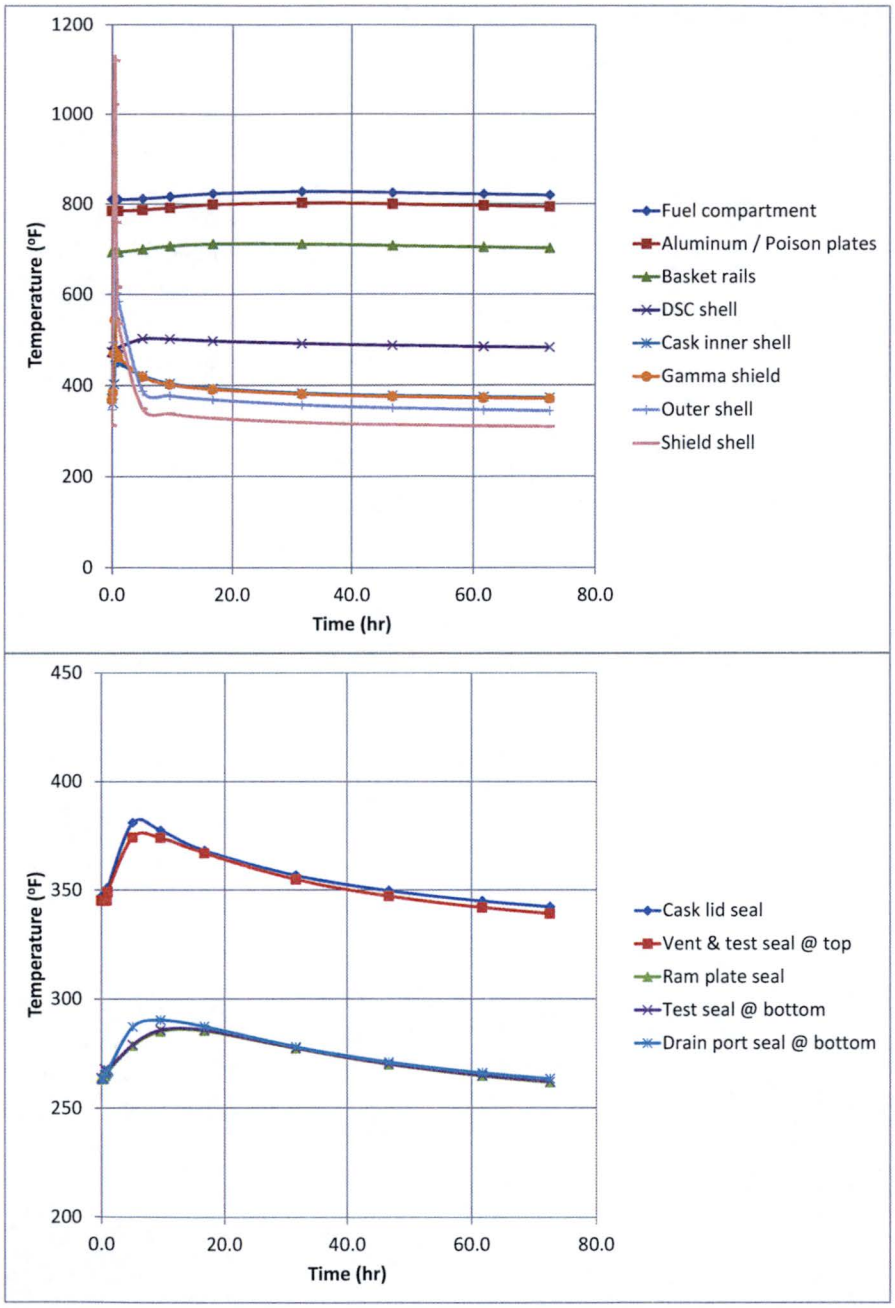

Figure A.3-58
Temperature Time History for MP197HB Transport Cask
HAC, 69BTH DSC, 26 kW, without External Fins (Load Case U1A)

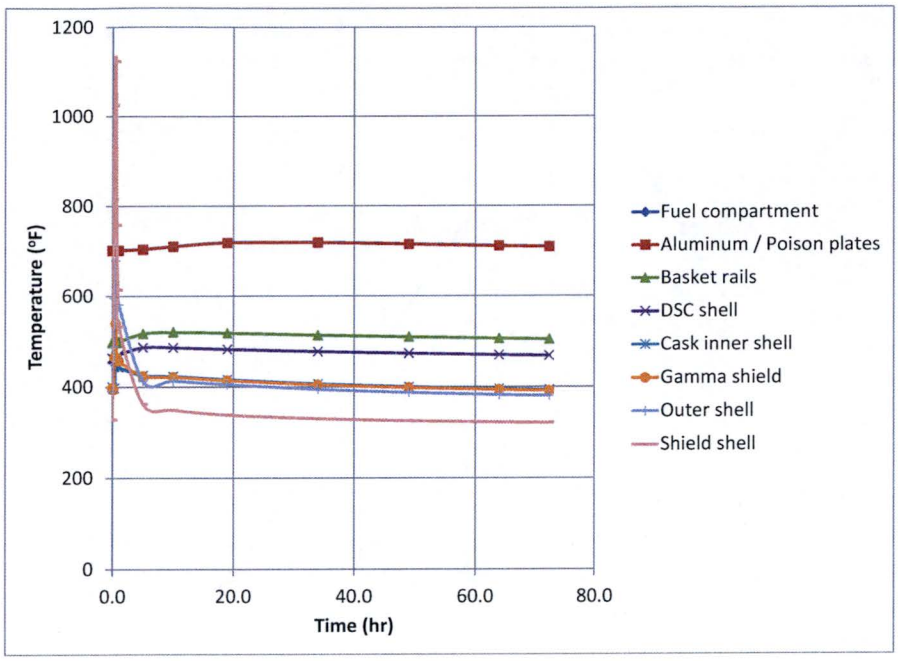

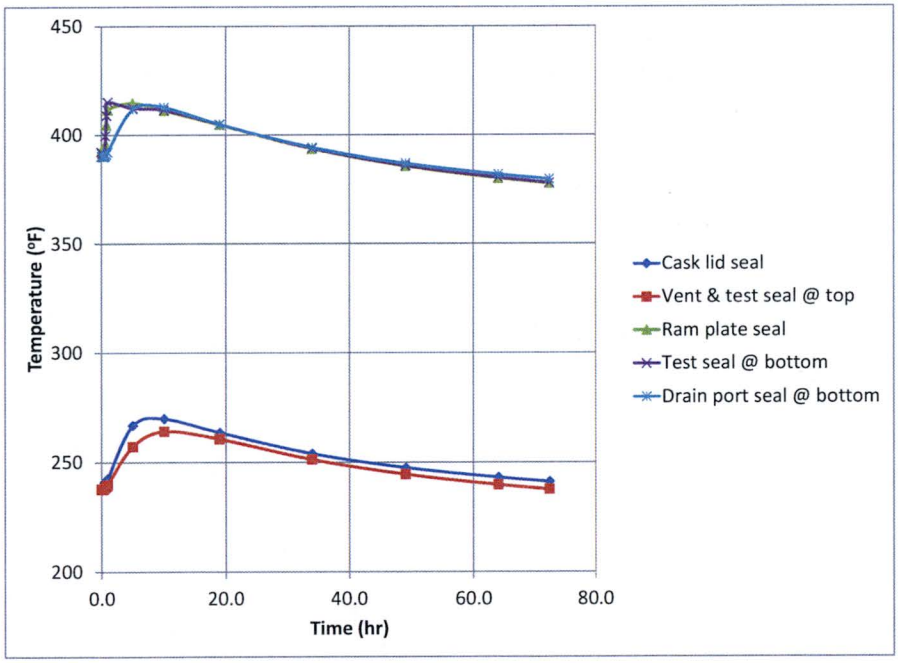

Figure A.3-59
Temperature Time History for MP197HB Transport Cask
HAC, 69BTH DSC, 26 kW, without External Fins (Load Case U2A)

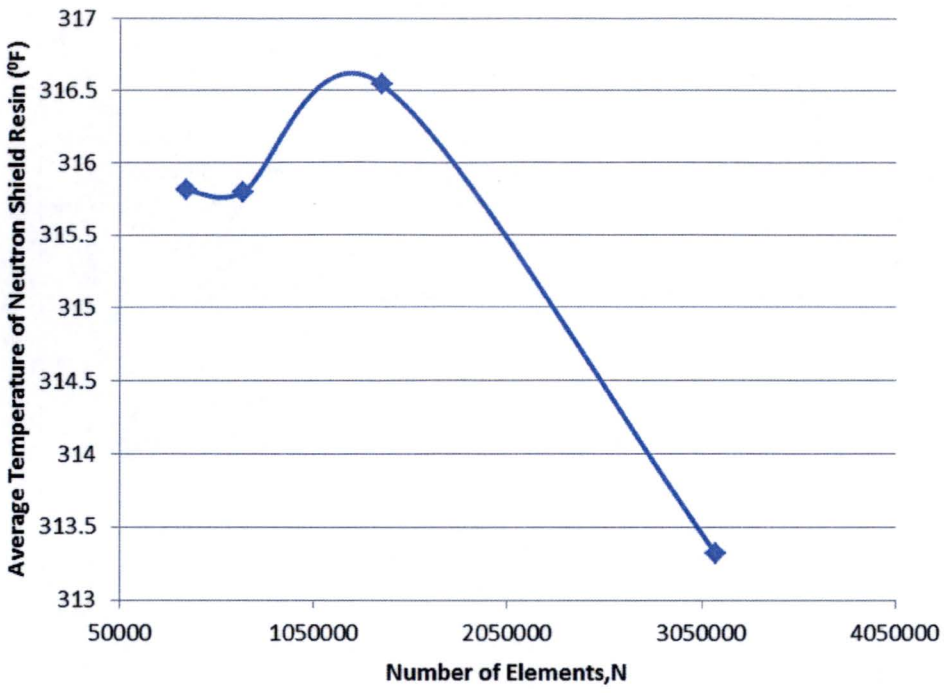

Figure A.3-60
Temperature vs. Number of Elements

Chapter A.5
Shielding Evaluation

TABLE OF CONTENTS

A.5.1 Description of the Shielding Design A.5-1b
A.5.1.1 Package Design Features A.5-1b
A.5.1.2 Codes and Standards A.5-2
A.5.1.3 Summary Table of Maximum Radiation Levels A.5-2
A.5.2 Source Specification A.5-3
A.5.2.1 Gamma Source A.5-4
A.5.2.2 Neutron Source A.5-7
A.5.2.3 Axial Source Distribution A.5-8
A.5.2.4 Axial Blankets A.5-10
A.5.2.5 HAC Sources A.5-11
A.5.3 Model Specification A.5-12
A.5.3.1 Configuration of Source and Shielding A.5-12
A.5.3.2 Material Properties A.5-14
A.5.4 Evaluation A.5-15
A.5.4.1 Methods A.5-15
A.5.4.2 Flux-to-Dose-Rate Conversion A.5-30a
A.5.4.3 Radiation Levels A.5-31
A.5.5 Appendix A.5-33
A.5.5.1 VYAL-B Mixing and Installation A.5-33
A.5.5.2 Fuel Qualification Results A.5-33
A.5.5.3 Decay Heat Restrictions A.5-35
A.5.5.4 Fission gas for BWR fuel at 70 GWd/MTU A.5-38a
A.5.6 References A.5-39

LIST OF TABLES

Table A.5-1 Summary of MP197HB NCT Dose Rates for Intact Fuel A.5-41
Table A.5-1a Summary of MP197HB NCT Dose Rates for Reconfigured Fuel, 50% Void Fraction A.5-41a
Table A.5-1b Summary of MP197HB NCT Dose Rates for Reconfigured Fuel, 50% Void Fraction, Additional Results A.5-41b
Table A.5-1c Summary of MP197HB NCT Dose Rates for Reconfigured Fuel, Reconfiguration Compliant with Enclosure 2 of the US NRC RIS 2015-XX [28] A.5-41c
Table A.5-2 Summary of MP197HB HAC Dose Rates A.5-42
Table A.5-2a Summary of MP197HB HAC Dose Rates for Reconfigured Fuel A.5-42a
Table A.5-3 Not used A.5-43
Table A.5-4 MP197HB Cask/69BTH DSC Shielding Materials A.5-44
Table A.5-5 Composition of VYAL-B A.5-45
Table A.5-6 DB PWR Fuel Assembly Material Mass A.5-46
Table A.5-7 DB BWR Fuel Assembly Material Mass A.5-47
Table A.5-8 TRITON Input Parameters A.5-48
Table A.5-9 Material Compositions for Fuel Assembly Hardware Materials A.5-49
Table A.5-10 BWR Axial Source Distributions for Intact Fuel A.5-50
Table A.5-10a BWR Axial Source Distributions for Reconfigured Fuel A.5-50
Table A.5-11 PWR Axial Source Distributions for Intact Fuel A.5-51
Table A.5-11a PWR Axial Source Distributions for Reconfigured Fuel A.5-51
Table A.5-12 Fuel Assembly Materials for MCNP A.5-52
Table A.5-13 Package Materials Input for MCNP A.5-54
Table A.5-14 Fuel Compositions for Burned Fuel Sensitivity Study A.5-55
Table A.5-15 Burned Fuel Sensitivity Study Dose Rate Results A.5-55
Table A.5-16 Flux-to-Dose Rate Conversion Factors for Gamma A.5-56
Table A.5-17 Flux-Dose-Rate Conversion Factors for Neutron A.5-57
Table A.5-18 CC Radiological Source A.5-58
Table A.5-19 Dry k_{eff} Results for the PWR DBFA A.5-59
Table A.5-20 Dry k_{eff} Results for the BWR DBFA A.5-60
Table A.5-21 Bounding Response Function NCT Dose Rates at 2 Meters from Surface of the Cask Containing 24PT4 DSC A.5-61
Table A.5-22 Bounding Response Function NCT Dose Rates at 2 Meters from Surface of the Cask Containing 24PTH DSC A.5-62
Table A.5-23 Bounding Response Function NCT Dose Rates at 2 Meters from Surface of the Cask Containing 32PT DSC A.5-63
Table A.5-24 Bounding Response Function NCT Dose Rates at 2 Meters from Surface of the Cask Containing 32PTH DSC A.5-64
Table A.5-25 Bounding Response Function NCT Dose Rates at 2 Meters from Surface of the Cask Containing 32PTH1 DSC A.5-65
Table A.5-26 Bounding Response Function NCT Dose Rates at 2 Meters from Surface of the Cask Containing 37PTH DSC A.5-66

Table A.5-27 Bounding Response Function NCT Dose Rates at 2 Meters from Surface of the Cask Containing 61BT DSC A.5-67
Table A.5-28 Bounding Response Function NCT Dose Rates at 2 Meters from Surface of the Cask Containing 61BTH Type 1 DSC A.5-68
Table A.5-29 Bounding Response Function NCT Dose Rates at 2 Meters from Surface of the Cask Containing 61BTH Type 2 DSC A.5-69
Table A.5-30 Bounding Response Function NCT Dose Rates at 2 Meters from Surface of the Cask Containing 69BTH DSC A.5-70
Table A.5-31 PWR Applied keff A.5-71
Table A.5-32 BWR Applied keff A.5-72
Table A.5-33 Matrix Showing Additional to the Transportation FQTs Cooling Times for Selected Cooling Times of CCs A.5-73
Table A.5-34 Summary of Maximum Dose Rates of the Cask Containing the Radioactive Waste Canister A.5-74
Table A.5-35 *Amount of Moles of Gases released as Result of Irradiation for GE7x7 BWR Fuel Assembly at 0.198 MTU, 3.7 wt % U-235, and 70 GWd/MTU* A.5-75
Table A.5-36 Bounding NCT Source for the 37PTH DSC in the MP197HB Transportation Package, Intact Fuel A.5-76
Table A.5-37 Bounding NCT Source for the 69BTH DSC in the MP197HB Transportation Package, Intact Fuel A.5-77
Table A.5-38 Bounding NCT and HAC Source for the 37PTH DSC, Reconfigured Fuel, 21 Inner Compartments A.5-78
Table A.5-38a Bounding NCT and HAC Source for the 37PTH DSC, Reconfigured Fuel, 16 Peripheral Compartments A.5-78
Table A.5-39 Bounding NCT and HAC Source for the 69BTH DSC, Reconfigured Fuel, 45 Inner Compartments A.5-79
Table A.5-39a Bounding NCT and HAC Source for the 69BTH DSC, Reconfigured Fuel, 24 Peripheral Compartments A.5-79
Table A.5-39b Bounding NCT and HAC Source for the 69BTH DSC, Reconfigured Fuel, 24 Peripheral Compartments A.5-79a
Table A.5-40 Photon Dose Rates Computed with C/M Average minus Standard Deviation A.5-80
Table A.5-40a Neutron Dose Rates Computed with Minimum C/M Ratios A.5-80aa
Table A.5-40b Cm-244 Samples Available for Low Burnup Fuel A.5-80ab
Table A.5-40c Cm-244 Samples Available for High Burnup Fuel A.5-80ac
Table A.5-41 Number of Samples Used for Each Isotope A.5-80a
Table A.5-41a Summary of Experimental Samples as a Function of Burnup Range A.5-80a
Table A.5-42 C/M Results from NUREG/CR-7012 ..... A.5-80b
Table A.5-43 C/M Results from NUREG/CR-7013 ..... A.5-80c
Table A.5-44 C/M Results from NUREG/CR-6968 ..... A.5-80d
Table A.5-45 Experimental Error Applied to the Isotopic C/M Data A.5-80f
Table A.5-46 Dose Rate Contribution for Isotopes of Interest (mrem/hr) A.5-80g
Table A.5-47 Not used A.5-80h
Table A.5-48 Selected TN-68 Dose Rates A.5-80i

Table A.5-49 MCNP Benchmark Results for HSM Model 80 ..... A.5-80j

Table A.5-50 ORIGEN-ARP Input Parameters for the Design Basis Sources A.5-80k

Table A.5-51 D_{NCI} Neutron Dose Rate Values for Various Active Fuel Compressions A.5-80l

Table A.5-52 "B" Parameters to Determine Additional Cooling Time for Reconfigured BWR Fuel (years) A.5-80m

Table A.5-53 "B" Parameters to Determine Additional Cooling Time for Reconfigured PWR Fuel (years) A.5-80n

Table A.5-54 Key Parameters of Compressed Fuel for 69BTH DSC Fuel Reconfiguration A.5-80o

Table A.5-55 NCT Reconfigured Fuel Dose Rates for MP197HB Containing 69BTH DSC with Compressed Fuel Configuration, 41% Void Fraction by Volume (30% Fuel Compaction) A.5-80p

Table A.5-56 NCT Reconfigured Fuel Dose Rates for MP197HB Containing 69BTH DSC with Compressed Fuel Configuration, 17% Void Fraction by Volume (50% Fuel Compaction) A.5-80q

Table A.5-57 HAC 1 Meter Dose Rates of MP197HB Containing 69BTH DSC with Compressed Fuel Configuration, 41% Void Fraction by Volume (30% Fuel Compaction) A.5-80r

Table A.5-58 HAC 1 Meter Dose Rates of MP197HB Containing 69BTH DSC with Compressed Fuel Configuration, 17% Void Fraction by Volume (50% Fuel Compaction) A.5-80s

Table A.5-59 69BTH NCT 17% Compressed Fuel – Neutron and Secondary Gamma – Burned Fuel Composition and MCNP Fission Neutron Multiplication Evaluation – Design Basis Source 2.6 wt. % U-235 / 62 GWd/MTU A.5-80t

Table A.5-60 69BTH NCT 17% Compressed Fuel – Neutron and Secondary Gamma – Burned Fuel Composition and MCNP Fission Neutron Multiplication Evaluation – High Enriched and High Burnup Fuel (5.0 wt. % U-235 / 70 GWd/MTU) A.5-80t

LIST OF FIGURES

Figure A.5-1 MP197HB Transport Cask with 69BTH DSC Model, Axial View A.5-81
Figure A.5-2 MP197HB Transport Cask with 69BTH DSC Model, Top View Showing Cask Lid with Gap, Top Nozzle, and Plenum A.5-82
Figure A.5-3 MP197HB Transport Cask with 69BTH DSC Model, Bottom View Showing Cask Bottom and Bottom Nozzle A.5-83
Figure A.5-4 MP197HB within 69BTH DSC Model, Cross Section View A.5-84
Figure A.5-5 Details of DSC Basket with Fuel Lattice Unit Cell in MCNP Model A.5-85
Figure A.5-6 MP197HB Transport Cask within 69 BTH DSC: MCNP Model Cut-through XY Plane (Z=25.12 cm), Normal Condition A.5-86
Figure A.5-7 MP197HB Bottom and Top Trunnion Attachment Block and Plug Geometry, Normal Condition A.5-87
Figure A.5-8 69BTH DSC and MP197HB Bottom Plugs with Grapple Ring Cut-Out A.5-88
Figure A.5-9 MP197HB Shear Key A.5-89
Figure A.5-10 Dose Rate Location Terminology A.5-90
Figure A.5-11 24PT4 DSC Radial Zones A.5-91
Figure A.5-12 24PTH and 24PTHF DSC Radial Zones A.5-91
Figure A.5-13 32PT, 32PTH, and 32PTH1 DSC Radial Zones A.5-92
Figure A.5-14 37PTH DSC Radial Zones A.5-92
Figure A.5-15 61BT, 61BTH (Type 1 and Type 2) and 61BTHF DSC Radial Zones A.5-93
Figure A.5-16 69BTH DSC Radial Zones A.5-94
Figure A.5-17 MCNP vs. Response Function for 37PTH DSC A.5-95
Figure A.5-18 MCNP vs. Response Function for 69BTH DSC A.5-96
Figure A.5-19 Peaking Factors for BWR fuel A.5-97
Figure A.5-20 Peaking Factors for PWR fuel A.5-98
Figure A.5-21 37PTH DSC Neutron Fraction of Total Dose Rate A.5-99
Figure A.5-22 69BTH DSC Neutron Fraction of Total Dose Rate A.5-100
Figure A.5-23 NCT MCNP Models (x-y View) A.5-101
Figure A.5-24 NCT 69BTH DSC MCNP Models (x-z View) A.5-102
Figure A.5-24a NCT 69BTH DSC MCNP Model for Heat Load Zone Configuration No. 8 with High-Burnup Reconfigured Fuel in Zone 5 (x-y and x-z views) A.5-102a
Figure A.5-25 NCT 37PTH DSC MCNP Models (x-z View) A.5-103
Figure A.5-26 HAC MCNP Models for Reconfigured Fuel (x-z View) A.5-104
Figure A.5-27 NCT Configurations for *Radial* Fuel Reconfiguration (x-y View) A.5-105
Figure A.5-28 Peripheral and Inner Fuel Locations for the 24PT4 and 24PTH DSCs A.5-106
Figure A.5-30 Correction Factors vs. Burnup–Cm-244 ..... A.5-108
Figure A.5-31 Correction Factors vs. Burnup–Cs-134 ..... A.5-108

Figure A.5-32 Correction Factors vs. Burnup–Cs-137 ..... A.5-109
Figure A.5-33 Correction Factors vs. Burnup–Ce-144 ..... A.5-109
Figure A.5-34 Correction Factors vs. Burnup–Eu-154 ..... A.5-110
Figure A.5-35 Correction Factors vs. Burnup–Ru-106 ..... A.5-110
Figure A.5-36 Correction Factors vs. Burnup–Sm-147 ..... A.5-111
Figure A.5-37 Correction Factors vs. Burnup–Sr-90 ..... A.5-111
Figure A.5-38 Correction Factors vs. Burnup for Each Reactor–Cs-137 ..... A.5-112
Figure A.5-39 Cooling Time Comparison–Trending Evaluation A.5-113
Figure A.5-40 25-Node MCNP Burned Fuel Model A.5-114

Chapter A.5
Shielding Evaluation

NOTE: References in this chapter are shown as [1], [2], etc. and refer to the reference list in Section A.5.6.

This chapter describes the shielding evaluation of the NUHOMS® MP197HB transportation package. The MCNP computer program is used to calculate the dose rates using a detailed three-dimensional model [1]. The source terms are generated with TRITON/ORIGEN-ARP sequence of SCALE [2]. The dose rates are in compliance with the applicable requirements of 10 CFR Part 71 for exclusive-use transportation in an open transport vehicle [3].

[

]

Proprietary Information Withheld Pursuant to 10 CFR 2.390

Proprietary Information Withheld Pursuant to 10 CFR 2.390

A.5.1 Description of the Shielding Design

The MP197HB cask is designed to transport one of several NUHOMS® DSCs loaded with spent fuel assemblies or dry irradiated and/or contaminated non-fuel bearing solid materials in a radioactive waste canister (RWC) in accordance with the requirements of the 10 CFR 71. The authorized contents acceptable for transport are described in Chapter A.1, Section A.1.2.3, including appendices A.1.4.1 through A.1.4.9A. A complete list of the NUHOMS® DSCs authorized for transport is provided in Chapter A.1, Section A.1.2.3.1. Chapter A.1, Section A.1.2.3.2 (also in Appendix A.1.4.9A) provides a description of the irradiated and/or contaminated non-fuel bearing solid materials authorized for transport in the RWC as well as its respective physical dimensions.

Radiological sources used for the calculation of the dose rates presented in this chapter are determined through ranking using the response function methodology to develop the fuel qualification tables (FQT). Response function results are compared with direct MCNP analysis using a discrete MP197HB transportation package model as described in Section A.5.4.1.2.3.

By definition of the FQTs, the minimum cooling times are determined so that the maximum NCT dose rates for intact fuel at 2 m from the side of the vehicle are ≤ 8.2 mrem/hr. For fuel in the peripheral basket locations, additional cooling time is needed for some burnup, enrichment, and cooling time (BECT) combinations due to fuel reconfiguration, as defined using the methodology in Section A.5.4.1.3.3. Further discussion of the fuel qualification methodology is contained in Section A.5.4.1.3 and FQT results are discussed in Section A.5.5.2.

A.5.1.1 Package Design Features

Shielding for the MP197HB transportation package is provided mainly by the cask body. Shielding against gamma radiation is provided by the lead and stainless steel shells that comprise the cask wall. For the neutron shielding, a borated VYAL-B resin compound surrounds the cask body radially. Gamma shielding in the cask ends is provided by the steel top and bottom assemblies of the transportation cask and axial ends of the DSCs. Additional shielding is provided by the steel outer shell surrounding the resin layer, the steel and aluminum structure of the fuel basket and optional heat dissipation fins surrounding the cask side between impact limiters.

For transport, wood filled impact limiters are installed on either end of the cask and provide additional shielding for the ends and some radial shielding for the areas at either end of the radial neutron shield.

Important-to-shielding dimensions are shown in Table A.5-4.

A full discussion and description of the models used in the shielding evaluation is contained in Section A.5.3.1.

Material properties used in the evaluation of the MP197HB transportation package are described in Section A.5.3.2.

A.5.1.2 Codes and Standards

ANSI/ANS-6.1.1-1977 flux-to-dose rate conversion factors are utilized for both gamma and neutron radiation [4]. These factors are provided in Table A.5-16 and Table A.5-17, respectively.

A.5.1.3 Summary Table of Maximum Radiation Levels

A.5.1.3.1 Regulatory Limits

The dose rates limits for the transportation of the MP197HB package, in an open vehicle, are obtained from 10 CFR 71.47(b) and 10 CFR 71.51(a)(2) and are listed as follows [3].

- Dose rate at any point on the external surface of the package under normal conditions is 200 mrem/hr (maximum).
- Dose rate at any point on the vertical planes projected from the outer edges, including the top and underside, under normal conditions is 200 mrem/hr (maximum).
- Dose rate at any point 2 m from the vertical planes projected from the outer edges, excluding the top and underside, under normal conditions is 10 mrem/hr (maximum).
- External dose rate at any point 1 m from the surface of the package under hypothetical accident conditions is 1000 mrem/hr (maximum).

A.5.1.3.2 Maxima

Normal conditions of transport (NCT) dose rates are computed for exclusive-use transport in an open vehicle. For the purposes of the shielding evaluation, the package surfaces, as shown in drawing MP197HB-71-1001, are conservatively assumed to be the vehicle surfaces. The package is assumed to be as wide as the open vehicle. Either end of the vehicle is assumed to be at the end of the impact limiters. The underside (floor) and top of the vehicle are assumed to correspond to the radius of the impact limiters. The package is assumed to be under the control of a private carrier and any operator in an occupied position will wear a dosimeter and be subject to a dose program to satisfy the requirements of 10 CFR 20.1502.

The maximum radiation dose rates for intact fuel during NCT are provided in Table A.5-1. The 37PTH DSC dose rates bound all PWR-type DSCs, and the 69BTH DSC dose rates bound all BWR-type DSCs. Dose rates are computed to bound all authorized burnup and enrichment combinations defined in the fuel qualification tables in Chapter A.1.

The maximum radiation dose rates for reconfigured fuel during NCT are provided in Table A.5-1a *and Table A.5-1b.* [

] In the reconfigured fuel models *for Table A.5-1a and Table A.5-1b,* the active fuel length is compressed until 50% void volume is reached. Fifty percent void volume is considered the design basis reconfiguration. Fuel reconfiguration increases the dose rates compared to the intact fuel models. To reduce the dose rates, in the reconfigured fuel models a

two-zone loading approach is utilized. Fuel in the inner zone is governed by the FQT cooling times, while fuel in the peripheral zone is cooled for a longer time. The FQT methodologies in the appendices of Chapter A.1 are modified to reflect the two-zone loading requirement.

Hypothetical accident condition (HAC) dose rates are calculated 1 m from the surface of the cask body. No credit is taken for the neutron shield or impact limiters. Both intact and reconfigured fuel are considered. The maximum radiation dose rates for HAC are shown in Table A.5-2 [ ] *and Table A.5-2a* [ ]

Dose rates for RWC are provided in Table A.5-34. This table contains both NCT and HAC dose rate results. Compared to spent fuel, RWC dose rates are low.

A.5.2 Source Specification

There are five principal sources of radiation associated with transport of spent nuclear fuel that are of concern for radiation protection.

1. Primary gamma radiation from spent fuel.
2. Primary neutron radiation from spent fuel (both alpha-n reactions and spontaneous fission).
3. Gamma radiation from activated fuel structural materials and fuel inserts.
4. Capture gamma radiation produced by attenuation of neutrons by shielding material of the cask.
5. Neutrons produced by sub-critical multiplication in the fuel.

There are three source configurations used in the evaluation of the shielding performance of the MP197HB transportation package. These configurations are selected because of their respective bounding parameters on all authorized contents. The bounding configurations are as follows:

- 8,182 A_2 (90,000 Ci of Co-60) in the RWC,
- 69 GE-2,3 7x7 Type G2A BWR spent fuel assemblies in the 69BTH DSC, and
- 37 B&W 15x15 Mark B-10 PWR spent fuel assemblies in the 37PTH DSC.

For the spent fuel assemblies listed, design basis sources which encompass the allowable burnup and enrichment combinations for the authorized contents are developed in the following subsections. The spent fuel assembly types are selected as bounding mainly because their respective initial uranium loading bounds all others.

For the 37PTH and 69BTH DSCs in the MP197HB transportation package, design basis BWR and PWR spent fuel sources are developed based on a bounding assembly average burnup, initial enrichment, and cooling time. These parameters are selected based on the fuel qualification method discussed in Section A.5.4.1.3. The B&W 15x15 Mark B10 and the GE-2, 3 7x7 Type G2A fuel assemblies contain the maximum heavy metal weight for their type, nearly 490 and 198 kgU, respectively. They result in bounding neutron and gamma source terms for PWR and BWR type of assemblies, respectively. Therefore, B&W 15x15 Mark B10 and the GE 2, 3 7x7 are evaluated as the design basis (DB) PWR and BWR fuel assembly (FA) in the shielding evaluation of MP197HB transportation package, respectively.

The fuel assembly hardware for the GE 7x7 fuel assembly is bounding as it contains the maximum amount of steel and inconel than any other BWR fuel design. For the PWR fuel assembly designs with cooling times greater than 15 years, the contribution from the fuel assembly hardware becomes less important due to substantial decay of the Co-60 source from hardware irradiation.

Generation of the source terms is a two-step process. First, two-dimensional TRITON/T-DEPL models are developed for the GE 7x7 and B&W 15x15 fuel assembly types. These computationally intensive models are used to generate burnup-dependent data libraries. The 44GROUPNDF5 cross section library *is* used *in the* TRITON/T-DEPL depletion calculations. *The TRITON/T-DEPL input parameters are summarized in Table A.5-8. Second, the source terms are computed using ORIGEN-ARP and utilize the data libraries developed above. The ORIGEN-ARP input parameters for the design basis sources are summarized in Table A.5-50.*

A.5.2.1 Gamma Source

The gamma sources used in the analysis are described in the following sections. The gamma radiation spectrum is presented *with* an 18 energy group structure consistent with the SCALE 27n-18g cross section library energy grouping structure. The lower boundary energy range in this library is 0.05 MeV. It corresponds to Group 45. The upper energy range is 8.00 to 10.00 MeV. It corresponds to Group 28. The conversion of the source spectra is performed directly through the ORIGEN-S code. The gamma source for the fuel assembly hardware is primarily from the activation of cobalt. This activation contributes primarily to energy Groups 36 and 37 of the SCALE 27n-18g library

A.5.2.1.1 24PTH

Partial length shielding assemblies (PLSAs) are only authorized for the 24PTH DSC and are Westinghouse 15x15 design fuel assemblies that consist mostly of stainless steel. They are restricted to a maximum burnup of 40 GW*d*/MTU and a maximum MTU loading of 0.330 as shown on Chapter A.1, Appendix A.1.4.3. Therefore, they are bounded by the design basis B&W 15x15 fuel assemblies.

A.5.2.1.2 37PTH

The NCT PWR design basis fuel assembly gamma source in the 37PTH DSC in the MP197HB transportation package is shown in Table A.5-36. This source is for intact fuel and is calculated at a burnup of 60 GWd/MTU, an initial enrichment of 3.9 wt. % U-235, and a cooling time of 15.7 years. This table includes the gamma contribution of all four homogenized fuel assembly regions.

The bounding PWR design basis gamma source terms for reconfigured fuel are shown in Table A.5-38 and Table A.5-38a for the inner and peripheral zones, respectively. These source terms are used in both NCT and HAC calculations that utilize reconfigured fuel. The inner zone consists of the inner 21 fuel assemblies, and the peripheral zone consists of the outer 16 fuel assemblies (see Figure A.5-29a). Both sources are calculated at a burnup of 62 GWd/MTU and an initial enrichment of 3.4 wt.%. Fuel with a cooling time of 20.7 years is placed in the inner zone, while fuel with a cooling time of 29.5 years is placed in the peripheral zone.

It is demonstrated in Section A.5.4.1.3.3 that fuel placed in the peripheral zone requires additional cooling time for some BECT combinations in order to meet the HAC dose rate limits. For a burnup of 62 GWd/MTU and an initial enrichment of 3.4 wt. %, Table A.5-53 indicates that 9.0 years of additional cooling time is needed in the peripheral zone. Because the inner zone contains fuel with a cooling time of 21.7 years, the minimum cooling time in the outer zone is then 21.7+9.0 = 29.7 years, which is conservatively rounded down to 29.5 years.

[

]

A.5.2.1.3 69BTH

The spent fuel payload consists of various DSCs with BWR fuel assemblies with or without channels and is specified in Chapter A.1, Appendix A.1.4.7 through A.1.4.9. The source term calculations for DSCs with the BWR fuel payload include the contribution from the channel (Table A.5-8) while the shielding calculations do not take credit for them. This represents conservatism in the gamma dose rate calculations by approximately 15% for fuel assemblies with channels (typically the most representative of all loaded BWR fuel assemblies).

The NCT BWR design basis gamma source for intact fuel is shown in Table A.5-37. This source is calculated at a burnup of 59 GWd/MTU, an initial enrichment of 2.8 wt. % U-235, and a cooling time of 13.7 years. This table includes the gamma contribution of all four homogenized fuel assembly regions.

The bounding BWR design basis gamma source terms for reconfigured fuel are shown in Table A.5-39 and Table A.5-39a for the inner and peripheral zones, respectively. These source terms are used in both NCT and HAC calculations that utilize reconfigured fuel. The inner zone consists of the inner 45 fuel assemblies, and the peripheral zone consists of the outer 24 fuel assemblies (see Figure A.5-29c). Both sources are calculated at a burnup of 62 GWd/MTU and an initial enrichment of 2.6 wt. %. Fuel with a cooling time of 18.5 years is placed in the inner zone, while fuel with a cooling time of 35.0 years is placed in the peripheral zone.

[ ]

It is demonstrated in Section A.5.4.1.3.3 that *reconfigured* fuel placed in the peripheral zone requires additional cooling time for some BECT combinations in order to meet the NCT and HAC dose rate limits. For a burnup of 62 GWd/MTU and an initial enrichment of 2.6 wt.%, Table A.5-52 indicates that *10.5* years of additional cooling time is needed in the peripheral zone. Because the inner zone contains fuel with a cooling time of 18.5 years, the minimum cooling time in the outer zone is then 18.5+*10.5* = *29.0* years.

A.5.2.1.4 Control Components

The spent fuel payload consists of various DSCs with PWR fuel assemblies and associated control components (CCs) and is specified in Chapter A.1, Appendix A.1.4.1 through A.1.4.6. For the PWR fuel assemblies, the various authorized CCs are listed in the above appendices. These include PWR burnable poison rod assemblies *(BPRAs)*, thimble plug assemblies, control rod assemblies, control rod cluster assemblies, axial power shaping rods, orifice rod assemblies, vibration suppression inserts, neutron source assemblies, and neutron sources. The CCs are typically solid or hollow rods of stainless steel or Zircaloy containing neutron absorbing or neutron source materials. Typically, the source term from these CCs is dominated by the Co-60 spectrum. Therefore, a separate material composition and irradiation history is not necessary for characterizing all of these CCs.

Radiological source in Table A.5-18 bounds any CC authorized for loading. The source in this table is referred to as design basis CC source. Guidelines for adjustment of FQT cooling times due to presence of DB CC sources are provided in Section *A.5.5.2.1.*

DB PWR FA *BPRAs* with burnup between 36,000 MWd/MTU and 45,000 MWd/MTU are bounded by the design basis CC source after 8 years decay. All other BPRAs irradiated between 36,000 MWd/MTU and 45,000 MWd/MTU would require 13 years of decay to be bounded by the design basis CC source. All other CCs would need to be examined on a case-by-case basis.

Combinations of radiological sources due DB PWR assembly and the DB CC source result in bounding dose rates when evaluating shielding performance of MP197HB transportation package loaded with DSCs containing PWR FAs with DB CC sources.

A.5.2.1.5 RWC

The NUHOMS®-MP197HB is designed to transport a payload of *56.0* tons of dry irradiated and/or contaminated non-fuel bearing solid materials in the RWC. The safety analysis of the cask takes no credit for the containment provided by the RWC. The quantity of radioactive material is limited to a maximum of 8,182 A_2 (90,000 Ci of Co-60). A list of typical components and their associated activities is shown in Section A.1.4.9A.3.

Co-60 emits two photons per disintegration, one at 1.17 *MeV* and one at 1.33 MeV. *Because Co-60 emits highly energetic photons, 90,000 Ci Co-60 bounds any potential non-fuel bearing solid material for the purposes of dose rate calculations.*

The decay heat load of the radioactive material is expected to be less than 5 kW, which is well below the 26 kW limit for the cask.

A.5.2.1.6 Reconstituted Fuel Assemblies

Reconstituted fuel assemblies are those where one or more fuel rods are replaced with non-fuel rods that displace the same amount of moderator in the active fuel region. Table A.5-6 of the SAR provides material details of a reconstituted fuel assembly where the rods are replaced with solid stainless steel after one cycle of irradiation. This assembly undergoes two additional cycles of irradiation where the source terms of the original and reconstituted fuel assemblies are compared. The summary of these evaluations is discussed in Section A.5.5.2.

A.5.2.2 Neutron Source

The neutron source energy distribution used in the shielding analysis is based on the Cm-244 Watt fission spectrum in the MCNP models. Cm-244 spontaneous fission represents approximately 90% of the neutron source in the active fuel region of the used nuclear fuel. It can be expressed in the following relationship:

$$p(E) \sim \exp\left(\frac{-E}{a}\right)\sinh\sqrt{bE} \ ,$$

where $a = 0.906\,\text{MeV}$ and $b = 3.8486\,(\text{MeV})^{-1}$ [1].

The strength of the neutron sources used in the shielding analysis was calculated using ORIGEN-ARP.

Sub-critical multiplication of the neutron and (n,γ) source terms was developed according to the methodology in Section A.5.4.1.1.4. Neutron peaking factors to account for the burnup dependent, neutron axial profile were developed and discussed in Section A.5.4.1.1.5.

A.5.2.2.1 37PTH

The intact fuel PWR NCT neutron source in the 37PTH DSC is provided in Table A.5-36. This source is calculated at a burnup of 60 GWd/MTU, an initial enrichment of 3.9 wt. % U-235, and a cooling time of 15.7 years. The k_{eff} value used to account for subcritical neutron multiplication is 0.2678 and the peaking factor employed is 1.152.

In calculations with reconfigured fuel, the neutron source term is dominant. The source in the inner zone corresponds to the largest FQT neutron source. The PWR design basis neutron source terms for reconfigured fuel are shown in Table A.5-38 and Table A.5-38a for the inner and peripheral zones, respectively. These source terms are used in both NCT and HAC calculations that utilize reconfigured fuel. The inner zone consists of the inner 21 fuel assemblies, while the peripheral zone consists of the outer 16 fuel assemblies (see Figure A.5-29a). Both sources are calculated at a burnup of 62 GWd/MTU and an initial enrichment of 3.4 wt. %. Fuel with a cooling time of 20.7 years is placed in the inner zone, while fuel with a cooling time of 29.5 years is placed in the peripheral zone. The k_{eff} value used to account for subcritical neutron multiplication is 0.2812 and the peaking factor employed is 1.152.

[**Proprietary Information Withheld Pursuant to 10 CFR 2.390**]

A.5.2.2.2 69BTH

The intact fuel BWR NCT neutron source in the 69BTH DSC is provided in Table A.5-37. This source is calculated at a burnup of 59 GWd/MTU, an initial enrichment of 2.8 wt. % U-235, and a cooling time of 13.7 years. The k_{eff} value used to account for subcritical neutron multiplication is 0.1699 and the peaking factor employed is 1.212.

In calculations with reconfigured fuel, the neutron source term is dominant. The source in the inner zone corresponds to the largest FQT neutron source. The BWR design basis neutron source terms for reconfigured fuel are shown in Table A.5-39 and Table A.5-39a for the inner and peripheral zones, respectively. These source terms are used in both NCT and HAC calculations that utilize reconfigured fuel. The inner zone consists of the inner 45 fuel assemblies, while the peripheral zone consists of the outer 24 fuel assemblies (see Figure A.5-29c). Both sources are calculated at a burnup of 62 GWd/MTU and an initial enrichment of 2.6 wt. %. Fuel with a cooling time of 18.5 years is placed in the inner zone, while fuel with a cooling time of 35.0 years is placed in the peripheral zone. [

] The k_{eff} value used to account for subcritical neutron multiplication is 0.1858 and the peaking factor employed is 1.212.

A.5.2.3 Axial Source Distribution

Source terms are developed for configurations with spent fuel assemblies in two dimensions using the ORIGEN-ARP sequence in SCALE. Axial profiles and peaking factors are employed to transform the source into three dimensions. The peaking factor multiplied by the source strength calculated in two dimensions is applied to the three dimensional MCNP model as the total source

strength. The axial profile in the MCNP model provides the sampling basis in the source description to properly model the distribution. A methodological development of the burnup dependent peaking factors is discussed in Section A.5.4.1.1.5.

A.5.2.3.1 PWR

A.5.2.3.1.1 Gamma

For the intact fuel models, the burnup profile is obtained from Table 2 of NUREG/CR-6801 [16] for burnups greater than 46 GWd/MTU. This burnup profile is replicated in Table A.5-11. The gamma axial source distribution is assumed to be the same as the axial burnup profile. The gamma axial source distribution is also provided normalized to a total of 1.000. When the distribution is normalized to a total of 1.000, the relative number of particles in each zone is represented. For example, in Zone 1 the distribution is 0.0318; therefore, 3.18% of the fuel gamma source is in Zone 1. The axial source distribution is applied to the active fuel in the MCNP models.

For the reconfigured fuel models, the burnup profile is obtained from Table 20 of ORNL/TM-12793 [26] for burnups between 44 and 55 GWd/MTU. This data is replicated in Table A.5-11a. The gamma axial source distribution is assumed to be the same as the axial burnup profile. The gamma axial source distribution is presented normalized to a total of 1.000. The axial source distribution is applied to the active fuel in the MCNP models.

A.5.2.3.1.2 Neutron

The neutron source is proportional to the fourth power of the axial burnup profile, as indicated in NUREG/CR-6802 [22]. The axial burnup profiles are the same as those utilized in Section A.5.2.3.1.1, Gamma. The non-normalized neutron axial source distribution is developed by raising the burnup profile to the fourth power. When the distribution is normalized to a total of 1.000, the relative number of particles in each zone is represented. This normalized profile is also provided. The neutron axial source distributions for intact and reconfigured fuel are provided in Table A.5-11 and Table A.5-11a, respectively. These axial source distributions are applied to the active fuel in the MCNP models.

A different burnup profile is used for reconfigured fuel primarily due to the effect on the neutron axial source distribution. The number of neutrons in the zone closest to the end of the neutron shield (Zone 1) becomes important for reconfigured fuel because the neutron shield stops at the impact limiter and the fuel is compressed in this direction. Comparing the two normalized PWR axial neutron source distributions (compare Table A.5-11 with Table A.5-11a), 0.52% of the neutrons are in Zone 1 in the intact fuel distribution, while 0.8% of the neutrons are in Zone 1 in the reconfigured fuel distribution.

A.5.2.3.2 BWR

A.5.2.3.2.1 Gamma

For the intact fuel models, the axial burnup profile is based on a representative fuel assembly with an average burnup of 40 GWd/MTU. The burnup profile is provided in Table A.5-10 and is divided into 12 axial zones. Rather than simply assume the gamma axial source distribution follows the axial burnup profile, an ORIGEN run is developed for each axial zone, taking account the burnup, water density, and temperature of each zone. The axial gamma source distribution is then derived from the explicit gamma sources from the ORIGEN outputs. The explicitly derived axial source distribution is provided in Table A.5-10. It may be observed that the axial source distribution is almost identical to the axial burnup profile. The gamma axial source distribution is also provided normalized to a total of 1.000. When the distribution is normalized to a total of 1.000, the relative number of particles in each zone is represented. For example, in Zone 1 the distribution is 0.0113; therefore, 1.13% of the fuel gamma source is in Zone 1. The axial source distribution is applied to the active fuel in the MCNP models.

Proprietary Information Withheld Pursuant to 10 CFR 2.390

A.5.2.3.2.2 Neutron

The neutron source is proportional to the fourth power of the axial burnup profile, as indicated in NUREG/CR-6802 [22]. The non-normalized neutron axial source distribution for intact fuel is provided in Table A.5-10 and is developed by raising the gamma axial source distribution to the fourth power (the gamma axial source distribution is nearly identical to the axial burnup profile). The non-normalized neutron axial source distribution for reconfigured fuel is provided in Table A.5-10a and is also developed by raising the axial burnup profile to the fourth power. When the distribution is normalized to a total of 1.000, the relative number of particles in each zone is represented.

A different profile is used for reconfigured fuel primarily due to the effect on the neutron axial source distribution. The number of neutrons in the zone closest to the end of the neutron shield (Zone 1) becomes important for reconfigured fuel because the neutron shield stops at the impact limiter and the fuel is compressed in this direction. Comparing the two normalized BWR axial neutron source distributions (compare Table A.5-10 with Table A.5-10a), 0.009% of the neutrons are in Zone 1 in the intact fuel distribution, while 0.7% of the neutrons are in Zone 1 in the redistributed fuel distribution. This represents a significant shift in the neutron distribution, resulting in conservative dose rates for reconfigured fuel.

A.5.2.4 Axial Blankets

Axial blankets in the fuel are authorized provided the minimum initial enrichment of U-235 in the blanket is 0.7 wt. %. Further, to account for the uncertainty associated with the depletion of

fuel assemblies with large (>5% active fuel length) natural uranium blankets, the fuel qualification is based on the maximum burnup instead of the assembly average burnup.

A.5.2.5 HAC Sources

There are several types of DSCs considered for loading in the transportation cask. The FQTs for each payload are defined so that the total NCT dose rate for intact fuel does not exceed the specified dose rate limit of 8.2 mrem/hr. Therefore, any source from any FQT resulting in the specified dose rate limit of 8.2 mrem/hr can be used to perform the intact fuel NCT shielding analysis. However, the bounding fractions of the total NCT dose rate at the location of interest (2 m from the vehicle) due to the neutron source are different for different BECT combinations, as shown in Figure A.5-21 for the 37PTH DSC and Figure A.5-22 for the 69BTH DSC.

Therefore, for the case when neutron shielding is completely lost or severely degraded during HAC, one would have to maximize D^n for Equation (A.5.29), not just from any FQT but from the FQT having the largest D^n. Among all the radiological sources from all the BECTs in all the FQTs, the radiological source corresponding to 62 GWd/MTU, 2.6 wt. %, 18.5 years cooling in the FQT for the 69BTH DSC payload results in the largest neutron fraction.

This source is appropriate both for HAC analysis and NCT reconfiguration analysis because the neutron component also becomes dominant in the NCT reconfiguration analysis. To reduce the dose rates it is necessary to use a zoned loading configuration. The source described above is used in the inner 45 compartments of the 69BTH DSC, while fuel with the same enrichment and burnup cooled to 35.0 years is placed in the 24 peripheral locations. The 69BTH HAC source terms are provided in Table A.5-39 and Table A.5-39a.

[

]

For the 37PTH DSC, the bounding neutron source occurs at a burnup of 62 GWd/MTU, an initial enrichment of 3.4 wt. % U-235, and a cooling time of 20.7 years. As with the 69BTH DSC, a two-zoned loading is utilized to reduce the dose rates. The inner 21 compartments utilize the maximum neutron source, and the peripheral 16 compartments utilize fuel with the same enrichment and burnup cooled to 29.5 years. The 37PTH HAC source terms are provided in Table A.5-38 and Table A.5-38a.

[

]

A.5.3 Model Specification

A.5.3.1 Configuration of Source and Shielding

The 3-D Monte Carlo computer code MCNP is used for calculating response functions and, the gamma and neutron radiation dose rates for the bounding shielding analysis of the cask [1]. This section provides details of the geometry, material, source term configurations, physics and tallies description employed in the shielding models to determine the dose rates and response functions used for qualification of fuel assemblies for transportation based solely on the dose rate limits.

The model geometry of the shielding configuration can be viewed on Figure A.5-1 through Figure A.5-9*, and Figure A.5-23 through Figure A.5-25*. Thicknesses of the major shielding components of the cask and 69BTH DSC are summarized in Table *A.5-4*.

Variance reduction was accomplished by means of importance zoning in all MCNP models. The importance function was created to keep balance of the particles (per volume) throughout the problem geometry. The process used to do this was an iterative approach starting with basic attenuation factors for the shielding materials. The neutron importance function developed was also applied to the secondary gammas.

The cask is secured in a horizontal position on a skid attached to a railcar or other trailer with a deck or floor during transportation. However, the package and its contents are modeled as a stand alone entity, without any surroundings in computational models for bounding shielding evaluation and determination of the response functions. Therefore, effect of transportation equipment on dose rate distributions below the cask (which can be especially important for the close, less than 2 meters distances) is conservatively not accounted for in the current analysis.

Sections *A.5.3.1.1* and *A.5.3.1.2* describe the shielding model developed for the MP197HB under NCT and HAC, respectively. Described models were used to calculate the axial and radial dose rates in the bounding shielding evaluation. Similar models are used for calculating response functions, with the differences in the description of DSC basket compartments, fuel regions, shielding materials densities and the thickness on ends of the cask, and axial burn-up profile variation (BWR vs. PWR) of the radiological source. Such a difference is due to the fact that the cask is designed for the transportation of the various DSCs designed for BWR and PWR FAs. Presented description of NCT model is applicable to the models employed for calculating response functions used for transportation qualification of BWR assemblies with the difference in number and arrangement of fuel compartments and aluminum transition rails in DSCs. The PWR model is very similar with exceptions for burn-up profile, fuel region materials densities, and composition.

A.5.3.1.1 NCT

The geometry of NCT model for the bounding shielding evaluation is a complete three dimensional simulation of the MP197HB transportation package loaded with 69BTH DSC containing design basis BWR assemblies. The cask, the DSC and its contents are modeled with a discrete representation of the basket and fuel structure. Each fuel assembly is divided into four axial zones. The bottom zone represents the lower end fittings, the middle zone represents the active fuel region and the upper zones represent the plenum and upper end fittings, respectively. The modeled active fuel length is 144 inches for intact fuel and the plenum length is 12.93

inches. The modeled bottom end fitting and top end fitting lengths are 6.65 inches and 12.62 inches, respectively. The fuel, end fittings and plenum are homogenized within each assembly envelope and the axial length of their respective zones. All of the above is applicable to MCNP models used for calculation of the response functions with the exception for axial extents of fuel regions, which are different in the models corresponding to the cask with DSCs containing PWR fuel.

A fuel basket assembly is designed to locate and support fuel assemblies. For NUHOMS® 69BTH, the basket structure consists of welded stainless steel tubes (fuel compartments) separated by aluminum-poison plates. Fuel compartments are arranged in 2 arrays (full 3×3 fuel compartment array and partial 3x3 fuel compartment array) surrounded by stainless steel wrap. These compartment arrays are separated by 0.375" thick aluminum plates. Solid aluminum transition rails centers fuel compartments clusters inside of the DSC. Fuel compartments are modeled as square stainless steel tubes separated by aluminum sheets. Thickness of the compartments and aluminum plates in MCNP model is 0.20" and 0.12", respectively. This description also applies for the MCNP model used for calculation of response function related to MP197HB\69BTH DSC shielding configuration. This is a conservative modeling approach for representing DSC fuel compartments in the shielding calculations.

Proprietary Information Withheld Pursuant to 10 CFR 2.390

External fins for excessive heat dissipation on outer surface of the cask are not modeled. MCNP simulation suggests that it may result in up to 15% (depending on burn-up\enrichment combination from FQT) of conservatism in calculated dose rates.

The borated neutron shielding material (VYAL-B) is embedded into 0.12" thick aluminum boxes. There are 60 such boxes around the side of the cask perimeter between impact limiters. Sides of the boxes adjacent to 2.50" thick cask Outer Shell and 0.375" Shield Shell are modeled as 0.125" thick aluminum cylindrical shells. The neutron shielding resin and the boxes are modeled explicitly. Information regarding the composition of the neutron shielding material is discussed in Section A.5.3.2.1.

Trunnion plugs are assumed to be made from the same neutron shielding material that is on the side of the cask. The same amount of the neutron shielding material of the plugs is assumed lost during HAC on the cask side. The plug is encased with 0.0625" thick steel shell. The shell portion at the bottom of the plug is placed on top of the plug in MCNP models. This preserves the total thickness of the steel on top and the bottom of the plug. Assumed configuration of the trunnion plugs in MCNP models is shown on Figure A.5-7.

Geometry of the grapple ring cut-out on the cask bottom and shear key cut out on the side in MCNP models are shown on sketches of Figure A.5-8 and Figure A.5-9.

The impact limiters are modeled as wood surrounded by a 0.25 in. thick steel shell. The interior steel gussets are conservatively neglected. Wood thickness between end of the impact limiters and the cask ends is 26.25" in MCNP models. The outer diameter is 125.53".

The fuel pins and fuel assembly hardware (end fittings and plenum materials) are homogenized within each assembly envelope and the axial length of their respective axial zones in MCNP models. This is a conservative modeling approach for representing fuel regions in the shielding calculations.

A.5.3.1.2 HAC

Proprietary Information Withheld Pursuant to 10 CFR 2.390

Pages A.5-12c through A.5-12d are proprietary information withheld pursuant to 10 CFR 2.390.

A.5.3.1.3 RWC

The geometry of the RWC and the volume occupied by the irradiated\contaminated hardware are specified in MCNP models using the following assumptions. The canister *is* modeled as a carbon steel cylinder with 70.50" diameter and 189.19" height. The cylinder is centered at the cask axis and it is 2.71" from the cask bottom plug. The thickness of the cylindrical shell on side of the canister is 1.75". Thickness of shield plugs on bottom and top of the canister is 5.75" and 7.00", respectively, as specified in Appendix A.1.4.9A. Radioactive waste occupies only a portion of the inner volume of the canister. It is assumed that the waste is distributed within a cylindrical volume with 66.0" diameter and 168" height. The bottom of that cylindrical region is in contact with the bottom plug of the canister. The rest of the inner volume of the canister is occupied with air.

A.5.3.1.4 Tallies

Bounding dose rates are computed at various distances from MP197HB transportation package. Mesh tallies calculate neutron, primary and secondary gamma radiation dose rates and distributions at various distances from the side and ends of the package. Cylindrical and rectangular mesh types are used. *Dose rate location terminology is shown on Figure A.5-10.*

Locations of mesh nodes are defined either in cylindrical or rectangular (Cartesian) coordinate systems. The Z-axis of the rectangular coordinate system is along the cask axis. The X-axis is on an imaginary plane through the cask axis and trunnions. It is perpendicular to the cask axis. The XZ plane is a horizontal plane and the Y axis runs in vertical elevation when the cask is in the transportation position. Rectangular (X-Y) mesh tallies are used to calculate spatial distributions at distances less than or equal to two meters from the cask ends. Size of the mesh unit segment is 30x30 cm. The central node of the grid is symmetric around the cask axis. The mesh grid extends up to 12 feet from the cask axis in X and Y directions.

The cylindrical (angular-axial) mesh is used for determining the dose rate distribution along the cask side between the ends of impact limiters and at various radial distances from the cask side. The dose rate around the cask is the highest along the cask side, and the cylindrical (angular-axial) mesh tally along the side of the cask between ends of impact limiters was also employed for determining response functions used for fuel assemblies qualification for transportation purpose. The Z-axis of the cylindrical coordinate system coincides with the cask axis. The axial coordinates of the mesh nodes are measured from the end of the bottom impact limiter. The axial distance between nodes of the cylindrical mesh between impact limiters is 32 cm, except for over the shear key cut-out, where the axial distance between nodes is 22 cm, and area over impact limiters. Axial spacing between nodes of the mesh grid over the impact limiters is 33.5 cm. The

angular coordinate is measured in counter-clockwise direction from an imaginary plane through the cask axis and the shear key, which is the YZ plane in the rectangular coordinate system. For the dose rates at less than or equal to two meters from the cask side, segmentation of the angular coordinate is performed to keep an arch length on the cylindrical grid constant (~30 cm).

A.5.3.1.5 Physics Specification

Upper energy limit for detailed photon physics treatment during MCNP calculation is set to 20.0 MeV. Photons with energy less than 0.001 MeV are cut off. This covers energy spectrum from the fuel assemblies in storage or qualified for transportation. Physics photon treatment accounts for coherent scattering and Doppler energy broadening. It does not account for bremmstrahlung and photonuclear collisions photons because dose rates are negligible from gamma radiation sources at energy less than 0.8 MeV and greater than 5.0 MeV, respectively. MCNP default parameters for neutron transport physics are used: no lower cut off or upper limit for the neutron source energy, neutrons are treated with implicit capture, *and* no delayed neutrons since the fission is turned off by using *nonu* card in MCNP input decks for neutron transport. *Subcritical multiplication is accounted in the neutron and (n,γ) sources as discussed in Section A.5.2.2 and Section A.5.4.1.1.4.*

A.5.3.2 *Material Properties*

The following materials were used in the development of the models of the MP197HB transportation package and its associated authorized conents for the purpose of evaluating the external dose rates.

A.5.3.2.1 VYAL-B

The borated neutron shielding material (VYAL-B) is a vinylester resin mixed with alumina hydrate and zinc borate which is added for their fire retardant properties. The elemental composition of the VYAL-B resin is shown in Table A.5–5. Additional notes regarding the use of this material are discussed in Section A.5.5.1.

A.5.3.2.2 RWC Assumed Composition

It is assumed the elemental composition of the smeared material *in the RWC* is identical to that of carbon steel. The density of smeared material is 1.0 g/cc in MCNP models. The material modeling consideration employed reasonably represents irradiated non-fuel hardware.

A.5.3.2.3 Homogenized Assembly Materials

The fuel assembly is homogenized into four source regions as described in Section A.5.4.1.1.1. The resulting composition and densities of these regions are shown in Table A.5-12 for the BWR and PWR DBFA described in Section A.5.2.

A.5.3.2.4 Shielding Materials

The elemental composition and densities of the materials used for the package evaluation beyond the neutron shielding and fuel assembly are shown in Table A.5-13.

A.5.4 Evaluation

A.5.4.1 Methods

The following sections describe individual methods used in the evaluation of the MP197HB transportation package.

A.5.4.1.1 Source Methodology

Developing the source requires the use of several different methods and programs to evaluate the authorized contents are acceptable for use and the MP197HB transportation package dose rates are below the regulatory limits as shown in Section A.5.1.3.1.

For the purposes of this section, design basis source may refer to the bounding PWR or BWR assemblies, as the method to generate the sources is equivalent.

A.5.4.1.1.1 Source Homogenization

For the dose calculation around the MP197HB, the source is divided into four separate regions: fuel, plenum, top end fitting, and bottom end fitting for primary gammas. For neutrons, the source is only the active fuel region. The densities of the homogenized regions are calculated by summing all of the material in the region and dividing by the volume. This volume spans the volume of a cuboid that spans the outer envelope of the fuel assembly. The spacing between the fuel pins or other components of the fuel assembly is included in the homogenized volume.

Homogenized assembly region compositions for the BWR *and PWR* design basis fuel assembl*ies* are described in Section A.5.3.2.3.

A.5.4.1.1.2 Burned Fuel Isotopic Composition

Proprietary Information Withheld Pursuant to 10 CFR 2.390

Proprietary Information Withheld Pursuant to 10 CFR 2.390

A.5.4.1.1.3 TRITON validation

The TRITON/T-DEPL sequence of SCALE has been validated against publicly available information to assess the uncertainties associated with the source terms.

Almost 100% of the gamma spectrum from light elements is in the range of 0.70 to 1.33 MeV which corresponds exactly to the two most prominent lines of Co-60. Shortly after discharge the emission at higher energies is dominated by actinides. This is true for energies >4 MeV at all cooling times and energy above 3.5 MeV for cooling times greater than 10 years [17]. As for fission products, the main contributors after six years with a fraction greater than 5% in the range of 0.01 to 0.90 MeV are: Sr-90, Y-90, Rh-106 (Ru-106), Cs-137, Pr-144 (Ce-144), Eu-154, and Eu-155. Contributions from Y-90, Rh-106, Cs-137, Pr-144, and Eu-154 are dominant in the range of 0.90 to 1.50 MeV. Rh-106 (Ru-106), Sm-147, Ce-142 and Pr-144 (Ce-144) are the strongest emitters at energies greater than 2.0 MeV. The accuracy of the gamma spectrum is dependent upon the energy. Photon rates computed for fission products tend to be more accurate than those for actinides because the calculation of their inventory has less uncertainty [17].

At discharge, the neutron source is almost equally produced from Cm-242 and Cm-244. The other strong contributor is Cf-252, which is approximately 1/10 of the Cm intensity, but its share vanishes after 6 years of cooling time because the half-life of Cf-252 is 2.65 years. The half-lives of Cm-242 and Cm-244 are 163 days and 18 years, respectively. Contributions from the next strongest emitters, Pu-238 and Pu-240, are lower by a factor of 1000 and 100, respectively, relative to Cm-244. For the ranges of exposures, enrichments, and cooling times in the fuel qualification tables, Cm-244 represents more than 90% of the total neutron source. The neutron spectrum is, therefore, relatively constant for the fuel parameters addressed herein.

The benchmark evaluation is performed using publicly available data provided in reference [19] for fuel samples obtained from the Calvert Cliffs, TMI, and Takahama reactors, reference [21] for high burnup fuel obtained from the Vandellos reactor, and reference [20] for fuel samples obtained from Gosgen and GKN II reactors. The burnup and enrichment combinations evaluated are representative of the combinations analyzed for fuel transport in the MP197HB. *A summary of the experimental samples utilized in the benchmark evaluation is provided in Table A.5-41a.*

Pages A.5-16a through A.5-19 are proprietary information withheld pursuant to 10 CFR 2.390.

Proprietary Information Withheld Pursuant to 10 CFR 2.390

A.5.4.1.1.6 Flux Factors

Fuel assembly hardware is also included in the source term calculation. The hardware source term is primarily due to Co-60. The fuel assembly hardware material masses are provided in Table A.5-6 and Table A.5-7 for PWR and BWR fuel, respectively, and the compositions used to compute the light element masses are provided in Table A.5-9. To account for the reduced neutron flux in the non-active fuel regions of the homogenized assembly, flux factors are employed to scale the light element masses of those regions in the ORIGEN-ARP input. The masses for the materials in the top end fitting, the plenum, and the bottom fitting regions are multiplied by 0.1, 0.2, and 0.15, respectively [15] in the BWR FA model. The PWR FA model uses the same flux factors for the top fitting and plenum, and 0.2 for the bottom fitting [15].

Proprietary Information Withheld Pursuant to 10 CFR 2.390

Pages A.5-20a through A.5-27 are proprietary information withheld pursuant to 10 CFR 2.390.

Proprietary Information Withheld Pursuant to 10 CFR 2.390

A.5.4.1.3 Fuel Qualification Methodology

The fuel qualification methodology is a process by which authorized contents are verified to be bounded by their respective design basis. The method ties together many different components in a way that efficiently ranks sources based on their corresponding dose rate at the most critical location. The critical location is defined to be the location where, if the critical location meets the regulatory dose rate limits, all other regulatory dose rate limits would be met. For the purposes of the shielding analysis of the MP197HB transportation package, the critical location is at the active fuel midplane, two meters from the projected vertical side surface of the vehicle. This is also referred to as the *location of interest* in the current chapter. For the purposes of fuel qualification, the output from the method generates equivalent sources that result in the same dose rate at any location along the package.

For discussion, the methodology can be split into two parts. As shown in the response function methodology, Section A.5.4.1.2, and specifically, equation (A.5.25*a, b, and c*), both the source and the set of linear, energy-dependent response functions must be known in order to determine the dose rate using this method.

A.5.4.1.3.1 Response Function

The MCNP model for NCT was utilized to calculate a response function at 2 meters from the transportation vehicle. The MCNP model specification regarding axial *burnup* profile variation along in-core axial region of fuel and correction to neutron source strength due to the *burnup* profile variation, treatment of neutron subcritical multiplication, described earlier in Section A.5.2.1 *through* Section A.5.2.3 *are* applicable. MCNP model description in Section A.5.3 regarding radial shielding configuration of the cask and 69BTH DSC, physics specification is applicable.

Considerations and a specification of cylindrical (with *"angular-axial"* segmentation) mesh tallies set up along side of the cask between ends of impact limiters at 2 meters radial distance from surface of impact limiters provided in Section *A.5.3.1.4* is applicable. Fine axial and angular segmentation with 20 axial and 71 angular segments are used, respectively. Size, (*axial length* × *arc length*), of the cylindrical mesh tally grid segments is approximately 34x32 cm. and 38x32 cm over the cask side between impact limiters and over impact limiters, respectively.

Fuel assemblies are grouped by certain radial zones in a description of the radiological sources in MCNP models for calculating response functions. The zoning scheme is very similar to that employed for definition of heat loading zones in DSCs loading options provided in Section A.1.4. There are three and four radial zones for DSCs containing PWR and BWR FAs, respectively. The inner zone encompasses fuel assemblies in 4 central compartments of 24PT4, 24PTH, 32PT, 32PTH and 32PTH1 DSCs and 9 central compartments of 37PTH DSC and DSCs containing BWR FAs. Such a definition of response functions provides flexibility in increasing the overall radiation capacity of the system. Results indicate that more than 93% of the radial dose rates around the cask are due to fuel assemblies in outer radial zones. Therefore, it would be possible to increase the source terms for the fuel assemblies located in the inner zone by a factor of 2.0 and still do not significantly increase the overall dose rate distribution around the cask due to self-shielding provided by the surrounding assemblies.

For each radial zone, response function entries are calculated for neutron, secondary gamma and the following 4 primary gamma radiation energy groups:

- 1.00 – 1.33 MeV,
- 1.33 – 1.66 MeV,
- 2.00 – 2.50 MeV,
- 2.50 – 3.00 MeV.

Response functions are calculated with MCNP for each cask\DSC shielding configuration. Entries of the response functions are essentially source to dose conversion factors as a function of energy (for gamma). The "conversion factors" corresponding to neutron radiation source are multiplied by "*peaking*" factors to account for the axial *burnup* profile of the fuel and subcritical *neutron* multiplication to obtain the response functions that are used for the fuel qualification evaluation. For neutrons and associated (n,γ) radiation, since a bounding energy spectrum is used, the response function calculated is just a total source to dose factor.

Alternatively, the response functions can be thought of as a 2D matrix which converts a source vector to a dose vector. The components of the dose vector are the dose rate values at the various angular and axial locations around the transportation package. The fuel qualification methodology is to select sources such that the largest component of the dose rate vector does not exceed 8.2 mrem/hr.

Results of the fuel qualification methodology are shown in Section A.5.5.2 for the MP197HB transportation package.

A.5.4.1.3.2 Source

The source portion of the fuel qualification method first requires that the proposed contents be known. Specifically, all the physical parameters of the fuel assembly, included isotopic composition of all the materials, should be well understood. The design basis assembly is depleted using the TRITON/T-DEPL sequence of SCALE to create an ORIGEN-ARP library for that specific assembly type. As the assembly is burned to generate the source, operational parameters such as assembly specific power and duration of cycle are controlled to bound the source as well as get the appropriate burnup.

The result of the application of this portion of the fuel qualification method is a primary gamma source for the four homogenized burned assembly regions as described in Section A.5.4.1.1.1, a primary neutron source, and a (n,γ) source.

A.5.4.1.3.3 Additional Cooling Time for Reconfigured Fuel

[

]

Pages A.5-29b through A.5-29f are proprietary information withheld pursuant to 10 CFR 2.390.

Proprietary Information on This Page
Withheld Pursuant to 10 CFR 2.390

A.5.4.1.3.4 Cooling Time Derivation for 69BTH DSC using Heat Load Zone Configuration 8

[

]

A series of verification cases are run for both NCT and HAC configurations using Heat Load Zone Configuration No. 8 to ensure that FQT based cooling times comply with NCT and HAC dose rate limits.

A.5.4.1.4 Dose Calculation Methodology

MCNP5 v1.40 is used for the shielding analysis [1]. MCNP5 is a standard, well-accepted shielding program utilized to compute dose rates for radiation protection. A three-dimensional model is developed that captures all of the relevant design parameters of the package. Dose rates are calculated by tallying the neutron and gamma fluxes over surfaces of interest and converting

these fluxes to dose rates using flux-to-dose rate conversion factors as described in Section A.5.4.2. Secondary gammas resulting from neutron capture are also tallied.

Separate models are developed for neutron and gamma source terms. Simple Russian roulette is used as a variance reduction technique for most tallies and geometric based splitting.

A loaded NUHOMS®-24P in the HSM Model 80 loaded with B&W 15x15 Mark B fuel was compared against an MCNP model of the same. The MCNP model was developed to calculate dose rates at the locations where the dose rates were measured on the real system. The results of this comparison are shown in Table A.5-49 as reproduced from Chapter M.5 of the Standardized NUHOMS® System UFSAR [23]. This validation was previously employed to qualify the MCNP methodology for the Standardized NUHOMS® System. The results show that MCNP conservatively predicts total dose rates compared to the measured data. Some conservatism in the methodology used to calculate the source terms still exists and likely contributed to the general over-prediction of the calculated dose rates when compared to the measured dose rates.

MCNP5 was also benchmarked using data from the TN-68 storage system [24]. This is performed by comparing measured dose rates to calculated dose rates at the

surface of the TN-68 cask at the approximate mid-plane of the active fuel. The results of these comparisons are shown in Table A.5-48 and confirm that the MCNP dose rate calculation methodology employed does not add any adverse uncertainty.

The fuel qualification methodology, as described in Section A.5.4.1.3 is also used to generate dose rates for specific configurations as validated by the response function methodology, described in Section A.5.4.1.2. Results of the fuel qualification methodology are discussed in Section A.5.5.2.

A.5.4.2 Flux-to-Dose-Rate Conversion

ANSI/ANS-6.1.1-1977 flux-to-dose rate conversion factors are utilized for both gamma and neutron radiation [4]. These factors are provided in Table A.5-16 and Table A.5-17, respectively.

A.5.4.3 Radiation Levels

A.5.4.3.1 Shear Key

As a result of the shear key cut-out on the side of the cask, the shielding properties in this area vary significantly. Depending on the neutron or gamma radiation source contribution to the total dose rate, the position of the maximum dose rate along the cask side may vary depending not only on axial but also the angular location. The transport cask shear key faces down during the transport. Neutron radiation streaming through the shear key cut-out of the neutron shielding on side of the cask will be within a solid angle not encompassing the accessible area near the transportation package. Therefore, the maximum dose rates determined with cylindrical mesh tallies around the cask side and reported in this chapter are at angular coordinates marked on Figure A.5-6 with P_x, where P_x corresponds to some angular coordinate between 0.25 and 0.75 rotations (including $P_{0.25}$ and $P_{0.75}$) if measuring counter clockwise from an imaginary plane through the cask axis and the shear key (which is designated with P_o on Figure A.5-6). The similar applies to interpretation of dose rates obtained with the response functions during qualification of assemblies for transportation. Due to symmetry of the dose rate distribution, dose rates angular coordinate between 0.25 and 0.50 rotations (including $P_{0.25}$ and $P_{0.50}$) were considered during the qualification.

There is noticeable neutron radiation streaming through the transport cask shear key. On the other hand, when the cask is at a transportation condition the shear key faces down. There is also additional shielding from a trailer or railcar skid and deck. It is observed from the analysis of the shielding configuration with a metal cask on a trailer platform that radiation from bottom portion of the cask side, scattering from concrete surface on the ground is not significant at distances greater than 1 meter from outside boundary of the transportation package. Therefore it is justified to use mesh tally segments located at top quadrants of the cylindrical mesh when considering dose rates along the cask between ends of impact limiters. Since the radiological source term distribution inside of the cask is symmetric in the computation models, only segments within top quadrant(s) of the cylindrical mesh tallies are considered to locate the maximum.

When the cask is in the vertical position the shear key cut-out is closed with the shear key plug made of steel and the same neutron shielding material as on the cask side. Prior to being rotated to the horizontal position and placed on the transport platform, the shear key plug is removed. When the cask is positioned horizontally on the transporter the shear key cut out fits over the steel shear key on the transporter platform. When the cask is removed from the transport platform, the shear key plug is reinstalled.

A.5.4.3.2 NCT Fuel Reconfiguration

Proprietary Information Withheld Pursuant to 10 CFR 2.390

Pages A.5-32 through A.5-32b are proprietary information withheld pursuant to 10 CFR 2.390.

A.5.5 Appendix

A.5.5.1 VYAL-B Mixing and Installation

Proprietary Information Withheld Pursuant to 10 CFR 2.390

A.5.5.2 Fuel Qualification Results

An evaluation was performed using the methodologies described in Section A.5.4 as appropriate for fuel assembly parameters of burnup, percent initial enrichment U-235 and cooling time that would result in normal conditions of transport dose rate at 2.0 meters from the *vehicle* side not exceeding 8.2 mrem/hr. The results are expressed in tabular format showing the minimum required cooling times as a function of enrichment and burnup. Such tables are referred to as Fuel Qualification Tables (FQTs).

After the cooling times to meet 8.2 mrem/hr dose rate requirement were determined, they were rounded up to the nearest 0.5 year in the final transportation FQTs. For example 5.1 is rounded up to 5.5, 8.8 is rounded up to 9.0, etc.

Due to shielding properties of the cask and concentration of most of the radiological source strength in in-core region, dose rate values along the cask side between impact limiters are larger than dose rates at the same distances from ends of impact limiters, regardless of the fuel assembly types loaded, conditions of transport (NCT or HAC) and DSC types. Therefore, in general, if dose rates along the side of the package comply with conditions of transport dose rate restrictions specified at the end of Section A.5.1.3.1, it indicates that shielding performance of the cask meets the regulatory requirements.

The transportation FQTs are, therefore, a set of acceptable combinations of burnup, enrichment, and cooling times such that the expected NCT dose rates at two meters from the cask are the same, regardless of the canister type contained inside of the cask. Therefore, no bounding set of NCT source terms are generated – rather all the source terms are expected to result in similar dose rates – bounded only by the maximum dose rate limits.

The transportation FQT dose rates for all bounding authorized contents are shown in Table A.5-21 through Table A.5-30 for the authorized DSCs in the MP197HB transportation package as described in Section A.1.2.3 and Appendices A.1.4.1 through A.1.4.9. *The transportation FQT for the 69BTH using Heat Load Zone Configuration 8 is shown in Table A.1.4.9-5b of Section A.1.4.9.*

A.5.5.2.1 Fuel Qualification Adjustment for Control Components

The spent fuel assemblies transported in the cask may contain irradiated fuel inserts (BPRA, TPA, etc.). They are referred to as control components (CCs). Control components are also allowed to be stored or transported along with fuel assemblies. CCs include burnable poison rod assemblies (BPRAs), thimble plugs, neutron sources, control rods, etc. It is assumed in the assemblies' qualification that they are not necessarily bound to any specific fuel assembly and can be removed from the assembly in which they were generated. It is expected that, for example, a 3 year cooled assembly can be mixed with a 13 year cooled CC or 17 years cooled FA can be mixed with 15 years cooled CCs.

From the shielding stand point, it is permissible to place CCs in any number of the fuel compartments not in a periphery, in any DSC Transport Cask shielding configuration. CCs in those compartments may affect a shape of the dose rates distribution near the transportation package but they will have a negligible effect on the dose rate maximums at the location of interest. When the CC sources are in outer peripheral DSCs' fuel compartments, the dose rate increase is entirely due radiation in 1.00 to 1.66 MeV energy range.

The following guidelines should be applied when fuel assemblies with CCs are considered for transportation in MP197HB transportation cask.

- CCs include burnable poison rod assemblies (BPRAs), thimble plugs, neutron sources, control rods, etc.
- CCs are not necessarily bounded to any specific fuel assembly and can be removed from the assembly in which they were generated. It is expected that, for example, a 3 year cooled assembly can be mixed with a 13 year cooled CC or 17 years cooled FA can be mixed with 15 years cooled CC, etc.
- The maximum number of fuel assemblies with CCs that can be loaded per DSC is equal to the number of assemblies per DSC.
- Additional cooling time is required for assemblies only in peripheral locations of the DSCs. There are 12 peripheral compartments in DSCs with 24 FA locations and 16 peripheral compartments in DSCs with 32 or 37 locations. Number of peripheral fuel compartments in DSCs containing BWR FAs is 24. The peripheral fuel compartments are shown in Figures A.5-28 through A.5-29c.
- No additional cooling time is required for assemblies with CCs in 24PT4 DSC because the transportation FQT already accounts for presence of 24PT4 design basis CC sources.

- A matrix shown in Table *A.5-33* provides additional cooling times at selected cooling times of CCs. The additional times shown are bounding even when all the fuel outer peripheral compartments contain CCs.
- For PWR fuel assemblies containing CCs, no additional cooling time is needed when they are loaded with cooling times greater than or equal to 15 years.

Note: the guidelines are based **only** on shielding performance evaluation.

A.5.5.2.2 Fuel Qualification Adjustment for Assemblies with Damaged or Reconstituted Rods

The following guidelines should be applied when fuel assemblies with reconstituted rods are considered for transportation in the MP197HB Transportation Cask:

- The maximum number of reconstituted fuel assemblies that can be loaded per DSC is equal to number of assemblies per DSC.
- PWR fuel assemblies may contain up to 10 rods and BWR fuel assemblies may contain up to four rods that are reconstituted with stainless steel that is irradiated.
- There is no limit on a number of rods reconstituted with un-irradiated stainless steel or Zircaloy or low enriched (lower than of an original, un-reconstituted, FA), natural uranium, UO_2 or other non-fuel material.
- There is no effect on the source terms due to the position of the reconstituted rods in the fuel rod array.
- Additional cooling time is required for assemblies in outer peripheral fuel compartments only. *The peripheral fuel compartments are shown in Figures A.5-28 through A.5-29c.*
- For cooling times greater than or equal to 10 years no extra cooling is required and the FQT cooling times for un-reconstituted FAs are also applicable for reconstituted FAs.
- One more year of cooling time is required for reconstituted fuel assemblies cooled for less than 10 years and located in outer peripheral fuel compartments.
- The maximum number of fuel assemblies with irradiated stainless steel reconstituted rods is restricted to four (Chapter A.1, Appendix A.1.4.1 through A.1.4.9) thereby ensuring that the analysis is conservative.

Note: the guidelines are based **only** on shielding performance evaluation.

A.5.5.3 Decay Heat Restrictions

The various DCS payloads allowed for transportation in the MP197HB cask have individual decay heat load limitations. There are numerous DSC loading options to meet those restrictions.

Decay heat values for various discrete decay heat power levels per fuel assembly can be obtained using the decay heat equations.

The decay heat equation (DHE) is established to calculate the decay heat of spent fuel assemblies as a function of enriched, burnup, and cooling time. Two DHEs are established: for BWR (maximum of 0.198 MTU) and PWR (maximum of 0.490 MTU) fuel assemblies. Decay heat data sets for various burn-up, enrichment and cooling time combinations are generated using DB BWR and DB PWR FA SAS2H\ORIGEN-S models *[17]*. A non linear regression analysis was performed on those data sets to obtain a fit of BWR and PWR decay heat data as a function of burnup, enrichment and cooling time. An uncertainty of 10 and 20 watts should be added to the calculated with the DHE decay heat values for BWR and PWR FAs when using the equations, respectively. These values are 2.5 and 2.3 times the standard deviations from the corresponding regression calculations. These uncertainties ensure that the calculated decay heat values from the DHEs are bounding for the DB BWR and PWR FAs. *T*he DHEs are established on data relevant to DB FAs. *As a result,* the equations predict conservative decay heat values for all other FA designs.

Thermal power was validated in reference [18]. The results show that the decay heat predicted by ORIGEN-S is within the range of uncertainty of the measurements in the reference. Specifically, the mean error was shown to be 0.7 W with an uncertainty of 17.6 W. Additionally, very similar calculated results were obtained using SAS2H and TRITON physics models. The difference was found to be less than 2% between the sequences.

A.5.5.3.1 BWR Decay Heat Equation

A nonlinear regression analysis was performed to obtain a fit of the BWR decay heat data as a function of burnup, initial enrichment, and cooling time. A very good fit was obtained based on an iterative evaluation using a 9-parameter model. The functional form is expressed below.

The decay heat (DH) in watts is expressed as:

$$DH_{BWR} = F_1 \exp\left[G\left(1 - \frac{1.2}{x_3}\right)(x_3 - 4.5)^H \left(\frac{x_2}{x_1}\right)^I \right] + 10,$$

where,

- $F_1 = A + Bx_1 + Cx_2 + Dx_1^2 + Ex_1x_2 + Fx_2^2$,
- x_1 equals the assembly average burnup in GWd/MTU,
- x_2 equals the initial enrichment in wt. % U-235,
- x_3 equals the cooling time in years,
- $A = -59.1$,
- $B = 23.4$,
- $C = -21.1$,
- $D = 0.280$,
- $E = -3.52$,
- $F = 12.4$,
- $G = -0.720$,
- $H = 0.157$, and
- $I = -0.132$.

The calculation uncertainty is 10 watts. It is added to the equation above as the last term. The minimum cooling time for *decay* heat calculation is 5 years.

Alternatively, the decay heat can be calculated without employing the decay heat equation, using an approved methodology with actual spent fuel parameters instead of bounding spent fuel parameters.

A.5.5.3.2 PWR Decay Heat Equation

A nonlinear regression analysis was performed to obtain a fit of the PWR decay heat data as a function of burnup, initial enrichment, and cooling time. A very good fit was obtained based on an iterative evaluation using a 9-parameter model. The functional form is expressed below.

The decay heat (DH) in watts is expressed as:

$$DH_{PWR} = F_1 \exp\left[G\left(1 - \frac{1.8}{x_3}\right)(x_3 - 4.5)^H \left(\frac{x_2}{x_1}\right)^I \right] + 20,$$

where,

- $F_1 = A + Bx_1 + Cx_2 + Dx_1^2 + Ex_1x_2 + Fx_2^2$,
- x_1 equals the assembly average burnup in GWd/MTU,
- x_2 equals the initial enrichment in wt. % U-235,
- x_3 equals the cooling time in years,
- $A = -44.8$,
- $B = 41.6$,
- $C = -37.1$,
- $D = 0.611$,
- $E = -6.80$,
- $F = 24.0$,
- $G = -0.575$,
- $H = 0.169$, and
- $I = -0.147$.

The calculation uncertainty is 20 watts. It is added to the equation above as the last term. The minimum cooling time for *decay* heat calculation is 5 years.

Alternatively, the decay heat can be calculated without employing the decay heat equation, using an approved methodology with actual spent fuel parameters instead of bounding spent fuel parameters.

A.5.5.4 Fission gas for BWR fuel at 70 GWd/MTU

The bounding quantity of gases released as a result of irradiation for the "generic" GE 7x7 BWR fuel assembly is evaluated.

Since the amount of released fission gases is conservative on the basis of lowest enrichment for a given burnup, the quantity of gases released is evaluated for a burnup and enrichment combination of 70 GWd/MTU and 3.70 wt% initial U-235, per BWR FQT in Tables A.1.4.9-4 to A.1.4.9-5a.

The total bounding amount of moles of gases released as a result of irradiation for one fuel assembly is presented in Table A.5-35; data presented in the table corresponds to 3.0 and 5.0 years of cooling time and 0.198 MTU.

The amount of gas produced for a "generic" BWR fuel assembly, 0.198 MTU, at 70 GWd/MTU, 3.70 wt% initial U-235 is 23.0 g-moles.

A.5.6 References

1. MCNP/MCNPX – Monte Carlo N-Particle Transport Code System Including MCNP5 1.40 and MCNPX 2.5.0 and Data Libraries, CCC-730, Oak Ridge National Laboratory, RSICC Computer Code Collection, January 2006.

2. SCALE 6: Modular Code System for Performing Standardized Computer Analyses for Licensing Evaluation for Workstations and Personal Computers, Oak Ridge National Laboratory, Radiation Shielding Information Center Code Package CCC-750, February 2009.

3. Title 10, Code of Federal Regulations, Part 71, *Packaging and Transportation of Radioactive Materials.*

4. American Nuclear Society, ANSI/ANS 6.1.1, *American National Standard for Neutron and Gamma-ray Flux to Dose Factors,* La Grange Park, IL, 1977.

5. *Deleted.*

6. *Deleted.*

7. Lewis, E.E. and W.F. Miller, Jr. Computational Methods of Neutron Transport. La Grange Park, Ill.: American Nuclear Society, Inc., 1993.

8. Bell, George I. and Samuel Glasstone. Nuclear Reactor Theory. New York: Van Nostrand Reinhold Company, 1970.

9. Duderstadt, James J. and Louis J. Hamilton. Nuclear Reactor Analysis. Hoboken, New Jersey: John Wiley and Sons, Inc., 1976.

10. Duderstadt, James J. and William R. Martin. Transport Theory. New York: John Wiley and Sons, Inc., 1979.

11. Shultis, J. Kenneth and Richard E. Faw. Radiation Shielding. La Grange Park, Ill.: American Nuclear Society, Inc., 2000.

12. Knoll, Glenn F. Radiation Detection and Measurement, 3rd ed. Hoboken, New Jersey: John Wiley and Sons, Inc., 2000.

13. *Deleted.*

14. *Deleted.*

15. Luksic, "Spent Fuel Assembly Hardware: Characterization and 10 CFR 61 Classification for Waste Disposal," PNL-6906, UC-85, June 1989.

16. NUREG/CR-6801 (ORNL/TM-2001/273), March 2003, "Recommendations for Addressing Axial Burnup in PWR Burnup Credit Analyses."

17. SCALE 4.4, "Modular Code System for Performing Standardized Computer Analyses for Licensing Evaluation for Workstations and Personal Computers," CCC-545, ORNL.

18. NUREG/CR-6972, February 2010, "Validation of SCALE 5 Decay Heat Predictions for LWR Spent Nuclear Fuel," ORNL.

19. U.S. Nuclear Regulatory Commission, "Analysis of Experimental Data for High Burnup PWR Spent Fuel Isotopic Validation—Calvert Cliffs, Takahama, and Three Mile Island Reactors," NUREG/CR-6968, Published February 2010, ORNL-TM-2008-71.

20. U.S. Nuclear Regulatory Commission, "Uncertainties in Predicted Isotopic Compositions for High Burnup PWR Spent Nuclear Fuel," NUREG/CR-7012, Published January 2011, ORNL-TM-2010-41.

21. U.S. Nuclear Regulatory Commission, "Analysis of Experimental Data for High-Burnup PWR Spent Fuel Isotopic Validation — Vandellós II Reactor," NUREG/CR-7013, Published January 2011, ORNL-TM-2009-321.

22. NUREG/CR-6802 (ORNL/TM-2002/31), May 2003, "Recommendations for Shielding Evaluations for Transport and Storage Packages."

23. Updated Final Safety Analysis Report for the Standardized NUHOMS® Horizontal Modular Storage System for Irradiated Nuclear Fuel, NUH-003, Rev. 12.

24. Transnuclear, Inc., "TN-68 Dry Storage Cask, Updated Final Safety Analysis Report," Revision 6. Certificate of Compliance No. 1027.

25. NOK Document "Technical Specification for the Supply of Transportable Casks for the Storage of Kernkraftwerk Leibstardt (KKL) Spent Fuel in ZWILAG." TS 07/01, Rev. 1.

26. M. D. DeHart, "Sensitivity and Parametric Evaluations of Significant Aspects of Burn-up Credit for PWR Spent Fuel Packages," ORNL/TM-12973, Lockheed Martin Energy Research Corp., Oak Ridge National Laboratory, May 1996.

27. NUREG/CR-6835, September 2003, "Effects of Fuel Failure on Criticality Safety and Radiation Dose for Spent Fuel Casks."

28. U.S. Nuclear Regulatory Commission, "NRC Draft Regulatory Issue Summary 2015-XX Considerations In Licensing High Burnup Spent Fuel in Dry Storage and Transportation.", Regulations.gov. Document ID: NRC-2015-0047-0002. Accessed April 27, 2016. URL: https://www.regulations.gov/document?D=NRC-2015-0047-0002 (NRC ADAMS Accession Number, ML14175A205).

Table A.5-1
Summary of MP197HB NCT Dose Rates for Intact Fuel

(Exclusive Use Package for Transportation)

37PTH DSC in the MP197HB Transportation Package			
Vehicle (Package) Surface[2] (mrem/hr), Limit = 200 mrem/hr			
	Top End	**Side**	**Bottom End**
Gamma	1.00 ± 0.056	24.5 ± 0.74	2.29 ± 0.025
Neutron	3.79 ± 0.10	*45.37 ± 1.01*	9.99 ± 0.13
(n,g)	1.54 ± 0.023	9.82 ± 0.098	4.29 ± 0.035
Total[1]	6.33 ± 0.12	*53.02 ± 1.02*	16.6 ± 0.13
2 m from Vehicle Surface (mrem/hr), Limit = 10 mrem/hr			
	Top End	**Side**	**Bottom End**
Gamma	0.243 ± 0.020	2.35 ± 0.071	0.335 ± 0.0041
Neutron	0.773 ± 0.019	4.75 ± 0.067	1.54 ± 0.022
(n,g)	0.177 ± 0.0044	1.74 ± 0.016	0.488 ± 0.0044
Total[1]	1.06 ± 0.032	8.25 ± 0.085	2.36 ± 0.023

69BTH DSC in the MP197HB Transportation Package			
Vehicle (Package) Surface[2] (mrem/hr), Limit = 200 mrem/hr			
	Top End	**Side**	**Bottom End**
Gamma	1.67 ± 0.15	*19.52 ± 0.56*	8.25 ± 0.073
Neutron	1.55 ± 0.037	*37.49 ± 0.65*	9.82 ± 0.11
(n,g)	0.731 ± 0.010	8.29 ± 0.06	4.15 ± 0.025
Total[1]	3.62 ± 0.041	*46.10 ± 0.72*	22.2 ± 0.013
2 m from Vehicle Surface (mrem/hr), Limit = 10 mrem/hr			
	Top End	**Side**	**Bottom End**
Gamma	0.344 ± 0.0040	3.86 ± 0.11	0.972 ± 0.013
Neutron	0.504 ± 0.0092	3.36 ± 0.045	1.47 ± 0.023
(n,g)	0.119 ± 0.0027	1.35 ± 0.011	0.464 ± 0.0030
Total[1]	0.917 ± 0.037	8.16 ± 0.10	2.91 ± 0.026

1. The total is not necessarily the sum of the corresponding dose rates listed. The total is the greatest total dose rate at any location, while the components of the dose rates are the respective maxima and may occur at different locations.
2. Dose rates are computed on the surfaces of the impact limiters and on the surface of the neutron shield. These package surface dose rates are conservatively reported as vehicle surface dose rates.

Table A.5-1a
Summary of MP197HB NCT Dose Rates for Reconfigured Fuel, 50% Void Fraction
(Exclusive Use Package for Transportation)

37PTH DSC in the MP197HB Transportation Package			
Vehicle (Package) Surface[1] (mrem/hr), Limit = 200 mrem/hr			
	Top End	**Side**	**Bottom End**
Gamma	0.154 ± 0.015	*0.844 ± 0.066*	1.30 ± 0.012
Neutron	3.77 ± 0.11	*80.49 ± 1.37*	24.0 ± 0.22
(n,g)	1.53± 0.024	*7.54 ± 0.07*	8.78 ± 0.051
Total	5.46 ± 0.11	*88.88 ± 1.38*	34.1 ± 0.22
2 m from Vehicle Surface (mrem/hr), Limit = 10 mrem/hr			
	Top End	**Side**	**Bottom End**
Gamma	0.143 ± 0.00033	0.387 ± 0.015	0.163 ± 0.0020
Neutron	0.748 ± 0.015	5.54 ± 0.067	3.40 ± 0.036
(n,g)	0.133 ± 0.0026	1.74 ± 0.016	0.947 ± 0.0060
Total	0.895 ± 0.015	7.44 ± 0.082	4.51 ± 0.036

69TH DSC in the MP197HB Transportation Package			
Vehicle (Package) Surface[1] (mrem/hr), Limit = 200 mrem/hr			
	Top End	**Side**	**Bottom End**
Gamma	0.0233 ± 0.00098	*0.213 ± 0.020*	2.68 ± 0.027
Neutron	1.69 ± 0.058	*107.35 ± 1.69*	43.0 ± 0.33
(n,g)	0.303 ± 0.0073	*11.17 ± 0.10*	15.3 ± 0.072
Total	2.01 ± 0.058	*118.74 ± 1.70*	61.0 ± 0.034
2 m from Vehicle Surface (mrem/hr), Limit = 10 mrem/hr			
	Top End	**Side**	**Bottom End**
Gamma	0.00602 ± 0.0011	0.126 ± 0.0083	0.280 ± 0.0049
Neutron	0.701 ± 0.014	6.64 ± 0.011	5.95 ± 0.056
(n,g)	0.110 ± 0.0024	1.74 ± 0.016	1.62 ± 0.0084
Total	0.817± 0.015	8.50 ± 0.11	7.85 ± 0.057

1. Dose rates are computed on the surfaces of the impact limiters and on the surface of the neutron shield. These package surface dose rates are conservatively reported as vehicle surface dose rates.

Table A.5-1b
Summary of MP197HB NCT Dose Rates for Reconfigured Fuel, 50% Void Fraction, Additional Results
(Exclusive Use Package for Transportation)

[ ]

69TH DSC in the MP197HB Transportation Package			
Vehicle (Package) Surface(1) (mrem/hr), Limit = 200 mrem/hr			
	Top End	**Side**	**Bottom End**
Gamma	0.065 ± 0.023	1.596 ± 0.072	2.753 ± 0.020
Neutron	1.727 ± 0.008	113.051 ± 0.453	39.964 ± 0.088
(n,g)	0.445 ± 0.003	10.379 ± 0.026	13.674 ± 0.019
Total(2)	2.025 ± 0.011	123.770 ± 0.454	56.391 ± 0.092
2 m from Vehicle Surface (mrem/hr), Limit = 10 mrem/hr			
	Top End	**Side**	**Bottom End**
Gamma	0.014 ± 0.004	0.306 ± 0.014	0.288 ± 0.003
Neutron	0.697 ± 0.003	6.727 ± 0.031	5.597 ± 0.014
(n,g)	0.126 ± 0.001	1.671 ± 0.004	1.453 ± 0.002
Total(2)	0.802 ± 0.004	8.533 ± 0.031	7.338 ± 0.015

1. *Dose rates are computed on the surfaces of the impact limiters and on the surface of the neutron shield. These package surface dose rates are conservatively reported as vehicle surface dose rates.*
2. *Spatial locations of maximums of components of the total dose rate are generally different. Because of this, the maximum of the total dose rate is generally not equal to the sum of maximums of the components.*

Table A.5-1c
Summary of MP197HB NCT Dose Rates for Reconfigured Fuel, Reconfiguration Compliant with Enclosure 2 of the US NRC RIS 2015-XX [28]

(Exclusive Use Package for Transportation)

[ ]

69TH DSC in the MP197HB Transportation Package			
Vehicle (Package) Surface(1) (mrem/hr), Limit = 200 mrem/hr			
	Top End	**Side**	**Bottom End**
Gamma	0.365 ± 0.002	2.875 ± 0.089	2.742 ± 0.016
Neutron	2.933 ± 0.018	107.463 ± 0.432	39.740 ± 0.078
(n,g)	1.305 ± 0.005	9.757 ± 0.024	13.233 ± 0.016
Total(2)	4.602 ± 0.019	117.526 ± 0.443	55.716 ± 0.081
2 m from Vehicle Surface (mrem/hr), Limit = 10 mrem/hr			
	Top End	**Side**	**Bottom End**
Gamma	0.076 ± 0.001	0.420 ± 0.019	0.284 ± 0.002
Neutron	0.794 ± 0.004	6.730 ± 0.029	5.572 ± 0.013
(n,g)	0.169 ± 0.001	1.771 ± 0.004	1.401 ± 0.002
Total(2)	0.968 ± 0.004	8.648 ± 0.031	7.257 ± 0.014

1. *Dose rates are computed on the surfaces of the impact limiters and on the surface of the neutron shield. These package surface dose rates are conservatively reported as vehicle surface dose rates.*
2. *Spatial locations of maximums of components of the total dose rate are generally different. Because of this, the maximum of the total dose rate is generally not equal to the sum of maximums of the components.*

Table A.5-2
Summary of MP197HB HAC Dose Rates

(Exclusive Use Package for Transportation)

	37PTH DSC in the MP197HB Transportation Package		
	1 m from Package Surface (mrem/hr), Limit = 1000 mrem/hr		
	Top(1)	**Side(1)**	**Bottom(2)**
Gamma	0.44 ± 0.09	5.99± 0.48	3.23 ± 0.10
Neutron	70.73± 1.41	843.57 ± 8.44	266.98 ± 2.67
(n,g)	0.20 ± 0.02	1.98 ± 0.06	1.00 ± 0.01
Total	71.36 ± 1.43	851.53 ± 8.52	271.22 ± 2.71

	69BTH DSC in the MP197HB Transportation Package		
	1 m from Package Surface (mrem/hr), Limit = 1000 mrem/hr		
	Top(1)	**Side(1)**	**Bottom(2)**
Gamma	0.25 ± 0.08	2.78 ± 0.31	3.66 ± 0.07
Neutron	61.78 ± 1.24	844.39 ± 8.44	333.65 ± 3.34
(n,g)	0.21 ± 0.02	2.37 ± 0.07	1.25 ± 0.01
Total	62.24 ± 1.24	849.54 ± 8.50	338.56 ± 3.39

Notes:
1. From Configuration 1 model (intact fuel).
2. From Configuration 3 model (reconfigured fuel, *50% void fraction,* flat axial source distribution.)

Table A.5-2a
Summary of MP197HB HAC Dose Rates for Reconfigured Fuel
(Exclusive Use Package for Transportation)

[ ]

69TH DSC in the MP197HB Transportation Package			
1 m from Package Surface (mrem/hr), Limit = 1000 mrem/hr			
	Top End(2)	**Side(1,2)**	**Bottom End(3)**
Gamma	0.759 ± 0.211	4.542 ± 0.455	3.717 ± 0.063
Neutron	65.074 ± 1.405	825.304 ± 5.934	318.511 ± 2.589
(n,g)	0.174 ± 0.014	1.907 ± 0.047	1.102 ± 0.008
Total(4 (5))	65.519 ± 1.406	830.920 ± 5.942	323.330 ± 2.590

Notes:
1. *Dose rates are at radial distance measured from the location corresponding to the shell of the neutron shielding on side of the cask.*
2. *From the cask containing not reconfigured fuel.*
3. *From the cask containing reconfigured fuel and having "flat" axial distribution of radiological sources in active regions of the fuel assemblies.*
4. *Spatial locations of maximums of components of the total dose rate are generally different. Because of this, the maximum of the total dose rate is generally not equal to the sum of maximums of the components.*
5. *Dose rates bound dose rates calculated with fuel reconfiguration approach in compliance with recommendations in Enclosure 2 of the US NRC RIS 2015-XX [28]*

Table A.5-3
Not used

Table A.5-*4*
MP197HB Cask/69BTH DSC Shielding Materials

69BTH DSC shielding	**Materials**	**Thickness, inches**
Outer Side Shell	Stainless Steel(1)	0.5
Bottom Shield Plug/Covers	Stainless Steel(1)	7.25(2)
Top Shield Plugs/Covers	Stainless Steel(1)	9.75(2)
MP197HB shielding	**Materials**	**Thickness, inches**
Inner Shell	Carbon Steel	1.25
Gamma Shield	Lead	3.00
Outer Shell	Carbon Steel	2.75
Neutron Shield	VYAL-B	6.0(3)
Neutron Shield Shell	Carbon Steel	0.375
Cask Bottom	Carbon Steel	6.5" 3" if below grapple ring cut-out
Cask Lid	Carbon Steel	4.5
Impact Limiters Outer Shell	Stainless Steel(1)	0.25
Impact Limiters	Wood	26.25(4) –axial Ø125.53"

Notes:
(1) Modeled as carbon steel.
(2) This is a combined thickness of shield plugs and cover plates.
(3) Neutron shielding material VYAL-B resin (composition shown below) is inside of 0.125" thick neutron shield box.
(4) This is measured from ends of the cask to ends of Impact Limiters.

Proprietary Information Withheld Pursuant to 10 CFR 2.390

Table A.5-*6*
DB PWR Fuel Assembly Material Mass

Fuel Assembly Region, length	**Fuel Assembly Part**	**Material**	**Standard Mass (kg)**	**Mass of Reconstituted Fuel Assembly (kg)**
Top Nozzle, 6.23 in.	Top Nozzle/Misc. Steel	SS-304	9.2	9.2
	Hold Down Spring	Inconel-718	1.8	1.8
Plenum, 8.73 in.	Upper Spring	Inconel-718	4.3	4.3
	Upper End Cap	Zircaloy-4	1.0	1.0
	Encompassing Clad.	Zircaloy-4	5.8	5.5
	Upper End Grid	Inconel-718	1.1	1.1
	Stainless Steel Rods	SS304	n/a	1.7
In-core Region, 142.29 in.	Fuel Stack	Uranium	490(1)	466(1)
	Encompassing Clad.	Zircaloy-4	101.1	96.2
	Encompassing Guide Tube	Zircaloy-4	6.3	6.3
	Spacer Grids	Inconel-718	5.0	5.0
	Grid Supports	Zircaloy-4	0.64	0.64
	Stainless Steel Rods	SS304	n/a	27.2
Bottom Nozzle, 8.38 in.	Lower End Plug	Zircaloy-4	8.9	8.5
	Encompassing Guide Tube	Zircaloy-4	0.1	0.1
	Lower Guide Tube Plugs	Zircaloy-4	1.4	1.4
	Lower End Fitting	SS 304	8.2	8.2
	Lower End Grid	Inconel-718	1.1	1.1
	Stainless Steel Rods	SS304	n/a	0.5

(1) wt. of UO_2 = 555.93 kg (Standard Mass) and 528.70 kg (Reconstituted)

Table A.5-7
DB BWR Fuel Assembly Material Mass

Hardware Item	Material	Average Mass, (kg/FA)	Comments
In-core Zone, (144.00 inch long, **4.73** g/FA total cobalt content)			
Cladding	Zircaloy-2	49.2	
Fuel Channel Sleeve	Zircaloy-4	37.1	
Grid Spacers	Zircaloy-4	1.95	7 spacers*~0.28 kg/spacer
Spacer Springs	Inconel X-750	0.36	7 springs*0.051 kg/spring
Channel Spring & Bolt	Inconel X-750	0.13	
Channel Fastener Guard	Stainless Steel	0.46	
Channel Spacer & Rivert	Stainless Steel	0.13	
Fuel	Uranium	198	wt. of UO_2=224.643 kg.=0.198 mtu/0.8814
Gas Plenum Zone, (12.93 inch long, **0.89** g/FA total cobalt content)			
Cladding	Zircaloy-2	4.89	
Fuel Channel	Zircaloy-4	0.00	
Plenum Springs	Stainless Steel	1.05	
Top End Fitting Zone, (12.62 inch long, **4.51** g/FA total cobalt content)			
Upper Tie Plate	Stainless Steel	2.08	
Lock Tab Washers & Nuts	Stainless Steel	0.05	
Expansion Springs	Inconel X-750	0.43	
End Plugs	Zircaloy	1.26	
Bottom End Fitting Zone, (6.65 inch long, **4.10** g/FA total cobalt content)			
Finger Springs	Inconel	0.05	
End Plugs	Zircaloy	1.26	
Lower Tie Plate	Stainless Steel	4.7	
Total, kgs.(1)		329.7	
Total, lbs.(1)		726.3	

Note:
(1) This mass is very conservative for the source term calculation because the maximum weight of fuel assembly with or without channel is limited to 705 lbs.

Table A.5-8
TRITON Input Parameters

(Part 1 of 2)

GE 7x7	
Parameter	***Value***
Assembly Pitch (cm)	*15.24*
Number of Fuel Rods	*49*
Fuel Cell Pitch (cm)	*1.87452*
Pellet OR (cm)	*0.61849*
Fuel Rod Cladding IR (cm)	*0.63373*
Fuel Rod Cladding OR (cm)	*0.71501*
Cladding Thickness (cm)	*0.08128*
Fuel Rod Cladding Material	*Zirc-4*
Square Channel Inside Dimension (cm)	*13.40612*
Channel Thickness (cm)	*0.2032*
Channel Material	*Zirc-4*
Specific Power (MW/MTU)	*40.0*
Average Fuel Temperature (K)	*850.0*
Average Cladding Temperature (K)	*620.0*
Average Moderator Temperature (K)	*560.0*
Average Moderator Density (g/cm^3)	*0.20, 0.43, and 0.80*

(Part 2 of 2)

B&W 15x15	
Parameter	***Value***
Assembly Pitch (cm)	*21.79690*
Number of Fuel Rods	*208*
Guide Tubes per Assembly	*17*
Fuel Cell Pitch (cm)	*1.44272*
Pellet OR (cm)	*0.473329*
Fuel Rod Cladding IR (cm)	*0.478790*
Fuel Rod Cladding OR (cm)	*0.546100*
Cladding Thickness (cm)	*0.067310*
Fuel Rod Cladding Material	*Zirc-4*
Guide Tube IR (cm)	*0.635000*
Guide Tube OR (cm)	*0.670560*
Guide Tube Thickness (cm)	*0.035560*
Guide Tube Material	*Zirc-4*
Specific Power (MW/MTU)	*40.0*
Average Fuel Temperature (K)	*950.0*
Average Cladding Temperature (K)	*640.0*
Average Moderator Temperature (K)	*575.0*
Average Moderator Density (g/cm^3)	*0.7232*

Table A.5-*9*
Material Compositions for Fuel Assembly Hardware Materials

Element	Atomic Number	Material Composition, grams per kg of material				
		Zircaloy-4	Inconel-718	Inconel X-750	Stainless Steel 304	UO_2 Fuel (per kg U)
H	1	1.30E-02	-	-	-	-
Li	3	-	-	-	-	1.00E-03
B	5	3.30E-04	-	-	-	1.00E-03
C	6	1.20E-01	4.00E-01	3.99E-01	8.00E-01	8.94E-02
N	7	8.00E-02	1.30E+00	1.30E+00	1.30E+00	2.50E-02
O	8	9.50E-01	-	-	-	1.34E+02
F	9	-	-	-	-	1.07E-02
Na	11	-	-	-	-	1.50E-02
Mg	12	-	-	-	-	2.00E-03
Al	13	2.40E-02	5.99E+00	7.98E+00	-	1.67E-02
Si	14	-	2.00E+00	2.99E+00	1.00E+01	1.21E-02
P	15	-	-	-	4.50E-01	3.50E-02
S	16	3.50E-02	7.00E-02	7.00E-02	3.00E-01	-
Cl	17	-	-	-	-	5.30E-03
Ca	20	-	-	-	-	2.00E-03
Ti	22	2.00E-02	7.99E+00	2.49E+01	-	1.00E-03
V	23	2.00E-02	-	-	-	3.00E-03
Cr	24	1.25E+00	1.90E+02	1.50E+02	1.90E+02	4.00E-03
Mn	25	2.00E-02	2.00E+00	6.98E+00	2.00E+01	1.70E-03
Fe	26	2.25E+00	1.80E+02	6.78E+01	6.88E+02	1.80E-02
Co	27	1.00E-02	4.69E+00	6.49E+00	8.00E-01	1.00E-03
Ni	28	2.00E-02	5.20E+02	7.22E+02	8.92E+01	2.40E-02
Cu	29	2.00E-02	9.99E-01	4.99E-01	-	1.00E-03
Zn	30	-	-	-	-	4.03E-02
Zr	40	9.79E+02	-	-	-	-
Nb	41	-	5.55E+01	8.98E+00	-	-
Mo	42	-	3.00E+01	-	-	1.00E-02
Ag	47	-	-	-	-	1.00E-04
Cd	48	2.50E-04	-	-	-	2.50E-02
In	49	-	-	-	-	2.00E-03
Sn	50	1.60E+01	-	-	-	4.00E-03
Gd	64	-	-	-	-	2.50E-03
Hf	72	7.80E-02	-	-	-	-
W	74	2.00E-02	-	-	-	2.00E-03
Pb	82	-	-	-	-	1.00E-03
U	92	2.00E-04	-	-	-	1.00E+03

Table A.5-10
BWR Axial *Source Distributions for Intact Fuel*

Zone	*Fraction of Core Height*	*Fractional Width of Zone*	*Axial Burnup Profile for 40 GWd/MTU*	*Gamma Axial Source Distribution (normalized to avg = 1.0)*	*Gamma Axial Source Distribution (normalized to sum = 1.0)*	*Neutron Axial Source Distribution (not normalized)*	*Neutron Axial Source Distribution (normalized to sum = 1.0)*
1	*0.05*	*0.05*	*0.2357*	*0.2256*	*0.0113*	*0.0026*	*9.181E-05*
2	*0.1*	*0.05*	*0.7746*	*0.7674*	*0.0384*	*0.3468*	*0.0123*
3	*0.2*	*0.1*	*1.0750*	*1.0854*	*0.1085*	*1.3879*	*0.0984*
4	*0.3*	*0.1*	*1.1836*	*1.2027*	*0.1203*	*2.0923*	*0.1483*
5	*0.4*	*0.1*	*1.2000*	*1.2223*	*0.1222*	*2.2321*	*0.1582*
6	*0.5*	*0.1*	*1.2000*	*1.2244*	*0.1224*	*2.2475*	*0.1593*
7	*0.6*	*0.1*	*1.1912*	*1.2164*	*0.1216*	*2.1893*	*0.1552*
8	*0.7*	*0.1*	*1.1515*	*1.1227*	*0.1123*	*1.5887*	*0.1126*
9	*0.8*	*0.1*	*1.0766*	*1.0964*	*0.1096*	*1.4450*	*0.1024*
10	*0.9*	*0.1*	*0.8973*	*0.9053*	*0.0905*	*0.6717*	*0.0476*
11	*0.95*	*0.05*	*0.6330*	*0.6255*	*0.0313*	*0.1531*	*0.0054*
12	*1.0*	*0.05*	*0.2410*	*0.2303*	*0.0115*	*0.0028*	*9.970E-05*
Total	-	-	-	-	*1.000*	-	*1.000*

Proprietary Information Withheld Pursuant to 10 CFR 2.390

Table A.5-11
PWR Axial *Source Distributions for Intact Fuel*

Zone	*Active Fuel Zone Center (% of Height)*	*Fractional width of Zone*	*Axial Burnup Profile for >46 GWd/MTU[16]*	*Gamma Axial Source Distribution (normalized to sum = 1.0)*	*Neutron Axial Source Distribution (not normalized)*	*Neutron Axial Source Distribution (normalized to sum = 1.0)*
1	*2.78*	*0.056*	*0.573*	*0.0318*	*0.108*	*0.0052*
2	*8.33*	*0.056*	*0.917*	*0.0509*	*0.707*	*0.0341*
3	*13.89*	*0.056*	*1.066*	*0.0592*	*1.291*	*0.0623*
4	*19.44*	*0.056*	*1.106*	*0.0614*	*1.496*	*0.0721*
5	*25.00*	*0.056*	*1.114*	*0.0619*	*1.540*	*0.0743*
6	*30.56*	*0.056*	*1.111*	*0.0617*	*1.524*	*0.0735*
7	*36.11*	*0.056*	*1.106*	*0.0614*	*1.496*	*0.0721*
8	*41.69*	*0.056*	*1.101*	*0.0612*	*1.469*	*0.0708*
9	*47.22*	*0.056*	*1.097*	*0.0609*	*1.448*	*0.0698*
10	*52.78*	*0.056*	*1.093*	*0.0607*	*1.427*	*0.0688*
11	*58.33*	*0.056*	*1.089*	*0.0605*	*1.406*	*0.0678*
12	*63.89*	*0.056*	*1.086*	*0.0603*	*1.391*	*0.0671*
13	*69.44*	*0.056*	*1.081*	*0.0601*	*1.366*	*0.0659*
14	*75.00*	*0.056*	*1.073*	*0.0596*	*1.326*	*0.0639*
15	*80.56*	*0.056*	*1.051*	*0.0584*	*1.220*	*0.0588*
16	*86.11*	*0.056*	*0.993*	*0.0552*	*0.972*	*0.0469*
17	*91.67*	*0.056*	*0.832*	*0.0462*	*0.479*	*0.0231*
18	*97.22*	*0.056*	*0.512*	*0.0284*	*0.069*	*0.0033*
Total	*-*	*-*	*-*	*1.000*	*-*	*1.000*

Table A.5-11a
PWR Axial Source Distributions for Reconfigured Fuel

Zone	*Fraction of Core Length from Bottom Nozzle (%)*	*Axial Burnup Profile for 44-55 GWd/MTU [26]*	*Gamma Axial Source Distribution (normalized to sum = 1.0)*	*Neutron Axial Source Distribution (not normalized)*	*Neutron Axial Source Distribution (normalized to sum = 1.0)*
1	*5*	*0.655*	*0.033*	*0.183*	*0.008*
2	*10*	*0.911*	*0.046*	*0.687*	*0.032*
3	*15*	*1.009*	*0.050*	*1.037*	*0.048*
4	*20*	*1.041*	*0.052*	*1.175*	*0.054*
5	*25*	*1.069*	*0.053*	*1.308*	*0.060*
6	*30*	*1.072*	*0.054*	*1.322*	*0.061*
7	*35*	*1.072*	*0.054*	*1.322*	*0.061*
8	*40*	*1.071*	*0.054*	*1.318*	*0.061*
9	*45*	*1.070*	*0.054*	*1.313*	*0.060*
10	*50*	*1.069*	*0.053*	*1.308*	*0.060*
11	*55*	*1.069*	*0.053*	*1.308*	*0.060*
12	*60*	*1.068*	*0.053*	*1.303*	*0.060*
13	*65*	*1.068*	*0.053*	*1.303*	*0.060*
14	*70*	*1.069*	*0.053*	*1.308*	*0.060*
15	*75*	*1.068*	*0.053*	*1.303*	*0.060*
16	*80*	*1.066*	*0.053*	*1.293*	*0.060*
17	*85*	*1.041*	*0.052*	*1.175*	*0.054*
18	*90*	*0.994*	*0.050*	*0.976*	*0.045*
19	*95*	*0.879*	*0.044*	*0.595*	*0.027*
20	*100*	*0.639*	*0.032*	*0.165*	*0.008*
Total	-	-	*1.000*	-	*1.000*

Table A.5-12
Fuel Assembly Materials for MCNP

(Part 1 of *4*)

BWR Assembly Region Material Densities					
Element/Isotope	**Atomic Number**	**Density (g/cm^3)**			
		Bottom Fitting	**Fuel**	**Plenum**	**Top Fitting**
C	6	1.166E-3	6.759E-6	1.340E-4	2.784E-4
O	8	-	3.806E-1	-	-
Si	14	1.496E-2	2.599E-4	1.675E-3	5.237E-3
P	15	6.558E-4	3.802E-6	7.535E-5	1.566E-4
Ti	22	3.876E-4	1.754E-4	-	1.757E-3
Cr	24	2.796E-1	3.390E-3	3.260E-2	7.687E-2
Mn	25	2.915E-2	1.690E-4	3.349E-3	6.961E-3
Fe	26	9.984E-1	7.806E-3	1.161E-1	2.433E-1
Ni	28	1.498E-1	5.925E-3	1.591E-2	8.435E-2
Zr	40	3.838E-1	7.195E-1	7.660E-1	2.022E-1
Sn	50	5.665E-3	1.062E-2	1.131E-2	2.985E-3
Hf	72	3.907E-5	7.325E-5	7.799E-5	2.059E-5
U-234	92	-	1.008E-3	-	-
U-235	92	-	1.132E-1	-	-
U-236	92	-	5.209E-4	-	-
U-238	92	-	2.716E+0	-	-
Total		1.864	3.960	0.947	0.624

Table A.5-12
Fuel Assembly Materials for MCNP

(Part 2 of *4*)

BWR Assembly Region Material Densities					
Element/Isotope	**Atomic Number**	**Composition By Weight Fraction**			
		Bottom Fitting	**Fuel**	**Plenum**	**Top Fitting**
C	6	0.00063	0.000002	0.00014	0.00045
O	8	-	0.096131	-	-
Si	14	0.00803	0.000066	0.00177	0.00839
P	15	0.00035	0.000001	0.00008	0.00025
Ti	22	0.00021	0.000044	-	0.00281
Cr	24	0.15004	0.000856	0.03441	0.12316
Mn	25	0.01564	0.000043	0.00354	0.01115
Fe	26	0.53574	0.001971	0.12259	0.38983
Ni	28	0.08037	0.001496	0.01679	0.13514
Zr	40	0.20594	0.181709	0.80866	0.32400
Sn	50	0.00304	0.002682	0.01194	0.00478
Hf	72	0.00002	0.000018	0.00008	0.00003
U-234	92	-	0.000255	-	-
U-235	92	-	0.028599	-	-
U-236	92	-	0.000132	-	-
U-238	92	-	0.685995	-	-
Gram Density (g/cc)		1.864	3.960	0.947	0.624

Table A.5-12
Fuel Assembly Materials for MCNP

(Part 3 of 4)

PWR Assembly Region Material Densities					
		Number Density (atom/b-cm)			
Element	**Atomic Number**	**Bottom End Fitting**	**Fuel**	**Plenum**	**Top End Fitting**
O	8	-	1.47E-02	-	-
Al	13	1.43E-05	3.93E-06	6.95E-05	3.24E-05
Ti	22	1.07E-05	2.95E-06	5.22E-05	2.43E-05
Cr	24	2.05E-03	7.19E-05	1.15E-03	3.25E-03
Mn	25	1.79E-04	-	-	2.71E-04
Fe	26	6.48E-03	9.19E-05	1.40E-03	9.97E-03
Ni	28	1.31E-03	1.56E-04	2.76E-03	2.42E-03
Zr	40	6.77E-03	4.12E-03	4.23E-03	-
Mo	42	2.01E-05	5.53E-06	9.77E-05	4.56E-05
Sn	50	8.49E-05	5.16E-05	5.30E-05	-
U-235	92	-	3.69E-04	-	-
U-238	92	-	6.93E-03	-	-
Total		1.69E-02	2.65E-02	9.81E-03	1.60E-02

Table A.5-12
Fuel Assembly Materials for MCNP

(Part 4 of 4)

PWR Assembly Region Material Densities				
Element	**Bottom Region**	**In-Core Region**	**Plenum Region**	**Top Region**
H	-	-	-	-
B-10	-	-	-	-
C	-	-	-	-
O	-	3.89E-01	-	-
Al	6.40E-04	1.76E-04	3.11E-03	1.45E-03
Ti	8.54E-04	2.35E-04	4.15E-03	1.94E-03
Cr	1.77E-01	6.21E-03	9.93E-02	2.80E-01
Mn	1.63E-02	-	-	2.47E-02
Fe	6.01E-01	8.52E-03	1.30E-01	9.25E-01
Ni	1.28E-01	1.52E-02	2.69E-01	2.35E-01
Zr	1.03E+00	6.24E-01	6.41E-01	-
Mo	3.20E-03	8.80E-04	1.56E-02	7.26E-03
Sn	1.67E-02	1.02E-02	1.04E-02	-
U-235	-	1.44E-01	-	-
U-238	-	2.74E+00	-	-
Total	1.969	3.938	1.172	1.476

Table A.5-13
Package Materials Input for MCNP

Element	Atomic Number, Z	Weight fraction, (%)					
		Air	**Lead**	**Carbon Steel**	**Stainless Steel**	**Aluminum**	**Wood**
H	1						6.218
C	6	0.01		1	2		44.450
N	7	75.52					
O	8	23.18					49.333
Al	13					100	
Ar	18	1.29					
Cr	24				19		
Fe	26			99	69.5		
Ni	28				9.5		
Pb	82		100				
Density, g/cm^3		1.127E-3	11.34	7.82	7.92	2.72(1)	0.125

Notes:
(1) Aluminum density is 2.702 g/cc. This discrepancy does not affect dose rates significantly.
(2) For VYAL-B, see Table A.5-5.

Proprietary Information Withheld Pursuant to 10 CFR 2.390

Table A.5-*16*
Flux-to-Dose Rate Conversion Factors for Gamma

Photon Energy (MeV)	**Conversion Factor (mrem/hr)/(γ/cm^2-s)**
0.01	3.96E-03
0.03	5.82E-04
0.05	2.90E-04
0.07	2.58E-04
0.1	2.83E-04
0.15	3.79E-04
0.2	5.01E-04
0.25	6.31E-04
0.3	7.59E-04
0.35	8.78E-04
0.4	9.85E-04
0.45	1.08E-03
0.5	1.17E-03
0.55	1.27E-03
0.6	1.36E-03
0.65	1.44E-03
0.7	1.52E-03
0.8	1.68E-03
1	1.98E-03
1.4	2.51E-03
1.8	2.99E-03
2.2	3.42E-03
2.6	3.82E-03
2.8	4.01E-03
3.25	4.41E-03
3.75	4.83E-03
4.25	5.23E-03
4.75	5.60E-03
5	5.80E-03
5.25	6.01E-03
5.75	6.37E-03
6.25	6.74E-03
6.75	7.11E-03
7.5	7.66E-03
9	8.77E-03
11	1.03E-02
13	1.18E-02
15	1.33E-02

Table A.5-*17*
Flux-Dose-Rate Conversion Factors for Neutron

Neutron Energy (MeV)	**Conversion Factor (mrem/hr)/(n/cm^2-s)**
2.50E-08	3.67E-03
1.0E -07	3.67E-03
1.00E-06	4.46E-03
1.00E-05	4.54E-03
1.00E-04	4.18E-03
1.00E-03	3.76E-03
1.00E-02	3.56E-03
1.00E-01	2.17E-02
5.00E-01	9.26E-02
1	1.32E-01
2.5	1.25E-01
5	1.56E-01
7	1.47E-01
10	1.47E-01
14	2.08E-01
20	2.27E-01

Table A.5-*18*
CC Radiological Source

E_{upper} (MeV)	E_{mean} (MeV)	Top Region γ/s/CC	Plenum Region γ/s/CC	Fuel Region γ/s/CC
0.05	0.025	8.484E+10	1.382E+11	1.170E+12
0.1	0.075	8.191E+09	5.176E+09	1.142E+11
0.2	0.15	1.217E+09	3.534E+09	1.697E+10
0.3	0.25	2.060E+08	3.482E+09	2.872E+09
0.4	0.35	7.014E+07	2.431E+10	9.776E+08
0.6	0.5	3.235E+07	3.854E+10	4.508E+08
0.8	0.7	4.155E+09	1.783E+10	2.835E+09
1	0.9	6.951E+09	4.180E+09	4.699E+09
1.33	1.165	1.690E+12	9.340E+11	2.356E+13
1.66	1.495	7.138E+11	3.946E+11	9.953E+12
2	1.83	9.577E+01	8.812E+01	9.153E-05
2.5	2.25	1.274E+07	7.040E+06	1.775E+08
3	2.75	3.942E+04	2.179E+04	5.495E+05
4	3.5	3.947E-15	6.520E-14	7.266E-18
Total		2.509E+12	1.564E+12	3.483E+13

Pages A.5-59 through A.5-72 are proprietary information withheld pursuant to 10 CFR 2.390

Table A.5-*33*
Matrix Showing Additional to the Transportation FQTs Cooling Times
for Selected Cooling Times of CCs

Cooling Time of CCs, years	**Additional Cooling Time in Years for FAs with Burn-Up**	
	<=40 GWD/MTU	**>40 GWD/MTU**
3.0	0.8	2.5
5.0	0.6	2.0
10.0	0.3	1.0
15.0	0.15	0.5

Notes: To find additional to the transportation FQT cooling times when the cooling times of Control Components (CCs) are not shown in the first column of the table use the nearest higher CC cooling time available in the table. For example, if cooling time of CCs is 8.0 years use data in the table relevant to 10.0 years cooled CCs.

Table A.5-34
Summary *of* Maximum Dose Rate*s* of the Cask Containing *the Radioactive* Waste Canister

Radial Distance from Side of ILs or Body [1], m	Normal Conditions of Transport (NCT)		Hypothetical Accident Condition	
	Dose Rate, mrem/hr	Relative Error	Dose Rate, mrem/hr	Relative Error
Shield Shell	64.0	0.01	103.0	0.01
Package Side Perimeter	30.2	0.01	103.0	0.01
0	24.1	0.01	74.3	0.01
1	12.7	0.005	49.1	0.01
2	8.33	0.01	31.2	0.01
2.7	6.4	0.01	20.9	0.01

[1] HAC dose rates for distances equal to 1 and 2 meters correspond to radial distances measured from the cask body (Shield Shell), not from side of Impact Limiters.

Axial Distance from IL, m	Bottom at NCT		Top at NCT	
	Dose Rate, mrem/hr	Relative Error	Dose Rate, mrem/hr	Relative Error
0	72.2	0.002	37.1	0.002
1	18.1	0.002	14.9	0.002
2	8.29	0.003	7.7	0.002
2.7[2]	5.4	0.004	5.2	0.003
4.3	2.7	0.006	2.7	0.005
5.8	1.6	0.007	1.7	0.006
7.3	1.1	0.003	1.1	0.007

Axial Distance from IL, m	Bottom at HAC		Top at HAC	
	Dose Rate, mrem/hr	Relative Error	Dose Rate, mrem/hr	Relative Error
0	198.7	0.003	68.5	0.003
1	37.3	0.003	28.4	0.003
2	15.7	0.005	14.1	0.004
3.0[2]	8.4	0.01	8.1	0.005
4.6	4.3	0.01	4.3	0.007
6.1	2.6	0.01	2.7	0.010
7.6	1.7	0.01	1.8	0.004

(2) Dose rates at distances greater than 2 meters from ends of the Impact Limiters correspond to edges of 40, 50, 60 feet long transportation "platform," respectively.

Table A.5-35

Amount of Moles of Gases released as Result of Irradiation for GE7x7 BWR Fuel Assembly at 0.198 MTU, 3.7 wt % U-235, and 70 GWd/MTU

Nuclide	Atomic Number	Initial Amount of Fission Gases		Amount of Fission Gases at 3 Years after Discharge		Amount of Fission Gases at 5 Years after Discharge	
		grams	gram-moles	grams	gram-moles	grams	gram-moles
Due to "Light" Elements							
H	1	1.23E+00	1.23E+00	1.23E+00	1.23E+00	1.23E+00	1.23E+00
H	2	7.48E-03	3.74E-03	7.48E-03	3.74E-03	7.48E-03	3.74E-03
H	3	6.48E-03	2.16E-03	5.47E-03	1.82E-03	4.89E-03	1.63E-03
He	3	2.40E-05	8.01E-06	1.03E-03	3.43E-04	1.61E-03	5.37E-04
He	4	1.81E+00	4.53E-01	1.81E+00	4.53E-01	1.81E+00	4.53E-01
N	14	1.55E+01	1.10E+00	1.55E+01	1.10E+00	1.55E+01	1.10E+00
N	15	7.13E-02	4.75E-03	7.13E-02	4.75E-03	7.13E-02	4.75E-03
F	19	2.40E+00	1.26E-01	2.40E+00	1.26E-01	2.40E+00	1.26E-01
Ne	20	2.83E-04	1.41E-05	2.83E-04	1.41E-05	2.83E-04	1.41E-05
Ne	21	3.48E-05	1.66E-06	3.48E-05	1.66E-06	3.48E-05	1.66E-06
Ne	22	1.36E-05	6.18E-07	1.36E-05	6.18E-07	1.36E-05	6.18E-07
Cl	35	6.75E-01	1.93E-02	6.75E-01	1.93E-02	6.75E-01	1.93E-02
Cl	36	1.62E-01	4.49E-03	1.62E-01	4.49E-03	1.62E-01	4.49E-03
Cl	37	2.87E-01	7.75E-03	2.87E-01	7.75E-03	2.87E-01	7.75E-03
Ar	36	4.55E-07	1.26E-08	1.55E-06	4.31E-08	2.28E-06	6.34E-08
Ar	38	6.48E-04	1.70E-05	6.48E-04	1.70E-05	6.48E-04	1.70E-05
Ar	39	6.80E-07	1.74E-08	6.75E-07	1.73E-08	6.72E-07	1.72E-08
Ar	40	1.16E-05	2.90E-07	1.16E-05	2.90E-07	1.16E-05	2.90E-07
I	127	2.55E-04	2.00E-06	2.72E-04	2.14E-06	2.72E-04	2.14E-06
Xe	128	1.96E-05	1.53E-07	1.96E-05	1.53E-07	1.96E-05	1.53E-07
Xe	129	1.78E-07	1.38E-09	1.79E-07	1.39E-09	1.79E-07	1.39E-09
Due to Actinides							
He	4	1.87E-01	4.68E-02	4.76E-01	1.19E-01	6.02E-01	1.50E-01
Due to Fission Products							
H	3	2.66E-02	8.87E-03	2.25E-02	7.49E-03	2.01E-02	6.69E-03
Br	79	9.69E-06	1.23E-07	2.24E-05	2.84E-07	3.09E-05	3.91E-07
Kr	80	2.87E-05	3.59E-07	2.87E-05	3.59E-07	2.87E-05	3.59E-07
Br	81	7.77E+00	9.59E-02	7.77E+00	9.59E-02	7.77E+00	9.59E-02
Kr	81	7.89E-06	9.74E-08	7.89E-06	9.74E-08	7.89E-06	9.74E-08
Kr	82	4.88E-01	5.95E-03	4.91E-01	5.99E-03	4.91E-01	5.99E-03
Kr	83	1.04E+01	1.25E-01	1.04E+01	1.25E-01	1.04E+01	1.25E-01
Kr	84	4.75E+01	5.66E-01	4.75E+01	5.66E-01	4.75E+01	5.66E-01
Kr	85	8.96E+00	1.05E-01	7.38E+00	8.69E-02	6.49E+00	7.63E-02
Kr	86	6.54E+01	7.61E-01	6.54E+01	7.61E-01	6.54E+01	7.61E-01
I	127	1.88E+01	1.48E-01	1.97E+01	1.55E-01	1.97E+01	1.55E-01
Xe	128	2.99E+00	2.34E-02	2.99E+00	2.34E-02	2.99E+00	2.34E-02
I	129	6.57E+01	5.09E-01	6.66E+01	5.16E-01	6.66E+01	5.16E-01
Xe	129	4.28E-02	3.31E-04	4.41E-02	3.42E-04	4.41E-02	3.42E-04
Xe	130	6.92E+00	5.33E-02	6.94E+00	5.34E-02	6.94E+00	5.34E-02
Xe	131	1.19E+02	9.05E-01	1.22E+02	9.33E-01	1.22E+02	9.33E-01
Xe	132	5.25E+02	3.98E+00	5.27E+02	3.99E+00	5.27E+02	3.99E+00
Xe	134	6.36E+02	4.75E+00	6.37E+02	4.75E+00	6.37E+02	4.75E+00
Xe	136	1.06E+03	7.82E+00	1.06E+03	7.82E+00	1.06E+03	7.82E+00
Total Amounts Due To Different Groups							
Total "Light" Elements		2.21E+01	2.95E+00	2.21E+01	2.95E+00	2.21E+01	2.95E+00
Actinides		1.87E-01	4.68E-02	4.76E-01	1.19E-01	6.02E-01	1.50E-01
Fission products		2.58E+03	1.98E+01	2.58E+03	1.99E+01	2.58E+03	1.99E+01
Total		2.60E+03	2.28E+01	2.61E+03	2.30E+01	2.61E+03	2.30E+01
Relative Amount of Different Groups from Total, %							
Total "Light" Elements		1%	13%	1%	13%	1%	13%
Actinides		0%	0%	0%	1%	0%	1%
Fission products		99%	87%	99%	87%	99%	86%
Total		100%	100%	100%	100%	100%	100%

Table A.5-36
Bounding NCT Source for the 37PTH DSC in the MP197HB Transportation Package, *Intact Fuel*

NCT Representative Radiological Source at 490 kgU/FA: 60 GWD/MTU, 3.9 wt. %, after 15.7 years of cooling. Generates 1.302 kWt/FA of decay heat. Results in 8.20 mrem/hr NCT total dose rate (~77.9 % is due to Neutron Source)						
E_{min}, MeV	to	E_{max}, MeV	Bottom Nozzle	In-core	Plenum	Top Nozzle
0.00e+00	to	5.00e-02	7.480E+10	1.061E+15	1.571E+11	4.590E+10
5.00e-02	to	1.00e-01	1.253E+10	2.932E+14	2.760E+10	8.664E+09
1.00e-01	to	2.00e-01	4.017E+09	2.059E+14	7.314E+09	2.095E+09
2.00e-01	to	3.00e-01	2.221E+08	6.129E+13	3.816E+08	1.049E+08
3.00e-01	to	4.00e-01	4.323E+08	3.961E+13	5.879E+08	1.366E+08
4.00e-01	to	6.00e-01	5.322E+09	6.678E+13	3.486E+09	9.999E+06
6.00e-01	to	8.00e-01	4.298E+09	2.006E+15	9.561E+09	1.295E+09
8.00e-01	to	1.00e+00	1.656E+09	4.291E+13	7.839E+09	1.372E+09
1.00e+00	to	1.33e+00	3.632E+12	8.431E+13	8.018E+12	2.523E+12
1.33e+00	to	1.66e+00	1.026E+12	1.560E+13	2.264E+12	7.126E+11
1.66e+00	to	2.00e+00	7.940E+01	1.034E+11	5.176E+01	1.232E-02
2.00e+00	to	2.50e+00	2.454E+07	6.388E+09	5.418E+07	1.705E+07
2.50e+00	to	3.00e+00	2.097E+04	5.143E+08	4.629E+04	1.457E+04
3.00e+00	to	4.00e+00	1.272E-05	8.797E+07	6.509E-05	1.047E-05
4.00e+00	to	5.00e+00	3.990E-34	2.666E+07	1.996E-34	0.0
5.00e+00	to	6.50e+00	1.150E-34	1.070E+07	5.750E-35	0.0
6.50e+00	to	8.00e+00	1.462E-35	2.099E+06	7.314E-36	0.0
8.00e+00	to	1.00e+01	1.951E-36	4.456E+05	9.761E-37	0.0
Total Gamma, g/(sec*FA)			4.761E+12	3.876E+15	1.050E+13	3.296E+12
(1)Total Neutrons, n/(sec*FA)			7.705E+8 *(raw)* *1.212E+9 (adjusted)*			

(1) *The "raw" source is calculated with ORIGEN-ARP. The adjusted source is the raw source multiplied by bpf/(1-k_{eff}) to account for subcritical neutron multiplication and an axial variation of the burnup profile in the active fuel region, where k_{eff} = 0.2678 and bpf = 1.152.*

Table A.5-37
Bounding NCT Source for the 69BTH DSC in the MP197HB Transportation Package, *Intact Fuel*

NCT Representative Radiological Source at *198kgU*/FA: 59 GW*d*/MTU, 2.8 wt. %, after 13.7 years of cooling. Generates 0.435 kWt/FA of decay heat. Results in 8.20 mrem/hr NCT total dose rate (~87.6% is due to Neutron Source).						
E_{min}, MeV	to	E_{max}, MeV	Bottom Nozzle	In-core	Plenum	Top Nozzle
0.00e+00	to	5.00e-02	3.310E+10	4.226E+14	1.831E+10	2.531E+10
5.00e-02	to	1.00e-01	6.247E+09	1.125E+14	1.978E+09	4.784E+09
1.00e-01	to	2.00e-01	1.660E+09	8.072E+13	1.401E+09	1.262E+09
2.00e-01	to	3.00e-01	8.565E+07	2.375E+13	8.963E+07	6.516E+07
3.00e-01	to	4.00e-01	1.333E+08	1.525E+13	2.504E+08	1.007E+08
4.00e-01	to	6.00e-01	7.952E+08	4.151E+13	4.962E+09	5.776E+08
6.00e-01	to	8.00e-01	4.271E+08	8.559E+14	2.588E+09	3.592E+08
8.00e-01	to	1.00e+00	1.421E+08	2.386E+13	4.260E+07	1.367E+08
1.00e+00	to	1.33e+00	1.817E+12	3.177E+13	5.593E+11	1.394E+12
1.33e+00	to	1.66e+00	5.132E+11	5.939E+12	1.579E+11	3.935E+11
1.66e+00	to	2.00e+00	7.616E+00	4.140E+10	5.025E+01	5.785E+00
2.00e+00	to	2.50e+00	1.228E+07	4.085E+09	3.779E+06	9.416E+06
2.50e+00	to	3.00e+00	1.049E+04	3.380E+08	3.229E+03	8.045E+03
3.00e+00	to	4.00e+00	1.297E-06	6.556E+07	9.489E-12	1.061E-05
4.00e+00	to	5.00e+00	0.0	1.595E+07	0.0	0.0
5.00e+00	to	6.50e+00	0.0	6.403E+06	0.0	0.0
6.50e+00	to	8.00e+00	0.0	1.256E+06	0.0	0.0
8.00e+00	to	1.00e+01	0.0	2.667E+05	0.0	0.0
Total Gamma, g/(sec*FA)			2.373E+12	1.614E+15	7.468E+11	1.820E+12
(1)Total Neutrons, n/(sec*FA)			4.636E+8 *(raw)* *6.769E+8 (adjusted)*			

(1) *The "raw" source is calculated with ORIGEN-ARP. The adjusted source is the raw source multiplied by bpf/(1-k_{eff}) to account for subcritical neutron multiplication and an axial variation of the burnup profile in the active fuel region, where k_{eff} = 0.1699 and bpf = 1.212.*

Table A.5-38
Bounding NCT and HAC Source for the 37PTH DSC, Reconfigured Fuel, 21 Inner Compartments

62 GWd/MTU, 3.4 wt. %, after 20.7 years of cooling.						
E_{min}, MeV	*to*	*E_{max}, MeV*	*Bottom Nozzle*	*In-core*	*Plenum*	*Top Nozzle*
0.00e+00	*to*	*5.00e-02*	*4.190E+10*	*9.278E+14*	*9.356E+10*	*2.741E+10*
5.00e-02	*to*	*1.00e-01*	*7.226E+09*	*2.580E+14*	*1.596E+10*	*5.008E+09*
1.00e-01	*to*	*2.00e-01*	*2.049E+09*	*1.726E+14*	*4.060E+09*	*1.211E+09*
2.00e-01	*to*	*3.00e-01*	*1.097E+08*	*5.205E+13*	*2.108E+08*	*6.122E+07*
3.00e-01	*to*	*4.00e-01*	*1.861E+08*	*3.394E+13*	*2.991E+08*	*7.931E+07*
4.00e-01	*to*	*6.00e-01*	*1.630E+09*	*3.412E+13*	*1.075E+09*	*6.543E+06*
6.00e-01	*to*	*8.00e-01*	*2.503E+09*	*1.814E+15*	*8.966E+09*	*1.404E+09*
8.00e-01	*to*	*1.00e+00*	*1.690E+09*	*2.333E+13*	*8.322E+09*	*1.418E+09*
1.00e+00	*to*	*1.33e+00*	*2.097E+12*	*5.405E+13*	*4.626E+12*	*1.457E+12*
1.33e+00	*to*	*1.66e+00*	*5.921E+11*	*9.141E+12*	*1.306E+12*	*4.113E+11*
1.66e+00	*to*	*2.00e+00*	*8.430E+01*	*8.750E+10*	*5.495E+01*	*1.278E-02*
2.00e+00	*to*	*2.50e+00*	*1.417E+07*	*4.707E+09*	*3.126E+07*	*9.842E+06*
2.50e+00	*to*	*3.00e+00*	*1.210E+04*	*4.287E+08*	*2.671E+04*	*8.409E+03*
3.00e+00	*to*	*4.00e+00*	*1.335E-05*	*8.973E+07*	*6.834E-05*	*1.100E-05*
4.00e+00	*to*	*5.00e+00*	*1.215E-33*	*3.018E+07*	*6.079E-34*	*0.0*
5.00e+00	*to*	*6.50e+00*	*3.502E-34*	*1.211E+07*	*1.752E-34*	*0.0*
6.50e+00	*to*	*8.00e+00*	*4.454E-35*	*2.376E+06*	*2.228E-35*	*0.0*
8.00e+00	*to*	*1.00e+01*	*5.944E-36*	*5.045E+05*	*2.973E-36*	*0.0*
*Total Gamma, g/(sec*FA)*			*2.746E+12*	*3.379E+15*	*6.065E+12*	*1.904E+12*
*(1)Total Neutrons, n/(sec*FA)*			*8.752E+08 (raw)* *1.345E+09 (adjusted intact)* *1.403E+09 (adjusted reconfigured)*			

(1) The "raw" source is calculated with ORIGEN-ARP. The adjusted source is the raw source multiplied by bpf/(1-k_{eff}) to account for subcritical neutron multiplication and an axial variation of burn-up profile in active fuel region, where bpf=1.152, k_{eff}=0.2505 if fuel is intact and k_{eff}=0.2812 if fuel is reconfigured. k_{eff} for reconfigured fuel includes an additional 12.25% increase to account for fuel compression.

Table A.5-38a
Bounding NCT and HAC Source for the 37PTH DSC, Reconfigured Fuel, 16 Peripheral Compartments

62 GWd/MTU, 3.4 wt. %, after 29.5 years of cooling.						
E_{min}, MeV	to	E_{max}, MeV	Bottom Nozzle	In-core	Plenum	Top Nozzle
0.00e+00	to	5.00e-02	1.405E+10	7.457E+14	3.435E+10	9.709E+09
5.00e-02	to	1.00e-01	2.282E+09	2.148E+14	5.081E+09	1.586E+09
1.00e-01	to	2.00e-01	5.854E+08	1.325E+14	1.260E+09	3.849E+08
2.00e-01	to	3.00e-01	3.130E+07	4.079E+13	6.798E+07	2.023E+07
3.00e-01	to	4.00e-01	4.449E+07	2.721E+13	8.651E+07	2.555E+07
4.00e-01	to	6.00e-01	1.780E+08	2.064E+13	1.229E+08	3.145E+06
6.00e-01	to	8.00e-01	1.746E+09	1.470E+15	8.468E+09	1.403E+09
8.00e-01	to	1.00e+00	1.625E+09	1.148E+13	8.178E+09	1.373E+09
1.00e+00	to	1.33e+00	6.589E+11	2.326E+13	1.454E+12	4.577E+11
1.33e+00	to	1.66e+00	1.861E+11	3.422E+12	4.105E+11	1.293E+11
1.66e+00	to	2.00e+00	6.787E+01	6.964E+10	4.424E+01	1.035E-02
2.00e+00	to	2.50e+00	4.452E+06	3.677E+09	9.823E+06	3.093E+06
2.50e+00	to	3.00e+00	3.804E+03	3.753E+08	8.393E+03	2.642E+03
3.00e+00	to	4.00e+00	1.109E-05	6.447E+07	5.677E-05	9.137E-06
4.00e+00	to	5.00e+00	1.215E-33	2.176E+07	6.079E-34	0.0
5.00e+00	to	6.50e+00	3.502E-34	8.734E+06	1.752E-34	0.0
6.50e+00	to	8.00e+00	4.454E-35	1.713E+06	2.228E-35	0.0
8.00e+00	to	1.00e+01	5.944E-36	3.638E+05	2.973E-36	0.0
Total Gamma, g/(sec*FA)			8.655E+11	2.690E+15	1.922E+12	6.015E+11
(1)Total Neutrons, n/(sec*FA)			6.324E+08 (raw) 9.720E+08 (adjusted intact) 1.014E+09 (adjusted reconfigured)			

(1) *The "raw" source is calculated with ORIGEN-ARP. The adjusted source is the raw source multiplied by bpf/(1-k_{eff}) to account for subcritical neutron multiplication and an axial variation of burnup profile in active fuel region, where bpf=1.152, k_{eff}=0.2505 if fuel is intact and k_{eff}=0.2812 if fuel is reconfigured. k_{eff} for reconfigured fuel includes an additional 12.25% increase to account for fuel compression.*

Table A.5-39
Bounding NCT and HAC Source for the 69BTH DSC, Reconfigured Fuel, 45 Inner Compartments

62 GWd/MTU, 2.6 wt. %, after 18.5 years of cooling						
E_{min}, MeV	*to*	*E_{max}, MeV*	*Bottom Nozzle*	*In-core*	*Plenum*	*Top Nozzle*
0.00e+00	*to*	*5.00e-02*	*1.916E+10*	*3.783E+14*	*8.447E+09*	*1.456E+10*
5.00e-02	*to*	*1.00e-01*	*3.637E+09*	*1.013E+14*	*1.130E+09*	*2.768E+09*
1.00e-01	*to*	*2.00e-01*	*9.263E+08*	*6.952E+13*	*5.678E+08*	*7.024E+08*
2.00e-01	*to*	*3.00e-01*	*4.731E+07*	*2.081E+13*	*3.469E+07*	*3.586E+07*
3.00e-01	*to*	*4.00e-01*	*6.872E+07*	*1.350E+13*	*8.793E+07*	*5.186E+07*
4.00e-01	*to*	*6.00e-01*	*2.571E+08*	*1.724E+13*	*1.586E+09*	*1.862E+08*
6.00e-01	*to*	*8.00e-01*	*1.480E+08*	*7.808E+14*	*8.274E+08*	*1.599E+08*
8.00e-01	*to*	*1.00e+00*	*6.221E+07*	*1.109E+13*	*1.490E+07*	*9.737E+07*
1.00e+00	*to*	*1.33e+00*	*1.059E+12*	*2.067E+13*	*3.239E+11*	*8.068E+11*
1.33e+00	*to*	*1.66e+00*	*2.992E+11*	*3.359E+12*	*9.148E+10*	*2.278E+11*
1.66e+00	*to*	*2.00e+00*	*8.137E+00*	*3.481E+10*	*5.299E+01*	*6.100E+00*
2.00e+00	*to*	*2.50e+00*	*7.158E+06*	*1.939E+09*	*2.189E+06*	*5.452E+06*
2.50e+00	*to*	*3.00e+00*	*6.116E+03*	*1.566E+08*	*1.870E+03*	*4.658E+03*
3.00e+00	*to*	*4.00e+00*	*1.374E-06*	*5.103E+07*	*1.198E-11*	*1.119E-05*
4.00e+00	*to*	*5.00e+00*	*0.0*	*1.697E+07*	*2.314E-33*	*0.0*
5.00e+00	*to*	*6.50e+00*	*0.0*	*6.811E+06*	*6.668E-34*	*0.0*
6.50e+00	*to*	*8.00e+00*	*0.0*	*1.336E+06*	*8.481E-35*	*0.0*
8.00e+00	*to*	*1.00e+01*	*0.0*	*2.837E+05*	*1.132E-35*	*0.0*
*Total Gamma, g/(sec*FA)*			*1.383E+12*	*1.417E+15*	*4.281E+11*	*1.053E+12*
*(1)Total Neutrons, n/(sec*FA)*			*4.958E+08 (raw)* *7.201E+08 (adjusted intact)* *7.380E+08 (adjusted reconfigured)*			

(1) The "raw" source is calculated with ORIGEN-ARP. The adjusted source is the raw source multiplied by bpf/(1-k_{eff}) to account for subcritical neutron multiplication and an axial variation of burn-up profile in active fuel region, where bpf=1.212, k_{eff}=0.1655 if fuel is intact and k_{eff}=0.1655(1+0.1225)=0.1858 if fuel is reconfigured. k_{eff} for reconfigured fuel includes an additional 12.25% increase to account for fuel compression.*

Table A.5-39a
Bounding NCT and HAC Source for the 69BTH DSC, Reconfigured Fuel, 24 Peripheral Compartments

62 GWd/MTU, 2.6 wt. %, after 35.0 years of cooling						
E_{min}, MeV	to	E_{max}, MeV	Bottom Nozzle	In-core	Plenum	Top Nozzle
0.00e+00	to	5.00e-02	2.534E+09	2.507E+14	8.099E+08	1.894E+09
5.00e-02	to	1.00e-01	4.166E+08	7.103E+13	1.278E+08	3.170E+08
1.00e-01	to	2.00e-01	1.011E+08	4.284E+13	3.525E+07	7.712E+07
2.00e-01	to	3.00e-01	5.433E+06	1.328E+13	1.956E+06	4.110E+06
3.00e-01	to	4.00e-01	7.162E+06	8.920E+12	3.183E+06	5.389E+06
4.00e-01	to	6.00e-01	5.200E+06	6.427E+12	2.437E+07	3.690E+06
6.00e-01	to	8.00e-01	1.708E+07	5.261E+14	1.277E+07	6.506E+07
8.00e-01	to	1.00e+00	1.934E+07	2.893E+12	1.730E+06	6.510E+07
1.00e+00	to	1.33e+00	1.209E+11	4.682E+12	3.697E+10	9.208E+10
1.33e+00	to	1.66e+00	3.414E+10	5.966E+11	1.044E+10	2.600E+10
1.66e+00	to	2.00e+00	5.420E+00	2.270E+10	3.529E+01	4.064E+00
2.00e+00	to	2.50e+00	8.169E+05	1.206E+09	2.498E+05	6.222E+05
2.50e+00	to	3.00e+00	6.980E+02	1.115E+08	2.134E+02	5.316E+02
3.00e+00	to	4.00e+00	9.708E-07	2.735E+07	8.459E-12	7.901E-06
4.00e+00	to	5.00e+00	0.0	9.232E+06	2.314E-33	0.0
5.00e+00	to	6.50e+00	0.0	3.705E+06	6.668E-34	0.0
6.50e+00	to	8.00e+00	0.0	7.268E+05	8.481E-35	0.0
8.00e+00	to	1.00e+01	0.0	1.543E+05	1.132E-35	0.0
Total Gamma, g/(sec*FA)			1.581E+11	9.275E+14	4.843E+10	1.205E+11
(1)Total Neutrons, n/(sec*FA)			2.699E+08 (raw) 3.920E+08 (adjusted intact) 4.018E+08 (adjusted reconfigured)			

(1) *The "raw" source is calculated with ORIGEN-ARP. The adjusted source is the raw source multiplied by bpf/(1-k_{eff}) to account for subcritical neutron multiplication and an axial variation of burn-up profile in active fuel region, where bpf=1.212, k_{eff}=0.1655 if fuel is intact and k_{eff}=0.1655*(1+0.1225)=0.1858 if fuel is reconfigured. k_{eff} for reconfigured fuel includes an additional 12.25% increase to account for fuel compression.*

Table A.5-39b
Bounding NCT and HAC Source for the 69BTH DSC, Reconfigured Fuel, 24 Peripheral Compartments:

[ ]

62 GWd/MTU, 2.6 wt. %, after 29.0 years of cooling						
E_{min}, MeV	to	E_{max}, MeV	Bottom Nozzle	In-core	Plenum	Top Nozzle
0.00e+00	to	5.00e-02	5.075E+09	2.898E+14	1.728E+09	3.835E+09
5.00e-02	to	1.00e-01	9.146E+08	8.044E+13	2.810E+08	6.961E+08
1.00e-01	to	2.00e-01	2.239E+08	5.062E+13	8.827E+07	1.705E+08
2.00e-01	to	3.00e-01	1.158E+07	1.555E+13	4.938E+06	8.784E+06
3.00e-01	to	4.00e-01	1.559E+07	1.035E+13	9.402E+06	1.179E+07
4.00e-01	to	6.00e-01	1.943E+07	7.871E+12	1.107E+08	1.401E+07
6.00e-01	to	8.00e-01	2.441E+07	6.053E+14	5.777E+07	7.039E+07
8.00e-01	to	1.00e+00	2.581E+07	4.238E+12	3.710E+06	7.004E+07
1.00e+00	to	1.33e+00	2.662E+11	7.793E+12	8.140E+10	2.027E+11
1.33e+00	to	1.66e+00	7.517E+10	1.055E+12	2.299E+10	5.725E+10
1.66e+00	to	2.00e+00	6.283E+00	2.644E+10	4.091E+01	4.711E+00
2.00e+00	to	2.50e+00	1.799E+06	1.409E+09	5.500E+05	1.370E+06
2.50e+00	to	3.00e+00	1.537E+03	1.240E+08	4.699E+02	1.170E+03
3.00e+00	to	4.00e+00	1.102E-06	3.405E+07	9.599E-12	8.966E-06
4.00e+00	to	5.00e+00	0.0	1.150E+07	2.314E-33	0.0
5.00e+00	to	6.50e+00	0.0	4.614E+06	6.668E-34	0.0
6.50e+00	to	8.00e+00	0.0	9.051E+05	8.481E-35	0.0
8.00e+00	to	1.00e+01	0.0	1.922E+05	1.132E-35	0.0
Total Gamma, g/(sec*FA)			3.477E+11	1.073E+15	1.067E+11	2.649E+11
(1)Total Neutrons, n/(sec*FA)			3.359E+08 (raw) 4.878E+08 (adjusted intact) 5.000E+08 (adjusted reconfigured)			

(1) *The "raw" source is calculated with ORIGEN-ARP. The adjusted source is the raw source multiplied by bpf/(1-k_{eff}) to account for subcritical neutron multiplication and an axial variation of burn-up profile in active fuel region, where bpf=1.212, k_{eff}=0.1655 if fuel is intact and k_{eff}=0.1655*(1+0.1225)=0.1858 if fuel is reconfigured. k_{eff} for reconfigured fuel includes an additional 12.25% increase.*

Pages A.5-80 through A.5-80t are proprietary information withheld pursuant to 10 CFR 2.390

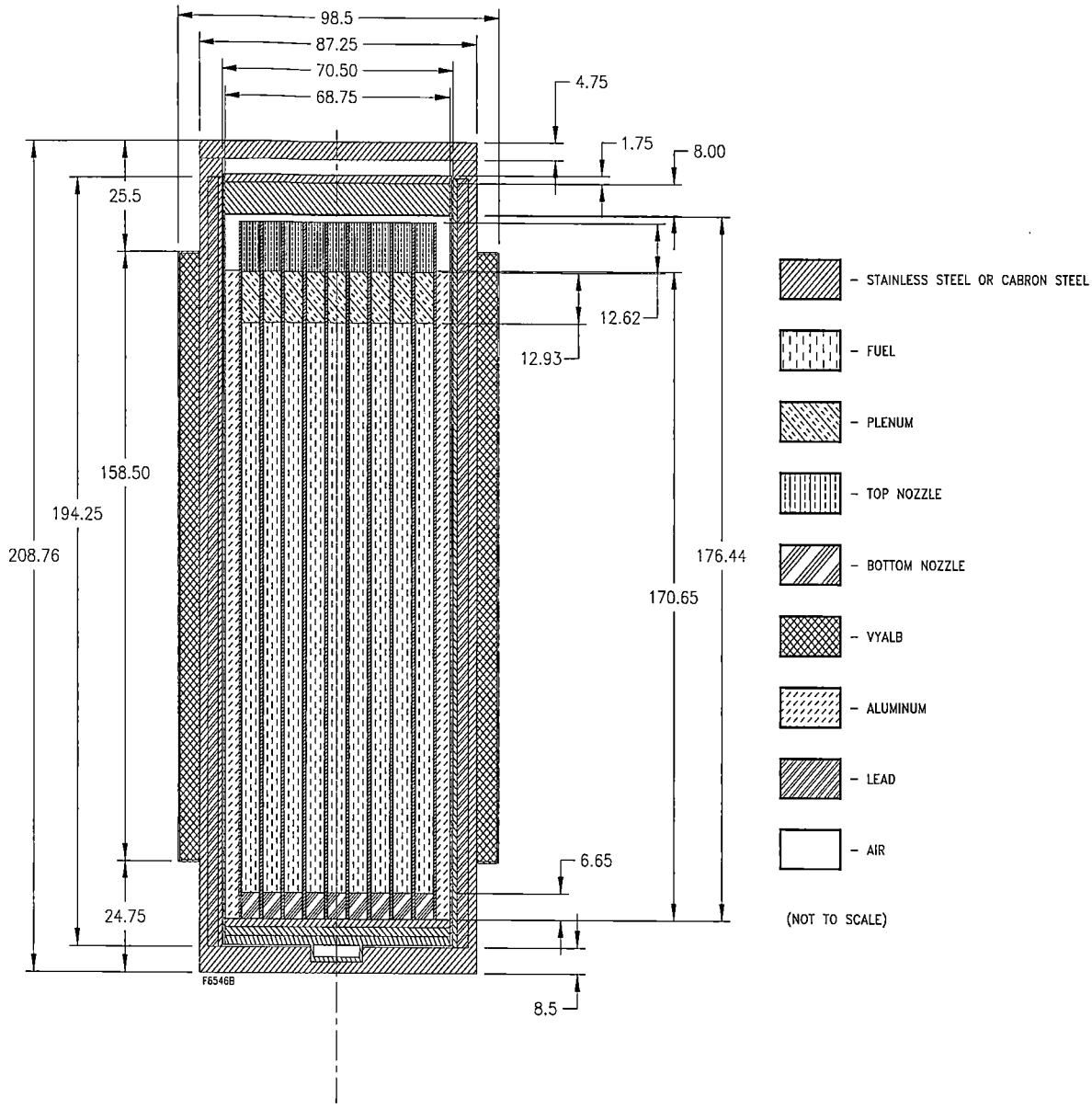

Figure A.5-1
MP197HB Transport Cask with 69BTH DSC Model, Axial View

Note: All dimensions are in inches. Impact Limiters are not shown.

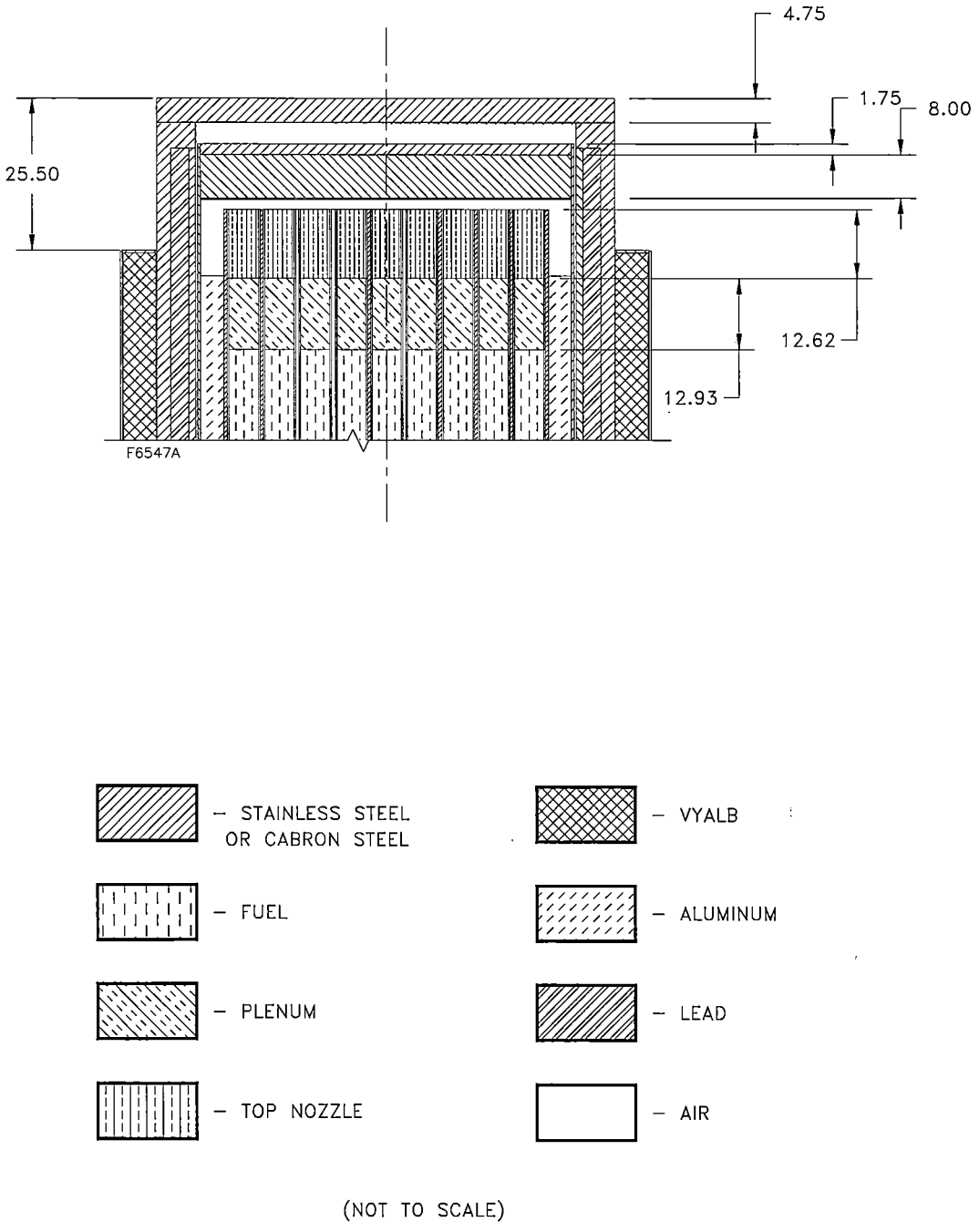

Figure A.5-2
MP197HB Transport Cask with 69BTH DSC Model, Top View Showing Cask Lid with Gap, Top Nozzle, and Plenum

Note: All dimensions are in inches. Top Impact Limiter is not shown.

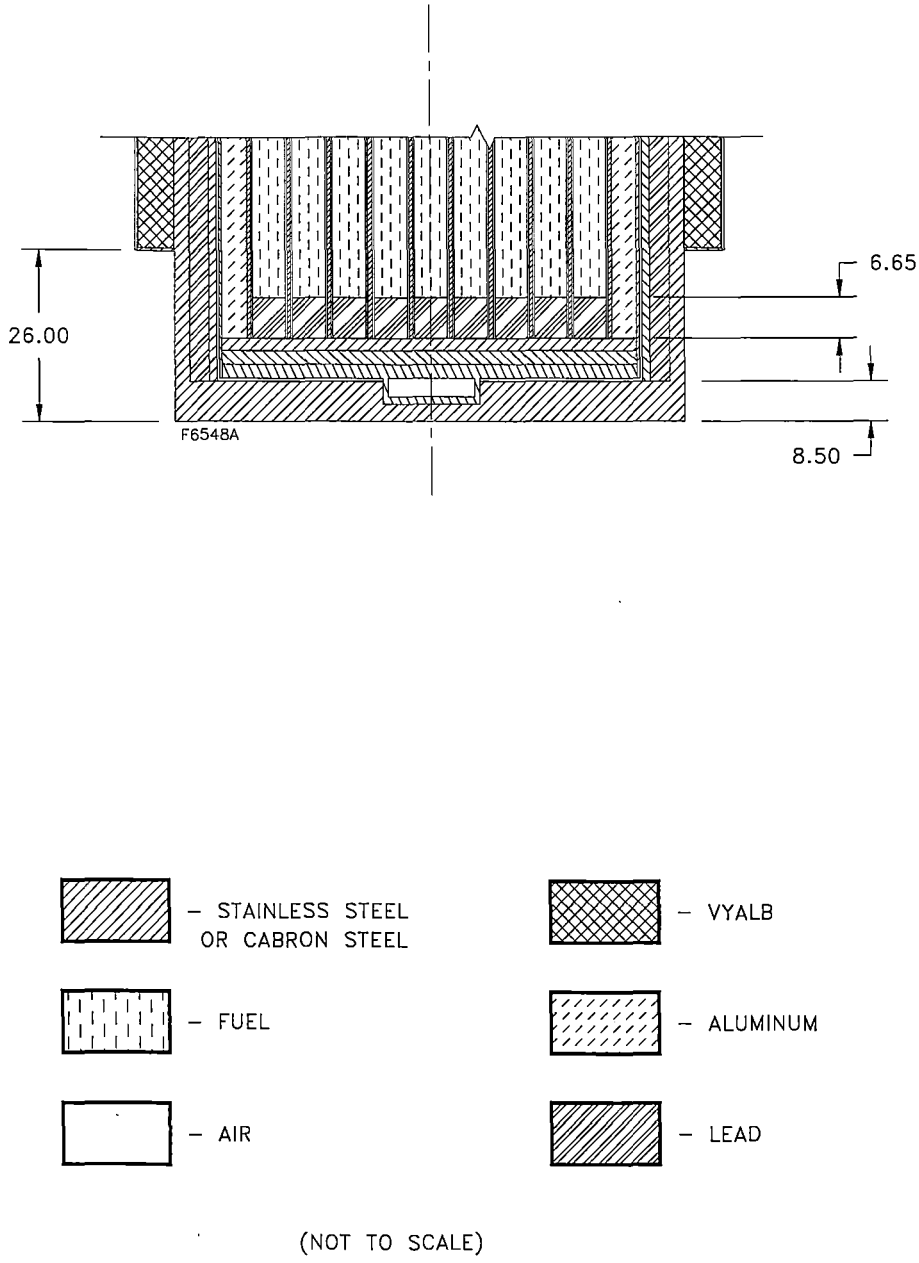

Figure A.5-3
MP197HB Transport Cask with 69BTH DSC Model, Bottom View Showing Cask Bottom and Bottom Nozzle

Note: All dimensions are in inches. Bottom Impact Limiter is not shown.

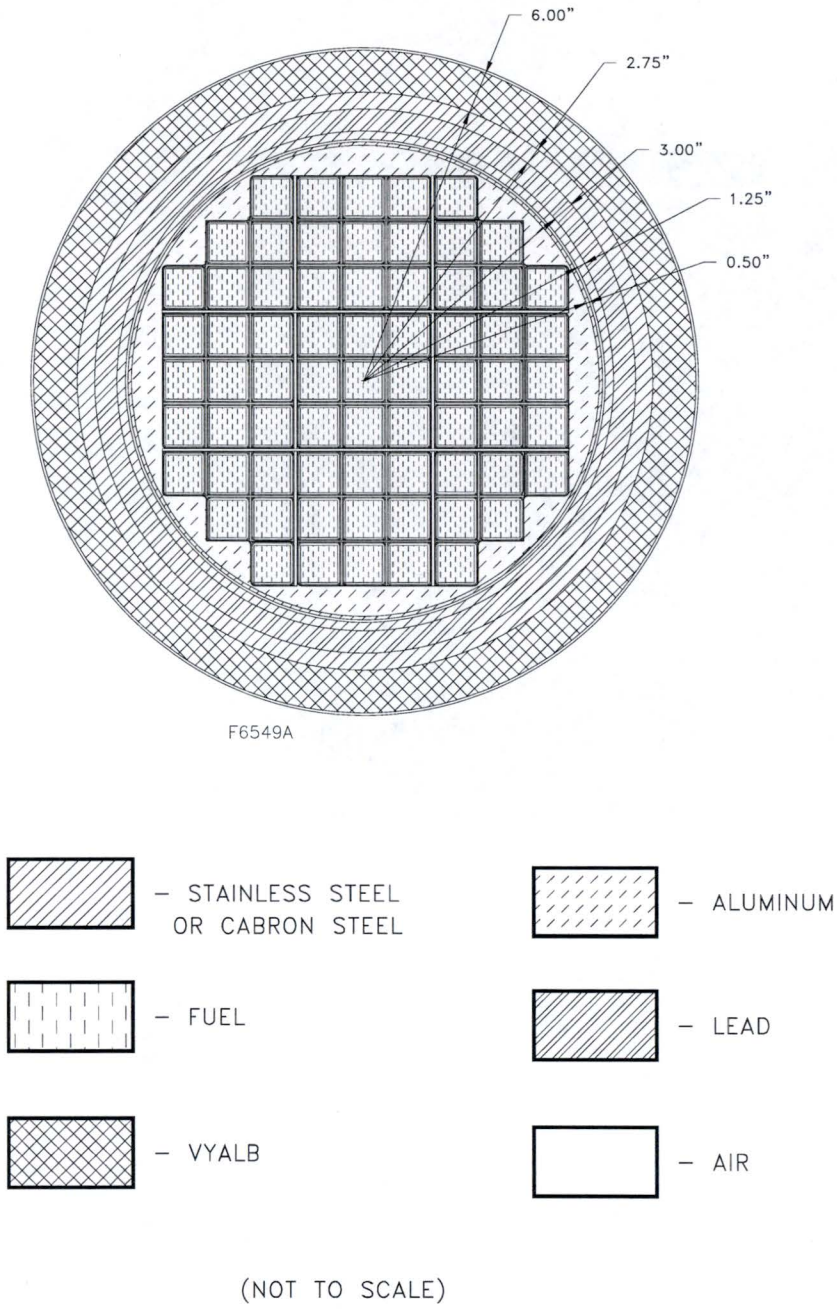

Figure A.5-4
MP197HB within 69BTH DSC Model, Cross Section View

Note: All dimensions are in inches

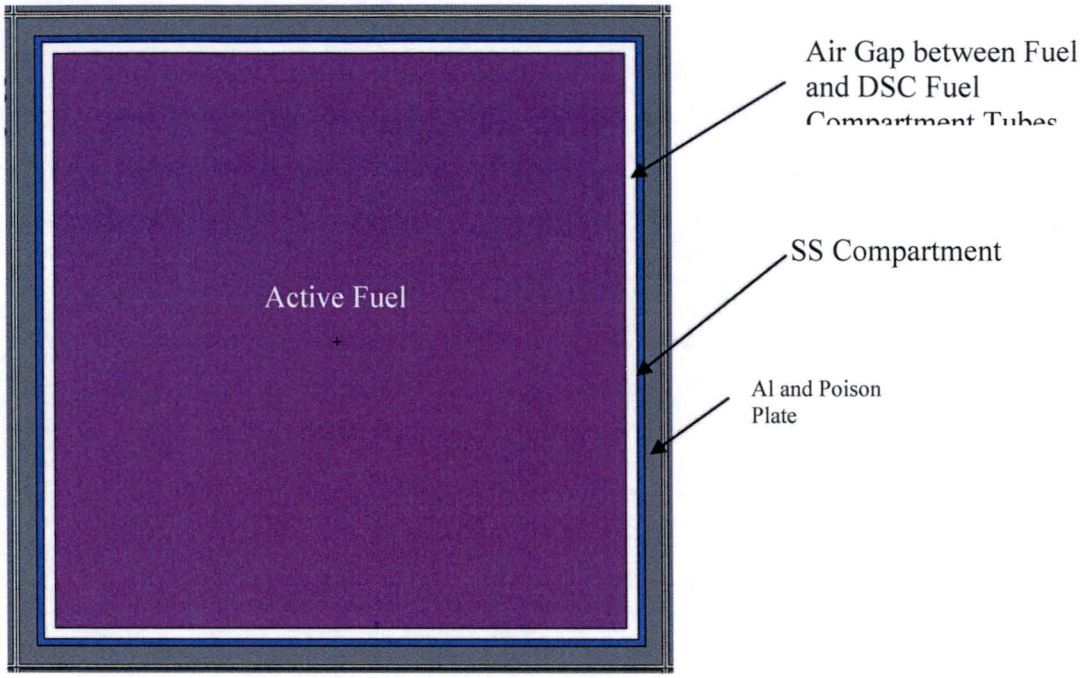

Figure A.5-5
Details of DSC Basket with Fuel Lattice Unit Cell in MCNP Model

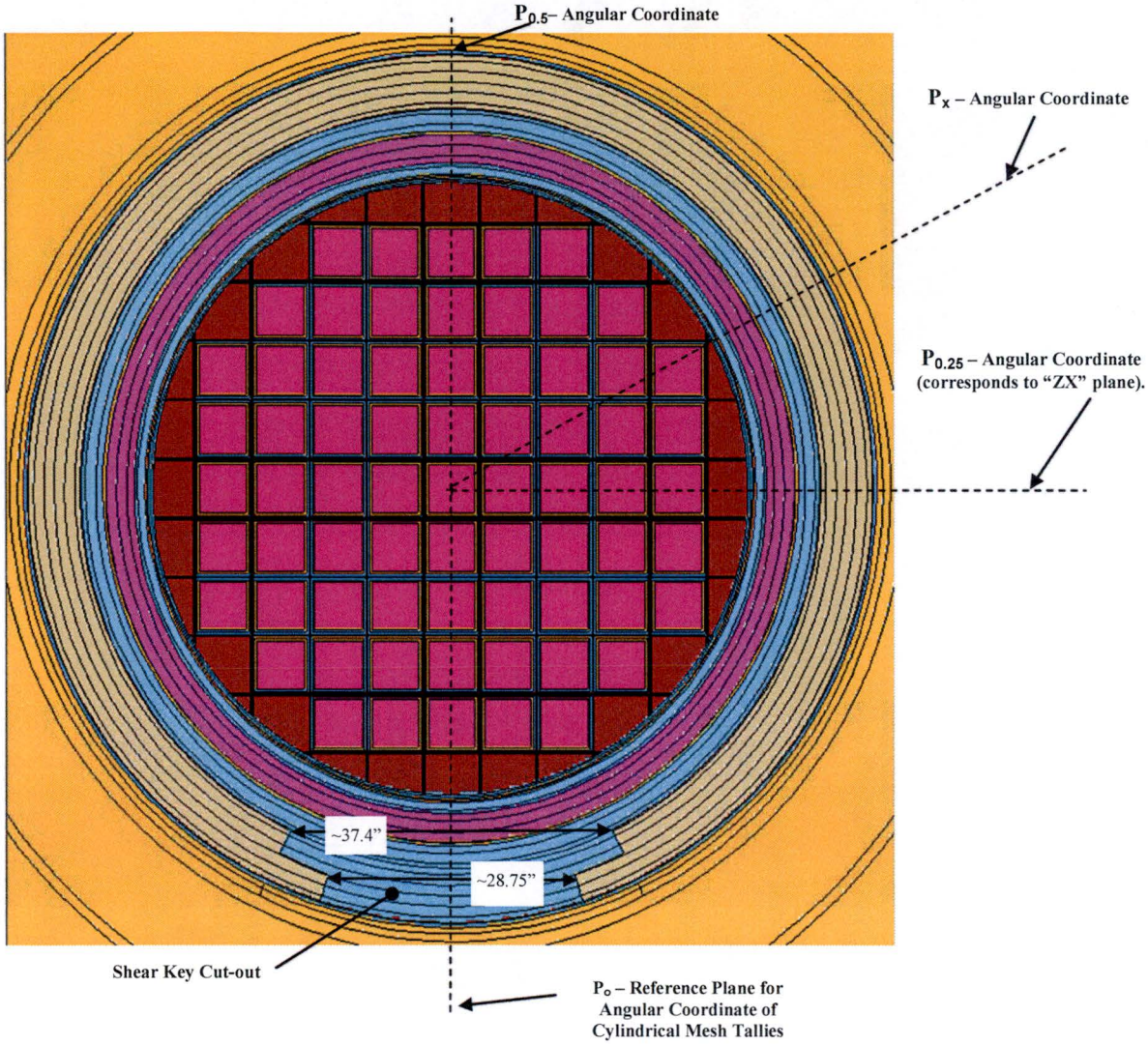

Figure A.5-6
MP197HB Transport Cask within 69 BTH DSC: MCNP Model Cut-through XY Plane (Z=25.12 cm), Normal Condition

Note: All dimensions are in inches

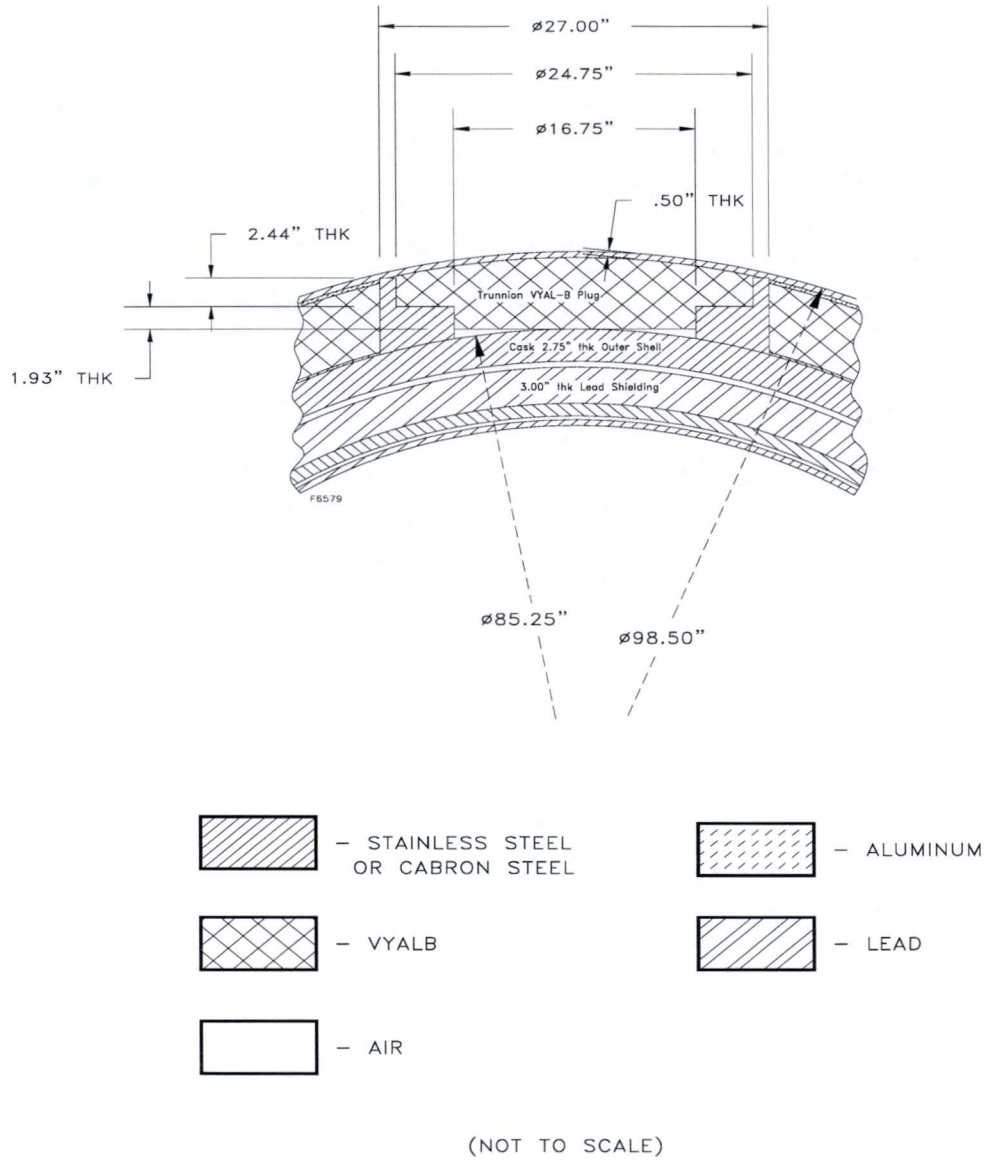

Figure A.5-7
MP197HB Bottom and Top Trunnion Attachment Block and Plug Geometry, Normal Condition

Note: All dimensions are in inches

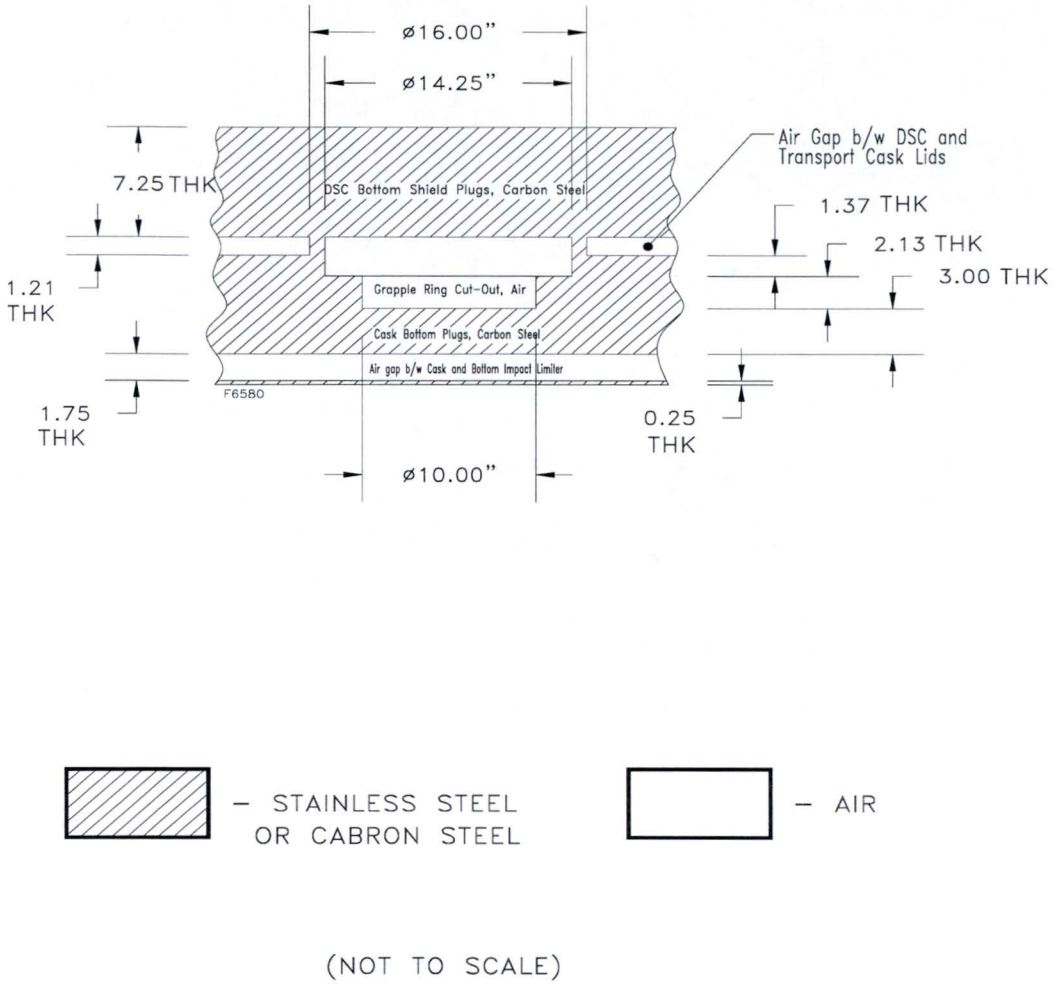

Figure A.5-8
69BTH DSC and MP197HB Bottom Plugs with Grapple Ring Cut-Out

Note: All dimensions are in inches

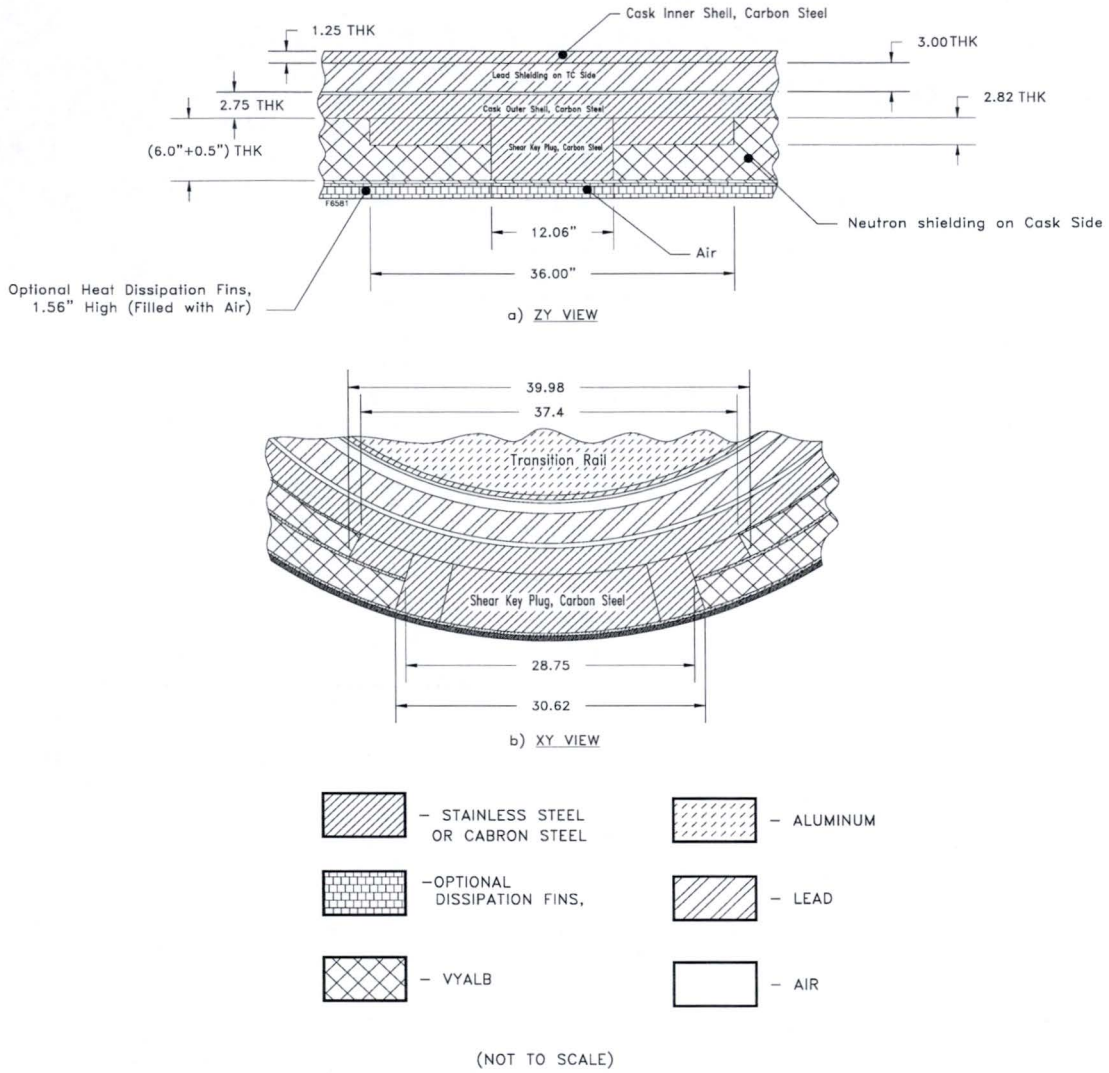

Figure A.5-9
MP197HB Shear Key

Note: 1) All dimensions are in inches
2) Two 0.125"aluminum shells from aluminum boxes encasing neutron shielding material, 0.375"cask outer shield shell as well as 0.375" air shell between lead shielding on cask side and cask outer shell are not seen.

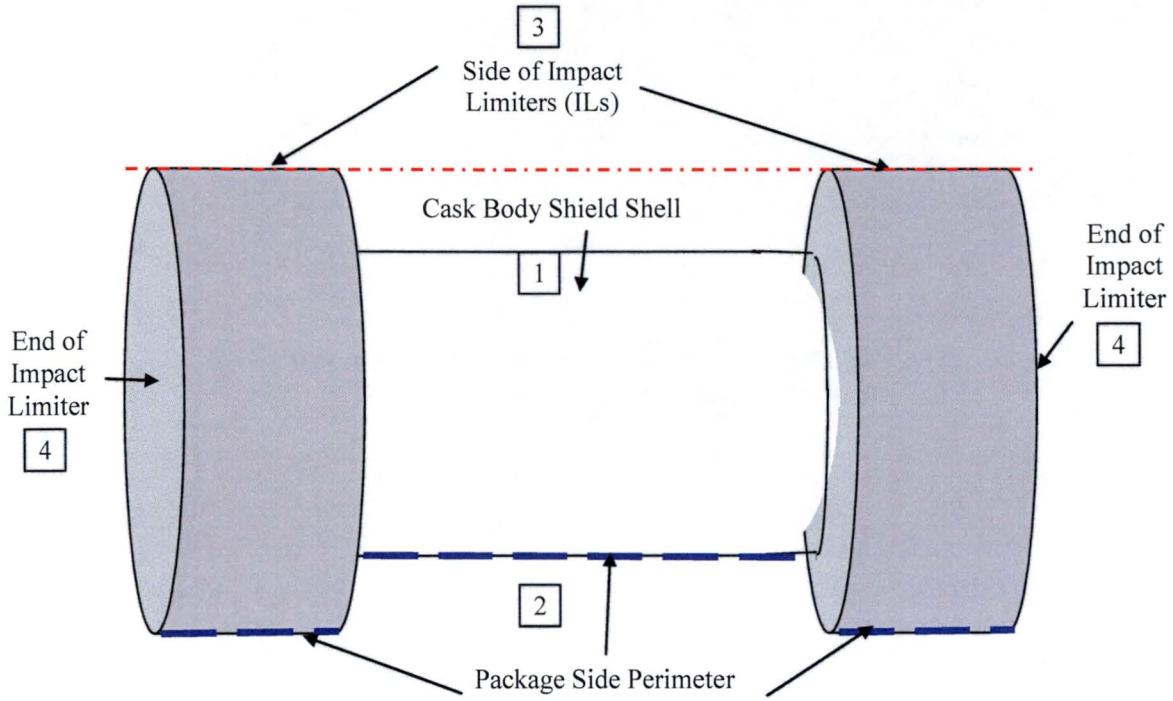

Figure A.5-10
Dose Rate Location Terminology

Pages A.5-91 through A.5-100 are proprietary information withheld pursuant to 10 CFR 2.390

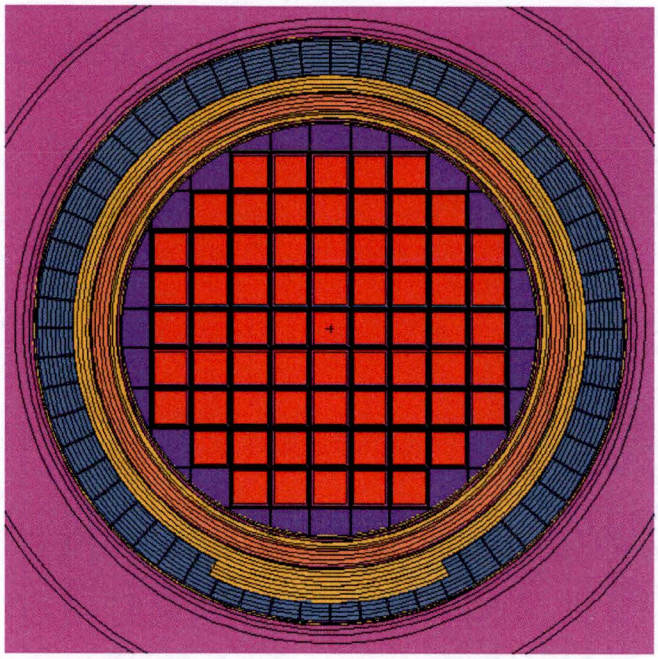

69BTH DSC

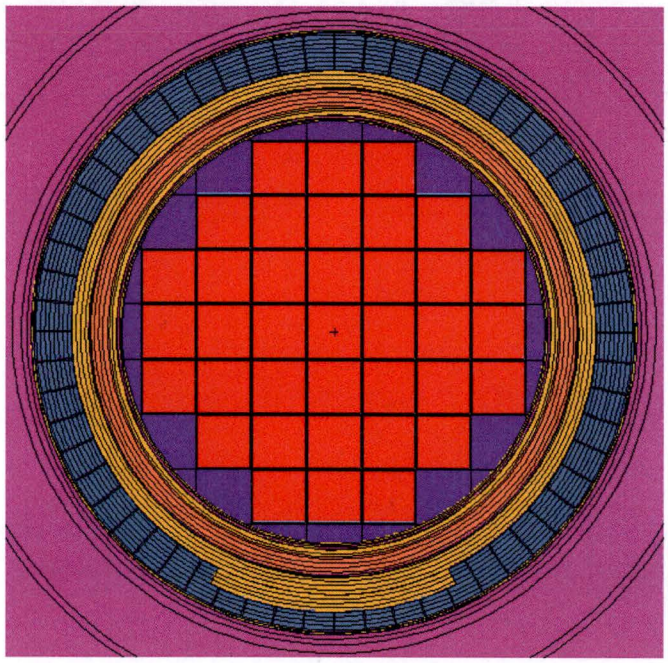

37PTH DSC

Figure A.5-23
NCT MCNP Models (x-y View)

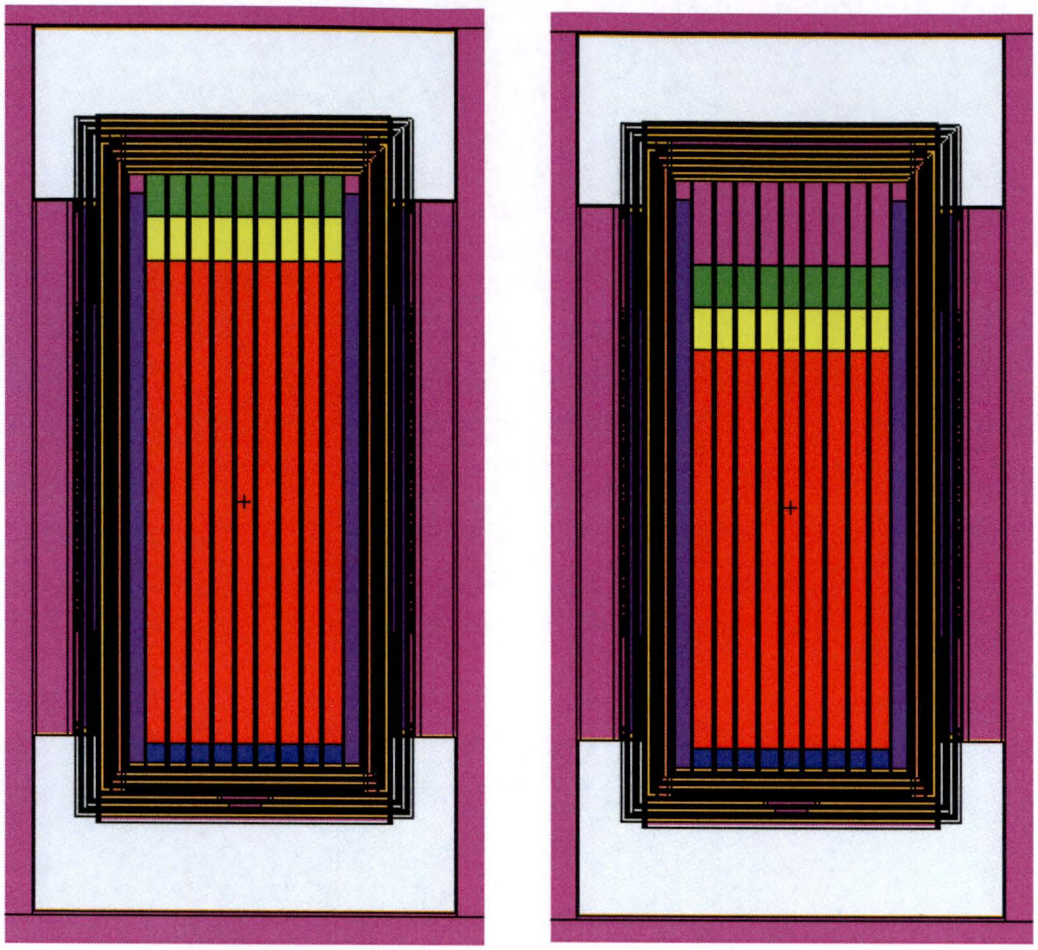

Intact Fuel Reconfigured Fuel

Figure A.5-24
NCT 69BTH DSC MCNP Models (x-z View)

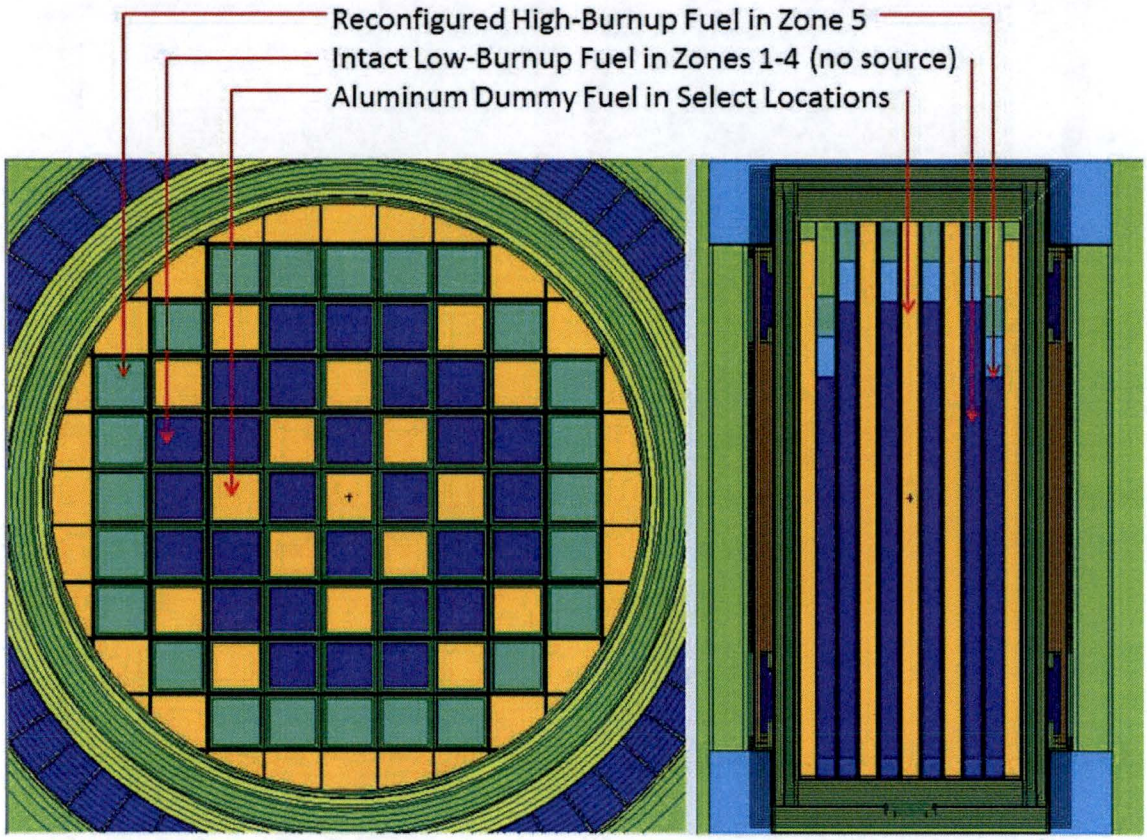

Figure A.5-24a
NCT 69BTH DSC MCNP Model for Heat Load Zone Configuration No. 8 with High-Burnup Reconfigured Fuel in Zone 5
(x-y and x-z views)

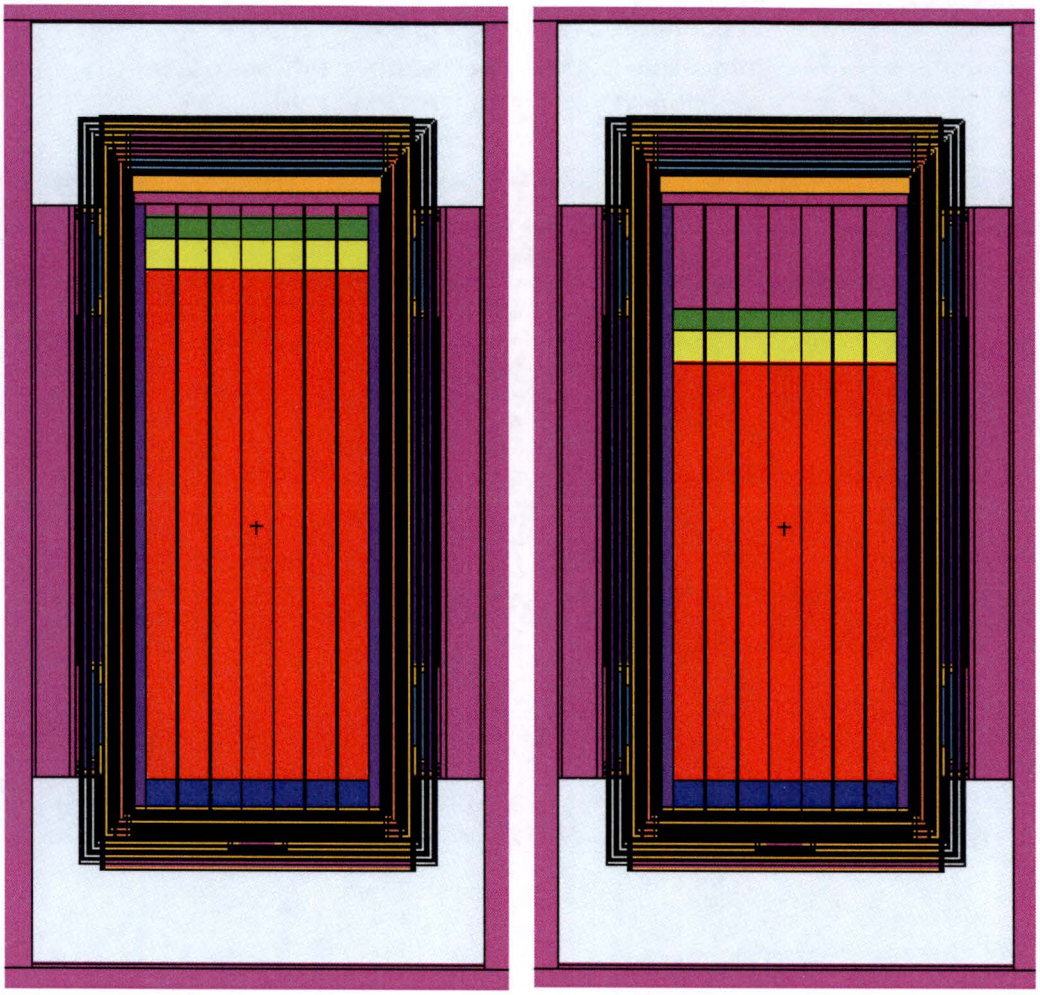

Intact Fuel Reconfigured Fuel

Figure A.5-25
NCT 37PTH DSC MCNP Models (x-z View)

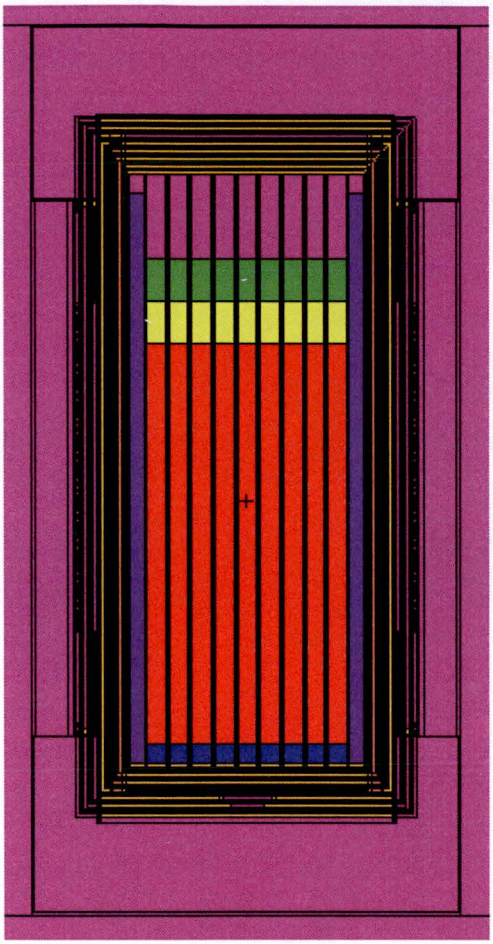

69BTH DSC

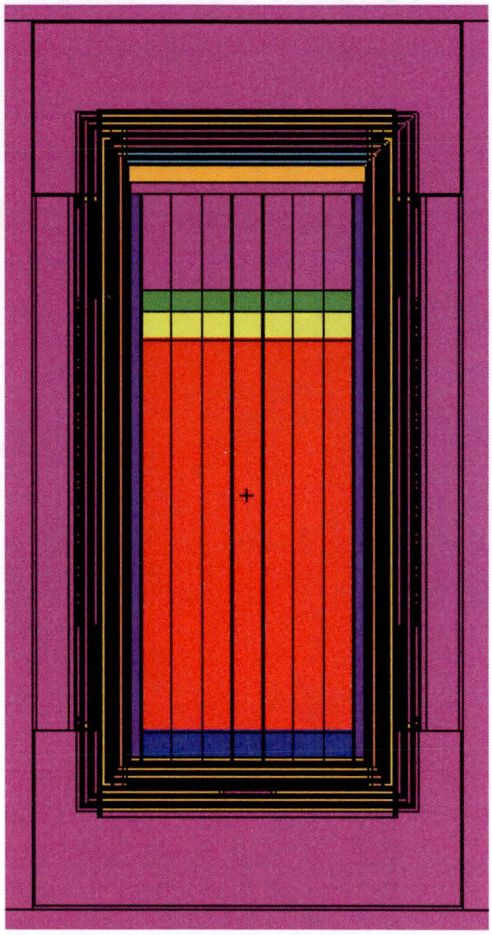

37PTH DSC

Note: All neutron shielding VYAL-B material, the aluminum boxes, the neutron shield steel skin, impact limiter wood, and impact limiter steel shell are modeled as air.

Figure A.5-26
HAC MCNP Models for Reconfigured Fuel (x-z View)

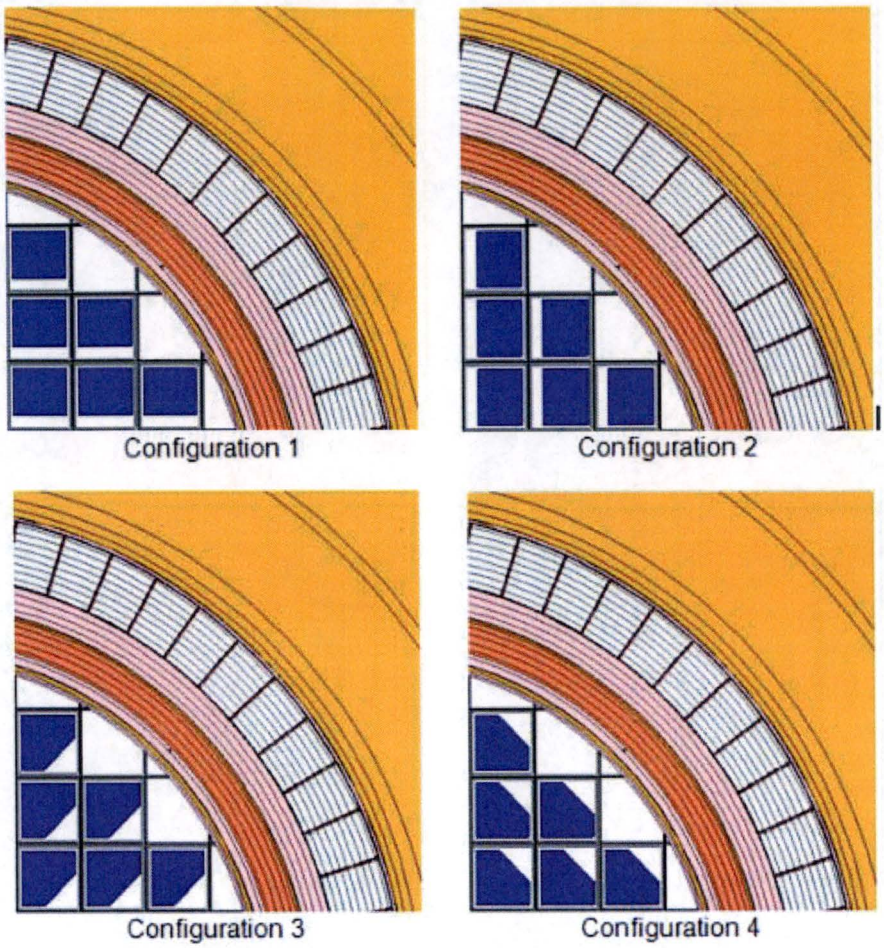

Figure A.5-27
NCT Configurations for *Radial* Fuel Reconfiguration (x-y View)

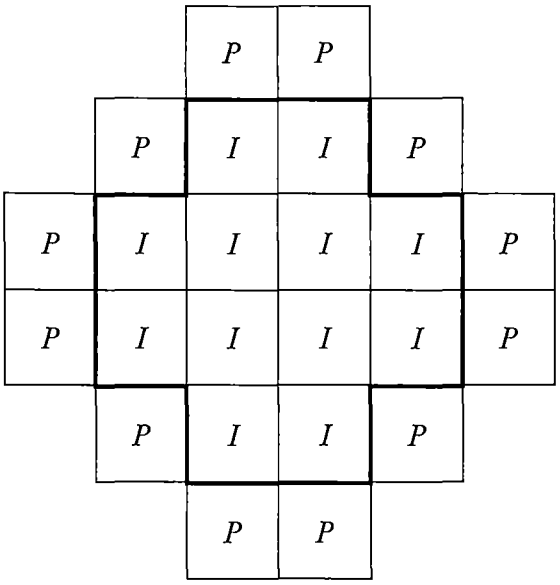

Figure A.5-28
Peripheral and Inner Fuel Locations for the 24PT4 and 24PTH DSCs

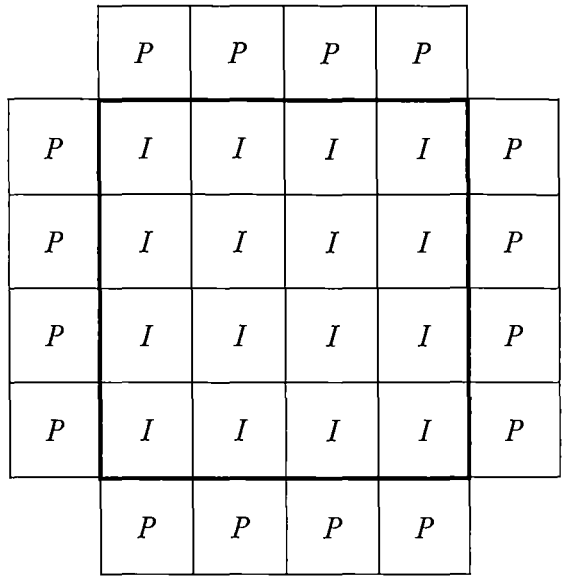

Figure A.5-29
Peripheral and Inner Fuel Locations for the 32PT, 32PTH, and 32PTH1 DSCs

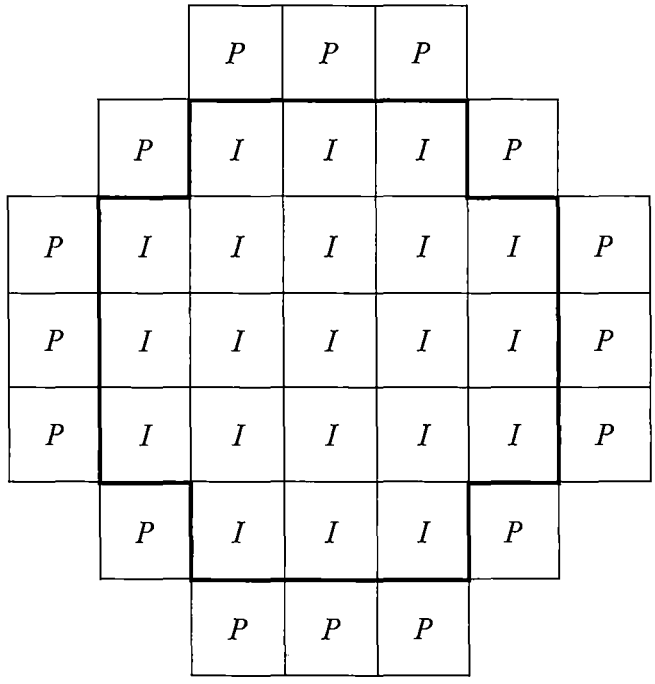

Figure A.5-29a
Peripheral and Inner Fuel Locations for the 37PTH DSC

			P	P	P			
	P	P	I	I	I	P	P	
	P	I	I	I	I	I	P	
P	I	I	I	I	I	I	I	P
P	I	I	I	I	I	I	I	P
P	I	I	I	I	I	I	I	P
	P	I	I	I	I	I	P	
	P	P	I	I	I	P	P	
			P	P	P			

Figure A.5-29b
Peripheral and Inner Fuel Locations for the 61BT and 61BTH DSCs

		P	P	P	P	P		
	P	I	I	I	I	I	P	
P	I	I	I	I	I	I	I	P
P	I	I	I	I	I	I	I	P
P	I	I	I	I	I	I	I	P
P	I	I	I	I	I	I	I	P
P	I	I	I	I	I	I	I	P
	P	I	I	I	I	I	P	
		P	P	P	P	P		

Figure A.5-29c
Peripheral and Inner Fuel Locations for the 69BTH DSC

Pages A.5-108 through A.5-111 are proprietary information withheld pursuant to 10 CFR 2.390

Proprietary Information Withheld Pursuant to 10 CFR 2.390

Figure A.5-38
Correction Factors vs. Burnup for Each Reactor–Cs-137

Proprietary Information Withheld Pursuant to 10 CFR 2.390

Figure A.5-39
Cooling Time Comparison–Trending Evaluation

Proprietary Information Withheld Pursuant to 10 CFR 2.390